THIOCYANATE LEACHING OF GOLD

by

OLAVO BARBOSA FILHO
B.Sc. Chem. Eng. (Faculdades de Engenharia FAAP - São Paulo)
M.Sc. Met. Eng. (Pontifícia Universidade Católica - Rio de Janeiro)

A Thesis submitted for the Degree of
Doctor of Philosophy of the University of London
and for the
Diploma of Membership of the Imperial College
of Science, Technology and Medicine

Department of Mineral Resources Engineering
Royal School of Mines
Imperial College of Science, Technology and Medicine
University of London

September 1991

To the memory of my father.
To those who in the quiet silence
of their hearts helped me to come
across.

ABSTRACT

The toxicity of cyanide has increasingly raised concerns with respect to environmental protection and operational safety, thus motivating a growing research activity towards alternative lixiviants for gold ores. The increasing interest in gold ores which are not amenable to cyanidation is another reason for the search for alternative lixiviants. One such lixiviant is thiocyanate. This thesis addresses the fundamental chemical, thermodynamic, kinetic and mechanistic aspects of the leaching of gold by thiocyanate.

The chemistry and thermodynamics of thiocyanate systems for leaching gold (and silver) ores was investigated, a number of Eh-pH diagrams, distribution curves and solubility diagrams having been drawn and used to support the experimental design and discussion of the subject. Gold is dissolved mainly as the auric, $Au(SCN)_4^-$, and aurous, $Au(SCN)_2^-$, complexes. The gold-thiocyanate system was found to be metastable, the metal being dissolved at potentials at which the oxidation of thiocyanate also takes place.

Considerable overpotentials are required for the oxidation of thiocyanate. An unified view is provided of the intermediate species in the oxidation of thiocyanate, particularly those responsible for the observed overpotentials, which are considered to have an important role in the mechanism of gold dissolution.

Iron(III) is the main oxidant investigated. The discussion of the iron-thiocyanate system is supported by thermodynamic calculations. An experimental programme was carried out to determine the redox processes in iron-thiocyanate solutions, namely, the reduction of iron(III) to iron(II) and the corresponding oxidation of thiocyanate. The effect of hydrogen peroxide in this context was also investigated. The overall stoichiometry of the process was established based on those experimental results. The progress of the reactions was related empirically to the observed changes in the electrochemical potentials in the system. The main intermediate species in the oxidation of thiocyanate by iron(III) were found to be $(SCN)_2$ and $(SCN)_3^-$, particularly the latter. The

mechanism of autoreduction of the iron(III)-thiocyanate complexes is discussed.

The kinetics of the dissolution of gold by iron(III)-thiocyanate solutions was studied extensively by means of a rotating gold disc. The process was found to be chemically controlled, with low rates of reaction, of the order of 10^{-10} mol/cm^2 s, at 25°C. Various attempts were made to improve the dissolution rates. Temperatures up to 85°C were tried, yielding initial rates of the order of 10^{-8} mol/cm^2 s with 0.10 mol/l SCN^-, which are similar to those obtained with the same concentration of thiourea. Another direction of investigation was the addition of small amounts of iodide or mixtures of iodine plus iodide, to the iron(III)-thiocyanate leaching system, at 25°C. These latter trials yielded initial gold dissolution rates similar to those obtained at 85°C without iodide/iodine addition, and average dissolution rates higher than those at 85°C. The improvement in the dissolution rates due to the iodide/iodine additions amounts to a synergistic effect. Accordingly, the chemistry of the mixed thiocyanate-iodide system is discussed in detail. Mechanisms of gold dissolution are discussed with reference both to the iron-thiocyanate and to the iron-thiocyanate-iodine systems.

Overall, thiocyanate proved to be a viable and interesting lixiviant for gold. The leaching rates are as high, or even higher, than those obtained with thiourea. Moreover, thiocyanate has the advantage of being considerably more stable than thiourea towards oxidation. The thiocyanate consumption, due to its decomposition through oxidation, was less than 4% in most of the experiments.

CONTENTS Page

ABSTRACT 3

LIST OF FIGURES 11

LIST OF TABLES 19

CHAPTER 1: INTRODUCTION 21

1.1. Previous Work on Gold Leaching by Thiocyanate 21
1.2. Thiocyanate as an Alternative Lixiviant for Gold 23
1.3. The Scope of the Present Work 24

CHAPTER 2: THERMODYNAMICS OF THIOCYANATE SYSTEMS FOR LEACHING GOLD AND SILVER ORES 31

2.1. Introduction 31
2.2. Metastable Eh-pH Diagrams 31
2.3. Thiocyanate Ion and Thiocyanic Acid 33
2.4. The SCN-H_2O System and its Comparison with the CN-H_2O System 36
2.5. The Au-H_2O and Ag-H_2O Systems 43
2.6. The Au-SCN-H_2O System 45
2.7. The Ag-SCN-H_2O System 49
2.8. Some Prospective Oxidants for the Thiocyanate Leaching of Gold and Silver 55
2.9. The Metastable Character of the Au-SCN-H_2O and Ag-SCN-H_2O Systems and its Comparison with the Homologous Cyanide Systems 58
2.10. Conclusions 61

CHAPTER 3: THE INTEMEDIATE SPECIES IN THE OXIDATION OF THIOCYANATE AND THEIR RELEVANCE FOR THE DISSOLUTION OF GOLD 63

3.1. Introduction 63

		Page
3.2.	The Postulation of Aqueous Thiocyanogen and its Hydrolysis	63
3.3.	Oxidation Overpotentials in Thiocyanate Solutions in Relation to Thiocyanogen	68
3.4.	The Anodic Oxidation of Thiocyanate: Early Work	71
3.5.	Pure Thiocyanogen and Thiocyanogen Solutions	74
3.6.	Thiocyanogen Hydrolysis	77
3.7.	The Transitory Forms Trithiocyanate, $(SCN)_3^-$, and Dithiocyanate, $(SCN)_2^-$	79
3.8.	The Anodic Oxidation of Thiocyanate: Recent Work	81
	3.8.1. Oxidation on Platinum Electrodes	82
	3.8.2. Oxidation on Gold Electrodes	87
	3.8.3. Characterization of Oxidation Intermediate Species in Aqueous Iron-Thiocyanate Solutions	99
3.9.	Some Final Comments on This Review	108
3.10.	Further Thermodynamic Calculations. Analogies with the Halide Systems. Some Mechanistical Ideas for the Thiocyanate Leaching of Gold	110
CHAPTER 4:	REDOX PROCESSES IN AQUEOUS IRON-THIOCYANATE SOLUTIONS	121
4.1.	Iron Complexation by Thiocyanate: Description and Thermodynamic Calculations	121
4.2.	Discussion of the Previous Work on the Oxidation of Thiocyanate by Iron(III)	126
4.3.	Analytical Techniques for Iron and Thiocyanate	132
	4.3.1. Standardization of Iron(III) Stock Solutions	132
	4.3.2. Volhard Method for the Determination of Thiocyanate	133
	4.3.3. Spectrophotometric Determination of Iron(III)	134
4.4.	Potential Readings in Iron(III)-Thiocyanate Solutions	134
	4.4.1. Potential Measurements: Practical Aspects	135
	4.4.2. A First Evaluation of the Potential Readings in Fresh Iron(III)-Thiocyanate Solutions	136

		Page
4.5.	Stability of Ferric Thiocyanate Solutions Towards Iron Precipitation: pH Constraint	142
4.6.	Thiocyanate Oxidation by Iron(III): Experimental	145
	4.6.1. Variables Studied and Respective Ranges	145
	4.6.2. Experimental Procedure	146
4.7.	Thiocyanate Oxidation by Iron(III): Results and Discussion	147
	4.7.1. Experimental Reproducibility	147
	4.7.2. Effect of the Concentrations of Thiocyanate and Iron(III)	150
	4.7.3. Effect of Temperature	160
4.8.	Thiocyanate Oxidation by Iron(III): Stoicheiometry of the Process	163
4.9.	Thiocyanate Hydrolysis	166
4.10.	Mechanistic Considerations	168
CHAPTER 5:	THE USE OF HYDROGEN PEROXIDE AS OXIDANT IN AQUEOUS IRON-THIOCYANATE SOLUTIONS	175
5.1.	Introduction	175
5.2.	Previous Work on Thiocyanate Oxidation by Hydrogen Peroxide	176
5.3.	Previous Work on the Oxidation of Iron(II) by Hydrogen Peroxide	177
5.4.	Experiments on Thiocyanate Oxidation by Hydrogen Peroxide	179
	5.4.1. Experimental and Analytical Procedures	180
	5.4.2. Results and Discussion	180
5.5.	The Action of Hydrogen Peroxide on Iron-Thiocyanate Solutions	182
	5.5.1. Experimental and Analytical Procedures	182
	5.5.2. Experimental Results and Discussion	185
CHAPTER 6:	AN INVESTIGATION OF THE DISSOLUTION OF GOLD BY IRON-THIOCYANATE AND IRON-THIOCYANATE-HYDROGEN PEROXIDE SOLUTIONS	189
6.1.	Introduction	189

		Page
6.2.	Rotating Disc Study: Experimental	189
	6.2.1. Equipment	189
	6.2.2. Experimental Procedure	190
	6.2.3. Experimental Conditions	193
	6.2.4. Gold Analysis	194
	6.2.5. Iron(II) and Thiocyanate Analysis	194
6.3.	Experimental Reproducibility	195
6.4.	Effect of the Rotation Speed	199
6.5.	Effect of the Concentration of Thiocyanate	205
6.6.	Effect of the Initial Concentration of Iron(III)	213
6.7.	Catalytic Effect of Gold Metal on the Autoreduction of Iron(III)-Thiocyanate Complexes	221
6.8.	Effect of Temperature	228
6.9.	Effect of Dissolved Oxygen	247
6.10.	The Consumption of Thiocyanate in the Rotating Disc Experiments	251
6.11.	Rotating Disc Experiments at Constant Potential	253
6.12.	Some Mechanistic Considerations	259
CHAPTER 7:	THE EFFECT OF IODIDE AND IODINE ADDITIONS ON THE DISSOLUTION OF GOLD BY IRON(III)-THIOCYANATE SOLUTIONS	269
7.1.	Introduction	269
7.2.	Previous Fundamental Research on the Iodide Leaching of Gold	270
7.3.	A Comparison between the Gold-Iodine-Water System and the Gold-Thiocyanate-Water System	272
7.4.	Experimental Conditions and Procedure. Analytical Techniques	275
7.5.	Gold Leaching with Iodide and Ferric Ions: Results and Discussion	276
7.6.	Gold Leaching by Iron(III)-Thiocyanate with Additions of Iodide or Iodine Solution: Results and Discussion	280

		Page
CHAPTER 8:	CONCLUSIONS. SUGGESTIONS FOR FURTHER WORK	301
8.1.	Conclusion	301
8.2.	Suggestions for Further Work	309
ACKNOWLEDGEMENTS		315
APPENDIX 1:	THERMODYNAMIC DATA AT 25°C USED IN THE PRESENT WORK	317
APPENDIX 2:	EQUILIBRIA APPEARING ON THE Eh-pH DIAGRAMS	321
APPENDIX 3:	STABILITY CONSTANTS CONSIDERED IN THE PRESENT WORK	325
APPENDIX 4:	TESTS OF IRON PRECIPITATION FROM IRON(III)-THIOCYANATE SOLUTIONS	329
APPENDIX 5:	RESULTS OF THE EXPERIMENTS WITH IRON(III)-THIOCYANATE SOLUTIONS (CHAPTER 4)	335
APPENDIX 6:	RESULTS OF THE GOLD ROTATING DISC EXPERIMENTS	343
APPENDIX 7:	REAGENTS USED IN THE PRESENT WORK	355
REFERENCES		359

LIST OF FIGURES

		Page
2.1	Distribution curve of thiocyanic acid	35
2.2	Eh-pH diagrams for the SCN-H_2O system at 25°C	37
2.3	Eh-pH diagrams for the CN-H_2O system at 25°C	42
2.4	Eh-pH diagrams for the Au-H_2O and Ag-H_2O systems at 25°C	44
2.5	Eh-pH diagrams for the Au-SCN-H_2O system at 25°C and activity of gold species of 10^{-4} mol/dm^3	46
2.6	Eh-pH diagrams for the Au-SCN-H_2O system at 25°C and activity of gold species of 10^{-5} mol/dm^3	47
2.7	Distribution curves for (a) gold(I)-thiocyanate and (b) gold(III)-thiocyanate complexes	48
2.8	Eh-pH diagrams for the Ag-SCN-H_2O system at 25°C and activities of silver species of 10^{-4} mol/dm^3	51
2.9	Eh-pH diagrams for the Ag-SCN-H_2O system at 25°C and activity of silver species of 10^{-5} mol/dm^3	52
2.10	Distribution curves for silver-thiocyanate complexes including precipitation of AgSCN	53
2.11	Solubility diagram for silver-thiocyanate species	54
2.12	Eh-pH diagrams indicating the thermodynamic feasibility of different oxidizing agents in the dissolution of gold and silver, and in the oxidation of thiocyanate	57
2.13	Eh-pH diagrams demonstrating the metastable character of the Au-SCN-H_2O, Ag-SCN-H_2O, Au-CN-H_2O and Ag-CN-H_2O systems	60
3.1	Current-potential curves obtained with a rotating platinum electrode at different concentrations of KSCN [49]	72
3.2	Current-potential curves with a stationary platinum electrode in KSCN solutions [50]	73
3.3	Current-potential curve obtained on a platinum rotating disc electrode in acetonitrile with $2x10^{-3}$ mol/dm^3 NH_4SCN [86]	83

		Page
3.4	Linear cyclic voltammograms on a stationary platinum electrode in acetonitrile with 2.028×10^{-3} mol/dm^3 NH_4SCN [81]	86
3.5	Cyclic voltammograms on a stationary gold electrode in DMSO containing 2.8×10^{-3} mol/dm^3 KSCN at 45.1°C [88]	88
3.6	Cyclic voltammograms on a stationary gold electrode at different triangular sweep rates in DMSO with 2.8×10^{-3} mol/dm^3 KSCN at 45.1°C [88]	89
3.7	Single triangular sweep voltammograms on gold in acetonitrile at 25°C: (a) Blank experiments in 0.1 mol/dm^3 $NaClO_4$; (b) Experiments in 1.98×10^{-3} mol/dm^3 NaSCN and 0.1 mol/dm^3 $NaClO_4$ [87]	91
3.8	Visible and u.v. spectra of acetonitrile solutions 2×10^{-3} mol/dm^3 in NaSCN after electrolysis at 0.4 to 0.6 V (vs. SCE) on a gold electrode at 25°C [87]	92
3.9	Absorption spectra (a) before and (b) after the oxidation of SCN^- at 0.500 V (vs. SCE) in aqueous solution 0.1 mol/dm^3 in NaSCN and 0.1 mol/dm^3 in $HClO_4$ [90]	96
3.10	Thin-layer cyclic voltammograms and absorbance potential curves monitored at 320 nm in 0.1 mol/dm^3 NaSCN and 0.1 mol/dm^3 $HClO_4$ [90]	97
3.11	Thin-layer cyclic voltammograms in aqueous solution 0.1 mol/dm^3 NaSCN and 0.1 mol/dm^3 $HClO_4$ (A) with and (B) without 2×10^{-3} mol/dm^3 Fe^{3+} [91]	100
3.12	Thin-layer absorption spectra in aqueous solution before and after electrolysis in 0.1 mol/dm^3 NaSCN and 0.1 mol/dm^3 $HClO_4$ (a-c) with and (d) without 2×10^{-3} mol/dm^3 Fe^{3+} [91]	101
3.13	Absorbance-potential curves in 0.1 mol/dm^3 NaSCN and 0.1 mol/dm^3 $HClO_4$ aqueous solutions (A, B) with and (A', B') without 2×10^{-3} mol/dm^3 Fe^{3+} [91]	102
3.14	Variation of absorbance with electrolysis time in 0.1 mol/dm^3 NaSCN and 0.1 mol/dm^3 $HClO_4$ at 0.500 V (vs. SCE) monitored at (a) 475 nm and (b) 320 nm [91]	104

		Page
3.15	Absorption spectra of fresh iron(III)-thiocyanate and iron(II)-thiocyanate solutions acidified with (a) hydrochloric acid; (b) sulphuric or acetic acid; (c) solution in ethyl acetate, no acid added [93-95]	106
3.16	Absorption spectra of fresh iron(III)-thiocyanate solutions 0.005 mol/dm^3 in Fe^{3+} and 0.05 mol/dm^3 in KSCN with varying concentrations of (a) hydrochloric acid and (b) sulphuric acid [93, 94]	107
3.17	Eh-pH diagrams for the SCN-H_2O system at 25°C considering only the intermediate species in the oxidation of thiocyanate	113
3.18	Eh-pH diagram for the bromine-water system at 25°C [97]	114
3.19	Eh-pH diagram for the iodine-water system at 25°C [98]	114
3.20	Eh vs. log {SCN^-} lines showing the potential zones of predominance of $Au(SCN)_2^-$, $Au(SCN)_4^-$ and $(SCN)_3^-$	119
4.1	Distribution curves for the iron(III)-thiocyanate complexes	123
4.2	Distribution curve for the iron(II)-thiocyanate complex	124
4.3	Average ligand numbers of thiocyanate complexes of iron(III) and iron(II) as a function of: (a) pSCN and (b) activity of SCN^-	125
4.4	Potential readings in fresh thiocyanate solutions on a platinum electrode, at pH 1.5 and 25°C	137
4.5	Autoreduction in ferric thiocyanate solutions demonstrated by (a) decrease in the potential readings and (b) increase in the percentage of Fe^{2+} with time, at pH 1.5 and 25°C	138
4.6	Eh-pH diagrams for the SCN-H_2O system	139
4.7	Effect of the iron(III) concentration on the potential readings in fresh thiocyanate solutions at pH 2 and 3 at 23°C	143
4.8	Variation in potential readings in fresh thiocyanate solutions as iron(III) is precipitated by raising the pH, at 23°C	144

		Page
4.9	Thiocyanate oxidation by iron(III): experimental reproducibility of (a) potential readings and (b) Fe^{3+} reduction (8 hours)	148
4.10	Thiocyanate oxidation by iron(III): experimental reproducibility of (a) potential readings and (b) Fe^{3+} reduction (18 days)	149
4.11	Effect of thiocyanate concentration on the autoreduction process: (a) potential readings; (b) Fe^{3+} reduction (24 hours)	152
4.12	Effect of thiocyanate concentration on the autoreduction process: (a) potential readings; (b) Fe^{3+} reduction (18 days)	153
4.13	Effect of Fe^{3+} concentration on the autoreduction process with predominance of the cationic complexes $FeNCS^{2+}$ and $Fe(NCS)_2^{+}$: (a) potential readings; (b) Fe^{3+} reduction (24 hours)	155
4.14	Effect of Fe^{3+} concentration on the autoreduction process with predominance of the cationic complexes $FeNCS^{2+}$ and $Fe(NCS)_2^{+}$: (a) potential readings; (b) Fe^{3+} reduction (18 days)	156
4.15	Effect of Fe^{3+} concentration on the autoreduction process with predominance of the anionic complexes: (a) potential readings; (b) Fe^{3+} reduction (24 hours)	157
4.16	Effect of Fe^{3+} concentration on the autoreduction process with predominance of the anionic complexes: (a) potential readings; (b) Fe^{3+} reduction (18 days)	158
4.17	Retarding effect of Fe^{2+} on the autoreduction process: (a) potential readings; (b) Fe^{3+} reduction	159
4.18	Effect of temperature on the autoreduction process with predominance of anionic complexes: (a) potential readings; (b) Fe^{3+} reduction	161
4.19	Arrhenius plot for the initial autoreduction reactions of iron(III)-thiocyanate complexes	162
4.20	Visible and u.v. spectrum of a freshly prepared solution containing *c.a.* 3.4×10^{-4} mol/dm^3 Fe^{3+} and 0.01 mol/dm^3 SCN^- in acetonitrile, at room temperature (*c.a.* 18°C)	172

		Page
4.21	Visible and u.v. spectrum of a ferric thiocyanate solution containing *c.a.* 3.4×10^{-4} mol/dm^3 Fe^{3+} and 0.01 mol/dm^3 SCN^- in acetonitrile, at room temperature (*c.a.* 18°C), taken 4 hours after the solution was prepared	173
5.1	Thiocyanate oxidation by hydrogen peroxide at pH 1.5 and 25°C	182
5.2	Thiocyanate oxidation by iron(III): (a) potential readings and (b) Fe^{3+} reduction, at 25°C	183
5.3	Experiments at constant potential: (a) concentration of SCN^- versus time and (b) consumption of H_2O_2 at pH 1.5 and 25°C	186
6.1	Schematic view of the system used in the rotating disc experiments	191
6.2	Reproducibility of gold leaching by ferric thiocyanate solution at pH 1.5 and 25°C	196
6.3	Reproducibility of (a) potential readings at the gold disc surface and (b) reduction of Fe^{3+} to Fe^{2+}, at pH 1.5 and 25°C	197
6.4	Effect of the rotation speed on the leaching of gold by ferric thiocyanate solution	202
6.5	Effect of the rotation speed on (a) potential readings at the gold disc surface and (b) reduction of Fe^{3+} to Fe^{2+}	203
6.6	Effect of the concentration of thiocyanate on the leaching of gold by ferric thiocyanate solutionat at pH 1.5 and 25°C	206
6.7	Effect of the concentration of thiocyanate on (a) potential readings at the gold disc and (b) reduction of Fe^{3+} to Fe^{2+} at pH 1.5 and 25°C	207
6.8	Logarithmic plots of dissolution rate versus thiocyanate concentration at 25°C, pH 1.5 and initial Fe^{3+} concentration of 0.055 mol/dm^3	212
6.9	Effect of the initial concentration of iron(III), using 0.275 mol/dm^3 SCN^-, on the leaching of gold by ferric thiocyanate solution, at pH 1.5 and 25°C	214

		Page
6.10	Effect of the initial concentration of iron(III), using 0.275 mol/dm^3 SCN^-, on (a) potential readings at the gold disc surface and (b) reduction of Fe^{3+} to Fe^{2+}, at pH 1.5 and 25°C	215
6.11	Effect of the initial concentration of iron(III), using 0.10 mol/dm^3 SCN^-, on the leaching of gold by ferric thiocyanate solution, at pH 1.5 and 25°C	217
6.12	Effect of the initial concentration of iron(III), using 0.10 mol/dm^3 SCN^-, on (a) potential readings at the gold disc surface and (b) reduction of Fe^{3+} to Fe^{2+}, at pH 1.5 and 25°C	219
6.13	Logarithmic plots of dissolution rate versus initial Fe^{3+} concentration at 25°C and pH 1.5 using (a) 0.275 mol/dm^3 SCN^- and (b) 0.10 mol/dm^3 SCN^-	220
6.14	Catalytic effect of gold metal on the autoreduction of iron(III)-thiocyanate complexes at 25°C and pH 1.5	222
6.15	Effect of temperature on the dissolution of gold with 0.10 mol/dm^3 SCN^- and 0.055 mol/dm^3 Fe^{3+}, at pH 1.5	229
6.16	Effect of temperature on (a) potential readings and (b) reduction of Fe^{3+} to Fe^{2+}, with 0.10 mol/dm^3 SCN^- and 0.055 mol/dm^3 Fe^{3+}, at pH 1.5	230
6.17	Effect of temperature on the dissolution of gold with 0.05 mol/dm^3 SCN^- and 0.055 mol/dm^3 Fe^{3+}, at pH 1.5	232
6.18	Effect of temperature on the dissolution of gold with 0.275 mol/dm^3 SCN^- and 0.055 mol/dm^3 Fe^{3+}, at pH 1.5	233
6.19	Effect of temperature on (a) potential readings and (b) reduction of Fe^{3+} to Fe^{2+}, with 0.275 mol/dm^3 SCN^- and 0.055 mol/dm^3 Fe^{3+}, at pH 1.5	235
6.20	Effect of temperature on (a) gold dissolution and (b) autoreduction of ferric thiocyanate, with 0.275 mol/dm^3 SCN^- and 0.055 mol/dm^3 Fe^{3+}, at pH 1.5	236
6.21	Effect of thiocyanate concentration at 25°C on (a) gold dissolution and (b) autoreduction of ferric thiocyanate	238

		Page
6.22	Effect of thiocyanate concentration at 85°C on (a) gold dissolution and (b) autoreduction of ferric thiocyanate	239
6.23	Arrhenius plots of the initial gold dissolution rates listed in Table 6.7	241
6.24	Arrhenius plots of the gold dissolution rates after 1 hour listed in Table 6.7	243
6.25	Arrhenius plots of the initial rates of autoreduction of the iron(III)-thiocyanate complexes in the runs listed in Table 6.7	244
6.26	Gold rotating disc after polishing	245
6.27	Gold rotating disc after leaching for 150 minutes at 85°C with 0.10 mol/dm^3 SCN^- and 0.055 mol/dm^3 Fe^{3+}, at pH 1.5	246
6.28	Effect of dissolved oxygen on the leaching of gold by ferric thiocyanate	248
6.29	Effect of dissolved oxygen on (a) potential readings at the gold disc surface and (b) reduction of Fe^{3+} to Fe^{2+}	249
6.30	Rotating disc runs at 25°C with 0.275 mol/dm^3 SCN^- and 0.055 mol/dm^3 of total iron: (a) runs at constant potentials and (b) comparison between runs at 703 mV and with spontaneous autoreduction	254
6.31	Rotating disc runs at 25°C with 0.10 mol/dm^3 SCN^- and 0.055 mol/dm^3 of total iron: (a) runs at constant potentials and (b) comparison between runs at 735 mV and with spontaneous autoreduction	255
6.32	Eh vs. log {SCN^-} lines showing the potential zones of predominance of $Au(SCN)_2^-$, $Au(SCN)_4^-$ and $(SCN)_3^-$	265
7.1	Eh-pH diagrams at 25°C for the (a) Au-I-H_2O system [187], (b) Au-SCN-H_2O system, and (c) Au-Br-H_2O system [187]	273
7.2	Effect of iodide concentration on the leaching of gold in presence of 0.055 mol/dm^3 (initial) Fe^{3+} at pH 1.5 and 25°C	276

		Page
7.3	Effect of iodide concentration on (a) potential readings at the gold disc surface and (b) reduction of Fe^{3+} to Fe^{2+}, at pH 1.5 and 25°C	277
7.4	Effect of iodide addition on the leaching of gold by ferric thiocyanate, using 0.10 mol/dm^3 SCN^- at pH 1.5 and 25°C	280
7.5	Effect of iodide addition on (a) potential readings and (b) Fe^{3+} reduction, in the leaching of gold at 25°C and pH 1.5	282
7.6	Effect of iodide addition on the leaching of gold by ferric thiocyanate, using 0.05 mol/dm^3 SCN^- at 25°C and pH 1.5	283
7.7	Effect of iodide addition on (a) potential readings and (b) Fe^{3+} reduction, in the leaching of gold by ferric thiocyanate, using 0.05 mol/dm^3 SCN^- at 25°C and pH 1.5	284
7.8	Effect of iodide concentration on the leaching of gold by ferric thiocyanate, using 0.10 mol/dm^3 SCN^- at 25°C and pH 1.5	291
7.9	Effect of thiocyanate concentration on the leaching of gold by ferric thiocyanate, with iodide addition at 25°C and pH 1.5	292
7.10	Gold rotating disc after leaching for 150 minutes at 25°C and pH 1.5 with 0.10 mol/dm^3 SCN^-, 0.0055 mol/dm^3 I^- and 0.055 mol/dm^3 Fe^{3+}	296

LIST OF TABLES

		Page
3.1	Standard Potentials for Half-Reactions of Several Halide and Thiocyanate Redox Couples in Aqueous Solution at 25°C	112
4.1	Activation Energies for the Initial Autoreduction Reactions of the Ferric Thiocyanate Complexes at pH 1.5	162
4.2	Thiocyanate Oxidation by Iron(III): Results of Some Argentimetric Titrations	164
4.3	Concentrations of Thiocyanate Estimated According to Reaction 4.19 from the Amounts of Fe^{2+} Produced (same experiments shown in Table 4.2)	164
5.1	Thiocyanate Oxidation by Hydrogen Peroxide: Experimental Results at pH 1.5 and 25°C	181
6.1	Gold Dissolution Rates Observed in the Experiments shown in Figure 6.2	199
6.2	Gold Dissolution Rates Observed with Several Rotation Speeds	202
6.3	Gold Dissolution Rates Observed with Several Concentrations of Thiocyanate	206
6.4	Gold Dissolution Rates Observed with Several Initial Concentrations of Iron(III) and 0.275 mol/dm^3 SCN^-	214
6.5	Gold Dissolution Rates Observed with Several Initial Concentrations of Iron(III) and 0.10 mol/dm^3 SCN^-	218
6.6	Catalytic Effect of Gold Metal on the Autoreduction of Iron(III)-Thiocyanate Complexes at 25°C. Extents of Autoreduction (in the Presence and Absence of Gold) and Gold Dissolution	225
6.7	Molar Ratios between Iron(III) Reduced and Gold Dissolved in Rotating Disc Runs at Several Temperatures	226

		Page
6.8	Gold Dissolution Rates Observed at Several Temperatures and SCN^- Concentrations	231
6.9	Apparent Activation Energies for the Gold Dissolution Process	241
6.10	Apparent Activation Energies for the Initial Overall (Homogeneous plus Heterogeneous) Autoreduction of the Iron(III)-Thiocyanate Complexes (estimates from Figure 6.25)	244
6.11	Gold Dissolution Rates Observed in the Experiments shown in Figure 6.28	250
6.12	Thiocyanate Consumption in the Rotating Disc Experiments: Results of Some Argentimetric Titrations	252
6.13	Gold Dissolution Rates Observed at Constant Potentials (by Addition of Hydrogen Peroxide) at 25°C	256
6.14	Thiocyanate Oxidation in the Runs at Constant Potential at 25°C	259
7.1	Standard Potentials for Half-Reactions of Several Bromide, Iodide and Thiocyanate Redox Couples in Aqueous Solution at 25°C	272
7.2	Gold Dissolution Rates Obtained with Several Iodide Concentrations and 0.055 mol/dm^3 Fe^{3+} at 25°C	278
7.3	Gold Dissolution Rates Observed with Several Concentrations of SCN^- and I^- (or Iodine) and 0.055 mol/dm^3 Fe^{3+} at 25°C	293

CHAPTER 1: INTRODUCTION

1.1. Previous Work on Gold Leaching by Thiocyanate

When considering different systems for the leaching of gold, Nicol, Fleming and Paul made the following remarks about the thiocyanate system, in a book published in 1987 [1] :

"..... *the oxidation of gold in acidic thiocyanate solutions can be expected to produce either the gold(I) complex* $Au(SCN)_2^-$ *or the gold(III) complex* $Au(SCN)_4^-$*..... Unfortunately, little has been published about this potentially important system other than a report (White, 1905) that leaching in thiocyanate solutions is faster than in solutions of thiosulphate..... At present, there are no published details regarding the nature of the products or the kinetics of these processes.....".* [1]

In the report mentioned in this quotation, dated from 1905, White [2] demonstrated the effectiveness of thiocyanate for dissolving gold. He worked with pieces of gold leaf and tested various oxidizing agents in solutions of ammonium thiocyanate. He also tested solutions of ferric thiocyanate alone as solvents for gold. The results were briefly and simply reported as weight loss of the pieces of gold leaf after different times. The conclusion was that, in the presence of a suitable oxidizing agent, gold is dissolved by thiocyanate solutions. Those pioneering trials were nevertheless forgotten over the following decades, which have seen the growth of cyanidation as the main gold extraction process worldwide.

The subject was revived only in 1986 with the publication by Fleming [3] of his investigation into the simultaneous recovery of gold and uranium from South African ores in sulphate-thiocyanate

media, using iron (III) as oxidant. The potential was kept constant by periodic additions of pyrolusite, MnO_2. To optimize the conditions for gold leaching, a series of experiments was run in which each parameter was varied in turn around the reference values and over the ranges reported below:

	Reference Value	Studied Range
Potential (mV vs. SHE)	700	640 - 730
NH_4SCN (mol/dm^3)	0.13	0.05 - 0.26
Fe^{3+} added (mol/dm^3)	0.045	0 - 0.233
pH	1.5	1.0 - 3.0
Temperature (°C)	22	20 - 60

The leaching tests were performed on one of the acidic pyritic gold-uranium ores from South Africa. The total iron concentration in solution before the addition of ferric sulphate varied with pH and was generally in the range of 2 to 5 g/l (i.e. 0.036 to 0.090 mol/dm^3). The leaching time was 6 hours for all experiments. With the above reference values, gold extractions somewhat higher than 80% were obtained. Variations in the thiocyanate concentration did not affect uranium extractions. Uranium was assumed to be dissolved as uranyl-sulphate complexes and gold as the complexes $Au(SCN)_2^-$ and $Au(SCN)_4^-$.

Nothing further has been reported or published on the thiocyanate leaching of gold, which renders the subject an unexplored field for investigation. This is particularly true of the fundamental chemical, thermodynamic and kinetic aspects of the process.

1.2. Thiocyanate as an Alternative Lixiviant for Gold

It is worthwhile paying attention to the circumstances that motivated the research on thiocyanate as a gold leachant in South Africa. They are explained by Fleming in the introduction to his paper [3], as follows:

"The uranium market has been in a recession for several years, and South Africa has remained a competitive producer only because most of its uranium resources are associated with gold-bearing reef and are mined as a byproduct of gold. However, while gold and uranium are mined from the same reef, the recovery of the two metals from the ore is carried out in separate tratment plants, and it is likely that further major reductions in the production cost of uranium will be achieved only if a method is developed for the leaching and concentration of the two metals together..... recent research has centred on the development of an aqueous chemical environment in which the two metals would dissolve simultaneously. Possible solvents include an alkaline solution of cyanide and carbonate and an acidic solution of thiourea and sulphate. The former solution suffers from the drawback that it is not well suited to the acidic pyritic ores that are commom in South Africa, and the high consumption of carbonate renders the process uneconomic; the latter solvent suffers from several drawbacks, the most serious of which is that thiourea is unstable at the potential required for effective uranium oxidation." [3]

This case history is particularly interesting as it shows that the consideration of thiocyanate was not directly raised by environment protection reasons. Thiocyanate was chosen because of a double constraint: first, the alkaline cyanidation medium did not suit the acidic nature of the ore; and second, the potential required to oxidize uranium would cause unacceptably high comsumption of thiourea through oxidation. The first constraint alone would perhaps lead to the use of the better known and already tested thiourea

system. The second constraint, however, ruled out that option.

The South African case is a rather specific one in the sense that the reasons behind the search for an alternative to cyanidation were different from those frequently invoked, namely: (1) protection of the environment against the high toxity of cyanide; (2) refractoriness of the gold ore; (3) use of solution mining techniques for gold extraction.

There may be, however, different contexts in which thiocyanate can be considered as an alternative lixiviant for gold. Besides being far more acceptable environmentally than cyanide, it enables the use of oxidizing agents such as iron(III) and hydrogen peroxide, once the leaching is effected in acidic media, at pH 2 or lower. This feature obviously favours the treatment of acidic ores. Furthermore, the high overpotential necessary for the oxidation of thiocyanate makes it particularly stable in leaching systems requiring high potentials. By not requiring oxygen, thiocyanate is also a suitable reagent for solution mining, as well as eliminating aeration problems in heap leaching.

The thiocyanate salts of Na^+, K^+ and NH_4^+ ions have high solubilities in aqueous solution and to a lesser extent in polar organic solvents.

1.3. The Scope of the Present Work

The scope of the present work includes the fundamental chemical, thermodynamic and kinetic aspects of the leaching of gold by thiocyanate. It is, in fact, the first fundamental study to be published on this specific subject.

There have been passing references to the possibility of gold leaching by thiocyanate, either in reviews of the chemistry of gold extraction [1, 4-8] or in papers about the prospects for alternative leaching systems in general [9, 10] . But apart from the two papers already mentioned [2,3], one from 1905 and the other from 1986, no experimental results have been reported so far. More specifically, no fundamental investigation on the chemistry, thermodynamics or kinetics of the process has ever been published.

The research work that has been carried out on thiocyanate over the last 30 or 40 years has mostly been concerned with applications to analytical chemistry or to other areas not closely related, if related at all, to hydrometallurgy. One of the features of this Thesis is the collection of information scattered over several different areas, such as chemistry, electrochemistry and biochemistry, and the attempt to put this unrelated information together into a framework oriented towards the specific aim of the leaching of gold. This is particularly true of the descriptive chemistry and thermodynamics of the relevant thiocyanate systems.

A substantial part of the work involved in the preparation of this Thesis was invested in the thermodynamic study of the thiocyanate systems with gold and silver. Thermodynamic data had to be retrieved from many different sources before being processed and presented in Eh-pH diagrams, solubility diagrams, distribution curves for the relevant series of complexes, all used in an overall thermochemical description of the thiocyanate systems for leaching gold (and silver) ores, part of which has already been published [11] . Most of this subject, which demanded a great number of thermodynamic calculations, is treated in **Chapter 2**.

Chapter 3 focuses the search for the intermediate species in the oxidation of thiocyanate. This matter had to be dealt with in depth in order to explain some observed experimental facts. The first of these was the high overpotential required for oxidizing thiocyanate, which suggested that some intermediate step would be

controlling the rate of the overall oxidation process. The second fact, observed since the first gold rotating disc experiments were conducted in this project, was the decrease in the rate of gold dissolution with time, which took place simultaneously with the reduction of the iron(III) to iron(II) and the consequent decrease in the potential readings in the solution. This fact suggested that the higher initial rates of gold dissolution would be, at least partially, due to the higher initial production of some intermediate species of thiocyanate oxidation, such as $(SCN)_3^-$ and/or $(SCN)_2$, which would be more active than SCN^- itself in the gold dissolution process. Accordingly, gold would be dissolved predominantly as the auric complex, $Au(SCN)_4^-$, at those higher potentials, and as the aurous complex, $Au(SCN)_2^-$, at lower potentials. To clarify this question it was necessary, as a first step, to review, criticize and attempt to unify the previous contributions by several researchers to the knowledge of the intermediate species in the oxidation of thiocyanate. Relating those species with the dissolution of gold is one of the contributions of the present Thesis. Further thermodyamic calculations are then presented, also in **Chapter 3**, involving the intermediate species $(SCN)_3^-$ and $(SCN)_2$. The pseudohalide character of thiocyanate is emphasized and several analogies are put forward with the corresponding species in the halide systems, X_3^- and X_2 (X = Cl, Br, I).

The redox processes in acidified iron-thiocyanate solutions are covered in **Chapter 4**. Due to its considerable complexity, it was necessary to treat the iron-thiocyanate system separately beforehand. It would be difficult, if not impossible, to provide a proper interpretation of the results of gold dissolution in the ferric-thiocyanate system before knowing the intricacies of the ferric-thiocyanate system itself. There was not sufficient information on the autoreduction of the ferric-thiocyanate complexes in solution. There was no information at all on matters such as the potential readings obtained in iron-thiocyanate solutions and how those readings relate to the progress of the autoreduction

process and to the concentrations of the species in solution. The stability of iron(III) towards precipitation from thiocyanate solutions was another point to be clarified. Each one of these aspects had to be approached experimentally. The reduction of iron(III) to iron(II) and the corresponding oxidation of thiocyanate was studied through a series of experiments which were extended up to 18 days to determine the long-term behaviour of the system. Potential measurements, iron precipitation and thiocyanate hydrolysis results are all included in this chapter. The experimental material presented is preceded by thermodynamic calculations leading to the distribution curves of the series of iron(III)-thiocyanate and iron(II)-thiocyanate complexes, as well as curves giving the average ligand number for each of these series as a function of the activity of free thiocyanate in solution. At the end of this chapter, a tentative mechanism is proposed for the oxidation of thiocyanate by iron(III).

Chapter 5 deals with the iron-thiocyanate-hydrogen peroxide system, and tries to correlate parameters such as the potential readings, peroxide consumption and thiocyanate oxidation. The mechanisms of oxidation of thiocyanate and ferrous ions by hydrogen peroxide are reviewed. Experimental results on the oxidation of thiocyanate by hydrogen peroxide, and on the effect of hydrogen peroxide in iron-thiocyanate solutions, are presented and discussed.

There is no previous information in the literature on the kinetics of gold dissolution by iron-thiocyanate and iron-thiocyanate-hydrogen peroxide solutions. **Chapter 6** provides a first contribution in this respect. For this purpose, the results from rotating gold disc experiments are presented and analysed. The dissolution of gold by ferric thiocyanate solutions was found to involve various simultaneous processes, namely, the reduction of iron(III) to iron(II), the corresponding oxidation of thiocyanate, the oxidation and the complexation of gold, etc. All the phenomena investigated separately in the previous chapters are combined here. Gold dissolution rates were determined. The parameters studied

included the concentrations of thiocyanate and iron(III), rotation speed and temperature. Some mechanistic ideas are proposed. The majority of the experiments were conducted in neutral (nitrogen) atmosphere. Aeration of the system did not increase the rates to any extent, indicating that oxygen is not required in the ferric thiocyanate system. Gold dissolution rates as fast as those obtained with thiourea were obtained with ferric thiocyanate solutions, but temperatures above the ambient (up to 85°C) were required for that. Particular emphasis was given to discussing the mechanism of the leaching process, in which the intermediate species of the oxidation of thiocyanate, particularly $(SCN)_3^-$, play an important role. Towards the end of **Chapter 6**, the relevance of the detailed investigation into the chemistry and electrochemistry of thiocyanate reported in **Chapter 3** becomes apparent.

Chapter 7 deals with a modified system, involving the addition of small quantities of iodide ions (or, alternatively, iodine solution) to the ferric thiocyanate system investigated in the previous chapter. The objective was to increase the gold dissolution rates while mantaining the temperature at 25°C. These experiments were very successful. Considerably higher rates, similar to those obtained with the plain ferric thiocyanate system at 85°C, were then obtained at 25°C. These rates are comparable to those obtained with similar concentrations of thiourea. The role of the iodide/iodine system, its thermodyamics and its interactions with the thiocyanate system are discussed in this chapter. Special emphasis is put in the discussion of mixed thiocyanate-iodine species as they are considered to account for the synergistic effect on the gold dissolution observed when iodide ions or iodine were added to the iron(III)-thiocyanate lixiviant.

In **Chapter 8**, the final conclusions of this project are presented, with some suggestions for further research. The overall experimental results demonstrated that thiocyanate is a viable and interesting option for the leaching of gold ores, providing leaching rates comparable to those obtained with thiourea. The pH should be

kept between 1 and 2.5, approximately, should iron(III) be used as oxidant. Oxygen is not required with the ferric thiocyanate system. The consumption of thiocyanate through oxidation by iron(III) is minimal, and its hydrolysis at pH 1 or higher is negligible.

The scope of this work was considerably enlarged in order to contain those basic aspects of the chemistry, thermodynamics, kinetics and mechanism of the thiocyanate leaching of gold which are relevant for an eventual future work of process development. With such a wide scope, several fundamental aspects could not be dealt with in depth due to the obvious limitations of time in a project of this nature. But even in such cases, initial guidelines for future fundamental research can be derived from the work presented here. The references surveyed and quoted throughout this work probably include the main body of published information presently available on the aqueous chemistry of thiocyanate as relevant to the leaching of gold.

The information contained in the text is complemented by seven Appendices, which contain the thermodynamic data used in the calculations, the reactions corresponding to the lines appearing in the Eh-pH diagrams, a series of experiments on the iron precipitation from iron(III)-thiocyanate solutions, experimental data, and a list of the chemicals used in the experimental work.

CHAPTER 2: THERMODYNAMICS OF THIOCYANATE SYSTEMS FOR LEACHING GOLD AND SILVER ORES

2.1. Introduction

The work reported in this chapter is an attempt to provide the thermodynamic basis for the thiocyanate leaching of gold and silver ores. The discussion of the chemistry of the relevant systems is supported by thermodynamic calculations which are presented as Eh-pH diagrams (also referred to as potential-pH or Pourbaix diagrams), distribution curves for the relevant series of complexes and solubility diagrams, all at 25°C. The thermodynamic data used in all calculations and the respective sources are reported in Appendices 1 and 3, and Appendix 2 reports the reactions corresponding to all lines appearing in the Eh-pH diagrams. Whenever possible, the thermodynamic data have been collected either from the most recent critical collection published [12] or from the U.S. National Bureau of Standards publications [13-15]. Other reliable sources have also been used [16-22]. The study considers only the series of homogeneous mononuclear complexes of gold and silver with thiocyanate. Polynuclear and mixed complexes have not been considered for the sake of simplicity and also because of the lack of thermodynamic data.

2.2. Metastable Eh-pH Diagrams

An unusual feature of the present study is the extensive use of metastable Eh-pH diagrams. The method is necessary to study systems like $CN\text{-}H_2O$, for instance, since cyanide is not

thermodynamically stable in water. This is true both if the ultimate oxidation step of cyanide to ammonia and carbonate is considered and also if cyanate, CNO^-, is regarded as the oxidation product. Cyanate in itself is a metastable species in aqueous solution, decomposing very slowly by reactions such as [23-26] :

$$CNO^- + H_2O = CO_3^{2-} + NH_4^+ \qquad (2.1)$$

Even if cyanate is considered as the final oxidation product, the (meta)stability area of cyanide lies below the stability area of water, as illustrated by **Figure 2.3a**. Thus, on strict thermodynamic grounds, a study of the system $CN\text{-}H_2O$ would finish at the very beginning since it is not stable in water.

In practice, the oxidation rate of cyanide is very low in air-sparged solutions. Thus, it is possible to disregard the decomposition of cyanide by oxidation and to consider definite concentrations (or, more accurately, activities) of this species in the calculation of Eh-pH diagrams for the systems $Au\text{-}CN\text{-}H_2O$ and $Ag\text{-}CN\text{-}H_2O$. The results are metastable diagrams (see **Figures 2.13b** and **2.13d**). The (meta)stability areas for the gold-cyanide and silver-cyanide complexes lie above that for cyanide. In other words, the redox potentials required for the dissolution of gold and silver are more than enough to oxidize cyanide. This means that the indications provided by those diagrams hold true as long as the cyanide concentration does not change appreciably through oxidation. This is a quasi-equilibrium (or metastable) situation.

The above remarks can be generalized. Metastable diagrams can be generated in cases in which the complexation of the metal by the ligand takes place at redox potentials higher than those required to oxidize the ligand. A basic requirement, however, is some kinetic evidence in support of the quasi-equilibrium assumptions made for the calculations.

In the thermochemical study presented in this chapter these

considerations have been adopted as a general method to investigate the behaviour of the thiocyanate systems for leaching gold and silver ores. Previous work [28, 36-46] on the oxidation of thiocyanate by several oxidizing agents justifies the non-consideration of its oxidation in the calculations of metastable diagrams for the systems Au-SCN-H_2O and Ag-SCN-H_2O.

The metastability of the diagrams for the systems Au-SCN-H_2O and Ag-SCN-H_2O, as well as of those for the systems Au-CN-H_2O and Ag-CN-H_2O, will be discussed further in Section 2.9.

2.3. Thiocyanate Ion and Thiocyanic Acid

The thiocyanate ion, SCN^-, has a linear structure with the carbon atom in the centre. It has the ability to form covalent compounds and complexes. The free ion may be regarded as the outcome of two resonance forms, $^-S\text{-}C{\equiv}N$ and $S{=}C{=}N^-$, on which the linearity of its structure is based [28]. A third structure with the triple bond between the S and C atoms is also mentioned [29, 30]. Thus, the thiocyanate ion is an ambidentate ligand, realizing its donor function either via the S or via the N atom. This results in two series of covalent complexes, the thiocyanates or S-thiocyanates and the isothiocyanates or N-thiocyanates. Regarding homogeneous complexes, it is usually observed that soft metal ions form S-thiocyanates, whereas hard metal ions prefer the N-thiocyanate coordination [31]. In the former are found more frequently - though not exclusively - second and third row transition elements including Au and Ag. In the later are often found metals of the first row of the transition series such as Mn, Fe, Ni, Cu and Zn [29, 30]. Thus, the thiocyanate ion is a soft ligand and the related metal complexes are represented as $M(SCN)_m^{n-}$, whilst isothiocyanate is considered a hard ligand and its complexes written as $M(NCS)_p^{q-}$. Cases in which

the bonding mode is not known or well defined have been classically indicated as $M(CNS)_r^{s-}$. Bridge-type complexes may also be formed in which both the S and the N atoms donate, M-N-C-S-M' [29, 30], but these complexes have not been considered in the present work. The same applies to mixed and polynuclear complexes which raise additional complications [31] that are beyond the scope of this work. Henceforth, the term thiocyanate will be used when referring to the different tautomeric forms of the ion, leaving implicit the distinctions described above.

Thiocyanate is a pseudohalide whose related pseudohalogen is thiocyanogen, $(SCN)_2$, and whose related acid is thiocyanic acid, HSCN. Thiocyanic acid exists in two tautomeric forms, H-S-C≡N and H-N=C=S in equilibrium with each other. They result from the protonation of thiocyanate ion at the S or N atom, and are named thiocyanic acid and isothiocyanic acid, respectively. Isothiocyanic acid predominates widely over thiocyanic acid [28]. However, the aqueous solution of the acid is usually referred to as thiocyanic acid and indicated as HSCN regardless of this structural distinction and this practice will also be adopted in this work.

Aqueous solutions of HSCN are stable up to concentrations of around 0.85 mol/dm^3. Attempts to reach higher concentrations cause decomposition [31]. This is certainly an additional source of error in the Eh-pH diagrams at the acidic end of the pH scale (besides the known deviations inherent to pH measurements in general at both extremes of the pH scale). A decomposition process reported [28] in acidic conditions is the hydrolysis according to the reaction (see Chapter 4, Section 4.8):

$$H^+ + HSCN + 2H_2O = H_2S + CO_2 + NH_4^+ \qquad (2.2)$$

At very high acidity there is also the possibility of further protonation of the thiocyanate ion to give H_2NCS^+ or even $HNC\overset{+}{S}H$ [28], but these higher acids have not been considered in the present work because of lack of thermodynamic data.

A first problem which arises in a thermodynamic study involving thiocyanic acid is to define its dissociation constant. There is no agreement on this subject. Boughton and Keller [32] determined pK_a = 0.97, a figure which is fairly consistent with pK_a = 0.85 by Suzuki and Hagisawa [33]. Morgan and Stedman [34] found pK_a = -1.84. Crowell and Hankins [35] proposed a pK_a from -2.0 to -2.3. These data and a few others are also quoted by Hughes [28], who suggests that pK_a should lie between -1.5 and -2.0. A calculation based on thermodynamic data from [12] and [13] yields pK_a = - 0.85. Smith and Martell [16] adopted the results reported in two of the above references [32, 33] and quoted pK_a = 0.9 ± 0.1 (25°C and zero ionic strength). This is also the value adopted in this work, on which basis the distribution curve shown in **Figure 2.1** was calculated. For the sake of consistency, this pK_a and $\Delta G°$ = 92.68 kJ/mol [12, 13, 15] for SCN^- were used to obtain $\Delta G°$ = 87.54 kJ/mol for HSCN.

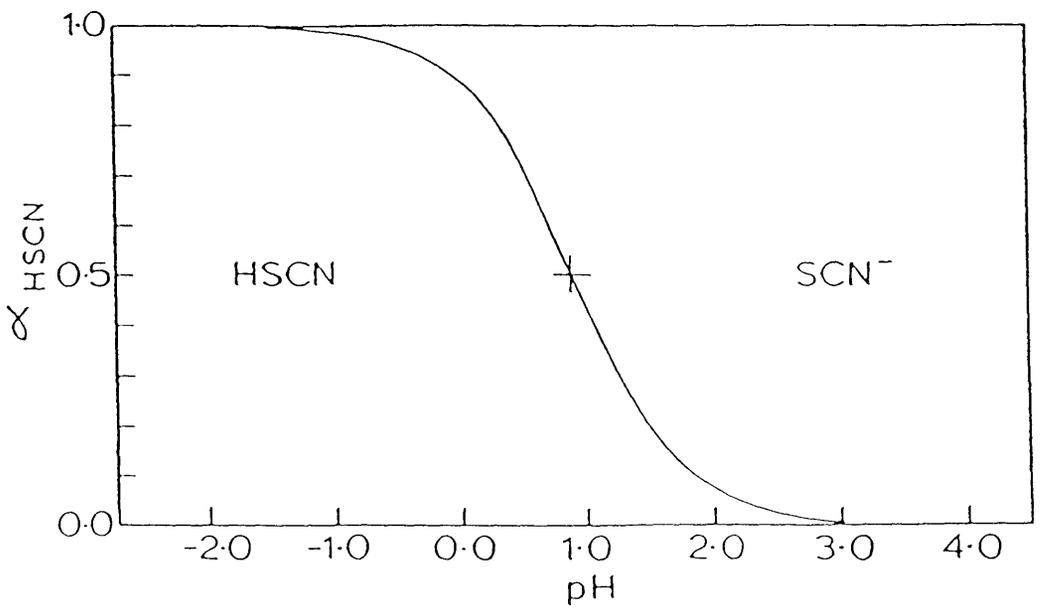


Figure 2.1 - Distribution curve of thiocyanic acid, calculated for pK_a = 0.9.

2.4. The SCN-H_2O System and its Comparison with the CN-H_2O System

The water stability boundaries are indicated in all Eh-pH diagrams presented in this work by lines 1 and 2. At potentials higher than those of line 1, water is oxidized to oxygen and at potentials lower than those of line 2, water is reduced to hydrogen. The fugacities are taken as one, i.e. $f_{O_2} = f_{H_2} = 1$ in these calculations.

The already known fact that thiocyanate participates in three redox systems with oxidation to sulphate was extensively discussed by Gauguin [47-49]:

$$SO_4^{2-} + CN^- + 8H^+ + 6e = SCN^- + 4H_2O \quad (2.3)$$

$$SO_4^{2-} + CNO^- + 10H^+ + 8e = SCN^- + 7H_2O \quad (2.4)$$

$$SO_4^{2-} + CO_3^{2-} + NH_3 + 11H^+ + 8e = SCN^- + 7H_2O \quad (2.5)$$

Using the thermodynamic data reported in Appendix 1, the Eh-pH diagrams corresponding to these three redox systems were drawn and are presented in **Figure 2.2**. The specific reactions corresponding to each individual line are listed in Appendix 2.

Reaction 2.3 (see **Figure 2.2a**) is irreversible as CN^- and SO_4^{2-} cannot be reduced back to SCN^- either chemically or electrochemically [48-50].

Reaction 2.4 (see **Figure 2.2b**) can be seen as a further irreversible oxidation step leading to cyanate, CNO^-, or cyanic acid, HCNO. **Figures 2.2a** and **2.2b** show that the lines corresponding the the metastable equilibria between thiocyanate and cyanate species are only slightly below those corresponding to the metastable equilibria between thiocyanate and cyanide species.

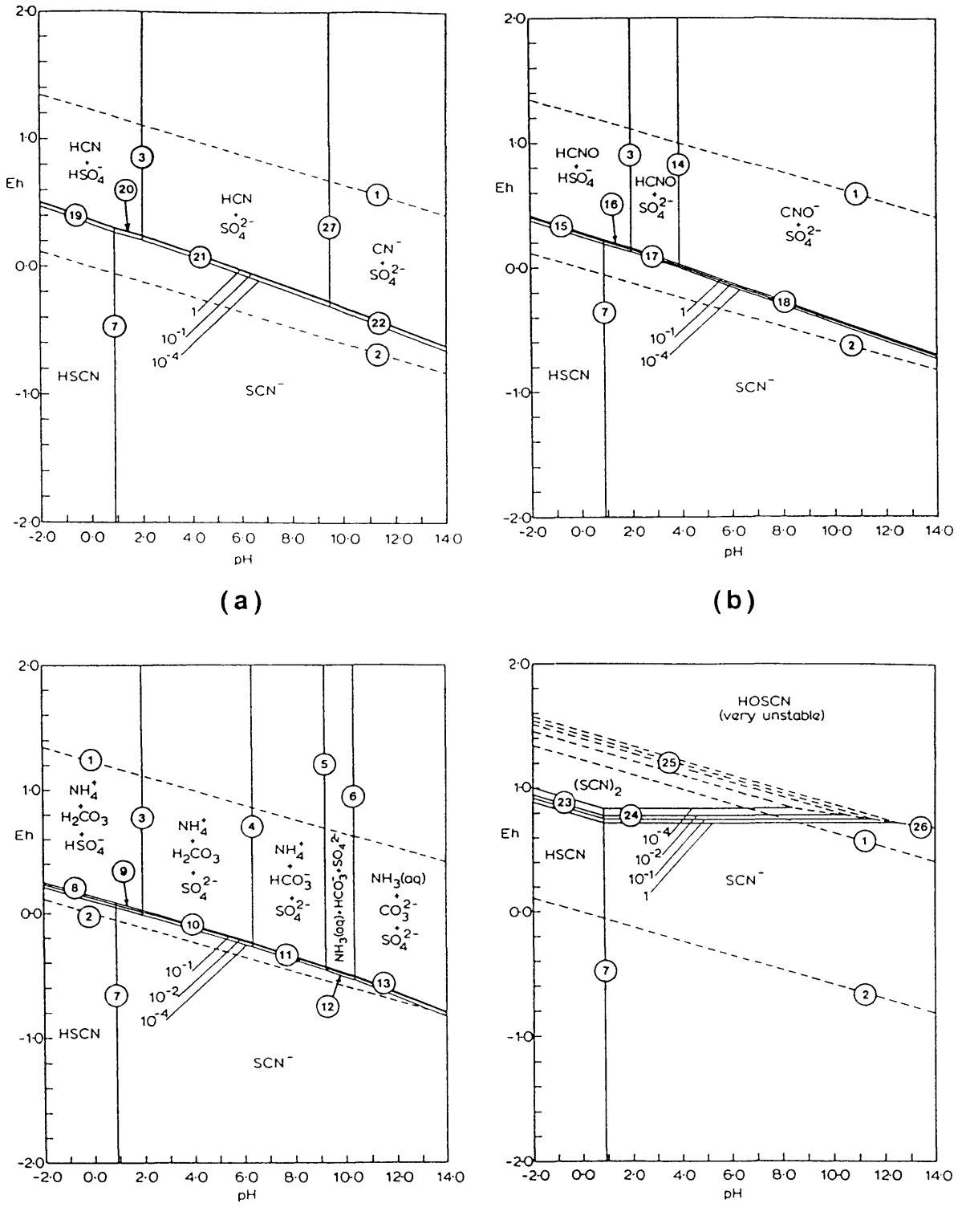


Figure 2.2 - Eh-pH diagrams for the SCN-H_2O system at 25°C: **(a)** metastable diagram considering cyanide as oxidation product; **(b)** metastable diagram considering cyanate as oxidation product; **(c)** stable homogeneous equilibrium diagram; **(d)** metastable diagram indicating the formation of thiocyanogen.

Cyanate and cyanic acid, in their turn, are metastable oxidation products whose irreversible decomposition into carbon dioxide and ammonia has been reported by different researchers [24-26]. This final condition, which corresponds to reaction 2.5, is represented in **Figure 2.2c**.

Cyanic acid, particularly, is very unstable in aqueous solution. According to Jolly [23], it may be looked upon as an aquo-ammono-carbonic acid, decomposing as follows:

$$HCNO + 2H_2O = H_2CO_3 + NH_3 \qquad (2.6)$$

Cyanic acid can also be seen as the dehydration product of carbamic acid, NH_2COOH, and equally as the deammoniation product of urea, $CO(NH_2)_2$ [23]. In fact, carbamic acid is sometimes referred to as an intermediate in the decomposition of cyanic acid [25] and the formation of urea is observed in aqueous solutions of ammonium thiocyanate [26, 27]. Cyanic acid has a pK_a of 3.91, as shown by the line 14 in **Figures 2.2b** and **2.3a.** Thus, below pH 3.91 the very unstable HCNO predominates and is rapidly decomposed into NH_4^+ and CO_2, as above discussed. At pH>3.91 the predominant form is the cyanate ion, CNO^-.

The cyanate ion is relatively more stable than cyanic acid and is usually considered to be the predominant oxidation product of cyanide in industrial practice such as in leaching circuits, where the oxidation is undesirable, or in effluent treatment plants for oxidative cyanide disposal. Nevertheless, CNO^- is metastable and ultimately decomposes into carbonate and ammonia, as indicated in **Figure 2.2c**.

It was experimentally demonstrated by Gauguin [47-49] and Nicholson [50] that the oxidation of thiocyanate in aqueous solution, both chemically and electrochemically, involves a considerable overpotential. According to their observations, the potentials for the

onset of oxidation were higher than those expected from calculations for the redox system shown in **Figure 2.2a**, although the final oxidation products were cyanide and sulphate, as indicated in that same Figure. It was then suggested that the oxidation of thiocyanate would proceed through the formation of some intermediate species, the most plausible one, according to Gauguin [47-49], being thiocyanogen, $(SCN)_2$. The existence of thiocyanogen, $(SCN)_2$, was proposed in 1918 by Bjerrum and Kirschner [51], who determined the standard potential E°=0.77 V (vs. SHE) for the couple:

$$(SCN)_{2(aq)} + 2e = 2SCN^- \qquad E° = 0.77\ V \qquad (2.7)$$

The formation of thiocyanogen as an intermediate species would then be responsible for the overpotential observed in the oxidation of thiocyanate [47-49]. Using this E° value and the remaining thermodynamic data listed in Appendix 1, the Eh-pH diagram corresponding to this processs of $(SCN)_2$ formation was drawn, as shown in **Figure 2.2d**. It should be kept in mind that the only usefulness of that diagram is to provide an insight into the mechanism of thiocyanate oxidation. Thiocyanogen can not even be regarded as metastable in water, because of its rapid hydrolysis according to the overall reaction [47-49, 51]:

$$3(SCN)_2 + 4H_2O = 5SCN^- + HCN + SO_4^{2-} + 7H^+ \qquad (2.8)$$

Thus, the overall thiocyanate oxidation process results from the addition of reactions 2.7 and 2.8 as follows:

$$3(SCN)_{2(aq)} + 6e = 6SCN^- \qquad (2.7)$$

$$5SCN^- + HCN + SO_4^{2-} + 7H^+ = 3(SCN)_2 + 4H_2O \qquad (2.8)$$

$$SO_4^{2-} + HCN + 7H^+ + 6e = SCN^- + 4H_2O \qquad (2.3)$$

This stoichiometry indicates the transfer of **6 electrons for each thiocyanate ion oxidized**. When cyanate is considered

as the oxidation product, **8 electrons** are involved, as indicated by reaction 2.4 and **Figure 2.2b**. **8 electrons** are also involved when the final oxidation products are considered to be carbonate, sulphate and ammonia, according to reaction 2.5 and **Figure 2.2c**.

Several papers [36-46] have been published on the oxidation of alkali metal and ammonium thiocyanates by a variety of reagents in aqueous solution, giving cyanide and sulphuric acid as the main products. Cyanate has also been found as a product [36-40]. Thus, the overall oxidation process corresponds to that described either by reaction 2.3 or by reaction 2.4 (**Figures 2.2a** and **2.2b**, respectively). Although, in thermodynamic terms, the most stable condition is that indicated by reaction 2.5 (**Figure 2.2c**).

The conversion to sulphate is often below 100%, some less oxidized sulphur species being found among the products. The main oxidation byproduct is sulphur dicyanide, $S(CN)_2$, as pointed out by several authors [36-40, 42, 43]. Sulphur dicyanide is produced in the course of the oxidation of thiocyanate, by the reaction of the intermediate species $(SCN)_2$ with the CN^- or HCN resulting from the oxidation process itself. $S(CN)_2$ has been detected as a byproduct of the oxidation of thiocyanate by hydrogen peroxide [36, 37], Caro's acid [38-40] and nitric and nitrous acids [42, 43], being responsible for the deviation of the observed stoicheiometry from that corresponding to reactions 2.3 and 2.4. These reactions, nevertheless, represent the prevailing process, the major oxidation products being sulphuric acid and cyanide and/or cyanate.

The reaction of $S(CN)_2$ with SCN^- may also produce thiocyanogen and cyanide, as follows [52]:

$$S(CN)_2 + SCN^- + H_3O^+ \rightarrow (SCN)_2 + HCN + H_2O \qquad (2.9)$$

Furthermore, $S(CN)_2$ slowly undergoes hydrolysis [53]:

$$S(CN)_2 + 2H_2O \rightarrow HOCN + HSCN \qquad (2.10)$$

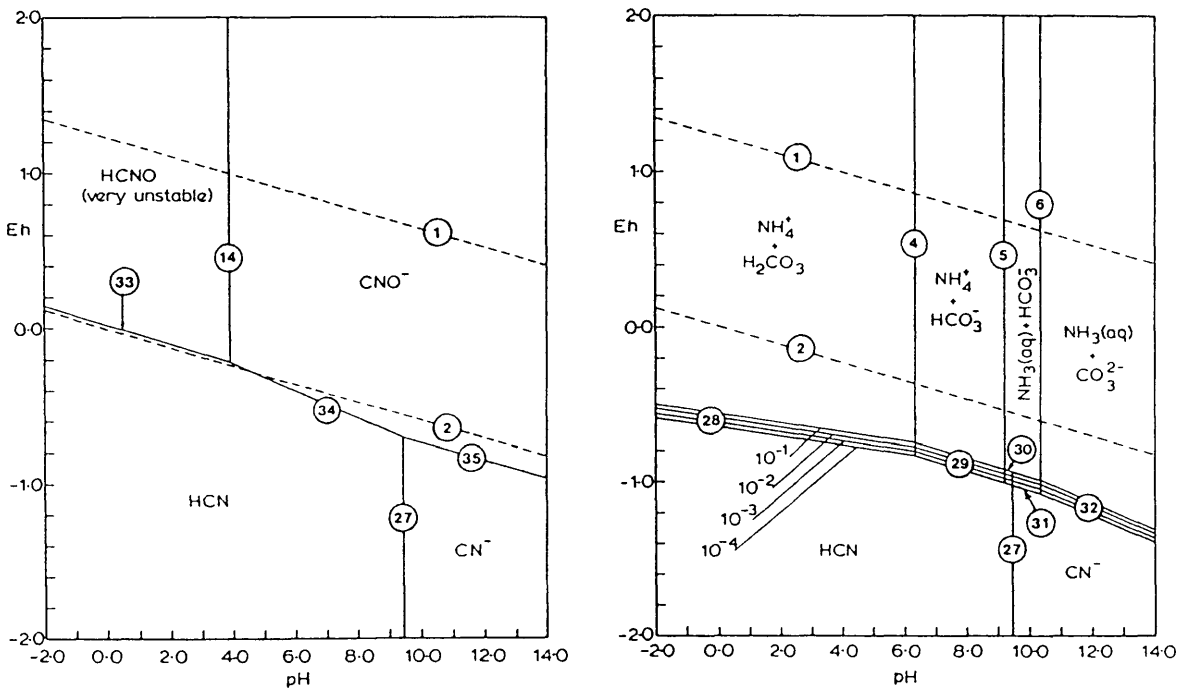
or:

$$S(CN)_2 + 4H_2O \rightarrow H_2SO_4 + HCN + HSCN + H^+ \qquad (2.11)$$

The formation of thiocyanogen as an intermediate species in the oxidation of thiocyanate is a sufficient explanation for the purpose of the present chapter, which is a general thermodynamic description. It is not sufficient, however, to explain the actual kinetics and mechanism of the oxidation of thiocyanate, which is a far more complex process involving several intermediate species. Hypothiocyanous acid, HSCNO, and the more hydrolyzed acids, $HSCNO_2$ and $HSCNO_3$, were proposed by Bjerrum and Kirschner [51] as intermediate species in the hydrolysis of $(SCN)_2$. The anion-radicals $(SCN)_2^-$ and $(SCN)_3^-$ are also quoted in the literature. They all have in common the fact of being unstable in aqueous solution, undergoing hydrolysis to yield the final oxidation products mentioned above. Despite being short-lived, these species are important for the interpretation of experimental results of gold leaching by thiocyanate solutions. They also provide a satisfactory explanation for the overpotentials required for SCN^- oxidation. Due to its importance, this subject will be treated in depth in the next chapter.

At this point, it is opportune to make some comments on the $CN\text{-}H_2O$ system whose diagrams, drawn using the data reported in Appendix 1, are shown in **Figure 2.3**. Diagrams including heterogeneous reactions with gaseous HCN and $(CN)_2$ have not been considered but can be found in the literature [59]. A comparison between **Figures 2.2c** and **2.3b** show that while SCN^-/HSCN have a narrow stability area in aqueous solution (bounded by lines 2 and 8-13), CN^-/HCN are not at all stable in water. If the oxidation to metastable CNO^-/HCNO is considered instead, a larger (meta)stability area for SCN^-/HSCN is found (**Figure 2.2b**) whereas CN^-/HCN still remain unstable in water (**Figure 2.3a**). One of the

consequences is that, starting from a mixed aqueous solution of thiocyanate and cyanide, it is possible to oxidize selectively cyanide leaving thiocyanate in solution. Another consequence is the possibility of converting CN^- into SCN^-, provided sulphur-containing species are available, as in the leaching of sulphur-containing ores, instead of converting CN^- directly to CNO^-; this conversion is in fact a side reaction observed in cyanidation plants. In any case, the redox potential gap for such reactions would be that between lines 15-18 (**Figure 2.2b**) and lines 33-35 (**Figure 2.3a**). A more complete analysis for cases involving external sources of sulphur-containing species would require further calculations on the CN-S-H_2O system including all possible species; but this is still to be done.



(a) **(b)**

Figure 2.3 - Eh-pH diagrams for the CN-H_2O system at 25°C: **(a)** metastable diagram considering cyanate as oxidation product; **(b)** stable homogeneous equilibrium diagram.

2.5. The $Au-H_2O$ and $Ag-H_2O$ Systems

Eh-pH diagrams for the $Au-H_2O$ and $Ag-H_2O$ systems are presented in **Figure 2.4**. The activities of all soluble gold and silver-containing species are taken as 10^{-4} and 10^{-5} mol/dm^3, as indicated in each diagram. Considering, as an approximation, the activity coefficients of all species as unity, those activities are, in the case of gold, equivalent to approximately 20 and 2 ppm, respectively. For silver, they are roughly equivalent to 11 and 1.1 ppm. These figures, particularly in the case of gold, are representative of the concentration range usually found in hydrometallurgical plants.

The diagrams in **Figure 2.4** are identical to those found in the literature [1, 4, 54-56]. The only change worth mentioning is the enhanced predominance area of $Au(OH)_3$ (s), which results from the use of $\Delta G° = -317.0$ kJ/mol for the formation of that species quoted in [12] and [14], in contrast to the traditionally adopted $\Delta G° = -290$ kJ/mol, given in [19]. The diagrams in **Figure 2.4** - as the other ones in this study - were drawn using the data given in Appendix 1.

The nobility of gold [1, 4, 5, 54-56] is apparent from **Figures 2.4a** and **2.4b**, which show that between the water stability lines 1 and 2 the predominant species is the native metal. Silver is comparatively less noble and shows a corrosion area partially bound by line 1 in which Ag^+ is stable in water (**Figures 2.4c** and **2.4d**); at higher pH the metal has a passivation area in which the oxide Ag_2O (s) is formed; at even higher pH, the soluble hydroxide $Ag(OH)_2^-$ is stable in water.

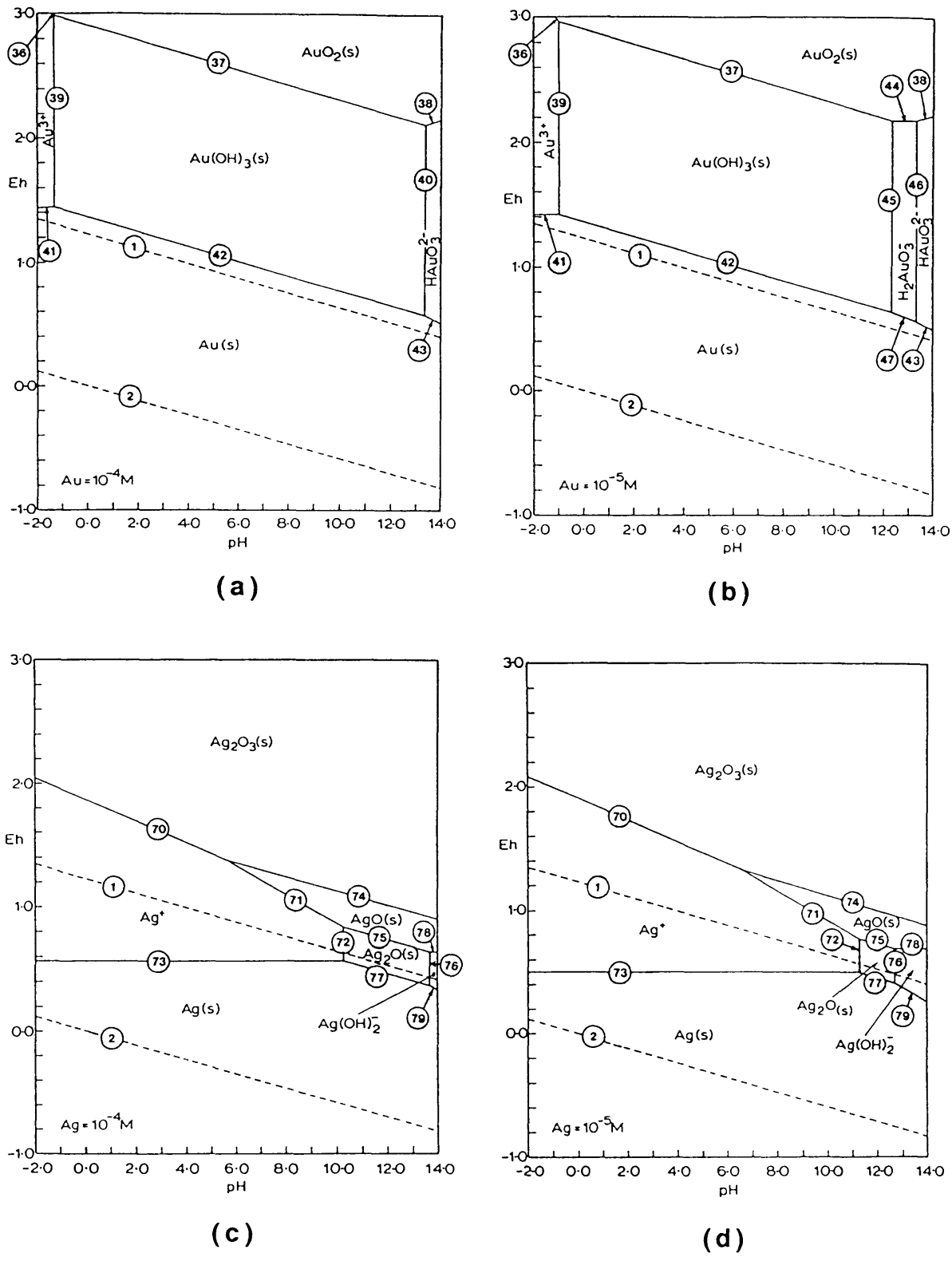


Figure 2.4 - Eh-pH diagrams for the Au-H_2O and Ag-H_2O systems at 25°C.

2.6. The Au-SCN-H_2O System

Eh-pH diagrams for this system are shown in **Figures 2.5** and **2.6** for activities of gold-containing species of 10^{-4} and 10^{-5} mol/dm^3, respectively (*c.a.* 20 and 2 ppm Au). The activities of either free SCN^- or HSCN are also indicated. At first sight, the similarities between these diagrams and those for the Au-Cl-H_2O, Au-Br-H_2O and Au-I-H_2O systems [4, 5, 183] highlight the pseudohalide character of thiocyanate (see Chapter 7, **Figure 7.1**).

A noticeable feature of the Au-SCN-H_2O system is that gold may be dissolved at pH values as low as 1 or 2, which enables the use of oxidants such as iron(III), hydrogen peroxide and manganese dioxide. The overall calculations also show that the redox potentials required for leaching are around 600-700 mV (vs. SHE).

The potentials required to reach 20 ppm of gold in solution (**Figure 2.5**) are higher than those necessary for reaching 2 ppm (**Figure 2.6**), which derives directly from the specific form of the Nernst equation as applied to reactions 56 and 57, and also 60 and 62, and 67 and 68. The reactions are all listed in Appendix 2. The resulting potentials are indicated in the Eh-pH diagrams by the lines with the same numbers, i.e. lines 56, 57, 60 and 62 (**Figures 2.5** and **2.6**), and 67 and 69 (**Figure 2.6d**). Conversely, for the same gold activity in solution, the potential required decreases as the thiocyanate concentration increases.

The complexes $Au(SCN)_2^-$ and $Au(SCN)_4^-$ are the most relevant among all those considered, since they are the only two appearing in the diagrams drawn for thiocyanate activities likely to be found in leaching operations, i.e. 10^{-1} to 10^{-2} mol/dm^3. A thiocyanate activity as high as 1 is not likely to be found in leaching circuits and was included in these calculations mainly to demonstrate tendencies of the system. On the other extreme, the activity 10^{-4} was included

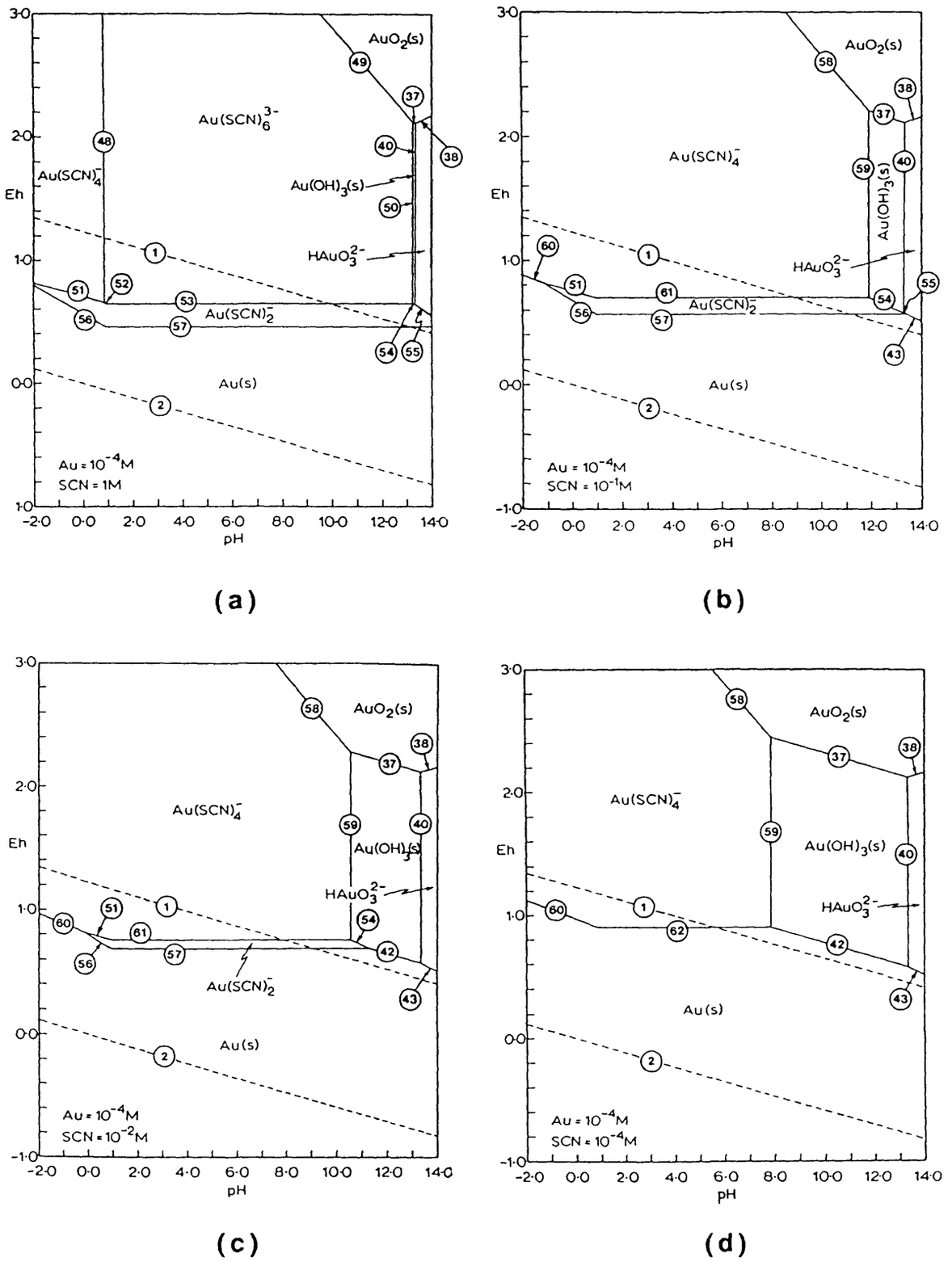


Figure 2.5 - Eh-pH diagrams for the Au-SCN-H_2O system at 25°C and activity of gold species of 10^{-4} mol/dm^3 (≈20 ppm).

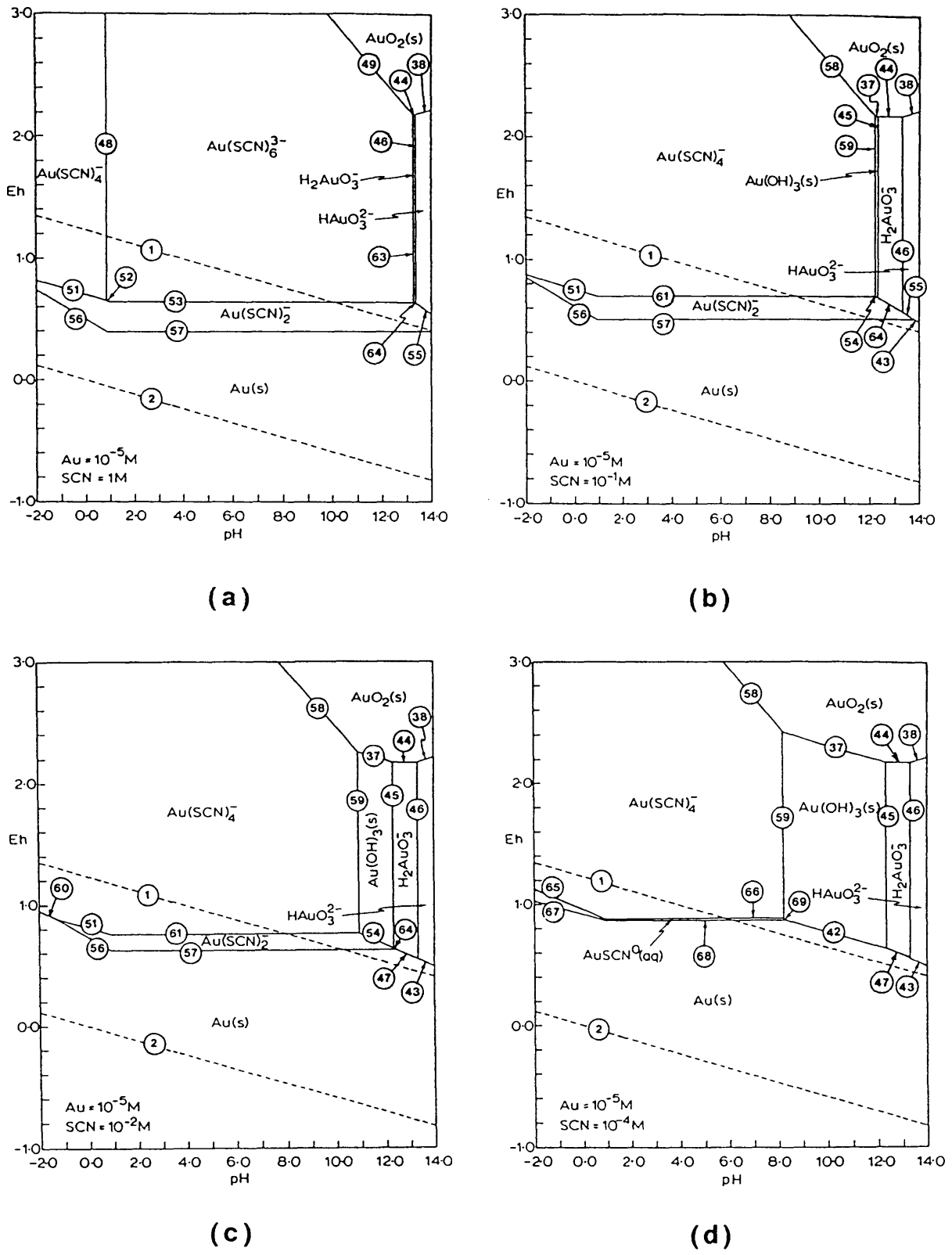
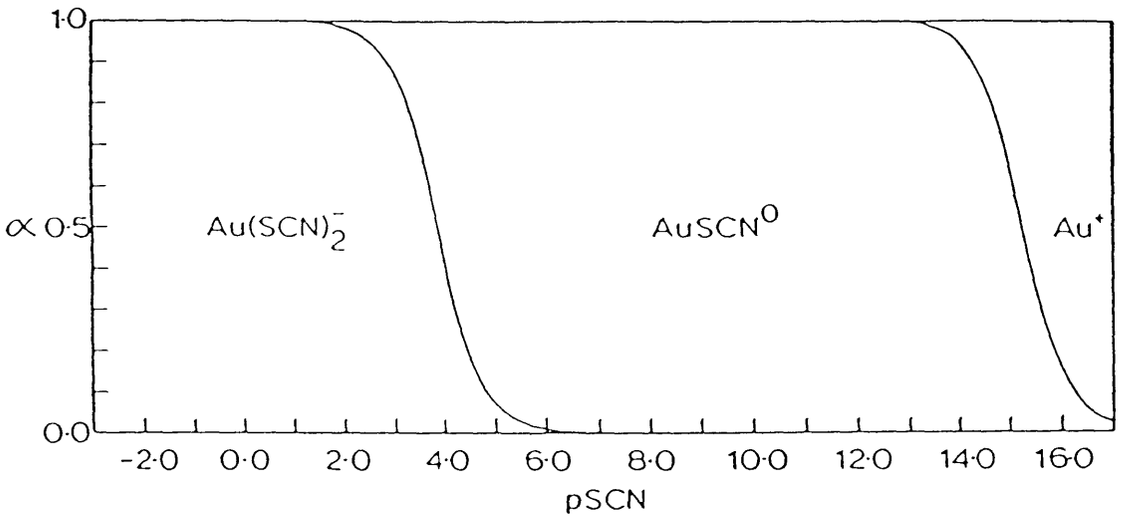
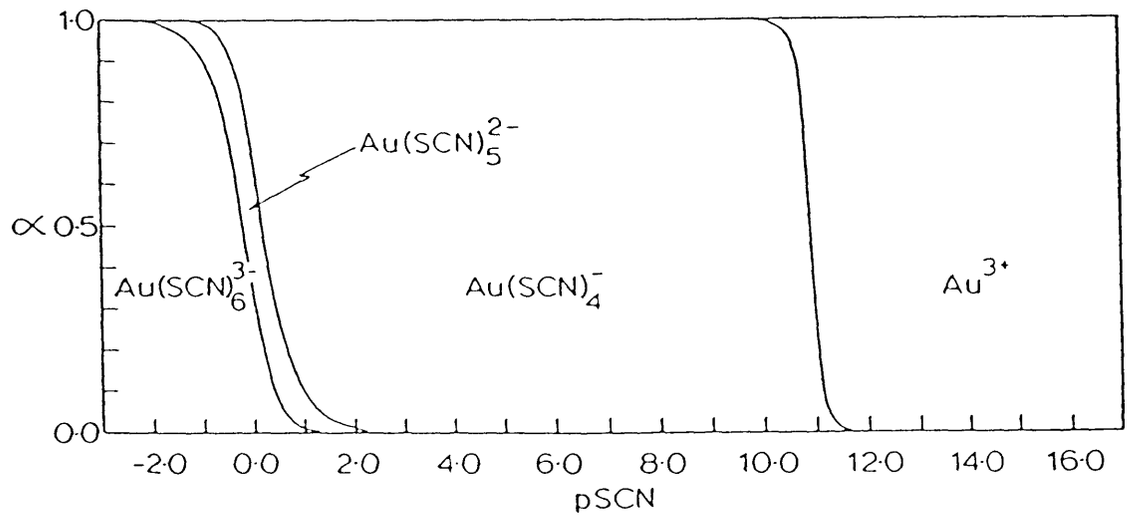


Figure 2.6 - Eh-pH diagrams for the Au-SCN-H_2O system at 25°C and activity of gold species of 10^{-5} mol/dm^3 (≈2 ppm).

to indicate the complexing behaviour of thiocyanate when it is present in small amounts, as is the case in cyanidation plants treating sulphur-containing ores.



(a)



(b)

Figure 2.7 - Distribution curves for **(a)** gold(I)-thiocyanate complexes and **(b)** gold(III)-thiocyanate complexes.

The species that appear in any Eh-pH diagrams are the predominant ones. This means that species responsible for as much as 49% or so of the total gold in solution may be omitted. For this reason, the distribution curves shown in **Figure 2.7** were calculated for **(a)** aurous and **(b)** auric thiocyanate complexes. By referring to such curves it is possible to know, for each activity of free thiocyanate (expressed as pSCN = -log a_{SCN^-}), the fractional contribution α of each complex, thereby complementing the information given in the Eh-pH diagrams. In **Figure 2.7**, the practical importance of the complexes $Au(SCN)_2^-$ and $Au(SCN)_4^-$ is once more observed. For free thiocyanate activities between 0.5 and 0.01 mol/dm^3 (i.e. pSCN between 0.3 and 2.0) these complexes are widely prevalent.

The relative stabilities of gold complexes with thiocyanate, cyanide and chloride may be compared by means of the stability constants given in Appendix 3. The stability of the gold(I) complexes with thiocyanate is greater than that of the chloride complex and smaller than that of the cyanide complex. The gold(III)-thiocyanate complex, $Au(SCN)_4^-$, is also more stable than the reported chloride complex $AuCl_4^-$.

2.7. The Ag-SCN-H_2O System

Eh-pH diagrams for this system are presented in **Figures 2.8** and **2.9** for silver activities of 10^{-4} and 10^{-5} mol/dm^3 (*c.a.* 11 and 1.1 ppm), respectively. Redox potentials for the dissolution of silver are much lower than those required for dissolving gold and, overall, they decrease as the dissolved silver activity decreases and/or the thiocyanate concentration increases. The figures are around 0-100 mV. The pH range for leaching is identical to that required for gold (pH 1 to 3), thereby also allowing the use of oxidizing agents such as iron(III) and hydrogen peroxide.

A major feature of this system is the marked insolubility of AgSCN. When the thiocyanate activity drops to 0.1 (**Figure 2.8c**) and 10^{-4} mol/dm^3 (**Figure 2.9d**), silver dissolution is no longer the prevalent process, the metal being kept as the solid phase AgSCN. To analyse this feature in detail the distribution curves shown in **Figure 2.10** were calculated; a_{Ag} is the analytical (i.e. total) activity of silver in solution. The curves corresponding to aqueous AgSCN are too close to those for solid AgSCN to appear distinctly in the drawings. Regarding **Figure 2.10a**, the curves on the left hand side indicate the fractional distribution α of the complexes at higher free thiocyanate activities, i.e. non-precipitation conditions. When the SCN^- activity drops to about 0.14 mol/dm^3 (pSCN = 0.86) precipitation starts, which is indicated by the discontinuity points on the curves for the soluble complexes. When the SCN^- activities reaches ≈0.09 mol/dm^3 or less (pSCN ≈ 1.05 or above), solid AgSCN predominates. The interpretation of **Figure 2.10b** is similar; for $a_{Ag} = 10^{-5}$ mol/dm^3, AgSCN precipitation takes place only when SCN^- activity drops below ≈0.033 mol/dm^3 (pSCN = 1.48), and becomes the predominant process (>50% of the silver as solid AgSCN) for $a_{SCN^-} \leq 0.019$, i.e. pSCN ≥ 1.73, approximately.

The behaviour of the Ag-SCN-H_2O system is also shown by **Figure 2.11**. Each straight line gives the logarithmic concentration of the related complex as a function of pSCN. The curve that surrounds the shaded area, in which solid AgSCN predominates, results from the addition of all soluble species for a given pSCN value.

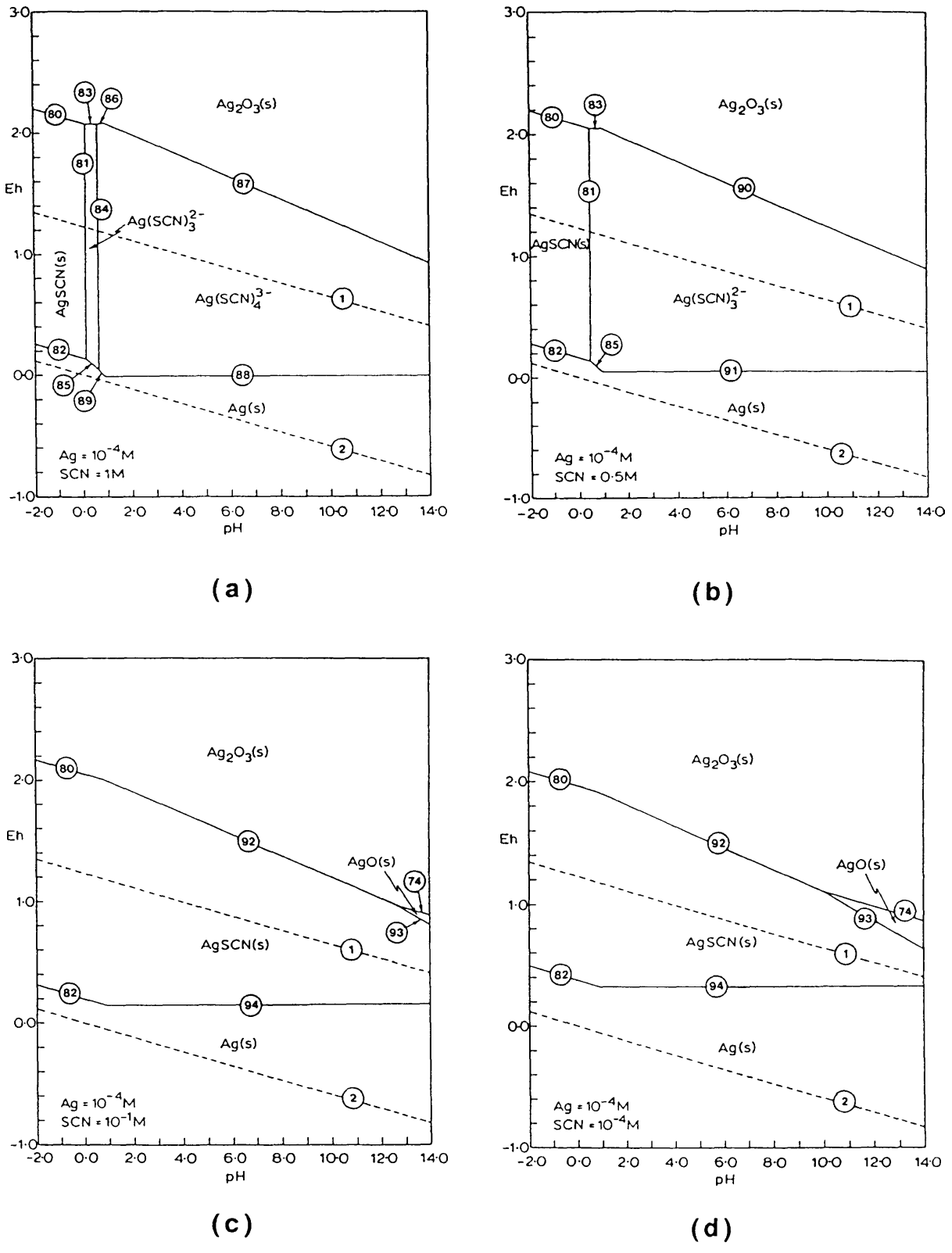


Figure 2.8 - Eh-pH diagrams for the Ag-SCN-H_2O system at 25°C and activities of silver species of 10^{-4} mol/dm^3 (≈11 ppm).

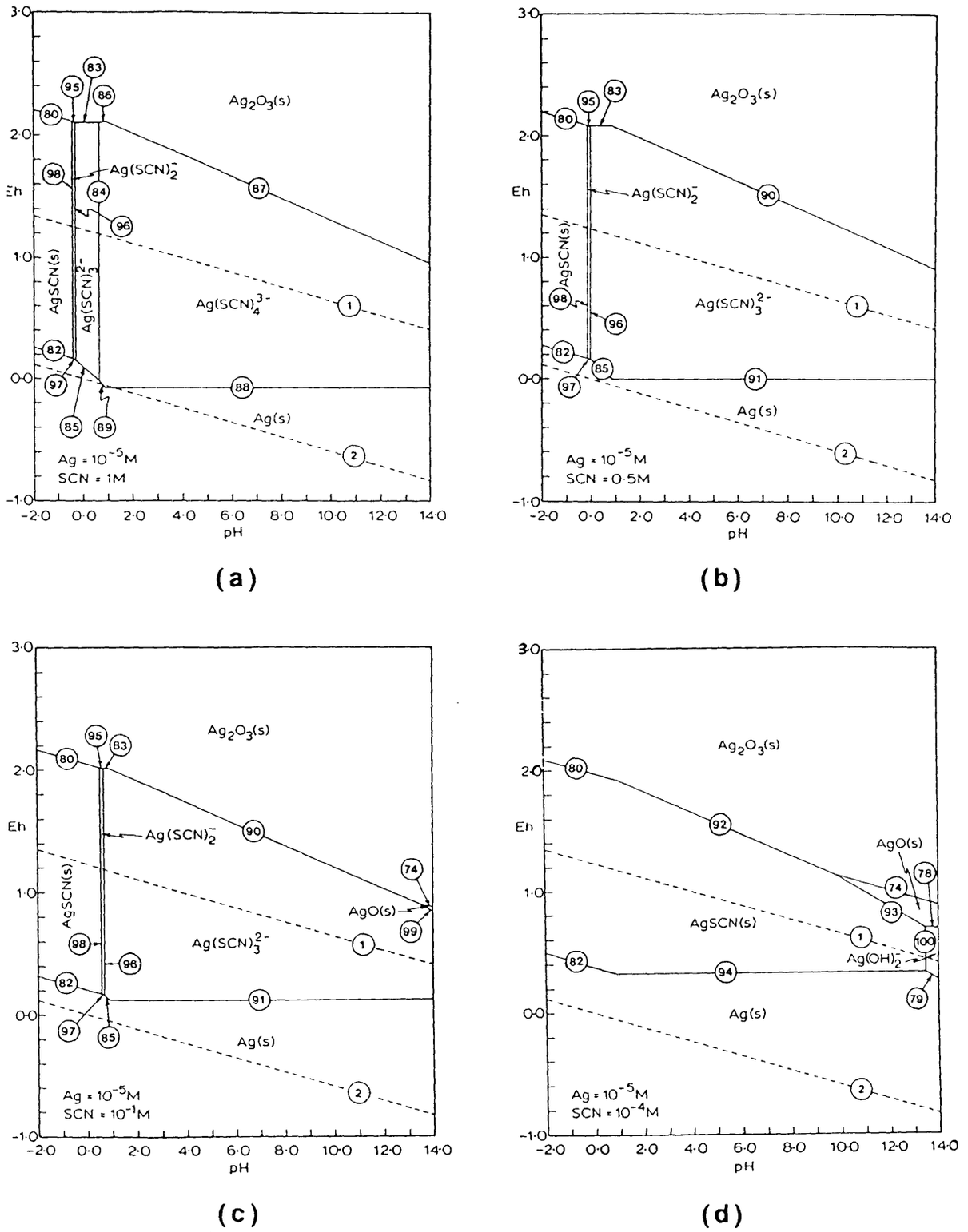
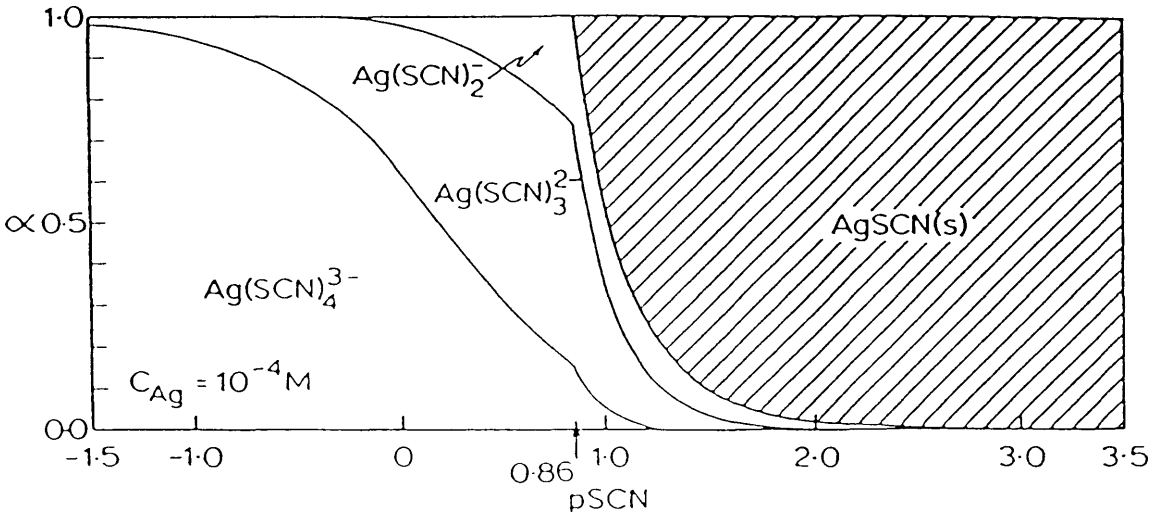
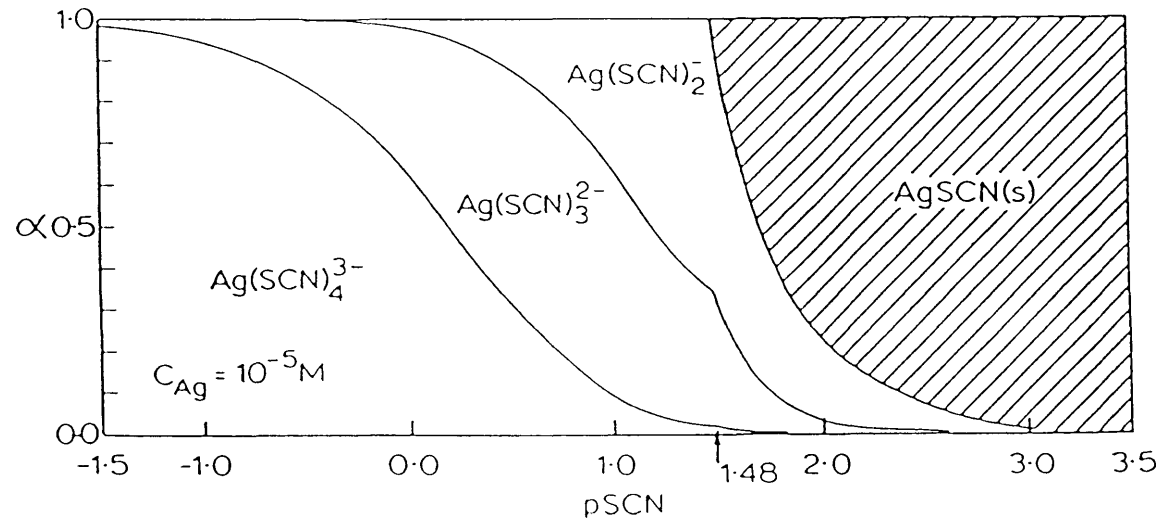


Figure 2.9 - Eh-pH diagrams for the Ag-SCN-H_2O system at 25°C and activity of silver species of 10^{-5} mol/dm^3 (≈1.1 ppm).



(a)



(b)

Figure 2.10 - Distribution curves for silver-thiocyanate complexes including precipitation of AgSCN. The analytical activity of silver, a_{Ag}, is **(a)** 10^{-4} and **(b)** 10^{-5} mol/dm^3. The activity of free thiocyanate ion is given by pSCN = - log a_{SCN^-}.

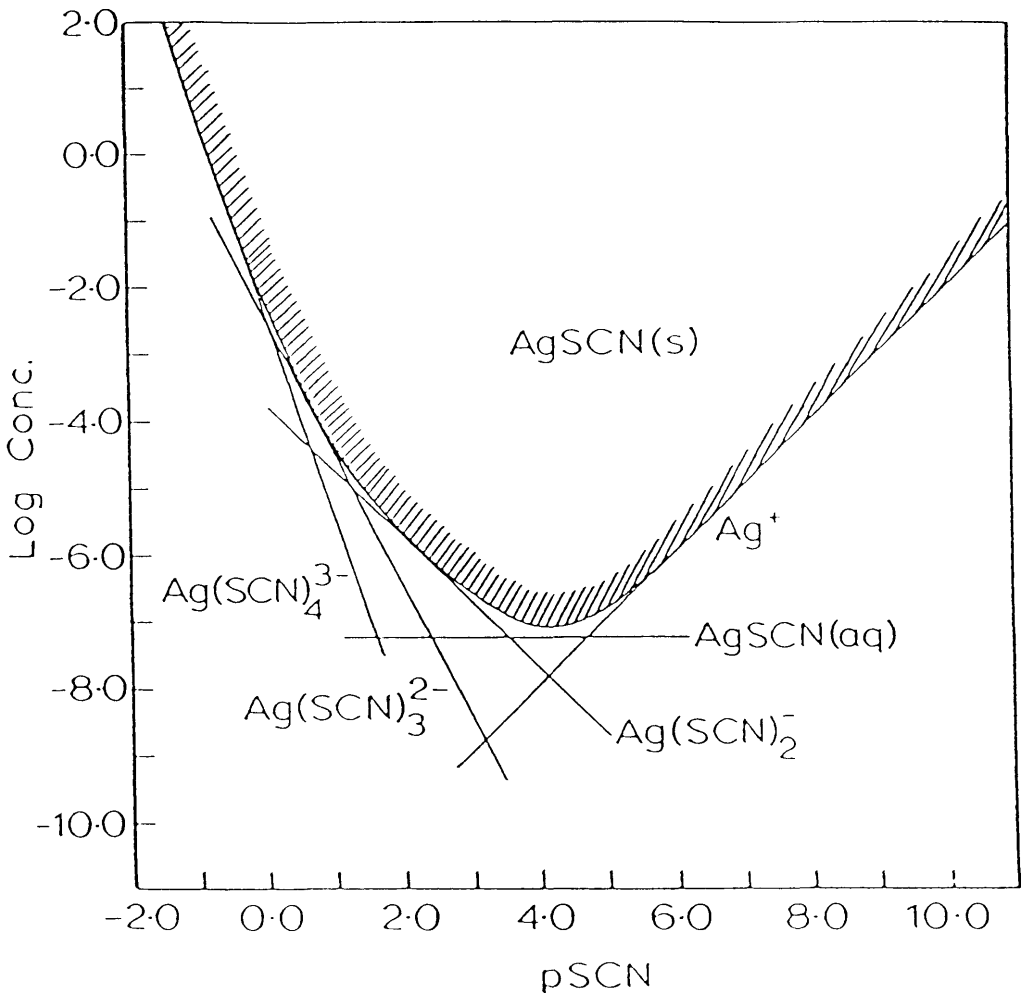


Figure 2.11 - Solubility diagram indicating the logarithmic activity of each silver species as a function of free thiocyanate ion activity, expressed as pSCN = - log a_{SCN^-}.

Thus, even when the redox potential is adequate, the dissolution of silver takes place only at fairly high thiocyanate activities. To achieve, for instance, a silver concentration of *c.a.* 11 ppm (as in **Figure 2.8**) and at the same time to prevent any AgSCN precipitation, a free thiocyanate activity not lower than 0.14 must be mantained, as shown by **Figures 2.10a** and **2.11**. In practice, the activity of the added thiocyanate salt must be higher to compensate for the protonation of part of the free thiocyanate into HSCN, which occurs below pH 3, as seen from **Figure 2.1**. If the expected silver activity is higher than that corresponding to approximately 11 ppm given in the example, the free thiocyanate level must be accordingly higher, probably too high from an economic point of view. The consequence is that thiocyanate leaching is not suitable for silver-rich ores or concentrates. The diagrams given here provide a basis for the assessment of each specific case.

The relative stabilities of silver complexes with thiocyanate, cyanide and chloride may be compared through the stability constants given in Appendix 3. Silver (I)-thiocyanate complexes are more stable than silver (I)-chloride complexes and less stable than silver (I)-cyanide complexes. An exception is aqueous AgCN, whose stability is notably low.

2.8. Some Prospective Oxidants for the Thiocyanate Leaching of Gold and Silver

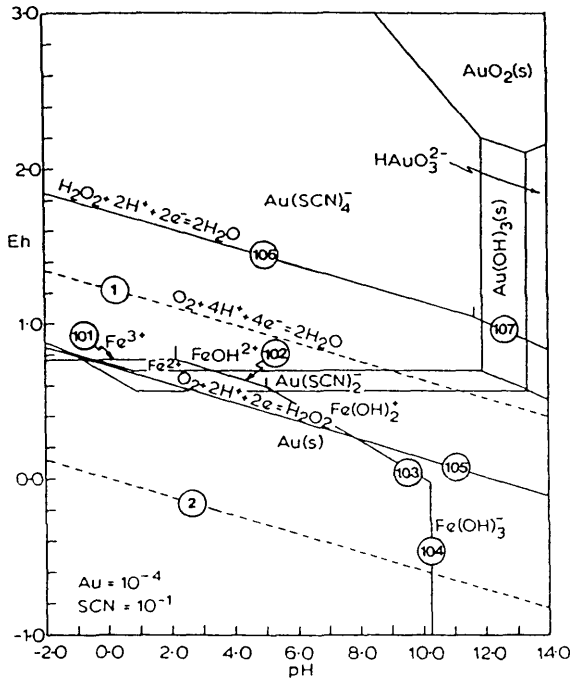
A frequent problem in cyanidation plants is the low solubility of oxygen in water. The alkalinity of the medium does not allow the use of a number of oxidants. Being effected in acidic media, thiocyanate leaching enables oxidizing agents such as ferric ions, hydrogen peroxide and MnO_2 to be used. This possibility has already been tried with results that justify further investigation [2, 3].

Figure 2.12 is a repetition of some of the diagrams already discussed upon which the lines for several oxidants have been overlaid. In the calculation of these lines, a 10^{-1} mol/dm^3 activity was adopted for all oxidants and their related reduced aqueous species; P_{O_2} = 1 atm or, more precisely, f_{O_2} = 1 was also taken (see reactions in Appendix 2).

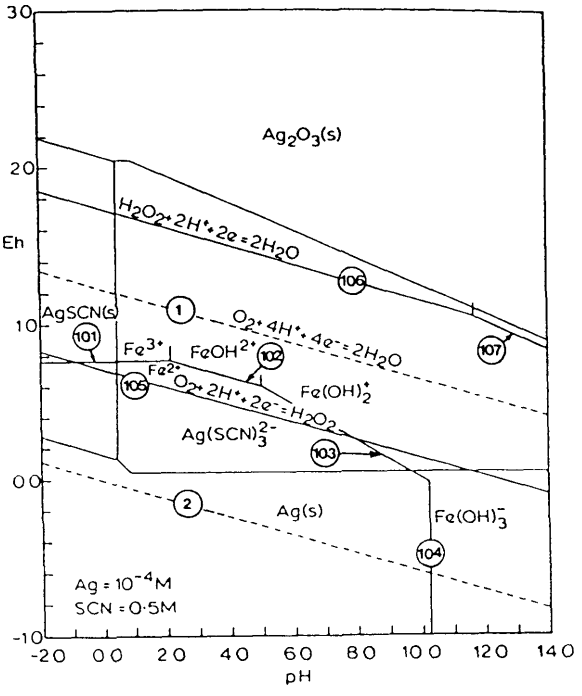
Lines 101 through 104 represent iron species, line 101 corresponding to the Fe^{3+}/Fe^{2+} redox pair. It is seen that Fe^{3+} is capable of oxidizing gold (**Figure 2.12a**) and silver (**Figure 2.12b**), the case of gold demanding a weakly acidic pH. These lines should be taken only as an indication, since in reality dissolved iron would be complexed by thiocyanate and other ligands and this would affect both the redox potential and the activity of free thiocyanate in the system. Nevertheless, thiocyanate complexes with iron are less stable than those with gold and silver, as demonstrated by the stability constants quoted in Appendix 3, which means that Au and Ag cations would be favoured in competition for thiocyanate ions in the presence of Fe cations. In any case, a more complete calculation is necessary to quantify the distribution of the species involved and the expected redox potential in a real or quasi-real system using iron (III) as the oxidizing agent.

Line 105 indicates the reduction of O_2 (g) to H_2O_2 (aq). This suggests that oxygen could be used as an oxidant, provided pH $\leq$ 2.5 in the case of gold. There remains, however, the drawback of its low solubility in water, particularly at atmospheric pressure.

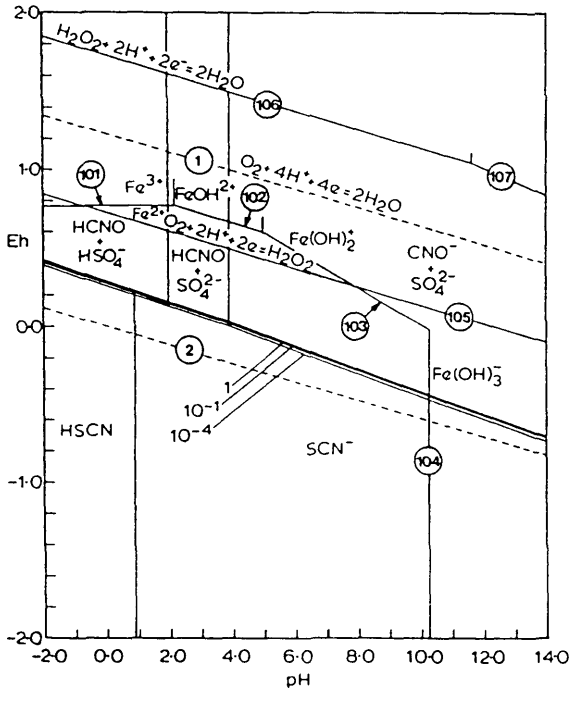
Line 106 represents the reduction of hydrogen peroxide to H_2O. The redox potentials observed when H_2O_2 is dissolved in water are in fact lower than those of line 106 and much closer to line 105. Regardless of any mechanistic hypothesis, the overall process of decomposition of hydrogen peroxide seems to comply with a reaction such as:



(a)



(b)



(c)

Figure 2.12 - Eh-pH diagrams indicating the thermodynamic feasibility of different oxidizing agents in the **(a)** dissolution of gold, **(b)** dissolution of silver and **(c)** oxidation of thiocyanate.

$$2\,H_2O_2 = 2\,H_2O + O_2(g) \qquad (2.12)$$

The diagrams suggest that hydrogen peroxide could be used in both gold and silver leaching, the former requiring a weakly acidic pH (pH $\leq$ 2.5 in the example of **Figure 2.12**). Caro's acid, H_2SO_5, would also be capable of oxidizing gold and silver in the systems studied, as it is a more powerful oxidizing agent than hydrogen peroxide.

A problem that arises when using any one of these oxidizing agents is depicted in **Figure 2.12c**. Potentials required for gold leaching are well above those required to oxidize thiocyanate. Even so, experiments [3] have shown that it is possible to attain efficient gold leaching with fairly low thiocyanate losses. Experimental work is required both on the kinetics of gold dissolution and on the kinetics of thiocyanate oxidation. It should be remembered that the cyanidation process is conducted at potentials high enough to oxidize cyanide and that, despite reagent losses, it is economically feasible.

Line 105 (**Figure 2.12a**) also shows that oxygen would not be effective in the thiocyanate leaching of gold in alkaline media. In fact, it is not expected to be effective at any pH above 2.5 or 3. Thus the SCN^- generated in cyanidation plants is not expected to participate in the gold dissolution process and simply reports as a cyanide loss.

2.9. The Metastable Character of the Au-SCN-H_2O and Ag-SCN-H_2O Systems and its Comparison with the Homologous Cyanide Systems

The Eh-pH diagrams presented in **Figure 2.13** were drawn by

superimposing those for the SCN-H_2O and CN-H_2O systems (in dashed lines) upon those for the related gold and silver systems.

Figure 2.13a shows that the stability areas for gold-thiocyanate complexes are well above those for SCN^- and HSCN. Even if cyanide species are considered instead of cyanate species as the products of thiocyanate oxidation, the situation remains practically the same. Thus, based on a thermodynamic reasoning alone, the leaching of gold by thiocyanate would be impossible. This fact emphasizes the importance of kinetic studies on the oxidation of thiocyanate at those potentials required for the oxidation and complexation of gold. This subject is dealt with extensively in Chapters 3, 4 and 5. At this stage it is sufficient to report that considerable overpotentials are involved in the oxidation of thiocyanate. Such overpotentials render the Au-SCN-H_2O system kinetically stable enough to make gold leaching a viable operation.

Figure 2.13c reveals a similar situation between HCN/CN^- and the aurocyanide complex. A comparison between **Figures 2.13c** and **2.13a** indicate that in the leaching of gold, thiocyanate is submitted to a higher oxidation driving force than is cyanide, i.e. the potential gap between the thiocyanate oxidation lines and the gold dissolution lines is greater than that between the cyanide oxidation lines and the gold dissolution lines in the case of cyanide leaching. This is a statement based on thermodynamics alone and nothing conclusive can be stated before kinetic studies are undertaken, specially those on real systems, involving specific ores and concentrates.

In the case of silver leaching (**Figures 2.13b** and **2.13d**), the conditions are much less aggressive (towards oxidation). However, in all cases considered, the predominance areas of the metal complexes lie above the predominance areas of the ligands. All the diagrams presented are metastable and this fact emphasizes the importance of kinetic studies for these systems.

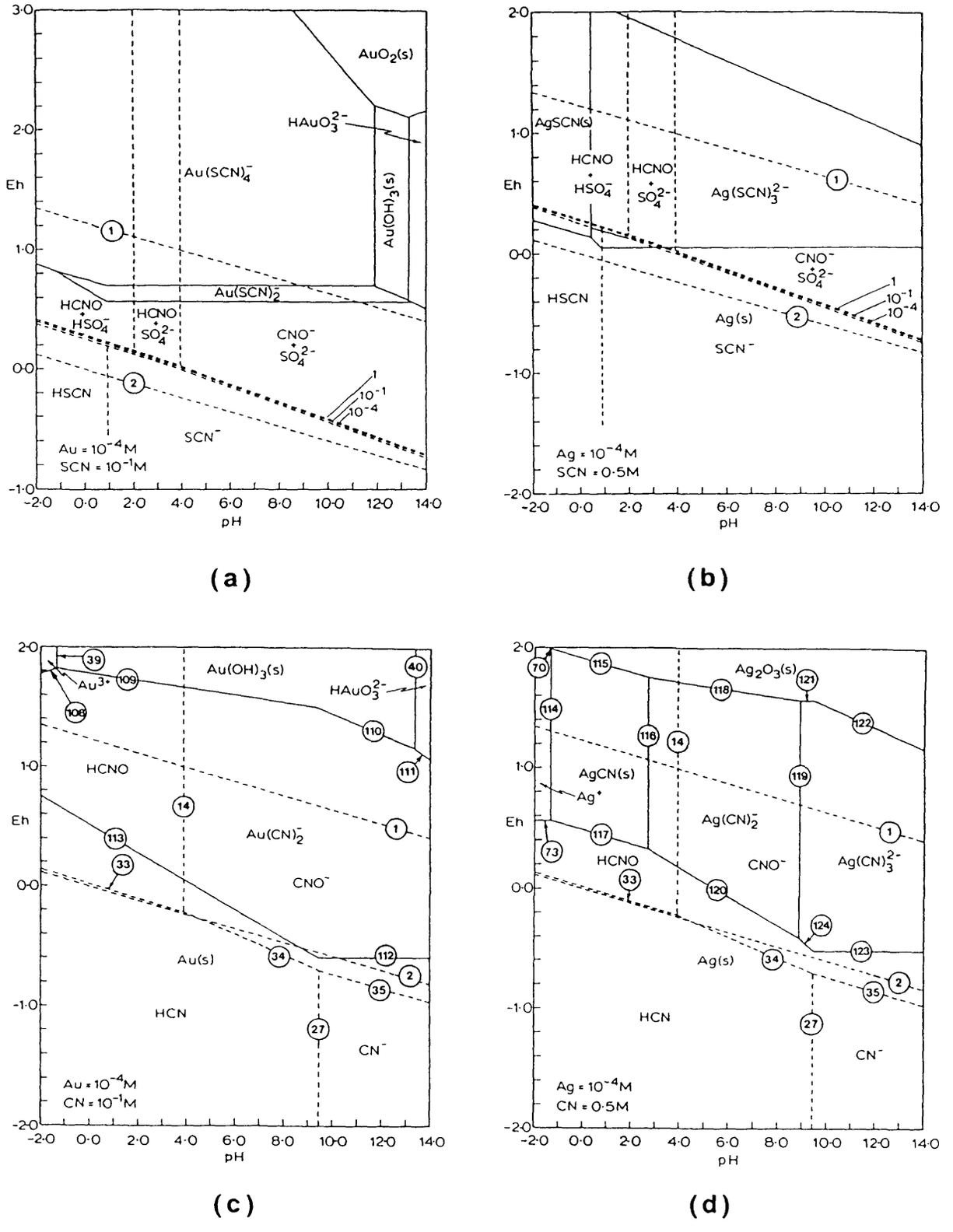


Figure 2.13 - Eh-pH diagrams demonstrating the metastable character of the Au-SCN-H_2O, Ag-SCN-H_2O, Au-CN-H_2O and Ag-CN-H_2O systems.

2.10. Conclusions

The thermodynamic study presented above predicts that:

(1) Gold can be leached effectively by thiocyanate at potentials around 600-700 mV (vs. SHE), at thiocyanate concentrations of 0.5-0.01 mol/dm^3 and under weakly acidic conditions (pH = 1 - 3). Gold is expected to dissolve mainly as the complexes $Au(SCN)_2^-$ and $Au(SCN)_4^-$.

(2) These low pH values enable the use of oxidants such as ferric ions, hydrogen peroxide, manganese dioxide or Caro's acid. Ferric ions will be totally or partly complexed by thiocyanate. The complexation may contribute to stabilize the ferric ions in solution and should also be considered in the formulation of any assumptions concerned with the leaching kinetics.

(3) Silver can also be leached by thiocyanate provided the required metal concentration in solution is low, as is the case with low grade ores. The redox potentials necessary are much lower (around 0-100 mV) than those for gold leaching, whereas the pH range is similar. The main drawback is the marked insolubility of AgSCN, which renders the process unsuitable for treating high grade ores. When applicable, silver is expected to be dissolved mainly as the complexes $Ag(SCN)_3^{2-}$ and $Ag(SCN)_4^{3-}$.

(4) As occurs with cyanidation, the leaching - especially of gold - takes place at potentials high enough to oxidize thiocyanate. Research on the kinetics of thiocyanate oxidation at those potentials should be done for each specific case, taking advantage of the fundamental studies reported in this work.

(5) The kinetics of gold and silver dissolution by thiocyanate also need to be investigated.

(6) Thiocyanate generated in conventional cyanidation plants by reaction of cyanide with sulphur-containing species^{-} is not expected to participate in the dissolution of gold because the mixed potentials produced by dissolved oxygen (i.e. air) in conventional cyanidation are too low.

CHAPTER 3: THE INTERMEDIATE SPECIES IN THE OXIDATION OF THIOCYANATE AND THEIR RELEVANCE FOR THE DISSOLUTION OF GOLD

3.1. Introduction

Most of the chemical species included in the thermodynamic description of the SCN-H_2O system presented in Chapter 2 are metastable. Their decomposition, however, is slow enough for them to be considered stable, from a practical standpoint. They are the species usually detected by conventional methods of chemical analysis during experiments on thiocyanate oxidation by several oxidizing agents. However, they are not capable of providing a complete mechanistic explanation of the process of thiocyanate oxidation. A considerable overpotential is required for that oxidation to take place and this fact alone suggests that some intermediate species are formed which are responsible for that overpotential. Such species have just been mentioned in the last chapter but their chemistry was not considered in detail. This is the objective of the present chapter. The intermediate species are relevant not only to explain the oxidation of thiocyanate, but also to provide a better understanding of the mechanism of gold leaching by it.

3.2. The Postulation of Aqueous Thiocyanogen and its Hydrolysis

The existence of free thiocyanogen, $(SCN)_2$, was first proposed by Bjerrum and Kirschner in 1918 [51], in a remarkable 76-page paper containing 55 tables of experimental results on gold-thiocyanate

solutions. Through spectrophotometric measurements in such solutions, they found that for $[SCN^-]$ = 0.1-0.4 mol/dm^3 the only complexes present are $Au(SCN)_2^-$ and $Au(SCN)_4^-$, the higher complexes $Au(SCN)_5^{2-}$ and $Au(SCN)_6^{3-}$ being present at higher free thiocyanate concentrations. They also observed that gold(III) thiocyanate solutions had a tendency towards autoreduction.

The conclusion that free thiocyanogen exists was reached as follows: analytical determinations consistently indicated that the autoreduction of 3 mol of $Au(SCN)_4^-$ produced 1 mol of H_2SO_4 and a total of 8 equivalents of acid. The course of the reaction could be followed either spectrophotometrically by the decrease of the absorption peak of $Au(SCN)_4^-$ at 578 nm or by titration with Na_2SO_3 of the unreduced gold. The velocity decreased with the progress of the reaction, which was attributed to the retarding effect of the $Au(SCN)_2^-$ produced. The overall autoreduction process was found to be irreversible and in agreement with the following reaction:

$$3Au(SCN)_4^- + 4H_2O \rightarrow 3Au(SCN)_2^- + 5HSCN + HCN + H_2SO_4 \qquad (3.1)$$

Potential measurements with platinum electrodes indicated that in fresh $Au(SCN)_4^-$ solutions 10-20 % of the Au was present as $Au(SCN)_2^-$, while sulphite titrations yielded titre consumptions as if all the Au were in the auric state. Spectrophotometric determinations agreed nearly quantitatively with the electrometric. The degree of dissociation was found to be independent of $[H^+]$ and $[SCN^-]$ and to agree with the Ostwald dilution law, showing that only two products were formed. Since one of the products was certainly $Au(SCN)_2^-$, the other was necessarily $(SCN)_2$. A mean value for the dissociation constant was then found as follows:

$$Au(SCN)_4^- = Au(SCN)_2^- + (SCN)_2 \qquad K = 0.49 \times 10^{-4} \qquad (3.2)$$

The value E° = 0.77 V for the couple $(SCN)_2/SCN^-$ was then calculated from the above constant and from the E° already determined (in the same work) for the couple $Au(SCN)_4^-/Au(SCN)_2^-$. Comparing this E° = 0.77 V with those for the halogens, Bjerrum and Kirschner placed thiocyanogen as an unstable halogen intermediate (currently termed a pseudohalide) between bromine and iodine, the E° values for the couples Br_2/Br^- and I_2/I^- being, respectively, 1.09V and 0.62V [12]. Consistently, Br_2 was found to be instantly reduced by a solution of NaSCN in HCl; the resulting colourless solution setting free I_2 from KI. This ability to displace iodine vanishes rapidly. The rate of the disapearance of this ability to oxidize I^- to I_2 was found to be approximately the same as the rate of the autoreduction of $Au(SCN)_4^-$. This further fact was regarded by Bjerrum and Kirschner as confirming the hypothesis that the autoreduction of $Au(SCN)_4^-$ was due to the formation of free $(SCN)_2$.

Once the halogenic character of thiocyanogen was established, it was possible to consider its hydrolysis, by analogy with Cl_2 for instance, to HOSCN and HSCN. A mechanism to explain reaction 3.1 was then proposed by Bjerrum and Kirschner [51], with the following steps:

$$Au(SCN)_4^- = Au(SCN)_2^- + (SCN)_2 \quad \text{(instantaneous)} \quad (3.2)$$

$$(SCN)_2 + H_2O = HOSCN + H^+ + SCN^- \quad \text{(instantaneous)} \quad (3.3)$$

$$2HOSCN \rightarrow HO_2SCN + H^+ + SCN^- \quad \text{(relatively slow)} \quad (3.4)$$

$$HOSCN + HO_2SCN \rightarrow HO_3SCN + H^+ + SCN^- \quad \text{(instantaneous)} \quad (3.5)$$

$$HO_3SCN + H_2O \rightarrow H_2SO_4 + HCN \quad \text{(instantaneous)} \quad (3.6)$$

Bjerrum and Kirschner [51] found that reaction 3.4 alone, due to

its relative slowness, determined the velocity of the irreversible autoreduction of auric thiocyanate.

The above partial reactions 3.3 to 3.6 constitute the mechanism of the hydrolysis of $(SCN)_2$, summarized by the overall reaction [51] :

$$3(SCN)_2 + 4H_2O = 5SCN^- + HCN + SO_4^{2-} + 7H^+ \quad (3.7)$$

There is a complete analogy between the above mechanism (reactions 3.3 to 3.6) for the hydrolysis of thiocyanogen and the similar process for chlorine, as follows [48, 51]:

$$Cl_2 + H_2O = Cl^- + HClO + H^+ \quad (3.8)$$

$$3HClO = Cl_2 + HClO_2 + H_2O \quad (3.9)$$

$$2HClO_2 = HClO + ClO_3^- + H^+ \quad (3.10)$$

$$2ClO_3^- + H^+ = ClO_4^- + HClO_2 \quad (3.11)$$

To better emphasize this analogy, which is only possible due to the pseudohalogenic character of thiocyanogen, Gauguin [48] rearranged the above steps of the hydrolysis mechanism in a slightly different way, as follows [48] :

$$(SCN)_2 + H_2O = SCN^- + HOSCN + H^+ \quad (3.3)$$

$$3HOSCN = (SCN)_2 + HO_2SCN + H_2O \quad (3.12)$$

$$2HO_2SCN = HOSCN + HO_3SCN \quad (3.13)$$

The above hydrolysis scheme is usually accepted even today

[28, 31]. This work was the starting point for the search for the intermediates in the oxidation of thiocyanate. The existence of free thiocyanogen and of its transitory hydrolysis products like hypothiocyanous acid, HOSCN, thiocyanous acid, HO_2SCN and thiocyanic acid, HO_3SCN, have been acknowledged in the mechanistic propositions of thiocyanate oxidation by several oxidizing agents [36-44, 47, 48]. It is, indeed, the corner stone of those mechanistic propositions whenever the chemical oxidation in aqueous solution is involved.

The identification of the series of gold-thiocyanate complexes by Bjerrum and Kirschner [51] has been confirmed by later work [20, 60, 61]. The same is true of the standard potentials for the gold-thiocyanate complexes, whose more recent determinations [20, 60, 61] are basically consistent with theirs [51].

Still as part of the same work [51], aurous thiocyanate solutions were found to deposit gold. But in this case the reaction is reversible since aurithiocyanate solutions dissolve gold metal with the formation of $Au(SCN)_2^-$. The process agrees with the following reaction, an approximate equilibrium constant having been determined [51]:

$$3Au(SCN)_2^- = 2Au + Au(SCN)_4^- + 2SCN^- \qquad K \approx 33 \qquad (3.14)$$

Starting from a solution with 0.1 mol/dm^3 HCl, 0.5 mol/dm^3 NaSCN and 0.1 mol/dm^3 Au(I) at 40°C, about 50% of the gold was observed to separate in 3 days [51].

From all the work reported above, it seems that the autoreduction of auric thiocyanate solutions takes place until the equilibrium defined by reaction 3.14 is established.

3.3. Oxidation Overpotentials in Thiocyanate Solutions in Relation to Thiocyanogen

Gauguin [47, 48] investigated the oxidation of thiocyanate and the significance of potential measurements on thiocyanate systems. The results were condensed in Eh-pH plots which were an interesting anticipation of the Eh-pH diagrams later proposed by Marcel Pourbaix. His main concern, however, were not the reversible equilibria that appear in a conventional Eh-pH diagram. Instead, he conducted his work on an entirely empirical basis, plotting his Eh-pH lines from a great number of measurements in thiocyanate and also in cyanide solutions. In the course of this work, he investigated the oxidation of thiocyanate by tetravalent cerium, iodine, permanganate, bromate, dichromate, hypochlorite, etc., comparing the overall stoichiometry of each one of these oxidation processes with the potential readings obtained in the course of the experiments.

Invariably, the overall oxidation process was found to be irreversible and to comply with the stoicheiometry already reported [47, 48]:

$$SCN^- + 4H_2O \rightarrow SO_4^{2-} + HCN + 7H^+ + 6e \qquad (3.15)$$

However, the potential readings taken from the oxidation experiments were higher than those expected from calculations using $\Delta G°$ data for the above reaction (see Figure 2.2, Chapter 2).

The readings were fitted into semi-empirical straight lines resembling the Nernst equation, enabling him to formulate hypotheses such as the number of electrons involved, the possible reactions ocurring, and so on. The following results, for example, were obtained [48]:

$$E = 0.564 - 0.058 \log [SCN^-] \qquad (3.a)$$

for the oxidation by Ce^{4+} in ≈0.1 N H_2SO_4 , and:

$$E = 0.566 - 0.054 \log [SCN^-] \qquad (3.b)$$

for the oxidation by iodine at pH 2.5.

Similar fits were obtained for all oxidizing agents investigated. The experiments consisted in adding a known amount of oxidant solution to the thiocyanate solution. The potential decay was followed until a stable value was obtained, which was used in the plots. The time elapsed until the reading was taken depended on the velocity of the oxidation process. For the oxidation by Ce^{4+}, for instance, the readings were taken about 30 minutes after the addition.

Potential readings in thiocyanate solutions at 0<pH<7 (without addition of any oxidant) were fitted by Gauguin [48] into the following semi-empirical equation:

$$E = 0.57 - 0.058 \log [SCN^-] \qquad (3.c)$$

for pH from 0 to 7.

Straight lines like the above ones indicate a considerable overpotential when related to those expected between SCN^- and $CN^- + SO_4^{2-}$ (see Eh-pH diagram in **Figure 2.2a**, Chapter 2). Additionally, the coefficient of the logarithimic term suggests a one-electron transfer process.

Gaugin [47, 48] related the overpotentials invariably detected in acidic medium to the presence of the pair $(SCN)_2/SCN^-$ proposed by Bjerrum and Kirschner [51] :

$$(SCN)_{2(aq)} + 2e = 2SCN^- \qquad E° = 0.77\ V \qquad (3.16)$$

This type of inference from experimental data led Gauguin to adopt in his work the mechanistic views on the oxidation of thiocyanate in acidic solutions earlier proposed by Bjerrum and Kirschner [51], with the production of thiocyanogen and its subsequent hydrolysis as indicated by reactions 3.3 to 3.6 above [47, 48].

In the alkaline range, however, the potential readings were fitted by Gauguin into the expression:

$$E = 1.17 + \frac{0.058}{6} \log \frac{[H^+]}{[SCN^-]} \qquad (3.d)$$

for pH from 9 to 14, corresponding to the process [48] :

$$SCN^- + 4H_2O \rightarrow SO_4^{2-} + CN^- + 8H^+ + 6e \qquad (3.17)$$

One of the limitations of the above proposals is that they do not consider the changes in potential with pH in the acidic range. Gauguin [48] observed variations ranging from 3 to 60 mV, but he did not try to explain them.

The different behaviours observed in acidic and alkaline solutions are related to the fact that the hydrolysis of $(SCN)_2$ inceases with decreasing $[H^+]$, as demonstrated later by Schöneshöfer et al. [72] (see Section 3.6 on the hydrolysis of thiocyanogen). At low pH, the production of $(SCN)_2$ is faster than its hydrolysis, which explains the influence of the pair $(SCN)_2/SCN^-$ on the potential readings, while in the alkaline range the two processes are of comparable rates [72], which may explain why the potentials at those pHs correspond better to reaction 3.17.

This work by Gauguin [47, 48] established that a considerable overpotential is required for the chemical oxidation of thiocyanate in acidic medium, and that it is due to an intermediate process

involving the tranfer of **approximately** one electron per SCN^- ion, as in the production of $(SCN)_2$.

3.4. The Anodic Oxidation of Thiocyanate: Early Work

The electrolysis of thiocyanate in methanolic solution on platinum and silver electrodes was studied by Kerstein and Hoffmann [70], who identified the product as being thiocyanogen, $(SCN)_2$.

Gauguin [49] also investigated the oxidation of thiocyanate electrochemically on a platinum electrode rotating at 600 rpm in aqueous solution, at 25°C and pH 1 adjusted with nitric acid. Again, an overpotential was found to be involved in the oxidation of thiocyanate, as shown in **Figure 3.1**. To explain this anodic overpotential, a mechanism was suggested including the production of the free radical $SCN^{\cdot}$ at the electrode surface followed by the dimerization of such free radicals to form thiocyanogen [49] :

$$SCN^- \rightarrow SCN^{\cdot} + e \qquad (3.18)$$

$$2SCN^{\cdot} \rightarrow (SCN)_2 \qquad (3.19)$$

The overall stoicheiometry, however, corresponded to the 6-electron transfer process leading to SO_4^{2-}, HCN and H^+ as oxidation products, which were formed by the hydrolysis of the $(SCN)_2$ subsequent to the electrode process.

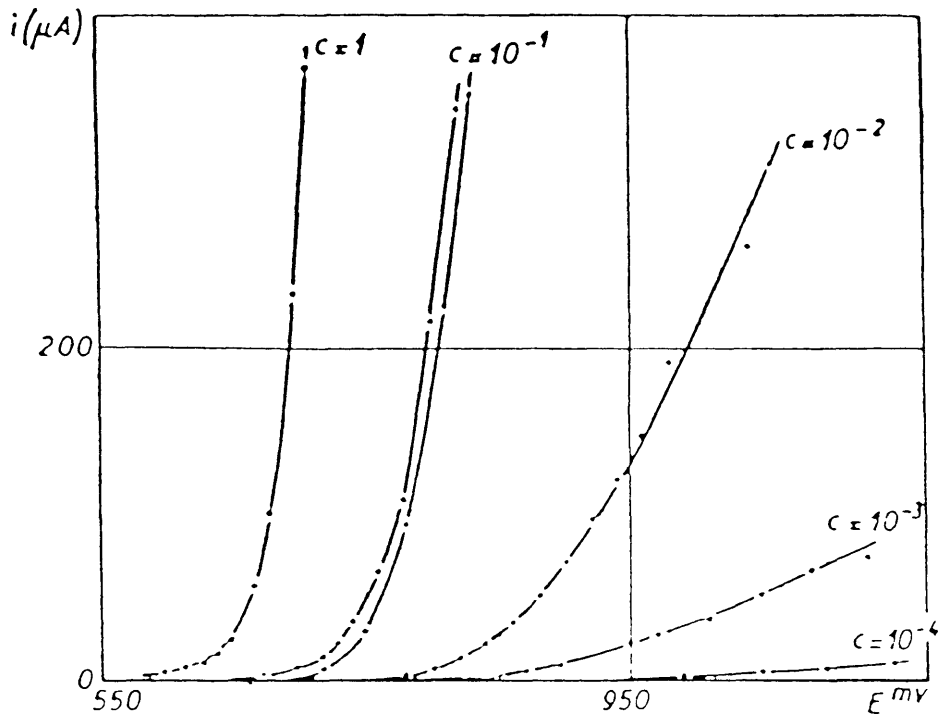


Figure 3.1 - Current-potential curves obtained with a rotating platinum electrode at different concentrations of KSCN, pH 1 adjusted with HNO_3, and temperature of 25°C (potentials vs. SHE) [49].

Nicholson [50] worked on the electrochemical oxidation of thiocyanate on a platinum electrode both in acidic and alkaline aqueous solutions. Several support electrolytes were tried and, in every case, an overpotential was required for the onset of oxidation. An electrode process such as the production of thiocyanogen was suggested as the cause of the overpotential observed, but a specific mechanism was not proposed. He also found the overall process to be the irreversible oxidation to cyanide and sulphuric acid, subsequent to the electrode process. Additionally, Nicholson investigated the influence of CN^-, Br^- and I^- on the anodic process and, particularly, on the overpotential observed. Some of the voltametric curves obtained by Nicholson are shown in **Figure 3.2**. The pH varied from 1

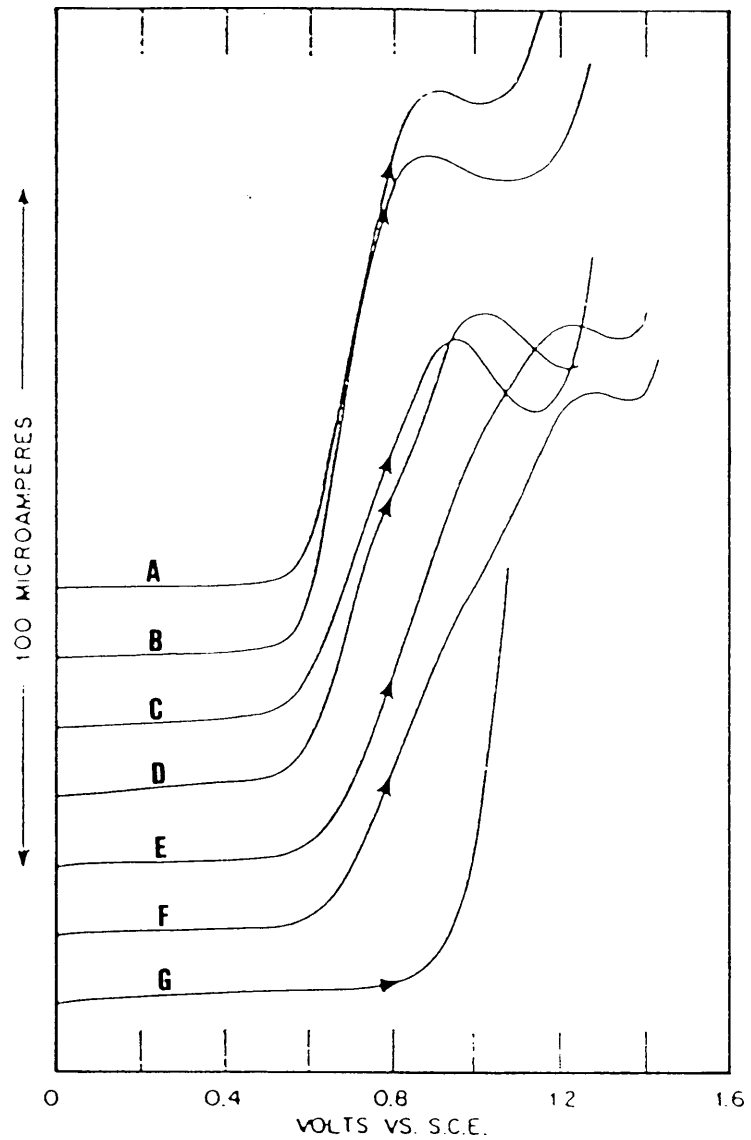


Figure 3.2 - Current-potential curves with a stationary platinum electrode in KSCN solutions containing the following supporting electrolytes (pH from 1 to 9) [50] : **(A)** 0.1 mol/dm^3 Pyridinium Chloride + 0.1 mol/dm^3 Pyridine; **(B)** 0.1 mol/dm^3 Pyridinium Nitrate + 0.1 mol/dm^3 Pyridine; **(C)** 0.1 mol/dm^3 NaAc + 0.1 mol/dm^3 HAc; **(D)** 0.1 mol/dm^3 KNO_3; **(E)** 0.1 mol/dm^3 H_2SO_4; **(F)** 0.1 mol/dm^3 HCl; **(G)** 0.04 mol/dm^3 NaOH + 0.1 mol/dm^3 H_3BO_3.

to 9, depending on the supporting electrolyte. The wave generally is not a simple form and its shape and position do not vary systematically with the pH or with the buffering capacity of the supporting electrolytes. The pH 9 was mantained by a borate buffer. Two waves are visible in several cases, being more clearly defined in the pyridine-pyridinium ion buffer. In most cases, the oxidation overpotential does not vary appreciably with the supporting electrolyte used.

The contributions by Kerstein and Hoffmann [70], Gauguin [49] and Nicholson [50] established that a considerable overpotential is also detected in the anodic oxidation of thiocyanate. The electrode process yields $(SCN)_2$ [49, 70], which then undergoes hydrolysis to SO_4^{2-}, HCN and H^+ ions.

3.5. Pure Thiocyanogen and Thiocyanogen Solutions

At almost the same time as Bjerrum and Kirschner [51] proposed the existence of free thiocyanogen as an unstable pseudohalogen in aqueous solution, an extensive study of the existence and properties of thiocyanogen was published by Söderbäck [62] , which reports the first successful isolation of yellowish crystals of $(SCN)_2$. He reacted iodine with silver thiocyanate in diethyl ether [28, 31, 62]:

$$2AgSCN + I_2 \longrightarrow (SCN)_2 + 2AgI \qquad (3.20)$$

Söderbäck showed that the compound was stable only in the absence of water and in the pure state only at temperatures much below ambient. His preparation, isolated from ether, melted between -2 and -3°C.

The above reaction, however, does not proceed to completion,

leaving some unreacted iodine. Better results are obtained by the action of chlorine or bromine on silver or lead thiocyanates suspended in either dry benzene, ether, carbon tetrachloride, glacial acetic acid or liquid SO_2 [28, 31, 63-69]:

$$2AgSCN + Br_2 \rightarrow 2AgBr + (SCN)_2 \qquad (3.21)$$

$$Pb(SCN)_2 + Br_2 \rightarrow PbBr_2 + (SCN)_2 \qquad (3.22)$$

One of the most recent studies on thiocyanogen is that published by Vanderzee and Quist [68]. They followed the procedure reported by Seel and Müller [64] , considered to be the easiest one, allowing Br_2 to act on AgSCN in liquid SO_2 (reaction 3.21). After filtering off the silver bromide, the SO_2 was evaporated under vacuum at -50°C. Those conditions of vacuum and temperature were mantained for 2 more hours, leaving white crystals of $(SCN)_2$. The crystals became yellow and melted at about -7°C to give an orange suspension. Cooling this to -70°C yielded white crystals and the colour disappeared. In the liquid form, $(SCN)_2$ was never observed to be stable for any length of time. In every case it gradually darkened and ultimately produced an orange-red powder.

Thiocyanogen is not usually isolated but is used in non-aqueous solutions up to 1 mol/dm^3, where it exists as the monomer. If these solutions are heated or if the concentration is too high, then polymerization takes place giving an orange-red precipitate. Addition of a small amount of KSCN to a $(SCN)_2$ solution in acetic acid produces a brilliant and clear yellow-orange solution which becomes cloudy within minutes and yields a burnt-orange precipitate in a few hours This yellow-orange colour is attributed to a species such as $(SCN)_3^-$ resulting from the addition of SCN^- to $(SCN)_2$ in a process similar to the formation of thiocyanogen halides [28, 31, 65, 66, 68, 71].

Thiocyanogen has a characteristic u.v. peak at 283 nm in

acetonitrile [84] . This peak is shifted to 288 nm in acetic acid [68] and to 296 nm in carbon tetrachloride [66, 68]. Vanderzee and Quist [68] also observed the appearence of a sharp spike at 250 nm in thiocyanogen solutions in acetic acid, simultaneously with the bright orange colour reported above, which led them to attribute this peak to $(SCN)_3^-$. However, this wavelength of 250 nm is typical of aliphatic disulphide bonds and the gradual appearance of this peak could as well indicate a reorganization of thiocyanogen itself between the structures N≡C-S-S-C≡N and S=S$(CN)_2$. The structure of thiocyanogen is still controversial. The disulphide structure is usually regarded as the correct one [28, 31] although some authors prefer the first structure, with the -S-S- link [67, 68]. As will be discussed later (see Section 3.7), the u.v. peak usually considered to characterize $(SCN)_3^-$ is around 320 nm [84, 90, 91]. This fact, however, does not rule out the possibility of $(SCN)_3^-$ having another absorption peak at 250 nm.

The use of non-aqueous solvents is required to prevent the fairly rapid hydrolysis of thiocyanogen. Thus, solutions of acetic anhydride showed about 2% decomposition (by I_2 titration) in 20 hours at 20°C; in acetic acid the decomposition under the same conditions was 10% [65, 66].

Non-aqueous solvents have also been used to prevent hydrolytic reactions in order to permit mechanistic studies of the anodic oxidation of thiocyanate, the preferred solvents being acetonitrile [81, 87, 204] and dimethylsulphoxide [82, 88, 204]. But even in a solvent like acetonitrile, anodically generated intermediate species are to some extent unstable at room temperature. Therefore, temperatures as low as 0°C or lower have been used in electrochemical studies of thiocyanate oxidation [81, 84, 86, 87]. Acetonitrile has also allowed the spectrophotometric determination of intermediate species such as $(SCN)_2$, $(SCN)_2^-$ and $(SCN)_3^-$ [84].

3.6. Thiocyanogen Hydrolysis

The mechanism of hydrolysis of thiocyanogen described by reactions 3.3 to 3.6, which was first proposed by Bjerrum and Kirschner [51], was also adopted by Stedman and Whincup [42]. They proposed the following rate law for the hydrolysis process [42] :

$$\text{Rate} = k \frac{[(SCN)_2]^2}{[H^+]^2 \ [SCN^-]^2} \qquad (3.e)$$

Stedman and Whincup [42] found k = 0.001 $mol^3\ dm^{-3}\ s^{-1}$ from measurements of the initial rates at 0°C and 1 mol/dm^3 ionic strength. They started with solutions of thiocyanogen in glacial acetic acid, prepared by the method of Gardner and Weinberger [69]. These were added to solutions of perchloric or sulphuric acid and sodium thiocyanate. Samples were taken and quenched in an excess of potassium iodide, the iodine liberated being titrated with thiosulphate. As the reaction progresses, however, complications arise from the fact that the HCN produced by hydrolysis reacts with the $(SCN)_2$ present yielding sulphur dicyanide, $S(CN)_2$, which also liberates iodine. Therefore, only initial rate measurements were used [42].

The interpretation of the rate law (equation 3.e) requires a knowledge of the speciation of aqueous solutions of thiocyanogen in the presence of an excess of thiocyanate ion, which is not a simple task. The suggestion was made of the existence of an equilibrium involving other species [42] :

$$(SCN)_3^- \underset{SCN^-}{\rightleftharpoons} (SCN)_2 \overset{H_2O}{\rightleftharpoons} HOSCN + H^+ + SCN^- \qquad (3.23)$$

The identification of intermediate species in the oxidation of thiocyanate has progressed in the last three decades. New

contributions came through the incorporation of more sophisticated techniques such as pulse radiolysis in aqueous solution [72-74, 76-80] and also through the use of non-aqueous solvents in order to stabilize the intermediates and enable their spectrometric detection in the course of chemical or electrochemical work.

Using the technique of pulse radiolysis combined with spectrophotometric and conductometric measurements, Schöneshöfer et al. [72] proposed that in acidic solution the formation of $(SCN)_2$ is much faster than its hydrolysis, whereas in alkaline solution, the two processes are of comparable rates.

In either case, the following equilibrium would be established:

$$(SCN)_2 + H_2O = H^+ + SCN^- + HOSCN \qquad K = 6x10^{-13} \text{ mol} \qquad (3.24)$$

The subsequent hydrolysis of HOSCN in acidic medium would proceed according to [72] :

$$HOSCN + H_2O \rightarrow HSO_2^- + HCN + H^+ \qquad (3.25)$$

In alkaline medium, the equilibrium (reaction 3.24) would be shifted to the right, which could be due to the dissociation of HOSCN [72] . Then:

$$(SCN)_2 + H_2O \rightarrow 2H^+ + SCN^- + OSCN^- \qquad (3.26)$$

In strongly alkaline solution, HCN would appear in its ionised form [72] :

$$OSCN^- + H_2O \rightarrow HSO_2^- + H^+ + CN^- \qquad (3.27)$$

3.7. The Transitory Forms Trithiocyanate, $(SCN)_3^-$, and Dithiocyanate, $(SCN)_2^-$

The possible existence of the trithiocyanate ion, $(SCN)_3^-$, was first suggested by Kerstein and Hoffmann [70] to explain some unexpected results in the electrolytic oxidation of a methanolic solution of potassium thiocyanate.

Cauquis and Pierre [84] used spectrophotometry to observe the behaviour of a thiocyanate solution in acetonitrile during electrolysis at 0.600 V and -15°C and found u.v. peaks at 320 nm and 283 nm, which were assigned to the species trithiocyanate, $(SCN)_3^-$, and thiocyanogen, $(SCN)_2$, respectively, and estimated the following equilibrium constant at 20°C in acetonitrile:

$$K = \frac{[(SCN)_2]\,[SCN^-]}{[(SCN)_3^-]} = (2\pm1) \times 10^{-2} \qquad (3.f)$$

Although qualitatively sound, this work by Cauquis and Pierre had to face accuracy limitations which were reported by the authors themselves. The main problems are the small magnitude of the coefficient of absorption of $(SCN)_3^-$ at 320 nm, the background absorption of the dimer at that same wavelength, and the instability of the latter [84].

The oxidation of SCN^- by $OH^\bullet$ radicals produced by the radiolysis of water (by gamma rays) was first investigated by Adams et al. [78]. They observed the formation of a transient species which absorbed strongly in the visible at λ_{max} = 480 nm. This absorption was first assigned to the $SCN^\bullet$ radical but it was pointed out that it was also consistent with the transient species being the dithiocyanate ion, $(SCN)_2^-$.

Baxendale et al. [73] carried out pulse radiolysis of aqueous KSCN solutions of pH 2 and 7, made with perchloric acid and a phosphate buffer, respectively. The oxidizing action of $OH^{\cdot}$ radicals upon SCN^- ions yielded a highly absorbing species at 475 nm. This species was proposed to be the $(SCN)_2^-$ ion, according to the following steps:

$$H_2O \xrightarrow{\gamma} H^+, OH^{\cdot}, e^-_{aq} \qquad (3.28)$$

$$SCN^- + OH^{\cdot} \longrightarrow SCN^{\cdot} + OH^- \qquad (3.29)$$

$$SCN^{\cdot} + SCN^- = (SCN)_2^- \qquad K=2.0\times10^5\ mol^{-1} \qquad (3.30)$$

The lifetimes of these free radicals and of the anion-radical $(SCN)_2^-$ are very short. The rate constants for the above reactions at 22°C are: 2.8×10^{10} $mol^{-1}s^{-1}$(reaction 3.29), 7.0×10^9 $mol^{-1}s^{-1}$ (reaction 3.30, from left to right) and 3.4×10^4 s^{-1} (reaction 3.30, from right to left). The three reactions were found to be first order with respect to SCN^- [73]. A similar value for the disproportionation rate constant for $(SCN)_2^-$ was determined by Nord et al. [74]. The equilibrium constant 2.0×10^5 mol^{-1} for reaction 3.30 was determined at 22°C and is the same at pH 2 and 7 [73].

The transitory form $(SCN)_2^-$ decays according to the reaction [73] :

$$2(SCN)_2^- = (SCN)_2 + 2SCN^- \qquad (3.31)$$

This reaction was found to be second order with respect to $(SCN)_2^-$, and is an alternative pathway for the formation of thiocyanogen, additional to the suggestion of dimerization of the uncharged radicals $SCN^{\cdot}$.

The behaviour of iodine was found by Baxendale et al. [73] to be analogous to that of thiocyanate, with I_2^- being found as a transitory form. It was this sort of analogy with the halides that led Betts and Dainton [41] to propose the participation of $(SCN)_2^-$ in the mechanism of oxidation of thiocyanate by Fe^{3+} years before the actual spectrophotometric detection of this species by pulse radiolysis.

A further pulse radiolysis study by Behar et al. [76] agreed with the above results and established a more detailed mechanism including precursors of $(SCN)_2^-$. Such precursors would be the anion-radicals $HOSCN^-$ and $OSCN^{2-}$, produced by the action of the OH free radicals on the SCN^- ion.

Duonghong et al. [75] confirmed the existence of $(SCN)_2^-$ by means of a different technique (laser photolysis) coupled with the spectrophotometric detection of $(SCN)_2^-$ at 470 nm.

3.8. The Anodic Oxidation of Thiocyanate: Recent Work

More recent work on the anodic oxidation of thiocyanate has been performed almost exclusively in non-aqueous solvents and on platinum or gold electrodes. Several researchers [81, 82, 87, 88, 90, 91] have tried to determine the mechanism of the electrode process and the probable species being generated in that process. There are differences between the results and the related mechanistic proposals resulting from experiments done on platinum [81, 82, 86] or on gold [87, 88, 90, 91] electrodes. Such differences are expected because of the reactivity of gold with thiocyanate, which causes an enhanced surface adsorption of thiocyanate species and the dissolution of the electrode, thus affecting the experimental results. Therefore, the studies carried out with platinum and gold

electrodes will be treated separately in this section.

3.8.1. Oxidation on Platinum Electrodes

Cauquis and Pierre [86] worked with acetonitrile as the solvent with 10^{-1} mol/dm^3 $LiClO_4$ as the supporting electrolyte. The solutions were $2x10^{-3}$ mol/dm^3 in LiSCN or NH_4SCN. The curves shown in **Figure 3.3** were obtained on a platinum rotating disc electrode. Curve A corresponds to the oxidation of SCN^-, whose half-wave potential was found to be $E_{1/2} = 0.320 \pm 0.020$ V (vs. Ag/Ag^+ 10^{-2} mol/dm^3); the current plateau indicates a condition of diffusion control. By comparing this curve with that obtained [111] for the iodide ion, I^-, they estimated that it would correspond to an one-electron transfer process. The cathodic curve A' was assigned to the reduction of the NH_4^+ ion from the NH_4SCN.

The oxidation of thiocyanate in acetonitrile on a stationary platinum electrode of large surface area at a constant potential of 0.600 V was found by Cauquis and Pierre [86] to depend on the operational conditions. At room temperature and normal daylight, a precipitate was formed which was identified as the polymer parathiocyanogen, $(SCN)_x$, which is known as a product of the decomposition of thiocyanogen. But when the electrolysis was carried out at -10°C and in the absence of light, the solution remained bright and the species $(SCN)_2$ was characterized through its infrared and ultraviolet spectra. In both of the above conditions, the electrolysis of more concentrated thiocyanate solutions was accompanied by a rapid current drop caused by a yellow insulating layer of $(SCN)_x$ forming on the surface of the electrode.

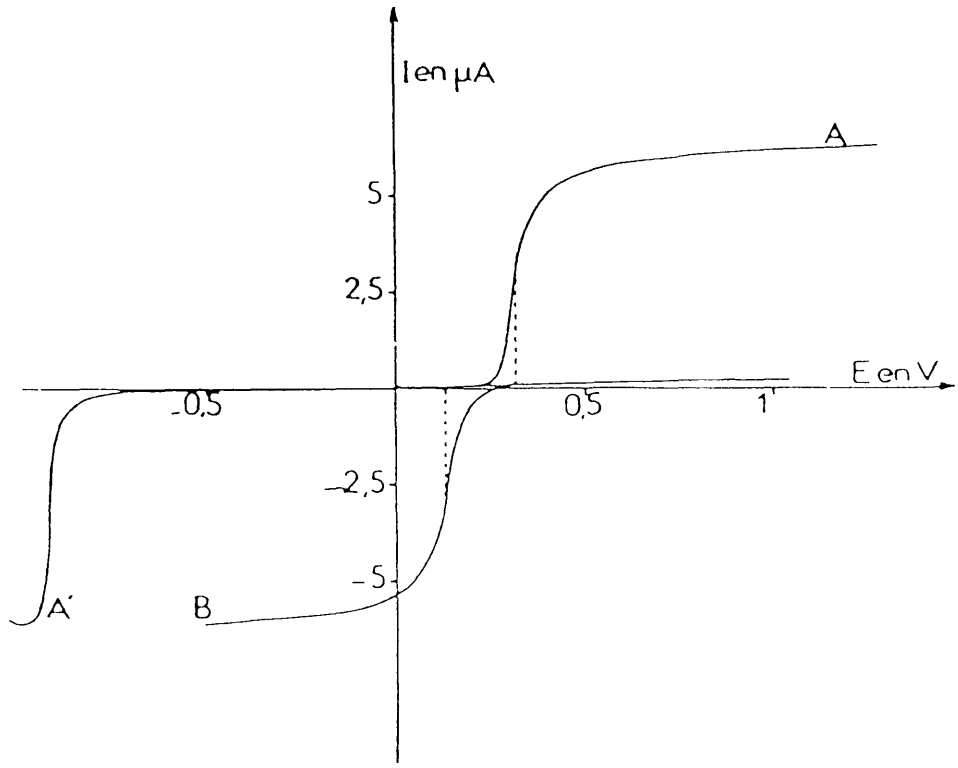


Figure 3.3 - Current-potential curve obtained on a platinum rotating disc electrode in acetonitrile containing $2x10^{-3}$ mol/dm^3 NH_4SCN and 0.1 mol/dm^3 $LiClO_4$ [86]. Potentials measured against an Ag/Ag^+ 10^{-2} mol/dm^3 reference electrode (add 0.68 V to obtain reading vs. SHE).

Curve A: Oxidation of the SCN^- ion
Curve A': Reduction of the NH_4^+ ion
Curve B: Reduction of $(SCN)_2$, about 10^{-3} mol/dm^3.

Coulometric measurements of thiocyanate oxidation also indicated an electrode process with the transfer of one electron per SCN^- ion.

Curve B in **Figure 3.3** corresponds to the reduction of electrolytically generated thiocyanogen. The same curve was obtained from a thiocyanogen solution prepared chemically. The curve has $E_{1/2}$ = 0.140 ± 0.020 V (vs. Ag^+/Ag 10^{-2} mol/dm^3), which was assigned to thiocyanogen. The cathodic reduction of thiocyanogen to thiocyanate was found to be quantitative if carried out immediately after the anodization and the coulometry of this reduction corresponded to one electron per SCN^- originally present. However, when such a solution containing *c.a.* 10^{-3} mol/dm^3 $(SCN)_2$ was left standing for 48 hours after addition of *c.a.* 0.05 mol/dm^3 H_2O, the curve B could no longer be obtained. Instead, the ions SO_4^{2-} and CN^- were found in that solution, obviously resulting from the hydrolysis of the $(SCN)_2$ initially produced [86].

The mechanism suggested by Cauquis and Pierre [86] is the same previously suggested by Gauguin [49], with the production of free radicals $SCN^{\bullet}$, followed by the dimerization of these radicals to $(SCN)_2$.

The kinetics of the couple $SCN^-/(SCN)_2$ on platinum in acetonitrile was also investigated by Pereiro et al. [81]. They worked at temperatures from -12 to -3°C, at different concentrations of NH_4SCN and 0.1 mol/dm^3 $[(C_2H_5)_4N]ClO_4$ (tetra-ethylammonium perchlorate, TEAP) as supporting electrolyte. The final product of the oxidation of SCN^- at platinum anodes was found to be thiocyanogen, which can be cathodically reduced. The overall reversible electrode process is [81]:

$$2\ SCN^- = (SCN)_2 + 2e \qquad (3.32)$$

Two possible mechanisms were suggested [81] :

I. $$SCN^- + Pt \xrightarrow{rds} (SCN)Pt + e \qquad (3.33)$$

$$2(SCN)Pt = (SCN)_2 + 2Pt \qquad (3.34)$$

II. $SCN^- + Pt = (SCN)Pt + e$ (3.35)

$(SCN)Pt + SCN^- \xrightarrow{rds} (SCN)_2 + (e)Pt$ (3.36)

Pt represents an active site at the electrode surface; (SCN) means an adsorbed radical formed during an initial electron-transfer step; rds stands for "rate determining step". The difference between the mechanism **II** and those previously proposed by Gauguin [49] and Cauquis and Pierre [86] is that thiocyanogen is not formed by the dimerization of free radicals but by the reaction between one adsorbed free radical and one SCN^- ion, leaving an adsorbed electron.

Some of the cyclic voltammograms are shown in **Figures 3.4a** and **3.4b**. The anodic waves correspond to the oxidation of thiocyanate with production of $(SCN)_2$, which is reduced in the reverse scan as shown by the cathodic waves. Pereiro et al.[81] concluded that both the anodic and cathodic reactions are slow electrochemical processes. At low potentials they are under activation control and at high potentials, due to depletion of the reacting species at the electrode surface, they become diffusion-controlled [81]. The **diffusion coefficient** of the SCN^- ion in acetonitrile was estimated in $D_{SCN^-} = 2.14 \times 10^{-5}$ cm^2/s [81].

Holtzen and Allen [83] working in aqueous thiocyanate solutions with a vitreous carbon electrode determined the **diffusion coefficient** of SCN^- ion to be 1.37×10^{-5} cm^2 s^{-1} in 0.1 mol/dm^3 KCl and 1.33×10^{-5} cm^2 s^{-1} in 0.1 mol/dm^3 KNO_3.

The anodic oxidation of thiocyanate dissolved as KSCN in dimethylsulphoxide (DMSO) was studied by Martinez et al. [82], at temperatures ranging from 25 to 160°C. The anodic process observed at *c.a.* 25°C was similar to that observed at low temperature in acetonitrile [40]. The main anodic product was found to be $(SCN)_2$ and the possible mechanisms proposed by Martinez et al. [82] are the same as those previously proposed by Pereiro et al. (reactions 3.33

to 3.36) [81]. Film formation was found to be favoured at 60°C though not leading to a total blockage of the electrode surface, which mantained an overall kinetic behaviour consistent with the reactions at 25°C. At *c.a.* 162°C, however, the SCN^- oxidation produced a $(SCN)_x$ film which caused the total passivation of the electrode. The oxidation overpotential was found to be lower at 162°C [82].

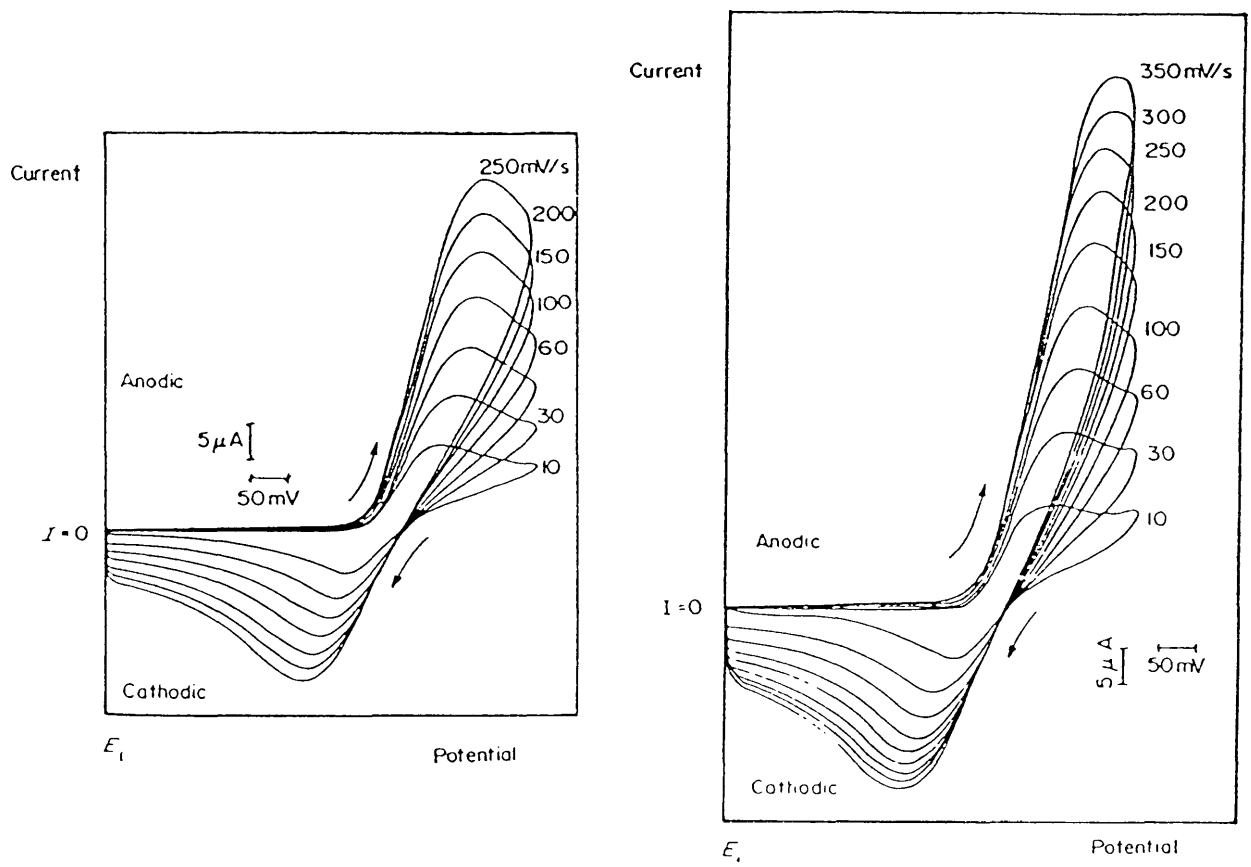


Figure 3.4 - Linear cyclic voltammograms on a stationary platinum electrode (0.071 cm^2) at different sweep rates in acetonitrile containing 2.028×10^{-3} mol/dm^3 NH_4SCN and 0.1 mol/dm^3 TEAP; **(a)** -10°C and **(b)** -3.0°C [81].

3.8.2. Oxidation on Gold Electrodes

The electrochemical kinetics of gold electrodes in SCN^-/DMSO solutions at temperatures between 25 and 65°C was studied by Martins et al. [88], who used both stationary and rotating disc electrodes. They proposed that the main electrode process at potentials between -0.2 and 0.8 V (vs. SCE) corresponds to:

$$(SCN)_3^- + 2e = 3SCN^- \qquad (3.37)$$

A mechanism for this electrode process was not proposed.

Typical voltammograms are shown in **Figure 3.5**. The authors found the process to be reversible, at least within the duration of the experiments, as shown by the reverse sweeps of the cyclic voltammograms, the cathodic peaks corresponding to the reduction of $(SCN)_3^-$ back to SCN^-. There is no mention to film formation at the electrode surface in this paper by Martins et al. [88].

Blank experiments (with only the solvent and supporting electrolyte) run at 25°C between -0.6 V and 1.2 V (vs. SCE) at different sweep rates exhibited a relatively small current contribution, either cathodic or anodic, within the -0.3 V to 0.9 V range. Traces of water were present in the solvent [88].

According to the authors [88], the electrooxidation of SCN^- ion took place at potentials between 0.1 V and 0.75 V (vs. SCE) without gold dissolution, while the electrodissolution of gold only occurred beyond 0.75 V (vs. SCE). This was supposed to be due to some inhibiting effect of the solvent, DMSO. Accordingly, the small cathodic peak at *c.a.* 0.85 V (vs. SCE), shown in **Figure 3.6**, was assigned by Martins et al. [88] to the reduction of dissolved gold species, but they did not comment on which species these could be. Separate current contributions from the two main anodic processes

considered, i.e. the oxidation of SCN^- and the dissolution of gold, were not determined experimentally [88].

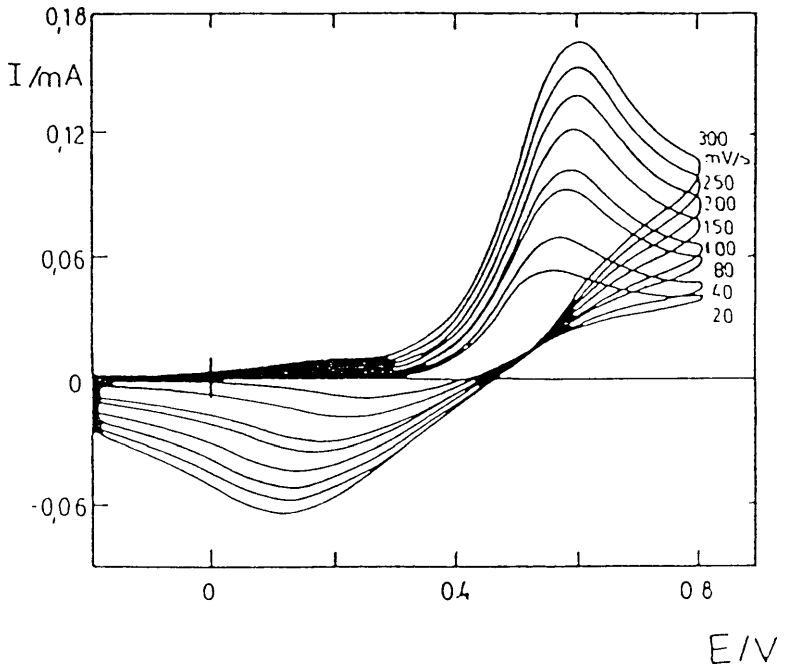


Figure 3.5 - Cyclic voltammograms on a stationary gold electrode (0.301 cm^2) with different triangular sweep rates in DMSO containing $2.8x10^{-3}$ mol/dm^3 KSCN and 0.5 mol/dm^3 $KClO_4$ at 45.1°C [88].

It is important here to note that the anodic sweeps in **Figure 3.6** were extended to potentials as high as 1.2 V (vs. SCE) or so. At such high potentials at least two other processes were taking place. First, the reactions with the solvent, whose current contribution, as reported by the authors, was relatively small up to 0.9 V. Second, the formation of some $Au(OH)_3$ by interaction with the residual water in the solvent. The small cathodic peak at 0.85 V could as well be due to the reduction of some oxidized species produced in one or both of these processes. Probably, there would be some solubilized

gold. However, it seems unlikely that thiocyanate complexes of gold would be reduced at that potential (cathodic peak at 0.85 V) because, according to the evidence presented in the thermodynamic study (Chapter 2), the potentials for the reduction of those complexes (in water) would be lower. Gold-thiocyanate complexes possibly present would, most probably, be reduced in a potential range below that for the reduction of $(SCN)_3^-$ and/or $(SCN)_2$.

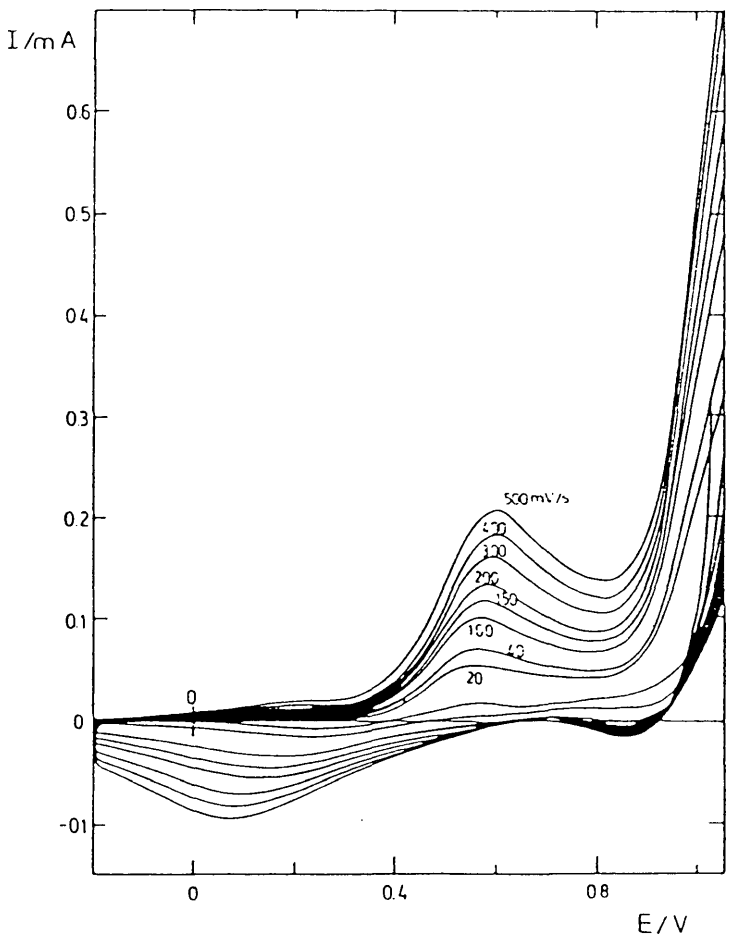
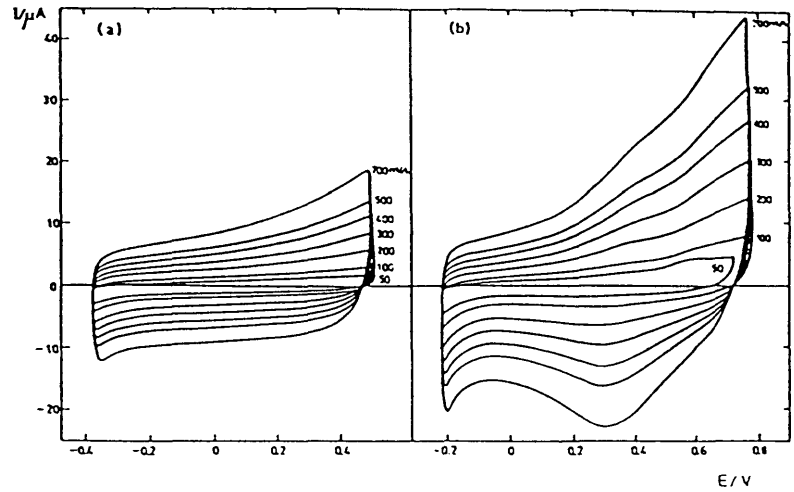


Figure 3.6 - Cyclic voltammograms on a stationary gold electrode (0.301 cm^2) with different triangular sweep rates in DMSO containing 2.8×10^{-3} mol/dm^3 KSCN and 0.5 mol/dm^3 $KClO_4$ at 45.1°C [88].

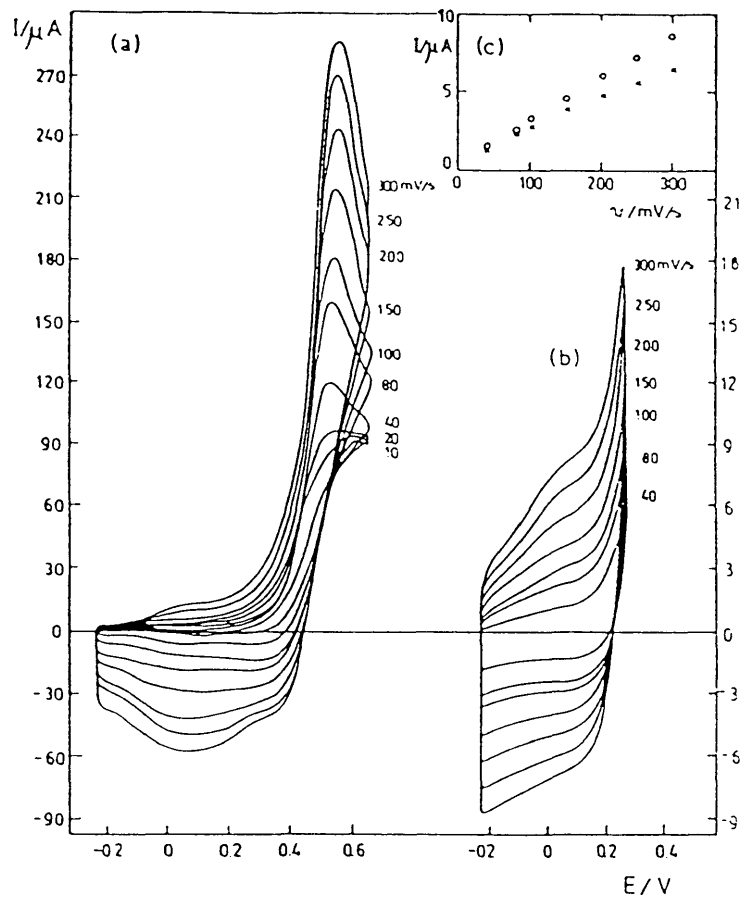
The thiocyanate oxidation process takes place in a potential range which overlaps the potential range for the gold dissolution by thiocyanate. On the other hand, oxidized species like $(SCN)_2$ and $(SCN)_3^-$, by analogy with the halogens I_2, Br_2 and Cl_2 and the respective trihalides, may be considered as oxidants for gold. Therefore, gold-thiocyanate complexes, if present in any appreciable amount, are not expected to undergo reduction at a potential as high as 0.85 V (vs. SCE), which lies much above those in which the production of $(SCN)_3^-$ takes place.

Martins et al. [87] also studied the electrochemistry of gold in acetonitrile solutions containing thiocyanate ions at 25°C The solutions were made up to contain from $1x10^{-3}$ mol/dm^3 to $5x10^{-3}$ mol/dm^3 NaSCN and 0.1 mol/dm^3 $NaClO_4$ as supporting electrolyte. Blank experiments are shown in **Figure 3.7a**. There is a relatively small current contribution between -0.39 and 0.50 V (vs. SCE). An increase in the current contribution was observed beyond 0.50 V, which was attributed by the authors [87] to the formation of a reaction product which probably changed the electrode surface. The surface coverage, either by electrosorption or by the formation of a surface compound was, however, slow [87].

Typical voltammograms in the presence of thiocyanate are shown in **Figure 3.7b**. The anodic current becomes appreciable beyond 0.4 V (vs. SCE), which corresponds to a considerable overpotential for the oxidation of thiocyanate. An anodic peak at 0.56 V becomes well defined at sweep rates above 40 mV/s. The cathodic peak, around 0.10 V (vs. SCE), indicates the reduction of the oxidized species produced during the anodic scan.



(a)



(b)

Figure 3.7 - Single triangular sweep voltammograms on gold covering different sweep rates and anodic potential limits in acetonitrile at 25°C: **(a)** Blank experiments in 0.1 mol/dm^3 $NaClO_4$; **(b)** Experiments in 1.98x10^{-3} mol/dm^3 NaSCN and 0.1 mol/dm^3 $NaClO_4$ (up on the right hand corner: dependence of the (o) anodic and (x) cathodic current peaks on the potential sweep rate) [87].

Coulometric measurements were also made by anodizing a gold electrode in the potential range between 0.4 and 0.6 V using a solution of $2x10^{-3}$ mol/dm^3 NaSCN in acetonitrile at 25°C. The authors considered that the anodic process corresponded to the production of Au(I), which would partially disproportionate, yielding a fine gold suspension and the auric complex according to the equilibrium [87]:

$$3Au(SCN)_2^- = 2SCN^- + 2Au + Au(SCN)_4^- \qquad (3.38)$$

The electrolysed solution had a yellow-orange colour and presented the u.v. and visible spectra shown in **Figure 3.8** [87].

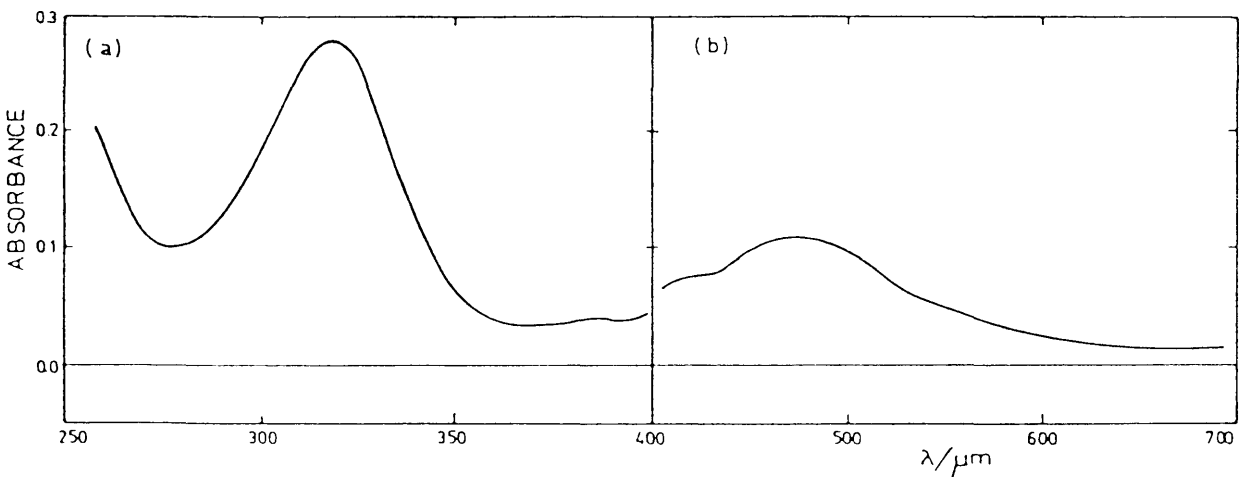


Figure 3.8 - Visible and u.v. spectra of acetonitrile solutions $2x10^{-3}$ mol/dm^3 in NaSCN after electrolysis at 0.4 to 0.6 V (vs. SCE) on a gold electrode at 25°C [87].

The authors concluded that the coulometry and u.v. spectrophotometry revealed that the anodic reaction taking place between 0.10 and 0.60 V (vs. SCE) was the electrodissolution of gold and put forward the following mechanism [87]:

$$Au + (SCN^-) = Au(SCN^-)_{ads} \quad (3.39)$$

$$Au(SCN^-)_{ads} = Au(SCN)_{ads} + e \quad (3.40)$$

$$Au(SCN)_{ads} + SCN^- = Au(SCN)_2^- \quad (3.41)$$

$$3Au(SCN)_2^- = 2SCN^- + 2Au + Au(SCN)_4^- \quad (3.42)$$

This mechanism was probably inspired by another one previously suggested by the same group for the dissolution in chloride medium [89].

The above mechanism seems feasible only as far as the production of adsorbed AuSCN is concerned (reactions 3.39 and 3.40). Reaction 3.41 also seems to be feasible as one of the possible ways of formation of the aurous complex. The disproportionation reaction 3.42, however, seems very unlikely, as already pointed out by Nicol [6] when discussing the similar mechanism for the chloride system proposed by the same group [89]. The early work by Bjerrum and Kirschner [51] already demonstrated that such disproportionation is comparatively slow even in gold solutions as concentrated as 0.1 mol/dm^3. Reaction 3.42 is none other than reaction 3.14, proposed by Bjerrum and Kirschner [51] and already discussed in Section 3.2. Furthermore, this reaction is not really part of the electrode process, which is then unable to account for the possible production of the Au(III) complex.

A drawback of this work by Martins et al. is the absence of any consideration of the anodic oxidation of thiocyanate and of the role played by oxidation products such as $(SCN)_2$, $(SCN)_3^-$ and $(SCN)_2^-$ in

the mechanism of the electrode process of gold dissolution. The u.v. peaks at 320 nm and 480 nm (see **Figure 3.8**) which were assigned by the authors to gold species in solution have been previously reported as corresponding to $(SCN)_3^-$ [84, 90, 91] and $(SCN)_2^-$ [73-75, 76] respectively, both in the presence and in the absence of a gold electrode. These species were not mentioned in the paper. The yellow-orange colour of the electrolysed solution, which was ascribed to solubilized gold species, is also characteristic of some solutions containing $(SCN)_3^-$ or a similar oxidized species (see Section 3.5) [28, 68]. No reference to the spectrophotometric behaviour of the aurous thiocyanate complexes was found in the literature. The auric thiocyanate complexes were measured by Bjerrum and Kirschner [51] at 578 nm. The possibility of the low-intensity peak at 480 nm being also due to a gold-thiocyanate complex can not be excluded, however, on the basis of the information available. Attempts were not made to determine the amount of gold actually present in solution by a different technique (e.g. atomic absorption spectrophotometry).

A more likely interpretation of the experimental results obtained by Martins et al. [87] seems to be the simultaneous thiocyanate oxidation and gold dissolution at least in part of the potential range 0.1 to 0.6 V (vs. SCE), the Au(III) complex being produced at the higher potentials within this range. Furthermore, most of the effective charge transfer in the anodic and cathodic processes seems to correspond to the oxidation of SCN^- and subsequent reduction of the oxidation products. This can be inferred from comparisons with the similar experiments on platinum electrodes already discussed, from the spectrophotometric follow-up of the electrolytic solution (see **Figure 3.8**). A further argument is the slow rate of gold dissolution by thiocyanate observed when using iron(III) as oxidant. In those chemical experiments, which will be extensively discussed in Chapter 6, the charge transfer rate involved in thiocyanate oxidation (corresponding to the Fe^{3+} reduction) was of the order of one hundred times greater than that corresponding to the gold dissolution.

An important contribution to the identification of the SCN^- electrooxidation products was made by Itabashi [90], by means of a spectroelectrochemical technique which is a combination of voltametry and spectrophotometry. For this purpose he used an OTTLE (Optically Transparent Thin Layer Electrode) cell, with a thickness of only 0.17 mm. The working electrode was a gold minigrid through which passed the light beam of a spectrophotometer, providing a spectrophotometric monitoring of the potential sweeps. This arrangement, which is described in the literature [152], allowed the instantaneous identification of the species being produced by the electrode process. This work is particularly relevant to the present study because it was performed in acidic aqueous solution, the hydrolytic reactions being naturally present. All the solutions reported contained 0.1 mol/dm^3 NaSCN and 0.1 mol/dm^3 $HClO_4$ as supporting electrolyte.

Typical absorption spectra before and after the oxidation of SCN^- under potential step control in the OTTLE cell are shown in **Figure 3.9**. The acidic solution containing the oxidation products exhibits a symetrical peak at 320 nm and a broad peak at 420 ± 5 nm. These peaks disappear completely upon electroreduction of the oxidized species to yield a spectrum which agrees with that of the SCN^- solution before the anodization [90].

Cyclic voltammograms and the corresponding absorbance-potential curves of SCN^- are shown in **Figure 3.10**. The anodic current increases up to the anodic switching potential, which is between 0.500 and 0.540 V (vs. SCE), whereas the cathodic wave gives a peak near 0.27 V. The sweep rate was 2 mV/s. Coulometric measurements at these conditions indicated reduction efficiencies of the oxidized species of SCN^- of 96, 93 and 92% for the anodic switching potentials of 0.500, 0.520 and 0.540 V, respectively. This suggests that, even in the acidic aqueous environment, the oxidation products are stable at least during the time of the experiment, which is more than 4 minutes [90].

The absorbance monitored at 320 nm (see **Figure 3.10**) increases as the anodic potential becomes more positive, reaches a maximum during the reverse sweep at a potential near that for a zero-current condition (in the voltammogram), and falls back to zero at the potential at which the cathodic current drops to almost zero [90].

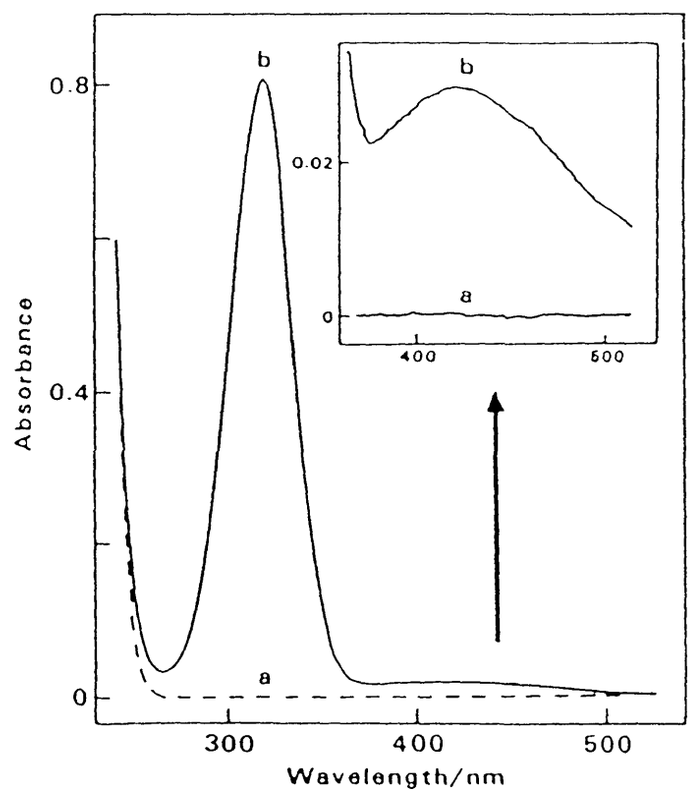


Figure 3.9 - Absorption spectra **(a)** before and **(b)** after the oxidation of SCN^- at 0.500 V (vs. SCE) in aqueous solution 0.1 mol/dm^3 in NaSCN and 0.1 mol/dm^3 in $HClO_4$. Cell thickness, 0.017 cm; anodic charge, *c.a.* 20 mC [90].

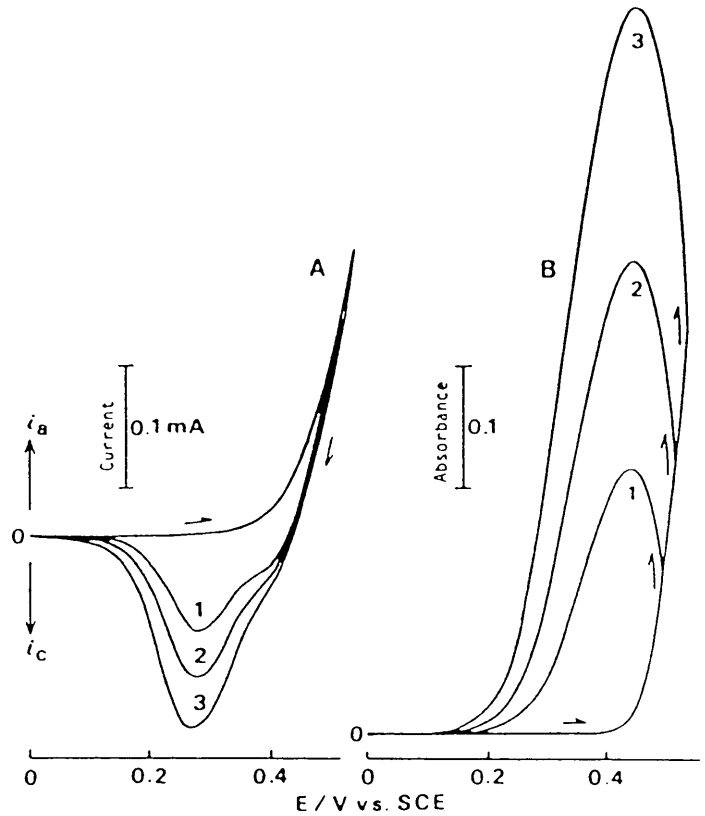


Figure 3.10 - Thin-layer cyclic voltammograms and absorbance potential curves monitored at 320 nm in 0.1 mol/dm^3 NaSCN and 0.1 mol/dm^3 $HClO_4$ at the sweep rate of 2 mV/s. Cell thickness, 0.017 cm. Anodic switching potential: **(1)** 0.500 V; **(2)** 0.520 V; **(3)** 0.540 V (vs. SCE) [90].

By reference to the work by Cauquis and Pierre [84] already discussed (Section 3.7), Itabashi [90] assigned the 320 nm peak to $(SCN)_3^-$. He suggested that the peak at 420 nm would also be due to $(SCN)_3^-$ because the optical density monitored at this wave length begins to rise immediately upon initiation of the controlled

potential oxidation of SCN^- and also because the voltammograms give a single cathodic peak. However, the assignement of the 420 nm peak to $(SCN)_3^-$ has no support in the earlier literature.

The mechanism proposed for the electrode process is [90]:

$$SCN^- \rightarrow SCN^{\cdot} + e \qquad (3.43)$$

$$SCN^{\cdot} + SCN^- \rightarrow (SCN)_2^- \qquad (3.44)$$

$$2(SCN)_2^- \rightarrow (SCN)_3^- + SCN^- \qquad (3.45)$$

Reaction 3.45 is an alternative path to that proposed by Baxendale et al. [73] for the decay of the transitory form $(SCN)_2^-$:

$$2(SCN)_2^- \rightarrow (SCN)_2 + 2SCN^- \qquad (3.46)$$

From the slope of the linear portion of the plot of absorbance versus anodic charge for SCN^- oxidation at 0.500 V, Itabashi calculated the molar adsorptivities of $(SCN)_3^-$ at 420 and 320 nm as being 6.4×10^2 and 2.2×10^4 $mol^{-1}dm^3cm^{-1}$, respectively [90].

The yield of $(SCN)_3^-$ in acidic thiocyanate solution under potential step control decreases drastically with decrease of hydrogen ion concentration below 0.04 mol/dm^3, which suggests its stabilization by associating with H^+ to form an acid molecule like $H(SCN)_3$ [90]. A similar behaviour had been found before for $(SCN)_2^-$ [75].

The products of the decomposition of $(SCN)_3^-$ were not reported by Itabashi, although it seems likely to undergo hydrolysis, rendering the overall SCN^- oxidation process irreversible, as extensively discussed previously in the case of $(SCN)_2$.

Itabashi [90] reported that no anodic dissolution of gold from the minigrid electrode took place during each anodic scan (see **Figure 3.9**) but did not mention the procedure used to make this determination. On the other hand, there is no previous reference in the literature to the peak at 420 nm as being due to $(SCN)_3^-$. At this point one could wonder if that low-absorbance broad peak at 420 nm was not due to a small amount of dissolved gold present as a thiocyanate complex.

3.8.3. Characterization of Oxidation Intermediate Species in Aqueous Iron-Thiocyanate Solutions

The spectroelectrochemical characterization of oxidized intermediate species in aqueous iron(III)-thiocyanate solutions was made by Itabashi [91] using the technique described above, i.e. the voltametry in the OTTLE cell simultaneous with the spectrophotometric determination of the species generated during the potential scan. He worked with solutions of NaSCN and $HClO_4$ as supporting electrolyte.

Figure 3.11 compares thin-layer cyclic voltammograms in thiocyanate solutions with and without Fe^{3+} added. The Fe^{3+} ions in the OTTLE cell were reduced to Fe^{2+} at 0.00 V (vs. SCE) before recording the voltammograms, which always started at this potential. The solution with Fe^{3+} gives a cathodic wave with two unresolved peaks at +0.33 V and +0.28 V on the reverse scan whereas the solution without Fe^{3+} gives a single cathodic peak at *c.a.* 0.27 V (vs. SCE), as already shown in the previous work by the same author (see **Figure 3.10**) [91].

Reduction efficiencies above 90% were obtained with concentrations of both NaSCN and $HClO_4$ of 0.1 mol/dm^3 or higher. The reduction efficiency was found to decrease with the increase of

the anodic switching potential, probably due to the decomposition (hydrolysis) of the oxidized species before the completion of the cycle. The efficiency was also found to decrease drastically with decrease in H^+ concentration below 0.04 mol/dm^3 [91].

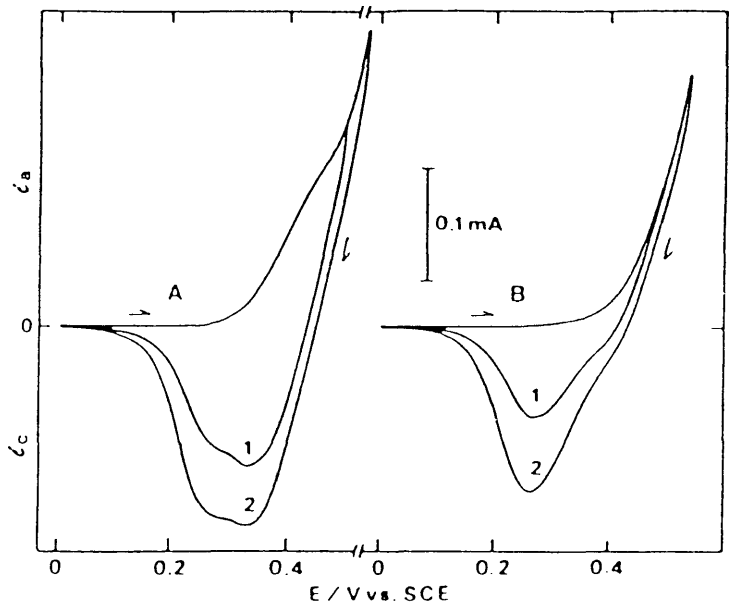


Figure 3.11 - Thin-layer cyclic voltammograms in aqueous solution 0.1 mol/dm^3 NaSCN and 0.1 mol/dm^3 $HClO_4$ **(A)** with and **(B)** without $2x10^{-3}$ mol/dm^3 Fe^{3+} present. Sweep rate, 2 mV/s; temperature, *c.a.* 18°C. Anodic switching potential: **(1)** 0.500 V; **(2)** 0.540 V (vs. SCE) [91].

Figure 3.12 shows thin-layer absorption spectra before and after electrolysis of solutions with 0.1 mol/dm^3 NaSCN and 0.1 mol/dm^3 $HClO_4$. Curves **a** to **c** were recorded from solutions containing 2 x 10^{-3} mol/dm^3 Fe^{3+} and curve **d** from a solution without Fe^{3+}. Curve **a** is a typical spectrum of an iron(III)-

thiocyanate solution showing characteristic peaks at 320 nm and 475 nm. These absorption peaks disappear completely upon electroreduction of the Fe^{3+} at 0.00 V (vs. SCE), as shown by curve **b**. The same previous peaks are again observed in curve **c**, obtained after reoxidation of Fe^{2+} under controlled potential step from 0.00 to 0.50 V (vs. SCE); the increase in the peak at 320 nm is due to the contribution of the electrogenerated oxidized species (which in curve **a** was generated by the autoreduction of Fe^{3+} only). Curve **d** shows the spectrum of the thiocyanate solution without any iron, with the peak at 320 nm corresponding to the electrogenerated oxidized species, and without the iron(III)-thiocyanate peak at 475 nm.

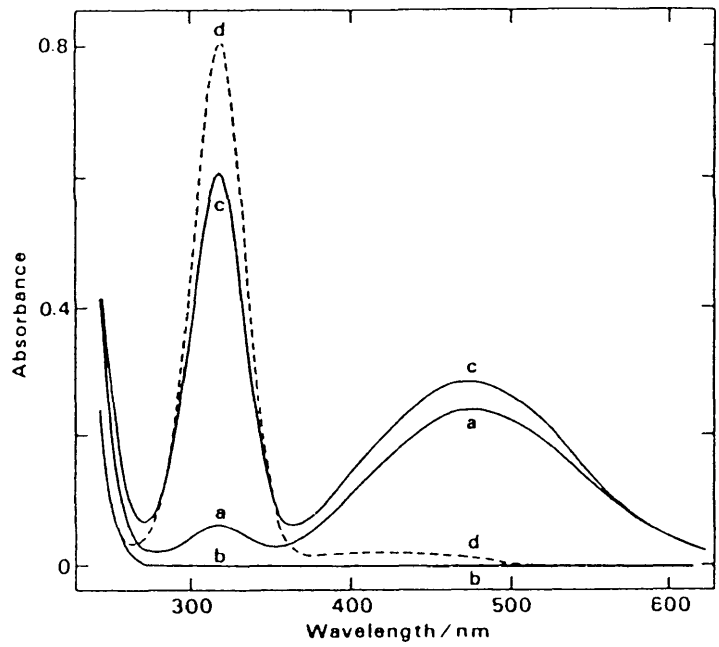


Figure 3.12 - Thin-layer absorption spectra in aqueous solution before and after the electrolysis in 0.1 mol/dm^{3}mol/dm^3 NaSCN and 0.1 mol/dm^3 $HClO_4$ **(a-c)** with and **(d)** without $2x10^{-3}$ mol/dm^3 Fe^{3+} present. **(a)** before electrolysis; **(b)** after reduction of Fe^{3+} at 0.00 V and cathodic charge of 8.1 mC; **(c)** after reoxidation of Fe^{2+} at 0.50 V and anodic charge of *c.a.* 20 mC; **(d)** after oxidation of SCN^- at 0.50 V (vs. SCE) [91].

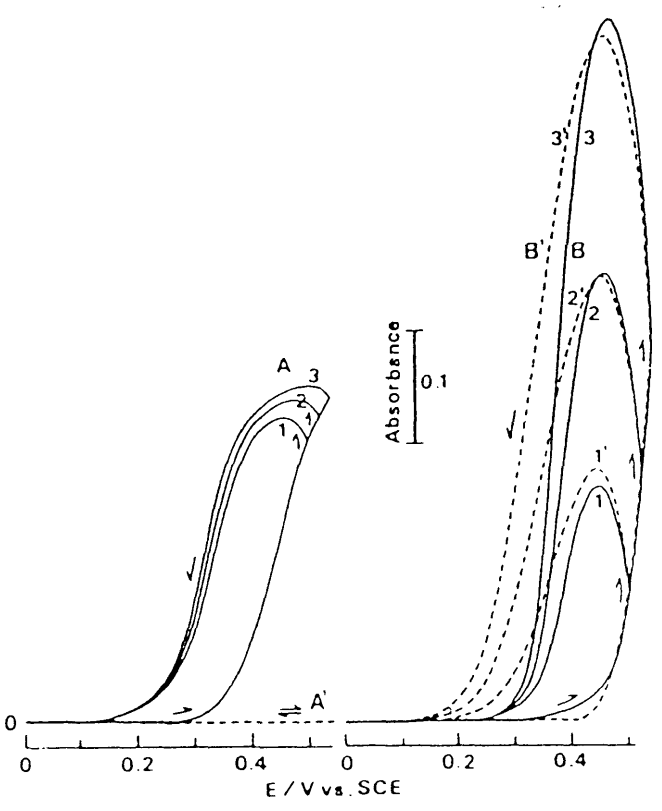


Figure 3.13 - Absorbance-potential curves in 0.1 mol/dm^3 NaSCN and 0.1 mol/dm^3 $HClO_4$ aqueous solutions **(A, B)** with and **(A', B')** without $2x10^{-3}$ mol/dm^3 Fe^{3+} present, at the sweep rate of 2 mV/s. Cell thickness, 0.017 cm. Wavelength monitored: **(A, A')** 475 nm; **(B, B')** 320 nm. Anodic switching potential: **(1, 1')** 0.500 V; **(2, 2')** 0.520 V; **(3, 3')** 0.540 V (vs. SCE) [91] .

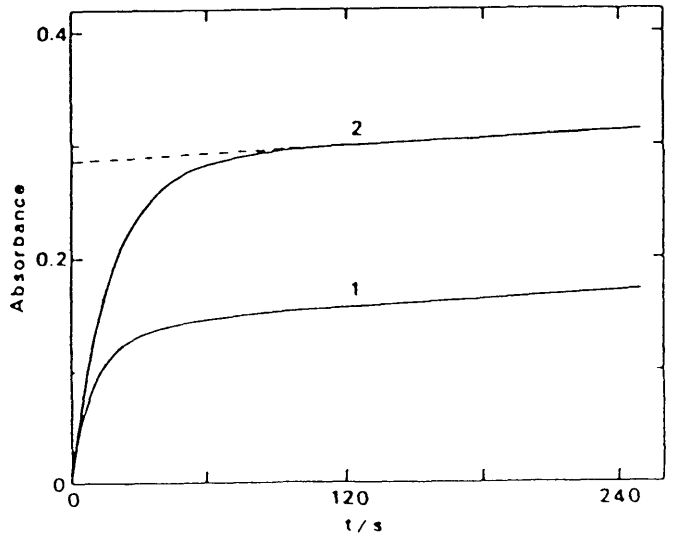
The peak at 475 nm is due to the iron(III)-thiocyanate complexes. The wavelength range around this value is used in the conventional spectrophotometric method of Fe^{3+} analysis [92]. It is interesting to note the coincidence between this peak for the iron(III)-thiocyanate complexes and that at the same wavelength for the anion-radical $(SCN)_2^-$ (see Section 3.7) [73, 76, 78]. This coincidence makes it practically impossible the separate

spectrophotometric detection of the anion $(SCN)_2^-$ in iron(III)-thiocyanate solutions.

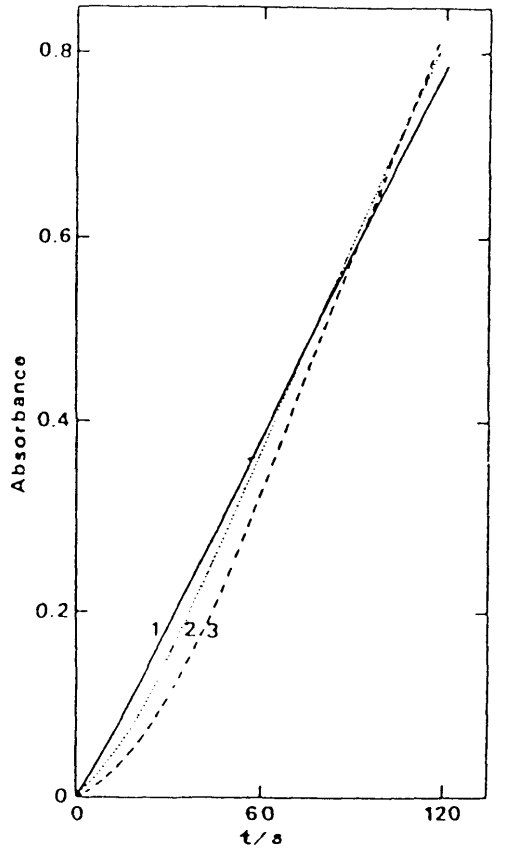
In the experimental conditions adopted by Itabashi [91], the peak at 475 nm is basically due to the iron(III)-thiocyanate complexes, as shown by **Figure 3.13**. The absorption-potential curves were recorded in the OTTLE cell under exactly the same conditions as those above reported for **Figure 3.11**. The Fe^{3+} was reduced at 0.00 V (vs. SCE) and then the potential sweep started with simultaneous recording of the absorbance curve. The broken lines show the absorbance changes monitored in acidic thiocyanate solution in the absence of iron, while the solid lines correspond to absorbance changes in similar solutions containing iron ions. At 475 nm (curves A and A'), a thiocyanate solution without any iron (curve A') did not give any detectable absorbance whereas the same thiocyanate solution with addition of $2x10^{-3}$ mol/dm^3 Fe^{3+} gave the curves A (1, 2 and 3 for anodic switching potentials of 0.500, 0.520 and 0.540 V, respectively). At 320 nm (curves B and B'), both solutions give absorption peaks during the negative scan; the iron(III)-thiocyanate solution (curves B) gave sharper peaks, the oxidized species being totally reduced in a relatively narrow potential region of 160 mV, whereas the thiocyanate solutions without iron (curves B') gave broader peaks, the oxidized species being reduced in a wider potential range of 250 mV [91].

The peak at 320 nm is the one previously assigned to $(SCN)_3^-$ [84, 90]. These measurements by Itabashi [91] showed that the trithiocyanate ion, $(SCN)_3^-$, is not only anodically generated but also produced by the spontaneous autoreduction of iron(III) in iron(III)-thiocyanate solutions.

The variation of absorbance at 475 nm and 320 nm with the time of electrolysis at the constant potential of 0.500 V (vs. SCE) is shown in **Figure 3.14** for acidic thiocyanate solutions containing **(1)** $1x10^{-3}$ mol/dm^3 Fe^{3+}, **(2)** $2x10^{-3}$ mol/dm^3 Fe^{3+} and **(3)** no iron.



(a)



(b)

Figure 3.14 - Variation of absorbance with electrolysis time in 0.1 mol/dm^3 NaSCN and 0.1 mol/dm^3 $HClO_4$ at 0.500 V (vs. SCE) monitored at **(a)** 475 nm and **(b)** 320 nm. Cell thickness, 0.017 cm. Fe^{2+} initially present: **(1)** 1x10^{-3} mol/dm^3; **(2)** 2x10^{-3} mol/dm^3; **(3)** none [91].

All Fe^{3+} was reduced to Fe^{2+} at 0.00 V before the potential step to 0.500 V. The absorbance at 475 nm increased rapidly until all Fe^{2+} was oxidized; then it tended to a constant value. The absorbance at 320 nm kept on increasing because of the high concentration of SCN^- in the solution (0.1 mol/dm^3); at the beginning, the rise was slower than that at 475 nm but after some time, it became faster. This was taken as an indication that Fe^{2+} is oxidized to Fe^{3+} in preference to SCN^- at 0.500 V and that the $(SCN)_3^-$ produced is stabilized by Fe^{3+} with the formation of an ion pair [91].

The concentration of $(SCN)_3^-$ at *c.a.* 30 min after the preparation of a solution containing $2x10^{-3}$ mol/dm^3 $Fe(ClO_4)_3$, 0.1 mol/dm^3 NaSCN and 0.1 mol/dm^3 $HClO_4$ was evaluated by Itabashi [51] as $1.7x10^{-4}$ mol/dm^3 by using the molar absorptivity of that species of $2.2x10^4$ mol^{-1} dm^3 cm^{-1} at 320 nm previously determined [90].

The following steps were proposed to explain the formation of $(SCN)_3^-$ in acidic iron(III)-thiocyanate solutions[91]:

$$Fe(NCS)_2^+ \longrightarrow Fe^{2+} + (SCN)_2^- \qquad \text{(slow)} \qquad (3.47)$$

$$2(SCN)_2^- \longrightarrow (SCN)_3^- + SCN^- \qquad \text{(fast)} \qquad (3.48)$$

Itabashi [91] estimated the normal potential for the redox couple $(SCN)_3^-/SCN^-$ as 0.68 V vs. SHE which is the potential at which the mixed current associated with the oxidation of SCN^- and the reduction of $(SCN)_3^-$ is experimentally observed.

After the discussion reported above, it is interesting to go back to the work published by Miyake [93-95] between 1960 and 1961, as it contains good spectrophotometric information on iron(III)-thiocyanate solutions in several media, both inorganic and organic. The data are presented in **Figures 3.15** and **3.16**. At first sight, the similarity of these spectra with the curve **a** of **Figure 3.12** is

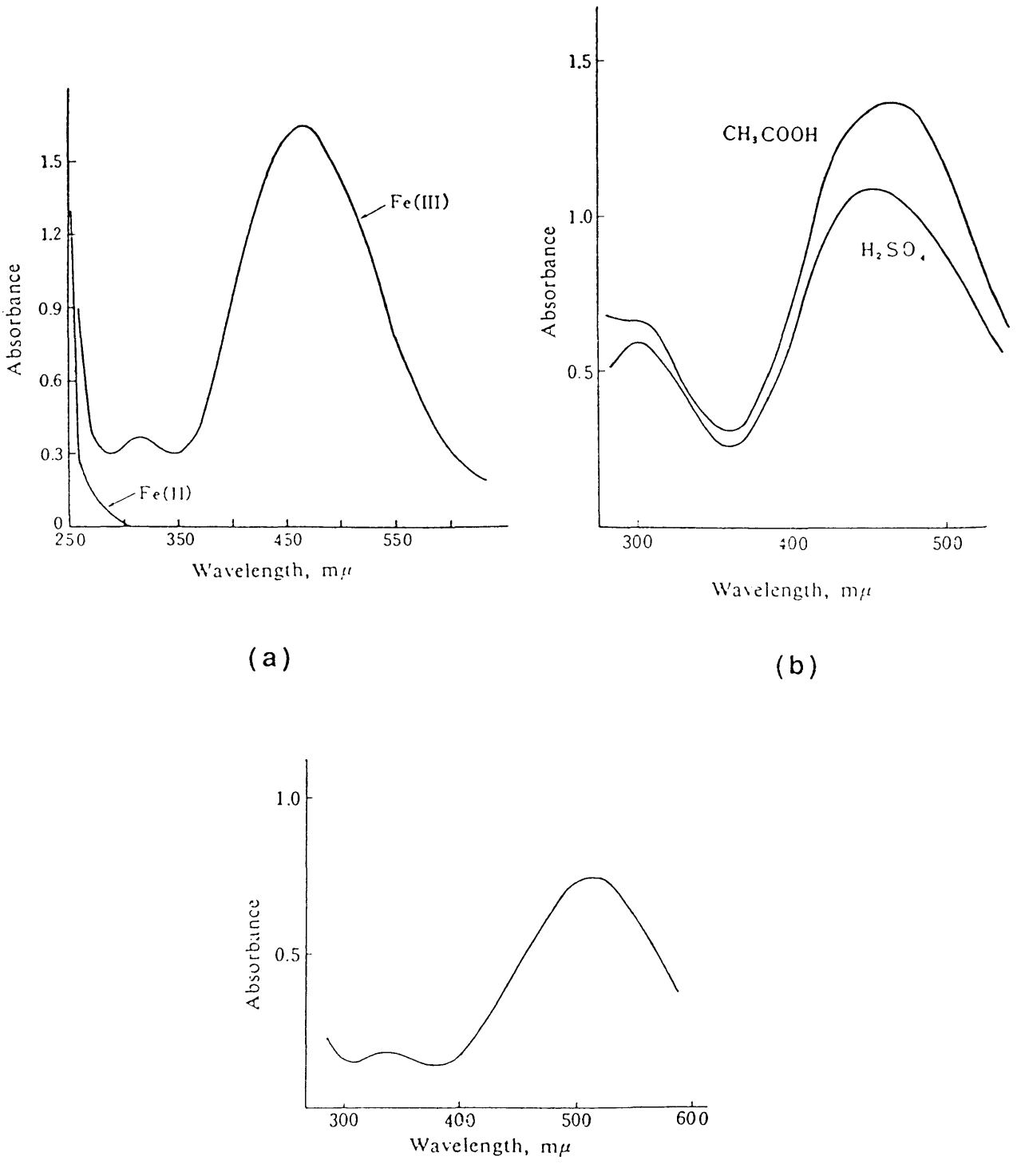
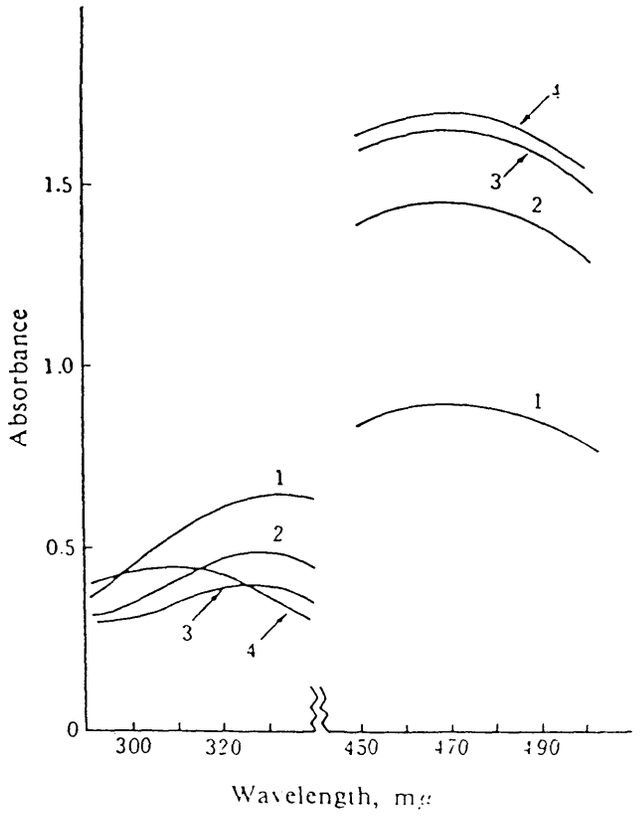
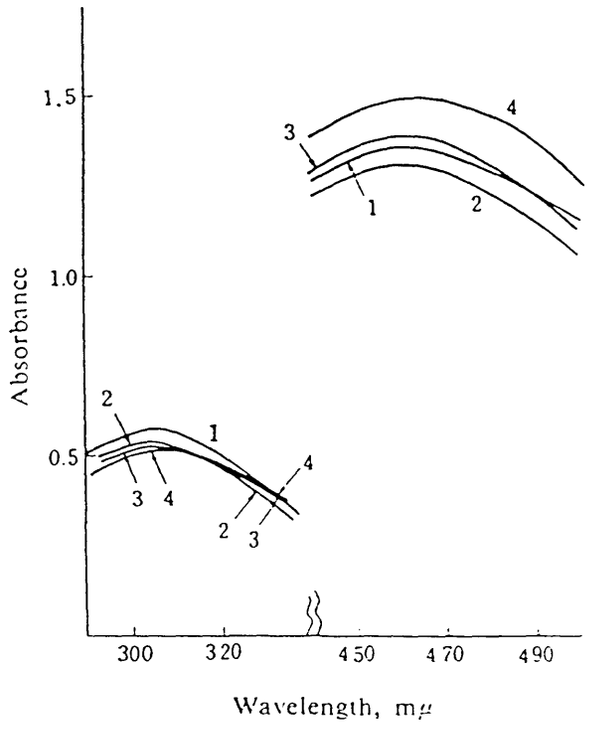


Figure 3.15 - Absorption spectra of fresh iron(III)-thiocyanate and iron(II)-thiocyanate solutions acidified with **(a)** hydrochloric acid; **(b)** sulphuric or acetic acid; **(c)** solution in ethyl acetate, no acid added [93-95].



(a)



(b)

Figure 3.16 - Absorption spectra of fresh iron(III)-thiocyanate solutions 0.005 mol/dm^3 in Fe^{3+} and 0.05 mol/dm^3 in KSCN with varying concentrations of **(a)** hydrochloric acid and **(b)** sulphuric acid, as follows: **(1)** 3.6 N; **(2)** 1.2 N; **(3)** 0.6 N; **(4)** 0.12 N [93, 94].

noticeable. They all present an intense peak around 475 nm, which is obviously due to the iron(III)-thiocyanate complexes, and a small peak around 320 nm, which is now assignable to the trithiocyanate ion, $(SCN)_3^-$. The lack of knowledge in the early 60's about the intermediate species of SCN^- oxidation led Miyake to assign consecutively that small peak to complexes of iron(III) with the anions of each one of the acids used, i.e. chloride, sulphate and acetate. Interestingly, he did not mention the small peak at all in the work in ethyl acetate solution [95], although it was present. The shift of the absorption maximum from about 470 nm in aqueous solution to 511 nm in ethyl acetate was ascribed to the formation of an iron(III)-thiocyanate complex higher than that prevailing in the aqueous solutions observed, a suggestion supported by magnetic measurements [95].

The changes in the 320 nm peak observed in **Figure 3.16a** with different concentrations of HCl may be explained by some interaction between the $(SCN)_3^-$ and Cl^- ions similar to those well known between $(SCN)_2$ and the halides, leading to the formation of the thiocyanogen halides [28, 31, 65-67]. It is noticeable that the interactions between $(SCN)_3^-$ and sulphate, shown in **Figure 3.16b**, are minimal, as expected.

3.9. Some Final Comments on this Review

The views on the intermediate species of the oxidation of thiocyanate have become increasingly complex since the early proposal of aqueous $(SCN)_2$ and its subsequent hydrolysis [51].

The electrochemical work, both in aqueous and in organic solvents, led to the confirmation of $(SCN)_2$ as the main product of the electrode process whenever a platinum electrode is used. The

work on gold electrodes has led to a different type of proposition, $(SCN)_3^-$ being the main oxidized product of the electrode process.

Spectrophotometric work in thiocyanate solutions electrolyzed on a platinum electrode in acetonitrile showed the coexistence of $(SCN)_2$, $(SCN)_3^-$ and SCN^-, an equilibrium constant being estimated for these three species in that solvent.

However, the work using pulse radiolysis of aqueous solutions permitted a more detailed observation of the formation of either $(SCN)_2$ or $(SCN)_3^-$, through the decay of the $(SCN)_2^-$ anion-radical, generated by the interaction of $OH^\bullet$ radicals with SCN^-. Going still deeper into this process, $HOSCN^-$ and $OSCN^{2-}$ were found to be precursors of the $(SCN)_2^-$ ion.

The later work in iron(III)-thiocyanate solutions demonstrated that $(SCN)_3^-$ is also generated by the oxidation of SCN^- by Fe^{3+}. The autoreduction of iron(III)-thiocyanate solutions yields $(SCN)_2^-$ by reaction of SCN^- with free radicals $SCN^\bullet$ released from the electron transfer within the iron(III)-thiocyanate complexes. The $(SCN)_2^-$ reacts further yielding $(SCN)_3^-$ and $(SCN)_2$.

An interesting aspect of the present subject is that the search for the different intermediate species has not been undertaken with a unified treatment, the only exception being the work by Cauquis and Pierre [84], who proposed the equilibrium between $(SCN)_2$, $(SCN)_3^-$ and SCN^- in acetonitrile, as mentioned above. This point deserves a more detailed treatment, as it provides a unified picture of the chemistry of thiocyanate oxidation, emphasizing its pseudohalide character. It is also relevant for the understanding of the thiocyanate leaching of gold.

3.10. Further Thermodynamic Calculations. Analogies with the Halide Systems. Some Mechanistical Ideas for the Thiocyanate Leaching of Gold

There has been no previous attempt to consider the existence of the intermediate species $SCN^{\cdot}$, $(SCN)_2$, $(SCN)_2^-$ and $(SCN)_3^-$ in the mechanism of dissolution of gold by thiocyanate solutions. The only proposed mechanism for the gold dissolution by thiocyanate [87] does not consider the oxidation of this ligand and the several intermediate species produced. The consideration of these species is important, as they seem to participate in the mechanism of gold dissolution.

The following equilibrium in acetonitrile was proposed by Cauquis and Pierre [48], who found the corresponding equilibrium constant at 20°C:

$$(SCN)_3^- = (SCN)_2 + SCN^- \qquad K=(2\pm1)\times10^{-2} \qquad (3.49)$$

Stedman and Whincup [42] suggested that aqueous solutions of thiocyanogen in the presence of an excess of thiocyanate ion could give rise to a metastable equilibrium involving several species such as:

$$(SCN)_3^- \underset{SCN^-}{\rightleftharpoons} (SCN)_2 \overset{H_2O}{\rightleftharpoons} HOSCN + H^+ + SCN^- \qquad (3.50)$$

The intervention of hydrolytic processes leading to the decomposition of these species can hardly permit such a condition to be regarded as an equilibrium. Despite this fact, the chemical composition of the species involved reveals a strong analogy with the halide systems.

The equilibrium expressed by reaction 3.49 is entirely analogous to those already proposed for the halides [12, 17, 96-98]:

$$Cl_3^- = Cl_2 + Cl^- \quad (3.51)$$

$$Br_3^- = Br_2 + Br^- \quad (3.52)$$

$$I_3^- = I_2 + I^- \quad (3.53)$$

A great deal of research has been done on these systems [96-119] and the analogies with the thiocyanate system are many. The hydrolysis of the halide species participating in the equilibria above yields oxygen-containing forms, according to a general scheme which inspired Bjerrum and Kirschener [51] and Gauguin [48] in the formulation of a mechanism to explain the hydrolysis of thiocyanogen (see Sections 3.2 and 3.6).

The standard potentials of several redox couples are given in **Table 3.1**, for comparative purposes. The figures listed there confirm early remarks [51] which place thiocyanogen as an unstable pseudohalogen between bromine and iodine. The overall thermodynamic analogy between the thiocyanate system and the bromide and iodide systems is illustrated by the Eh-pH diagrams in **Figures 3.17**, **3.18** and **3.19**. The diagrams in **Figures 3.18** and **3.19** are quoted from the literature [97, 98], while those in **Figure 3.17** were calculated as part of this work. It should be kept in mind that the diagrams in **Figure 3.17** do not represent equilibrium situations, since $(SCN)_2$ and $(SCN)_3^-$ are not stable in water. They are useful as a means of demonstrating the mechanistic steps involved in the oxidation of thiocyanate. For these intermediate species to appear in the diagrams, the metastable and stable oxidation products had to be disregarded in the calculations.

The value of the standard potential for the couple $(SCN)_3^-/SCN^-$ was estimated by Itabashi [91] as 0.68 V in aqueous solution.

Alternatively, the value 0.71 V was found by combining the equilibrium constant determined by Cauquis and Pierre [84] for reaction 3.49 (in acetonitrile) with the ΔG^o values reported in the Appendix 1. The estimate made by Itabashi was preferred in the present calculations. As a consequence, the ΔG^o for $(SCN)_3^-$ was found to be 409.3 kJ/mol (see Appendix 1).

The potentials for the oxidation of thiocyanate indicated by the lines 125 and 126 in **Figure 3.17** are considerably higher than those indicated by the lines 19, 20 and 21 in **Figure 2.2a** (see Chapter 2), which correspond to the metastable equilibra between SCN^- and HCN and H_2SO_4, the main oxidation products, formed through the hydrolysis of $(SCN)_2$ and $(SCN)_3^-$. The comparison between **Figures 3.17** and **2.2a** reveals the overpotentials involved in the oxidation of thiocyanate.

Table 3.1 - Standard Potentials for Half-Reactions of Several Halide and Thiocyanate Redox Couples in Aqueous Solution at 25°C

Half-Reaction	E° (V)	Reference
$I_{2(aq)} + 2e^- = 2I^-_{(aq)}$	0.621	12, 98
$I_3^-{}_{(aq)} + 2e^- = 3I^-_{(aq)}$	0.536	12, 98
$(SCN)_{2(aq)} + 2e^- = 2SCN^-_{(aq)}$	0.77	19, 51
$(SCN)_3^-{}_{(aq)} + 2e^- = 3SCN^-_{(aq)}$	0.68	91
$Br_{2(aq)} + 2e^- = 2Br^-_{(aq)}$	1.0874	12, 97
$Br_3^-{}_{(aq)} + 2e^- = 3Br^-_{(aq)}$	1.0503	12, 97
$Cl_{2(aq)} + 2e^- = 2Cl^-_{(aq)}$	1.396	12
$Cl_3^-{}_{(aq)} + 3e^- = 3Cl^-_{(aq)}$	1.4152	12

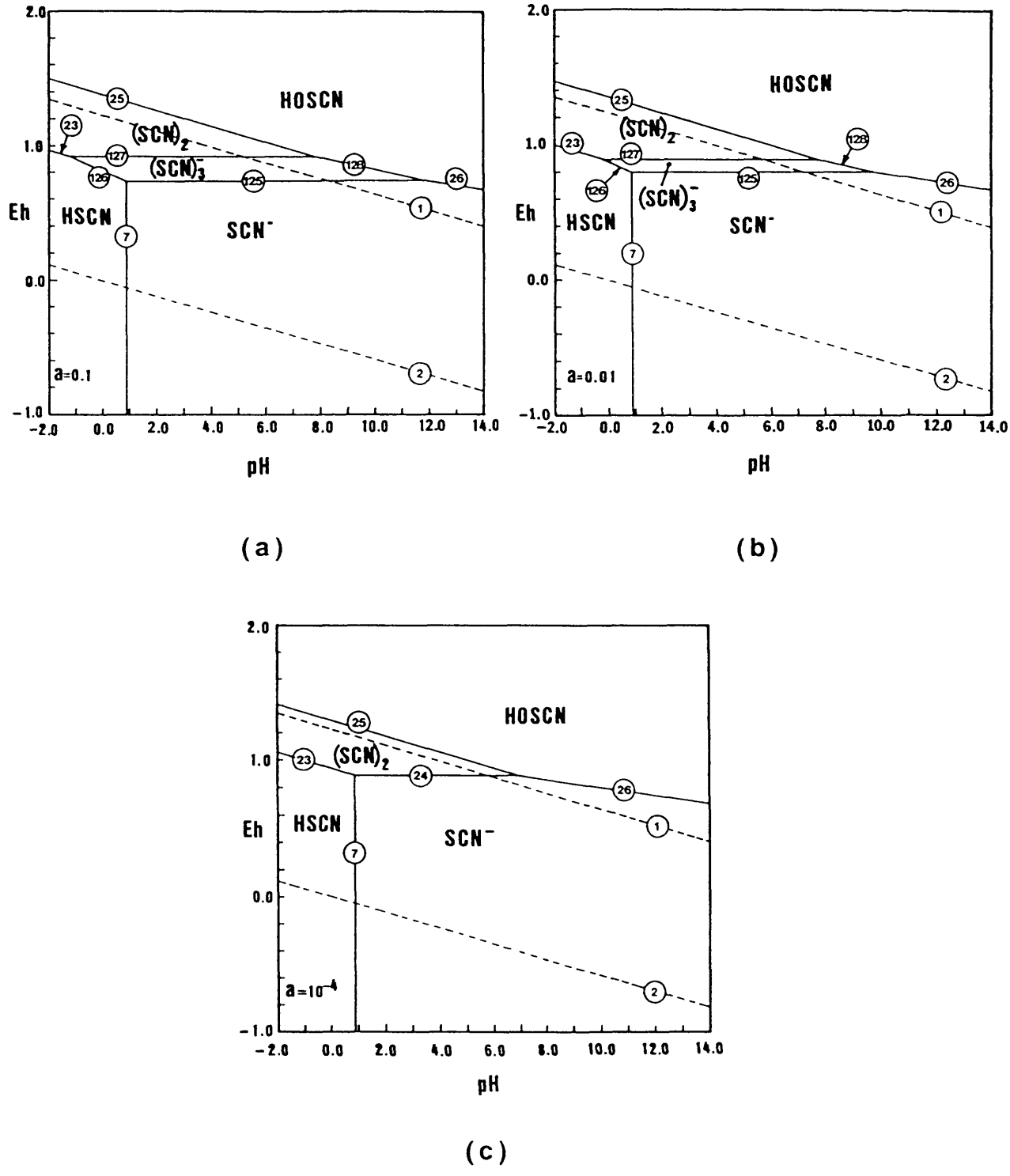


Figure 3.17 - Eh-pH diagrams for the SCN-H_2O system at 25°C considering only the intermediate species in the oxidation of thiocyanate (the metastable and stable oxidation products were not considered in the calculations).

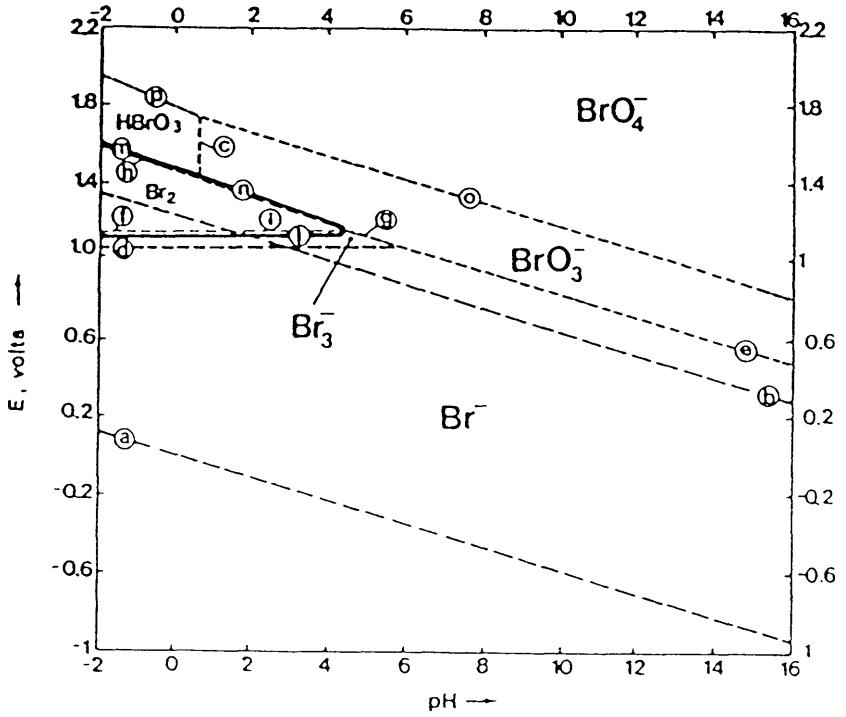


Figure 3.18 - Eh-pH diagram for the bromine-water system at 25°C (1 gram-atom of total dissolved bromine) [97].

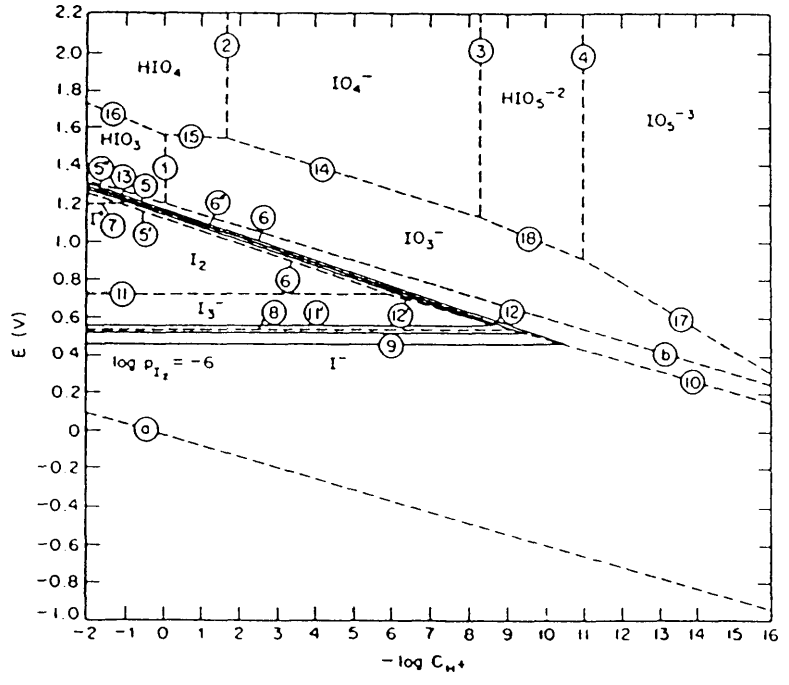


Figure 3.19 - Eh-pH diagram for the iodine-water system at 25°C (total iodine concentration of 0.5 mol/dm^3) [98].

Another interesting observation comes from the comparison between **Figure 3.17** and **Figures 2.5** and **2.6**. The potentials for the oxidation of thiocyanate to $(SCN)_3^-$ (lines 125 and 126 in **Figure 3.17**) roughly coincide with the lines between the aurous and auric complexes, $Au(SCN)_2^-$ and $Au(SCN)_4^-$ (lines 51 and 61 in **Figures 2.5** and **2.6**). This fact points to the following situation: gold dissolves predominantly as the auric complex, $Au(SCN)_4^-$, at potentials in which the predominant thiocyanate species is the oxidized form $(SCN)_3^-$. The aurous complex, $Au(SCN)_2^-$, is formed at potentials in which the predominant form is SCN^-. The transition between one condition and the other may not be sharp. It is reasonable to suppose the existence of a narrow potential band between the two conditions, within which gold dissolves as a mixture of both auric and aurous complexes.

A tentative mechanism to explain the thiocyanate leaching of gold under conditions in which SCN^- is predominant would then include the following steps:

$$Au_{(s)} + SCN^- = Au(SCN^-)_{(ads)} \quad (3.54)$$

$$Au(SCN^-)_{(ads)} = Au(SCN)_{(ads)} + e \quad (3.55)$$

$$Au(SCN)_{(ads)} \longrightarrow AuSCN_{(ads)} \quad (3.56)$$

$$AuSCN_{(ads)} + SCN^- \longrightarrow Au(SCN)_2^- \quad (3.57)$$

Reactions 3.54, 3.55 and 3.57 correspond to those proposed by Martins et al. [87] to explain the formation of the aurous complex. Reaction 3.55 corresponds to the formation of the free radical $SCN^{\bullet}$, which may either oxidize gold metal to form $AuSCN_{(ads)}$ (reaction 3.56) or to participate in other reactions with SCN^- to form intermediate species (see reactions 3.43 to 3.45). In fact, $(SCN)_3^-$

has been proposed both by Martins et al. [88] and by Itabashi [90] as product of the anodic oxidation of SCN^- on gold electrodes. In contrast, the formation of $AuSCN_{(ads)}$ as an intermediate species in the mechanism of gold dissolution corresponds to the propositions of analogous species in the halide systems, i.e. $AuCl_{(ads)}$, $AuBr_{(ads)}$ and $AuI_{(ads)}$ [6, 89, 188, 189], and in the cyanide system, i.e. $AuCN_{(ads)}$ [1, 4, 7, 183-186].

The auric complex would be formed at potentials high enough to oxidize thiocyanate to $(SCN)_3^-$. Thus, in the presence of $(SCN)_3^-$ the following reaction would ensue:

$$AuSCN_{(ads)} + (SCN)_3^- \longrightarrow Au(SCN)_4^- \qquad (3.58)$$

It is also possible to conceive the direct attack of $(SCN)_3^-$ to the metal surface, producing at the same time the aurous complex $Au(SCN)_2^-$ and the adsorbed compound $AuSCN_{(ads)}$, as follows:

$$2Au_{(s)} + (SCN)_3^- \longrightarrow Au(SCN)_2^- + AuSCN_{(ads)} \qquad (3.59)$$

This reaction can be dismembered into two steps, one leading to the formation of the complex $Au(SCN)_2^-$ and of the free radical $SCN^{\cdot}$, and the other yielding the adsorbed compound $AuSCN_{(ads)}$, as follows:

$$Au_{(s)} + (SCN)_3^- \longrightarrow Au(SCN)_2^- + SCN^{\cdot} \qquad (3.60)$$

$$Au_{(s)} + SCN^{\cdot} \longrightarrow AuSCN_{(ads)} \qquad (3.61)$$

The species $(SCN)_3^-$ and $SCN^{\cdot}$ work both as oxidants and complexants in reactions 3.60 and 3.61, respectively. The $AuSCN_{(ads)}$ formed in reaction 3.61 would then react according to reaction 3.57 or 3.58, yielding $Au(SCN)_2^-$ or $Au(SCN)_4^-$, respectively.

This mechanism can be further elaborated. For instance: what

is represented here by $AuSCN_{(ads)}$ may be more correctly seen not as a discrete unit but as a thin-layer of Au^+ and SCN^- ions bonded together and adsorbed on the gold metal surface. Any oxidizing species such as SCN^-, $(SCN)_2^-$, $(SCN)_2$ or $(SCN)_3^-$ could then react with (or be formed upon) that layer and promote further electron transfer and/or complexation, forming one of the gold complexes.

Returning now to the point mentioned above: gold dissolves predominantly as the auric complex, $Au(SCN)_4^-$, at potentials at which the predominant thiocyanate species is $(SCN)_3^-$; whereas the aurous complex, $Au(SCN)_2^-$, is formed at potentials at which the predominant form is SCN^-. The transition between one condition and the other may not be sharp. Some thermodynamic calculations (see data in Appendix 1) may illustrate this point.

The metastable equilibrium between solid gold and aqueous $Au(SCN)_2^-$ may be written as follows:

$$Au(SCN)_2^- + e = Au_{(s)} + 2SCN^- \qquad (3.62)$$

This reaction corresponds to the line 57 in the Eh-pH diagrams for the gold-thiocyanate-water system (see **Figures 2.5** and **2.6**). The form of the Nernst equation for this reaction, considering the activity of gold in solution as 10^{-5}, is:

$$E = 0.3952 - 0.1182 \log \{SCN^-\} \qquad (3.63)$$

The metastable equilibrium between the aurous and auric complexes, which corresponds to the line 61 in the Eh-pH diagrams for the gold-thiocyanate-water system (see **Figures 2.5** and **2.6**), is:

$$Au(SCN)_4^- + 2e = Au(SCN)_2^- + 2SCN^- \qquad (3.64)$$

The corresponding form of the Nerst equation, considering equal activities for the two gold complexes, is:

$$E = 0.6433 - 0.0591 \log \{SCN^-\} \quad (3.65)$$

The line 125 of the diagrams in **Figure 3.17** refer to the reaction:

$$(SCN)_3^- + 2e = 3SCN^- \quad (3.66)$$

This is not an equilibrium situation due to the instability of $(SCN)_3^-$ towards hydrolysis, but the application of the Nernst equation gives an indication of the overpotential for the oxidation of thiocyanate. The form of the Nernst equation, assuming the activity of $(SCN)_3^-$ as being 1% of that of SCN^- (which is a sensible assumption due to the fact that trithiocyanate is only slowly produced by the oxidation of thiocyanate) is then:

$$E = 0.6209 - 0.0591 \log \{SCN^-\} \quad (3.67)$$

Now, the formation of $Au(SCN)_2^-$, $Au(SCN)_4^-$ and $(SCN)_3^-$ can be compared by plotting together the equations 3.63, 3.65 and 3.67 for a range of SCN^- activities, as shown in **Figure 3.20**. The straight lines in this figure correspond to:

Line **A**: $Au(SCN)_2^- + e = Au_{(s)} + 2SCN^-$ (3.62)

$E = 0.3952 - 0.1182 \log \{SCN^-\}$ (3.63)

Line **B**: $Au(SCN)_4^- + 2e = Au(SCN)_2^- + 2SCN^-$ (3.64)

$E = 0.6433 - 0.0591 \log \{SCN^-\}$ (3.65)

Line **C**: $(SCN)_3^- + 2e = 3SCN^-$ (3.66)

$E = 0.6209 - 0.0591 \log \{SCN^-\}$ (3.67)

Figure 3.20 illustrates the point already mentioned: the aurous complex, $Au(SCN)_2^-$, is formed at potentials in which SCN^- predominates, in the area bound by lines **A** and **C**. Within this area, the gold dissolution mechanism is described by reactions 3.54 to 3.57. The same complex is also formed in the area between lines **B** and **C**, where $(SCN)_3^-$ predominates, which suggests the mechanism described by reactions 3.60 and 3.61, besides reaction 3.57. The auric complex, in its turn, is formed in the region above line **B**, and the main step involved is reaction 3.58.

The predominance of the auric complex, $Au(SCN)_4^-$, at redox potentials above line **B** of **Figure 3.20** was first demonstrated by the experimental work performed by Bjerrum and Kirschner [51] and, much later, by Pouradier and Gadet [60].

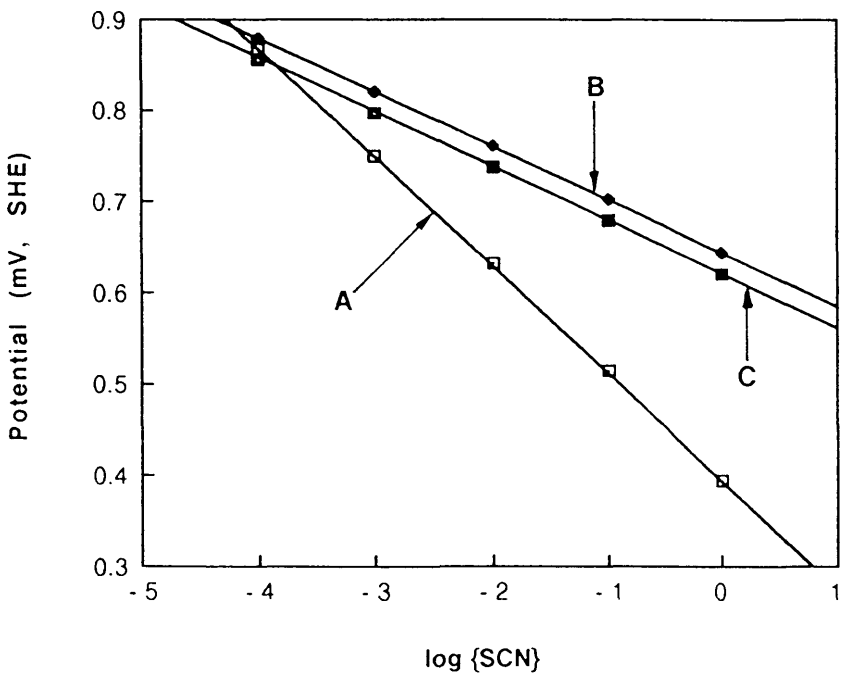


Figure 3.20 - Eh vs. log $\{SCN^-\}$ lines showing the potential zones of predominance of $Au(SCN)_2^-$ (above line **A**), $Au(SCN)_4^-$ (above line **B**) and $(SCN)_3^-$ (above line **C**), considering the total activity of gold in solution as 10^{-5} mol/dm^3, the activities of the gold complexes as being equal, and the activity of $(SCN)_3^-$ as 1% of that of SCN^-.

These simple calculations are useful in the interpretation of results of gold leaching by iron(III)-thiocyanate solutions (see Chapter 6). The mixed potentials in such solutions decrease with time due to the autoreduction of the iron(III)-thiocyanate complexes (see Chapter 4). Leaching experiments with a rotating gold disc revealed that in the beginning (i.e. during the first minutes), the mixed potentials correspond to the formation of $Au(SCN)_4^-$ and at the end, to formation of $Au(SCN)_2^-$, a transition zone existing between these two conditions. This subject will be resumed in Section 6.12, Chapter 6, when discussing the results of the rotating gold disc experiments with iron(III)-thiocyanate solutions.

The objectives of this chapter have been to demonstrate, on the basis of all the previous research work, the existence of several intermediate species in the oxidation of thiocyanate, particularly $(SCN)_3^-$ and $(SCN)_2$, and their relevance for the understanding of the mechanism of gold leaching by this reagent.

CHAPTER 4: REDOX PROCESSES IN AQUEOUS IRON-THIOCYANATE SOLUTIONS

4.1. Iron Complexation by Thiocyanate: Description and Thermodynamic Calculations

Early attempts to establish the compositions of the deep red complexes present in solutions of ferric thiocyanate can be traced back to the end of the last century [120]. Much research was carried out on the identification of the iron(III)-thiocyanate complexes before 1953 [120-126], the main contributions of that period having being reviewed by Lewin and Wagner [127]. By then, four iron(III)-thiocyanate complexes were confirmed as existent and two higher complexes hypothetically admitted [127].

Later work led to the confirmation of a series of six mononuclear iron(III)-thiocyanate complexes and to the determination of their stability constants [21, 22, 128-131]. Only two consistent sets of stability constants are reported in the literature, one including all the six complexes [16] and the other including all but the sixth complex [22] . Both were determined at 25°C and ionic strength 3.0 and are reported in Appendix 3. These two sets of stability constants are not only internally consistent but also mutually consistent to a fair extent.

The first step in the work reported in this chapter was to calculate, using the above mentioned stability constants, the **distribution curves** of the iron(III)-thiocyanate complexes, which are shown in **Figure 4.1**.

An entirely different situation is found when the complexation of iron(II) by thiocyanate is considered. The only iron(II)-thiocyanate

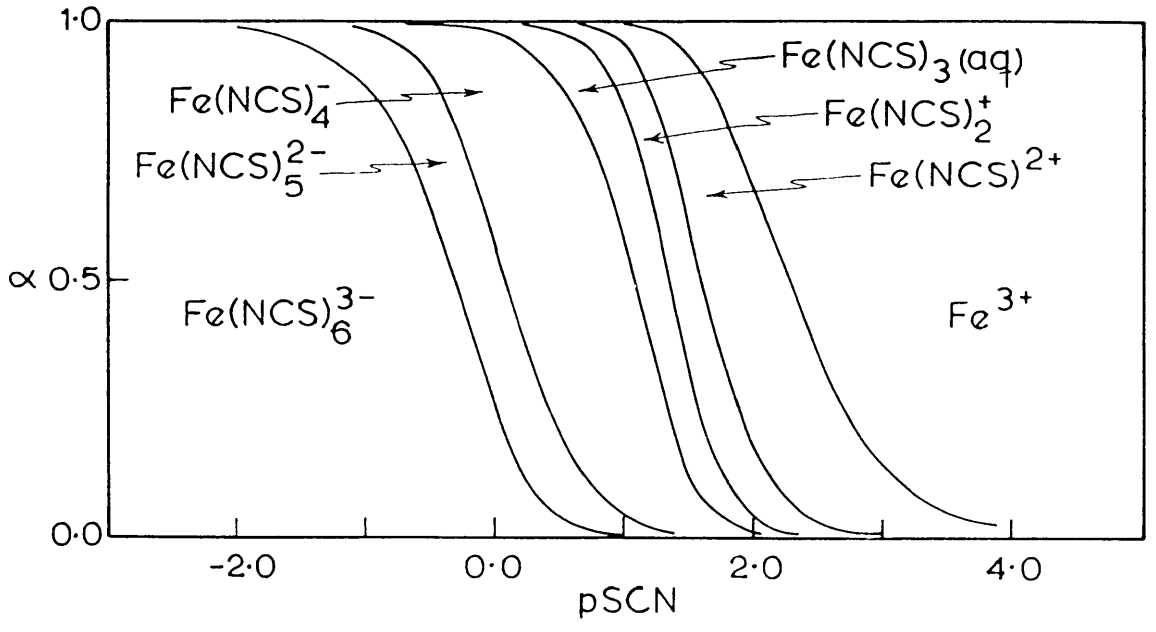
complex reported so far [16, 18, 138, 139] is $FeNCS^+$, whose stability constant is lower than that for the corresponding iron(III) monocomplex. This indicates that the ability of thiocyanate to complex ferrous ions is much smaller than that towards ferric ions.

Calculations for the ferrous complex led to the distribution curve shown in **Figure 4.2**. The value of the stability constant used is that selected by Smith and Martell [16] ionic strength 3.0, which is also included in Appendix 3.

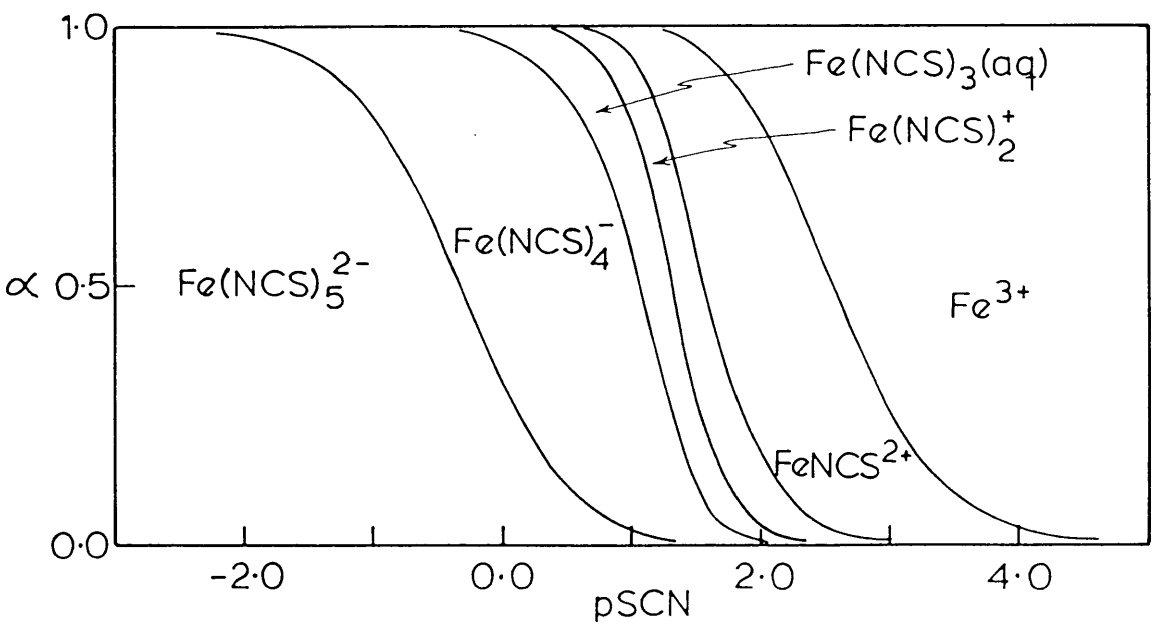
It is easy to see from **Figure 4.1** how diverse is the iron(III)-thiocyanate system. Low concentrations of free thiocyanate lead to the formation of cationic complexes. High thiocyanate concentrations yield anionic complexes. At any SCN^- activity between 10^{-3} and 10 mol/dm^3, which encompasses all pratical leaching systems, anionic and/or neutral and/or cationic complexes coexist in solution.

A comparison between **Figures 4.1** and **4.2** emphasizes the much greater ability of SCN^- to coordinate Fe^{3+} in comparison to Fe^{2+}. For all SCN^- activities above 0.01 or so, the average ligand number for the Fe^{3+} complexes is higher than that for Fe^{2+}. The practical consequence of this fact is that the reduction of complexed Fe^{3+} to Fe^{2+} releases SCN^-, thus increasing the concentration of free SCN^- in solution. If such a reduction progresses far enough, the predominant iron(III)-thiocyanate complex may change in the course of the process (see **Figure 4.1**), leading to a different sequential reaction. The autoreduction of iron(III)-thiocyanate solutions will be extensively explored in this chapter, the objective being to emphasize this shift in the predominant complex as the autoreduction proceeds. Each complex is expected to have an inherent autoreduction rate. The predominant complex or complexes at a certain time will naturally be more influential in determining the overall autoreduction rate at that time. The relevance of this fact will emerge in Chapter 6, where it will be shown that the rate of gold leaching is related to the rate of

autoreduction of the iron(III)-thiocyanate complexes.



(a)



(b)

Figure 4.1 - Distribution curves for the iron(III)-thiocyanate complexes calculated using stability constants from **(a)** Smith and Martell [16] and **(b)** Korondán and Nagypál [22] (data in Appendix 3).

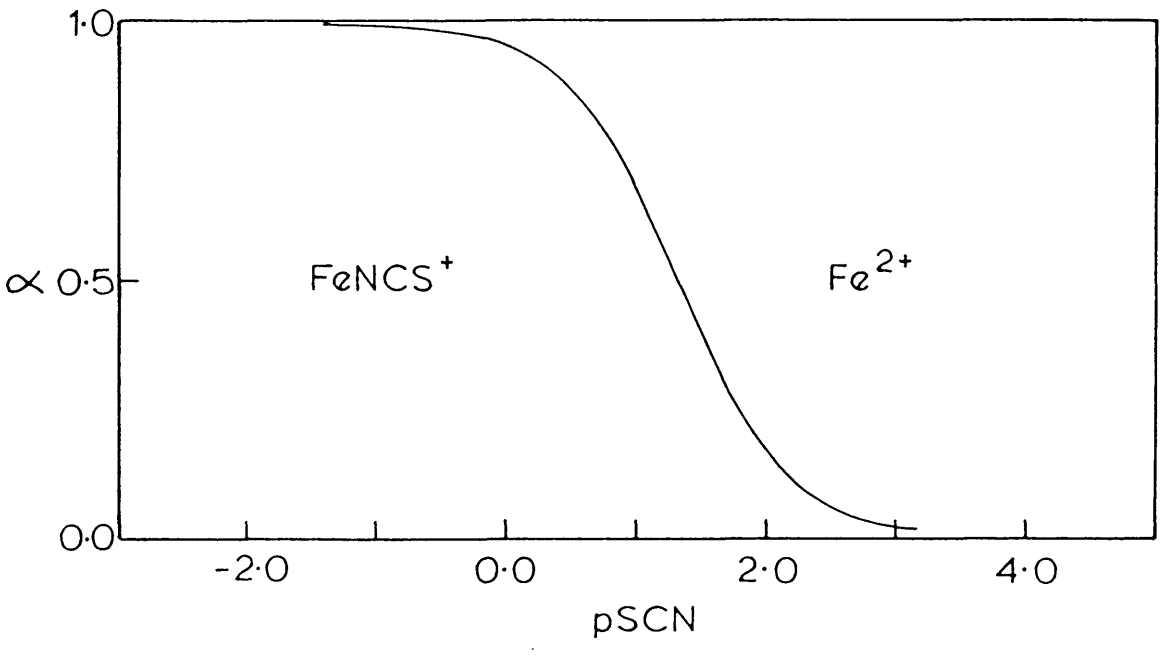
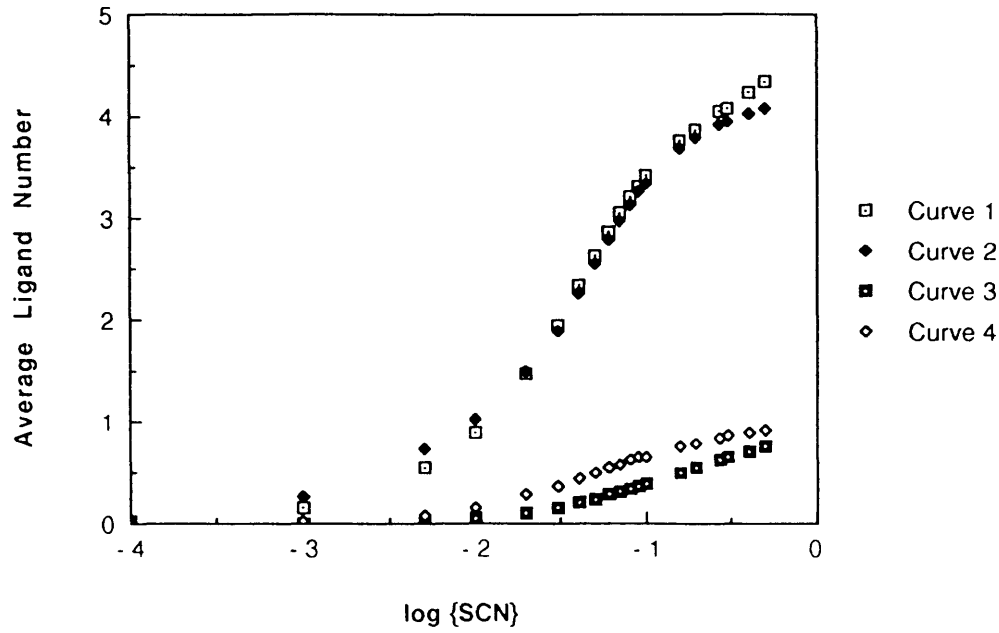
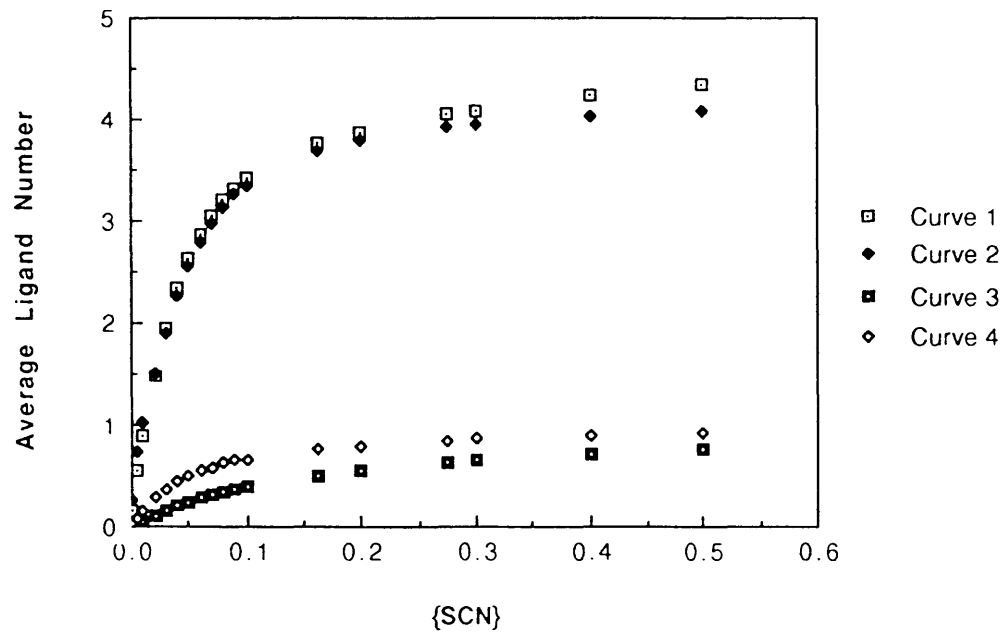


Figure 4.2 - Distribution curve for the iron(II)-thiocyanate complex calculated using data from Smith and Martell [16] (data in Appendix 3).

The occurrence of more than one stable complex under a wide range of conditions suggests that the **average ligand number** is a useful parameter to simplify the description of the system, indicating its average composition for a given set of activities or concentrations of Fe^{3+} and SCN^-. By a calculation procedure similar to that used to obtain the distribution curves (**Figures 4.1** and **4.2**), the average ligand numbers of the iron-thiocyanate complexes were estimated. The results are shown in **Figures 4.3a** and **b**. The greater ability of SCN^- to coordinate Fe^{3+} as compared with Fe^{2+} is apparent. Regarding the ferric complexes, there is a marked transition from cationic (ligand number up to 2) to anionic (ligand number above 3) complexes as the activity of free thiocyanate is increased from 0 to 0.1. For the ferrous complex, two different



(a)



(b)

Figure 4.3 - Average ligand numbers of thiocyanate complexes of iron(III) and iron(II) as a function of: **(a)** pSCN and **(b)** activity of SCN^-. Ferric complexes with data from [16] (curve 1) and [22] (curve 2), both at I=3. Ferrous complex with data from [16] for I=3 (curve 3) and I=0 (curve 4).

values of the stability constant, one for ionic strength 3.0 and other for ionic strength 0 [16] yield curves very close to each other.

The calculation procedures for obtaining the curves shown in **Figures 4.1** to **4.3** are described by several authors [134-136].

Mixed and polynuclear complexes of Fe^{3+} with SCN^- and SO_4^{2-} and/or OH^- are expected to exist [31, 131]. However, they are not considered here as this would raise additional complications that are beyond the scope of this project.

When solutions containing ferric ions and thiocyanate are mixed, the blood red colour which is characteristic of the iron(III)-thiocyanate complexes appears immediately. The kinetics of formation of the iron-thiocyanate complexes is very fast, the times involved being in the milisecond range [132-133]. For the purposes of the present work, the formation of the iron-thiocyanate complexes will be considered as instantaneous.

Inspection of the data in Appendix 3 will show that the gold-thiocyanate complexes are much more stable than the corresponding iron(III)-thiocyanate complexes. Thus, in thermodynamic terms, the ligand will preferentially complex gold cations, either when available in the free state or when already coordinating ferric ions.

4.2. Discussion of the Previous Work on the Oxidation of Thiocyanate by Iron(III)

Only two references are available on the oxidation of thiocyanate by ferric ions; one by Betts and Dainton [41] and the other by Ellis and Laurence [137].

The first paper on the subject was published by Betts and

Dainton [41] in 1953, concerned with the bleaching of iron(III)-thiocyanate solutions. In contrast to the iron(II)-thiocyanate complex, the iron(III)-thiocyanate complexes have a deep blood-red colour, resulting from an absorption peak in the visible region of the spectrum, around 475 nm. This is the basis of a standard spectrophotometric method for determination of iron(III) in solution, described in detail by Sandell [92]. One of the problems encountered in this method is the spontaneous bleaching of ferric thiocyanate solutions, due to the autoreduction of Fe^{3+} to Fe^{2+} with the corresponding oxidation of thiocyanate. Samples to be analyzed can not be left standing for long as this would change the relative concentration of Fe^{3+} by reduction to Fe^{2+}. The problem is then mainly related to the initial rates of the redox processes in fresh iron(III)-thiocyanate solutions.

Thus, Betts and Dainton [41] determined the initial rates of autoreduction of ferric thiocyanate in aqueous solutions of perchloric acid between 14.8 and 29.9°C. The concentration ranges investigated were 0.005-0.10 mol/dm^3 for SCN^- and 0.0005-0.01 mol/dm^3 for Fe^{3+}. They interpreted the results by proposing the following mechanism involving the $FeNCS^{2+}$ complex:

$$Fe^{3+} + SCN^- = FeNCS^{2+} \qquad (4.1)$$

$$FeNCS^{2+} + SCN^- \rightarrow Fe^{2+} + (SCN)_2^- \quad \text{(rate determining step)} \qquad (4.2)$$

$$Fe^{3+} + (SCN)_2^- \rightarrow Fe^{2+} + (SCN)_2 \qquad (4.3)$$

$$3(SCN)_2 + 4H_2O \rightarrow 5SCN^- + SO_4^{2-} + HCN + 7H^+ \qquad (4.4)$$

or, in the case of the $Fe(NCS)_2^+$ complex:

$$Fe^{3+} + 2SCN^- = Fe(NCS)_2^+ \qquad (4.5)$$

$$Fe(NCS)_2^+ + SCN^- \rightarrow Fe^{2+} + (SCN)_2^- \quad \text{(rate determining step)} \qquad (4.6)$$

$$Fe^{3+} + (SCN)_2^- \longrightarrow Fe^{2+} + (SCN)_2 \qquad (4.3)$$

$$3(SCN)_2 + 4H_2O \longrightarrow 5SCN^- + SO_4^{2-} + HCN + 7H^+ \qquad (4.4)$$

The relative balance between the contributions of the two sets of reactions above to the overall mechanism would be controlled by the equilibrium between the two complexes considered:

$$FeNCS^{2+} + SCN^- = Fe(NCS)_2^+ \qquad (4.7)$$

Reactions 4.1, 4.5 and 4.7 are the previously known equilibria of formation of the complexes $FeNCS^{2+}$ and $Fe(NCS)_2^+$, which were the only two considered by Betts and Dainton [41]. These are practically instantaneous reactions [132, 133]. Reaction 4.4 represents the overall hydrolysis of thiocyanogen proposed early by Bjerrum and Kirschner [51], which was extensively discussed in Chapter 3, Section 3.2. The rate determining step was suggested to be reaction 4.2 or 4.6, depending on the complex involved. These reactions correspond to the formation of the transitory form $(SCN)_2^-$ which is the key to the whole mechanism. It is interesting to notice that Betts and Dainton included this anion-radical in their mechanistic proposal by analogy with the already known species Br_2^-, I_2^- and $(CN)_2^-$.

As the main objective of their work was the determination of the initial autoreduction rate, most of the experiments performed by Betts and Dainton did not last more than 20 minutes. They also demonstrated that a considerable deviation occurred between the course of reaction extrapolated from the initial rate law proposed and that observed, particularly after 60 minutes. The course of reaction tended to slow down with time, an effect attributed to the increasing concentration of Fe^{2+} produced by the autoreduction process itself.

A rather complex initial rate law was proposed by Betts and Dainton [41], supported by the above quoted mechanism. However, considering the question from the point of view of today's accepted knowledge of the subject, the complexity of their scheme seems to have been overwhelmed by the higher complexity of the iron-thiocyanate system itself. The concentration ranges investigated were 0.005-0.10 mol/dm^3 for SCN^- and 0.0005-0.01 mol/dm^3 for Fe^{3+}. **Figures 4.1** through **4.3** show that at free SCN^- activities around *c.a.* 0.1 mol/dm^3, a fraction as large as 80% of the total Fe^{3+} in solution exists as neutral and anionic complexes with SCN^-, which are not covered by the above mechanism and, in quantitative terms, are not included in the expression proposed for the initial rate law [41].

Another point to be considered is the participation of the species $(SCN)_2^-$ in the mechanism proposed by Betts and Dainton. The spectroelectrochemical characterization of oxidized intermediate species in aqueous thiocyanate [90] and ferric thiocyanate [91] solutions made by Itabashi by means of voltametry in an OTTLE (Optically Transparent Thin Layer Electrode) cell led to the following mechanistic steps [91] :

$$Fe(NCS)_2^+ \longrightarrow Fe^{2+} + (SCN)_2^- \qquad \text{(slow)} \qquad (4.8)$$

$$2(SCN)_2^- \longrightarrow (SCN)_3^- + SCN^- \qquad \text{(fast)} \qquad (4.9)$$

It should be noted that, since Itabashi [91] worked with a solution 0.1 mol/dm^3 in NaSCN and $2 \cdot 10^{-3}$ mol/dm^3 in Fe^{3+}, the main complex - though not the only one - expected to be present in solution would be $Fe(NCS)_4^-$, instead of $Fe(NCS)_2^+$. Furthermore, most of the Fe^{2+} would be present as $FeNCS^+$ (see **Figures 4.1** through **4.3**). Such criticism, however, does not change the relevant fact that trithiocyanate, $(SCN)_3^-$, is produced by the anodic oxidation of both thiocyanate [90] and ferric thiocyanate solutions [91], giving an absorption peak at *c.a.* 320 nm. On the other hand, the U.V. spectra of freshly prepared acidic ferric thiocyanate solutions obtained both

by Itabashi [91], Miyake [93-95], and during the present work, also showed the absorption peak characteristic of $(SCN)_3^-$, at 320 nm. This demonstrates that trithiocyanate is produced not only anodically but also by the spontaneous autoreduction in ferric thiocyanate solutions. The participation of $(SCN)_3^-$ was not acknowledged in the above mechanism proposed by Betts and Dainton. The existence of this species was not yet proved at that time (see Chapter 3, Section 3.7).

The second paper on the oxidation of thiocyanate by ferric ions was published by Ellis and Laurence in 1967 [137]. They had a rather specific interest which was the photolysis of the complex $FeNCS^{2+}$ by light with wavelengths of 5461, 4358 and 3660 Å characteristic of the mercury arc. The photolysis starts with the the absorption of light in the charge transfer band of $FeNCS^{2+}$ followed by its breakdown into the ferrous ion and the free radical $SCN^{\cdot}$:

$$FeNCS^{2+} \xrightarrow{h\nu} Fe^{2+} + SCN^{\cdot} \qquad (4.10)$$

The free radical $SCN^{\cdot}$ was then considered to participate in several reactions, such as the formation of $(SCN)_2$ by reaction with $FeNCS^{2+}$, the formation of HOSCN by reaction with $FeOH^{2+}$, the reoxidation of Fe^{2+} into $FeNCS^{2+}$, and so on. Ellis and Laurence [137] included hypothiocyanous acid, HOSCN, in their mechanistic proposals, but omitted intermediate species like $(SCN)_2^-$ and $(SCN)_3^-$. The duration of the experiments were short, the results being interpreted in terms of initial rates.

Photolytic reactions are not exclusive to thiocyanate complexes. Similar well known reactions are [137]:

$$FeCl^{2+} \xrightarrow{h\nu} Fe^{2+} + Cl^{\cdot} \qquad (4.11)$$

$$FeOH^{2+} \xrightarrow{h\nu} Fe^{2+} + OH^{\cdot} \qquad (4.12)$$

Such reactions, however, require specific wavelengths. Reaction 4.11, for instance, is activated at 3130 Å and reaction 4.12 at 3660 Å [137].

The experiments reported in the present project were conducted under ordinary diffuse light, which is the condition expected to be found in any hydrometallurgical operation. A few replicates performed in the dark did not show any noticeable deviation from those results.

Despite the contributions by Betts and Dainton [41] and Ellis and Laurence [137], there are several points still to be investigated about the redox processes in thiocyanate solutions which are relevant for the gold leaching by thiocyanate. These points can be summarized as follows:

(1) What are the potential readings in iron(III)-thiocyanate solutions; how are they influenced by factors such as thiocyanate concentration, ferric ion concentration and pH; and how do they decrease as the autoreduction of the ferric complexes proceeds? These questions have not been previously answered.

(2) The behaviour of the autoreduction reaction over long periods of time (hours and days) and wide concentration ranges of Fe^{3+} and SCN^- has not yet been investigated. The few such experiments performed by Betts and Dainton [41] were exploratory and did not describe the behaviour of the system. They were mainly concerned with the initial rates and mechanism.

(3) In connection with the previous points, a thorough investigation of the stoichiometry of the oxidation of thiocyanate by ferric ions is required. Reagent consumption by oxidation is an important point to be evaluated from the point of view of thiocyanate leaching.

The objective of the following sections is to present and discuss experimental results in order to answer these (and a few more) questions.

4.3. Analytical Techniques for Iron and Thiocyanate

4.3.1. Standardization of Iron(III) Stock Solutions

In all experiments, additions of Fe^{3+} were made from a standard 1 mol/dm^3 stock solution which was standardized by the dichromate method [136, 142, 143] as follows: the samples were kept at 70-90°C and acidified to a concentration of 5 to 6 mol/dm^3 of HCl. All Fe^{3+} was then reduced to Fe^{2+} by stannous chloride, $SnCl_2$, whose excess was destroyed by oxidation to the stannic form by mercuric chloride, Hg_2Cl_2. The mixture now containing all iron as Fe^{2+} was then further acidified with HCl and cooled to room temperature. It was then further diluted with 1 mol/dm^3 H_2SO_4 and titrated with a standard solution of potassium dichromate, $K_2Cr_2O_7$. Diphenylbenzidinesulphonic acid was used as indicator. A small addition of concentrated phosphoric acid was required before the titration. The overall titration reaction is [136, 142, 143]:

$$Cr_2O_7^{2-} + 6Fe^{2+} + 14H^+ \longrightarrow 6Fe^{3+} + 2Cr^{3+} + 7H_2O \qquad (4.13)$$

This is a conventional and well proved method which gave excelent results in terms of accuracy and reproducibility.

4.3.2. Volhard Method for the Determination of Thiocyanate

The Volhard method is one of the volumetric argentimetric methods of determination of thiocyanate [136, 142-145]. It was exhaustively used throughout this experimental work.

The analyses were made as follows: an excess of standard 0.1 mol/dm^3 silver nitrate solution was added to the thiocyanate sample acidified with HNO_3, to precipitate the SCN^- ions as the solid AgSCN. The precipitation is quantitative due to the extremely low solubility product of AgSCN (see Appendix 3). The excess Ag+ ions were then back-titrated with standard 0.1 mol/dm^3 thiocyanate solution. Ferric alum was used as indicator, due to the strong colour of the iron(III)-thiocyanate complex which appears when the end point is reached.

Formaldehyde was added to the samples before the addition of silver nitrate, in order to prevent interference by any residual HCN dissolved as a product of the thiocyanate oxidation by iron(III). Formaldehyde keeps HCN/CN^- in solution by forming the compound $CN\text{-}CH_2OH$, which prevents its coprecipitation as AgCN (s) when the silver nitrate is added. This reaction is as follows [145]:

$$CN^- + CH_2O + H_2O \longrightarrow CN\text{-}CH_2OH + OH^- \qquad (4.14)$$

The presence of $HCNO/CNO^-$ was systematically checked by keeping the samples in a water bath at 70°C for 1 hour (or boiling them for a few minutes) before employing the above procedure. The heating destroys any cyanates or cyanides eventually present. In fact, such titrations never differed from those of samples not submitted to heating, indicating that cyanic acid or cyanate ion were not present in the samples.

4.3.3. Spectrophotometric Determination of Iron(II)

The rate of autoreduction of the ferric thiocyanate complexes was followed by determining the concentration of Fe^{2+} with time. This was done spectrophotometrically by measuring the absorbance of the orange-red o-phenanthroline complex $(C_{12}H_8N_2)_3Fe^{2+}$ at 508 nm. This complex is formed quantitatively in the pH range 2-9. Below pH 2 the colour develops slowly and is much weaker. The solutions show no change in colour after months and Beer's law is closely followed [92, 145-147].

Iron(II) determinations were performed as follows: samples were collected at certain times and run into a mixture which quenched the autoreduction reaction and, after dilution, permitted the spectrophotometric measurement. This quenching mixture contained sufficient ammonium fluoride to discharge completely the red colour of the ferric thiocyanate present (F^- is a stronger complexant of Fe^{3+} than SCN^- and forms colourless complexes). In addition, ammonium acetate buffer was present to keep the pH of the mixture at *c.a.* 4.7. The third component was o-phenanthroline. After addition of the sample the mixture was completed to volume with water and measured after at least 1 hour. All the cationic and anionic species in the mixture were kept within the non-interference levels recommended by Fortune and Mellon [146]. The procedure was extensively tested before being used. The method is remarkably accurate and reproducible.

4.4. Potential Readings in Iron(III)-Thiocyanate Solutions

The Eh-pH diagrams presented in Chapter 2 showed that gold is leached by thiocyanate at potentials above *c.a.* 600 mV. They also showed that at such potentials the $SCN\text{-}H_2O$ system is metastable,

which emphasizes the need for kinetic studies on the thiocyanate decomposition by oxidation. Fortunately, in the case of thiocyanate, the oxidation proceeds through several intermediate species whose formation demands considerable overpotentials.

Potential measurements are, consequently, an essential piece of information in this research of the thiocyanate leaching of gold, as this parameter affects both the gold dissolution and the thiocyanate oxidation.

4.4.1. Potential Measurements: Practical Aspects

Potentials were measured, throughout this project, against Ag/AgCl reference electrodes. Several such electrodes manufactured by Russell and Co. were used. The accuracy of the electrodes was frequently checked with standard solutions of $Fe(CN)_6^{3-}/Fe(CN)_6^{4-}$ in KCl, which are recommended in the literature [140]. Readings within ±5 mV of the standard value were considered acceptable [141]. Otherwise, the electrodes were serviced, which always included changing the $AgCl^-$saturated KCl solution.

The indicator electrodes were made of platinum (considered as inert) and gold. In most cases the readings were taken on both Pt and Au electrodes (in the same experiment). Exhaustive measurements (see Appendices 5 and 6) showed that the discrepancies between these two readings were minimal (less than 15 mV for iron concentrations from 0.01 to 0.10 mol/dm^3) and, in most cases, non-existent. Thus, the contribution of the dissolution of the gold electrode to the mixed potentials measured in the iron-thiocyanate system was found to be minimal, if not negligible.

The presence of the Fe^{3+}/Fe^{2+} couple provided a very stable and quick response. The potential readings were within ±5 mV no matter if the gold electrode was rotating or stationary, and no matter if the

solution was being stirred or at rest. The same was not true when the Fe^{3+}/Fe^{2+} couple was not present (for instance, in the experiments with hydrogen peroxide and without iron). In these cases the electrode response was slower, and the measurements were taken with the solution steadly stirred, for such readings proved to be more stable and reproducible than those tried with the system completely still.

In almost all experiments the Fe^{3+} stock solutions were made up with ferric alum (ammonium ferric sulphate). Ferric nitrate was used in a few preliminary tests but was discontinued to avoid any interference due to the oxidizing effect of the nitrate ion. Analytical grade reagents were used throughout this work and are all listed in the Appendix 7.

4.4.2. A First Evaluation of Potential Readings in Fresh Iron(III)-Thiocyanate Solutions

Exploratory experiments for measuring the mixed potentials produced in iron(III)-thiocyanate solutions were performed as follows: freshly prepared thiocyanate solutions were put into a thermostated stirred glass reactor which was fitted with pH, Ag/AgCl reference, Pt and Au electrodes. The system was acidified with H_2SO_4 to pH 1.5 and flushed with nitrogen for *c.a.* 45 minutes. The temperature was 25°C. An amount of 1 mol/dm^3 ferric alum stock solution was then added. Potential readings were taken as soon as the electrode response stabilized and considered to be the readings of the "freshly prepared solutions" (or zero time readings). Some results are shown in **Figure 4.4**.

Some experiments were extended to 4 hours so that the decrease of the potential with the progress of the autoreduction could be recorded, as seen in **Figure 4.5a**. The Fe^{3+} reduction in these same experiments is shown in **Figure 4.5b** in terms of the

precentage of Fe^{2+} produced with time.

Reference to the Eh-pH diagrams for the Au-SCN-H_2O system presented in Chapter 2 will also indicate that the potentials appearing in **Figures 4.4** and **4.5** are sufficiently high to oxidize gold to Au^{III} or to Au^{I}.

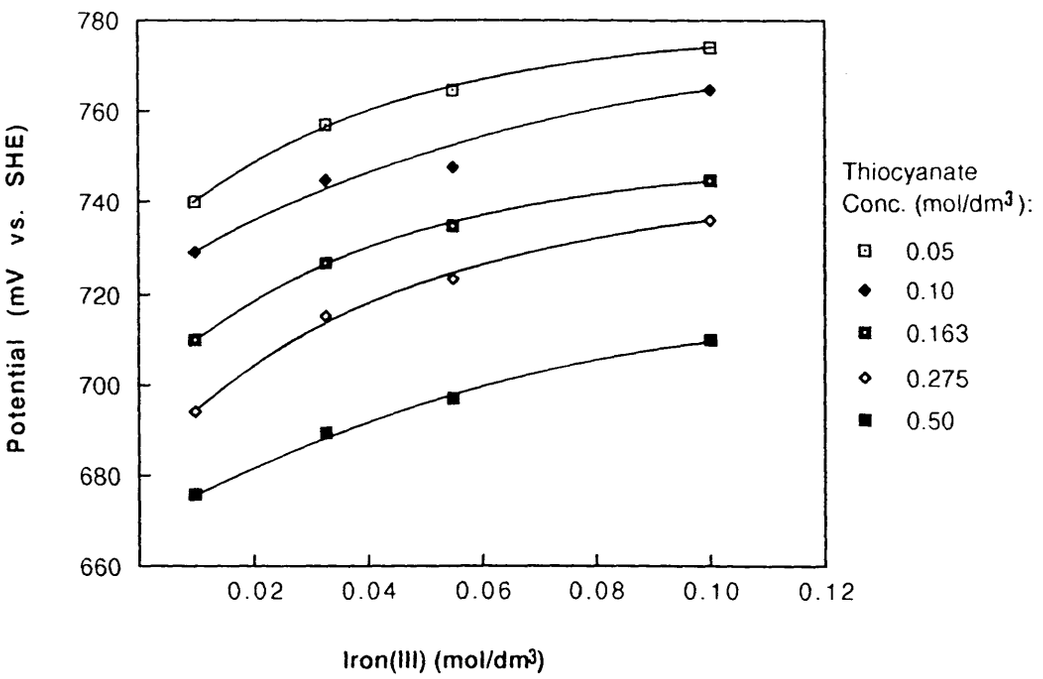
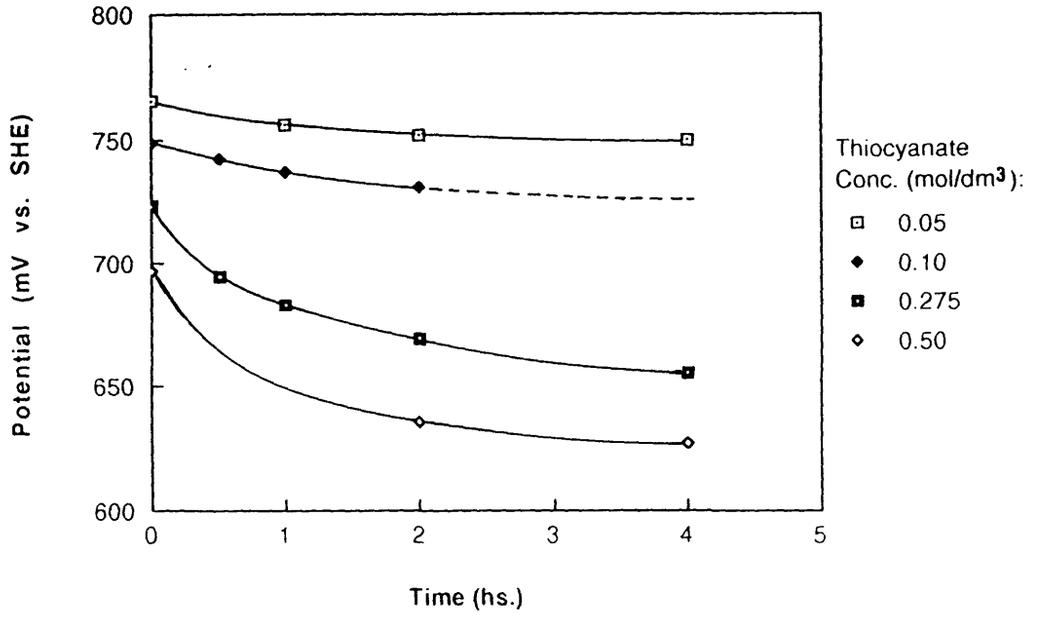
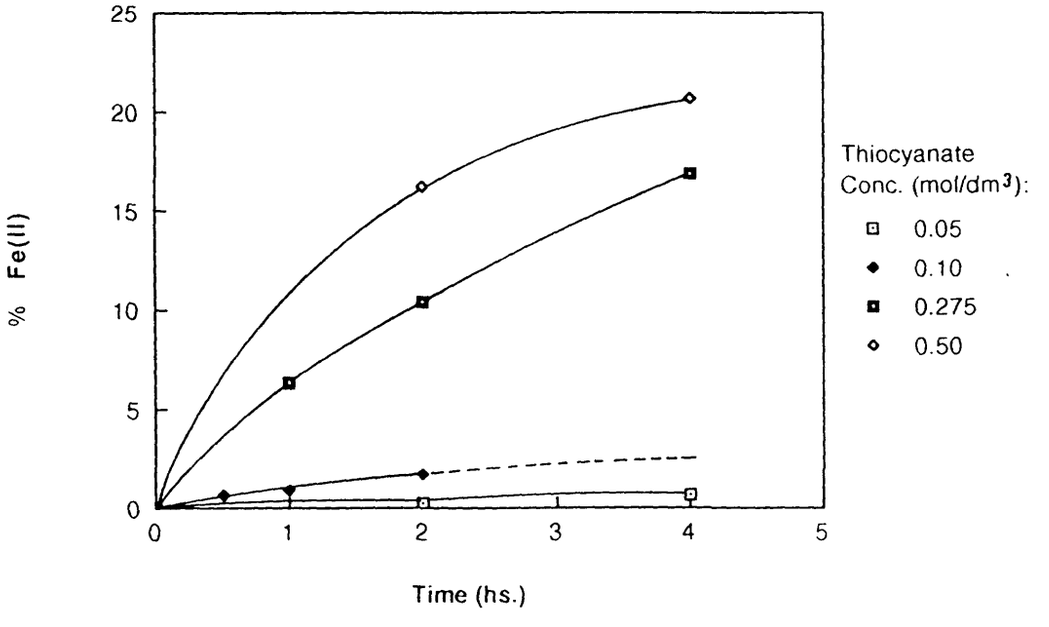


Figure 4.4 - Potential readings in fresh thiocyanate solutions on a platinum electrode, at pH 1.5 and 25°C. Readings on a gold electrode are practically the same.



(a)



(b)

Figure 4.5 - Autoreduction in ferric thiocyanate solutions demonstrated by **(a)** decrease in the potential readings and **(b)** increase in the percentage of Fe^{2+} with time (readings with Ag/AgCl-Pt electrode at pH 1.5 and 25°C). Initial Fe^{3+} concentration in all experiments: 0.055 mol/dm^3.

The thermodynamic basis of the autoreduction of ferric thiocyanate solutions is made evident by comparing the potential readings shown in **Figures 4.4** and **4.5a** with the Eh-pH diagrams shown in **Figure 4.6**, whose calculation was discussed in Chapters 2 and 3. The potentials measured are high enough to oxidize SCN^- to HCN (the same is true if the oxidation to $HCNO/CNO^-$ or $NH_3/CO_2/H_2SO_4$ is considered, as shown in Chapter 2, Section 2.4). Additionally, reference to **Figure 4.6b** shows that the potential readings are above the potentials involved in the oxidation of SCN^- to $(SCN)_3^-$ and $(SCN)_2$, whose formation is part of the autoreduction mechanism.

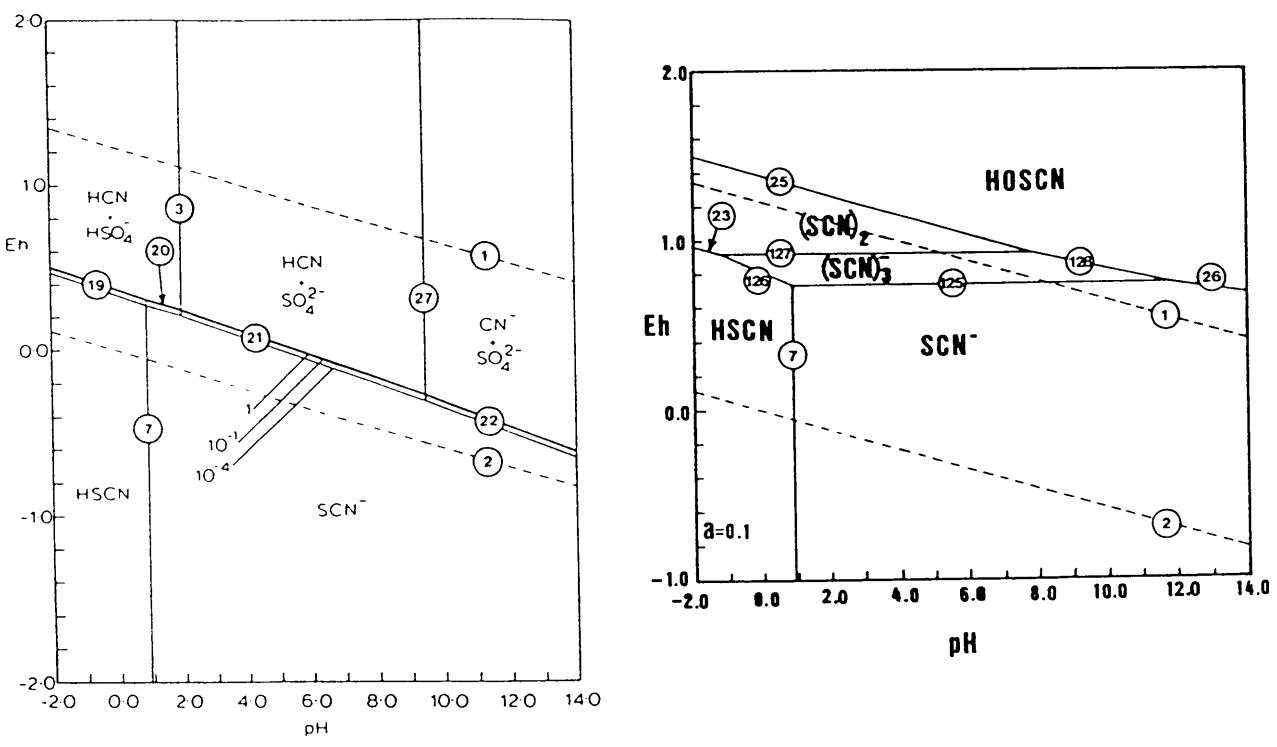


Figure 4.6 - Eh-pH diagrams for the $SCN-H_2O$ system: **(a)** metastable diagram considering oxidation to HCN/CN^- and **(b)** calculation considering only the intermediate species in the thiocyanate oxidation.

The standard potential for the redox couple Fe^{3+}/Fe^{2+} is [12, 19]:

$$Fe^{3+} + e = Fe^{2+} \qquad E^{o} = 0.771\ V \qquad (4.15)$$

By definition, this E° value corresponds to activity 1 for both cations. The specific form of the Nernst equation for this reversible couple is:

$$E = 0.771 - 0.0591 \log \frac{\{Fe^{2+}\}}{\{Fe^{3+}\}} \qquad (4.16)$$

The mixed potentials in iron-thiocyanate solutions are mainly determined by the redox couple Fe^{2+}/Fe^{3+}. However, both Fe^{3+} and Fe^{2+} cations are, to some extent, complexed by SCN^-. The effect of complexation on the reversible potential of an electrode is explained by Burkin [148]. It is usual, in order to calculate the electrode potential, to consider the uncomplexed cations as the only potential determining species, and to consider that the effect of complex formation is to reduce their activities [148]. In the present case, the electrode is the Fe^{3+}/Fe^{2+} couple. Therefore, for equation 4.16 to be valid for an iron(III)-thiocyanate solution, the logarithmic term $\{Fe^{2+}\}/\{Fe^{3+}\}$ must be related to the analytic concentrations of Fe^{2+} and Fe^{3+} in solution, to the stability constants of the several ferric and ferrous complexes with thiocyanate, and to the respective activity coefficients.

Due to the much greater ability of SCN^- to complex Fe^{3+} in comparison to Fe^{2+}, increases in the activity of free SCN^- cause reductions in the activity of Fe^{3+} which are more pronounced that the corresponding reductions in the activity of Fe^{2+}. This explains the lowering of potential with increasing free SCN^- concentration observed in **Figure 4.4**.

This explanation also applies to the decrease in the potential readings with the progress of the autoreduction, illustrated by **Figure 4.5**. The reduction of complexed Fe^{3+} to Fe^{2+} releases free

SCN^-, which causes a stronger complexation of the remaining Fe^{3+}. Thus, the decrease in the mixed potential with the progress of the autoreduction is due not only to the increase in the Fe^{2+}/Fe^{3+} molar ratio but also to the further decrease in the activity of the remaining Fe^{3+} caused by that stronger complexation.

At least two other redox couples contribute to the mixed potential readings:

$$(SCN)_3^- + 2e = 3\ SCN^- \qquad E° = 0.68\ V \qquad (4.17)$$

$$(SCN)_2 + 2e = 2\ SCN^- \qquad E° = 0.77\ V \qquad (4.18)$$

The intermediate species $(SCN)_3^-$ and $(SCN)_2$, which are responsible for the thiocyanate oxidation overpotentials, are produced as Fe^{3+} is reduced to Fe^{2+}.

Although the above reported experiments were conducted in a nitrogen atmosphere, aerated replicates did not shown any noticeable contribution of dissolved oxygen to the potential readings. The autoreduction rate was not affected either. This subject will be resumed in Section 4.7.

In view of the above analysis of the factors determining the mixed potentials in iron-thiocyanate solutions, a mathematical model for predicting them would have to include, at least, the standard potentials for the couples Fe^{3+}/Fe^{2+}, $(SCN)_3^-/SCN^-$ and $(SCN)_2/SCN^-$, the stability constants for the ferric thiocyanate complexes, the stability constant for the ferrous thiocyanate complex, the concentrations of free SCN^-, $(SCN)_3^-$ and $(SCN)_2$, and the activity coefficients of these species. The success of such an attempt does not seem to be certain. Activity coeffici ents are lacking for most species and concentrations of $(SCN)_3^-$ and $(SCN)_2$

are not stable due to hydrolysis. As the system as a whole is not in equilibrium, rate equations would have to be included. Despite all this complexity, any hydrometallurgical system would be even more complex, involving other constituents such as sulphur species, other metal redox couples, mixed complexes of Fe^{3+} and Fe^{2+} with SCN^-, OH^-, SO_4^{2-}, and so on. For all these reasons, attempts to build a mathematical model for the system were considered beyond the scope of this work.

For the present purposes it seems sufficient to recognize that the potential readings reported in this and the next chapters correspond to mixed potentials mainly determined by the Fe^{3+}/Fe^{2+} redox couple, plus its complexation by SCN^-, with the redox couples $(SCN)_3^-/SCN^-$ and $(SCN)_2/SCN^-$ also contributing to the measured values.

4.5. Stability of Ferric Thiocyanate Solutions Towards Iron Precipitation: pH Constraint

The effect of pH on the stability of iron(III)-thiocyanate solutions was initially demonstrated by a few experiments whose results are shown in **Figures 4.7** and **4.8**. These were aerated experiments conducted at room temperature (*c.a.* 23°C) in a stirred glass reactor fitted with pH, Ag/AgCl reference, and Pt electrodes.

In the case of **Figure 4.7**, the thiocyanate concentration was 0.10 mol/dm^3 and the pH was kept constant by additions of H_2SO_4 or NaOH, as applicable. A 1 mol/dm^3 Fe^{3+} alum solution was sequentially dispensed in order to obtain Fe^{3+} concentrations from 0.001 to 0.1 mol/dm^3, and the potential readings were taken as soon as the electrode response became stable (i.e. as soon as the potential reading stopped increasing). At pH 2 the potential

measurements increased steadly with the additions of Fe^{3+}. At pH 3 there was a slight increase at very low Fe^{3+} concentrations, but subsequent additions led to nucleation and precipitation, with corresponding decreases in the potential readings.

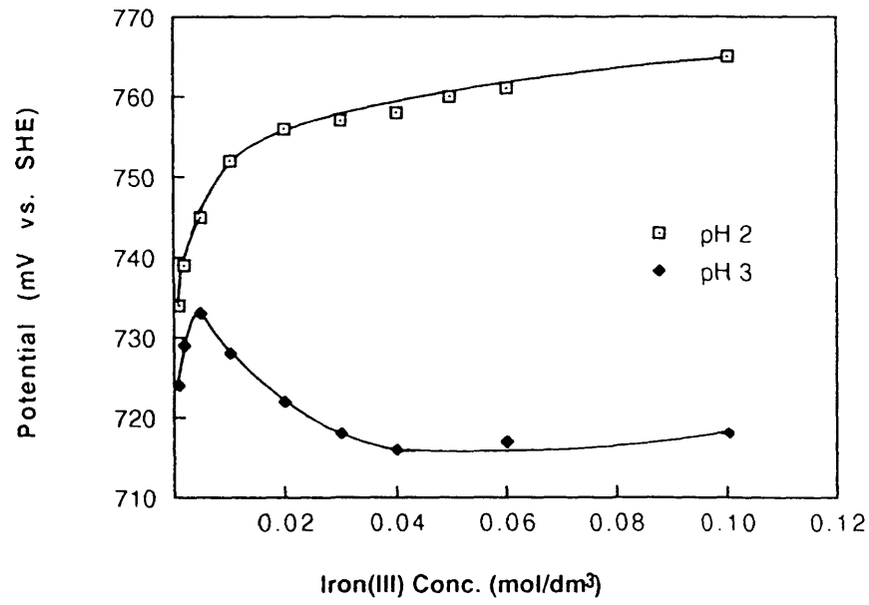


Figure 4.7 - Effect of the iron(III) concentration on the potential readings in fresh thiocyanate solutions at pH 2 and 3. Thiocyanate concentration: 0.10 mol/dm^3; temperature: *c.a.* 23°C.

The same behaviour is further demonstrated by **Figure 4.8**. In these experiments, both the Fe^{3+} and SCN^- concentrations were initially fixed. The pH was adjusted and the potential readings taken as above reported. In all cases, there was a sharp decrease in the potential readings above pH 2.5, corresponding to the precipitation of Fe^{3+}, which was easily observed above pH 2.5.

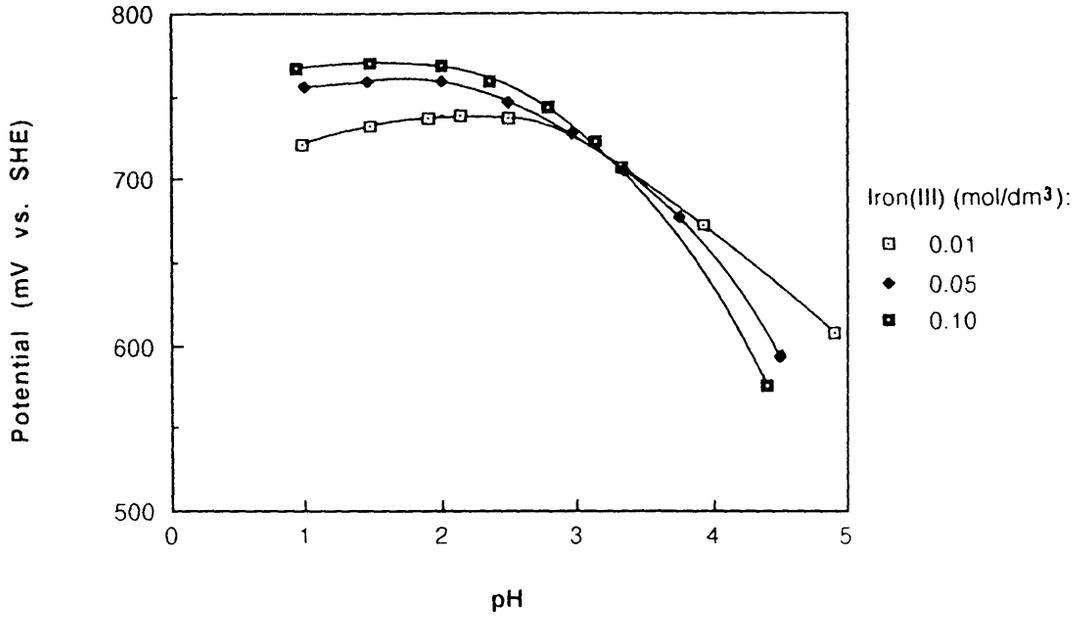


Figure 4.8 - Variation in potential readings in fresh thiocyanate solutions as iron(III) is precipitated by raising the pH, at *c.a.* 23°C. Thiocyanate concentration: 0.10 mol/dm^3.

A good review of the hydrolysis of inorganic iron(III) salts was made by Flynn [149], who quotes the following hydrolysis reactions as yielding species in aqueous solution:

$$Fe^{3+} + H_2O \rightarrow FeOH^{2+} + H^+ \qquad (4.19)$$

$$FeOH^{2+} + H_2O \rightarrow Fe(OH)_2^+ + H^+ \qquad (4.20)$$

$$Fe(OH)_2^+ + H_2O \rightarrow Fe(OH)_3 + H^+ \qquad (4.21)$$

$$Fe(OH)_3 + H_2O \rightarrow Fe(OH)_4^- + H^+ \qquad (4.22)$$

$$2Fe^{3+} + 2H_2O \rightarrow Fe_2(OH)_2^{4+} + 2H^+ \qquad (4.23)$$

$$3Fe^{3+} + 4H_2O \longrightarrow Fe_3(OH)_4^{5+} + 4H^+ \qquad (4.24)$$

In thiocyanate solutions the reactions are certainly more complex due to the formation of mixed complexes such as $[Fe(OH)(NCS)(H_2O)_4]^+$ and others [31, 131], besides the iron(III)-thiocyanate complexes already considered. Addition of base displaces the above reactions to the right and causes precipitation. The characterized crystalline Fe^{3+} oxides and hydrous oxides are Fe_2O_3 and FeO(OH), each of which is polymorphic. The phases important in the hydrolysis and precipitation of Fe^{3+} salts are listed by Flynn [149].

It was important to have, in all experiments reported in this work, a correspondence between iron additions and concentrations in solution, without any precipitation taking place. A series of experiments at 23-60°C was then conducted in order to determine the pH constraint towards iron(III) precipitation. This investigation and the results are reported in the Appendix 4. Infrared analysis of the material precipitated showed that it consisted mainly of goethite, FeO(OH). It was found that pH values above 2 would cause precipitation at higher temperatures. On the other hand, pHs below 1 would cause considerable protonation of SCN^- into HSCN (see Chapter 2, Section 2.3), which would reduce the activity of the ligand besides increasing the consumption of acid. As a consequence, most of the experiments were run at pH 1.5.

4.6. Thiocyanate Oxidation by Iron (III): Experimental

4.6.1. Variables Studied and Respective Ranges

The main purpose of the experimental work reported in this chapter was to investigate the autoreduction process in iron(III)-

thiocyanate solutions over long periods of time and wide concentration ranges of Fe^{3+} and SCN^-. The experiments were conducted at pH 1.5 (with a few exceptions at pH 1 and 2) and most of them were extended for 18 days. The variables studied and respective ranges were:

Thiocyanate concentration:	0.05 to 0.50 mol/dm^3
Iron(III) concentration:	0.01 to 0.10 mol/dm^3
Temperature:	25 to 55°C

4.6.2. Experimental Procedure

The initial experiments were performed in a stirred glass reactor fitted with pH, Ag/AgCl reference and Pt electrodes. The reactor was immersed in a thermostatically controlled water bath. The reactor was aerated (i.e., not sealed to the atmosphere). A freshly prepared potassium thiocyanate solution was put into the reactor and acidified with 1.8 mol/dm^3 H_2SO_4 to pH 1.5. Ferric alum was then added as a standard stock solution and this was considered the zero time. Comparative experiments were also made in nitrogen and in air sparged atmospheres, neither showing any significant alteration in the potential readings and autoreduction rates. Further comparative experiments were made in conical flasks placed in a thermostatically controlled shaker. These gave the same results as the respective replicate runs in the stirred reactor. As a consequence of these comparisons, most of the experiments (particularly those extended for 18 days) were aerated and conducted in the shaker. Samples were collected at regular times and analyzed spectrophotometrically for Fe^{2+} and argentimetrically for thiocyanate. Potential and pH readings were also taken at regular

times. The results are tabulated in Appendix 5. Analytical grade reagents were used in all experiments (see Appendix 7).

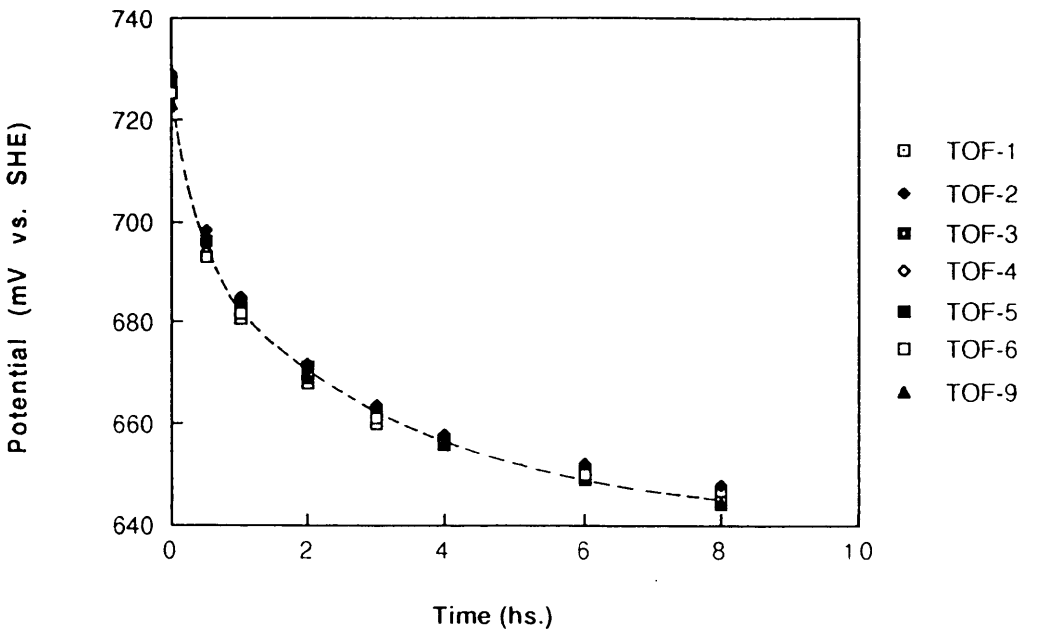
4.7. Thiocyanate Oxidation by Iron (III): Results and Discussion

4.7.1. Experimental Reproducibility

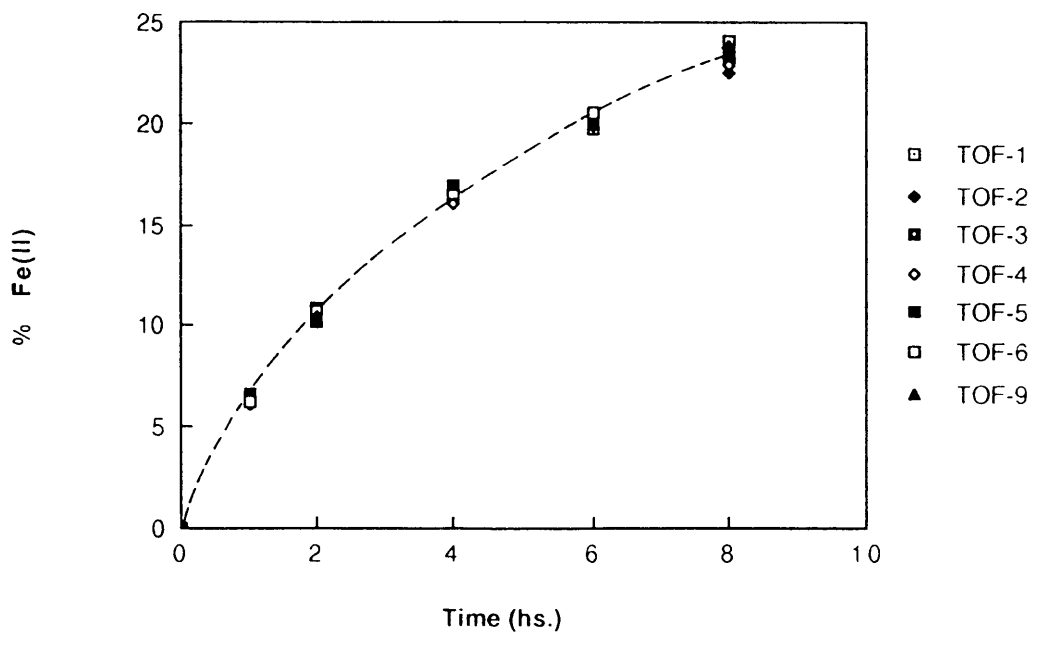
Reproducibility runs are shown in **Figure 4.9**. The potential readings appear in **Figure 4.9a**. The Fe^{2+} analyses appear in **Figure 4.9b** as the percentage of this cation over the total iron content which, at zero time, corresponded entirely to the ferric ions added. All the corresponding numerical data are reported in Appendix 5.

Figure 4.9 shows very good reproducibility. In fact, as far as potential readings and Fe^{2+} production (i.e. autoreduction rates) are concerned, reproducibility was never a problem with such experiments.

Most of the runs shown in **Figure 4.9** were aerated (reactor open to the atmosphere). In one of the runs (TOF-5), the reactor was thoroughly flushed with N_2 but the results were the same, suggesting that oxygen practically does not interfere in the autoreduction process. In another run (TOF-6), air was bubbled in order to assure an oxygen saturated solution, and the results did not change either. The possibility of interference of oxygen was checked in several other tests and was proved to be non-existent under the experimental conditions used in this work. This observation is in agreement with previous experimental results which demonstrate that, in the absence of a suitable catalyst, the oxidation of Fe^{2+} by molecular oxygen is a very slow process in acidic solutions, particularly under atmospheric conditions [179-182]. Such slow

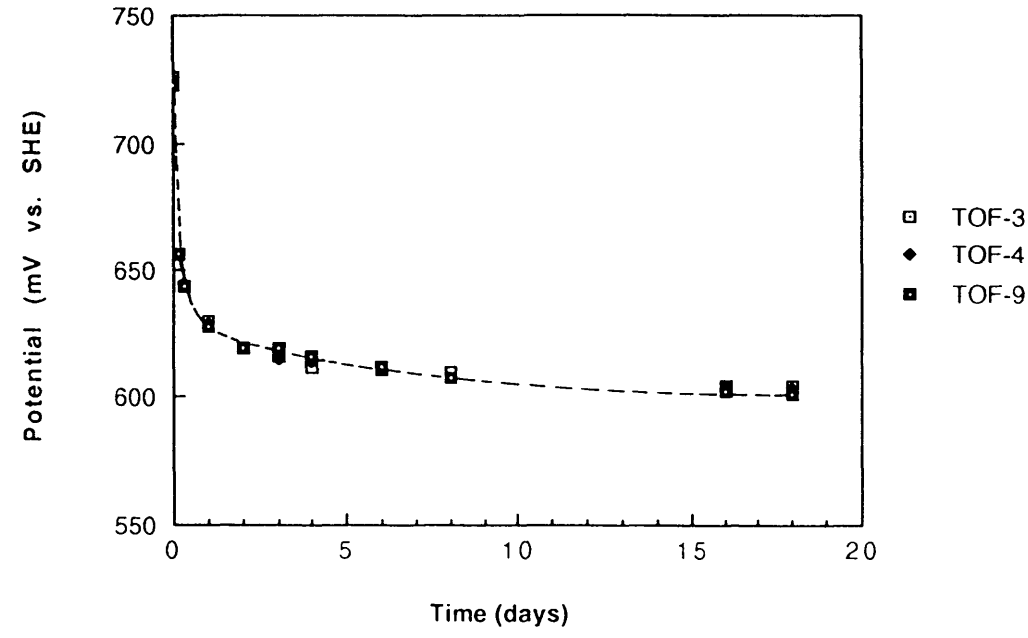


(a)

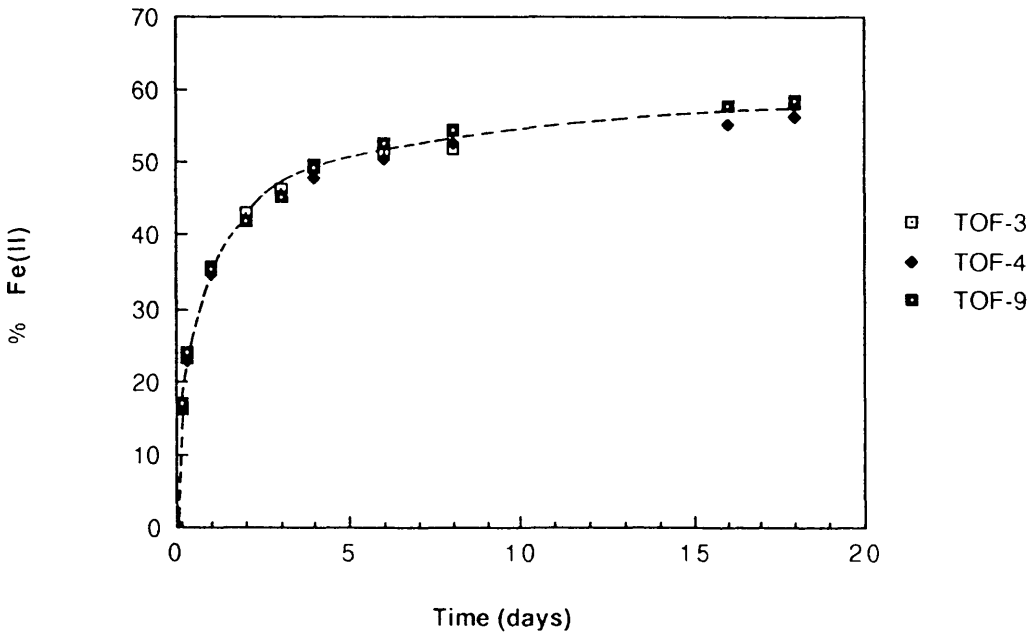


(b)

Figure 4.9 - Thiocyanate oxidation by iron(III): experimental reproducibility of **(a)** potential readings and **(b)** Fe^{3+} reduction. For all experiments: pH 1.5; temperature, 25°C; 0.275 mol/dm^3 SCN^- and 0.055 mol/dm^3 Fe^{3+} (initial concentrations).



(a)



(b)

Figure 4.10 - Thiocyanate oxidation by iron(III): experimental reproducibility of **(a)** potential readings and **(b)** Fe^{3+} reduction. For all experiments: pH 1.5; temperature, 25°C; 0.275 mol/dm^3 SCN^- and 0.055 mol/dm^3 Fe^{3+} (initial concentrations).

oxidation is even more difficult to be observed amidst the autoreduction of ferric thiocyanate.

Among the five aerated runs presented in **Figure 4.9**, three were performed in the stirred reactor and two in conical flasks kept in a thermostatically controlled shaker, as described above. The results were practically the same.

When the runs were prolonged for several days, the autoreduction process slowed down and tended to a condition of metastable equilibrium (the potential was still above that required for thiocyanate oxidation, as already shown in the Eh-pH diagrams) As seen in **Figures 4.10a** and **b**, most of the Fe^{3+} reduction and potential drop took place in the first 2 or 3 days, and the first 4 or 8 hours contributed more than the last 15 days. After some Fe^{2+} is produced, the Fe^{3+} reduction is counteracted by the reverse reaction, i.e. the reoxidation of Fe^{2+}, which is not sufficient to reverse the overall tendency but causes a marked decrease in the autoreduction rate. Reaction mechanisms both for the autoreduction and the reoxidation of Fe^{2+} will be discussed below, in Section 4.10.

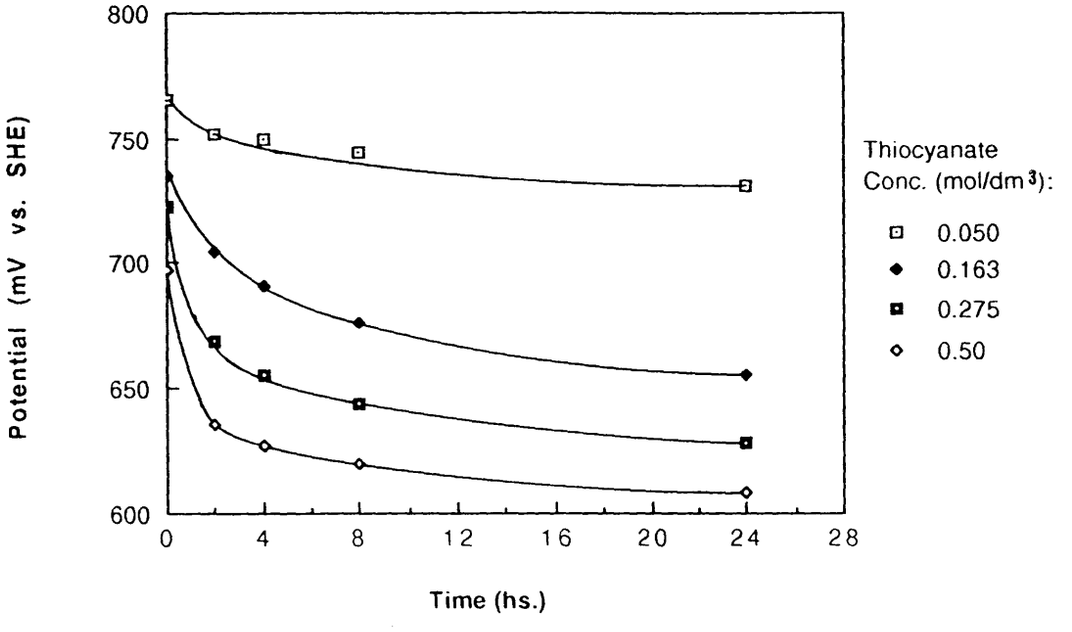
4.7.2. Effect of the Concentrations of Thiocyanate and Iron(III)

The effect of thiocyanate concentration on the potential readings and Fe^{3+} reduction is seen in **Figures 4.11a** and **b**. Data from the same experiments, which lasted 18 days, are also shown in **Figures 4.12a** and **b**. The initial concentration of Fe^{3+} is 0.055 mol/dm^3 in the four experiments. The upper curve (0.05 mol/dm^3 thiocyanate) corresponds to the formation of the cationic complexes $FeNCS^{2+}$ and $Fe(NCS)_2^{+}$, besides some uncomplexed Fe^{3+}. In the runs with higher total thiocyanate, the free thiocyanate concentration is accordingly higher and the neutral and anionic complexes,

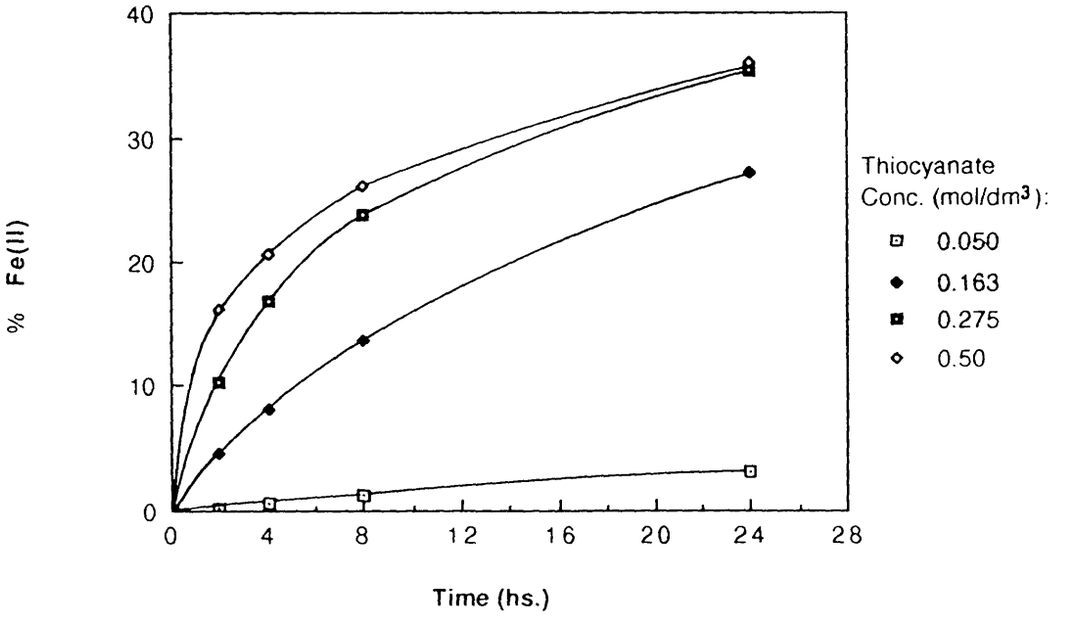
particularly $Fe(NCS)_4^-$, predominate (see **Figures 4.1** through **4.3**). As the autoreduction proceeds, both Fe^{2+} and $FeNCS^+$ are also found in solution.

The first fact to be noticed in **Figures 4.11a** and **4.12a** is the lowering of the initial potential readings due to the increasing ligand number of the complexes formed, an effect already discussed. The second fact is the increase in the initial rate of potential drop with increasing ligand number of the predominant complex. This corresponds to increasing initial autoreduction rates with increasing thiocyanate concentrations (**Figures 4.11b** and **4.12b**). It is apparent that the higher the ligand number, the faster the inherent autoreduction rate of the ferric thiocyanate complex. The Fe^{2+} and $FeNCS^+$ produced in solution tend to counteract the reduction process. As a consequence, in the runs with higher free thiocyanate concentrations, the overall autoreduction process is much faster in the initial moments and then slows down drastically, due to the marked Fe^{2+} and $FeNCS^+$ build up in solution. For lower free thiocyanate concentrations, on the other hand, the initial autoreduction rate is lower and, as the Fe^{2+} and $FeNCS^+$ production is also slower, the overall rate decrease is more gradual.

It should be noticed that in all autoreduction experiments discussed here there is a change in the speciation of the system as the reactions proceed. In the beginning of each experiment, there is a certain distribution of complexes in solution (see **Figures 4.1** through **4.3**). Because thiocyanate complexes Fe^{3+} much more strongly than Fe^{2+}, the progress of the autoreduction process releases SCN^- and causes an increase in the free thiocyanate concentration. Consequently, there is a continuous shift in the distribution of the ferric complexes towards higher ligand numbers, simultaneously with the production of Fe^{2+} and $FeNCS^+$. This causes a continuous change in the speciation of the system. Considering now, from the kinetic standpoint, that each ferric complex has an inherent autoreduction rate, the overall rate of the autoreduction process appears to be the resultant of several simultaneous individual rates. Furthermore, the overall autoreduction rate changes

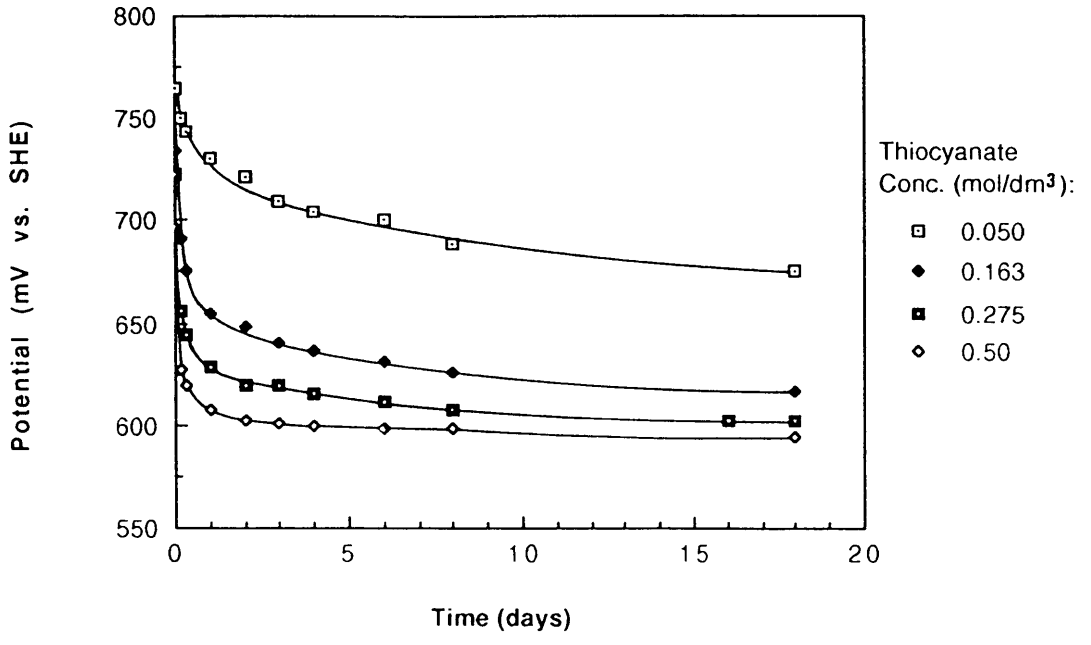


(a)

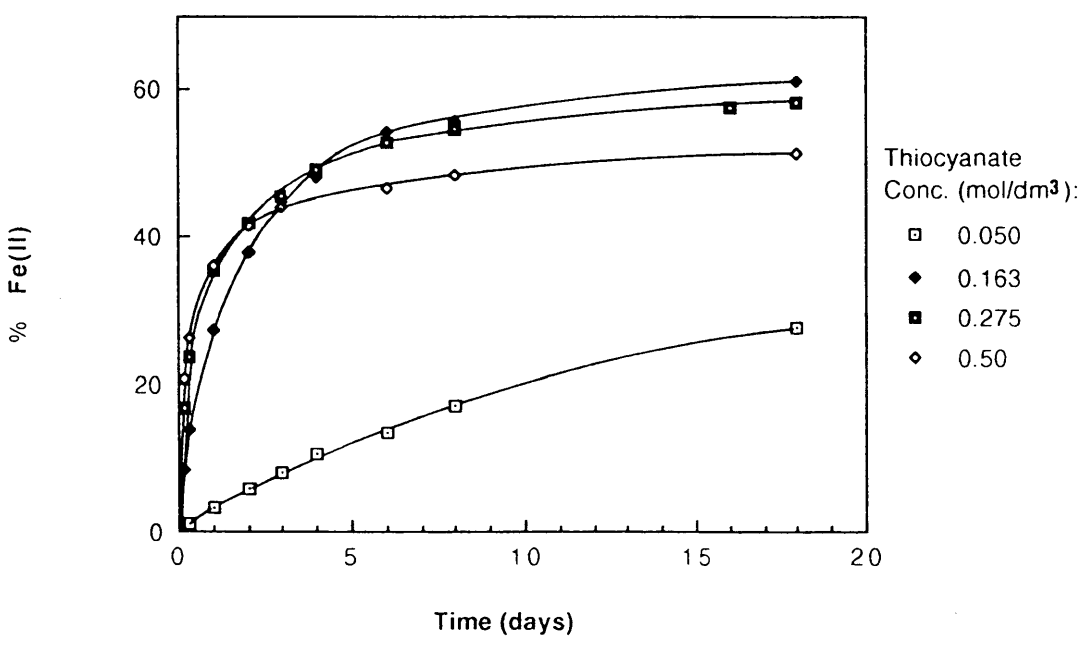


(b)

Figure 4.11 - Effect of thiocyanate concentration on the autoreduction process: **(a)** potential readings; **(b)** Fe^{3+} reduction. For all experiments: pH 1.5; temperature, 25°C; 0.055 mol/dm^3 Fe^{3+} (initial concentration).



(a)



(b)

Figure 4.12 - Effect of thiocyanate concentration on the autoreduction process: **(a)** potential readings; **(b)** Fe^{3+} reduction. For all experiments: pH 1.5; temperature, 25°C; 0.055 mol/dm^3 Fe^{3+} (initial concentration).

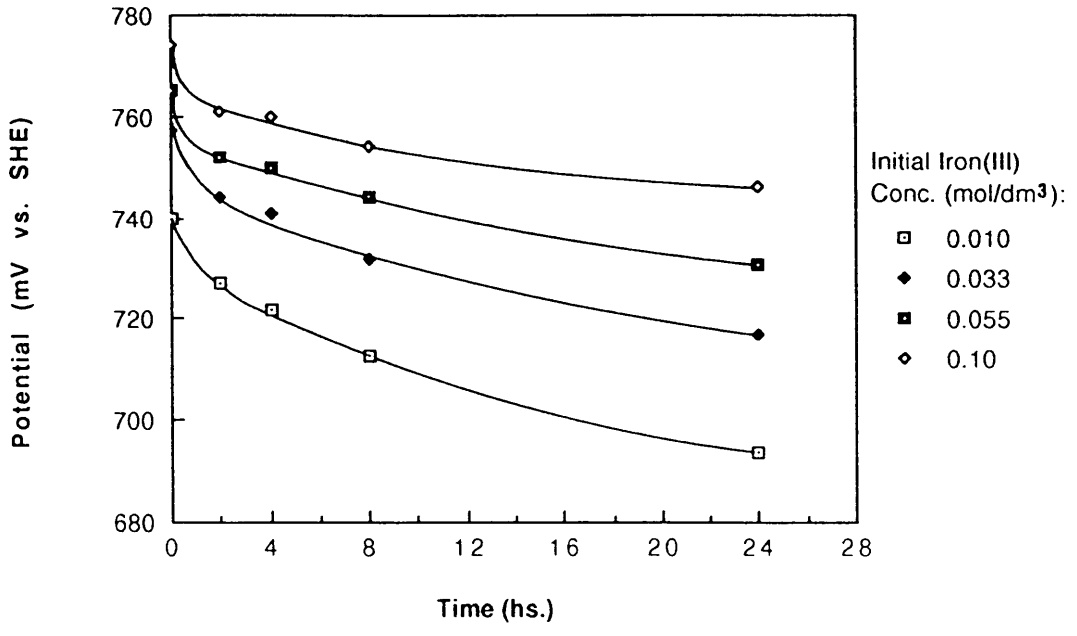
not only due to the build up of Fe^{2+} and $FeNCS^{+}$ (reverse reactions), but also due to that shift in the distribution of ferric complexes with time.

Three more series of four 18-day long experiments each, like the ones shown in **Figures 4.11** and **4.12**, were performed with initial Fe^{3+} concentrations of 0.010, 0.033 and 0.10 mol/dm^3 for each series, respectively. The results are similar, and the numerical data are all tabulated in Appendix 5.

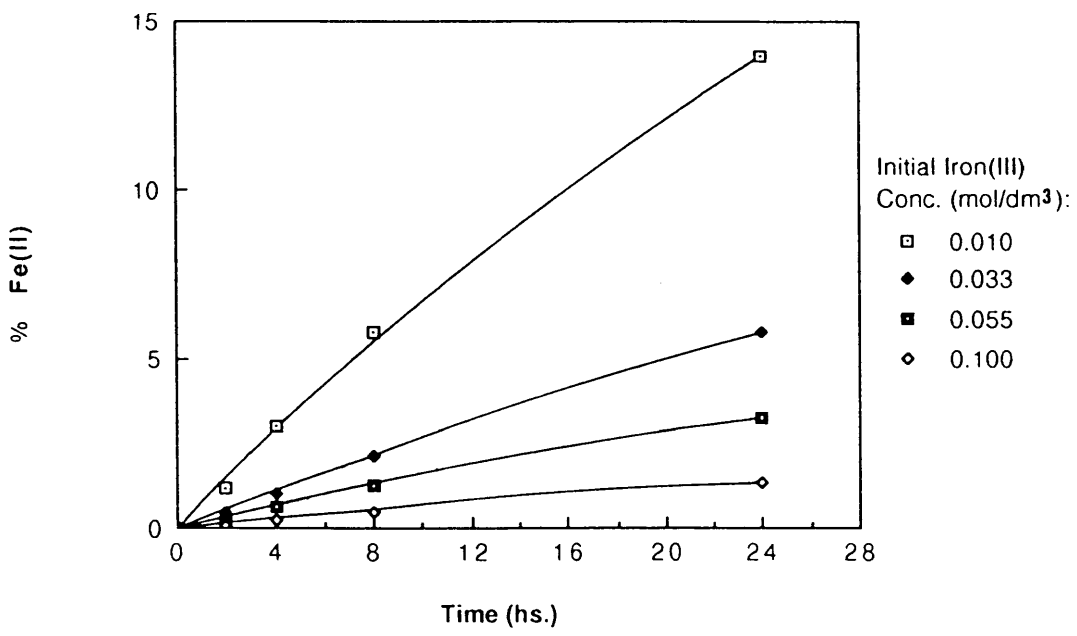
A different way of visualizing the same behaviour described above is by considering a fixed thiocyanate concentration and increasing the initial Fe^{3+} concentration. This is seen in **Figures 4.13** and **4.14** for 0.05 mol/dm^3, and in **Figures 4.15** and **4.16** for 0.275 mol/dm^3 of thiocyanate.

The cationic complexes $FeNCS^{2+}$ and $Fe(NCS)_2^{+}$ are practically the only two formed in the experiments shown in **Figures 4.13** and **4.14**. The initial rates of potential drop and Fe^{3+} reduction are slow (compared with those shown in **Figures 4.15** and **4.16**) and decrease very gradually with the progress of the autoreduction process. When, instead, the total thiocyanate concentration is fixed in 0.275 mol/dm^3, as in **Figures 4.15** and **4.16**, the initial rates are much faster but soon slow down drastically due to the also much faster build up of Fe^{2+} and $FeNCS^{+}$.

The retarding effect of ferrous species on the autoreduction of ferric species is further demonstrated in **Figures 4.17a** and **b**. These three runs were started with 10, 30 and 50% of the total iron content respectively being present as Fe^{2+}. The higher the initial percentage of Fe^{2+}, the slower the autoreduction rate and potential drop.

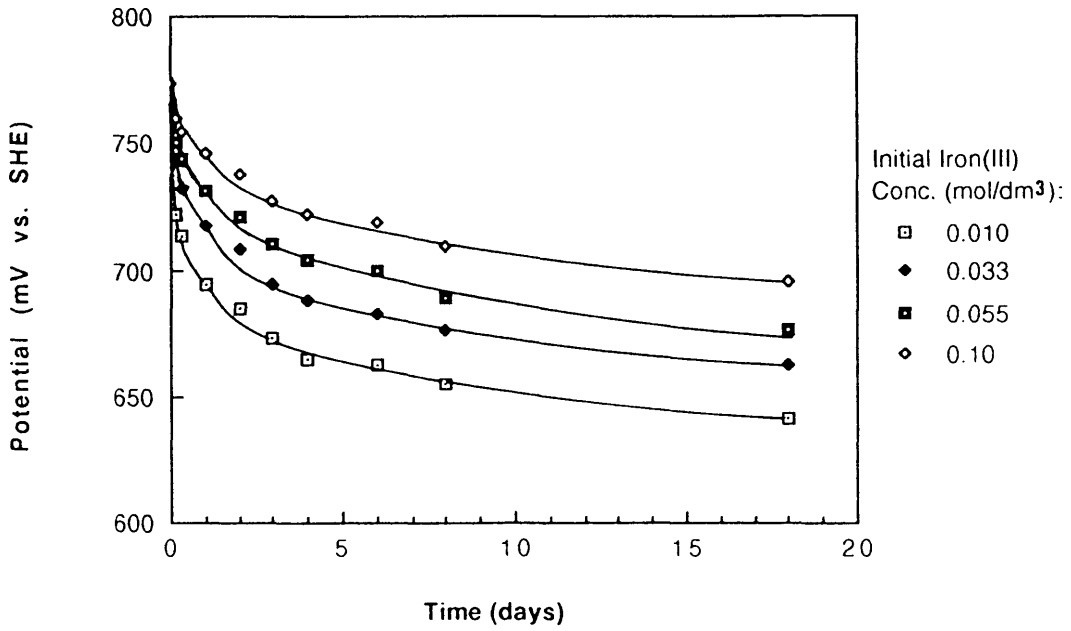


(a)

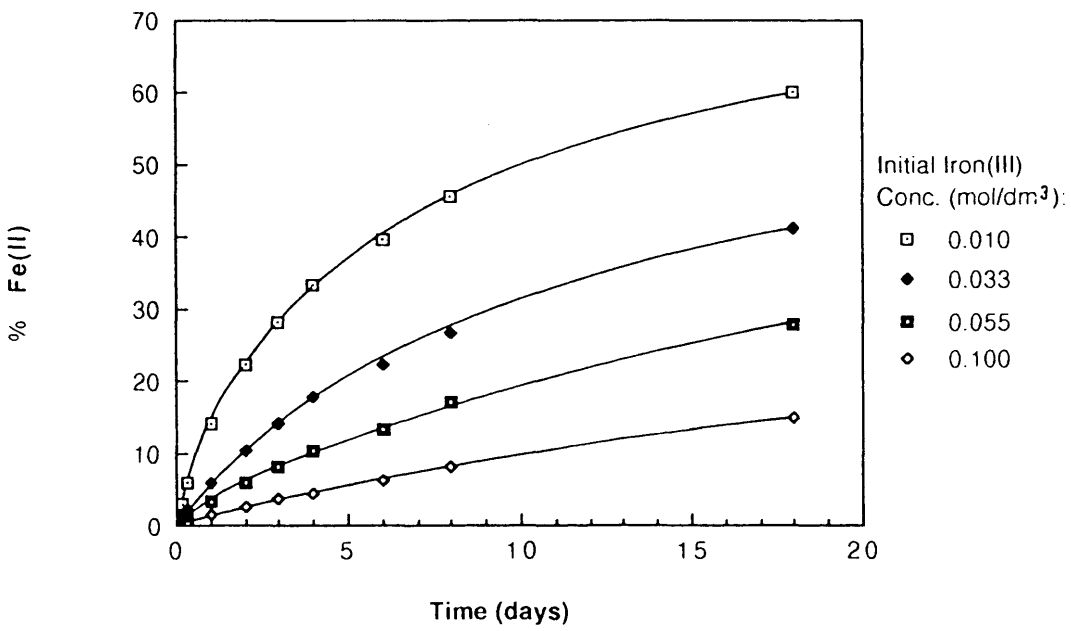


(b)

Figure 4.13 - Effect of Fe^{3+} concentration on the autoreduction process with predominance of the cationic complexes $FeNCS^{2+}$ and $Fe(NCS)_2^{+}$: **(a)** potential readings; **(b)** Fe^{3+} reduction. For all experiments: pH 1.5; temperature, 25°C; 0.050 mol/dm^3 SCN^- (initial concentration).

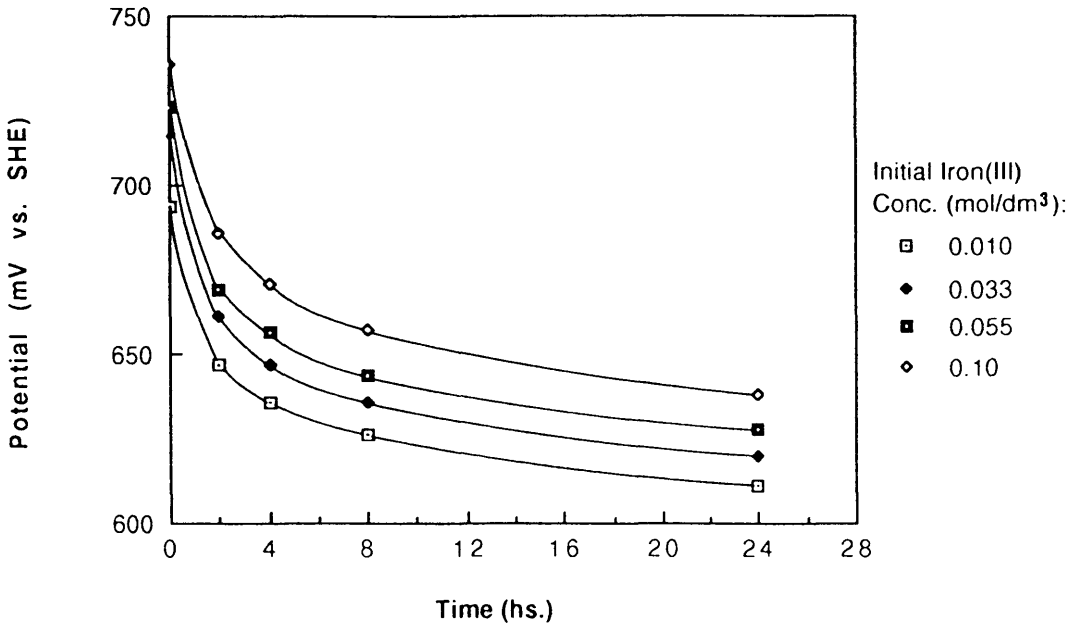


(a)

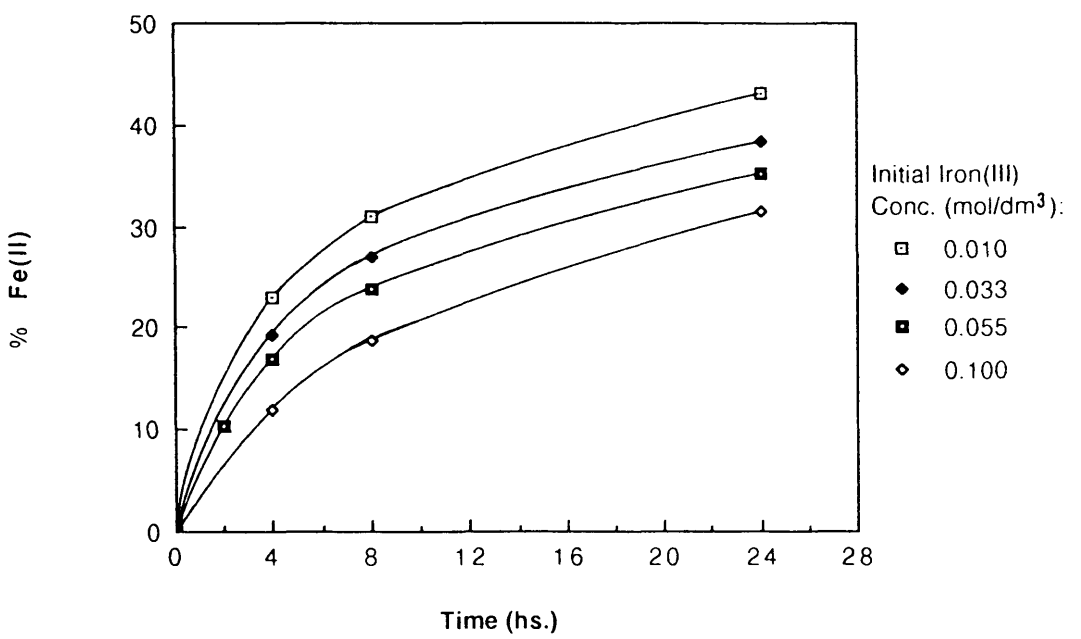


(b)

Figure 4.14 - Effect of Fe^{3+} concentration on the autoreduction process with predominance of the cationic complexes $FeNCS^{2+}$ and $Fe(NCS)_2^{+}$: **(a)** potential readings; **(b)** Fe^{3+} reduction. For all experiments: pH 1.5; temperature, 25°C; 0.050 mol/dm^3 SCN^- (initial concentration).

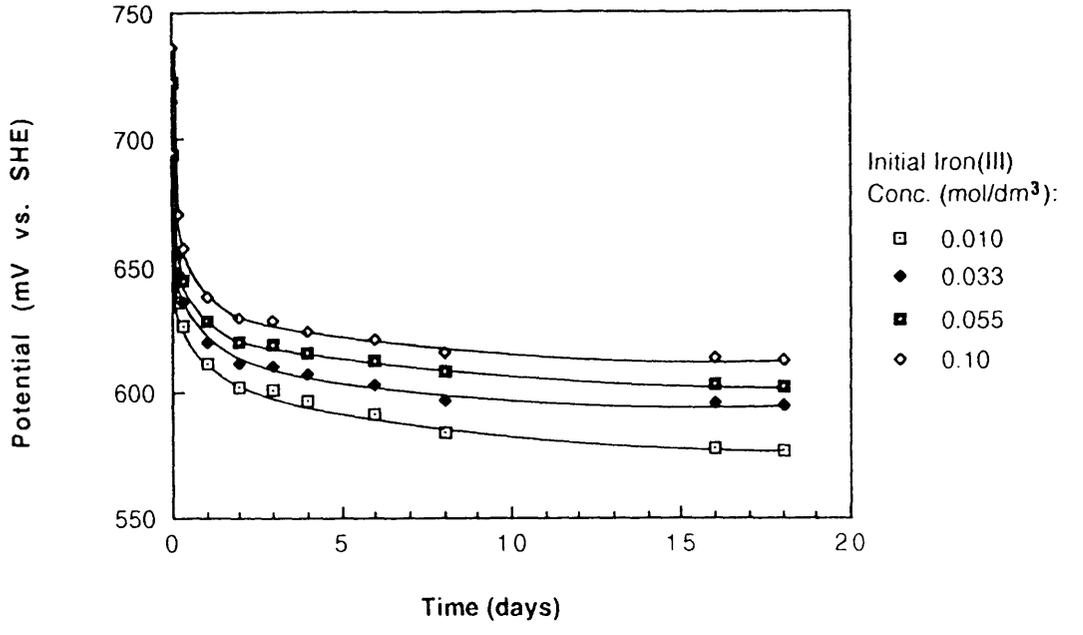


(a)

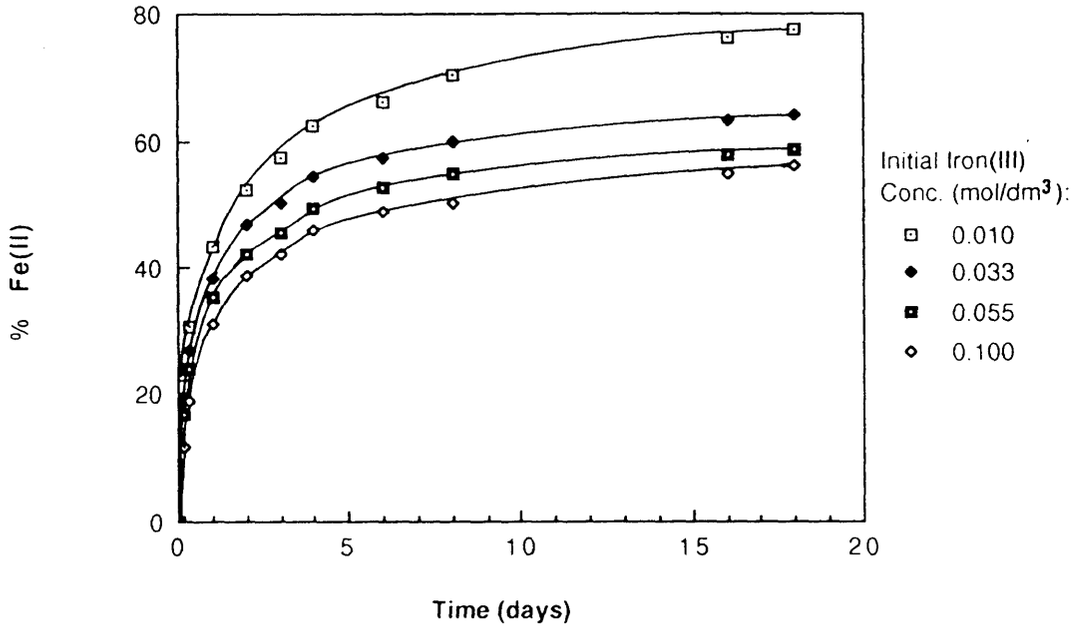


(b)

Figure 4.15 - Effect of Fe^{3+} concentration on the autoreduction process with predominance of the anionic complexes : **(a)** potential readings; **(b)** Fe^{3+} reduction. For all experiments: pH 1.5; temperature, 25°C; 0.275 mol/dm^3 SCN^- (initial concentration).

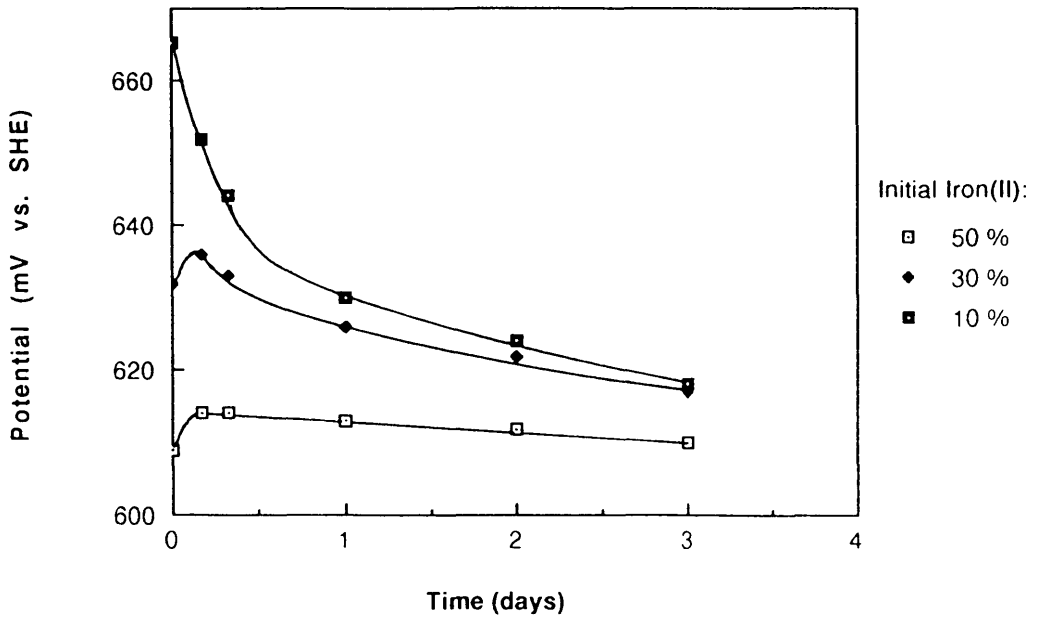


(a)

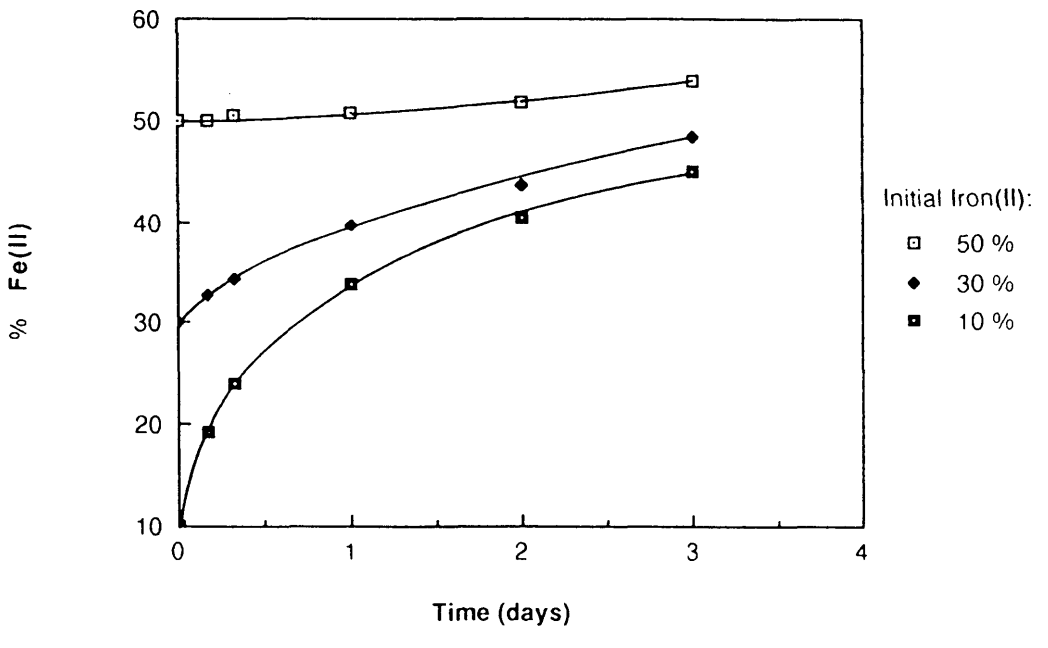


(b)

Figure 4.16 - Effect of Fe^{3+} concentration on the autoreduction process with predominance of the anionic complexes: **(a)** potential readings; **(b)** Fe^{3+} reduction. For all experiments: pH 1.5; temperature, 25°C; 0.275 mol/dm^3 SCN^- (initial concentration).



(a)



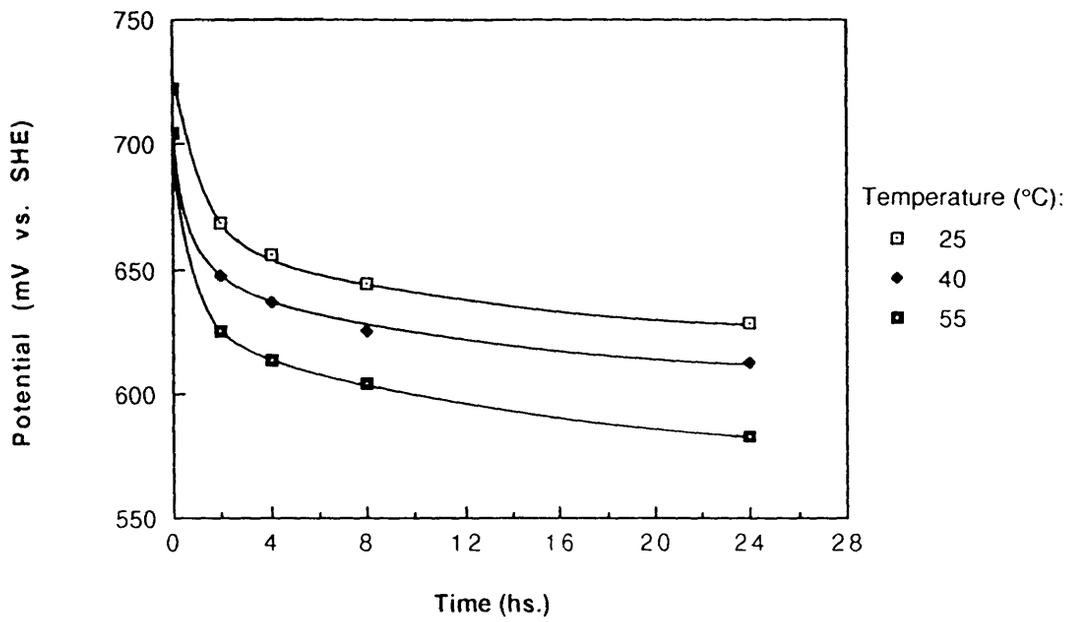
(b)

Figure 4.17 - Retarding effect of Fe^{2+} on the autoreduction process: **(a)** potential readings; **(b)** Fe^{3+} reduction. For all experiments: pH 1.5; temperature, 25°C; total iron in solution, 0.055 mol/dm^3; 0.275 mol/dm^3 SCN^- (initial concentration).

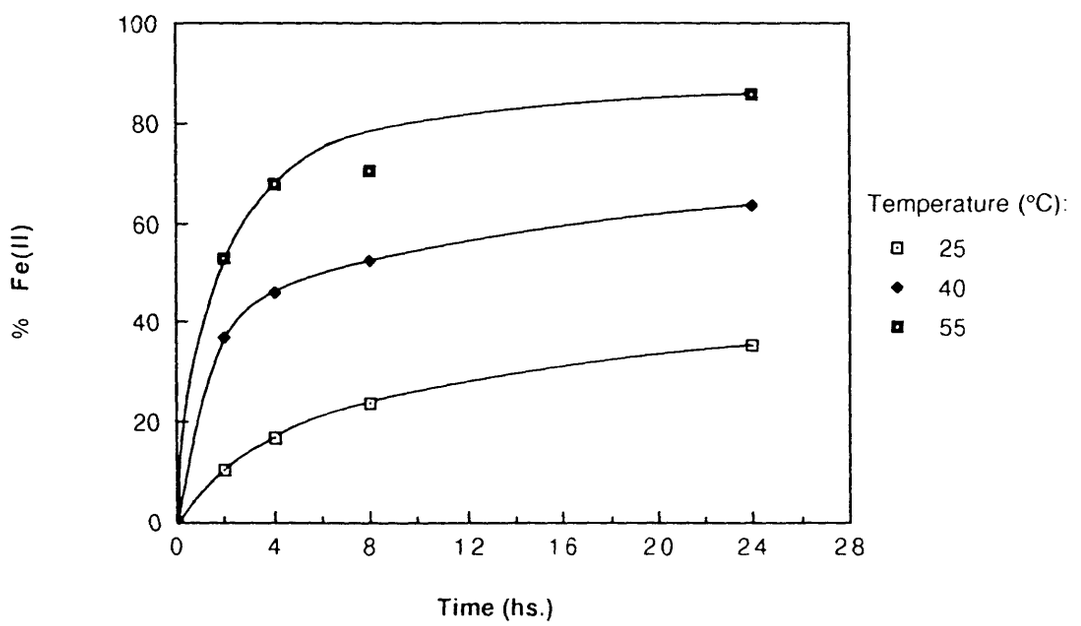
4.7.3. Effect of Temperature

The effect of temperature on the autoreduction process is illustrated in **Figures 4.18a** and **b**. Initial autoreduction rates from three series of experiments at several temperatures were used in the Arrhenius plot shown in **Figure 4.19**, the respective activation energies being listed in **Table 4.1**.

The experiments illustrated in **Figures 4.18a** and **b** started with 0.275 mol/dm^3 of SCN^- and 0.055 mol/dm^3 Fe^{3+}, which are the same concentrations used to demonstrate the experimental reproducibility (**Figures 4.9** and **4.10**). It means that the predominant complex is the anion $Fe(NCS)_4^-$. Other complexes should also be present in minor amounts, according to the distribution curves (see **Figures 4.1** through **4.3**). The activation energy for the initial autoreduction process in these conditions was estimated to be 85.5 kJ/mol. In contrast, the activation energy for the initial process with 0.05 mol/dm^3 SCN^- and 0.055 mol/dm^3 Fe^{3+}, corresponding mainly to the complex $FeNCS^{2+}$, was estimated in 142.8 kJ/mol, while the value found with 0.10 mol/dm^3 SCN^- and 0.055 mol/dm^3 Fe^{3+}, corresponding to the predominance of the complex $Fe(NCS)_2^+$, was 110.1 kJ/mol. The activation energy of the initial autoreduction reaction decreases with increasing ligand number of the predominant complex involved. This is a further indication (see **Table 4.1**), consistent with the experimental results discussed in the previous section, that each complex has an inherent autoreduction rate, which is higher for the complexes with higher ligand numbers.



(a)



(b)

Figure 4.18 - Effect of temperature on the autoreduction process with predominance of anionic complexes : **(a)** potential readings; **(b)** Fe^{3+} reduction. For all experiments: pH 1.5; 0.275 mol/dm^3 SCN^- and 0.055 mol/dm^3 Fe^{3+} (initial concentrations).

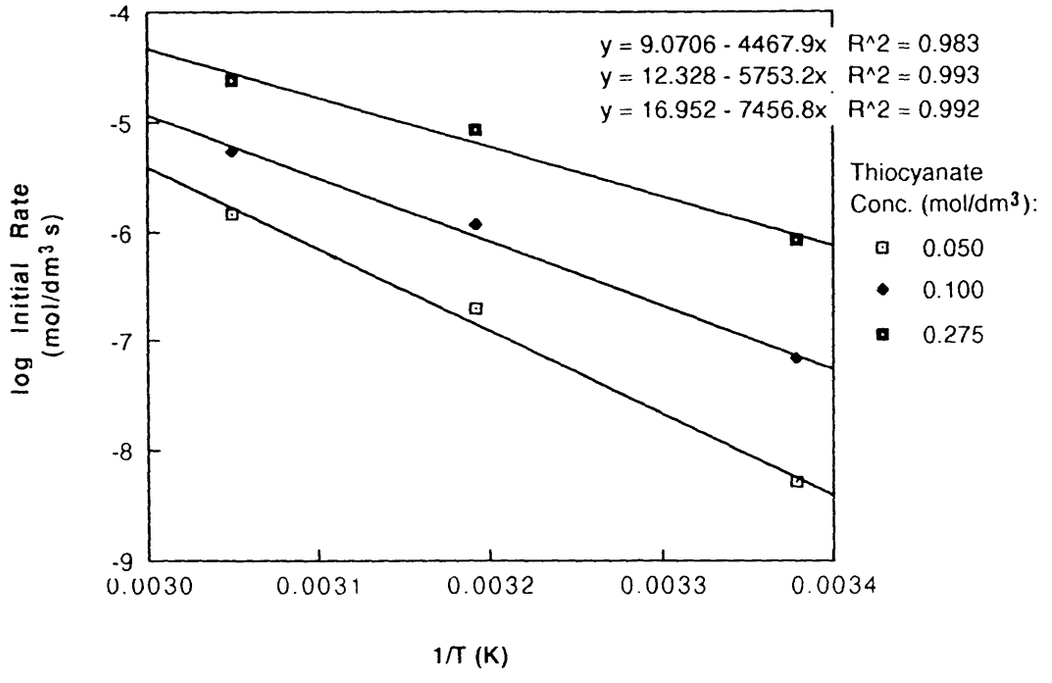


Figure 4.19 - Arrhenius plot for the initial autoreduction reactions of iron(III)-thiocyanate complexes. Experimental conditions: 0.055 mol/dm^3 Fe^{3+} (initial) and pH 1.5.

Table 4.1 - Activation Energies for the Initial Autoreduction Reactions of the Ferric Thiocyanate Complexes at pH 1.5

Initial Concentrations (mol/dm^3)		Predominant Complex	Activation Energy
[SCN^-]	[Fe^{3+}]		(kJ/mol)
0.050	0.055	$FeNCS^{2+}$	142.8
0.100	0.055	$Fe(NCS)_2^+$	110.1
0.275	0.055	$Fe(NCS)_4^-$	85.5

4.8. Thiocyanate Oxidation by Iron(III): Stoicheiometry of the Process

During autoreduction experiments such as those described above, Fe^{3+} is reduced to Fe^{2+} and SCN^- is oxidized. Argentimetric determinations of thiocyanate were carried out extensively in order to determine the stoicheiometry of its oxidation by ferric ions. The results are all tabulated in Appendix 5. Some of them are seen in **Table 4.2**. All the results reveal a minimal consumption of thiocyanate even when the autoreduction experiments are prolonged for 18 days. When confronted with the amount of Fe^{2+} produced at the same time, these titrations suggest that several electrons have to be transferred (i.e. several ferric ions have to be reduced to the ferrous state) in order to oxidize a single thiocyanate ion.

The overall results show a very small consumption of thiocyanate by oxidation by Fe^{3+} during the autoreduction process. Most of the oxidation takes place during the first hours (or days), which is consistent with the higher rates of Fe^{2+} production and potantial decrease observed in the beginning of the experiments. These conclusions are better illustrated by the results listed in Appendix 5. The analytical results are consistent with the redox system:

$$SO_4^{2-} + CN^- + 8H^+ + 6e = SCN^- + 4H_2O \qquad (4.19)$$

If the thiocyanate concentration at each time is estimated by this 6-electron transfer reaction and the spectrophotometric readings of Fe^{2+} produced, instead of by the argentimetric titration, the results are very consistent with the argentimetric ones. **Table 4.3** contains such estimates corresponding to the same experiments shown in **Table 4.2**. More data of this type are reported in Appendix 5. The overall results suggest that the stoicheiometry corresponds to reaction 4.19.

Table 4.2 - Thiocyanate Oxidation by Iron(III): Results of Some Argentimetric Titrations.

Initial Conc. (mol/dm^3)		Temp.	Thiocyanate Conc. (mol/dm^3) and % Oxidized					
			24 hs.		72 hs		18 days	
[SCN$^-$]	[Fe^{3+}]	(°C)	[SCN$^-$]	% Cons.	[SCN$^-$]	% Cons.	[SCN$^-$]	% Cons.
0.050	0.055	25	0.049	2.00	0.049	2.00	0.047	6.00
0.163	0.10	25	-	-	0.157	3.69	0.153	5.85
0.275	0.055	25	0.272	1.09	0.272	1.09	0.270	1.82
0.50	0.10	25	0.494	1.20	0.492	1.60	0.491	1.80
0.275	0.055	40	0.270	1.82	-	-	-	-
0.050	0.10	55	0.046	8.00	-	-	-	-
0.50	0.10	55	0.487	2.60	-	-	-	-

Table 4.3 - Concentrations (mol/dm^3) of Thiocyanate Estimated According to Reaction 4.19 from the Amounts of Fe^{2+} Produced (same experiments shown in **Table 4.2**).

Initial Conc. (mol/dm^3)		Temp.	Fe^{2+} Analyses and Estimation of SCN^- (mol/dm^3)					
			24 hs.		72 hs		18 days	
[SCN$^-$]	[Fe^{3+}]	(°C)	[Fe^{2+}]	[SCN$^-$]	[Fe^{2+}]	[SCN$^-$]	[Fe^{2+}]	[SCN$^-$]
0.050	0.055	25	0.0018	0.050	0.0044	0.049	0.0152	0.047
0.163	0.10	25	0.0174	0.160	0.0343	0.157	0.0556	0.153
0.275	0.055	25	0.0195	0.272	0.0256	0.271	0.0319	0.270
0.50	0.10	25	0.0352	0.494	0.0405	0.493	0.0474	0.492
0.275	0.055	40	0.0387	0.269	-	-	-	-
0.050	0.10	55	0.0299	0.045	-	-	-	-
0.50	0.10	55	0.0774	0.487	-	-	-	-

At pH around 1.5, which is the value adopted in the present work, the cyanide produced will be protonated to HCN and released from solution. This is sometimes noticed as a faint smell of cyanide, fortunately a very small amount indeed, since the overall reaction involves the transfer of six electrons. This means that six Fe^{3+} are required to be reduced to Fe^{2+} in order to oxidize a single SCN^-. As a consequence, the thiocyanate consumption by oxidation is rather small even in those experiments showing extensive autoreduction, such as those at higher temperatures.

Some contribution from a second redox system cannot be ruled out:

$$SO_4^{2-} + CNO^- + 10H^+ + 8e = SCN^- + 7H_2O \qquad (4.20)$$

At the pH value adopted, however, cyanate is protonated to HCNO, which is quickly decomposed to ammonia, and carbonic and sulphuric acids, leading to the system:

$$SO_4^{2-} + CO_3^{2-} + NH_3 + 11H^+ + 8e = SCN^- + 7H_2O \qquad (4.21)$$

Many samples were analyzed for cyanate but it was never detected. Thus, either it was not produced or, if so, was quickly decomposed.

In purely stoicheiometric terms, the autoreduction process is consistent with the following:

$$6Fe^{3+} + SCN^- + 4H_2O \longrightarrow 6Fe^{2+} + HCN + SO_4^{2-} + 7H^+ \qquad (4.22)$$

This overall process is irreversible, as HCN and SO_4^{2-} cannot be reduced back to SCN^-. Reaction 4.20 can be seen as a further irreversible oxidation step leading to cyanate or cyanic acid, which undergo hydrolysis to carbonate and ammonia (reaction 4.21). Thus, the overall oxidation process is irreversible.

4.9. Thiocyanate Hydrolysis

The subject treated in this section is the hydrolysis of SCN^- in acidic medium. It is a process distinct from the hydrolysis of intermediate species in the mechanism of oxidation of thiocyanate by various oxidizing agents, such as Fe^{3+}. The destruction of SCN^- directly by hydrolysis proved to be negligible under the conditions studied here. The hydrolysis of thiocyanic acid in hydrochloric, phosphoric and sulphuric acids was studied by Crowell and Hankins [35] and by Stedman et al. [42]. The hydrolysis proceeds according to the equation:

$$H^+ + HNCS + 2H_2O \longrightarrow H_2S + CO_2 + NH_4^+ \qquad (4.23)$$

The actual mechanism is substantially more complex than this overall reaction, and involves a number of intermediate species whose consideration would go much beyond the scope of the present work. A concise description with the available references is given by Hughes [28]. However, the acid concentrations adopted in the hydrolysis studies mentioned above [35, 42] were generally much higher than those found in a system at pH between 1 and 2, as is the case of the present work. Crowell and Hankins [35] used acid concentrations from 0.05 to 11.11 mol/dm^3. Similarly high concentrations were used by Stedman et al. [42].

The hydrolysis reaction was found to be first order in relation to thiocyanate or thiocyanic acid. On the other hand, the rate was found to increase markedly with the acid concentration. For instance, the rate constant increased from 4.90×10^{-8} s^{-1} at 1.94 mol/dm^3 HCl to 4.48×10^{-4} s^{-1} at 11.1 mol/dm^3 HCl, at 25°C, a 9140-fold increase [35]. With 0.05 mol/dm^3 HCl, the rate constant was estimated to be 4.12×10^{-9} s^{-1} [35]. The behaviour was identical when the other acids quoted above were used [28]. This latter figure also indicates that the hydrolysis rate at acid concentrations below

0.05 mol/dm^3, i.e. pH>1.5, is expected to be minimal.

To investigate this effect, a series of experiments was conducted between 25 and 55°C, at pH 1.5 (*c.a.* 0.022 mol/dm^3 H_2SO_4), and thiocyanate concentrations ranging from 0.05 to 0.50 mol/dm^3. The runs lasted 24 hours and were conducted in neutral (nitrogen) atmosphere, in a stirred reactor immersed in a thermostatically controlled water bath. The thiocyanate concentrations in the samples were determined argentimetrically. The solutions from the runs were then kept for several weeks in stoppered bottles at room temperature (*c.a.* 18°C), and again titrated for thiocyanate.

All the results indicated that, within the investigated conditions, hydrolysis was negligible. No hydrolysis at all was titrimetrically detected in the 24 hour samples. The only evidence of some hydrolysis taking place was a very faint smell of H_2S emanating from the reactor during the runs at higher temperature and higher thiocyanate concentration. The titrations after 8 days did not indicate any hydrolysis either, except for a couple of runs (higher thiocyanate concentrations) which showed 1.8% and 1.5% thiocyanate decomposed. Small amounts of H_2S accumulated in the stoppered bottles after 8 days. Solutions from a couple of runs were left in the bottles for 2 months and then titrated again, showing no further hydrolysis at all.

4.10. Mechanistic Considerations

The autoreduction of ferric thiocyanate complexes can be explained by the following mechanism:

$$Fe(NCS)_n^{3-n} \longrightarrow Fe^{2+} + (n-1)\ SCN^- + SCN^{\cdot} \qquad (4.24)$$

$$Fe(NCS)_n^{3-n} \longrightarrow FeNCS^+ + (n-2)\ SCN^- + SCN^{\cdot} \qquad (4.25)$$

$$SCN^{\cdot} + SCN^- = (SCN)_2^- \qquad (4.26)$$

$$2(SCN)_2^- \longrightarrow (SCN)_2 + 2SCN^- \qquad (4.27)$$

$$2(SCN)_2^- \longrightarrow (SCN)_3^- + SCN^- \qquad (4.28)$$

$$(SCN)_3^- = (SCN)_2 + SCN^- \qquad (4.29)$$

$$3(SCN)_2 + 4H_2O \longrightarrow 5SCN^- + HCN + SO_4^{2-} + 7H^+ \qquad (4.30)$$

Reactions 4.24 and 4.25 correspond to the rate controlling step of the overall process [49, 81, 82, 86]. They indicate basically the production of the free radical $SCN^{\cdot}$ through the breakdown of the ferric thiocyanate complexes. The Fe^{3+} cation shares covalent bonds with n SCN^- anions through the N atoms. The transfer of one of the shared electrons into it causes its reduction to Fe^{2+}. As the ability of SCN^- to complex Fe^{2+} is much smaller than that to complex Fe^{3+}, the ferric thiocyanate complex breaks down releasing (n-1) or (n-2) (reaction 4.24 or 4.25, respectively) free SCN^- ions plus one free radical $SCN^{\cdot}$. The experimental results presented in the previous sections suggest that the ability of a ferric thiocyanate complex to undergo this electron transfer step increases with the number of

SCN^- coordinating the Fe^{3+} ion or, in other words, with increasing concentration of free SCN^- in solution. Thus, the autoreduction of the ferric thiocyanate complexes is a typical inner-sphere transfer mechanism with change in the geometry of the product, differently from what happens, for instance, in the autoreduction of $Fe(CN)_6^{3-}$ to $Fe(CN)_6^{4-}$, where the electron transfer takes place in the outer sphere of the complex and both oxidized and reduced species have basically the same geometry [150, 151].

There is unanimity among researchers about the proposition of formation of the free radical $SCN^{\cdot}$ as the first mechanistic step in the oxidation of SCN^-, which is also regarded as the rate controlling step. This proposition comes from the electrochemical work performed by Gauguin [49], by Cauquis and Pierre [86], by several researchers from Arvia's group [81, 82], and by Itabashi [90, 91]. It also comes from the contributions, using pulse radiolysis and similar techniques, given by Adams et al. [78], Baxendale et al. [73], Schöneshöfer et al. [72, 77], and others [74-76], all of which were discussed in Chapter 3.

The reaction of the free radical $SCN^{\cdot}$ with SCN^- to produce the transitory form $(SCN)_2^-$ (reaction 4.26) was proposed both by Adams et al. [78] and Baxendale et al. [73].

The intermediate species thiocyanogen, $(SCN)_2$, and trithiocyanate, $(SCN)_3^-$, are then formed according to reactions 4.27 and 4.28, which were respectively proposed by Baxendale et al. [73] in 1968 and by Itabashi in 1984 [90] and 1985 [91].

Reaction 4.29 is the equilibrium proposed by Cauquis and Pierre [84] in acetonitrile. This equilibrium is not expected to be established in aqueous solution due to the hydrolysis of those intermediate species. The hydrolysis of $(SCN)_2$ is likely to be faster than that of $(SCN)_3^-$ in acidic medium, due to the relative stabilization of the latter by H^+ observed by Itabashi [90]. This

observation, however, does not rule out the direct hydrolysis of $(SCN)_3^-$. In this context, reaction 4.29 can be taken merely as an indication of the interconvertion between the intermediate species as the overall process progresses.

Reaction 4.30 represents the overall process of $(SCN)_2$ hydrolysis, which in its turn comprises several individual steps, as already described in Chapter 3, Sections 3.1 and 3.5. A similar overall reaction can be conceived for the hydrolysis of $(SCN)_3^-$.

The formation of the intermediate species $(SCN)_3^-$ and $(SCN)_2$ is, as far as the mechanism of gold leaching is concerned, the most relevant feature of the autoreduction process. The history of their discovery, the experimental evidences and the main aspects of their chemistry were all reviewed in Chapter 3. Further spectrophotometric evidence was collected during this work, as illustrated in **Figures 4.20** and **4.21**.

Figure 4.20 is the spectrum of a freshly prepared solution of ferric thiocyanate containing *c.a.* 3.4×10^{-4} mol/dm^3 Fe^{3+} and 0.01 mol/dm^3 SCN^- in acetonitrile, at room temperature (*c.a.* 18°C). The large peak at 475 nm corresponds to the ferric thiocyanate complexes and is normally used in spectrophotometric determinations of Fe^{3+} [92]. The two small unresolved peaks on the left, at 320 nm and 285 nm, correspond to $(SCN)_3^-$ and $(SCN)_2$, respectively [84, 90, 91]. In acidic aqueous solution, only the peak at 320 nm appears (i.e., its shoulder at *c.a.* 285 nm can not be distinguished), which is probably due to the hydrolysis of $(SCN)_2$ being faster than that of $(SCN)_3^-$, which would be relatively stabilized by the presence of H^+ and/or by the formation of ion pairs with other cations [90].

The spectrum shown in **Figure 4.21** was produced by the same solution used to obtain **Figure 4.20**, but was taken 4 hours after its

preparation. The absorbance scale was magnified so that the peaks in the u.v. region could be better observed. The u.v. peaks are more intense due to the progress of the autoreduction, with the consequent production of $(SCN)_3^-$ and $(SCN)_2$. A full display of the absorbance scale would also show a slight decrease in intensity of the peak at 475 nm, due to the corresponding reduction of Fe^{3+} (the ferrous thiocyanate complex does not absorb in any of the wavelengths considered). The spectra in **Figures 4.20** and **4.21** are similar to those obtained by Miyake [93, 94, 95] both in acidic aqueous solutions and in ethyl acetate (see **Figures 3.15** and **3.16**, Chapter 3).

One of the main characteristics of the autoreduction process, amply demonstrated by the experimental results presented in the previous sections, is the decrease in the overall rate with time, due to the increasing concentration of Fe^{2+} in solution. It is believed here, in accordance with the above mechanistic views (equations 4.23 through 4.29), that the reverse reaction responsible for the retardation of the autoreduction process is:

$$(SCN)_2^- + Fe^{2+} \longrightarrow Fe(NCS)_2^+ \qquad (4.31)$$

or, alternatively,

$$(SCN)_2^- + Fe^{2+} \longrightarrow FeNCS^{2+} + SCN^- \qquad (4.32)$$

The ferric thiocyanate complexes formed may then be coordinated by additional SCN^- ions, depending on the free thiocyanate concentration in the system.

Reactions 4.31 and 4.32 become increasingly important with time, due to the build up of Fe^{2+} in the system, as the autoreduction progresses. $(SCN)_2^-$ is a highly oxidizing species whose E° was estimated in 1.29 V by Stanbury et al. [45]. Its is not possible to rule out reactions in which other oxidized species such as $(SCN)_2$ and

$(SCN)_3^-$ would also oxidize Fe^{2+}. The overall picture would then show Fe^{3+} as the primary oxidant, and the oxidized intermediate species as also having the ability to act as oxidizing agents.

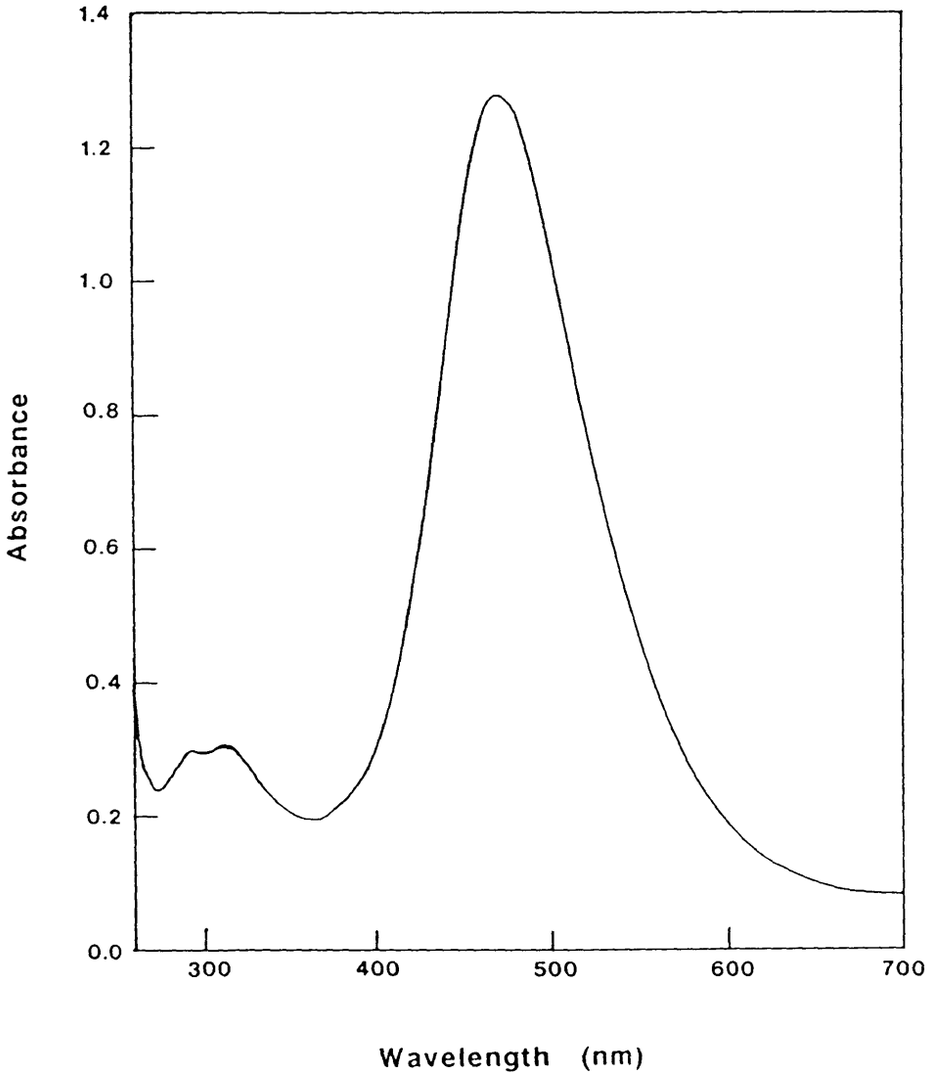


Figure 4.20 - Visible and u.v. spectrum of a freshly prepared solution containing *c.a.* 3.4×10^{-4} mol/dm^3 Fe^{3+} and 0.01 mol/dm^3 SCN^- in acetonitrile, at room temperature (*c.a.* 18°C).

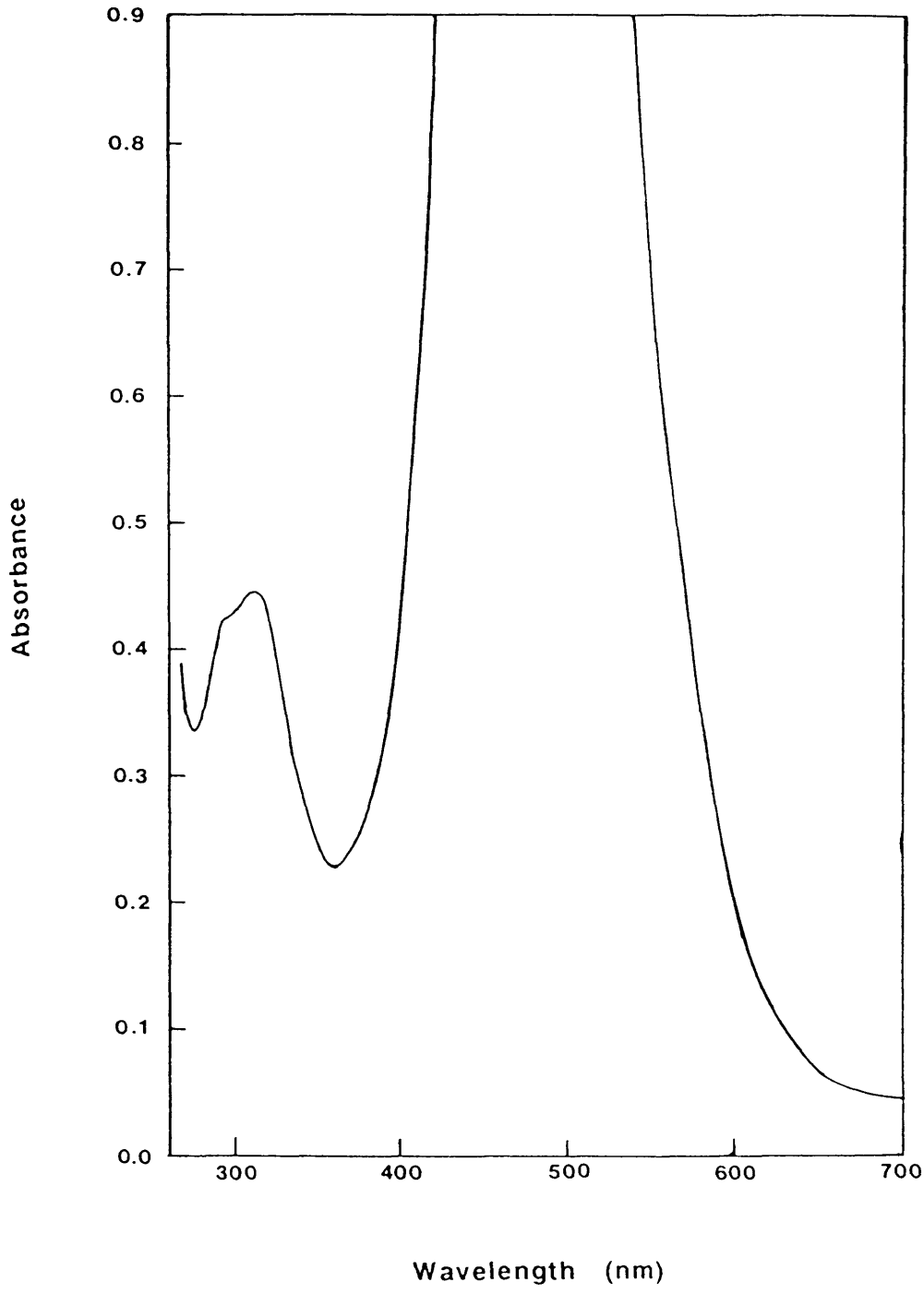


Figure 4.21 - Visible and u.v. spectrum of a ferric thiocyanate solution containing *c.a.* 3.4×10^{-4} mol/dm^3 Fe^{3+} and 0.01 mol/dm^3 SCN^- in acetonitrile, at room temperature (*c.a.* 18°C), taken 4 hours after the solution was prepared.

CHAPTER 5: THE USE OF HYDROGEN PEROXIDE AS OXIDANT IN AQUEOUS IRON-THIOCYANATE SOLUTIONS

5.1. Introduction

The redox processes in iron-thiocyanate solutions were discussed in the previous chapter. Freshly prepared ferric thiocyanate solutions were observed to undergo autoreduction, with conversion of Fe^{3+} to Fe^{2+} and the corresponding oxidation of SCN^-. The potential readings in such solutions decrease with the progress of the autoreduction. As the mixed potential is a key parameter in the leaching of gold, it is necessary to maintain it either around a constant value or, at least, at a value situated within some convenient limits. The objective of this chapter is to investigate the use of hydrogen peroxide for that purpose.

Hydrogen peroxide is known to oxidize both SCN^- and Fe^{2+}. The investigation has then to be addressed in three stages: **(1)** the oxidation of SCN^- by H_2O_2; **(2)** the oxidation of Fe^{2+} by H_2O_2; **(3)** the oxidizing effect of H_2O_2 in iron-thiocyanate solutions. As far as stage **(1)** is concerned, the scarcity of previous experimental results on the oxidation of thiocyanate by hydrogen peroxide demanded a series of experiments to be performed as part of the present work. The same is true as regards stage **(3)**. The results of the experiments are presented and discussed in this chapter.

The starting point is a review of the previous contributions on the oxidation of SCN^- and Fe^{2+} by hydrogen peroxide.

5.2. Previous Work on Thiocyanate Oxidation by Hydrogen Peroxide

The earliest study on the oxidation of thiocyanate by hydrogen peroxide was published by Kastle and Smith in 1904 [153]. They reported HCN and H_2SO_4 as the oxidation products, according to the overall reaction:

$$HSCN + 3H_2O_2 \rightarrow H_2SO_4 + HCN + 2H_2O \qquad (5.1)$$

Sant [154] presented a short communication in 1957 containing a mechanistic proposal which was supposed to comply with the above overall reaction, with HOSCN and H_2SO_3 as intermediate species, although he did not report any stoicheiometric data.

The most complete investigation on the subject is that published by Wilson and Harris [36, 37]. They observed that the oxidation is catalyzed by H^+ ions at pH below 2. Above pH 4, the reaction was observed to be pH independent. A comprehensive mechanism was proposed for both pH ranges, as follows:

$$SCN^- + H_2O_2 \rightarrow HOSCN + OH^- \qquad (pH>4) \qquad (5.2)$$

$$H_3O^+ + SCN^- + H_2O_2 \rightarrow HOSCN + 2H_2O \qquad (pH<2) \qquad (5.3)$$

$$HOSCN + H_2O_2 \rightarrow HOOSCN + H_2O \qquad (5.4)$$

$$HOOSCN + H_2O_2 \rightarrow H_2SO_3 + HOCN \qquad (pH>4) \qquad (5.5)$$

$$HOOSCN + H_3O^+ \rightarrow H_2SO_3 + HCN + H^+ \qquad (pH<2) \qquad (5.6)$$

$$HOSCN + HCN \rightarrow S(CN)_2 + H_2O \qquad (5.7)$$

$$HOCN + 2H_2O \rightarrow HCO_3^- + NH_4^+ \qquad (5.8)$$

$$H_2SO_3 + H_2O_2 \rightarrow H_2SO_4 + H_2O \qquad (5.9)$$

The rate determining reactions would be 5.2 and 5.3 for the pH-independent (pH>4) and the acid catalyzed (pH<2) reactions, respectively.

In agreement with the above mechanism, it was found that at 4<pH<12 the oxidation products are sulphate, cyanate, ammonia and carbonate [36]. At pH<2, the main products are sulphate and hydrogen cyanide, plus a minor byproduct, sulphur dicyanide, $S(CN)_2$, which was analytically detected [37]. HOSCN and HOOSCN are the main intermediate species proposed by Wilson and Harris. The reactions and products relevant to the present work are those occurring at pH<2, which corresponds to the pH range for the gold leaching.

It is currently accepted that the oxidative action of hydrogen peroxide takes place through the free radicals $OH^{\cdot}$ and $HO_2^{\cdot}$ [155-163]. This consideration, apparently disregarded in the above mechanism, could lead to the inclusion of hypothetical intermediate species such as $HOSCN^-$ and $OSCN^{2-}$, whose existence was later proposed on an experimental basis by Behar et. al. [76]. However, all the final products, including sulphur dicyanide, were analytically determined by Wilson and Harris [36, 37]. An account of the stoicheiometry of the oxidation process was not produced by these authors.

5.3. Previous Work on the Oxidation of Iron(II) by Hydrogen Peroxide

Harber and Weiss [155] proposed a mechanism for the oxidation of Fe^{2+} by H_2O_2 which, after being modified by Kolthoff and Medalia [157-159] and Barb et al. [160], acquired the form currently accepted:

$$Fe^{2+} + H_2O_2 \rightarrow Fe^{3+} + OH^{\cdot} + OH^{-} \quad (5.10)$$

$$Fe^{2+} + OH^{\cdot} \rightarrow Fe^{3+} + OH^{-} \quad (5.11)$$

$$OH^{\cdot} + H_2O_2 \rightarrow H_2O + HO_2^{\cdot} \quad (5.12)$$

$$Fe^{2+} + HO_2^{\cdot} \rightarrow Fe^{3+} + HO_2^{-} \quad (5.13)$$

$$Fe^{3+} + HO_2^{\cdot} \rightarrow Fe^{2+} + O_2 + H^{+} \quad (5.14)$$

The kinetics of the system has been investigated in perchloric, sulphuric and phosphoric acid solutions, both in the presence and absence of oxygen. The stoicheiometric ratio is $2Fe^{2+}$ for each H_2O_2 and the effect of dissolved oxygen is minimal [136, 156-160]. At very low peroxide/ferrous ion ratios only the steps 5.10 and 5.11 occur, the reaction is second order (i.e., first order to Fe^{2+} and H_2O_2) and no oxygen is evolved [159].

The stoicheiometry of the reaction changes considerably when a compound subject to oxidation is added to the system. This effect has been studied with a number of organic compounds. In such cases, the presence or absence of oxygen may change both the mechanism and the stoicheiometry of the oxidation process [136, 156-159, 161-163]. A good summary of such changes in mechanism and H_2O_2/Fe^{2+} ratio is offered by Kolthoff et al. [136].

The oxidation of an organic compound by a mixture of H_2O_2 and Fe^{2+} is usually called the Fenton reaction, and the oxidizing mixture is called Fenton's reagent (after H. J. H. Fenton, who was the first to describe the reaction in 1894 [164]). A great deal of work has been performed on this subject [156-159, 161-163].

The effect of H_2O_2 upon iron(II)-thiocyanate solutions could then be referred to as the oxidation of thiocyanate by Fenton's

reagent. The mechanisms developed to explain the oxidation of organic compounds by Fenton's reagent invariably involve the formation of organic radicals and other steps [136, 161-163] which do not apply to the oxidation of an inorganic compound such as thiocyanate. However, changes in the Fe^{2+}/H_2O_2 stoicheiometry in acidic medium are expected to occur when thiocyanate is added, as both the H_2O_2 and the Fe^{3+} produced have the ability to oxidize it.

5.4. Experiments on Thiocyanate Oxidation by Hydrogen Peroxide

The aim of these experiments is to provide a quantitative assessment of the oxidation of thiocyanate by hydrogen peroxide over several hours, within concentration ranges expected to be found in a leaching circuit. The only experimental results of this nature are those published by Kastle and Smith [153] in 1904. They determined the amount of thiocyanate oxidized by titrating with potassium hydroxide the acidity produced by reaction 5.1, using phenolphthalein as indicator. The method does not seem very accurate as it involves the dissociation contants of the acids, particularly of HSCN, HCN and H_2O_2, whose determination was not certain by 1904. The dissociation constant of HSCN was determined much later [32-35] (see Chapter 2, Section 2.3). Sant [154] did not report any results in terms of the extent of thiocyanate oxidation. Wilson and Harris [36, 37] were basically concerned with mechanisms and initial rates, not having concentrated on the stoicheiometry of the process. Furthermore, they used peroxide concentrations higher than the ones considered in this work. Redox potentials were also measured during the present experiments and are reported in Appendix 5.

5.4.1. Experimental and Analytical Procedures

The experiments were performed in conical flasks placed in a thermostatically controlled shaker and had a duration of 24 hours. Freshly prepared potassium thiocyanate solutions were acidified with 1.8 mol/dm^3 H_2SO_4 to pH 1.5. The required amount of hydrogen peroxide 30% w/v (i.e. 8.82 mol/dm^3) was then added and this was taken as the zero time. The temperature was 25°C in all experiments.

Thiocyanate was determined argentimetrically. The samples were titrated directly with a standard solution of $AgNO_3$ using eosin (tetrabrom-fluorescein) as indicator. Eosin is an adsorption indicator. Silver nitrate precipitates thiocyanate quantitatively as the white solid AgSCN. The end point is indicated by the colour change of the precipitate from white to pink, caused by the adsorption of the indicator, which takes place as soon as the titre is in (slight) excess. The end point is sharp and reproducible.

5.4.2. Results and Discussion

Results of several runs are shown in **Table 5.1**. The hydrogen peroxide concentrations tried were 0.009, 0.029 and 0.088 mol/dm^3, which correspond respectively to 0.3, 1.0 and 3.0 g/l.

The oxidation is practically completed after 4 hours. Samples collected 2 hours from the beginning of the runs revealed that most of the oxidation had already occurred by then. The typical pattern of the progress of the reaction is shown in **Figure 5.1**. These observations emphasize the fact that, for practical purposes, the oxidation of thiocyanate by hydrogen peroxide is a relatively fast reaction.

There was no peroxide left after 24 hours in the last six runs of **Table 5.1**. The ratios between peroxide consumed and thiocyanate oxidized varied from 1.3 to 3.14. It was observed that, for a particular initial SCN^- concentration, the higher the initial H_2O_2 concentration, the higher the observed ratio, and the closer it would get to equation 5.1. This suggests that when there is more H_2O_2 available (for the same SCN^- concentration), the reaction proceeds with the formation of more oxidized products, whereas a larger amount of intermediate products is found (after the same 24 hours) when relatively smaller amounts of H_2O_2 are initially added. This short term behaviour diverges considerably from reaction 5.1. A better explanation would be provided by the mechanism described above (reactions 5.2 to 5.9), the degree of completion of the overall process being dependent on the H_2O_2 and SCN^- concentrations initially present.

Table 5.1 - Thiocyanate Oxidation by Hydrogen Peroxide: Experimental Results at pH 1.5 and 25°C (concentrations in mol/dm^3)

Initial Concentrations (mol/dm^3)		Thiocyanate Concentration (mol/dm^3) and % Consumption					
		4 hs.		8 hs		24 hs	
$[SCN^-]$	$[H_2O_2]$	$[SCN^-]$	% Cons.	$[SCN^-]$	% Cons.	$[SCN^-]$	% Cons.
0.050	0.009	0.048	4.0	0.047	6.0	0.047	6.0
0.050	0.029	0.042	16.0	0.041	18.0	0.041	18.0
0.050	0.088	0.029	42.0	0.029	42.0	0.026	48.0
0.10	0.009	0.094	6.0	0.094	6.0	0.094	6.0
0.10	0.029	0.088	12.4	0.088	12.4	0.088	12.4
0.10	0.088	0.068	32.0	0.068	32.0	0.068	32.0
0.275	0.009	-	-	0.268	2.5	0.268	2.5
0.275	0.029	0.266	3.3	0.262	4.7	0.262	4.7
0.275	0.088	0.249	9.5	0.247	10.2	0.247	10.2

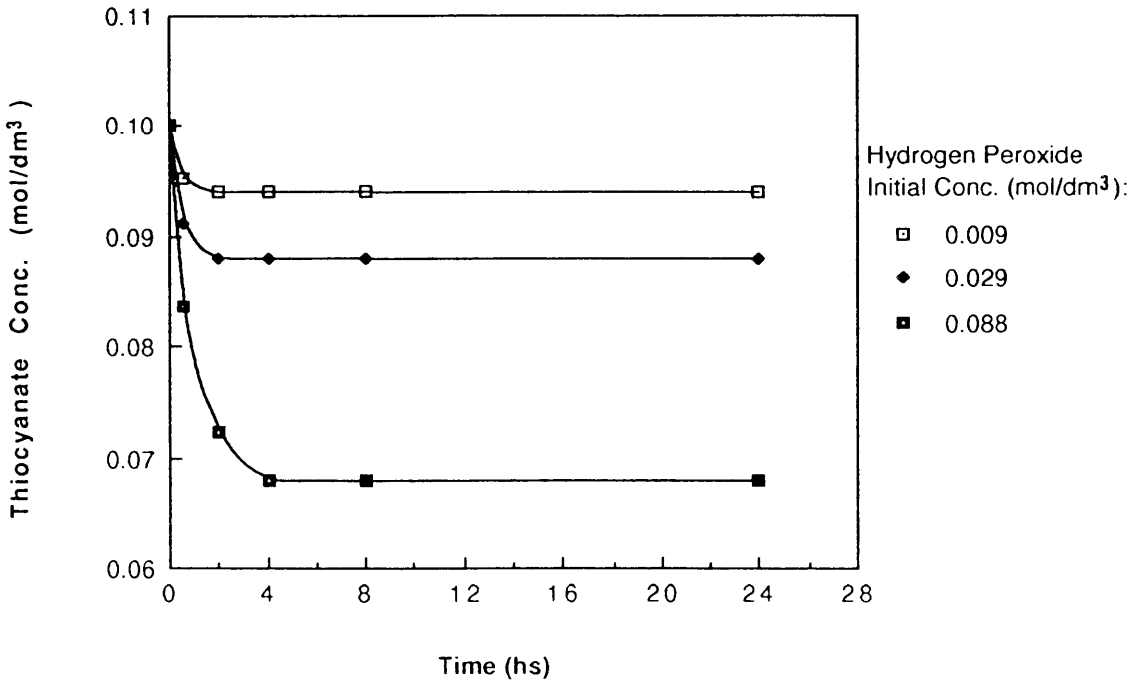
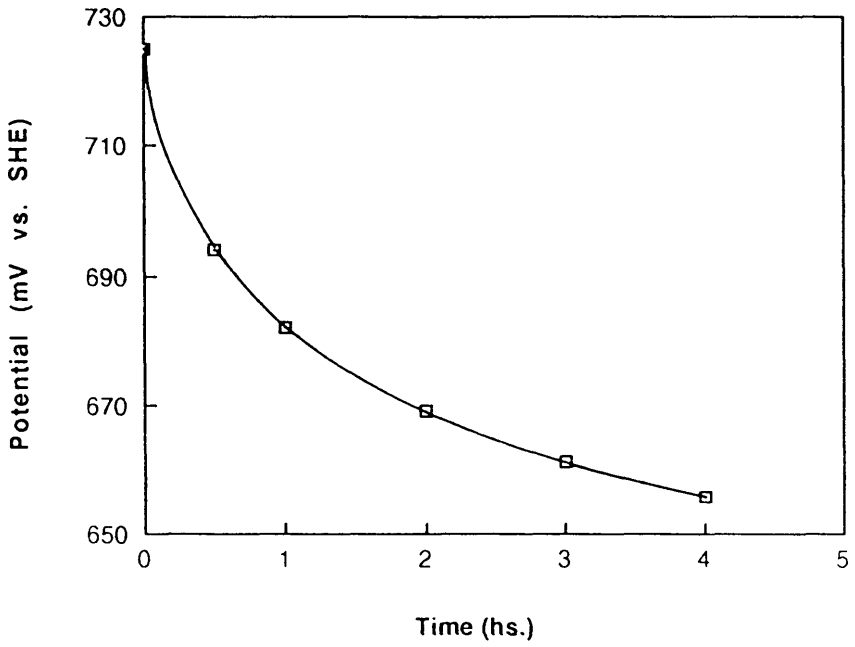


Figure 5.1 - Thiocyanate oxidation by hydrogen peroxide at pH 1.5 and 25°C. The initial thiocyanate concentration is 0.10 mol/dm^3 for all experiments. The initial peroxide concentrations correspond to 0.3, 1.0 and 3.0 g/l (i.e. 0.009 to 0.088 mol/dm^3, respectively).

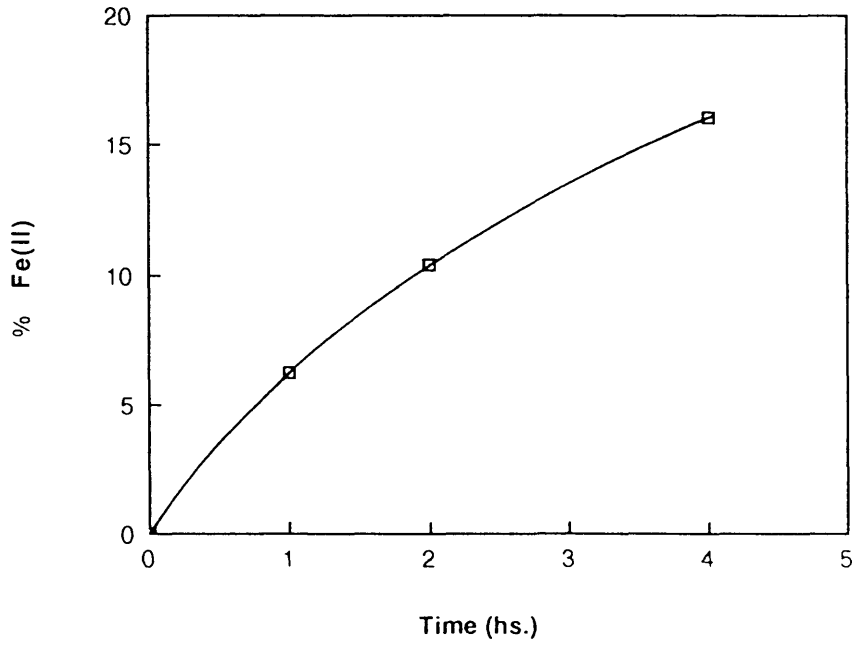
5.5. The Action of Hydrogen Peroxide on Iron-Thiocyanate Solutions

5.5.1. Experimental and Analytical Procedures

The best way to explain this procedure is to consider first the normal course of the autoreduction of a freshly prepared ferric thiocyanate solution, as shown in **Figure 5.2**. In such an experiment, all the iron is added initially as Fe^{3+}. As the reaction proceeds, it is



(a)



(b)

Figure 5.2 -Thiocyanate oxidation by iron(III): **(a)** potential readings and **(b)** Fe^{3+} reduction. Initial concentrations: 0.275 mol/dm^3 SCN^- and 0.055 mol/dm^3 Fe^{3+}; pH 1.5; temperature, 25°C.

gradually reduced to Fe^{2+} (**Figure 5.2b**), with a corresponding decrease in the potential readings (**Figure 5.2a**).

Figure 5.2 indicates that the reaction is faster in the beginning and slows down with time. This means that attempts to mantain a constant potential close to that at zero time (which corresponds to Fe^{2+} percentages close to zero) will cause higher thiocyanate consumption by oxidation. In such conditions there is a fast reduction of Fe^{3+} to Fe^{2+}. The Fe^{2+} reoxidized by H_2O_2 is rapidly reduced again. The electron transfer reactions involving the Fe^{3+}/Fe^{2+} redox couple are then very fast in such conditions, increasing both the decomposition of H_2O_2 and the oxidation of SCN^-.

On the other hand, if a lower potential is maintained, which corresponds to a higher percentage of Fe^{2+}, the whole process becomes slower, with less peroxide consumed and less thiocyanate oxidized.

In each of the experiments described in this section, the percentage of ferrous ions (and consequently the potential) was kept constant by sequential additions of hydrogen peroxide.

The experiments were performed in a stirred glass reactor fitted with pH, Ag/AgCl reference and Pt electrodes, and immersed in a thermostatically controlled water bath which was set to 25°C in all runs. The reactor was aerated (i.e., not sealed to the atmosphere). Once in the reactor, freshly prepared thiocyanate solutions were acidified to pH 1.5 with 1.8 mol/dm^3 H_2SO_4. Ferric and ferrous alum solutions were then added, at zero time, in a suitable proportion to provide the Fe^{2+}/Fe^{3+} ratio (and potential) to be mantained constant throughout the experiment. Additions of 5% w/v (i.e. 1.47 mol/dm^3) hydrogen peroxide were made from a precision burette. The experiments lasted 4 hours.

Thiocyanate samples were analysed according to the Volhard method described in Section 4.3, Item 4.3.2.

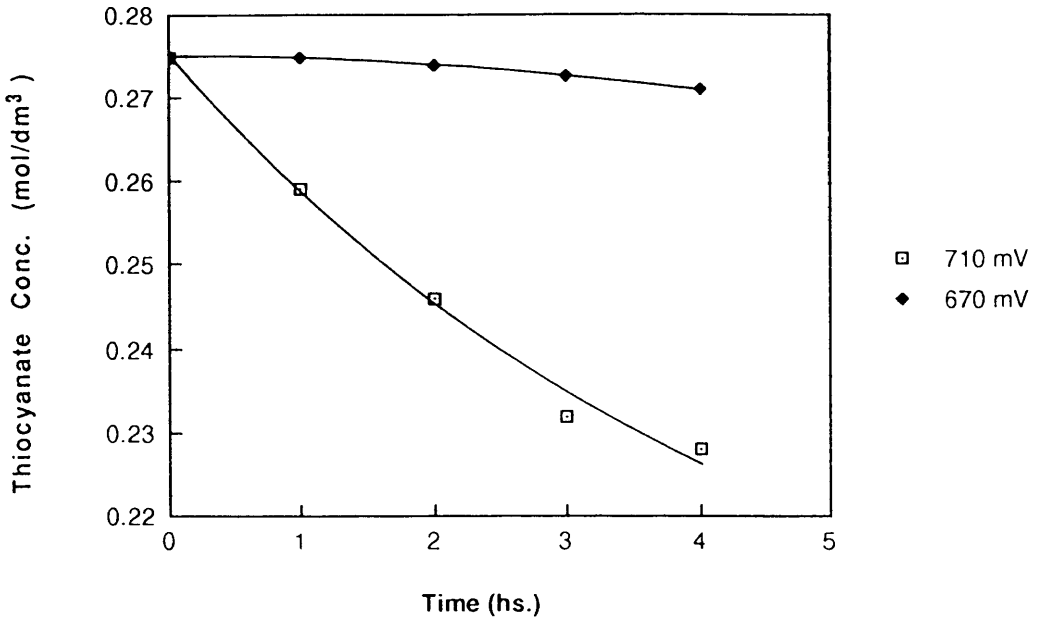
5.5.2. Experimental Results and Discussion

Typical results are shown in **Figure 5.3**. In one of the runs, the potential was kept constant at 670 mV, which corresponds to 10% of the iron as Fe^{2+} (i.e. 0.0495 mol/dm^3 Fe^{3+} and 0.0055 mol/dm^3 Fe^{2+}). With such a relative amount of Fe^{2+}, the autoreduction of Fe^{3+} was slow. Consequently, the oxidation of SCN^- (**Figure 5.3a**) and the consumption of H_2O_2 (**Figure 5.3b**) were very low.

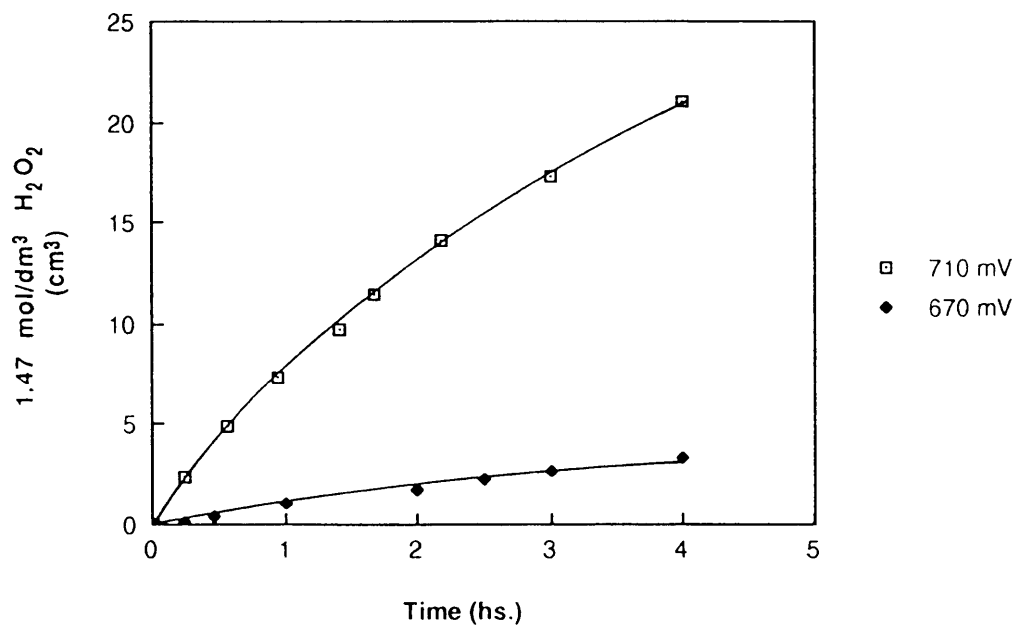
In the other run shown in **Figure 5.3**, the potential was kept constant at 710 mV, which corresponds to only 1.5% of Fe^{2+}. Under these conditions, the fast kinetics of the Fe^{3+}/Fe^{2+} couple caused a considerably higher oxidation of SCN^- and consumption of H_2O_2.

Experiments starting with 20% or more of Fe^{2+} (potential of 650 mV or lower) did not consume any peroxide in 4 hours, so slow was the autoreduction process and the potential decrease.

Further information was sought by making potentiometric titrations with H_2O_2 of acidified (pH 1.5) thiocyanate solutions containing Fe^{2+} or mixtures of Fe^{2+} and Fe^{3+} ions (50% or more of Fe^{2+}). Thiocyanate samples were collected at different stages of each titration and immediately analysed. In no case there was an end point. The titration was ended when the potential reached the value corresponding to all iron as Fe^{3+} (from comparison with similar freshly prepared ferric thiocyanate solutions). At the beginning of the titrations, due to the relatively high concentration of Fe^{2+}, the H_2O_2 oxidized mainly these cations and only secondarily oxidized SCN^- (the potential response was fast and stable and the decrease in the thiocyanate concentration was minimal). Towards the end of the titration, with most of the Fe^{2+} already oxidized, there was a much higher consumption of SCN^- per cm^3 of H_2O_2 solution added. However, it was impossible to distinguish this effect from the oxidation SCN^-



(a)



(b)

Figure 5.3 - Experiments at constant potential: **(a)** concentration of SCN^- versus time and **(b)** consumption of 1.47 mol/dm^3 H_2O_2. Initial concentrations: 0.275 mol/dm^3 SCN^- and 0.055 mol/dm^3 total iron; pH 1.5; temperature, 25°C. Fe^{2+}: 10% and 1.5% at 710 and 670 mV, respectively.

by the autoreduction of Fe^{3+}, which becomes very fast when the Fe^{2+} concentration becomes relatively small. Nor was it possible to determine the ratios between H_2O_2, Fe^{2+} and SCN^-, which anyway seemed to vary according to the concentrations of the species involved. This would require information about the concentrations of SCN^- and Fe^{2+} at a given time, but difficulties appeared in determining Fe^{2+} in the presence of H_2O_2. Attempts were made to use the o-phenanthroline method for this purpose, but the H_2O_2 present also oxidized the Fe^{2+}-o-phenanthroline complex, causing underestimation of the Fe^{2+} concentration (this reaction is indeed one of the spectrophotometric methods for determining ppm amounts of H_2O_2 [165]).

As far as practical applications are concerned, the overall conclusion is that a compromise should be sought between the potential required for effective gold leaching and the consumption of SCN^- and H_2O_2. As shown in **Figure 5.3**, the consumption of both reagents decreases with increases of the Fe^{2+}/Fe^{3+} molar ratio.

CHAPTER 6: AN INVESTIGATION OF THE DISSOLUTION OF GOLD BY IRON-THIOCYANATE AND IRON-THIOCYANATE-HYDROGEN PEROXIDE SOLUTIONS

6.1. Introduction

The aim of this chapter is to present the first contribution to the understanding of the kinetics of gold dissolution by thiocyanate. Experiments were performed with a rotating gold disc in order to determine the dissolution rates and hence to propose some mechanistic ideas to explain the leaching of gold by ferric thiocyanate solutions.

The literature review is limited to the two papers [2, 3] already discussed in Chapter 1 (Introduction). No fundamental kinetic study on this system has been published so far. Thus, this chapter is entirely concerned with the description of the experiments performed as part of the present work, and with the presentation and discussion of the results. All the numerical data are reported in Appendix 6. The numbers of the experiments, when quoted, correspond to those used in the Appendix.

6.2. Rotating Disc Study: Experimental

6.2.1. Equipment

The basic arrangement used in the experiments is shown schematically in **Figure 6.1**. The main items of equipment are:

- Oxford Rotating Disc System Model MC5/88, comprising an electronic motor controller (1, see **Figure 6.1**) connected to a motor (2) and gold disc assembly (3). The gold rotating disc had a diameter of 1.4 cm and was constructed as an electrode, i.e. it was provided with an external electric contact so that the potential on the disc surface could be measured. The gold was 99.99% pure.

- pH meter (4) fitted with glass electrode (Russell and Co.)

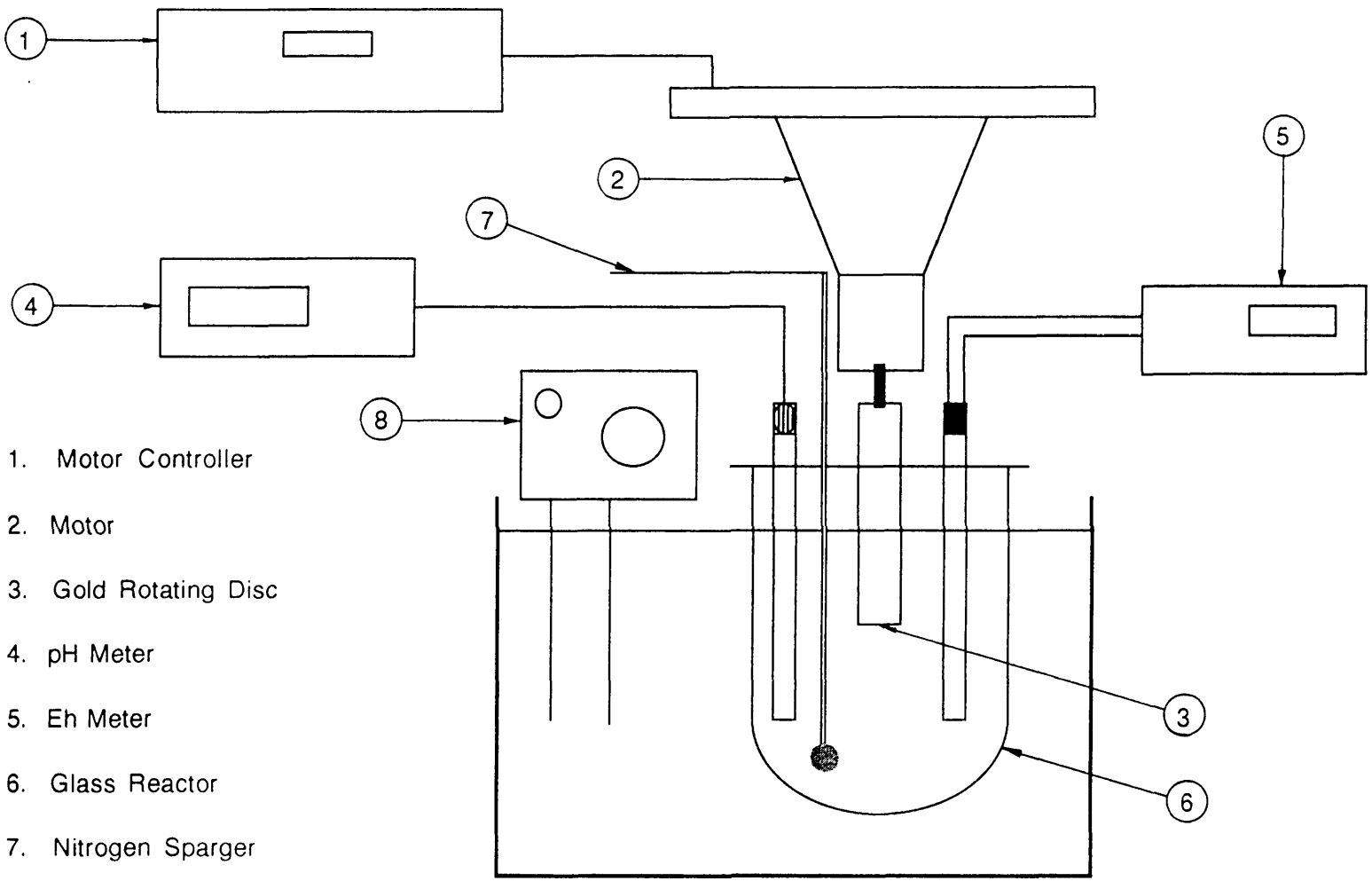
- Eh meter (5) fitted with an Ag/AgCl reference electrode. A Pt indicator electrode was also included in order to compare the potential readings on the Au and Pt surfaces against the reference electrode.

- Glass reactor with lid (6), fitted with a gas sparger (7) to introduce nitrogen whenever an inert atmosphere was required. The reactor capacity was 250 cm^3.

- Thermostatically controlled water bath (8). In the experiments at 85°C, the water bath was replaced by a heating mantle coupled with a Fimonitor automatic temperature controller and mercury thermometer.

6.2.2. Experimental Procedure

Analytical grade reagents were used in all experiments (see Appendix 7). A freshly prepared solution of potassium thiocyanate was acidified with 1.8 mol/dm^3 H_2SO_4. The initial pH was 1.5. Nitrogen was sparged into the solution for 45-60 minutes before starting the experiment and once it was started, the gas was sparged over the solution, keeping the neutral atmosphere inside the reactor. The rotating disc was then lowered into the solution and the required amount of ferric alum stock solution was added. The



1. Motor Controller
2. Motor
3. Gold Rotating Disc
4. pH Meter
5. Eh Meter
6. Glass Reactor
7. Nitrogen Sparger
8. Water Bath with Thermostat

Figure 6.1 - Schematic view of the system used in the rotating disc experiments

rotation was started immediately and that was considered the zero time. The overall initial volume of the liquid phase was 180 cm^3.

This same type of experiment was also performed with the reactor aerated (i.e. open to the atmosphere) for comparison with those under nitrogen atmosphere.

Potential readings were made throughout the experiments both on the Au disc and on the Pt electrode. Regular pH readings were also made. The autoreduction of the ferric thiocyanate solutions was monitored spectrophotometrically by the o-phenanthroline method already described (see Chapter 4, Item 4.3.3). Thiocyanate was analyzed argentimetrically (see Chapter 4, Item 4.3.2). Gold was analyzed by atomic absorption spectrophotometry. Volume corrections were applied to all analytical results.

Some experiments at constant potential were included in the programme. These were performed with the reactor aerated and the potential was mantained constant by additions of hydrogen peroxide. In these experiments, both Fe^{3+} and Fe^{2+} alum solutions were added initially in a ratio suitable to provide the desired potential from the beginning.

The gold disc was polished before each experiment with water-based diamond compounds. Coarser grades of compound were first used depending on how etched the disc was from the previous experiment. But in all cases the polishing was finished with a 3 μm compound, which imparted a mirror finish to the disc surface. The use of a 1 μm compound was tried but yielded the same experimental results, thus leading to the adoption of 3 μm as the finishing grade. Polishing was carried out on silk cloths, using water-based polishing lubricant. After polishing, the disc was rinsed with distilled water, dipped for *c.a.* 1 minute in chromic sulphate solution and finally rinsed again, as recommended in the literature [204]. It has been reported that the current responses of gold and platinum rotating disc electrodes did not change when the polishing

was carried out with abrasive sizes from 0.5 to 14 μm, even when the rotation speed was varied in the range 400-8100 rpm [166].

Great care was taken to assessing the suitability of this disc conditioning procedure. This was done in two different ways. First, by checking the reproducibility of the overall gold dissolution experiments with ferric thiocyanate solutions (see Section 6.3). Second, electrochemically, by running several voltammograms with the freshly polished disc in 0.1 mol/dm^3 sulphuric acid in order to check the reproducibility of the surface conditioning and to compare the results with those from similar voltammetric studies reported in the literature [167, 168]. In both cases the procedure was found to be adequate.

Another treatments used consisted in submitting the gold disc to four or five consecutive cyclic sweeps between -0.4 and +1.6 V (vs. SHE) or, alternatively, to maintain the gold disc at 0.0 V (vs. SHE) for 1 minute, both in 0.1 mol/dm^3 H_2SO_4. These procedures were applied after the disc had been polished, dipped in chromic sulphate solution and rinsed with water, as described above. The objective of the consecutive sweeps was to verify the effectiveness of the chemical treatment with chromic sulphate solution in destroying any organic substances. The potential step to 0.0 V aimed to ensure that there was no oxidation of the gold disc surface by the chromic sulphate solution. These latter procedures proved to be unnecessary.

6.2.3. Experimental Conditions

The variables included in this kinetic investigation and their respective ranges were:

Rotation Speed	18.8 to 157 rad/s (180 to 1500 rpm)

Thiocyanate concentration:	0.05 to 0.50 mol/dm^3
Iron(III) concentration:	0.01 to 0.10 mol/dm^3
Temperature:	25 to 85°C

The variation of the rotation speed was intended for the application of Levich's theory of the rotating disc [152, 169-176] in the interpretation of the experimental results. This approach will be discussed in Section 6.5, in connection with the observed gold dissolution rates. The concentration ranges for iron(III) and thiocyanate were the same as those adopted in Chapter 4. The temperature range was extended up to 85°C, rather than only up to 55°C, as in Chapter 4.

6.2.4. Gold Analysis

Gold was analyzed by atomic absorption spectrophotometry (AAS) in all samples collected from the rotating disc experiments, using a Perkin-Elmer spectrophotometer Model 1100B. Standards for the calibration of the spectrophotometer were prepared by dilution of a primary 100 ppm gold standard in ferric thiocyanate solutions with compositions similar to those used as leach liquors in the experiments, in order to minimize matrix effects. Besides this, background correction was used in all the measurements. Overall, the readings gave standard deviations below 2%.

6.2.5. Iron(II) and Thiocyanate Analysis

The progress of the autoreduction of the ferric thiocyanate solutions during the rotating disc experiments was followed by

analyzing the increase in the Fe^{2+} concentration. The 1,10-phenanthroline method described in Chapter 4, Item 4.3.3, was used for this purpose.

Thiocyanate was analyzed argentimetrically, by the Volhard method described in Chapter 4, Item 4.3.2. Special attention was paid to the thiocyanate consumption during the experiments at higher temperatures (i.e. 55-85°C) and to those at constant potential (to which hydrogen peroxide was added).

6.3. Experimental Reproducibility

A great deal of information is provided by each rotating disc experiment. The first piece of information comes from the gold analysis (AAS). The second, from the potential readings. The third, from the spectrophotometric determinations of Fe^{2+}. Thiocyanate determinations and pH readings complement the information. The discussion of the experimental results requires the display and correlation of all these pieces of information, particularly the first three mentioned. The objective of this section is, besides considering the reproducibility, to demonstrate the way in which the experimental results are presented in the following sections.

Gold dissolution results of three similar runs are shown in **Figure 6.2**. The corresponding potential readings and Fe^{2+} analyses are shown in **Figures 6.3a** and **6.3b**, respectively.

Figures 6.2 and **6.3** demonstrate the reproducibility both of the gold leaching and of the simultaneous autoreduction of the ferric thiocyanate solution, as indicated by the potential decrease and Fe^{2+} production with time.

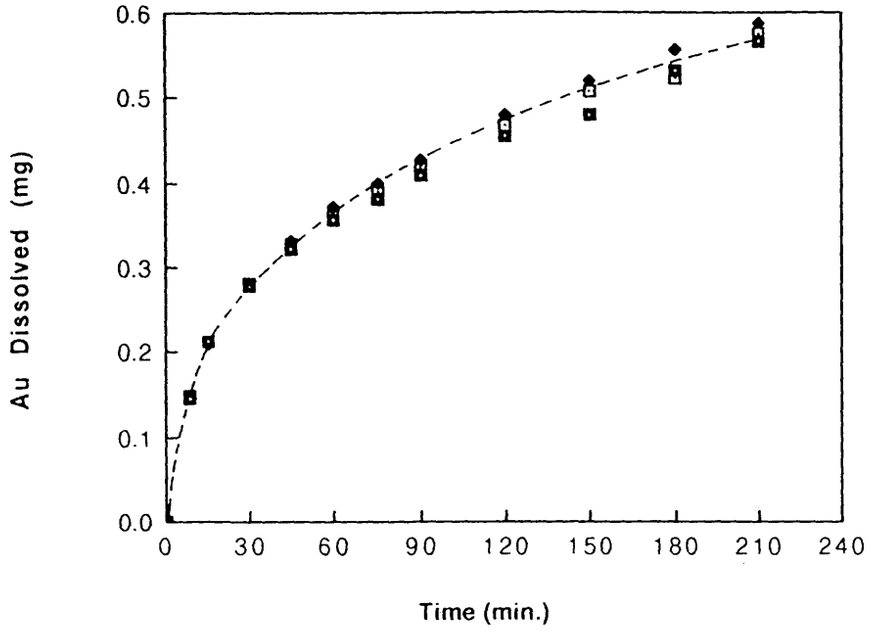
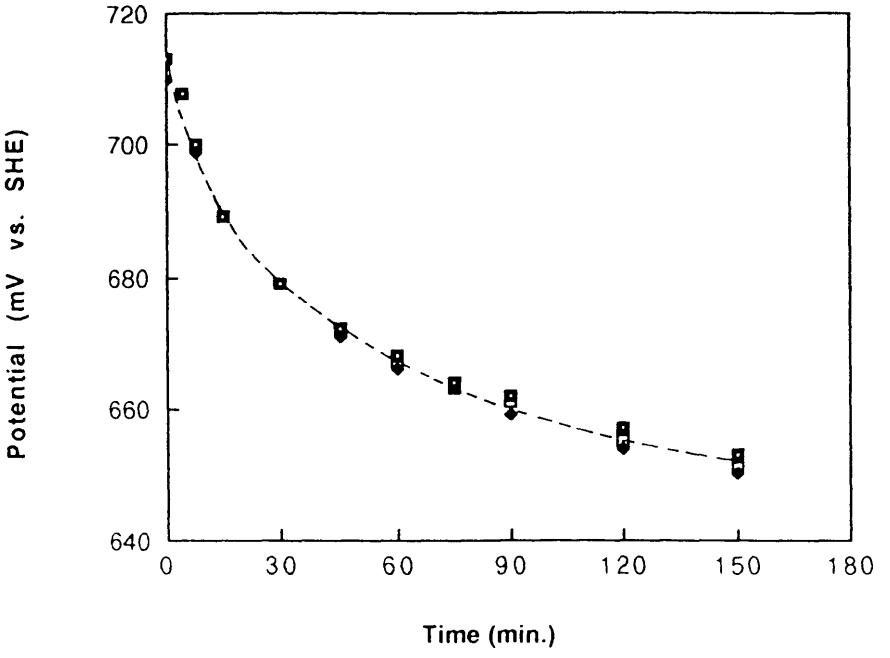
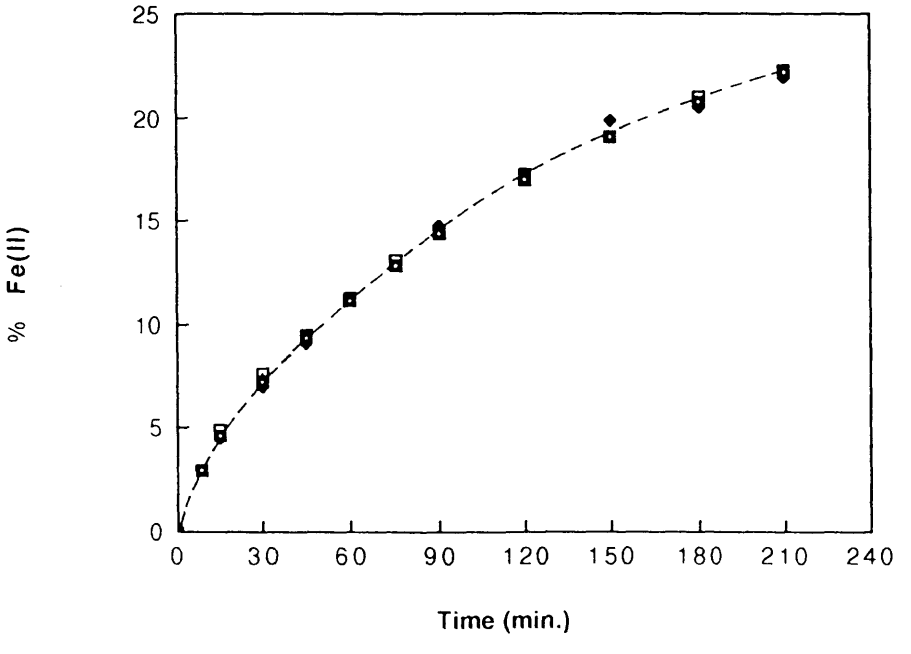


Figure 6.2 - Reproducibility of gold leaching by ferric thiocyanate solution. Initial concentrations: 0.275 mol/dm^3 SCN^- and 0.055 mol/dm^3 Fe^{3+}; pH 1.5; temperature, 25°C; rotation speed, 75.4 rad/s (720 rpm). N_2 atmosphere.

A most noticeable feature of such experiments appears in these graphs, which is the correlation between the gold dissolution rate and the autoreduction process. At the beginning, the potentials and the autoreduction rate were higher, causing a higher gold dissolution rate. After some time both rates decreased, which was also true of the potential readings. This simple observation becomes more meaningful when compared with the thermodynamic study made in Chapter 2 and with the further calculations made in Chapter 3, Sections 3.10 and 3.11. At the beginning of the experiments, the potentials correspond with the predominance area of the auric complex, $Au(SCN)_4^-$ (see **Figures 2.5** and **2.6**) and simultaneously, there was a larger production of oxidizing intermediate species of thiocyanate, particularly $(SCN)_3^-$ and $(SCN)_2$, due to autoreduction.



(a)



(b)

Figure 6.3 - Reproducibility of **(a)** potential readings at the gold disc surface and **(b)** reduction of Fe^{3+} to Fe^{2+}. Initial concentrations: 0.275 mol/dm^3 SCN^- and 0.055 mol/dm^3 Fe^{3+}; pH 1.5; temperature, 25°C; rotation speed, 75.4 rad/s (720 rpm). N_2 atmosphere.

As the runs progressed, formation of the aurous complex, $Au(SCN)_2^-$, became more likely due to the decrease in the potential and in the autoreduction rate.

The significance of the potential readings taken in these rotating disc experiments was discussed in Chapter 4, Item 4.4.2. They are basically mixed potentials whose main cathodic process corresponds to the reduction of Fe^{3+} and whose anodic process corresponds to the oxidation of thiocyanate. The main potential-determining couples are Fe^{2+}/Fe^{3+}, plus the effect of complexation of these cations by SCN^-, and the couples $(SCN)_3/SCN^-$ and $(SCN)_2/SCN^-$. Dissolved oxygen, in the aerated experiments, did not affect the potential readings.

Although the potential readings in **Figure 6.3a** are the ones taken from the gold disc, the readings at the Pt electrode, which is inert under the same conditions, are very similar (see Appendix 6). The readings on the Au and Pt electrodes showed a non-reproducible discrepancy of the order of 15 mV or less at zero time, which decreased steadly over the first 15 minutes or so in all experiments, after which the two readings were invariably the same (within 5 mV) and very reproducible. The vast majority the readings did not differ from each other by more than 1 or 2 mV.

The numerical data from **Figure 6.2** were used to calculate the dissolution rates at the beginning of the experiments and after 1 hour. The results are given in **Table 6.1**. Initial rates were estimated from samples collected after 8 minutes of the beginning of the runs. Rates after 1 hour were estimated by linear regression including gold samples collected from 1 hour to the end of the runs. The correlation coefficients correspond to these linear fittings.

Table 6.1 - Gold Dissolution Rates Observed in the Experiments shown in **Figure 6.2**

Run Number	Initial Rate $J \times 10^{10}$ (mol/cm^2 s)	Rate after 1 Hour $J \times 10^{11}$ (mol/cm^2 s)	Linear Correlation Coefficient, R^2 after 1 Hour
Au-1	10.2	7.50	0.98
Au-2	10.2	8.00	0.99
Au-3	9.91	7.63	1.00

The experimental error estimated from **Table 6.1** is 1.7% for the initial rates and 3.4% for the rates after 1 hour. The experimental reproducibility was also confirmed in a series of four aerated experiments, all the other conditions remaining identical with those of **Figure 6.2**. The experimental errors estimated from this additional series were 3.8% for the initial rates and 4.7% for the rates after 1 hour. The results of the aerated experiments will be discussed in Section 6.9, where the effect of dissolved oxygen will be evaluated. Replicates were also conducted under several other conditions within this experimental programme, in order to ensure the consistency of the results.

6.4. Effect of the Rotation Speed

The solution of the hydrodynamic problem of defining the flow pattern imposed by a rotating disc was initially proposed by Levich in 1942 [169, 170] and has been extensively considered in the specialized literature [152, 169-176]. According to Levich's theory, there is a linear dependence between the flux of a given species to (or from) the rotating disc, J (mol/cm^2 s), and the square root of the

angular velocity, $\omega^{1/2}$ (ω in rad/s). This was demonstrated by the equation:

$$J = 0.62\ D^{2/3}\ \nu^{-1/6}\ \omega^{1/2}\ c_o \qquad (6.1)$$

D is the diffusion coefficient of the species considered and c_o its concentration in solution; ν is the kinematic viscosity of the solution. This equation is only valid for a regime of laminar flow. Under such conditions, it is capable of predicting the rate of a solid-liquid reaction on a rotating disc, provided the process is transport controlled. It should be noticed that J is not necessarily the flux of material dissolving from the disc, but the flux of the species which plays the key role in the rate controlling step of the overall leaching mechanism. Thus, equation 6.1 can be used to investigate the extent to which the dissolution process is transport controlled. For a dissolution reaction entirely transport controlled, the observed rates should agree with those estimated by the equation 6.1.

The rotation speed range within which there is laminar flow can be estimated by equation 6.2, which relates the Reynolds number, Re, the rotation speed, ω, the radius of the disc, r, and the kinematic viscosity of the solution, ν [152]:

$$Re = \omega\ r^2/\nu \qquad (6.2)$$

The critical Reynolds number, at which the flow regime changes from laminar to turbulent, is $Re_{crit} \approx 2 \times 10^5$ [152, 171, 173]. A typical value of kinematic viscosity of an aqueous medium is 10^{-2} cm^2/s [152]. The radius of the gold disc set-up used in the present work is 1.0 cm. When applied to equation 6.2, these figures yield ω = 2,000 rad/s, which is *c.a.* 19,000 rpm. This is a rough estimate of the maximum theoretical rotation speed at which the transition from laminar to turbulent flow would take place. In practice, this speed tends to be lower because of imperfections in the construction of the rotating disc assembly and also because of vortex formation around the sheath. This estimate is more than 6

times the highest speed experimentally accessible, which is 3,000 rpm. This is the maximum rotation speed provided by the equipment used. In the present work, the rotation speed was varied from 180 to 1500 rpm, which is well within the range for laminar flow.

Results of experiments at several rotation speeds are shown in **Figure 6.4**. Apart from the rotation speed, all the remaining conditions are the same as used in the reproducibility tests showed in **Figures 6.2** and **6.3**. There is practically no change in the gold dissolution rate with the rotation speed. The same is true of the rate of autoreduction of the ferric thiocyanate solutions, which does not present any change with the rotation speed, as shown both by the potential readings (**Figure 6.5a**) and the reduction of Fe^{3+} to Fe^{2+} (**Figure 6.5b**).

Gold dissolution rates calculated from the numerical data used to plot the curves of **Figure 6.4** appear in **Table 6.2**.

Observation of **Figure 6.4** and **Table 6.2** shows that there is no appreciable effect of the hydrodynamic conditions, as determined by the rotation speed, in the gold dissolution rate. This is an indication that mass transport does not play any significant role in the control mechanism of the dissolution process.

An important point of comparison can now be established. The rates reported in **Table 6.2** were calculated from the gold analyses. The comparison between these and the rate estimated according to the Levich equation can give an indication about the type of control mechanism.

Under the conditions used in these experiments (**Figure 6.4**), the average ligand number is *c.a.* 3.4 and the free SCN^- concentration is *c.a.* 0.09 mol/dm^3. The predominant ferric thiocyanate complex is $Fe(NCS)_4^-$. These estimates were derived from the calculations presented in the **Figures 4.1** to **4.3**, Chapter

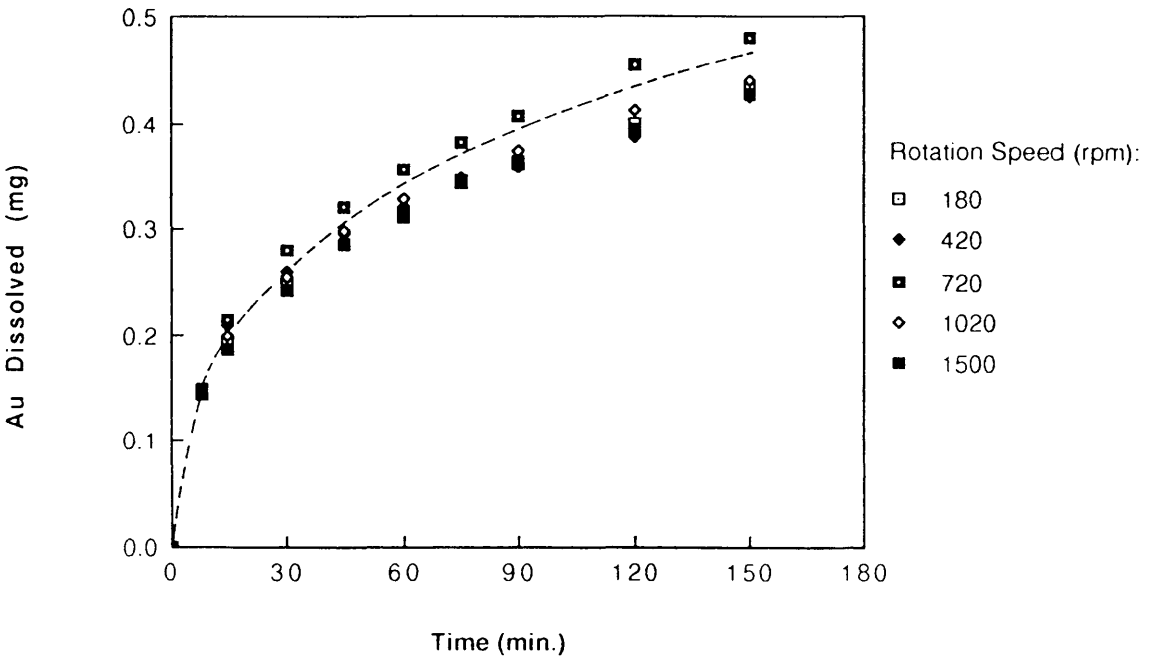
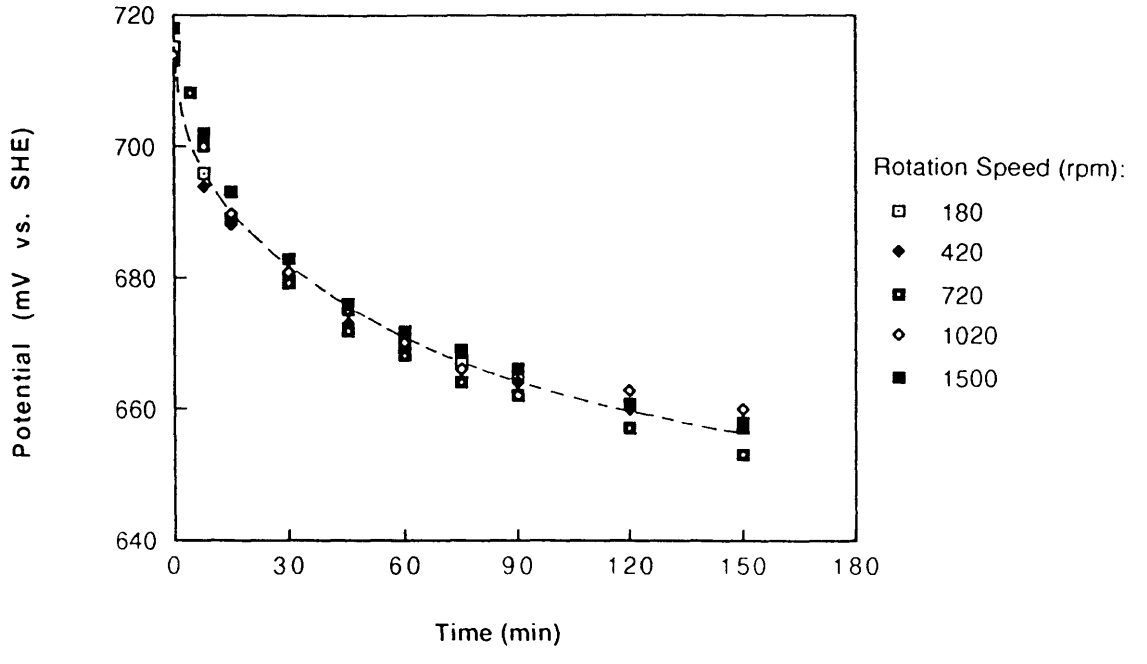


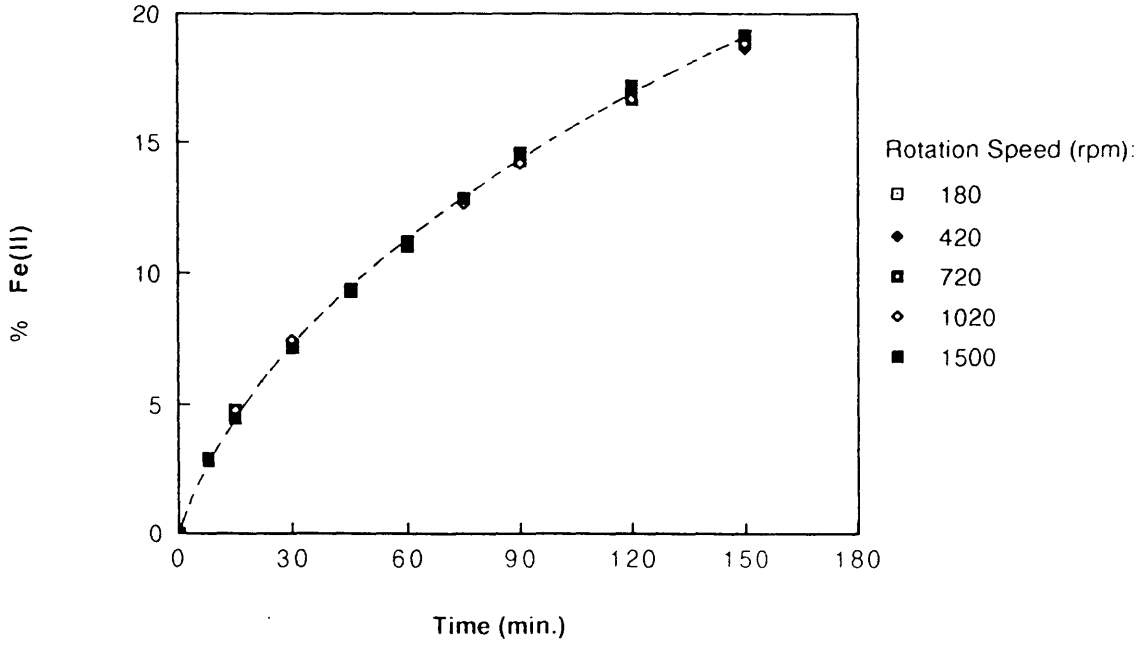
Figure 6.4 - Effect of rotation speed on the leaching of gold by ferric thiocyanate solution. Initial concentrations: 0.275 mol/dm^3 SCN^- and 0.055 mol/dm^3 Fe^{3+}; pH 1.5; temperature, 25°C. N_2 atmosphere.

Table 6.2 - Gold Dissolution Rates Observed with Several Rotation Speeds (experimental conditions indicated in **Figure 6.4**)

Rotation Speed (rpm)	Initial Rate J x 10^{10} (mol/cm^2 s)	Rate after 1 Hour J x 10^{11} (mol/cm^2 s)	Linear Correlation Coefficient, R^2 after 1 Hour
180	10.2	6.98	0.99
420	10.2	5.99	0.99
720	9.91	7.63	0.98
1020	10.0	6.86	0.99
1500	9.88	6.68	0.98



(a)



(b)

Figure 6.5 - Effect of rotation speed on **(a)** potential readings at the gold disc surface and **(b)** reduction of Fe^{3+} to Fe^{2+}. Initial concentrations: 0.275 mol/dm^3 SCN^- and 0.055 mol/dm^3 Fe^{3+}; pH 1.5; temperature, 25°C. N_2 atmosphere.

4. The diffusion coefficient of the SCN^- ion in aqueous solution, as determined by Holtzen and Allen [83], is 1.37 x 10^{-5} cm^2 s^{-1}. The kinematic viscosity can be assumed to be *c.a.* 10^{-2} cm^2 s^{-1} [152]. Substitution of these figures in equation 6.1 yields, for the rotation speed range from 180 to 1500 rpm (18.8 to 157 rad s^{-1}), gold dissolution rates from 3.0 x 10^{-7} to 8.6 x 10^{-7} mol cm^{-2} s^{-1}, respectively. The first of these figures, corresponding to 180 rpm, is more than 300 times the initial observed rate, and more than 4,700 times the rate after 1 hour. The second figure, corresponding to 1500 rpm, is 970 times the observed initial rate and 14,370 times the observed rate after 1 hour.

The observed rates are several orders of magnitude lower than those estimated by Levich equation. These comparisons, plus the lack of response of the observed rates towards the rotation speed (**Figure 6.4**), clearly suggest that the dissolution process is not transport controlled. It is rather **chemically controlled**.

In the above calculation, the term c_0 of the Levich equation (equation 6.1) was taken as the 0.09 mol/dm^3 estimated as the concentration of free SCN^-. In practice, however, the availability of thiocyanate is probably higher. The stability constants of $Au(SCN)_2^-$ and $Au(SCN)_4^-$ are some 15 to 35 orders of magnitude higher than those of similar iron(III)-thiocyanate complexes, as reported in Appendix 3. As a consequence, iron-complexed SCN^- is also available, at least to some extent, to complex gold. Which means that the term c_0 in equation 6.1 would in practice be higher than the 0.09 adopted.

Comparison of **Figures 6.4** and **6.5** indicates the same behaviour already noticed in the previous section. The higher dissolution rates at the beginning were coupled with higher potential readings and autoreduction rates and, thermodynamically, with the predominance of the auric complex, $Au(SCN)_4^-$. There was also a larger production of thiocyanate intermediate species such as

$(SCN)_3^-$ and $(SCN)_2$, due to the faster autoreduction. As the experiments progressed, the autoreduction rates decreased and, simultaneously, the dissolution rates decreased more than 10 times. Due to the lower potential readings, the aurous complex, $Au(SCN)_2^-$, became predominant on thermodynamic grounds. These joint observations point to a connection between the dissolution rate, the oxidation state in which gold is dissolved (i.e. Au^+ and/or Au^{3+}), and the availability of intermediate species such as $(SCN)_3^-$ and $(SCN)_2$, which are both oxidants and sources of the ligand, SCN^-. However, the effects of the remaining variables have to be considered before coming to any conclusion about these observations.

6.5. Effect of the Concentration of Thiocyanate

Experiments at several concentrations of thiocyanate are shown in **Figure 6.6**. The corresponding potential readings and Fe^{2+} fractions appear in **Figure 6.7**. From the numerical data used in **Figure 6.6**, the gold dissolution rates were calculated and are listed in **Table 6.3**.

These gold dissolution results look odd at first sight. Some of the runs were replicated and confirmed the behaviour pattern (see Appendix 6). As regards the initial rates, a tenfold increase in the thiocyanate concentration (from 0.05 to 0.50 mol/dm^3, see **Table 6.3**) causes only approximately a twofold increase in the rate. Furthermore, there seems to be no simple relation between the increases in the concentration of thiocyanate and the corresponding increases in the initial rates. A more awkward pattern is found when considering the rates after 1 hour, in the same table. The irregularities in the behaviour are then pronounced and dismiss any simple correlation.

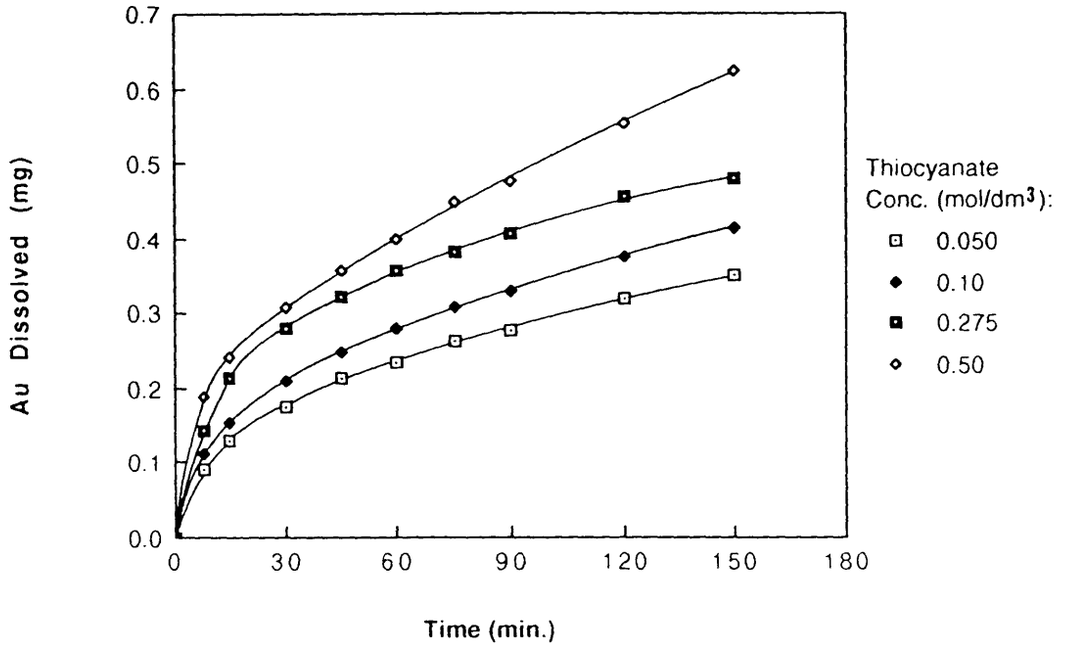
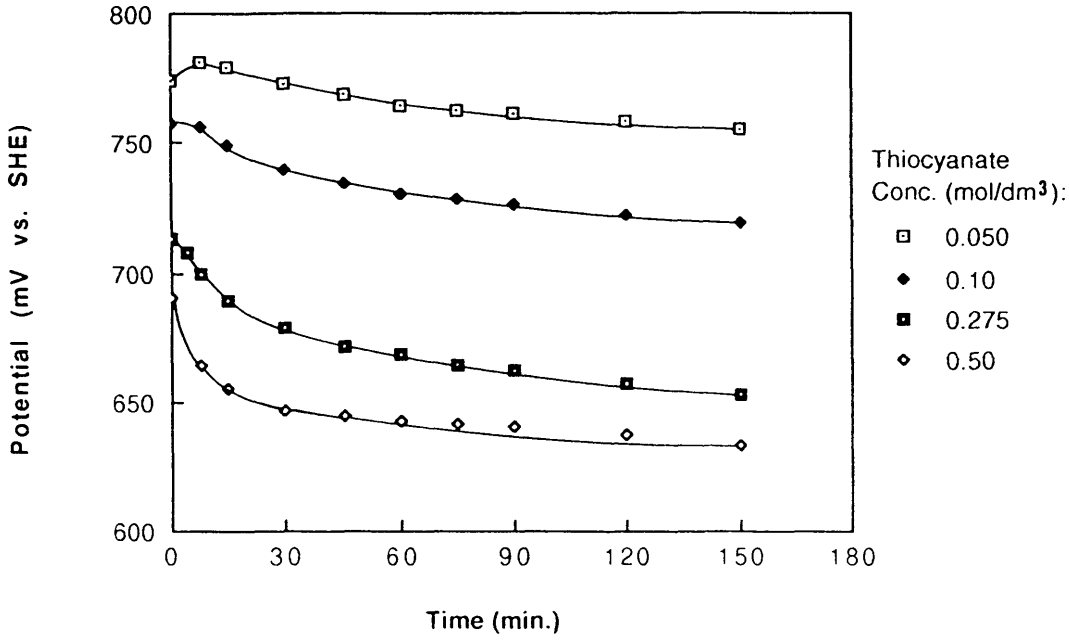


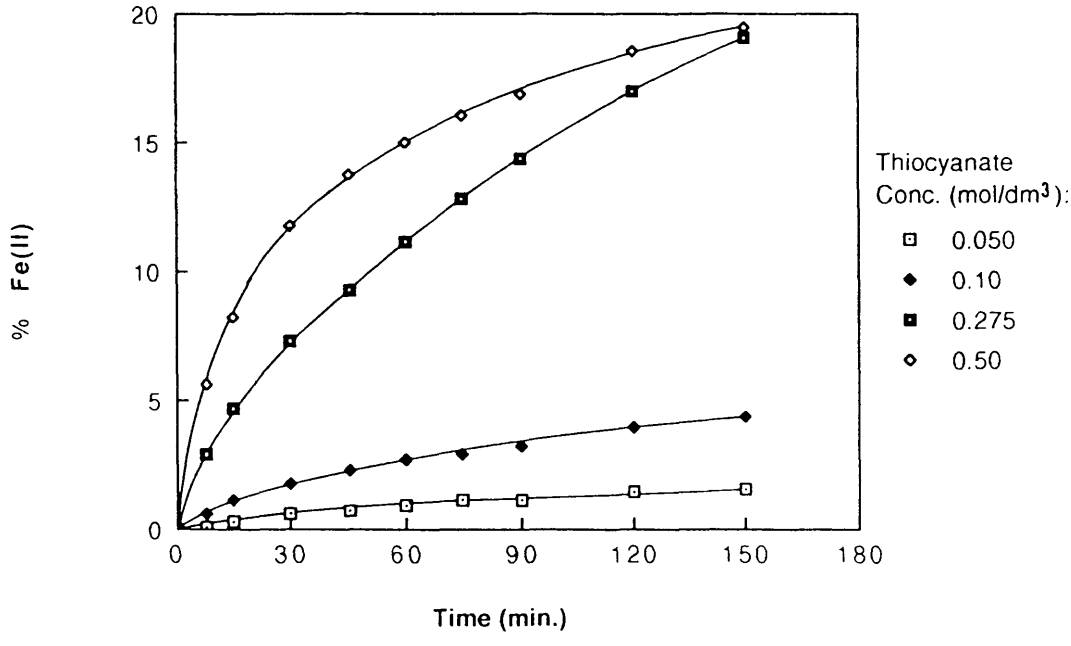
Figure 6.6 - Effect of the concentration of thiocyanate on the leaching of gold by ferric thiocyanate solution. For all runs: 0.055 mol/dm^3 Fe^{3+} (initial); pH 1.5; temperature, 25°C; rotation speed, 75.4 rad/s (720 rpm). N_2 atmosphere.

Table 6.3 - Gold Dissolution Rates Observed with Several Concentrations of Thiocyanate (experimental conditions indicated in **Figure 6.6**)

Thiocyanate Conc. (mol/dm^3)	Initial Rate J x 10^{10} (mol/cm^2 s)	Rate after 1 Hour J x 10^{11} (mol/cm^2 s)	Linear Correlation Coefficient, R^2 after 1 Hour
0.050	6.30	6.96	1.00
0.10	7.78	8.08	1.00
0.275	9.91	7.63	0.98
0.50	13.1	13.5	1.00



(a)



(b)

Figure 6.7 - Effect of the concentration of thiocyanate on **(a)** potential readings at the gold disc and **(b)** reduction of Fe^{3+} to Fe^{2+}. For all runs: 0.055 mol/dm^3 Fe^{3+} (initial); pH 1.5; temperature, 25°C; rotation speed, 75.4 rad/s (720 rpm). N_2 atmosphere.

The complexity of this system defies a straightforward approach. It is believed here that there are three main factors which, put together, may provide an overall explanation for the observed behaviour. The first is the complexation of iron by thiocyanate. The second is the autoreduction of the ferric thiocyanate complexes. The third is the nature of the control of the dissolution kinetics, which is by chemical reaction.

The complexation of iron by thiocyanate can be referred back to **Figures 4.1** through **4.3**, in Chapter 4. The calculations represented in those figures are the basis for the estimates of the concentrations (or, more accurately, activities) of the iron species in solution, used in the present discussion. These estimates are necessarily approximate, due to the lack of activity coefficients for the species considered.

In the experiments with 0.05 and 0.10 mol/dm^3 of total SCN^- (see **Table 6.3**), the predominant ferric thiocyanate complex in solution is the cation $FeNCS^{2+}$. In the first of these experiments, about half of the Fe^{3+} remains uncomplexed by SCN^- and the activity of this ligand in the free state is around 0.005 mol/dm^3. In the second experiment, $FeNCS^{2+}$ is still the predominant iron species but there are considerable fractions of Fe^{3+}, $Fe(NCS)_2^+$ and $Fe(NCS)_3$ which, put together, total about 50% of the iron in solution; the activity of free SCN^- is roughly 0.02 mol/dm^3 (see **Figures 4.1** and **4.3**).

In the third and fourth experiments of **Table 6.3**, respectively with 0.275 and 0.50 mol/dm^3 of total SCN^-, the predominant complex is the anion $Fe(NCS)_4^-$. In the third experiment, about 20% of the initial Fe^{3+} exists as lower complexes, and the activity of free thiocyanate is *c.a.* 0.09 mol/dm^3. In the fourth experiment, the predominant complex is still $Fe(NCS)_4^-$, but there are also minor fractions of $Fe(NCS)_3$ and of the higher complexes $Fe(NCS)_5^{2-}$ and $Fe(NCS)_6^{3-}$. The activity of free SCN^- is *c.a.* 0.28 mol/dm^3 (see

Figures 4.1 and **4.3**).

All the conditions mentioned in the two previous paragraphs are initial conditions. Thus, as far as the iron complexation by thiocyanate is concerned, the experiments reported are not qualitatively homogeneous from the very beginning. The speciation of the system is different in each case. In this fact lies the difficulty in making comparisons between the initial rates reported in **Table 6.3**. The first and second experiments contain basically cationic ferric thiocyanate complexes, whereas the third and fourth contain different distributions with the predominance of $Fe(NCS)_4^-$. As the thiocyanate concentration is increased from 0.050 to 0.50 mol/dm^3, the whole range of iron(III)-thiocyanate complexes is formed, each experiment being unique according to the initial Fe^{3+}/SCN^- ratio. Due to the autoreduction of the ferric thiocyanate complexes, the speciation of the system also changes within each individual run as the reactions proceed. This brings about the discussion of the second factor mentioned above (i.e. the autoreduction process).

Each iron(III)-thiocyanate complex has an inherent autoreduction rate (see Chapter 4, Items 4.7.2 and 4.7.3). Additionally, the experimental results suggest a correlation between the gold dissolution rate and the autoreduction process. It follows that the initial dissolution rate will depend on the initial Fe^{3+}/SCN^- ratio and will vary consistently within a narrow concentration range. When, due to concentration changes, a new complex becomes predominant, the response of the dissolution rate to further increases in the SCN^- concentration will be accordingly different. Such functional changes tend to be smoothed by the overlapping of the fractions of different complexes, the overall autoreduction rate being the resultant of several individual rates, one for each complex present in solution. But the overall "overlapping function" does not promise to be simple at all. Hence the difficulty in generalizing the overall behaviour in a straightforward mathematical model.

Thus, as each run proceeds, the speciation changes. Fe^{2+} and $FeNCS^{+}$ are produced. Free SCN^{-} is released and there is a redistribution of the ferric thiocyanate complexes between themselves. The autoreduction rate decreases and so does the gold dissolution rate. But again, the way such decreases take place depends on the initial composition of the system. A look at the curves of **Figure 6.7** illustrates this point. The gold dissolution rates after 1 hour reported in **Table 6.3** are not directly consistent with the increasing thiocyanate concentrations, which suggests that the path followed by each run is unique to those initial conditions, both quantitatively and qualitatively. There are even cases, such as the third run of **Table 6.3**, in which a further increase in the thiocyanate concentration, despite producing a slightly higher initial rate, causes a decrease in the rate observed after 1 hour. This can only be understood by referring to the autoreduction process, i.e. to the potential readings and Fe^{3+} reduction illustrated in **Figure 6.7**. These three pieces of information (gold dissolution, potential readings and Fe^{3+} reduction) have to be put together in order to provide a suitable explanation. By increasing the thiocyanate concentration, the autoreduction rate and the corresponding potential decrease tend to become faster, leading to a situation in which the gold dissolution rate is lower than that obtained, after that same time (1 hour, in this case), with less thiocyanate.

Such changes in behaviour with the progress of the run were clearly demonstrated in the experiments at higher temperatures (up to 85°C), which are discussed in Section 6.7. In some of those experiments, as much as 80 or 90% of the Fe^{3+} initially added was reduced to Fe^{2+}. There was a wide variation of the Fe^{3+}/SCN^{-} ratio and, consequently, several complexes became successively predominant, within the same experiment. The autoreduction and the gold dissolution rates changed accordingly.

Attempts to work out kinetic data in terms of free SCN^{-} do not give accurate results. The stability constants of $Au(SCN)_2^{-}$ and

$Au(SCN)_4^-$ are some 15 to 35 orders of magnitude higher than those of similar iron(III)-thiocyanate complexes, as reported in Appendix 3. This means that not only free SCN^- but also iron-complexed SCN^- are available to complex gold. Additionally, gold metal catalyses the autoreduction of ferric thiocyanate complexes (see Section 6.7), which suggests that such complexes are easily adsorbed on the metal surface, where they are reduced and, at the same time, release "free" thiocyanate (or the free radical $SCN^\cdot$) which could complex gold cations. It may be argued that free thiocyanate is "more available" than iron-complexed thiocyanate, but due to the overwhelmingly higher stability constants of the gold-thiocyanate complexes as compared with the iron(III)-thiocyanate complexes, the border between the two degrees of "availability" becomes blurred enough to discourage any exactness in this respect.

The discussion above explains the ways in which the dissolution rate responds to the initial Fe^{3+}/SCN^- ratio. It does not explain, however, why the rates are so low (see **Table 6.3**), when cyanidation rates are known to be of the order of 10^{-9} mol/cm^2 s [177] and initial rates with thiourea are reported to reach a maximum of 10^{-8} mol/cm^2 s (with 0.1 mol/dm^3 thiourea and 0.01 mol/dm^3 formamidine disulphide) [177]. In the previous section, the gold dissolution by thiocyanate was found to be chemically controlled. In this section, a further step was taken with the discovery that the gold dissolution rate is rather insensitive to increases in the concentration of thiocyanate. This is better visualized in **Figure 6.8**. The logarithmic plot fits a straight line in the case of the initial rates (R^2 = 0.98) but the correlation is not as good for the rates after 1 hour (R^2 = 0.62). The overall reaction order with respect to SCN^- is just 0.30. It should be noticed that **Figure 6.8** gives only a rough estimate of the order of the overall reaction with respect to SCN^-. As mentioned above, different complexes take part in the process depending on the initial Fe^{3+}/SCN^- ratio, and the consideration of the process in overall terms omits such distinctions.

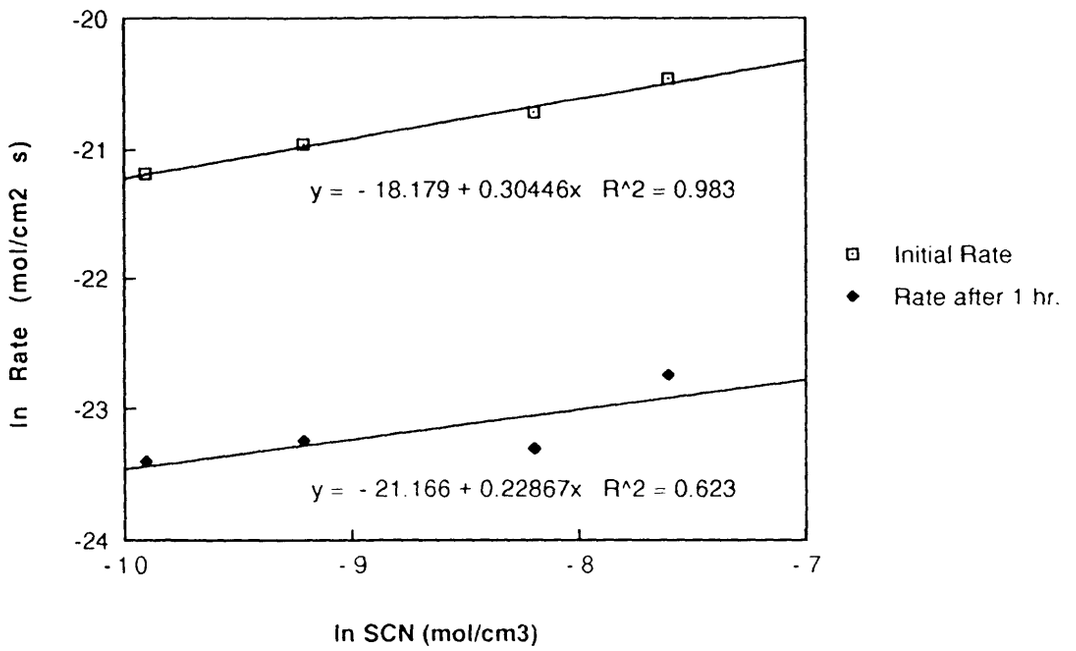


Figure 6.8 - Logarithmic plots of the dissolution rate versus thiocyanate concentration at 25°C, pH 1.5 and initial Fe^{3+} concentration of 0.055 mol/dm^3 (data from **Table 6.3**).

It is believed here that the chemical steps responsible for the low dissolution rates observed involve, on the one hand, the formation of a thin layer of $AuSCN_{(ads)}$ adsorbed on the surface of the metal and, on the other hand, the production of intermediate species such as $(SCN)_3^-$ and $(SCN)_2$ which are both oxidants and complexants of gold. This latter aspect is related to the autoreduction process. The higher initial autoreduction rates, which take place at the higher initial mixed potentials, correspond to higher production of active intermediate species. Under such conditions, the $AuSCN_{(ads)}$ layer is not allowed to stabilize and the gold is further oxidized to the auric state, being dissolved as $Au(SCN)_4^-$. With time, the autoreduction slows down, the potential drops, the production of active intermediate species decreases, and

the $AuSCN_{(ads)}$ becomes more stable, being acted upon mainly by SCN^-, which then dissolves gold as the aurous complex $Au(SCN)_2^-$. These mechanistic considerations were first mentioned in Section 3.11, Chapter 3, and will be resumed in Section 6.10.

6.6. Effect of the Initial Concentration of Iron(III)

The effect of the initial concentration of iron(III) on the gold dissolution rate is illustrated in **Figure 6.9**. The corresponding potential readings and reduction of Fe^{3+} to Fe^{2+} appear in **Figure 6.10**. The gold dissolution rates calculated from the same data are shown in **Table 6.4**. This set of experimental data was obtained with a thiocyanate concentration of 0.275 mol/dm^3.

A second set of experimental data was obtained with 0.10 mol/dm^3 SCN^- and is shown in **Figures 6.11** and **6.12**, and **Table 6.5**.

The analysis of these results is similar to that made in the previous section. Varying the concentration of SCN^- with constant initial concentration of Fe^{3+} or varying the latter while keeping SCN^- constant can both be put in terms of the initial Fe^{3+}/SCN^- ratios. The ferric thiocyanate complexes initially formed and the subsequent path followed by the autoreduction process will be set as a consequence.

In the first set of results (**Figures 6.9** and **6.10**, and **Table 6.4**), the complexes formed are anionic with a predominance of $Fe(NCS)_4^-$. The fractions of higher complexes increase as the initial concentration of Fe^{3+} is diminished or, within the same run, as the autoreduction proceeds. But at all times the predominant complex remains the same (refer to **Figures 4.1** through **4.3**).

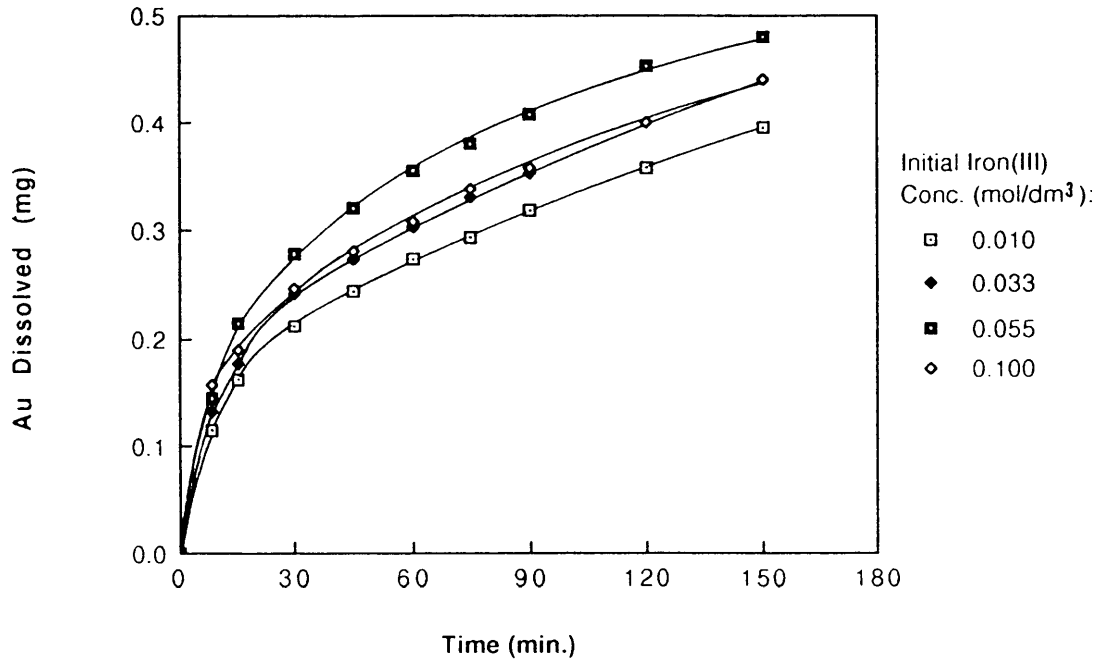
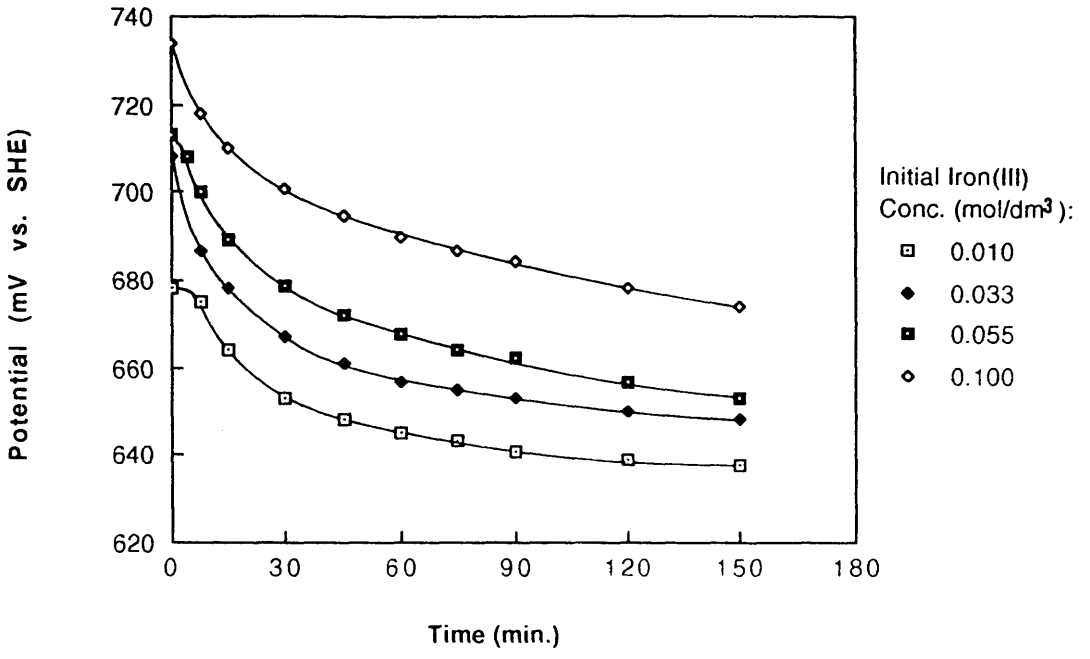


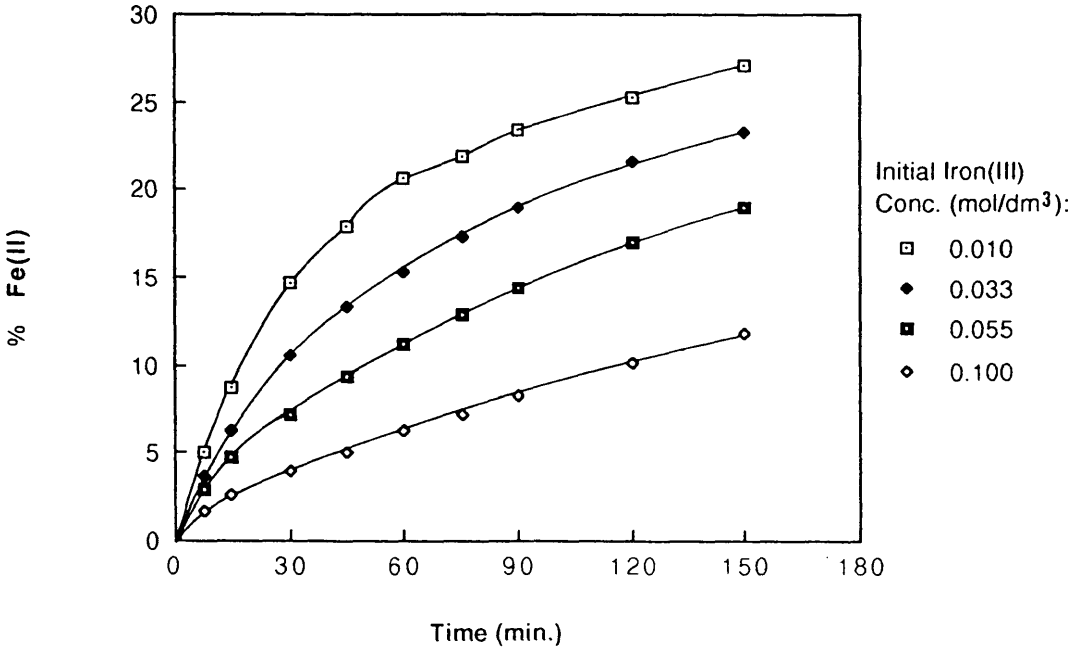
Figure 6.9 - Effect of the initial concentration of iron(III) on the leaching of gold by ferric thiocyanate solution. For all runs: 0.275 mol/dm^3 SCN^-; pH 1.5; temperature, 25°C; rotation speed, 75.4 rad/s (720 rpm). N_2 atmosphere.

Table 6.4 - Gold Dissolution Rates Observed with Several Initial Concentrations of Iron(III) and 0.275 mol/dm^3 SCN^- (experimental conditions indicated in **Figure 6.9**)

Initial Iron(III) Conc. (mol/dm^3)	Initial Rate J x 10^{10} (mol/cm^2 s)	Rate after 1 Hour J x 10^{11} (mol/cm^2 s)	Linear Correlation Coefficient, R^2 after 1 Hour
0.010	7.90	7.46	1.00
0.033	9.14	8.22	1.00
0.055	9.91	7.63	1.00
0.100	10.7	7.93	1.00



(a)



(b)

Figure 6.10 - Effect of the initial concentration of iron(III) with 0.275 mol/dm^3 SCN^- on **(a)** potential readings at the gold disc surface and **(b)** reduction of Fe^{3+} to Fe^{2+}. For all runs: pH 1.5; 25°C; 75.4 rad/s (720 rpm). N_2 atmosphere.

There is a moderate increase in the initial dissolution rate with increasing initial Fe^{3+} concentrations, i.e. with increasing mixed potentials, as shown in **Figure 6.10a**. The dissolution rates after 1 hour, in their turn, respond in a rather irregular way, which is attributed to the different paths followed by the autoreduction process, according to the initial Fe^{3+} and SCN^- concentrations. The rate after 1 hour is rather insensitive to variations in the initial Fe^{3+} concentration. This is illustrated by the logarithmic plot in **Figure 6.13a**, the order of the initial dissolution reaction being not more than 0.13 with respect to the overall Fe^{III} present. As regards the rate after 1 hour, the order (i.e., the slope of the straight line) is minimal and the correlation coefficient is poor, which may be interpreted as indicating no dependence at all of the rate after 1 hour on the initial concentration of Fe^{III}. Again, it should be emphasized that the logarithmic plots of dissolution rate versus total Fe^{III} shown in **Figure 6.13** provide only a rough estimate of the overall reaction order. In these experiments, practically all Fe^{III} is complexed by SCN^-. Thus, the Fe^{III} species acting as oxidant is basically the ferric thiocyanate complex which is predominant under those conditions (plus the other complexes also present as minor fractions). As each complex has its inherent autoreduction rate (see Chapter 4, Items 4.7.2 and 4.7.3), a different set of initial concentrations may give a different slope of the logarithmic plot. This is seen in **Figure 6.13b**, which was calculated from the second set of experimental data, represented in **Figures 6.11** and **6.12**, and **Table 6.5**. The order estimates in this second case are 0.17 for the initial reaction and 0.13 for the reaction after 1 hour.

The actual process of oxidation of gold should consist mainly of electron transfer steps involving intermediate species such as the free radical $SCN^{\cdot}$, $(SCN)_3^-$, $(SCN)_2$, etc., which can act both as oxidants and ligands in the make up of gold-thiocyanate complexes. The direct electron transfer from Au^0 or Au^I to Fe^{III} can not be ruled out, but does not seem sufficient to explain the behaviour observed. In fact, most of the electron transfer to Fe^{III} is related to the

autoreduction of the ferric thiocyanate complexes, as already pointed out in Section 6.5. This point will be further discussed in Section 6.7.

In the second set of results (**Figures 6.11**, **6.12** and **Table 6.5**) the concentration of thiocyanate is 0.10 mol/dm^3, whereas the same initial concentrations of Fe^{3+} were used. There is, in this case, a gradual shift from the predominance of the anionic complex $Fe(NCS)_4^-$ in the first run of **Table 6.5** to the predominance of the cationic complex $FeNCS^{2+}$ in the last run. The initial rates increase with the increasing initial concentration of Fe^{3+} up to a value around 0.055 mol/dm^3, and then decrease. The rates after 1 hour behave in the same way. Overall, the initial rates with 0.10 mol/dm^3 SCN^- are only about 1.5 times lower than those with 0.275 mol/dm^3.

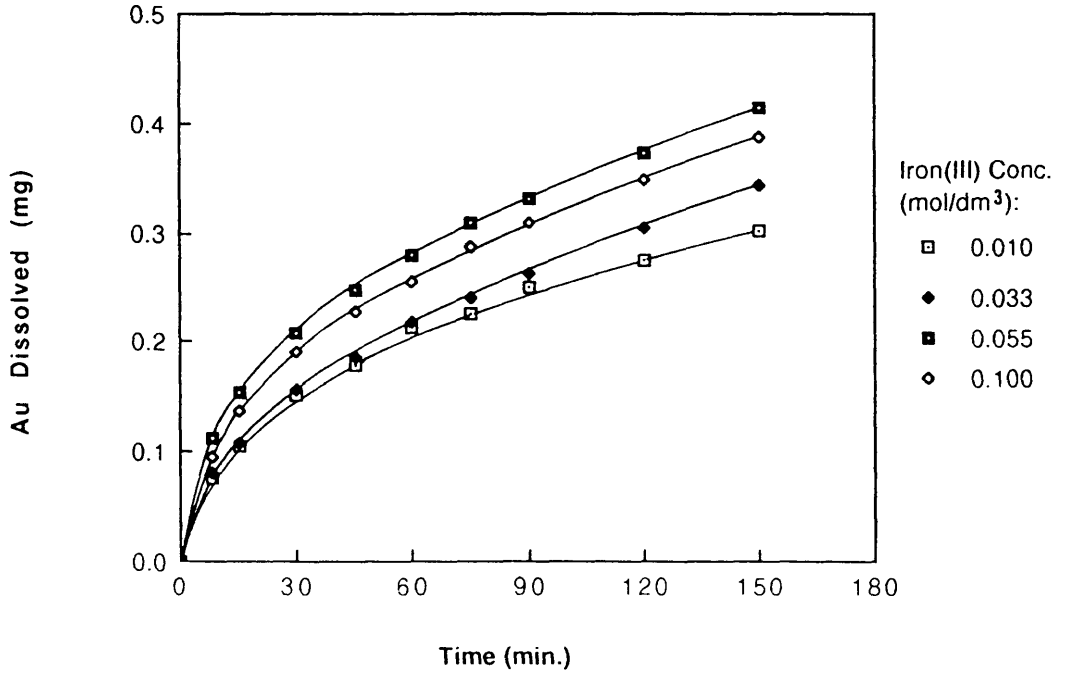


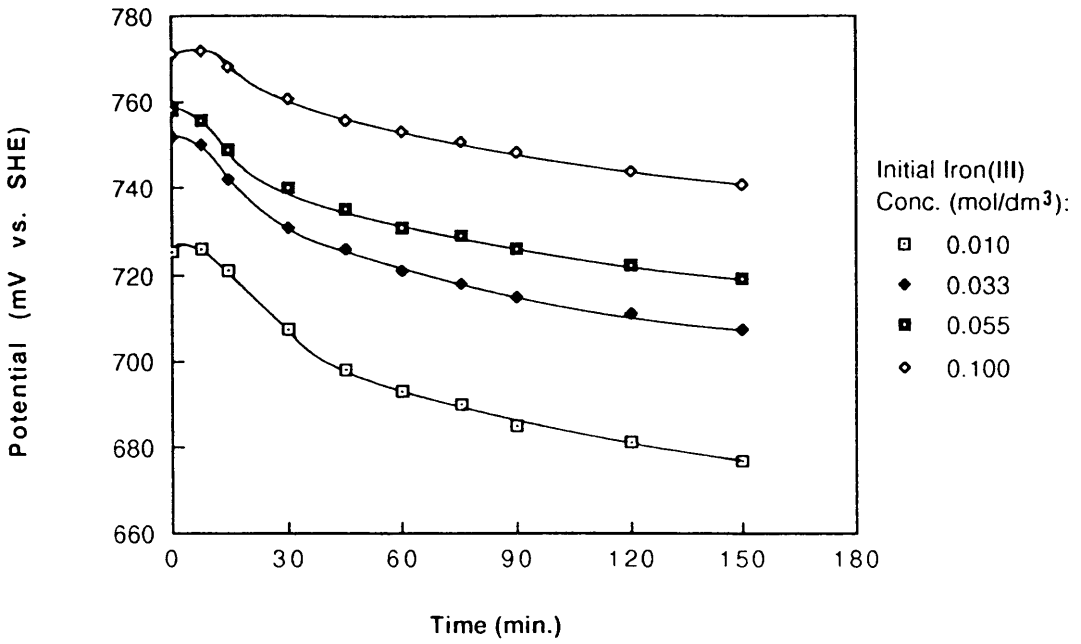
Figure 6.11 - Effect of the initial concentration of iron(III) on the leaching of gold by ferric thiocyanate solution. For all runs: 0.10 mol/dm^3 SCN^-; pH 1.5; temperature, 25°C; rotation speed, 75.4 rad/s (720 rpm). N_2 atmosphere.

Table 6.5 - Gold Dissolution Rates Observed with Several Initial Concentrations of Iron(III) and 0.10 mol/dm^3 SCN^- (experimental conditions indicated in **Figure 6.11**)

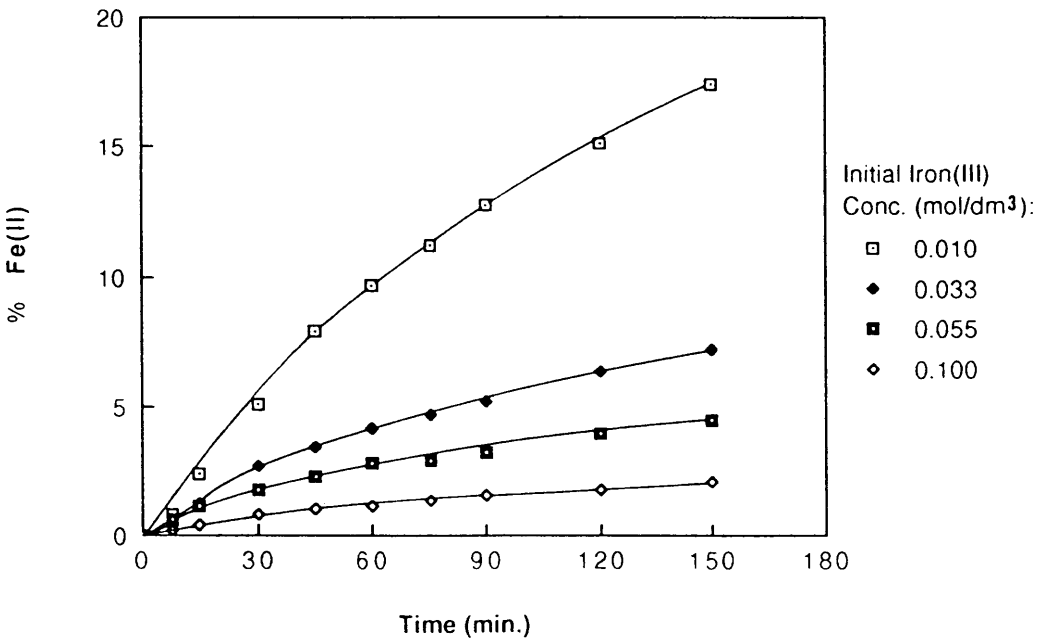
Initial Iron(III) Conc. (mol/dm^3)	Initial Rate J x 10^{10} (mol/cm^2 s)	Rate after 1 Hour J x 10^{11} (mol/cm^2 s)	Linear Correlation Coefficient, R^2 after 1 Hour
0.010	5.17	5.40	0.99
0.033	5.56	7.60	1.00
0.055	7.78	8.08	1.00
0.100	6.55	7.77	0.99

At this point it is interesting to compare **Figures 6.10a** and **6.12a** and to observe the relations between the thiocyanate concentration, the potential readings and the gold dissolution rates. The potential readings obtained when the concentration of thiocyanate is 0.275 mol/dm^3 (**Figure 6.10a**) are lower than with 0.10 mol/dm^3 (**Figure 6.12a**), but due to the greater availability of SCN^- in the first case, the initial dissolution rates are about 1.5 times higher than those in the second, despite the higher potential readings of the latter. The rates after 1 hour, in their turn, have about the same value in most cases (see **Tables 6.4** and **6.5**), despite the potential readings in **Figure 6.10a** being considerably lower than those in **Figure 6.12a**.

Overall, the dissolution rates presented in this section have the same magnitude, and in many cases about the same value, as those reported in the previous section, which dealt with the effect of the concentration of thiocyanate. Under the conditions studied, there is only a small effect of the initial concentration of Fe^{III} on the gold dissolution rate.

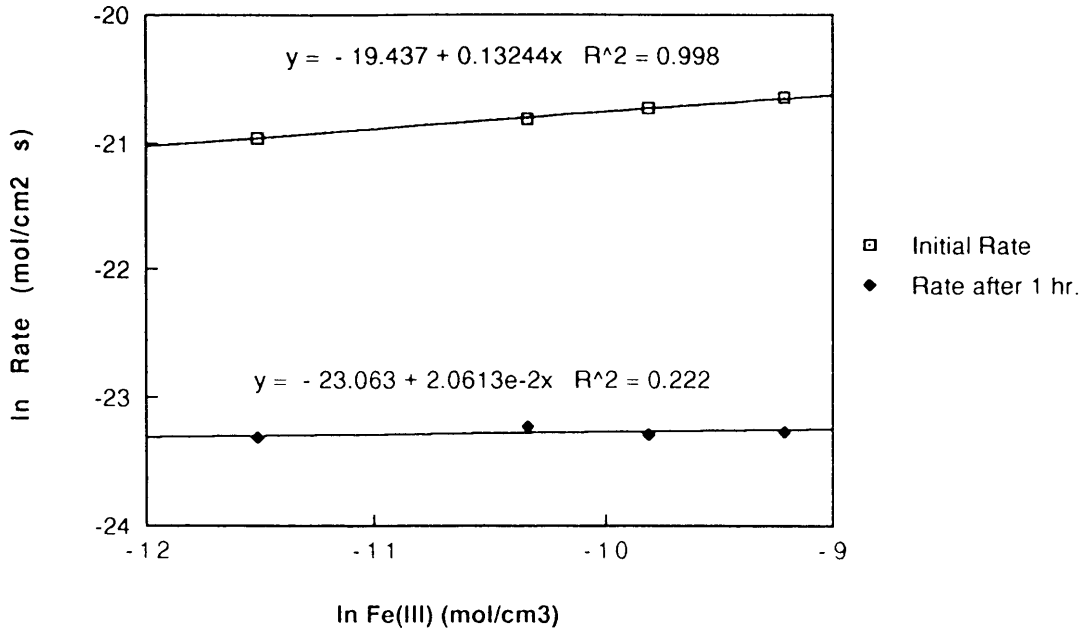


(a)

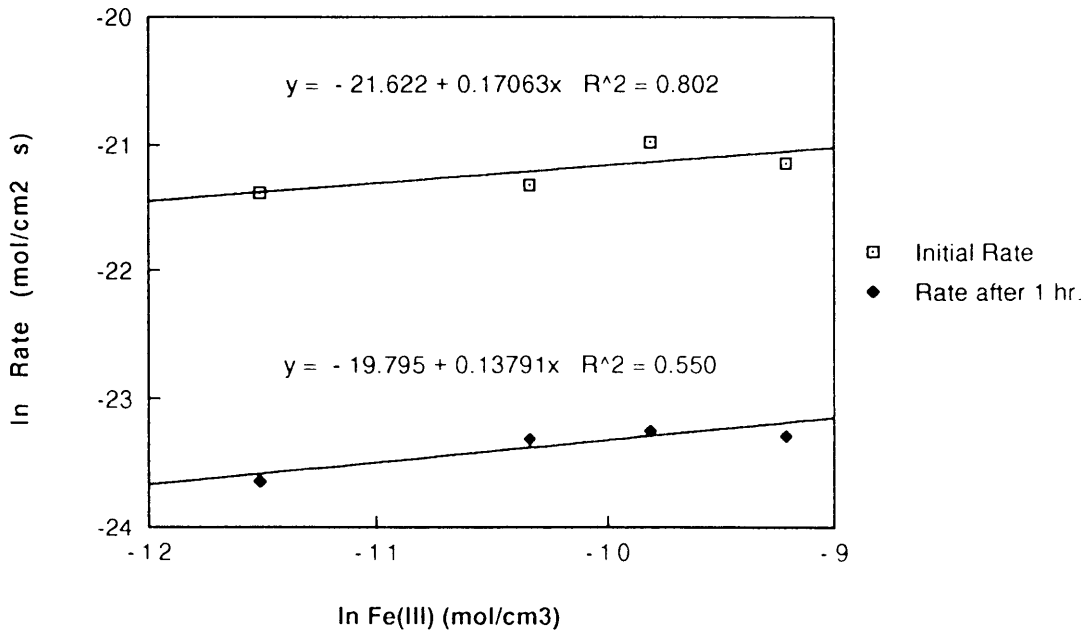


(b)

Figure 6.12 - Effect of the initial concentration of iron(III) with 0.10 mol/dm^3 SCN^- on **(a)** potential readings at the gold disc surface and **(b)** reduction of Fe^{3+} to Fe^{2+}. For all runs: pH 1.5; 25°C; 75.4 rad/s (720 rpm). N_2 atmosphere.



(a)



(b)

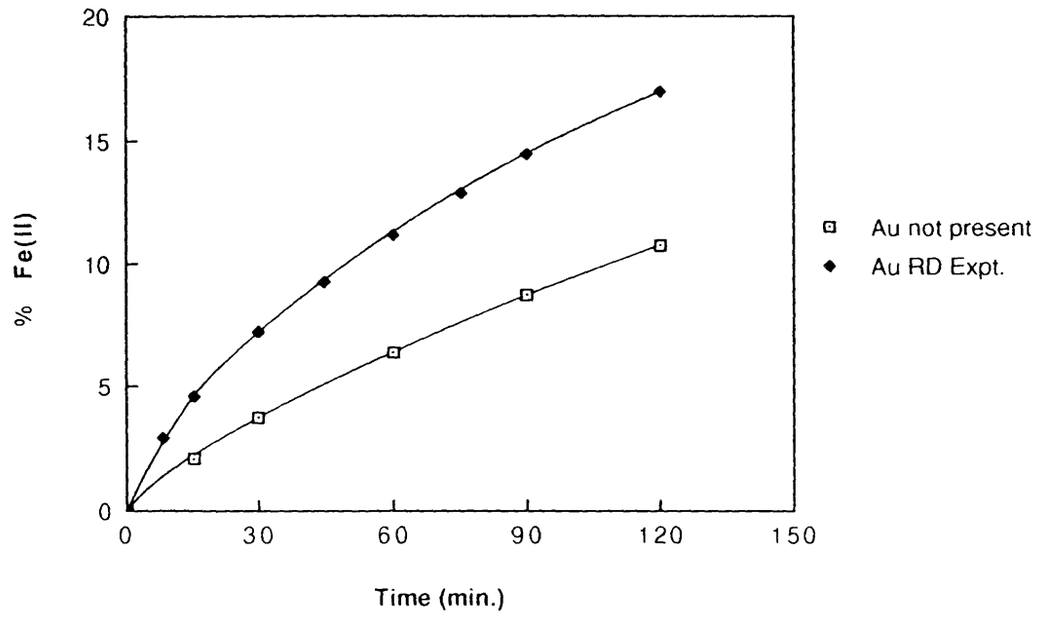
Figure 6.13 - Logarithmic plots of dissolution rate versus initial Fe^{3+} concentration at 25°C and pH 1.5 using **(a)** 0.275 mol/dm^3 SCN^- (data from **Table 6.4**) and **(b)** 0.10 mol/dm^3 SCN^- (data from **Table 6.5**).

The findings of this and the previous sections can be put together as follows: under the conditions investigated, there is little effect of the concentrations of Fe^{3+} and SCN^- on the gold dissolution rate. In all cases, the rates observed were at least one order of magnitude lower than those obtained with cyanide and even lower than the maximum initial rates obtained with 0.1 mol/dm^3 of thiourea (plus 0.01 mol/dm^3 formamidine disulphide) [177]. The dissolution of gold is related to the autoreduction of the ferric thiocyanate complexes, as expressed both by the potential readings and by the production of Fe^{2+}. Within the same run, higher potential readings and higher autoreduction rates correspond to higher dissolution rates and vice-versa. These observations indicate the participation of the intermediate species $(SCN)_3^-$ and $(SCN)_2$ (besides the free radical $SCN^{\cdot}$), which are produced by the autoreduction process, in the mechanism of gold dissolution. The complex $Au(SCN)_4^-$ is preferentially formed under the initial conditions, when the autoreduction is faster and the mixed potentials higher. As the run proceeds, the $Au(SCN)_2^-$ complex prevails (see Chapter 3, Sections 3.10, and Section 6.10).

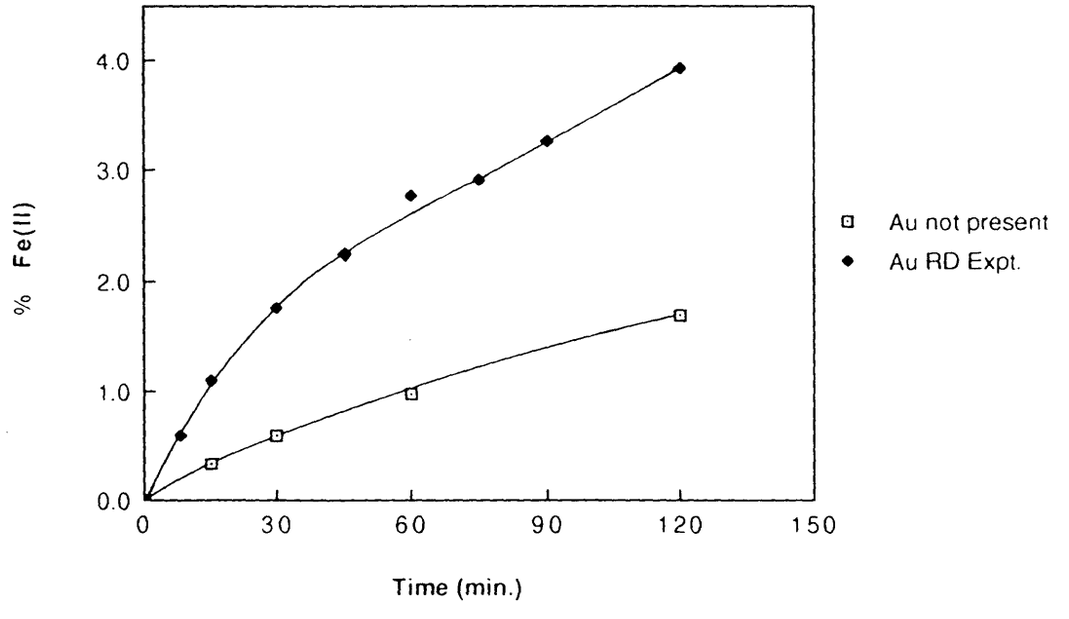
6.7. Catalytic Effect of Gold Metal on the Autoreduction of Iron(III)-Thiocyanate Complexes

The autoreduction of iron(III)-thiocyanate complexes was more extensive in the gold rotating disc experiments than in plain autoreduction experiments under the same conditions (except for the absence of the gold disc). This is illustrated in **Figure 6.14**.

One of the first thoughts to arise when analysing these results was whether the increase in the Fe^{3+} reduction in the presence of gold was due to the oxidation of gold during the dissolution process. If so, it could not be considered as autoreduction of ferric thiocyanate, neither could it be regarded as catalysis.



(a)



(b)

Figure 6.14 - Catalytic effect of gold metal on the autoreduction of iron(III)-thiocyanate complexes at 25°C and pH 1.5, with initial Fe^{3+} concentration of 0.055 mol/dm^3 and thiocyanate concentration of **(a)** 0.275 and **(b)** 0.10 mol/dm^3.

The answer to this question reveals a very interesting fact about the leaching of gold by ferric thiocyanate solutions. Taking as a first example the runs shown in **Figure 6.14a**: the amount of Fe^{3+} reduced to Fe^{2+} in the rotating disc experiment was *c.a.* $1.68x10^{-3}$ moles while in the corresponding autoreduction experiment this amount was $1.06x10^{-3}$ moles, which means an increase of $6.20x10^{-4}$ moles in the rotating disc run. The amount of gold dissolved after the same 2 hours was $2.3x10^{-6}$ moles. Thus in molar terms, the increase in the amount of Fe^{3+} reduced was about 270 times higher than the amount of gold dissolved; a quantity much bigger than that necessary to promote the oxidation of the gold dissolved. Even considering all the gold being dissolved in the auric state, the charge equivalent to the increase in Fe^{3+} reduction would still be *c.a.* 90 times the charge effectively involved in the gold oxidation. In other words, most of the Fe^{3+} was used to oxidize thiocyanate rather than to oxidize gold. Furthermore, the presence of the gold metal catalyzed the Fe^{3+} reduction and the corresponding thiocyanate oxidation, i.e. catalyzed the autoreduction process in the ferric thiocyanate solution. Considering now the rotating disc experiment separately, the overall amount of Fe^{3+} reduced is, in molar terms, about 730 times greater than the gold dissolved. In terms of charge transfer, the charge involved in the Fe^{3+} reduction is between 240 and 730 times that involved in the oxidation of gold (depending on its oxidation state). Most of the iron reduction is therefore related to the oxidation of thiocyanate, which shows that, while studing the leaching of gold, it is in the ferric thiocyanate solution itself that most of the transformations occur.

Similar observations can be made in the runs of **Figure 6.14b**. The total Fe^{3+} reduction was $3.88x10^{-4}$ moles in the rotating disc run and $1.67x10^{-4}$ moles in the autoreduction run. The amount of gold dissolved was $1.89x10^{-6}$ moles. This means that, in molar terms, the increase in Fe^{3+} reduction due to the presence of the gold disc was 117 times the amount of gold dissolved. Considering the rotating disc run alone, the overall charge transfer involved in the Fe^{3+} reduction was between 68 and 205 times greater than that

effectively required to oxidize the gold dissolved.

There is a catalytic effect of the gold metal on the autoreduction process. Furthermore, the overall charge transfer taking place in the system is mainly related to the autoreduction of ferric thiocyanate with only a minor part involved in the oxidation of gold. This observation is further demonstrated by the results shown in **Table 6.6**. The two columns on the right contain the molar ratios between the total iron(III) reduced (in the rotating disc experiments) and the gold dissolved, and between the fraction of the total autoreduction which is due to heterogeneous process and the gold dissolved, respectively. Some comments on **Table 6.6** should be added, as follows:

In all runs, a high fraction of the total autoreduction is due to heterogeneous process, which involves the adsorption of the iron(III)-thiocyanate complexes on the surface of the gold disc. In most of the runs at 25°C, that fraction is greater for higher complexes (i.e. $Fe(NCS)_4^-$ and higher, which are predominant in the runs with 0.275 mol/dm^3 SCN^-) than for lower complexes (i.e. $FeNCS^{2+}$ and $Fe(NCS)_2^+$, which are predominant in the runs with 0.10 mol/dm^3 SCN^-).

Comparison between the data in **Table 6.6** (obtained using a rotation speed of 75.4 rad/s) and those in **Figure 6.5** show that there was no variation in the extent of autoreduction when the rotation speed of the gold disc was varied in the range 19-157 rad/s (180-1500 rpm), which suggests that diffusion of the complexes plays no significant role in determining the rate of the heterogeneous process.

Thus, the total autoreduction of the iron(III)-thiocyanate complexes in a leaching experiment results from two distinct contributions. One comes from the autoreduction which takes place in the bulk of the solution due to electron transfer within the

Table 6.6 · Catalytic Effect of Gold Metal on the Autoreduction of Iron(III)-Thiocyanate Complexes at 25°C. Comparison between the Extents of Autoreduction (in the Presence and Absence of Gold) and Gold Dissolution. Experiment Time: 2 hours. Volume of Liquid Phase: 180 cm^3.

Initial Concentrations (mol/dm^3)		**Temp.**	**Fe(III) Reduced to Fe(II)** (mol/dm^3)		Increase in Autoreduction due to Au Catalysis (mol/dm^3)	Gold Dissolved (mol/dm^3)	Molar Ratio: Autoreduction (total) / Au Dissolved	Molar Ratio: Increase in Autoreduction/ Au Dissolved
SCN	Fe(III)	(°C)	Au Rotating Disc Runs	Autoreduction Runs (without Au Disc)				
0.10	0.010	25	0.0015	0.0004	0.0011	0.000008	197	142
0.10	0.033	25	0.0021	0.0009	0.0012	0.000009	246	136
0.10	0.055	25	0.0022	0.0009	0.0012	0.000011	206	117
0.10	0.100	25	0.0018	0.0006	0.0012	0.000010	182	119
0.275	0.010	25	0.0025	0.0012	0.0013	0.000010	250	127
0.275	0.033	25	0.0071	0.0042	0.0030	0.000011	628	261
0.275	0.055	25	0.0093	0.0058	0.0036	0.000013	730	278
0.275	0.100	25	0.0101	0.0071	0.0030	0.000011	894	266
0.275	0.055	40	0.0239	0.0202	0.0037	0.000029	815	125
0.275	0.055	55	0.0378	0.0290	0.0088	0.000122	309	72

complexes, and the other comes from the autoreduction of the complexes adsorbed on the surface of the gold disc. The contribution of this heterogeneous process to the total autoreduction varied from 15% to 73%, in the runs in **Table 6.6** only. The relative contributions of the homogeneous and heterogeneous autoreduction is affected by factors such as type of complex (i.e. cationic or anionic, ligand number, etc.) and temperature.

The fact that the amount of gold dissolved corresponds, on a molar basis, to less than 1% of the iron(III) reduced at the surface suggests a considerable degree of passivation of the gold metal, which might be taken as an indication of the formation of a thin-layer of adsorbed AuSCN on its surface (see Section 6.12).

Table 6.7 - Molar Ratios between Iron(III) Reduced and Gold Dissolved in Rotating Gold Disc Runs. Initial Iron(III) Concentration: 0.055 mol/dm^3 . Experiment Time: 2 hours.

Thiocyanate Concentration (mol/dm^3)	Temperature (°C)	Fe(III) Reduced to Fe(II) (mol/dm^3)	Gold Dissolved (mol/dm^3)	Molar Ratio: Fe(III) Reduced/ Au Dissolved
0.05	25	0.0008	0.000009	88
0.05	48	0.0036	0.000032	112
0.05	55	0.0063	0.000045	142
0.05	85	0.0479	0.000234	205
0.10	25	0.0022	0.000011	206
0.10	40	0.0065	0.000024	272
0.10	48	0.0122	0.000034	363
0.10	55	0.0170	0.000054	317
0.10	85	0.0494	0.000318	155
0.275	25	0.0093	0.000013	730
0.275	40	0.0239	0.000029	816
0.275	48	0.0297	0.000042	706
0.275	55	0.0374	0.000122	307
0.275	85	0.0540	0.000247	218

The data in **Table 6.6** show that, in molar terms, the amount of gold dissolved corresponds to only 0.72 ± 0.31% of the Fe^{3+} reduced in the heterogeneous process, and to 0.32 ± 0.17% of that reduced in the overall (homogeneous plus heterogeneous) process. The situation is similar for rotating disc experiments at several temperatures, as shown in **Table 6.7**, whose data indicate that, in molar terms, the gold dissolved corresponds to only 0.46 ± 0.30% of the total autoreduction.

Therefore, the dissolution of gold takes place at a rather complex interface at which are arriving both the intermediate species of SCN^- oxidation resulting from the autoreduction in the bulk of the solution, namely $(SCN)_3^-$ and $(SCN)_2$, and the various iron(III)-thiocyanate complexes present in solution. The complexes adsorbed on the gold surface also undergo autoreduction with the production of free radicals $SCN^{\cdot}$, from which $(SCN)_2^-$, $(SCN)_3^-$ and $(SCN)_2$ are produced. This heterogeneous mechanism includes reactions 3.43 to 3.45 proposed by Itabashi [90] (see Chapter 3, Item 3.8.2). Apart from the adsorption and desorption steps, the reaction steps of the heterogeneous mechanism are similar to those of the homogeneous mechanism, which was discussed in Chapter 4, Section 4.10. The active intermediate species of SCN^- oxidation, produced both in the homogeneous and heterogeneous processes, participate in the mechanism of gold dissolution.

The fact that the gold dissolved corresponds, on a molar basis, to less than 1% of the iron(III) reduced at the surface suggests a considerable degree of passivation of the gold metal. This passivation might suggest the formation of a thin-layer of adsorbed AuSCN on the surface.

6.8. Effect of Temperature

The low gold dissolution rates reported in the previous sections motivated attempts to improve the performance of the ferric thiocyanate system in this respect. Two main courses of investigation were adopted. The first one was to try higher temperatures. The second was to continue working at 25°C but making additions of iodide ions or iodine solution in order to chemically alter the leaching process. The first of these sets of results is discussed in this section. The results from iodide/iodine additions will be treated in the next chapter.

Gold dissolution results with 0.10 mol/dm^3 SCN^- and 0.055 mol/dm^3 Fe^{3+} at several temperatures are shown in **Figure 6.15**. The corresponding potential readings and Fe^{3+} reduction data are shown in **Figure 6.16**. The gold dissolution rates are listed in **Table 6.8**. There was a noticeable increase in the gold dissolution rate with temperature, particularly above 55°C. The same was observed with respect to the autoreduction process. About 93.1% of the Fe^{3+} was reduced to Fe^{2+} at 85°C, in comparison with only 4.4% at 25°C (see **Figure 6.16b**). The initial dissolution rate at 85°C was 1.80×10^{-8} mol cm^{-2} s^{-1}. A rate as high as 1.13×10^{-8} mol cm^{-2} s^{-1} was obtained using only 0.05 mol/dm^3 SCN^- at 85°C. These dissolution rates are comparable to the 1×10^{-8} mol cm^{-2} s^{-1}, which was the maximum rate obtained by Groenewald [177] using 0.1 mol/dm^3 thiourea and 0.01 mol/dm^3 formamidine disulphide at 25°C.

Gold dissolution results of the first four experiments listed in **Table 6.8**, with 0.05 mol/dm^3 SCN^-, are shown in **Figure 6.17**. The behaviour pattern is very similar to that obtained with 0.10 mol/dm^3 and illustrated in **Figures 6.15** and **6.16**. Plots of potential readings and Fe^{3+} reduction versus time are similar to those of **Figure 6.16** and were not included here to avoid repetition. The Fe^{3+} reduction in the experiment at 85°C reached 89.4%, a figure

which is very close to the 93.1% reported for the experiment with 0.10 mol/dm^3 SCN^- at the same temperature.

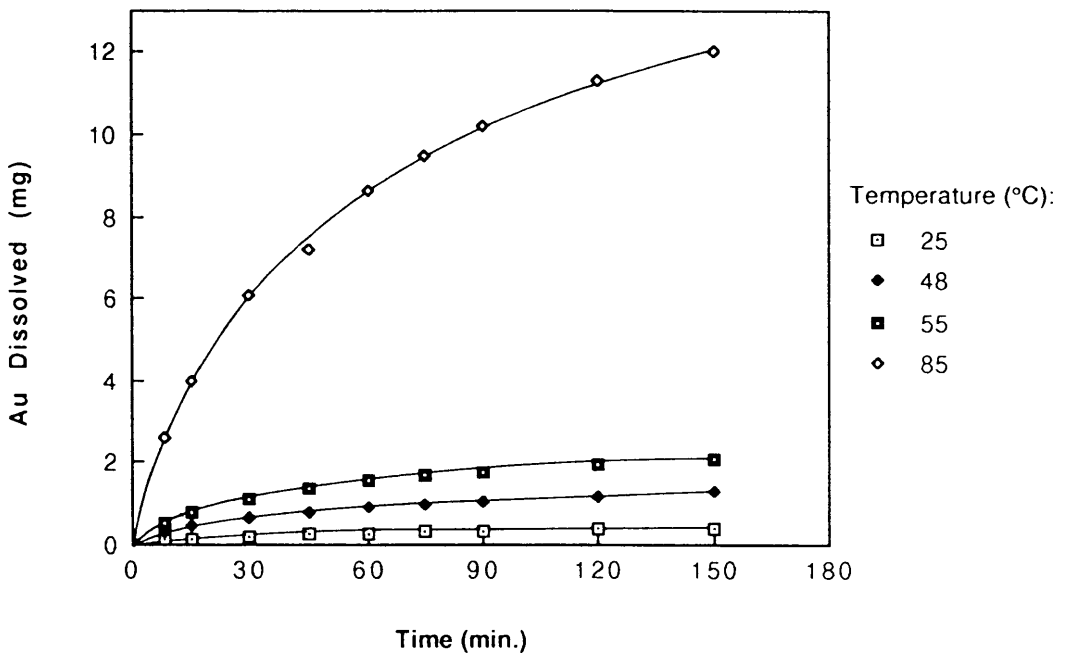
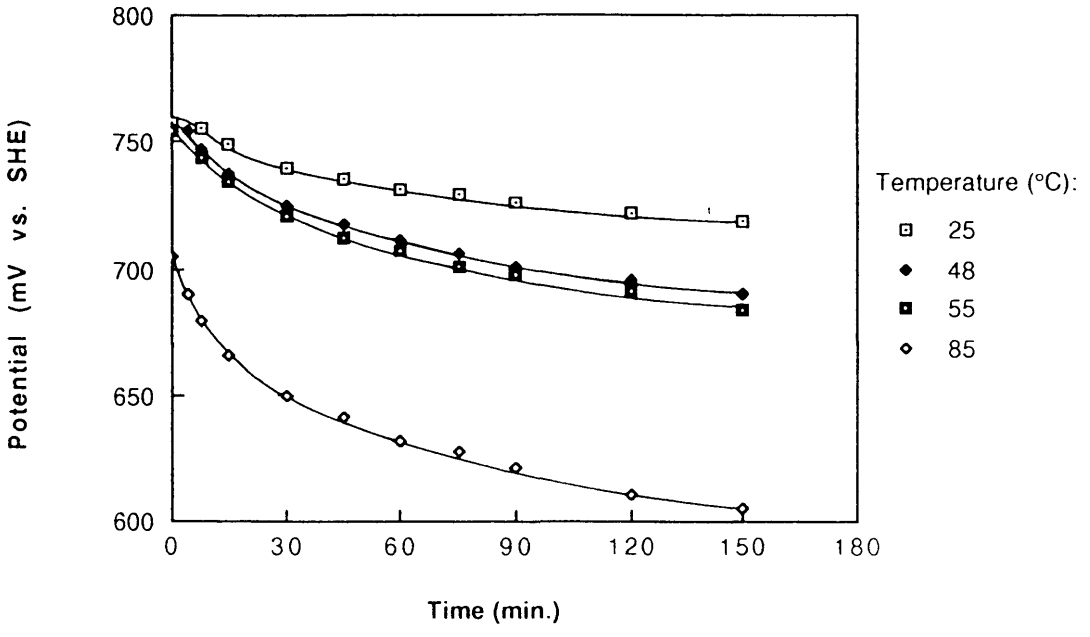
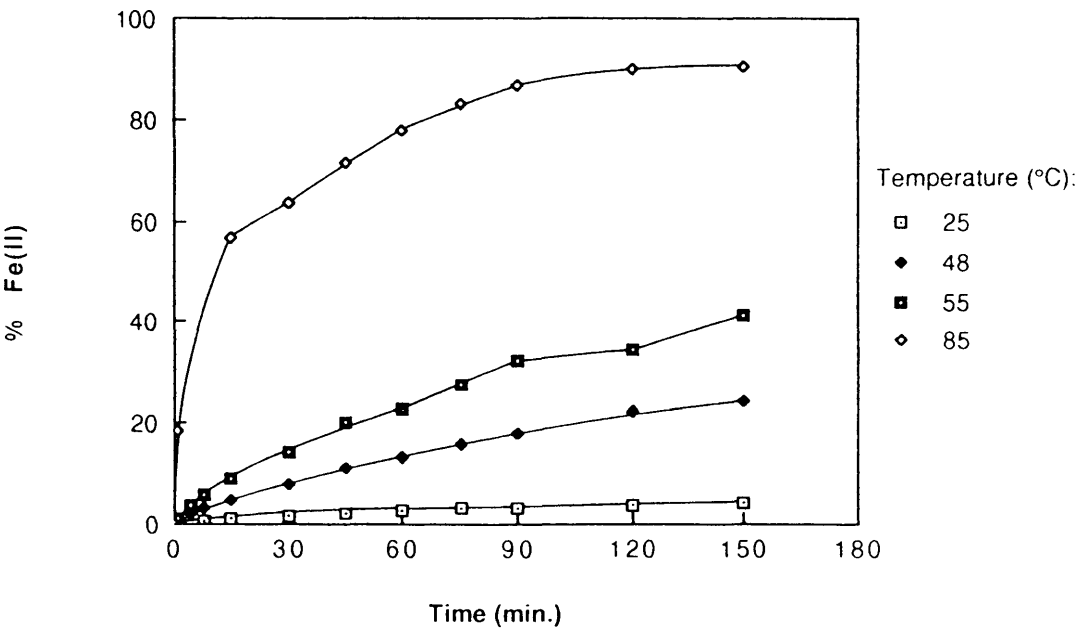


Figure 6.15 - Effect of temperature on the dissolution of gold with 0.10 mol/dm^3 SCN^- and 0.055 mol/dm^3 Fe^{3+} (initial), at pH 1.5 and 75.4 rad/s (720 rpm). N_2 atmosphere.

In both of these series, the predominant complex at zero time was the cation $FeNCS^{2+}$. There was also a considerable fraction of Fe^{3+} uncomplexed by SCN^- in the first series (with 0.05 mol/dm^3 SCN^-). In the second series (with 0.10 mol/dm^3), fractions of $Fe(NCS)_2^+$ and $Fe(NCS)_3$ were also initially present and there was a shift to the predominance of the anion $Fe(NCS)_4^-$ towards the end of the experiment at 85°C, due the conversion of more than 93.1% of the initial Fe^{3+} to Fe^{2+}, which drastically changed the Fe^{3+}/SCN^- ratio. This change, however, occurred gradually with time and did not affect the overall pattern of results, which was basically the same for the two series of experiments, as illustrated in **Figures 6.15** and **6.17**.



(a)



(b)

Figure 6.16 - Effect of temperature on **(a)** potential readings and **(b)** reduction of Fe^{3+} to Fe^{2+}. For all runs: 0.10 mol/dm^3 SCN^- and 0.055 mol/dm^3 Fe^{3+} (initial); pH 1.5; 75.4 rad/s (720 rpm); N_2 atmosphere.

Table 6.8 - Gold Dissolution Rates Observed at Several Temperatures and SCN^- Concentrations. In all runs the initial Fe^{3+} concentration was 0.055 mol/dm^3 (pH 1.5, 720 rpm, N_2 atmosphere)

Thiocyanate Conc. (mol/dm^3)	Temperature (°C)	Initial Rate J x 10^9 (mol/cm^2 s)	Rate after 1 Hour J x 10^{10} (mol/cm^2 s)
0.05	25	0.63	0.70
0.05	48	1.75	2.42 (*)
0.05	55	2.61	2.53 (*)
0.05	85	11.3	11.8 (*)
0.10	25	0.78	0.81
0.10	48	2.28	2.44 (*)
0.10	55	3.56	2.79 (*)
0.10	85	18.0	16.5
0.275	25	0.99	0.76
0.275	40	1.98	2.42 (*)
0.275	48	2.46	5.73 (*)
0.275	55	3.15	27.4 (*) (**)
0.275	85	20.6	0.83 (*)

(*) Samples considered in the linear regression are the ones collected at 90 minutes and after. The correlation coeffecients, R^2, for all the straight lines are 0.99 or 1.00.

(**) Three different dissolution stages could be distinguisehd in this run. A dissolution rate of 1.10×10^{-9} mol cm^{-2} s^{-1} was estimated for the intermediate stage, between 15 and 75 minutes

The effect of temperature in the distribution of the iron(III)-thiocyanate complexes has been disregarded, because of the lack of thermodynamic data. Since the temperature range is narrow (i.e. 25-35°C), it is reasonable to assume that there is no great variation in the stability constants.

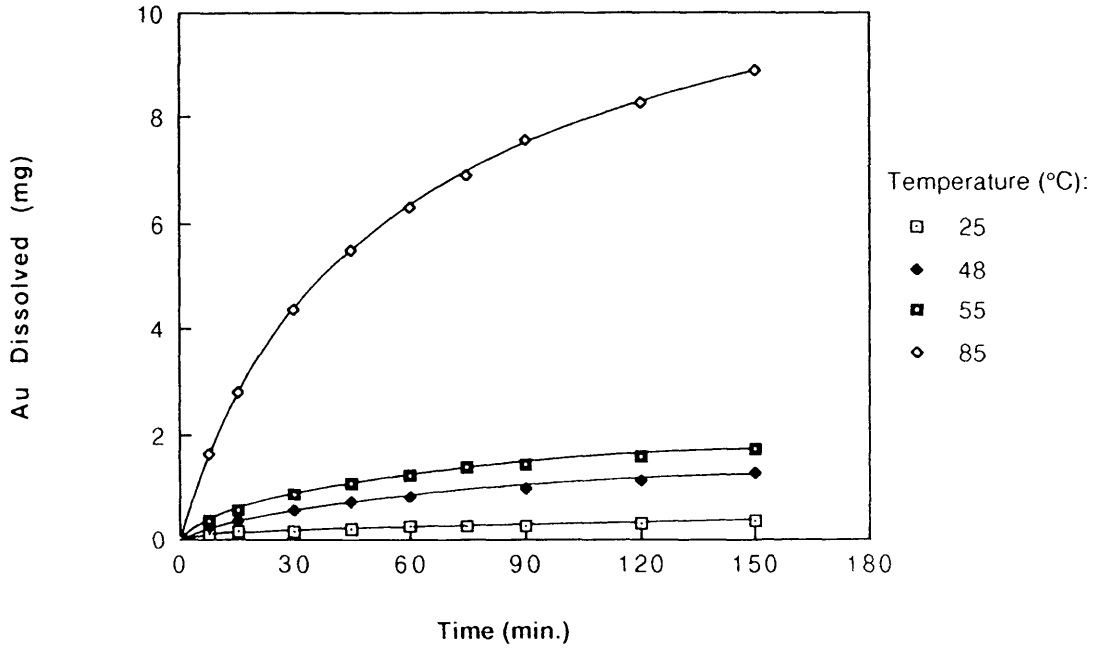


Figure 6.17 - Effect of temperature on the dissolution of gold with 0.05 mol/dm^3 SCN^- and 0.055 mol/dm^3 Fe^{3+} (initial), at pH 1.5 and 75.4 rad/s (720 rpm). N_2 atmosphere.

A rather different set of results was obtained from the third series of experiments, with 0.275 mol/dm^3 SCN^-, listed in **Table 6.8**. The gold dissolution results of this series are plotted in **Figure 6.18** and the related potential readings and Fe^{3+} reduction data are shown in **Figure 6.19**.

There is a marked change in shape of the gold dissolution curves in **Figure 6.18** as the temperature is increased. The change starts to appear at 40°C and becomes clear at 55°C. At this temperature, there seems to be three different stages of gold dissolution, the first relatively fast, the second slower and the third becoming almost as fast as the first one. The dissolution rates calculated for these three stages at 55°C are 3.15×10^{-9} (initial), 1.10×10^{-9} (from 15 to 60 minutes) and 2.74×10^{-9} (from 90 to 180 minutes), all expressed in mol cm^{-2} s^{-1}. These rates are also listed

in **Table 6.8**. When the temperature was further increased to 85°C (see **Figure 6.18**), the initial rate observed was the highest obtained in this work, 2.06×10^{-8} mol cm^{-2} s^{-1}. The three reaction stages observed at 55°C did not appear in this case. Due to the high rate of the dissolution process, the different stages seem to have occurred in a fast sequence in the beginning of the experiment, and are not distinguishable. The decrease of the rate with time was much more pronounced at 85°C, and after two hours the dissolution had almost completely stopped. The runs at 55°C and 85°C were replicated (in both the second and third series of **Table 6.8**) to confirm the reproducibility of the results. Additional data are reported in Appendix 6.

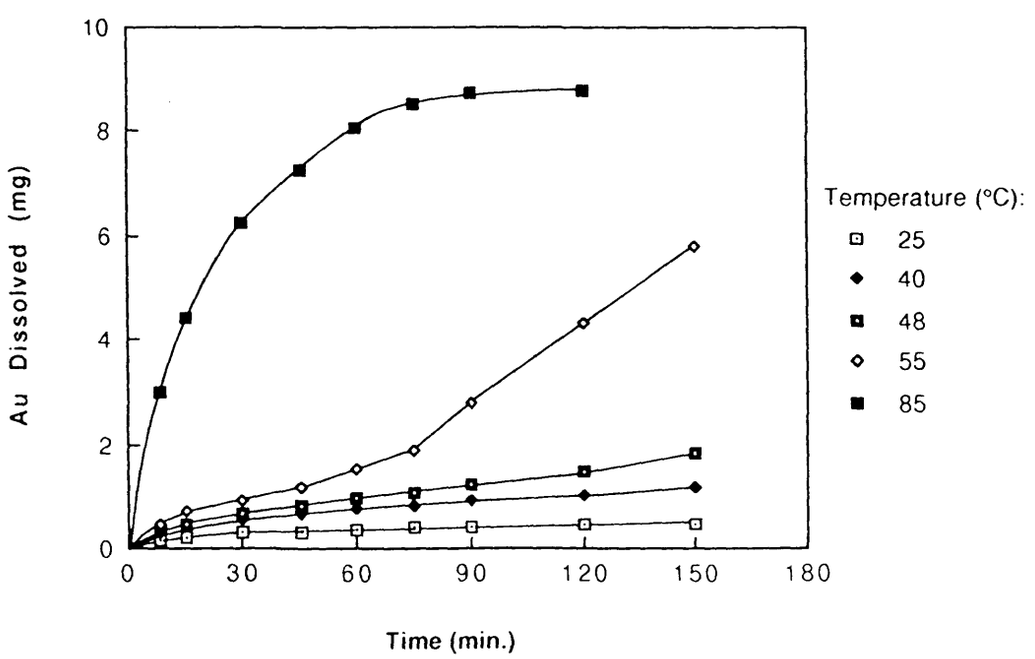
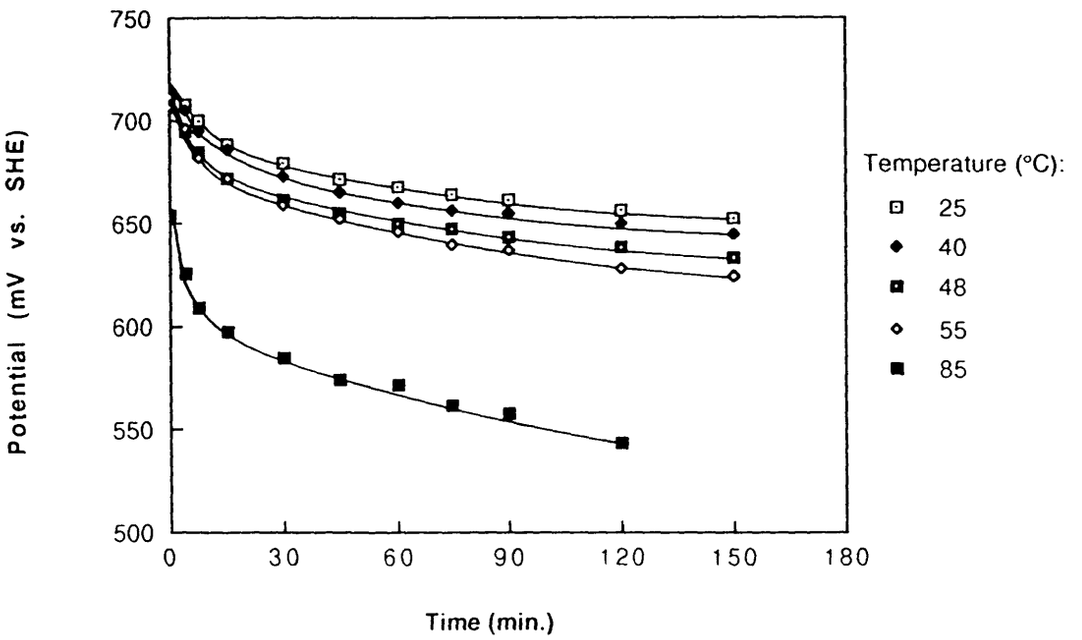


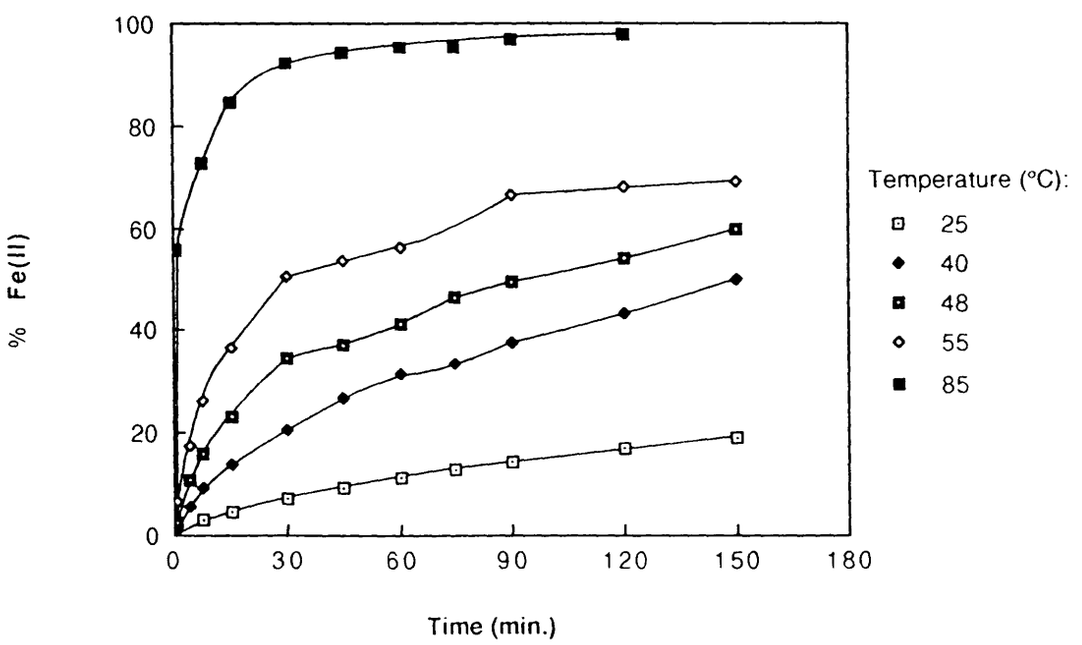
Figure 6.18 - Effect of temperature on the dissolution of gold with 0.275 mol/dm^3 SCN^- and 0.055 mol/dm^3 Fe^{3+} (initial), at pH 1.5 and 75.4 rad/s (720 rpm). N_2 atmosphere.

The main clue to the interpretation of the results of **Figure 6.18** is, again, the correlation between the gold dissolution and the simultaneous autoreduction of ferric thiocyanate, which is illustrated in **Figure 6.19**. At zero time, $Fe(NCS)_4^-$ is the predominant complex, about 20% of the Fe^{3+} exists as the lower complexes $FeNCS^{2+}$, $Fe(NCS)_2^+$ and $Fe(NCS)_3$, and the activity of free thiocyanate is *c.a.* 0.09 mol/dm^3. As the autoreduction proceeds, the Fe^{3+}/SCN^- ratio decreases and there is a shift towards the higher anionic complexes, $Fe(NCS)_5^{2-}$ and $Fe(NCS)_6^{3-}$. This shift was not pronounced at 25°C but was apparent at 55°C, for at this latter temperature the autoreduction was fast enough to show the differences as reflected in the three different stages of the gold dissolution process mentioned above. It is reasonable to suppose that, as each of the ferric thiocyanate complexes has its own structure, charge distribution and autoreduction characteristics, the successive shift from one predominant complex to another will reflect on the gold dissolution behaviour. At 85°C the autoreduction was very fast and most of it was completed within the first 15 minutes or so. The changes made apparent at 55°C occurred too rapidly to be observed as distinct stages.

The correlation between the gold dissolution and the autoreduction process can be better visualized in **Figure 6.20**, which was plotted with the same set of data of **Figures 6.18** and **6.19** but omitting the run at 85°C. Thus, due to the magnification of the vertical scales in **Figure 6.20**, the different stages (i.e., the changes in rate) of gold dissolution and autoreduction appear more clearly.

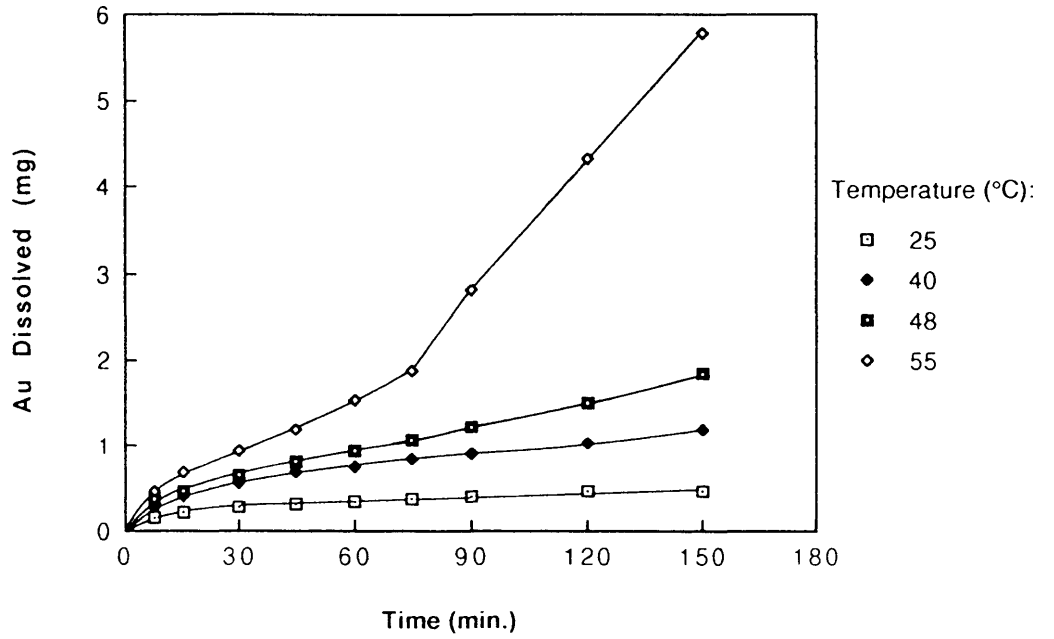


(a)

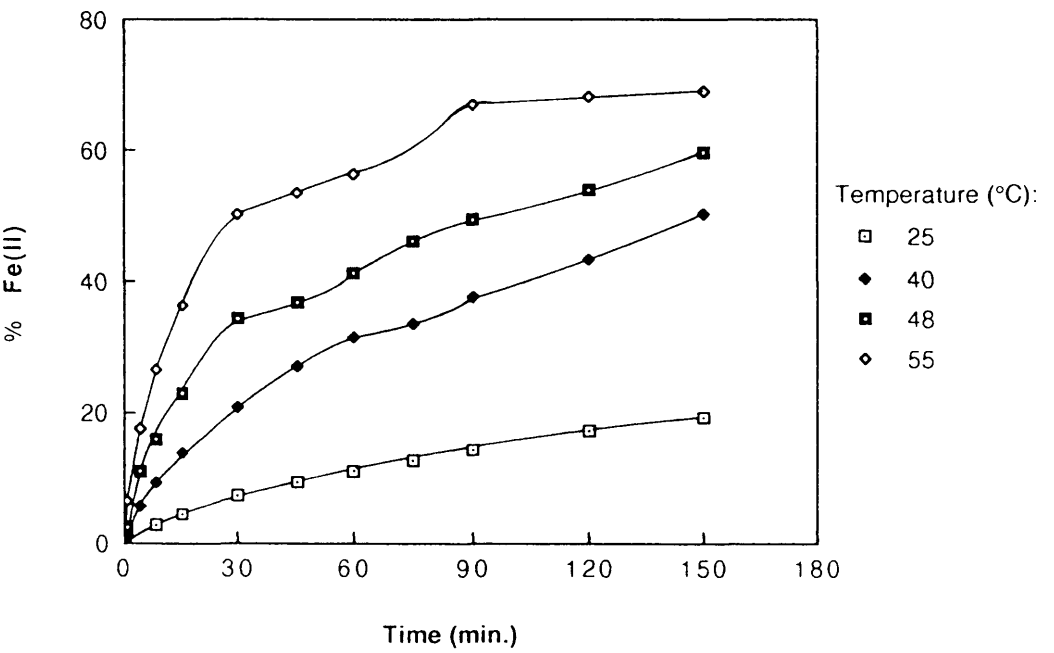


(b)

Figure 6.19 - Effect of temperature on **(a)** potential readings and **(b)** reduction of Fe^{3+} to Fe^{2+}. For all runs: 0.275 mol/dm^3 SCN^- and 0.055 mol/dm^3 Fe^{3+} (initial); pH 1.5; 75.4 rad/s (720 rpm); N_2 atmosphere.



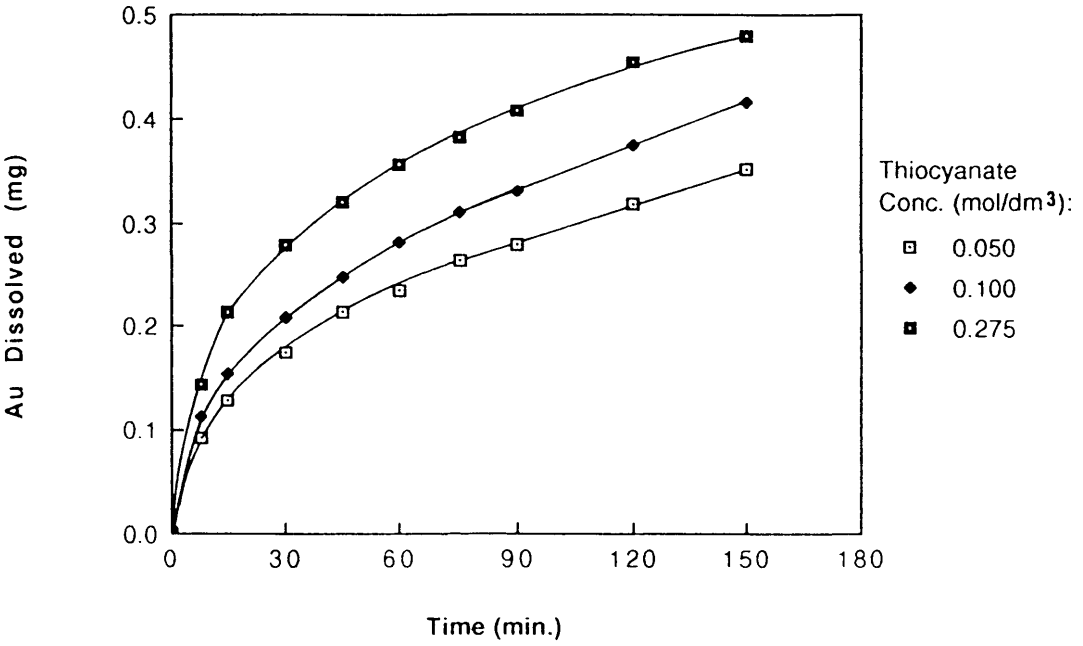
(a)



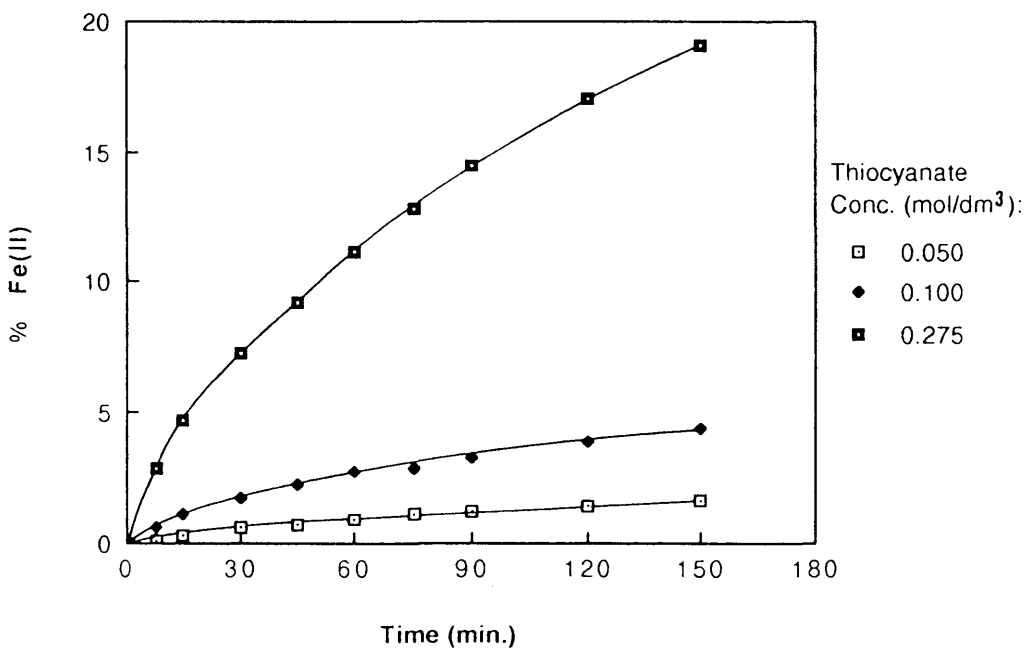
(b)

Figure 6.20 - Effect of temperature on **(a)** gold dissolution and **(b)** autoreduction of ferric thiocyanate. For all runs: 0.275 mol/dm^3 SCN^-, 0.055 mol/dm^3 Fe^{3+} (initial), pH 1.5, 75.4 rad/s (720 rpm) and N_2 atmosphere (same data used in **Figure 6.19**).

It is interesting now to observe the effect of thiocyanate concentration at several temperatures. It has already been emphasized that the specific way the autoreduction process takes place in a certain experiment depends on the initial complex distribution which, in its turn, is determined by the initial concentrations of Fe^{3+} and SCN^-. The gold dissolution rates are higher when the autoreduction rates are higher. For the same initial Fe^{3+} concentration and temperature, the initial autoreduction rate increases with the SCN^- concentration. It was also observed (see Chapter 4, Item 4.7.2) that when the initial autoreduction rate was higher, it tended to slow down more rapidly due to the faster build up of Fe^{2+} in the system. This overall behaviour pattern was also followed by the gold dissolution, which is illustrated by **Figure 6.21** for 25°C and, more clearly, by **Figure 6.22** for 85°C. At 25°C, the initial gold dissolution rates increased with increasing thiocyanate concentration, as expected. The rates after 1 hour, however, increased when the thiocyanate concentration was increased from 0.050 to 0.10 mol/dm^3 but decreased when it was further raised to 0.275 mol/dm^3, as indicated in **Table 6.8**. This behaviour became drastic at 85°C (see **Figure 6.22** and **Table 6.8**), due to the acceleration of the autoreduction of the ferric thiocyanate complexes. Despite this acceleration, the progress of the autoreduction was more gradual in the experiments with 0.050 and 0.10 mol/dm^3 SCN^-, due to the initial compositions of the system (predominance of the cationic complex $FeNCS^{2+}$). As a consequence, the decrease of the gold dissolution rate was also more gradual throughout the experiment. But when the thiocyanate concentration was further raised to 0.275 mol/dm^3, which corresponds to the predominance of the anionic complex $Fe(NCS)_4^-$, the autoreduction process became so fast that it was practically completed within the first 30 minutes. Accordingly, the gold dissolution rate was initially very high only to drop, after 90 minutes, to a value comparable to that obtained at 25°C and, this is the point, much lower than that obtained with only 0.10 or even 0.050 mol/dm^3 SCN^- (see **Table 6.8**). In other words: in the two

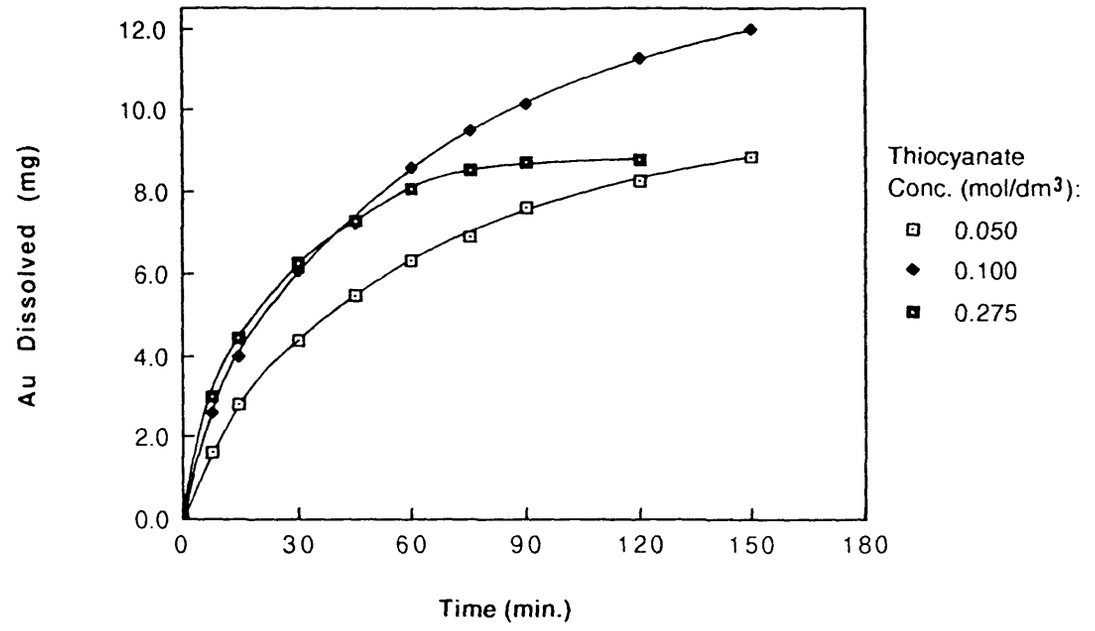


(a)

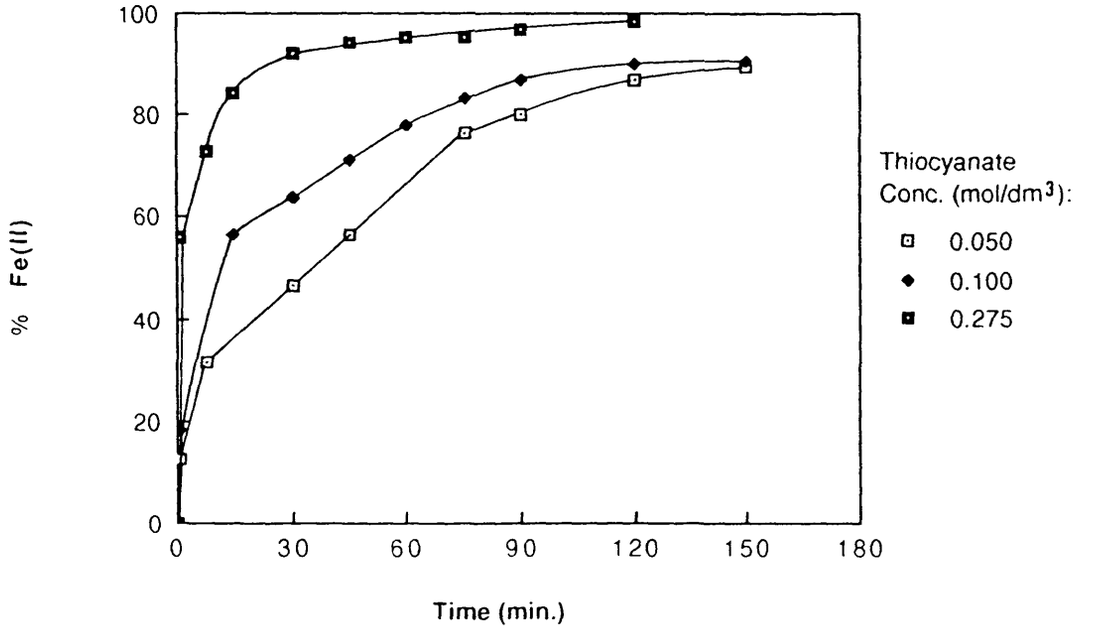


(b)

Figure 6.21 - Effect of thiocyanate concentration at 25°C on **(a)** gold dissolution and **(b)** autoreduction of ferric thiocyanate. For all runs: 0.055 mol/dm^3 Fe^{3+} (initial), pH 1.5, 75.4 rad/s (720 rpm) and N_2 atmosphere.



(a)



(b)

Figure 6.22 - Effect of thiocyanate concentration at 85°C on **(a)** gold dissolution and **(b)** autoreduction of ferric thiocyanate. For all runs: 0.055 mol/dm^3 Fe^{3+} (initial), pH 1.5, 75.4 rad/s (720 rpm) and N_2 atmosphere.

runs with 0.05 and 0.10 mol/dm^3 SCN^-, the initial autoreduction rates were lower but the process kept going and, throughout the experiment, the mixed potential decrease was slower and there was a continuous and more controlled production of active intermediate species such as $SCN^\cdot$, $(SCN)_3^-$ and $(SCN)_2$. In the experiment with 0.275 mol/dm^3 SCN^-, most of the autoreduction occurred during the first 15 minutes or so, which caused a drastic decrease in the mixed potential. As a result, the slightly higher initial dissolution rate decreased to a minimum after the first hour, and the overall gold dissolution was lower than that obtained using only 0.10 or 0.050 mol/dm^3 SCN^-.

A general conclusion is that by using higher temperatures, initial gold dissolution rates as high as 10^{-8} mol cm^{-2} s^{-1} can be obtained. Average gold dissolution rates of the magnitude of 10^{-9} mol cm^{-2} s^{-1} are also feasible, provided an optimum compromise between the temperature and the initial Fe^{3+} and SCN^- concentrations is achieved. The best SCN^- concentration is not necessarily the highest one. The improvement in the initial dissolution rate achieved by adding more thiocyanate may lead to poorer overall results due to the higher autoreduction rates. In such cases (higher autoreduction rates), attempts to keep a constant potential by adding a suitable oxidant are expected to result in higher thiocyanate consumption (see Sections 5.5 and 6.11).

The data presented in **Table 6.8** were used to calculate the activation energy of the gold dissolution process. The results are presented in **Figures 6.23** and **6.24**, and **Table 6.9**.

Figure 6.23 shows Arrhenius plots of the initial dissolution rates from the series of experiments with 0.050, 0.10 and 0.275 mol/dm^3 SCN^-. The respective apparent activation energies were practically coincident, with average 44.7 kJ/mol and standard deviation of 4.2%. These figures confirm the chemical control of the gold dissolution process, which has already been indicated by the

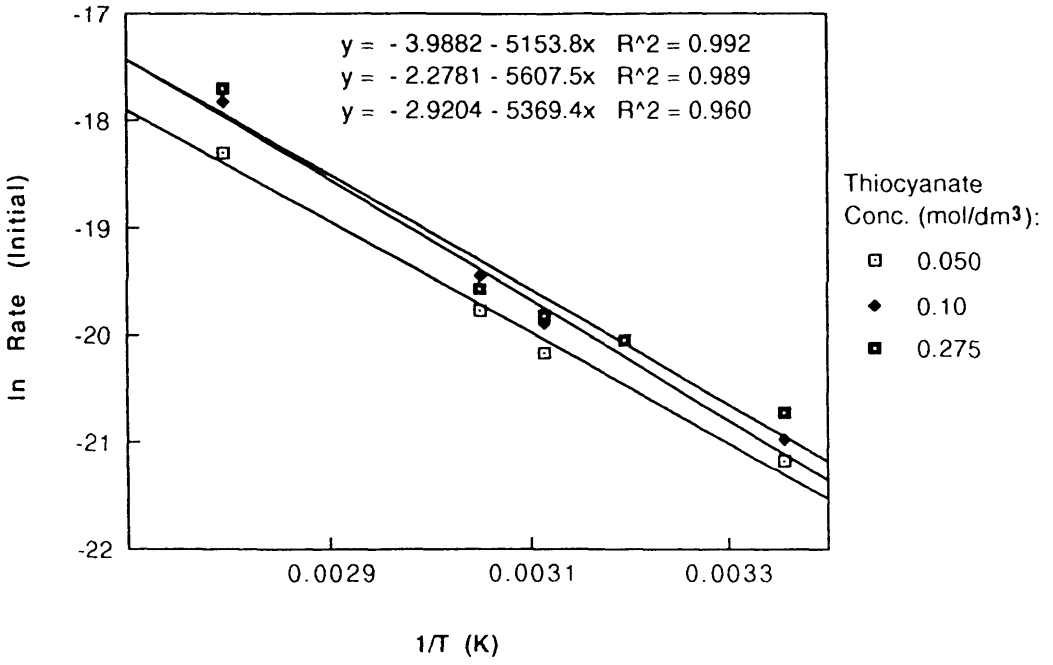


Figure 6.23 - Arrhenius plots of the initial gold dissolution rates listed in **Table 6.8**. The equations of the straight lines (upper right corner) correspond, from top to bottom, to 0.050, 0.10 and 0.275 mol/dm^3 SCN^-, respectively.

Table 6.9 - Apparent Activation Energies (kJ/mol) for the Gold Dissolution Process. Dissolution rates from **Table 6.8**. For all runs: initial Fe^{3+} concentration 0.055 mol/dm^3, pH 1.5, 75.4 rad/s and N_2atmosphere.

Thiocyanate Conc. (mol/dm^3)	Calculation from Initial Rates (**Figure 6.23**)	Calculation from Rates After 1 hour (**Figure 6.24**)
0.050	42.85	41.31
0.100	46.62	44.29
0.275	44.64	91.05 (*)

(*) This figure was obtained using data from the experiments from 25 to 55°C, i.e., by omitting the run at 85°C from the calculation.

experimental results discussed in Section 6.4. The small standard deviation suggests the same dissolution mechanism within the whole thiocyanate concentration range investigated. As already mentioned, this mechanism includes the species SCN , $(SCN)_2$ and $(SCN)_3^-$, which are produced by the autoreduction process.

Arrhenius plots of the gold dissolution rates after 60-90 minutes (see **Table 6.8**) are presented in **Figure 6.24**, which shows that the rates obtained with 0.050 and 0.10 mol/dm^3 thiocyanate could be satisfactorily fitted into straight lines. For these two series of experiments, the activation energies had approximately the same value of those calculated from the initial rates (see **Table 6.9**), suggesting that the same dissolution mechanism was operative throughout the experiments. However, the rates obtained with 0.275 mol/dm^3 SCN^- could not be fitted into a straight line and are indicated as scattered points in **Figure 6.24**. That scattering is not due to experimental error. Several of those experiments were replicated and confirmed the results. The fact was that in the experiments with 0.275 mol/dm^3 SCN^- the autoreduction of the ferric thiocyanate complexes was very fast, particularly above 40°C. This means that the system underwent composition changes (transformations in the complex distribution due to the increase in the Fe^{2+}/Fe^{3+} ratio) which somehow changed the dissolution mechanism after some time. Such composition changes were the most drastic at 85°C, as almost all Fe^{3+} was reduced to Fe^{2+} in 30 minutes or so. One of the factors to be considered in such a situation is that, due to the reduction of most of the iron to Fe^{2+}, the reoxidation (reverse reaction) of the Fe^{2+} to Fe^{3+} by intermediate species such as $SCN^{\cdot}$, $(SCN)_2$ and $(SCN)_3^-$ may become increasingly important. Additional factors are the formation of higher anionic complexes such as $Fe(NCS)_5^{2-}$ and $Fe(NCS)_6^{3-}$, the marked decrease in the potential readings due to the very high Fe^{2+}/Fe^{3+} ratio, the increasing tendency towards the complexation of Fe^{2+} with formation of $FeNCS^+$, the hydrolysis of the intermediate thiocyanate species, etc. There seems to be no simple explanation

for eventual changes in mechanism due to extensive transformations in the speciation of the system. Fortunately, the results obtained from the initial rates, as shown in **Figure 6.23**, are more relevant for leaching practice, in which the autoreduction of ferric thiocyanate would not be allowed to progress to almost completion, as this would almost stop the gold dissolution.

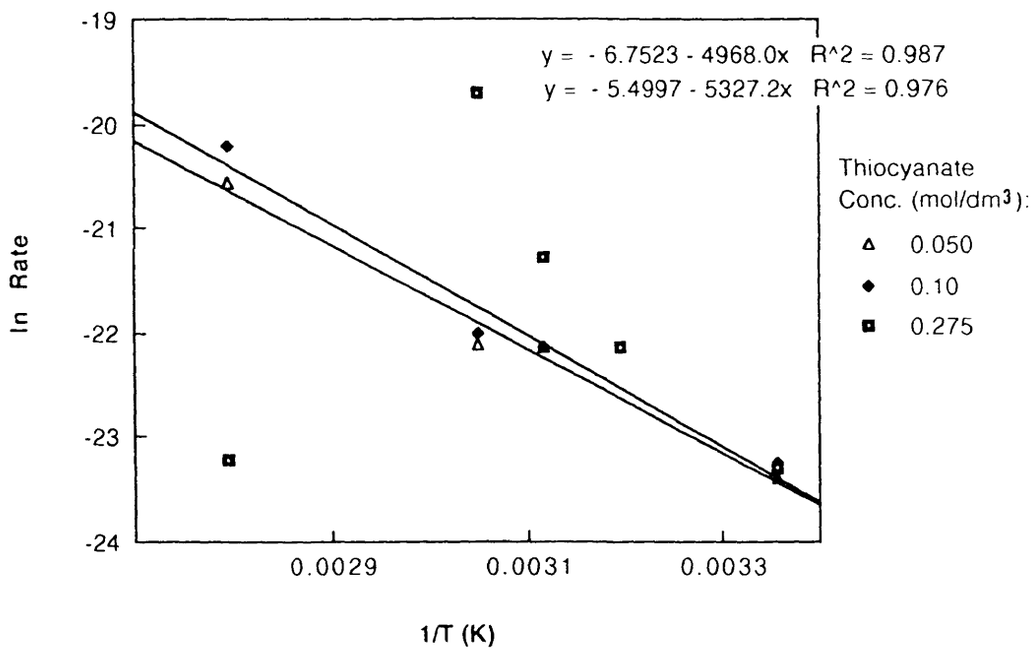


Figure 6.24 - Arrhenius plots of the gold dissolution rates after 1 hour listed in **Table 6.8**. The equations of the straight lines (upper right corner) correspond, from top to bottom, to 0.050 and 0.10 SCN^-, respectively. The scattered points correspond to the series of experiments with 0.275 mol/dm^3 SCN^-.

Arrhenius plots using the initial rates of autoreduction of the iron(III)-thiocyanate complexes in the rotating gold disc runs listed in **Table 6.8** are shown in **Figure 6.25**. The respective apparent activation energies are listed in **Table 6.10**.

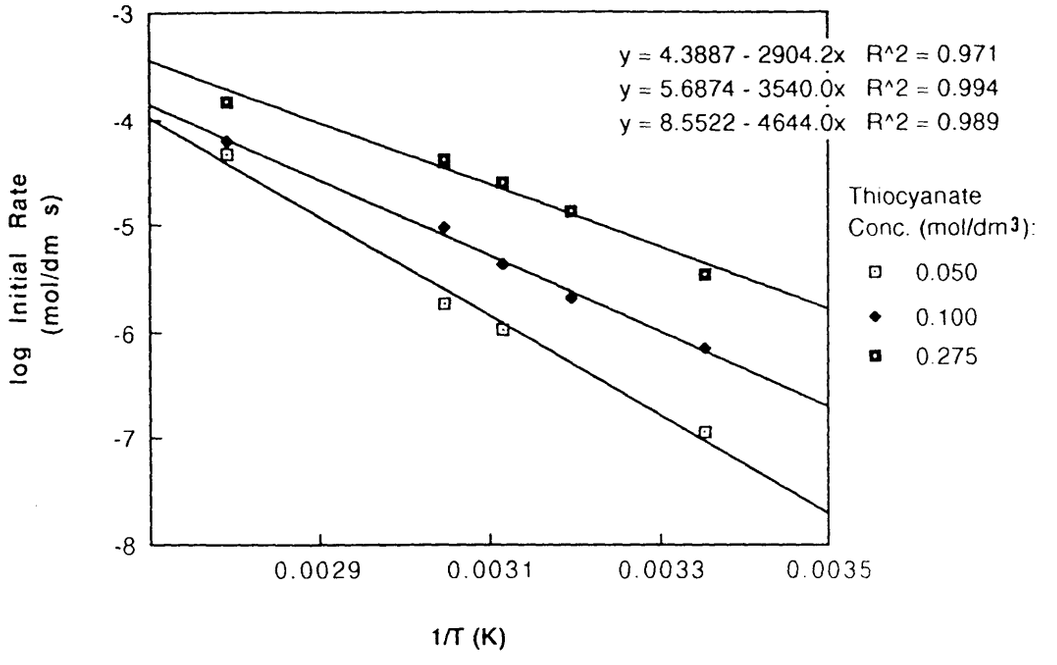


Figure 6.25 - Arrhenius plots of the initial rates of autoreduction of the iron(III)-thiocyanate complexes in the runs listed in **Table 6.8**. The respective apparent activation energies are listed in **Table 6.10**.

Table 6.10 - Apparent Activation Energies for the Initial Overall (Homogeneous plus Heterogeneous) Autoreduction of the Iron(III)-Thiocyanate Complexes at pH 1.5 (estimates from **Figure 6.25**).

Initial Concentrations (mol/dm^3)		Predominant Complex	Apparent Activation Energy
$[SCN^-]$	$[Fe^{3+}]$		(kJ/mol)
0.050	0.055	$FeNCS^{2+}$	88.9
0.100	0.055	$Fe(NCS)_2^+$	67.8
0.275	0.055	$Fe(NCS)_4^-$	55.6

The values in **Table 6.10** are a combination of two contributions: one from the homogeneous autoreduction, which takes place in the bulk of the solution, and another from the heterogeneous autoreduction of the iron(III)-thiocyanate complexes adsorbed on the surface of the rotating gold disc. Comparison between these values and those given in **Table 4.1** (see Section 4.7), which were estimated using the same initial concentrations of Fe^{3+} and SCN^-, indicate that the heterogeneous autoreduction has activation energies which are much lower than those for the homogeneous process. On the other hand, comparison between the activation energies for the dissolution of gold (**Table 6.9**) and for the autoreduction of the iron(III)-thiocyanate complexes (**Table 6.10**) suggests that this latter process includes the rate determining step of the overall gold dissolution process.

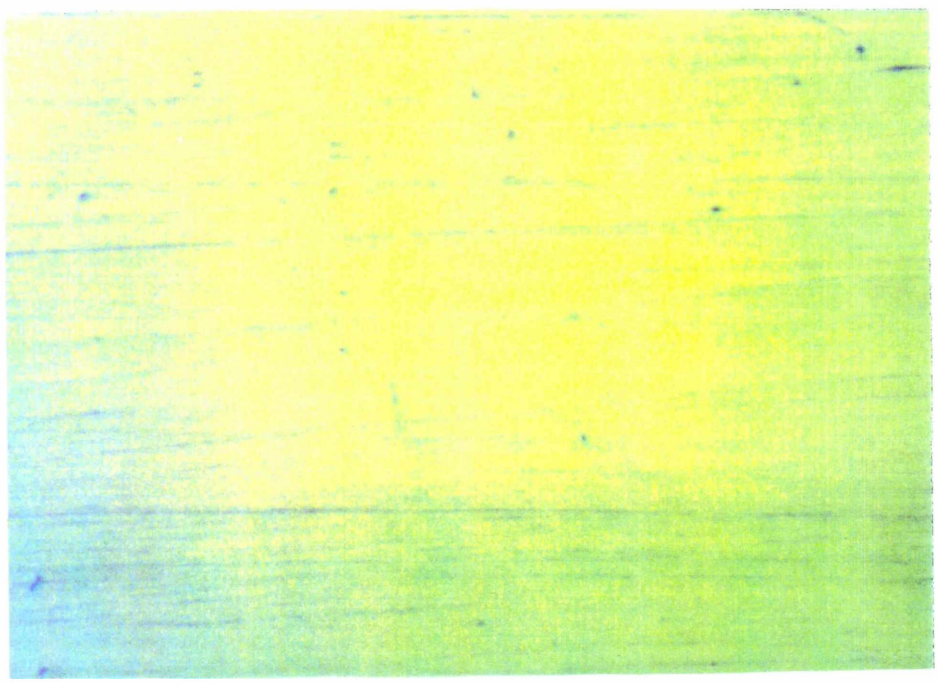
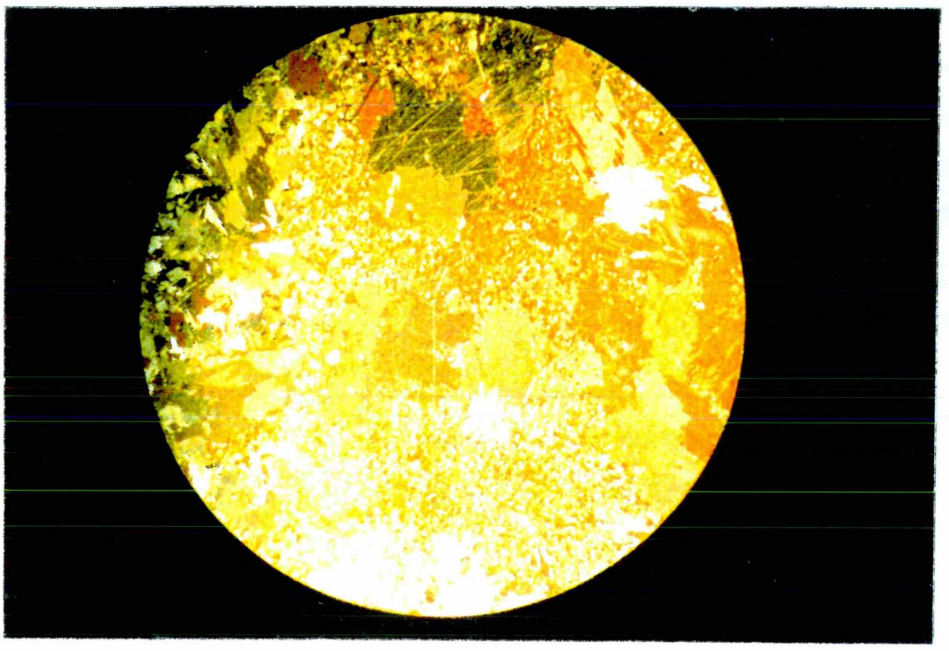
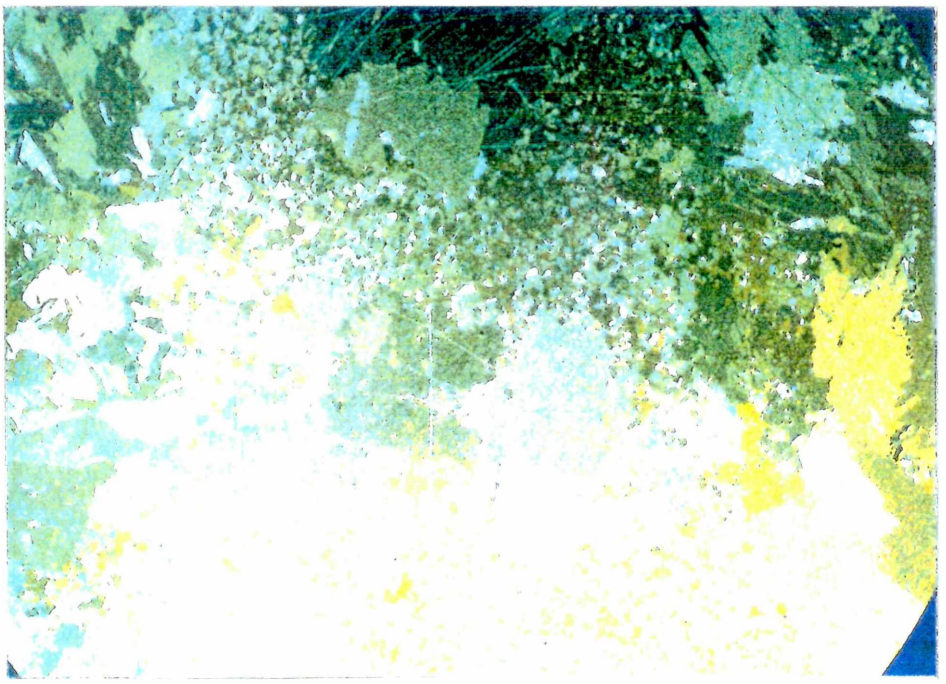


Figure 6.26 - Gold rotating disc after polishing (magnification: 50 x).



(a)



(b)

Figure 6.27 - Gold rotating disc after leaching for 150 minutes at 85°C with 0.10 mol/dm^3 SCN^- and 0.055 mol/dm^3 Fe^{3+} (initial), pH 1.5. Magnifications: **(a)** 6 x and **(b)** 50 x.

This section is completed by **Figures 6.26** and **6.27**, which are pictures of the rotating gold disc used in the experiments. **Figure 6.26** shows the disc after polishing. **Figure 6.27** shows it after having been leached for 150 minutes with 0.10 mol/dm^3 SCN^- and 0.055 mol/dm^3 Fe^{3+}, at pH 1.5 and 85°C. The pronounced etching of the gold disc was easily observable after runs at higher temperatures, such as 55°C or 85°C. But it was not perceptible after runs at 25°C, due to the low dissolution rates at this temperature.

6.9. Effect of Dissolved Oxygen

All the experiments reported in this chapter so far were conducted in nitrogen atmosphere in order to prevent any interference from oxygen. The effect of dissolved oxygen has been already mentioned when discussing the experimental reproducibility. Series of replicates were conducted both in nitrogen and aerated atmospheres. The gold dissolution results of these two series were put together in **Figure 6.28**. The corresponding potential readings and Fe^{3+} reduction data are shown in **Figure 6.29**. The experiments under nitrogen atmosphere are those shown in **Figures 6.2** and **6.3**, which are repeated here for comparison.

Curiously, the presence of dissolved oxygen was slightly detrimental to the dissolution of gold. The effect was mainly noticed on the initial dissolution rates, as shown in **Table 6.11**. The rates after 1 hour were almost unaffected. On the other hand, no effect was observed on the autoreduction process, which remained practically unaffected by the presence of oxygen, as shown in **Figure 6.29**.

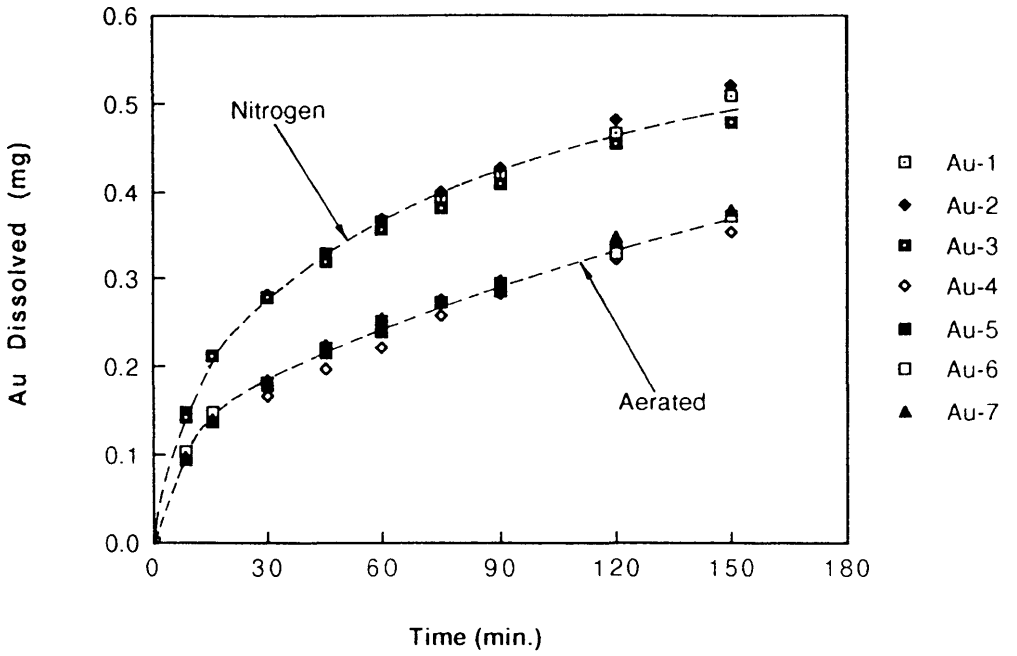
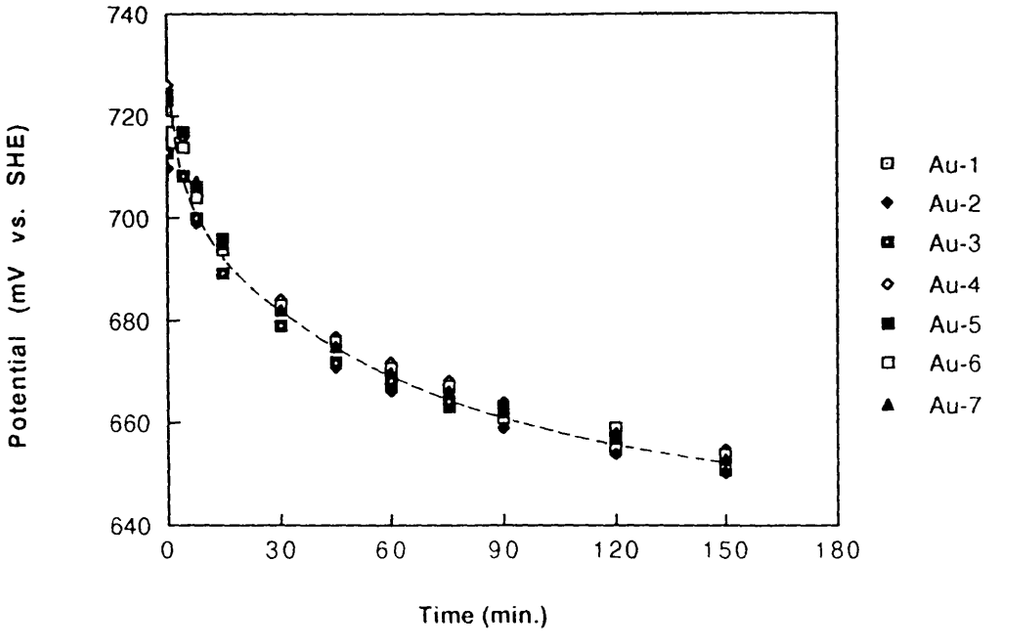
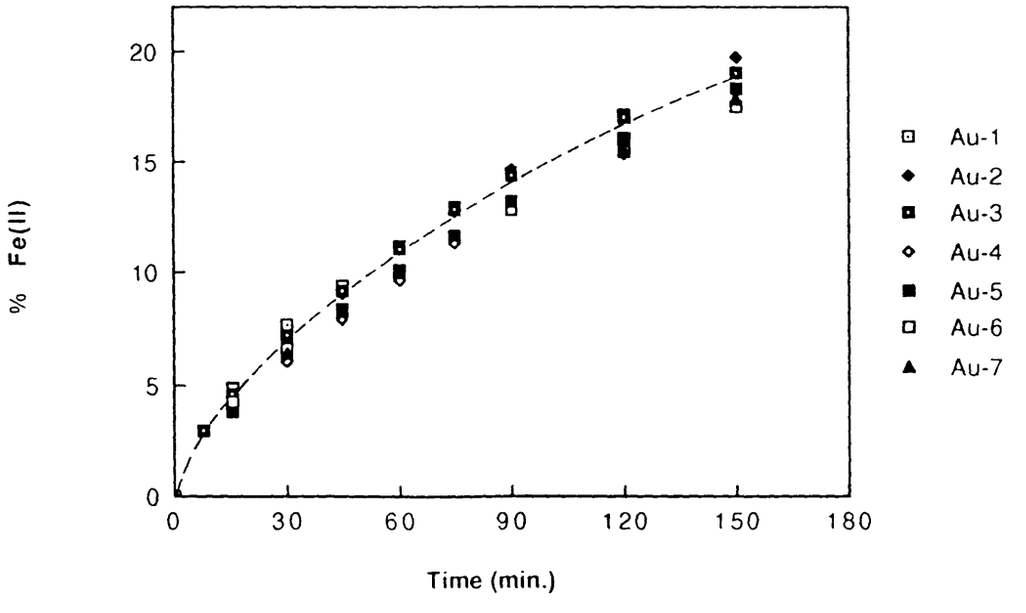


Figure 6.28 - Effect of dissolved oxygen on the leaching of gold by ferric thiocyanate. Au-1 to Au-3: N_2 atmosphere; Au-4 to Au-7: aerated runs. Initial concentrations: 0.275 mol/dm^3 SCN^- and 0.055 mol/dm^3 Fe^{3+}; pH 1.5; temperature, 25°C; rotation speed, 75.4 rad/s (720 rpm).

The presence of oxygen referred to in this section corresponds to the amount of oxygen which is naturally dissolved in the leaching solution when the reactor is not flushed with nitrogen but, instead, is simply left open to the atmosphere. Concentrations of dissolved oxygen were not measured during this work. Solubilities of oxygen in aqueous media were thoroughly investigated by Weiss [178], who published his results in comparison with a review of work done by several other researchers. In one of Weiss' tables, the solubility of oxygen from moist air at one atmosphere total pressure at 24°C is 5.88 ppm in pure water, lower values being found depending on the levels of salinity in the water. It is thus reasonable to assume that the initial levels of dissolved oxygen in the rotating disc experiments reported here should be between 5 and 6 ppm.



(a)



(b)

Figure 6.29 - Effect of dissolved oxygen on **(a)** potential readings at the gold disc surface and **(b)** reduction of Fe^{3+} to Fe^{2+}. Au-1 to Au-3: N_2 atmosphere; Au-4 to Au-7: aerated runs. Initial concentrations: 0.275 mol/dm^3 SCN^- and 0.055 mol/dm^3 Fe^{3+}; pH 1.5; temperature, 25°C; rotation speed, 75.4 rad/s (720 rpm).

Table 6.11 - Gold Dissolution Rates Observed in the Experiments shown in **Figure 6.28**

Run Number	Initial Rate J x 10^{10} (mol/cm^2 s)	Rate after 1 Hour J x 10^{11} (mol/cm^2 s)	Linear Correlation Coefficient, R^2 after 1 Hour
Au-1	10.2	7.50	0.98
Au-2	10.2	8.00	0.99
Au-3	9.91	7.63	1.00
Au-4	6.81	6.73	0.98
Au-5	6.55	7.25	1.00
Au-6	7.16	6.50	0.99
Au-7	6.73	6.98	0.99

A chemical explanation for this effect of oxygen is related to the active role of intermediate species such as $SCN^{\cdot}$, $(SCN)_3^{-}$ and $(SCN)_2$ in the leaching reactions. These species react with oxygen to yield a different group of intermediates such as hypothiocyanous acid, HOSCN, and its anion, $OSCN^-$, and anion-radicals such HO_2SCN^-, $HOSCN^-$ and $OSCN_2^-$. The first two species, among others, were early proposed by Bjerrum and Kirschner [51] when investigating the hydrolysis of $(SCN)_2$, and later by Gauguin [48]. Schöneshöfer et al. [72] also proposed the same species based on pulse radiolysis studies. The anion-radicals were proposed by Behar et al. [76] (see Chapter 3). The specific reaction of dissolved oxygen with $(SCN)_2$ yielding $OSCN^-$ was proposed by Seel and Müller [64] as one of the preliminary steps in the hydrolysis of thiocyanogen.

These oxygen-containing intermediate species are more subject to hydrolysis (for indeed they have been proposed as intermediates in the hydrolysis of the non-oxygenated species) and, it is supposed here, less active in the dissolution of gold. Furthermore, by being bonded to 1 or 2 oxygen atoms, the SCN^- group is not as readily available to act as a ligand in the formation of gold-thiocyanate complexes. This reasoning would then explain the poorer gold dissolution in the presence of dissolved oxygen. It would also explain why the initial rates are the mainly affected, because it is at the beginning of the experiments that the production of $SCN^\cdot$, $(SCN)_3^-$ and $(SCN)_2$ is greatest, due to faster autoreduction rates.

On the other hand, dissolved oxygen does not affect the potential readings and the autoreduction rates, as shown in **Figure 6.29**. This observation is consistent with the proposal of the production of the free radical $SCN^\cdot$ as being the rate controlling step in the oxidation of thiocyanate [82, 86, 90]. Dissolved oxygen participates in subsequent steps of the oxidation of thiocyanate and does not interfere with the autoreduction rate or the potential readings. Furthermore, dissolved oxygen does not seem to oxidize Fe^{2+} back to Fe^{3+} to an appreciable extent, under the conditions investigated here. One of the reasons for this behaviour is the relatively slow kinetics of the oxidation, in acidic solutions, of ferrous ions by molecular oxygen in the absence of a suitable catalyst (Cu^{2+} ions are one of such catalysts mentioned in the literature) [179-182].

6.10. The Consumption of Thiocyanate in the Rotating Disc Experiments

The leach solutions from the rotating disc experiments were analysed for thiocyanate by means of the Volhard method (see Chapter 4, Item 4.3.2). Some results are shown in **Table 6.12**.

These results simply reproduce those discussed in Chapter 4, Section 4.8, and the conclusions of that section are entirely valid in the present case. Thus, the consumption of thiocyanate in the rotating disc experiments is consistent with the following stoicheiometry:

$$6Fe^{3+} + SCN^- + 4H_2O \longrightarrow 6Fe^{2+} + HCN + SO_4^{2-} + 7H^+ \qquad (6.3)$$

The overall process is irreversible, as HCN and SO_4^{2-} cannot be reduced back to SCN^-. The stoicheiometry indicated by reaction 6.3 corresponds basically to the autoreduction of the iron(III)-thiocyanate complexes. As observed in Section 6.7, most of the reduction of Fe^{3+} in the rotating disc experiments corresponds to the oxidation of SCN^-, with only a very minor part being due to the oxidation of gold.

Table 6.12 - Thiocyanate Consumption in the Rotating Disc Experiments: Results of Some Argentimetric Titrations (Initial Fe^{3+} Concentration in All Runs: 0.055 mol/dm^3)

Initial Thiocyanate (mol/dm^3)	Temp. (°C)	Fe^{3+} Reduced %	Thiocyanate Conc. (mol/dm^3)	Thiocyanate Consumed %
0.050	25	1.59	0.050	0
0.10	25	4.42	0.10	0
0.275	25	19.81	0.272	1.09
0.050	55	14.72	0.049	2.00
0.10	55	34.29	0.097	3.13
0.275	55	66.75	0.269	2.55
0.050	85	89.46	0.044	12.0
0.10	85	90.57	0.093	6.85
0.275	85	98.18	0.265	3.64

Further oxidation of thiocyanate to cyanate or cyanic acid may also contribute to the overall stoicheiometry. This possibility has already been discussed in Section 4.8.

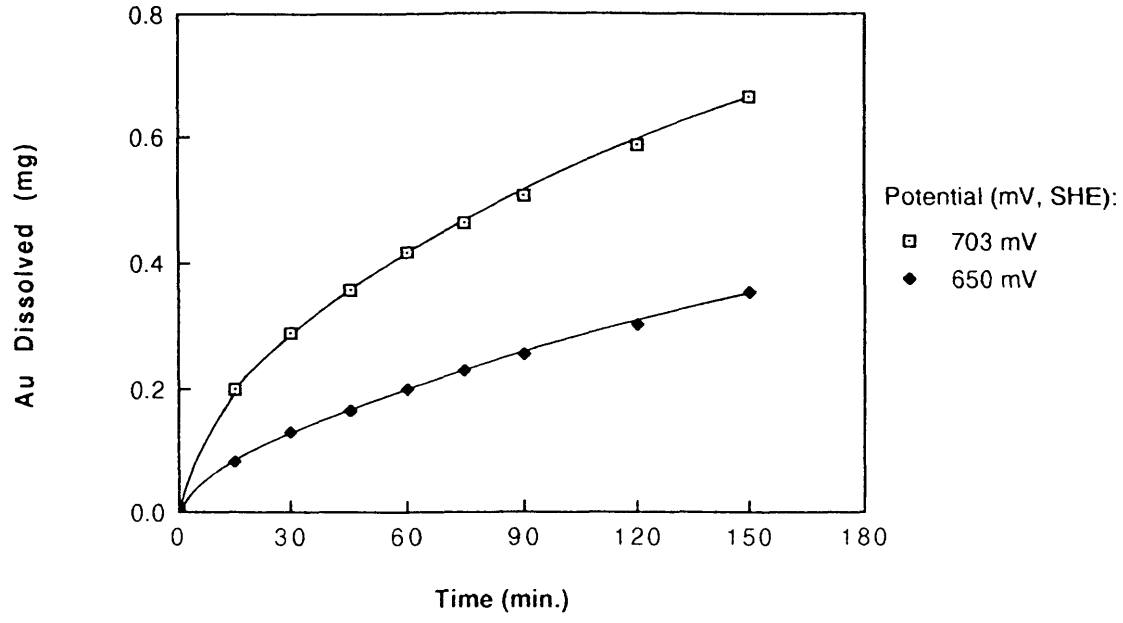
Thiocyanate hydrolysis was not observed even at the highest temperature investigated (85°C). Otherwise, it would have been noticed at once by the easily perceptible smell of H_2S produced or by the presence of suspended elemental sulphur in solution. Furthermore, the consistency between the reduction of Fe^{3+} and the oxidation of SCN^- rules out the occurrence of hydrolysis to any appreciable extent.

6.11. Rotating Disc Experiments at Constant Potential

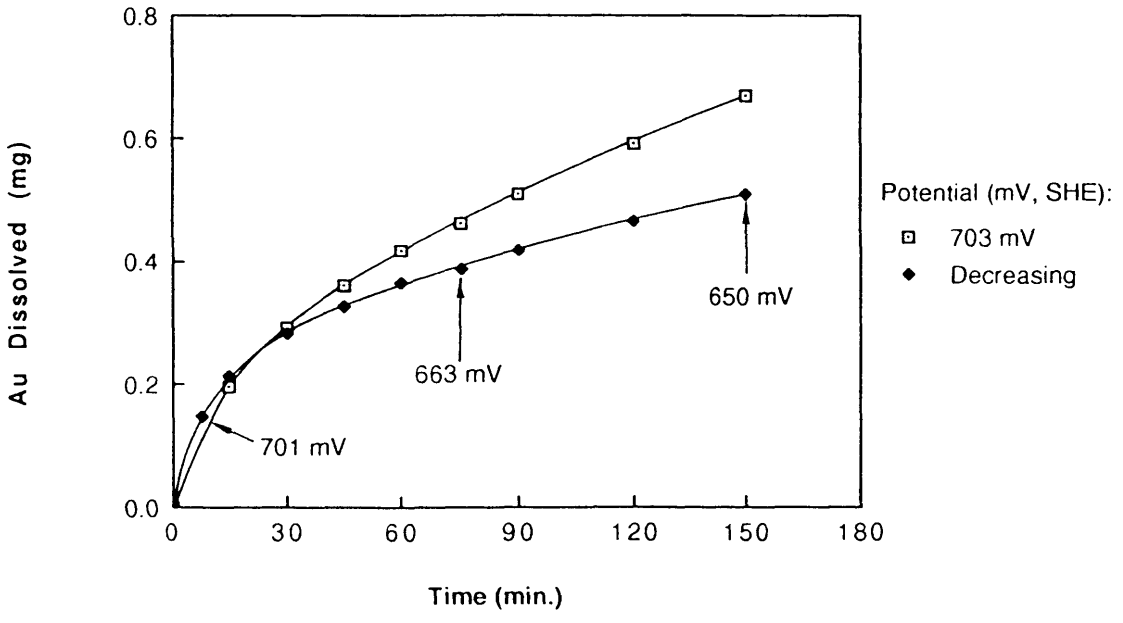
In these rotating disc experiments, potential readings were maintained constant by additions of hydrogen peroxide to the ferric thiocyanate solutions. Hydrogen peroxide oxidizes the Fe^{2+} produced by the autoreduction process, and can be used to keep a constant Fe^{2+}/Fe^{3+} ratio. The oxidizing effect of hydrogen peroxide on thiocyanate, on ferrous ions, and on iron-thiocyanate solutions was the subject of Chapter 5. This section is solely concerned with the performance of the system in terms of gold dissolution.

Results of experiments at constant potential are shown in **Figures 6.30** and **6.31**. The respective rates are shown in **Table 6.13** and the consumption of thiocyanate in **Table 6.14**.

Figure 6.30a shows runs with 0.275 mol/dm^3 SCN^- and 0.055 mol/dm^3 total iron. In the run at 703 mV, 2% of the iron was initially added as Fe^{2+} and the remainder as Fe^{3+}. In the run at 650 mV, the initial percentage of Fe^{2+} was 20%. As expected, the dissolution rate at 703 mV was higher.

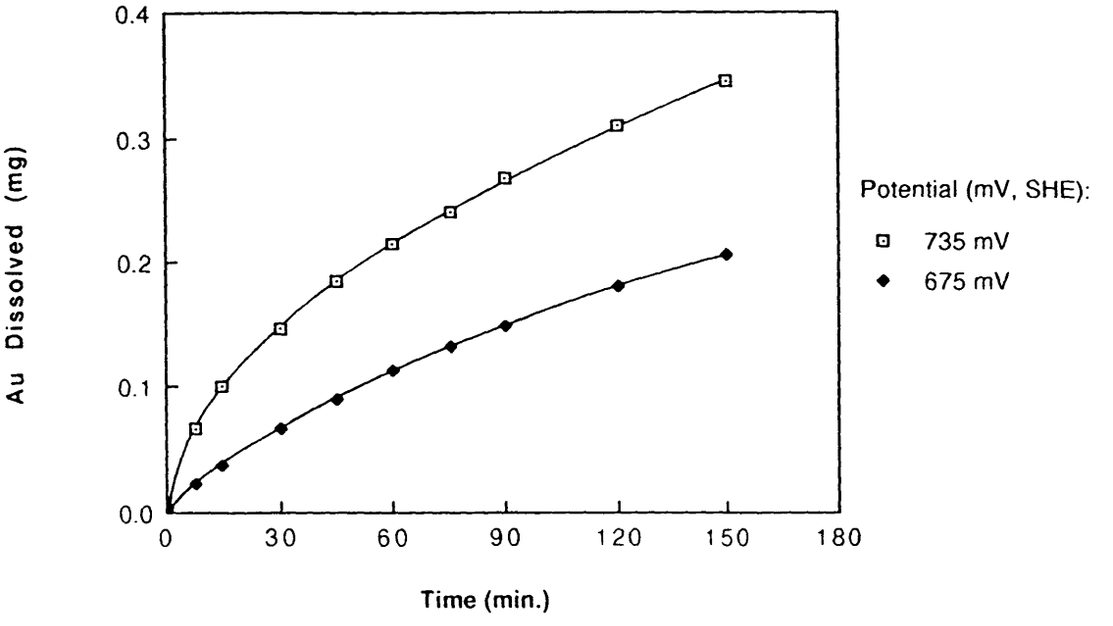


(a)

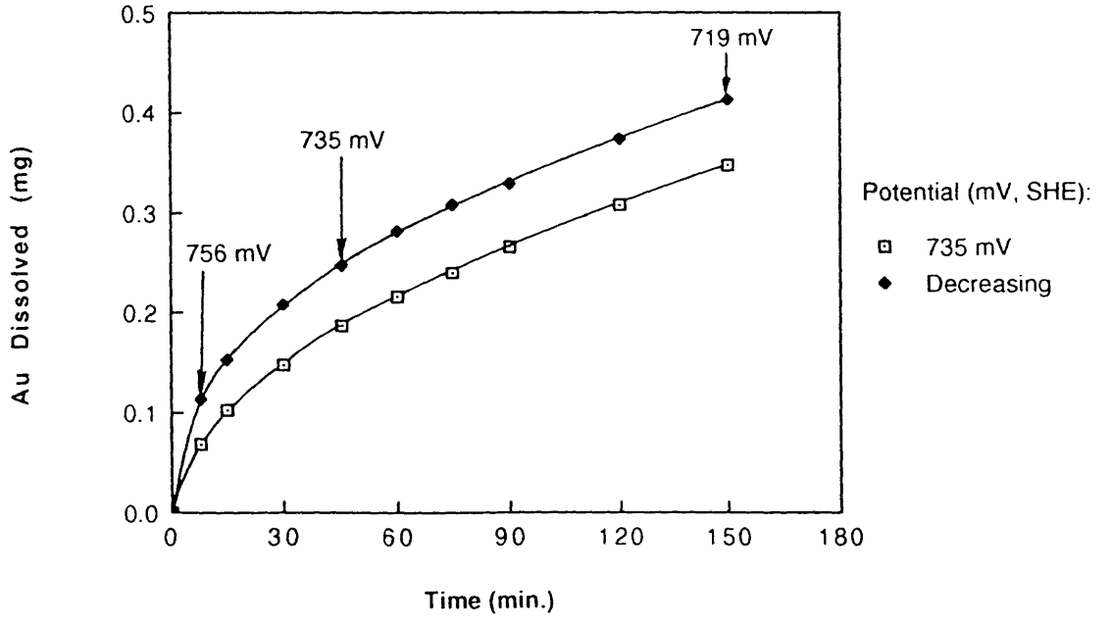


(b)

Figure 6.30 - Rotating disc runs at 25°C with 0.275 mol/dm^3 SCN^- and 0.055 mol/dm^3 of total iron: **(a)** runs at the constant potentials of 703 mV (2% Fe^{2+}) and 650 mV (20% Fe^{2+}) and **(b)** comparison between the run at 703 mV and a run with spontaneous autoreduction (decreasing potential, indicated by the arrows).



(a)



(b)

Figure 6.31 - Rotating disc runs at 25°C with 0.10 mol/dm^3 SCN^- and 0.055 mol/dm^3 of total iron: **(a)** runs at the constant potentials of 735 mV (2% Fe^{2+}) and 675 mV (20% Fe^{2+}) and **(b)** comparison between the run at 735 mV and a run with spontaneous autoreduction (decreasing potential, indicated by the arrows).

Table 6.13 - Gold Dissolution Rates Observed at Constant Potentials (by Addition of Hydrogen Peroxide) at 25°C. In all runs the initial Fe^{3+} concentration was 0.055 mol/dm^3; pH 1.5; 75.4 rad/s.

Thiocyanate Conc. (mol/dm^3)	Potential (mV vs. SHE)	%Fe^{2+}	Initial Rate J x 10^{10} (mol/cm^2 s)	Rate after 1 Hour (§) J x 10^{11} (mol/cm^2 s)	
0.10	735	2.00	4.69	8.03	
0.10	675	20.0	1.61	5.55	
0.10	Decreasing	Increasing	7.78	8.08	(*)
0.275	703	2.00	9.06	15.2	
0.275	650	20.0	3.47	9.33	
0.275	Decreasing	Increasing	10.2	8.00	(**)

(§) The correlation coeffecients, R^2, for all the straight lines are 0.99 or 1.00.

(*) No peroxide was added to this run. The autoreduction followed its normal course. The initial mixed potential was 758 mV (no Fe^{2+} in solution), dropping to 719 mV (4.42% Fe^{2+}) after 150 minutes.

(**) Same type of run as in the previous note.The initial mixed potential was 710 mV (no Fe^{2+} in solution), dropping to 650 mV (19.81% Fe^{2+}) after 150 minutes.

A comparison between the experiment at 703 mV and one in which all iron was initially added as Fe^{3+} and the autoreduction was allowed to follow its normal course is shown in **Figure 6.30b**. The initial rate at constant potential was lower because the initial potential in the other experiment was higher (710 mV). The situation was reversed after some time, as shown in **Table 6.13**.

A similar set of results is presented in **Figure 6.31**, in which the same total iron concentration was used but the thiocyanate concentration was reduced to 0.10 mol/dm^3. The percentages of Fe^{2+} in the experiments of **Figure 6.31a** were also 2% and 20%, which corresponded to potentials of 735 mV and 675 mV, respectively.

A comparison similar to that in **Figure 6.30b** is presented in **Figure 6.31b**. The initial rate was higher in the experiment in which all iron was initially added as Fe^{3+}, whose initial potential was 758 mV. Furthermore, as only 0.10 mol/dm^3 SCN^- was used, the autoreduction rate was slower, which kept the dissolution rate in this experiment higher than that in the experiment at constant potential, over the 150 minutes. However, the rates in **Table 6.13** indicate that if the experiments were extended for a longer time, this situation would be reversed and the dissolution rate at constant potential would become the higher one, which qualitatively corresponds to the same observation made for the experiments with 0.275 mol/dm^3 SCN^-.

Curiously, the gold dissolution rate in the runs at constant potential decreases with time. A straightforward supposition would be that, by keeping constant the Fe^{2+}/Fe^{3+} ratio and potential, the resulting rate would also be constant. This proved not to be so. There seems to be no isolated factor capable of explaining this behaviour. One of the probable factors is the gradual stabilization of a thin layer of adsorbed AuSCN, which obviously does not exist at zero time. This effect seems to be more pronounced in the runs with 20% Fe^{2+}, whose mixed potentials favour the existence of gold in the aurous state, resulting in the formation of both $AuSCN_{(ads)}$ and the complex $Au(SCN)_2^-$. A second factor is the modification of the chemistry of the system by the presence of hydrogen peroxide, whose oxidizing action takes place through the free radicals $OH^\cdot$ and $HO_2^\cdot$ [155-163] (see Chapter 5, Sections 5.2 and 5.3). This effect is more pronounced in the runs with only 2% Fe^{2+}, in which the consumption of H_2O_2 (and the corresponding thiocyanate oxidation) is higher, as shown in **Table 6.14**. Reactions of SCN^- with the free radical $OH^\cdot$ produced by the radiolysis of water were reported (see Chapter 3, Section 3.7) to result in the formation of oxidized thiocyanate species such as $SCN^\cdot$, $(SCN)_2^-$ and $(SCN)_2$, whose precursors would be species such as $OSCN^{2-}$ and $HOSCN^-$ [72, 73, 76, 77]. The oxidation of thiocyanate by hydrogen peroxide, on the other

hand, was reported to produce intermediate species such as HOSCN and HO_2SCN [36, 37]. In the present case, H_2O_2 is added to a system in which non-oxigenated intermediate species such as $(SCN)_2$ and $(SCN)_3^-$ are present as a result of the autoreduction of ferric thiocyanate complexes. Its action is intended to raise the potential reading back to the pre-established value, by reoxidizing Fe^{2+} to Fe^{3+}. What is actually achieved, however, is a combination of this desired action with the (undesired) attack of the free peroxide radicals on the non-oxygenated thiocyanate intermediate species, resulting in a different family of intermediates such as HOSCN, $OSCN^-$, $HOSCN^-$, $OSCN^{2-}$, HO_2SCN, O_2SCN^-, all these species having already been proposed in the references quoted above or in earlier references [48, 51]. Such oxygenated intermediate species seem to be less active than $(SCN)_3^-$ and $(SCN)_2$ in the mechanism of gold dissolution, which results in dissolution rates lower than those that would be expected according to the potential values. The effect of H_2O_2 is to some extent similar to that of dissolved oxygen discussed in the previous section. It tends, however, to have a stronger effect due to the high solubility of H_2O_2 in water and to the high reactivity of the free peroxide radicals which, additionally, have a strong oxidizing effect on SCN^- itself.

The consumption of thiocyanate, for a given total iron concentration, increases with the total thiocyanate concentration and with the potential, i.e. with the autoreduction rate. The behaviour is similar to that already observed in Chapter 5.

The experimental results discussed in this section point towards the need for investigation, in future projects, of oxidizing agents capable of maintaining the mixed potential of the system without, at the same time, impairing its ability to dissolve gold.

Table 6.14 - Thiocyanate Oxidation in the Runs at Constant Potential at 25°C. In all runs the Total Iron Concentration in Solution was 0.055 mol/dm^3; pH 1.5; 75.4 rad/s (720 rpm).

Initial Thiocyanate (mol/dm^3)	Potential (mV vs. SHE)	% Fe^{2+}	H_2O_2 0.9 M Added (cm^3)	Final Thiocyanate [SCN^-] (mol/dm^3)	% Cons.
0.100	735	2.00	2.10	0.098	2.00
0.100	675	20.0	0	0.100	0
0.275	703	2.00	5.67	0.253	8.00
0.275	650	20.0	0.60	0.273	0.73

6.12. Some Mechanistic Considerations

The results from the rotating disc experiments presented in this chapter indicate that the gold dissolution and the autoreduction of the ferric thiocyanate complexes are related phenomena. The autoreduction of ferric thiocyanate complexes can be explained by the following mechanism:

$$Fe(NCS)_n^{3-n} \longrightarrow Fe^{2+} + (n-1)\ SCN^- + SCN^{\cdot} \qquad (6.4)$$

$$Fe(NCS)_n^{3-n} \longrightarrow FeNCS^+ + (n-2)\ SCN^- + SCN^{\cdot} \qquad (6.5)$$

$$SCN^{\cdot} + SCN^- = (SCN)_2^- \qquad (6.6)$$

$$2(SCN)_2^- \longrightarrow (SCN)_2 + 2SCN^- \qquad (6.7)$$

$$2(SCN)_2^- \longrightarrow (SCN)_3^- + SCN^- \quad (6.8)$$

$$(SCN)_3^- = (SCN)_2 + SCN^- \quad (6.9)$$

$$3(SCN)_2 + 4H_2O \longrightarrow 5SCN^- + HCN + SO_4^{2-} + 7H^+ \quad (6.10)$$

One of the main characteristics of the autoreduction process, amply demonstrated by the experimental results of this work, is the decrease in the overall rate with time, due to the increasing concentration of Fe^{2+} in solution. The reverse reaction responsible for the retardation of the autoreduction process is:

$$(SCN)_2^- + Fe^{2+} \longrightarrow Fe(NCS)_2^+ \quad (6.11)$$

or, alternatively:

$$(SCN)_2^- + Fe^{2+} \longrightarrow FeNCS^{2+} + SCN^- \quad (6.12)$$

The ferric thiocyanate complexes formed in the two latter reactions may then be coordinated by additional SCN^- ions, depending on the activity of free thiocyanate in the system. Reactions 6.11 and 6.12 become increasingly important with time, due to the build-up of Fe^{2+} in the system as the autoreduction progresses. $(SCN)_2^-$ is a highly oxidizing species whose E° was estimated in 1.29 V by Stanbury et al. [45]. It is not possible to rule out reactions in which other oxidized species such as $(SCN)_2$ and $(SCN)_3^-$ would also oxidize Fe^{2+}.

This overall autoreduction mechanism was discussed in Chapter 4, Section 4.10, with reference both to experimental results obtained in this project and to the relevant literature available on the chemical [41, 137] and electrochemical [49, 81, 82, 86, 90, 91] oxidation of thiocyanate and on pulse radiolysis studies of thiocyanate [72-74, 76-78].

Reactions 6.4 and 6.5 correspond to the rate controlling step of the overall process [41, 49, 81, 82, 86, 90, 91], which is the production of the free radical $SCN^{\cdot}$ through the breakdown of the iron(III)-thiocyanate complexes. The free radical $SCN^{\cdot}$ is very short-lived and produces the transitory form $(SCN)_2^-$ (reaction 6.6) which, in its turn, decays to produce $(SCN)_2$ and $(SCN)_3^-$ through reactions 6.7 and 6.8.

It should be noticed that this overall mechanism applies both to the homogeneous autoreduction of the iron(III)-thiocyanate complexes and to the autoreduction of the complexes adsorbed on the surface of gold metal. The latter has received particular attention by Itabashi, who proposed a similar mechanism to explain the anodic behaviour both of thiocyanate [90] and iron(III)-thiocyanate [91] solutions on gold electrodes (see reactions 3.43 to 3.48 in Chapter 3). The only difference between the mechanisms for the homogeneous and heterogeneous autoreduction processes are the adsorption and desorption steps involved in the latter. These steps, however, do not seem to play any significant role in determining the rate of autoreduction, as observed in Section 6.7.

As far as gold dissolution is concerned, the main characteristic of the autoreduction of ferric thiocyanate is the production of the intermediate species $(SCN)_2$ and $(SCN)_3^-$, which are both oxidants and complexants for gold in a manner which is very similar to the action of the homologous halide species X_2 and X_3^- (X = Cl, Br, I). The analogies between the thiocyanate and the halide systems were explored in detail in Chapter 3, Section 3.10.

A preliminary discussion of the gold dissolution mechanism was also made in Chapter 3, Section 3.10, in which the following steps were considered:

$$Au_{(s)} + SCN^- = Au(SCN^-)_{(ads)} \qquad (6.13)$$

$$Au(SCN^-)_{(ads)} = Au(SCN)_{(ads)} + e \quad (6.14)$$

$$Au(SCN)_{(ads)} \longrightarrow AuSCN_{(ads)} \quad (6.15)$$

$$AuSCN_{(ads)} + SCN^- \longrightarrow Au(SCN)_2^- \quad (6.16)$$

Reactions 6.13, 6.14 and 6.16 correspond to those proposed by Martins et al. [87] to explain the formation of the aurous complex. Reaction 6.14 corresponds to the formation of the free radical $SCN^{\cdot}$, which may either oxidize gold metal to form $AuSCN_{(ads)}$ (reaction 6.15) or to participate in other reactions with SCN^- to form intermediate species. In contrast, the formation of $AuSCN_{(ads)}$ as an intermediate species in the mechanism of gold dissolution corresponds to the propositions of analogous species in the halide systems, i.e. $AuCl_{(ads)}$, $AuBr_{(ads)}$ and $AuI_{(ads)}$ [6, 89, 188, 189], and in the cyanide system, i.e. $AuCN_{(ads)}$ [1, 4, 7, 183-186]. Within this project, the only experimental observation that might be taken as an indication of the formation of that compound is the strong passivation of the gold metal, the amount of gold dissolved corresponding, on a molar basis, to less than 1% of the iron(III) reduced at the surface (see Section 6.7). The similar compounds of the other metals of the same periodic group, $CuSCN_{(s)}$ and $AgSCN_{(s)}$, are highly insoluble. The postulation of the formation of a thin-layer of AuSCN is therefore consistent with the passivating effect observed.

In the leaching of gold by iron(III)-thiocyanate solutions, the adsorption of SCN^- (reaction 6.13) is replaced by the adsorption of an iron(III)-thiocyanate complex which, through autoreduction, produces the adsorbed free radical $SCN^{\cdot}$, i.e. $Au(SCN)_{(ads)}$. This subsequently leads to the formation of either thiocyanate intermediate species (reactions 6.6 to 6.9) or $AuSCN_{(ads)}$ (reaction 6.15).

The auric complex would be formed at higher potentials, at which the predominant thiocyanate species is $(SCN)_3^-$. Then:

$$AuSCN_{(ads)} + (SCN)_3^- \longrightarrow Au(SCN)_4^- \qquad (6.17)$$

It is also possible to conceive the direct attack of $(SCN)_3^-$ on the metal surface producing, at lower potentials, the aurous complex $Au(SCN)_2^-$ and the adsorbed compound $AuSCN_{(ads)}$, as follows:

$$2Au_{(s)} + (SCN)_3^- \longrightarrow Au(SCN)_2^- + AuSCN_{(ads)} \qquad (6.18)$$

This reaction can be dismembered into two steps, one leading to the formation of the complex $Au(SCN)_2^-$ and the free radical $SCN^{\cdot}$, and the other yielding the adsorbed compound $AuSCN_{(ads)}$, as follows:

$$Au_{(s)} + (SCN)_3^- \longrightarrow Au(SCN)_2^- + SCN_{(ads)} \qquad (6.19)$$

$$Au_{(s)} + SCN_{(ads)} \longrightarrow AuSCN_{(ads)} \qquad (6.20)$$

The species $(SCN)_3^-$ and $SCN^{\cdot}$ act both as oxidants and complexants in reactions 6.19 and 6.20, respectively. The $AuSCN_{(ads)}$ formed in reaction 6.20 could then react according to reaction 6.16 or 6.17, yielding $Au(SCN)_2^-$ or $Au(SCN)_4^-$, respectively.

The aurous complex may also be formed by direct attack of the metal by the anion-radical $(SCN)_2^-$, as follows:

$$Au_{(s)} + (SCN)_2^- \longrightarrow Au(SCN)_2^- \qquad (6.21)$$

Thiocyanogen produced by reactions 6.7 and 6.9 may react on the metal surface, leading to the formation of $AuSCN_{(ads)}$:

$$2Au_{(s)} + (SCN)_2 \longrightarrow 2AuSCN_{(ads)} \qquad (6.22)$$

It is believed that $AuSCN_{(ads)}$ may be seen more correctly not as a discrete unit but as a thin-layer of Au^+ and SCN^- ions bond together and adsorbed on the gold metal surface. Any oxidizing species such as SCN^-, $(SCN)_2^-$ or $(SCN)_3^-$ could then react with that layer and promote further electron transfer and complexation, forming one of the gold complexes.

The main intermediate species generated by the autoreduction of ferric thiocyanate is $(SCN)_3^-$. The rotating disc experiments demonstrated that there is a correlation between the autoreduction rates and the gold dissolution rates. The higher dissolution rates in the beginning of the experiments were coupled with higher potential readings and autoreduction rates and, thermodynamically, with the predominance of the auric complex, $Au(SCN)_4^-$. This coincided with the greater production of $(SCN)_3^-$ due to the faster autoreduction. As the experiments progressed, the autoreduction rates decreased and, simultaneously, the dissolution rates decreased, usually more than 10 times. Due to the lower potential readings, the aurous complex, $Au(SCN)_2^-$, became the predominant one. These joint observations indicated the connection between the gold dissolution rates, the oxidation state in which gold is dissolved, and the availability of intermediate species such as $(SCN)_3^-$. The active role of such intermediate species was particularly apparent in the experiments at higher temperatures (such as 55-85°C), in which the autoreduction process occurs to a much greater extent than at 25°C.

The relation between the formation of $Au(SCN)_2^-$, $Au(SCN)_4^-$ and the oxidation of SCN^- to $(SCN)_3^-$ is illustrated in **Figure 6.32**, whose calculations were explained in Chapter 3, Section 3.10. The straight lines correspond to:

Line **A**: $Au(SCN)_2^- + e = Au_{(s)} + 2SCN^-$ (6.23)

$E = 0.3952 - 0.1182 \log \{SCN^-\}$ (6.24)

Line B: $Au(SCN)_4^- + 2e = Au(SCN)_2^- + 2SCN^-$ (6.25)

$E = 0.6433 - 0.0591 \log \{SCN^-\}$ (6.26)

Line C: $(SCN)_3^- + 2e = 3SCN^-$ (6.27)

$E = 0.6209 - 0.0591 \log \{SCN^-\}$ (6.28)

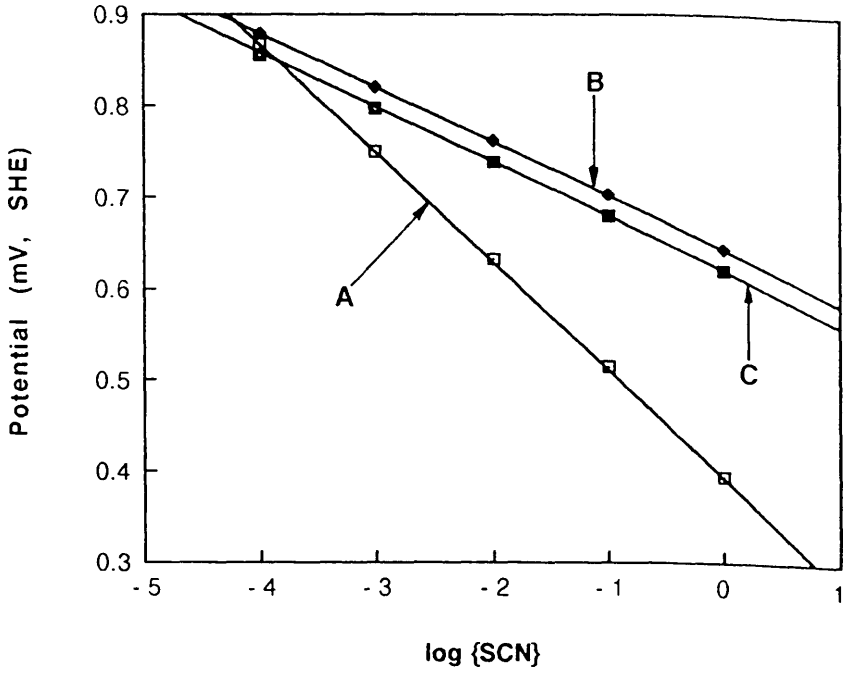


Figure 6.32 - Eh versus log $\{SCN^-\}$ lines showing the potential zones of predominance of $Au(SCN)_2^-$ (above line **A**), $Au(SCN)_4^-$ (above line **B**) and $(SCN)_3^-$ (above line **C**), considering the total gold activity in solution as 10^{-5} mol/dm^3, the activities of the two gold complexes as being equal, and the activity of $(SCN)_3^-$ as 1% of that of SCN^-.

Figure 6.32 illustrates the point mentioned above: the aurous complex, $Au(SCN)_2^-$, is formed at potentials in which SCN^- predominates, in the area bound by lines **A** and **C**. Within this area,

the gold dissolution mechanism is described by reactions 6.13 to 6.16. The same complex is also formed in the area between lines **B** and **C**, where $(SCN)_3^-$ predominates, which suggests the mechanism described by reactions 6.19 and 6.20. The auric complex, in its turn, is formed in the region above line **B**, and the main step involved is reaction 6.17.

Thus, in a typical rotating disc experiment at 25°C, three different stages seem to occur sequentially, as follows: **(1)** gold dissolution as $Au(SCN)_4^-$ in the first minutes, according to reaction 6.16, yielding the highest dissolution rates; **(2)** a transition stage in which the previous mechanism gradually gives way, as the mixed potential decreases and the autoreduction of ferric thiocyanate slows down, to the dissolution as $Au(SCN)_2^-$ according to reactions 6.18 and 6.19, yielding intermediate dissolution rates and leading to the gradual stabilization of a thin-layer of the intermediate compound $AuSCN_{(ads)}$, which has a passivating effect on the gold surface; **(3)** gold dissolution as $Au(SCN)_2^-$ according to reactions 6.13 through 6.15, yielding the lowest dissolution rates, which corresponds to the lowest mixed potentials and autoreduction rates. This is a simplified view which emphasizes the main trends of a rather complex and variable process. If the temperature is raised to 85°C, for instance, the autoreduction of ferric thiocyanate is carried out to near completion, which substantially extends the duration of stage **(2)**, resulting in high overall dissolution rates.

A mechanistic assumption included in stage **(3)** above would be the formation of the aurous complex according to reactions 6.13 to 6.16, the related cathodic process being the direct electron transfer from $Au_{(s)}$ to Fe^{III}, resulting in Fe^{II} and Au^{I}. The overall iron(III)-thiocyanate autoreduction process would be disregarded. This assumption can not be entirely ruled out, but its contribution to the overall gold dissolution seems to be minimal. The experimental evidence collected in this work shows a marked dependence of the rates of dissolution of gold on the rates of autoreduction of the

iron(III)-thiocyanate complexes. In fact, whenever the latter were low, the dissolution of gold took place at rates which were too low for any practical purposes. Overall, the main role of Fe^{III} seems to be that of a primary oxidant which acts upon SCN^- to generate thiocyanate intermediate species. These are the species directly responsible for the oxidation and dissolution of gold. The experiments at 85°C (see **Figures 6.15** through **6.19**) emphasize this point. The gold dissolution rates remain relatively high as long as the autoreduction process is kept going.

CHAPTER 7: THE EFFECT OF IODIDE AND IODINE ADDITIONS ON THE DISSOLUTION OF GOLD BY IRON(III)-THIOCYANATE SOLUTIONS

7.1. Introduction

The experimental results presented in the previous chapter demonstrated that initial gold dissolution rates of the order of 10^{-9} or even 10^{-8} mol/cm^{-2} s^{-1} could be obtained with ferric thiocyanate solutions, provided temperatures as high as 85°C were used. Those results were encouraging but the necessity for temperatures above ambient was a limitation, as it would add costs to conventional agitated leaching, while rendering the process unusable in circumstances requiring heap leaching or solution mining. The research was then oriented towards finding a way of increasing the gold dissolution rate at ambient temperature. Additions of small amounts of iodide or iodine were very successful in bringing about the desired results. The rates of gold leaching by ferric thiocyanate solutions with the addition of small amounts of iodide/iodine at 25°C were comparable to those obtained at 85°C with the plain ferric thiocyanate solutions. A first mention of the possibility of adding iodine to the thiocyanate leaching system was made by Fleming [198]. There seems to be no development in this respect, since nothing has been published on the subject so far.

In trying to understand how the iodide/iodine system works together with the thiocyanate system, it is advisable to first know how it works separately. The first step is then to investigate the basic aspects of the iodide/iodide leaching of gold, which is a relatively new area for hydrometallurgists. The first developments with this system were intended to recover gold from electronic or other scrap materials [193-196]. A process for hydrometallurgical

recovery of gold was then patented by McGrew and Murphy [192], in which the lixiviant was a mixture of iodide ions and elemental iodine, this latter working as oxidizing agent. The gold was subsequently recovered on activated charcoal and the excess iodide formed during the process was reoxidized to iodine electrochemically in a special diaphragm cell to regenerate the lixiviant. A study demonstrating the economic feasibility of the iodide/iodine system for in-situ leaching was published by Jacobson et al. [197] in 1987.

7.2. Previous Fundamental Research on the Iodide Leaching of Gold

Elemental iodine is scarcely soluble in water. Its solubility increases in presence of iodide ions. The dissolution process takes place through the formation of polyiodide ions such as I_3^-, I_4^{2-}, I_5^- and I_6^{2-}, besides aqueous I_2 [189]. However, species higher than I_3^- are not relevant for the present purposes, as the iodide concentrations used in leaching experiments are between 10^{-3} and 10^{-1} mol/dm^3. The relevant equilibrium is then [142, 189-191]:

$$I_{2(aq)} + I^- = I_3^- \qquad (7.1)$$

The value log K = 2.86 at 25°C is reported for the equilibrium constant of this reaction [18, 189]. A broader description of the iodine-water system is found in Chapter 3, Section 3.10, where an Eh-pH diagram including a larger number of species is provided (see **Figure 3.19**). An advantage of the iodine system when compared to the thiocyanate system is that the oxidized forms I_2 and I_3^- are very stable in water, which is not the case of $(SCN)_2$ and $(SCN)_3^-$, both being subject to hydrolysis and decomposition to sulphate and hydrogen cyanide.

In a recent review of the dissolution chemistry of gold and silver in different lixiviants, Hiskey and Atluri [187] showed that both the aurous, AuI_2^-, and the auric, AuI_4^-, complexes are formed with iodide. The aurous complex is the most likely to be found at redox potentials typical of iodine solutions, whose main oxidizing species are I_2 and I_3^- (see equation 7.1).

Experimental work was done by Qi and Hiskey on the electrochemistry [188, 190] and on the kinetics and mechanism [189, 190] of the iodide leaching of gold. These authors considered the triiodide ion, I_3^-, as the oxidizing agent and found that the gold dissolution process was first order with respect to this species and half order with respect to I^-. A comparison of gold leaching between iodide and cyanide was also presented, in which a rate of about 2.6×10^{-9} mol/cm^2 s was obtained with 10^{-2} mol/dm^3 NaI and 5×10^{-3} mol/dm^3 I_2. This value is similar to those found in cyanidation experiments [189]. Most of the experiments were performed with a rotating gold disc at 23°C and pH range from 2 to 10. The highest I^- concentration used was 0.01 mol/dm^3. The dissolution rate was practically insensitive to pH variations within this range. It is interesting to learn that almost no gold dissolution at all was obtained when oxygen or hydrogen peroxide were used as oxidant (instead of elemental iodine being added to the iodide solution) [189].

The iodide leaching of gold was also recently investigated by Davis and Tran [191]. Three different oxidizing agents were tried: iodine, hypochlorite and hydrogen peroxide. Elemental iodine was found to be the best oxidant over the pH range from 2.7 to 11.5. It also allowed higer oxidant concentrations to be used in solution, resulting in the highest dissolution rates. Hypochlorite yielded faster dissolution rates than iodine (for the same amount added) but this was observed only at pH 2.7 and with additions smaller than 0.025 mol/dm^3 (with 0.1 mol/dm^3 KI). The rates dropped drastically at OCl^- concentrations above 0.040 mol/dm^3, and proved to be strongly dependent upon the solution pH, falling to unacceptably low

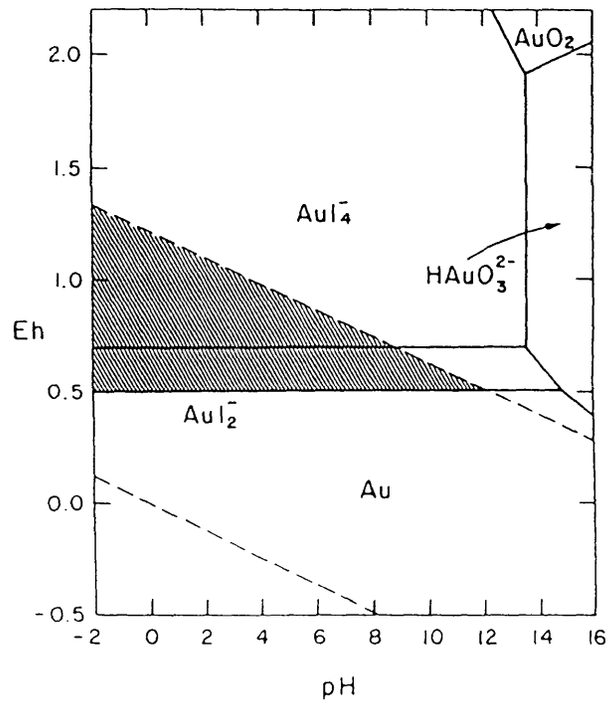
values at alkaline pHs, regardless of the OCl^- concentration. Hydrogen peroxide, on the other hand, proved to be unsuitable as an oxidant in the iodide system, the poor initial results discouraging further investigation. The optimum iodine-iodide mixture of 0.10 mol/dm^3 KI and 0.040 mol/dm^3 iodine could dissolve gold at a rate of 1.56×10^{-8} mol/cm^2 s from pH 2.7 to 10. With 0.02 mol/dm^3 KI, the dissolution rate was similar to the 2.6×10^{-9} mol/cm^2 s reported by Qi and Hiskey. [189, 190]. Davis and Tran [191] emphasized the importance of optimizing the iodine-iodide mole ratio for any given leaching conditions.

7.3. A Comparison between the Gold-Iodine-Water System and the Gold-Thiocyanate-Water System

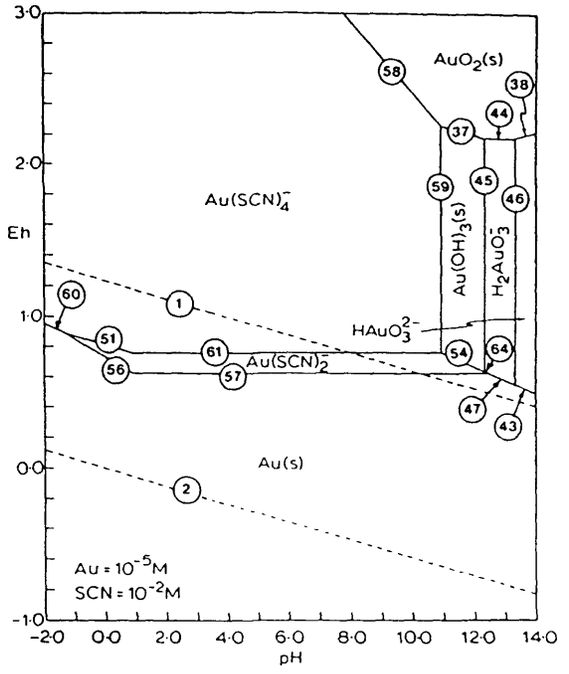
The standard potentials of several redox couples are reported in **Table 7.1**. The figures indicate that the (pseudo)halide character of thiocyanate lies between those of iodide and bromide.

Table 7.1 - Standard Potentials for Half-Reactions of Several Bromide, Iodide and Thiocyanate Redox Couples in Aqueous Solution at 25°C.

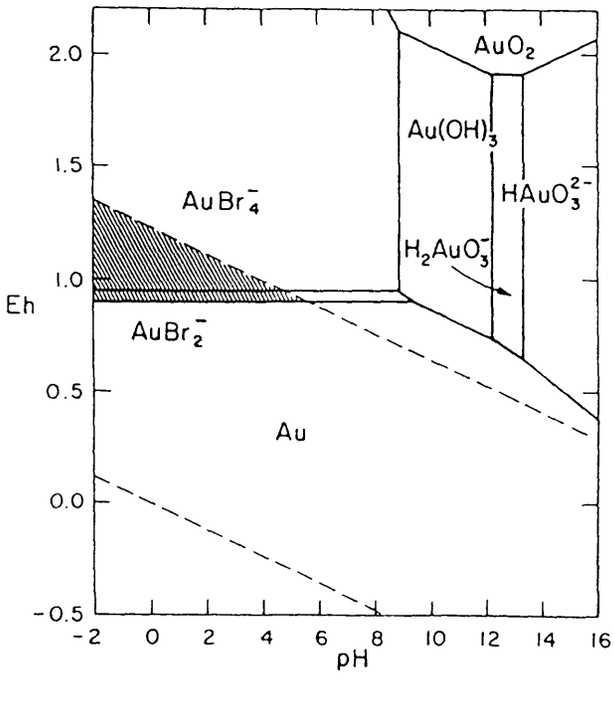
Half-Reaction	E° (V)	Reference
$I_{2(aq)} + 2e^- = 2I^-_{(aq)}$	0.621	12, 98
$I_3^-{}_{(aq)} + 2e^- = 3I^-_{(aq)}$	0.536	12, 98
$(SCN)_{2(aq)} + 2e^- = 2SCN^-_{(aq)}$	0.77	19, 51
$(SCN)_3^-{}_{(aq)} + 2e^- = 3SCN^-_{(aq)}$	0.68	91
$Br_{2(aq)} + 2e^- = 2Br^-_{(aq)}$	1.0874	12, 97
$Br_3^-{}_{(aq)} + 2e^- = 3Br^-_{(aq)}$	1.0503	12, 97



(a)



(b)



(c)

Figure 7.1 - Eh-pH diagrams at 25°C for the **(a)** Au-I-H_2O system [187], **(b)** Au-SCN-H_2O system (calculated as part of this work), and **(c)** Au-Br-H_2O system [187]. In all cases, the activities adopted were: {Au} = 10^{-5} and {L} = $!0^{-2}$ (L = I^-, SCN^- and Br^-).

Both bromide and iodide are lixiviants for gold and it is interesting to compare the Eh-pH diagrams drawn by Hiskey [187] for these two systems with those drawn for the gold-thiocyanate-water system as part of this work, which were presented in Chapter 2. A set of these diagrams is shown in **Figure 7.1**. The three diagrams are remarkably similar, once again demonstrating the pseudohalide character of thiocyanate. The main point from this comparison is that the potentials corresponding to the lines between solid gold and the aurous complexes, as expected, follow the same order as those for the redox couples in **Table 7.1**. The potentials for the formation of the three aurous complexes can then be arranged in the following increasing order: AuI_2^- < $Au(SCN)_2^-$ < $AuBr_2^-$.

The reason for trying iodide additions to the ferric thiocyanate lixiviant now becomes apparent. As demonstrated in the previous chapter, the gold dissolution rates are related to the ferric thiocyanate autoreduction. The low dissolution rates at 25°C and, particularly, the decrease of the initial dissolution rates with time are consequences of the observed autoreduction rates and their simultaneous decrease with time. Behind these observations stands the active role played by thiocyanate oxidation intermediate species, particularly $(SCN)_3^-$, in the mechanism of gold dissolution. **Table 7.1** and **Figure 7.1** show that, even when the potentials are too low to permit the formation of $(SCN)_3^-$, iodide species such as I_2 and I_3^- are still stable in solution and, coincidentially, the complex AuI_2^- is also stable. The presence of the iodide species in solution extends the potential range in which the gold dissolution is thermodynamically feasible to values as low as *c.a.* 500 mV. Such values are lower than those ever attained in the rotating disc runs reported in the previous chapter, througout the temperature range considered. Chemically, this means that the lack of $(SCN)_3^-$ due to the slowing down of the autoreduction process is counterbalanced by the presence of I_3^-, which is both oxidant and complexant for gold. As a consequence, the tendency towards the stabilization of the thin-layer of $AuSCN_{(ads)}$ with time is counterbalanced and that

intermediate compound is removed into solution probably as a mixed complex of gold with SCN^- and I^-.

The above thermodynamic reasoning supports initial trials with the mixed thiocyanate-iodide system. However, the chemistry actually involved is considerably more complex due to the production of mixed species of iodine with thiocyanate. This subject will be resumed in Section 7.6 when discussing the experimental results.

7.4. Experimental Conditions and Procedure. Analytical Techniques

Iodine, hypochlorite and hydrogen peroxide are the only oxidizing agents already tried experimentally in the iodide leaching of gold [189, 191]. In the present work, on the other hand, Fe^{3+} is considered as the main oxidant. Some iodide leaching runs using Fe^{3+} as oxidant were then conducted in the initial part of the experimental programme reported in this chapter. These were followed by the leaching runs with ferric thiocyanate solutions with additions of iodide or iodine. The same gold rotating disc equipment and experimental procedure described in Chapter 6, Section 6.2 were used in this part of the work. The analytical techniques for gold, ferric and ferrous ions, and thiocyanate, were also the same described in Section 6.2.

Analytical grade reagents were used in all experiments (see Appendix 7). The potassium salts of iodide and thiocyanate were used. All runs were conducted in an inert (nitrogen) atmosphere. The following conditions apply to all runs: temperature, 25°C; pH 1.5; initial Fe^{3+} concentration, 0.055 mol/dm^3 (as ferric alum); disc rotation speed, 75.4 rad/s (700 rpm).

7.5. Gold Leaching with Iodide and Ferric Ions: Results and Discussion

Results of iodide leaching runs, without addition of thiocyanate, are shown in **Figure 7.2**. The corresponding potential readings and reduction of Fe^{3+} to Fe^{2+} are presented in **Figure 7.3**. The dissolution rates obtained in these three experiments are given in **Table 7.2**, which also contains the correlation coefficients for the linear fits.

The behaviour observed in these iodide leaching runs was different from that observed in the ferric thiocyante leaching in two main respects: first, there was no marked variation in the gold dissolution rate within an individual run; second, the rates with iodide, shown in **Table 7.2**, were much higher than with thiocyanate.

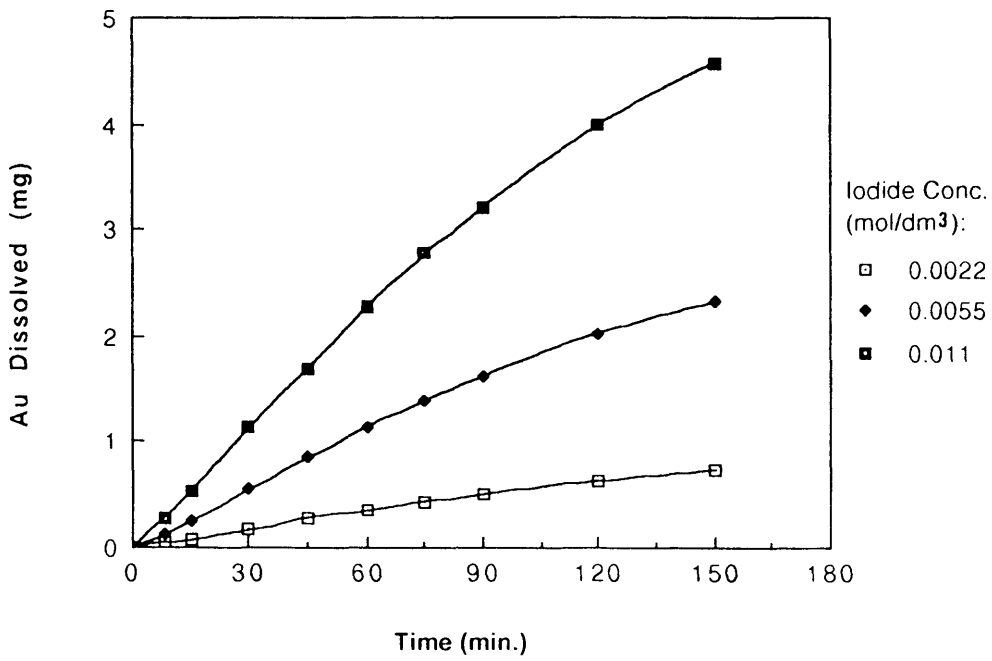
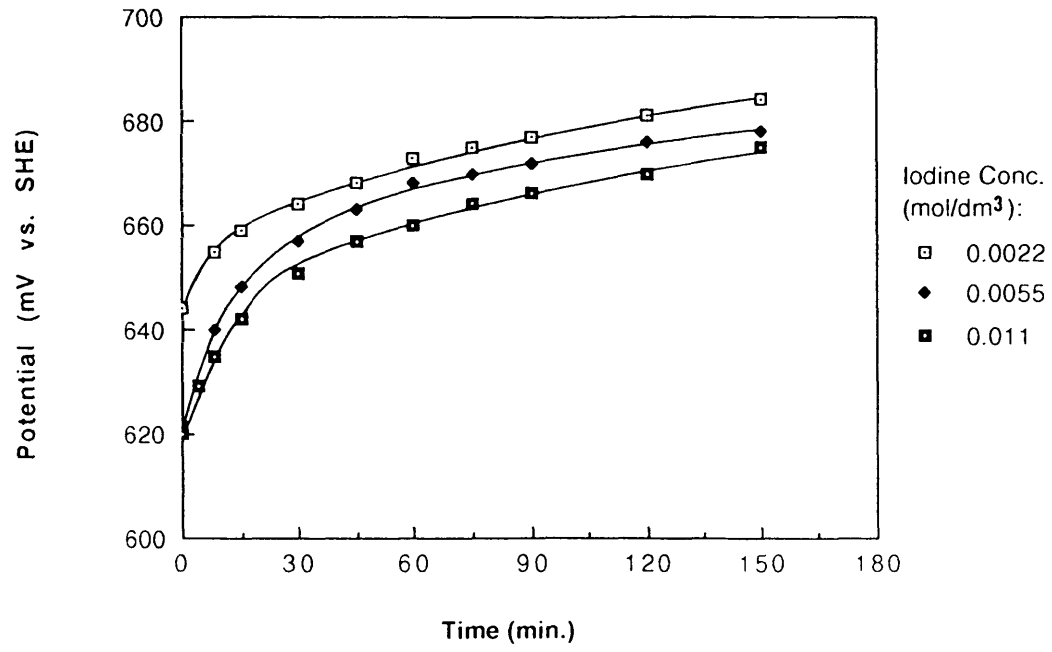
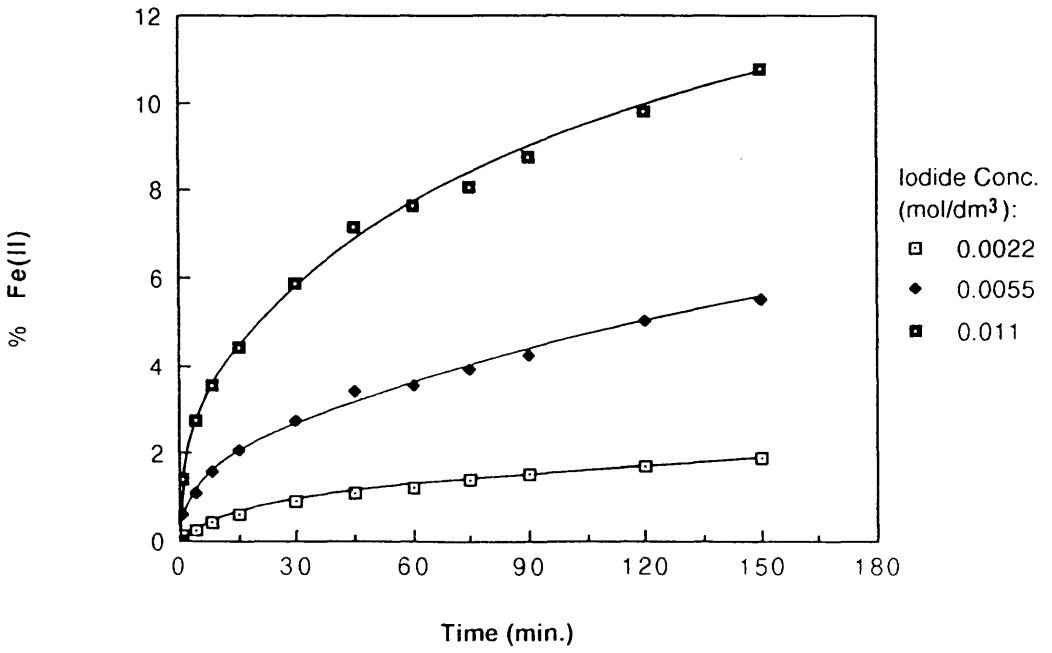


Figure 7.2 - Effect of iodide concentration on the leaching of gold in presence of 0.055 mol/dm^3 (initial) Fe^{3+} at 25°C. Rotation speed, 75.4 rad/s (700 rpm). Nitrogen atmosphere.



(a)



(b)

Figure 7.3 - Effect of iodide concentration on **(a)** potential readings at the gold disc surface and **(b)** reduction of Fe^{3+} to Fe^{2+}. For all runs: 0.055 mol/dm^3 Fe^{3+} (initial), pH 1.5, temperature 25°C, rotation speed 75.4 rad/s (700 rpm), N_2 atmosphere.

Table 7.2 - Gold Dissolution Rates Obtained with Several Iodide Concentrations at 25°C, pH 1.5 and 0.055 mol/dm^3 Fe^{3+}(experiments presented in **Figure 7.2**)

Iodide Concentration (mol/dm^3)	Gold Dissolution Rate J x 10^9 (mol/cm^2 s)	Linear Correlation Coefficient R^2
0.0022	0.28	0.989
0.0055	0.89	0.987
0.011	1.74	0.986

A comparison between the rates of **Table 7.2** and those of **Table 6.3** (Section 6.5, Chapter 6) shows that the dissolution rate obtained with a given iodide concentration was considerably higher than those obtained with thiocyanate concentrations 10 or more times larger than that of iodide. The constancy of the rates with iodide is demonstrated by the correlation coefficients being very close to 1.0 for the linear fits including all the sample points. The third rate value in **Table 7.2** compares very well with the 2.6×10^{-9} mol/cm^2 s obtained by Qi and Hiskey [189, 190] using 0.01 mol/dm^3 NaI and 0.005 mol/dm^3 I_2.

The complete behaviour pattern of the iodide experiments emerges when **Figure 7.2** is compared with **Figure 7.3**. It is interesting to notice that, while there was a decrease in the potential readings in the ferric thiocyanate solutions due to the progress of autoreduction, the reverse took place in the iodide system. The mixed potentials were low at zero time (shortly after the addition of Fe^{3+} to the iodide solution) and then increased and tended to a plateau (see **Figure 7.3a**). Such potential rise is due to the production of the species I_2 and I_3^-, which are generated by the

oxidation of I^- by Fe^{3+}. The corresponding Fe^{3+} reduction is shown in **Figure 7.3b**. Differently from $(SCN)_2$ and $(SCN)_3^-$, which are unstable and decompose through hydrolysis, I_2 and I_3^- are very stable and accumulate in solution as the iodide oxidation progresses. The potential determining couples are basically Fe^{3+}/Fe^{2+}, I_2/I^- and I_3^-/I^-. The measurements reported therefore correspond to mixed potentials, which are in fact nonequilibrium (irreversible) potentials. The anodic and cathodic processes involved are then the I^- oxidation and the Fe^{3+} reduction, respectively. The readings appearing in **Figure 7.3a**, as well as in the other graphs in this chapter, were taken at the surface of the gold rotating disc, against a Ag-AgCl reference electrode. Similar measurements were taken on a platinum electrode. The dissolution of the gold electrode did not contribute appreciably to the mixed potentials. Overall, the readings on the Au and Pt electrodes were very similar, as reported in Appendix 6.

The behaviour observed in the experiments reported in this section is similar to that reported both by Qi and Hiskey [189, 190] and by Davis and Tran [191], using iodine as oxidant. The only difference is that in the present case, and for the first time, Fe^{3+} was added instead of iodine, the species I_2 and I_3^- being produced in solution. These species, I_3^- in particular, are directly responsible for the oxidation and complexation of gold [189-191]. The relative constancy of the gold dissolution rate with time within each run is due to the stability of I_2 and I_3^- in solution. The mechanism of gold dissolution seems to be similar to that discussed in the previous chapter, Section 6.12, in which $(SCN)_3^-$ plays an important role.

The ability of I^- to complex Fe^{3+} and Fe^{2+} is very small compared to that of SCN^-, particularly in the case of Fe^{3+}, and was not considered in this section. A few complexes are reported in the literature [12, 18].

7.6. Gold Leaching by Iron(III)-Thiocyanate with Additions of Iodide or Iodine Solution: Results and Discussion

The effect of iodide addition on the leaching of gold by ferric thiocyanate is illustrated in **Figure 7.4**. The respective mixed potential and Fe^{3+} reduction patterns are shown in **Figure 7.5**.

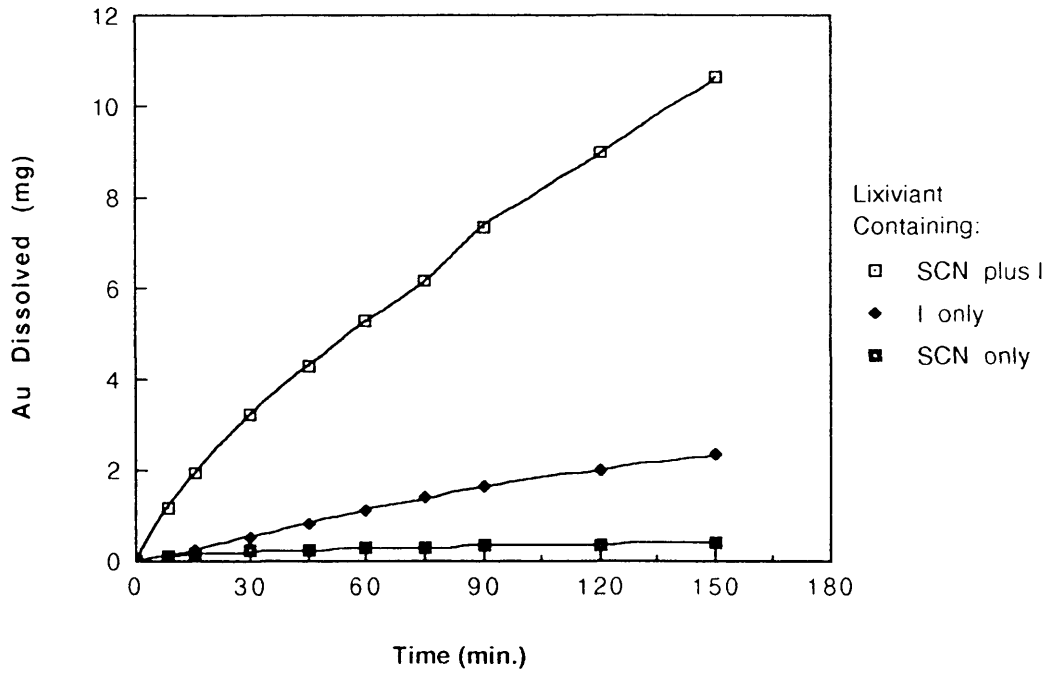
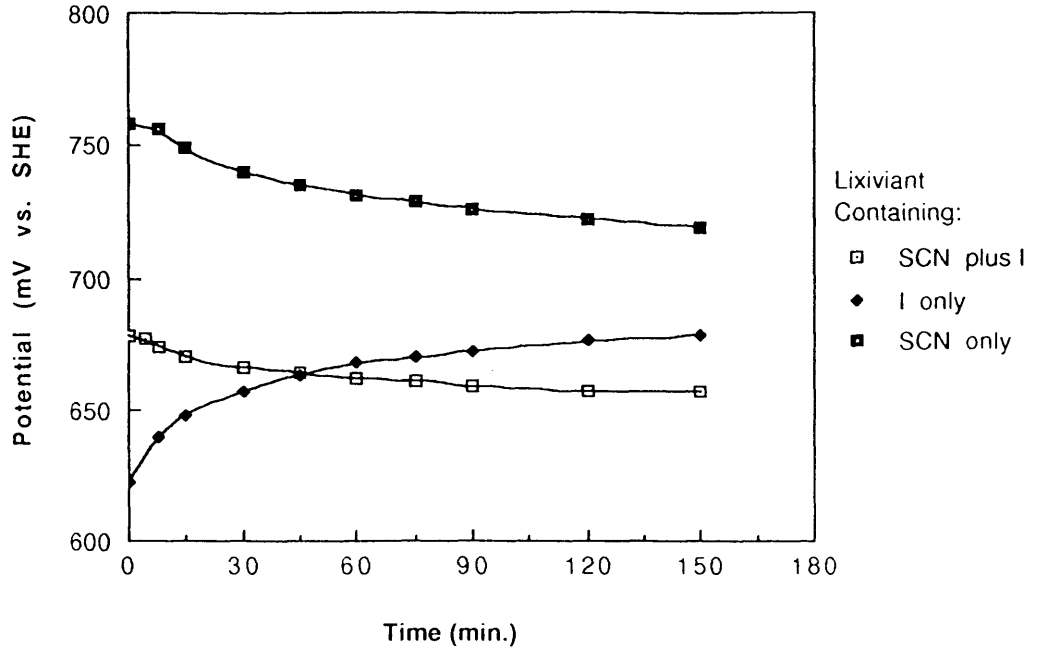


Figure 7.4 - Effect of iodide addition on the leaching of gold by ferric thiocyanate at 25°C and pH 1.5. Lixiviant concentrations: 0.10 mol/dm^3 SCN^- and 0.0055 mol/dm^3 I^-. Disc rotation speed: 75.4 rad/s (700 rpm). N_2 atmosphere.

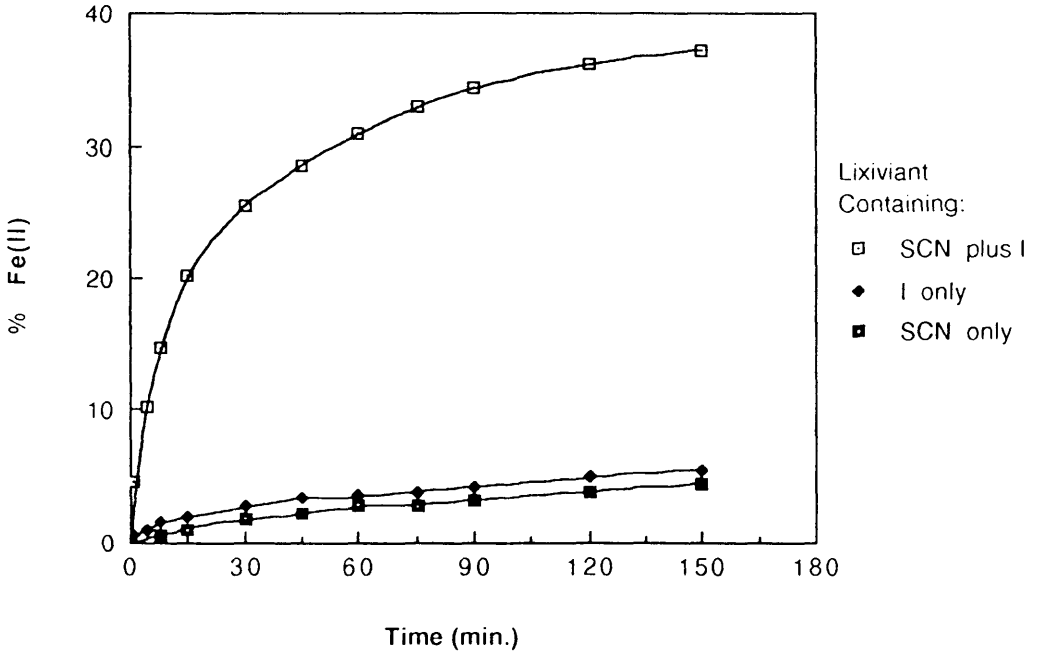
Figure 7.4 shows that the effect of adding iodide was drastic. The concentrations used were 0.10 mol/dm^3 SCN^- and 0.0055 mol/dm^3 I^-, which means a SCN^-/I^- ratio of 18.2. The leaching was poor when that amount of thiocyanate alone was used, revealing the

limitations of the ferric thiocyanate leaching at room temperature, already explored in Chapter 6. When, on the other hand, iodide alone was used, the results were remarkably better, despite the concentration of iodide being about 18 times lower than that of thiocyanate. When the two reagents were added together, the effect was considerably stronger than that of each of them individually, suggesting a synergistic effect. The initial rate in that experiment was 8.17×10^{-9} mol/cm^2 s. The decrease in the initial gold dissolution rate was much less pronounced than that observed with the ferric thiocyanate solutions alone, which can be explained in terms of I_3^- being stable at potentials lower than $(SCN)_3^-$, compensating for the decrease in the production of this latter species (and for its depletion through hydrolysis). Therefore, the rate after 1 hour was 3.26×10^{-9} mol/cm^2 s, which amounts to a decrease of the initial rate by a factor of 2.5, whereas this factor was around 10 in the runs with ferric thiocyanate alone (see, for instance, **Table 6.3** in Section 6.5). The average dissolution rate, obtained by including all sample points in the linear regression, was 3.78×10^{-9} mol/cm^2 s, with a correlation coefficient of 0.985 for the linear fit.

There was a basic difference in the way the mixed potentials varied in the experiments discussed here, as shown in **Figure 7.5a**. An initial potential drop followed by a tendency to stabilization was observed in the runs with ferric thiocyanate alone, whereas in the experiments with ferric ions and iodide the tendency towards stabilization was preceded by an initial potential rise. With the mixed system, both tendencies compensated for each other to some extent, resulting in a small net potential variation despite of the much higher Fe^{3+} reduction occurred in the mixed experiment, as shown in **Figure 7.5b**. These different patterns of potential variation can be explained in terms of the cathodic and anodic currents which determine the irreversible potentials. The main cathodic process was the reduction of Fe^{3+}. The corresponding anodic processes were, in one case, the oxidation of thiocyanate to $(SCN)_3^-$



(a)



(b)

Figure 7.5 - Effect of iodide addition on **(a)** potential readings and **(b)** Fe^{3+} reduction, in the leaching of gold at 25°C and pH 1.5. Lixiviant concentrations: 0.10 mol/dm^3 SCN^- and 0.0055 mol/dm^3 I^-. Disc rotation speed: 75.4 rad/s (700 rpm). N_2 atmosphere.

and $(SCN)_2$ and then to HCN and SO_4^{2-}, and in the other case, the oxidation of iodide to I_3^- and I_2. The much higher Fe^{3+} reduction in the mixed experiment indicates that the thiocyanate and iodide systems do not behave independently; they interact to produce new chemical species, not yet considered in this work.

The high dissolution rate obtained in the experiment with iodide addition shown in **Figure 7.4** encouraged a lower thiocyanate concentration to be tried. The results are presented in **Figure 7.6** and **7.7**, which show that the overall patterns of gold dissolution, potential variation and Fe^{3+} reduction were similar to those already observed in the previous set of experiments. The iodide concentration was again 0.0055 mol/dm^3, but the thiocyanate concentration was only 0.050 mol/dm^3.

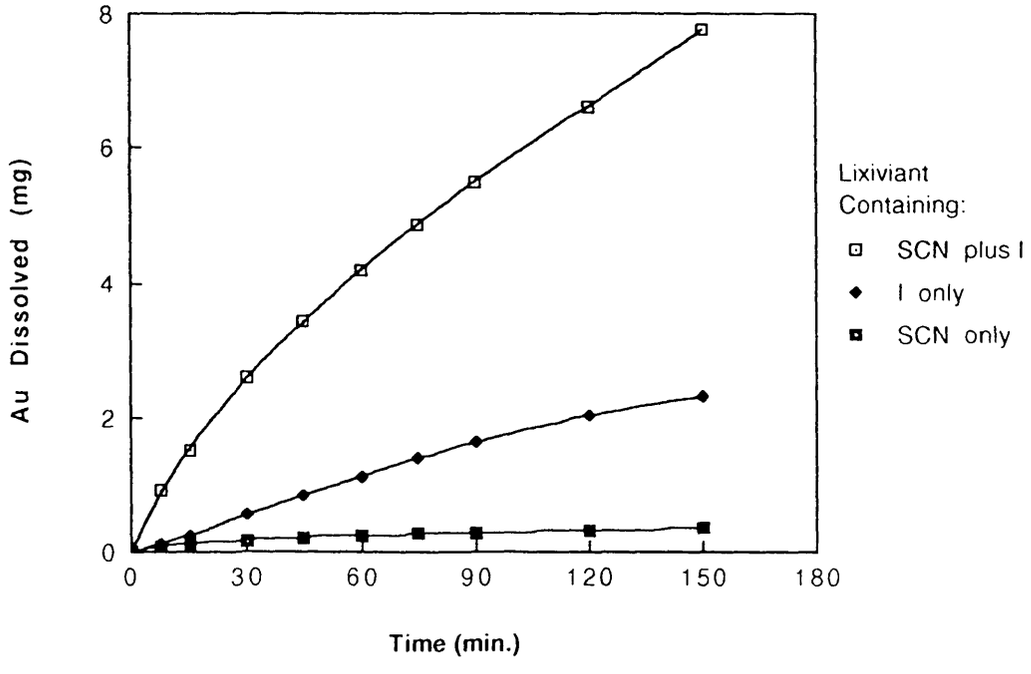
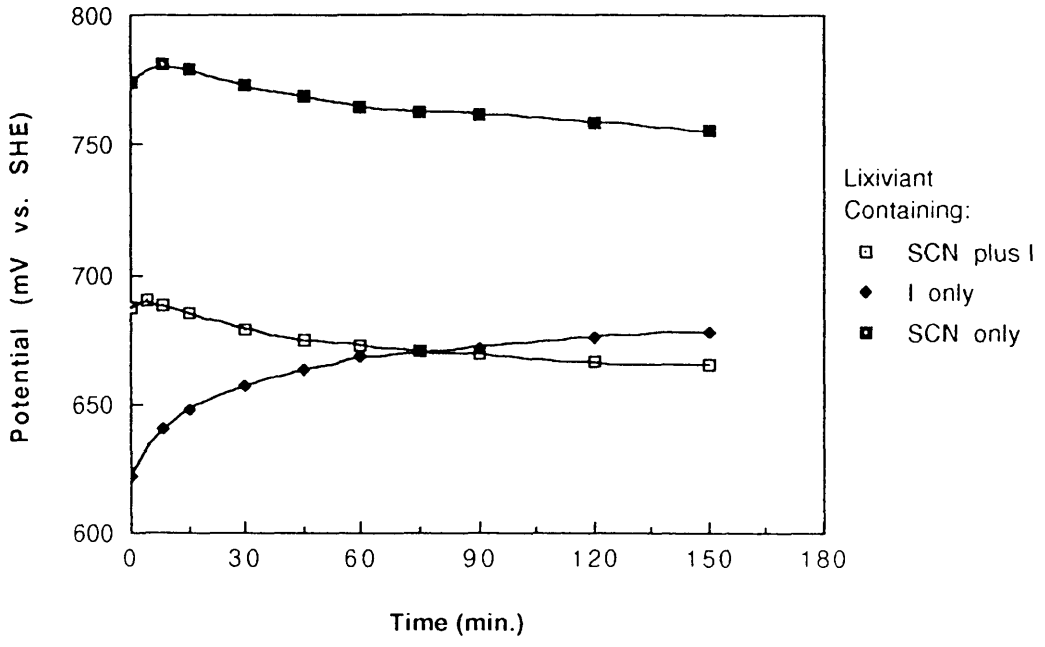
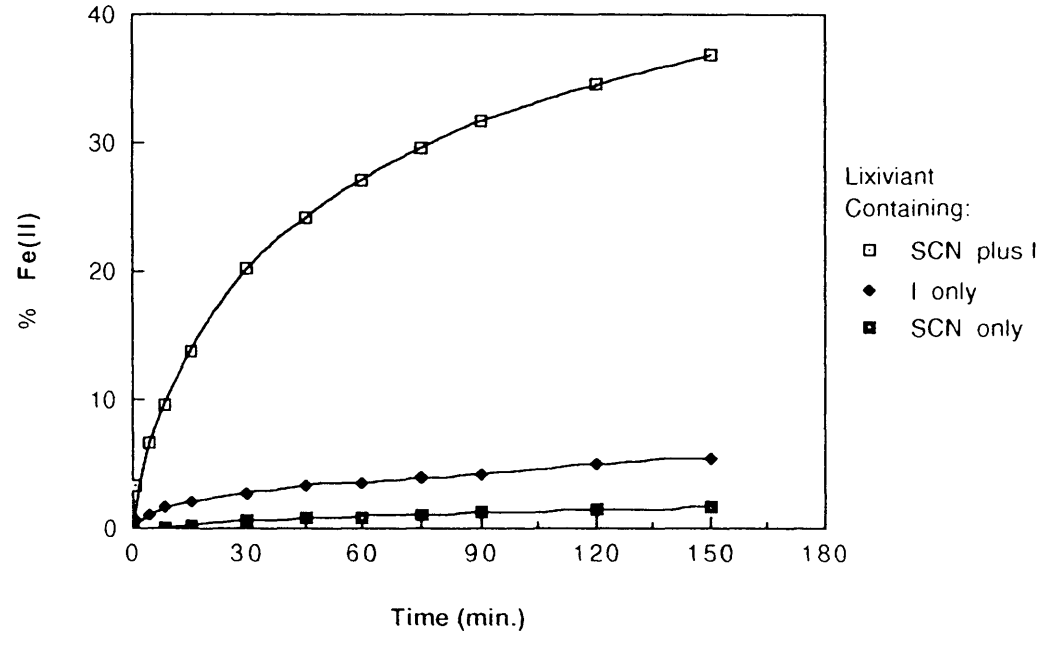


Figure 7.6 - Effect of iodide addition on the leaching of gold by ferric thiocyanate at 25°C and pH 1.5. Lixiviant concentrations: 0.050 mol/dm^3 SCN^- and 0.0055 mol/dm^3 I^-. In all runs: 0.055 mol/dm^3 Fe^{3+} (initial), 75.4 rad/s (700 rpm) and N_2 atmosphere.



(a)



(b)

Figure 7.7 - Effect of iodide addition on **(a)** potential readings and **(b)** Fe^{3+} reduction, in the leaching of gold at 25°C and pH 1.5. Lixiviant concentrations: 0.050 mol/dm^3 SCN^- and 0.0055 mol/dm^3 I^-. In all runs: 0.055 mol/dm^3 Fe^{3+} (initial), 75.4 rad/s (700 rpm) and N_2 atmosphere.

The initial dissolution rate obtained in the experiment with 0.050 mol/dm^3 SCN^- and 0.0055 mol/dm^3 I^- was 6.17×10^{-9} mol/cm^2 s, and the average rate, including all sample points in the linear regression, was 2.16×10^{-9} mol/cm^2 s. Again, the Fe^{3+} reduction in the experiment with the mixed thiocyanate-iodide system was much higher than that observed in either of the other two runs with thiocyanate or with iodide only, as illustated in **Figure 7.7b**.

As remarked above, the much higher Fe^{3+} reduction in the mixed experiments indicate an interaction between the thiocyanate and iodide systems, which produces chemical species not yet considered in the present work. The interaction between thiocyanate and iodine has received due attention in the chemical literature [28, 199-202].

As stated above, iodine is scarcely soluble in water, but becomes readily soluble if iodide ions are present in solution, the following equilibrium being established:

$$I_{2(aq)} + I^- = I_3^- \qquad (7.1)$$

Similarly, it was found that rather large quantities of iodine could be dissolved in aqueous potassium thiocyanate to give solutions which were yellow or orange in colour. These solutions were not very stable and underwent slow oxidation of SCN^- to HCN and SO_4^{2-}, which took several hours to reach completion. The overall process was irreversible and, in acidic medium, corresponded to the reaction [202]:

$$SCN^- + 3I_2 + 4H_2O \longrightarrow SO_4^{2-} + 6I^- + HCN + 7H^+ \qquad (7.2)$$

Thus, the rate of this reaction was not sufficiently high to account for the speed with which iodine dissolved in the thiocyanate solution. This observation led to the postulation of relatively stable intermediate species, particularly I_2SCN^- and ISCN [202].

Later work [199, 201] emphasized the formation of the complex I_2SCN^- as the predominant species, which presents a strong u.v. absorption peak at 303 nm. The following reversible equilibrium was found to be quickly established upon dissolution of iodine in an acidic thiocyanate solution [199, 201, 202]:

$$I_{2(aq)} + SCN^- = I_2SCN^- \qquad (7.3)$$

The value log K = 1.93 at 25°C for ionic strengths from 1 to 5 was estimated by Lewis and Skoog [201], while Orságh et al. [199] found log K = 1.72 at an ionic strength 0.11.

In a solution containing I^-, I_2 and SCN^-, the reversible equilibria expressed by reactions 7.1 and 7.3 exist simultaneously. Thus, addition of concentrated KSCN to a dilute solution of the triiodide-starch complex caused a rapid loss of the characteristic blue colour, due to consumption of I_2 to form I_2SCN^- and simultaneous conversion of I_3^- to I_2 and I^- to keep the equilibrium of reaction 7.1. Providing that not too much SCN^- had been added, the colour could be restored by addition of iodide ion. Besides this simple empirical procedure, the reversibility of reaction 7.3 was confirmed spectrophotometrically [199, 201].

A slightly different situation arose when iodide ions were added to an acidic solution containing thiocyanogen, $(SCN)_2$, the following reaction having being observed [200]:

$$(SCN)_{2(aq)} + I^- = I(SCN)_2^- \qquad (7.4)$$

The value log K = 4.10 at 25°C and ionic strength 1.2 was determined by Long and Skoog [200] for this equilibrium. This corresponds to an equilibrium constant of 1.25×10^4, which indicates the great ability of I^- to stabilize $(SCN)_2$ through complexation.

The species $I(SCN)_2^-$ has u.v. absorption characteristics which are very similar to I_2SCN^-, both presenting absorption peaks at 303 nm [199-201]. These two species can be seen as belonging to a substitution series whose extremes are I_3^- and $(SCN)_3^-$.

The difficulty in the experimental investigation of reaction 7.4 in aqueous solutions resides in the rapid decomposition of $(SCN)_2$ through hydrolysis. To produce this reaction, Long and Skoog [200] started from a thiocyanate solution to which a suitable oxidant was added in order to release $(SCN)_2$. Iodide ions were then added immediately and produced the u.v. peak characteristic of $I(SCN)_2^-$. However, if the iodide ions were introduced after the thiocyanate-oxidant mixture was left standing for a few minutes, the absorbance was appreciably less and was dependent on the time of standing. This decrease in absorbance was undoubtedly due to the relatively fast hydrolysis of $(SCN)_2$. Thus, $(SCN)_2$ is stabilized by the complexation with I^- to form $I(SCN)_2^-$, which results in a considerable benefit to the gold dissolution process.

Both I_2SCN^- and $I(SCN)_2^-$ are intermediate species which undergo irreversible decomposition, presumably to sulphate and other products of thiocyanate oxidation. The factors affecting the decomposition of both species are similar. The rate of decomposition is greatly reduced in the temperature range 0-10°C. Their stability also increases with ionic strength and H^+ concentration. Thus, with temperatures between 0 and 10°C, ionic strengths between 1 and 5 and H^+ concentrations from 1 to 2 mol/dm^3, the intensity of the absorption peak at 303 nm was observed to be practically constant (less than 0.1% decrease in 1 hour). Even at room temperature and with an acid concentration of 0.1 mol/dm^3, which are typical leaching conditions, the decrease in the intensity of the u.v. absorption peak of I_2SCN^- was less than 1% in 1 hour [200, 201]. These observations reveal a remarkable stability compared to $(SCN)_2$, whose hydrolysis is so much faster that it requires the experimental observations to be carried out in organic

solvents (see Chapter 3, Sections 3.5 and 3.6).

The foregoing discussion can be summed up in terms of the following reactions:

$$I_{2(aq)} + I^- = I_3^- \qquad \log K = 2.86 \qquad (7.1)$$

$$I_{2(aq)} + SCN^- = I_2SCN^- \qquad \log K = 1.93 \qquad (7.3)$$

$$(SCN)_{2(aq)} + I^- = I(SCN)_2^- \qquad \log K = 4.10 \qquad (7.4)$$

$$(SCN)_{2(aq)} + SCN^- = (SCN)_3^- \qquad \log K = 3.04 \qquad (7.5)$$

The value log K = 3.04 for reaction 7.5 was calculated from the $\Delta G°$ data reported in Appendix 1. The remaining ones are the quoted above in this section.

The considerably higher reduction of Fe^{3+} observed in the gold rotating disc experiments with the mixed thiocyanate-iodide system, as shown in **Figures 7.5b** and **7.7.b**, can now be explained in terms of the four reactions given above. Reaction 7.5 results from the autoreduction of the ferric thiocyanate complexes. The fast reaction of I^- with $(SCN)_2$ to give $I(SCN)_2^-$ (reaction 7.4) displaces reaction 7.5 to the left, thus causing further Fe^{3+} reduction to replace $(SCN)_3^-$ and reestablish the equilibrium (reaction 7.5). The same applies to the consumption of I_2 through reaction with SCN^- to yield I_2SCN^- (reaction 7.3), which displaces reaction 7.1 to the left and requires further Fe^{3+} reduction to replace I_3^- and reestablish that equilibrium. The overall consequence of that extensive Fe^{3+} reduction was an accumulation in the system of the relatively stable species X_3^- (where X = I and/or SCN). The stabilization of a considerable amount of $(SCN)_2$ through complexation by I^- is a particularly relevant fact, once this intermediate thiocyanate

species is regarded as more unstable towards hydrolysis than $(SCN)_3^-$ [42, 72, 90]. Anion-radicals having a net negative charge tend to be more stable in solution because of the formation of ionic pairs with H^+ and/or another cations available. Species of the type X_2 (where X = SCN, I, Br, Cl) present several inconveniences, such as easy hydrolysis in the case of $(SCN)_2$, or release to the gaseous phase, due to the relatively high partial pressures of the halogens. In these respects, thiocyanate works as a "carrier" for halide species in solution, which may be especially interesting due to its very low toxicity and consequent better environmental and operational acceptability.

In the case of the rotating disc experiments reported above in this section, the initial system contained SCN^- and I^-. The two main reactions likely to have taken place under the oxidizing effect of Fe^{3+} were:

$$I^- + 2SCN^- = I(SCN)_2^- + 2e \qquad (7.6)$$

$$2I^- + SCN^- = I_2SCN^- + 2e \qquad (7.7)$$

Although I_2SCN^- and $I(SCN)_2^-$ are the main mixed iodide-thiocyanate species found in solution, they are not the only ones. Several other species may be identified. ISCN is one of such species already mentioned in the literature [199-202].

The foregoing reasoning demonstrates that both the higher Fe^{3+} reduction and the synergistic effect on the gold dissolution caused by the addition of iodide to the iron(III)-thiocyanate system can be explained in terms of reactions 7.1 and 7.3 through 7.7 or, in other words, in terms of the production of mixed species of iodide or iodine and thiocyanate, I_2SCN^- and $I(SCN)_2^-$ being the the main ones. The experimental results indicated that these two species have

important roles in the mechanism of gold dissolution, similarly to that which happens with I_3^- and $(SCN)_3^-$. The overall oxidizing ability of the system is greatly enhanced by the accumulation, due to the establishment of the reversible equilibria shown by reactions 7.1, 7.3, 7.4 and 7.5, of the relatively stable series I_3^-, I_2SCN^-, $I(SCN)_2^-$ and $(SCN)_3^-$. As both SCN^- and I^- are ligands for gold, these species have not only oxidizing but also complexing ability, upon reduction.

Resuming now the discussion of the gold rotating disc experiments. The results presented in **Figures 7.4** through **7.7** revealed this very interesting chemistry involving the thiocyanate and iodide systems. Further experiments were then performed to further investigate the effects of the concentrations of thiocyanate and iodide on gold dissolution.

Experiments with several iodide concentrations and 0.10 mol/dm^3 SCN^- are shown in **Figure 7.8**. There is a pronounced increase in the gold dissolution rate with increasing iodide concentration. The run with 0.0055 mol/dm^3 I^- is the same as that plotted in **Figure 7.4**. The variation of the potential readings and the reduction of Fe^{3+} followed basically the same pattern already described for the similar experiments in **Figures 7.5** and **7.7** (see data in Appendix 6). The increase in the initial iodide concentration furthers the production of $I(SCN)_2^-$ and I_2SCN^- as shown by reactions 7.6 and 7.7 and redistributes the equilibria indicated by reactions 7.1, 7.3, 7.4 and 7.5, so that there is an increase in the overall concentration of X_3^- (X = I and/or SCN) in the system. The active role of such species in the mechanism of gold dissolution is demonstrated by the considerable increase in the dissolution rates in these series of experiments. The highest initial dissolution rate, obtained with 0.10 mol/dm^3 SCN^- and 0.011 mol/dm^3 I^-, was 1.07×10^{-8} mol/cm^2 s and the average rate in the same run was 5.42×10^{-9} mol/cm^2 s. This initial rate is the same as that obtained with 0.10 mol/dm^3 thiourea and 0.01 mol/dm^3 formamidine

disulphide [177]. It is also close to the optimum rate of 1.56×10^{-8} mol/cm^2 s obtained by Davis and Tran [191] with a iodine-iodide mixture of 0.10 mol/dm^3 KI and 0.040 mol/dm^3 iodine. Moreover, the present lixiviant is much more stable than thiourea and, on the other hand, contains much less I_2 in solution than the latter solution, which means much less I_2 loss to the gaseous phase.

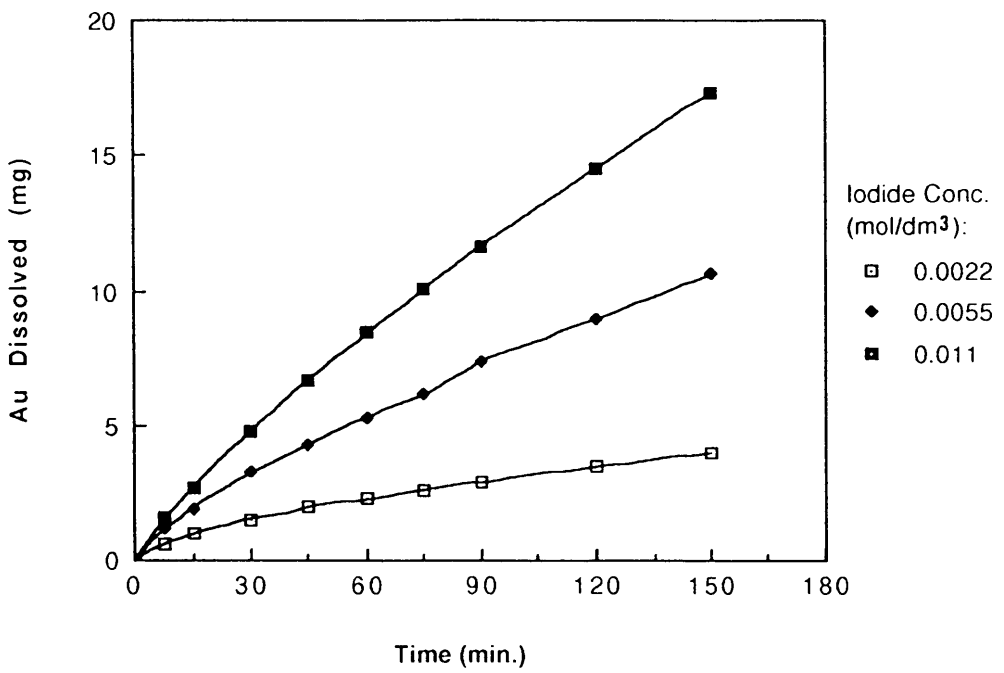


Figure 7.8 - Effect of iodide concentration on the leaching of gold by ferric thiocyanate at 25°C and pH 1.5. Lixiviant concentrations: 0.10 mol/dm^3 SCN^- and 0.055 mol/dm^3 Fe^{3+} (initial). Disc rotation speed: 75.4 rad/s (700 rpm). N_2 atmosphere.

Experiments with several thiocyanate concentrations and 0.0055 mol/dm^3 I^- are shown in **Figure 7.9**. It is interesting to compare this plot with **Figure 6.6**, and also to compare the rates reported in this chapter, which are all listed in **Table 7.3**, with

those in **Table 6.3**. It is seen that in the presence of iodide species, the gold dissolution rates are considerably more responsive to increases in the thiocyanate concentration. This effect can also be interpreted in terms of reactions 7.6 and 7.7 and redistribution the equilibria indicated by reactions 7.1, 7.3, 7.4 and 7.5. Increases in the thiocyanate concentration cause increases in the overall concentration of X_3^- (X = I and/or SCN) species in solution, which improves the gold leaching rate.

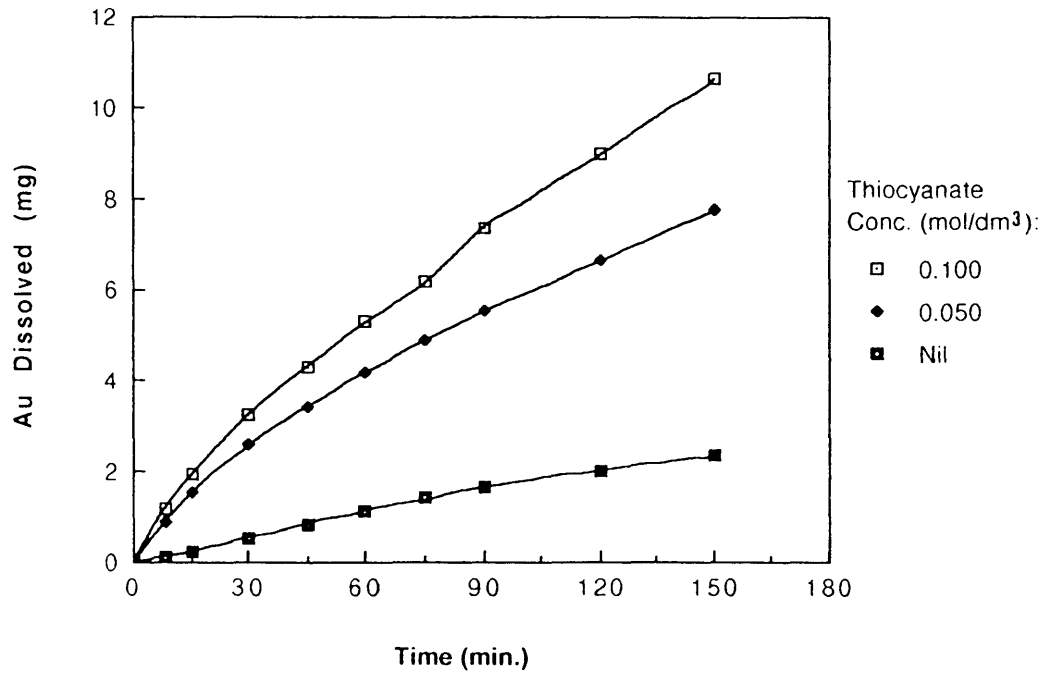


Figure 7.9 - Effect of thiocyanate concentration on the leaching of gold by ferric thiocyanate with iodide addition, at 25°C and pH 1.5. Lixiviant concentrations: 0.0055 mol/dm^3 I^- and 0.055 mol/dm^3 Fe^{3+} (initial). Disc rotation speed: 75.4 rad/s (700 rpm). N_2 atmosphere.

Table 7.3 - Gold Dissolution Rates Observed with Several Concentrations of SCN^- and I^- (or Iodine) and 0.055 mol/dm^3 Fe^{3+} at 25°C and pH 1.5

Concentrations (mol/dm^3)		Initial Rate J x 10^9	Rate after 1 Hour J x 10^9	Average Rate J x 10^9
SCN^-	I^-	(mol/cm^2 s)	(mol/cm^2 s)	(mol/cm^2 s)
0.050	0	0.63	0.07	-
0.10	0	0.78	0.08	-
0	0.0022	0.32	0.23	0.28
0	0.0055	0.89	0.72	0.89
0	0.011	1.92	1.41	1.74
0.050	0.0055	6.17	2.16	2.76
0.10	0.0022	4.43	1.03	1.37
0.10	0.0055	8.17	3.26	3.78
0.10	0.011	10.7	5.42	6.27
Runs with Addition of Iodine Solution (Normality Units) Instead of Iodide Ions:				
0.10	0.001 N (*)	4.91	1.54	1.93
0.10	0.005 N (*)	11.0	5.63	6.29

(*) 0.001 and 0.005 N of I_2 added as standard iodine solution correspond to 0.0022 and 0.011 mol/dm^3 of atomic I, respectively, which are the same concentrations used when I^- was added in some of the experiments above. This can be understood as follows: a 0.10 N iodine solution is made up by adding 12.7 g of solid I and 20 g of KI to one liter of water [136, 142, 143]. This amounts to 0.22 mol/dm^3 of atomic I.

The figures in **Table 7.3** summarize everything that has been said in this chapter about the synergistic effect of additions of iodide ions or iodine to the ferric thiocyanate leaching system. In

the last two runs reported in the table, iodine was added instead of iodide ions. Iodine was added from a standard 0.10 N stock solution prepared according to the conventional procedure adopted in volumetric analysis [136, 142, 143]. Thus, to make up one litre of 0.10 N standard iodine solution, 12.7 g of solid iodine were dissolved in a small volume of water already containing 20 g KI, which means that the mass balance for atomic iodine in solution was 0.22 mol/dm^3. The concentrations of 0.001 and 0.005 N of iodine reported in those two experiments are the same, in terms of atomic iodine, to the 0.0022 and 0.011 mol/dm^3 adopted when iodide was added. The reason for carrying out those two experiments was to check the extent of the improvement in the gold dissolution rates when the oxidized forms I_2 and I_3^- were added at once, at zero time, instead of being generated by the Fe^{3+} reduction. Therefore, the runs with 0.10 mol/dm^3 SCN^- and addition of 0.001 and 0.005 N iodine solution should be compared with those with the same SCN^- concentration and 0.0022 and 0.011 mol/dm^3 I^-, respectively. The figures in **Table 7.3** show that the increases in the gold dissolution rates were not very pronounced, particularly with 0.005 N I_2, which demonstrates the high rate at which the X_3^- (X = I and/or SCN) species are initially produced in solution through the reduction of Fe^{3+}, in the experiments with iodide addition.

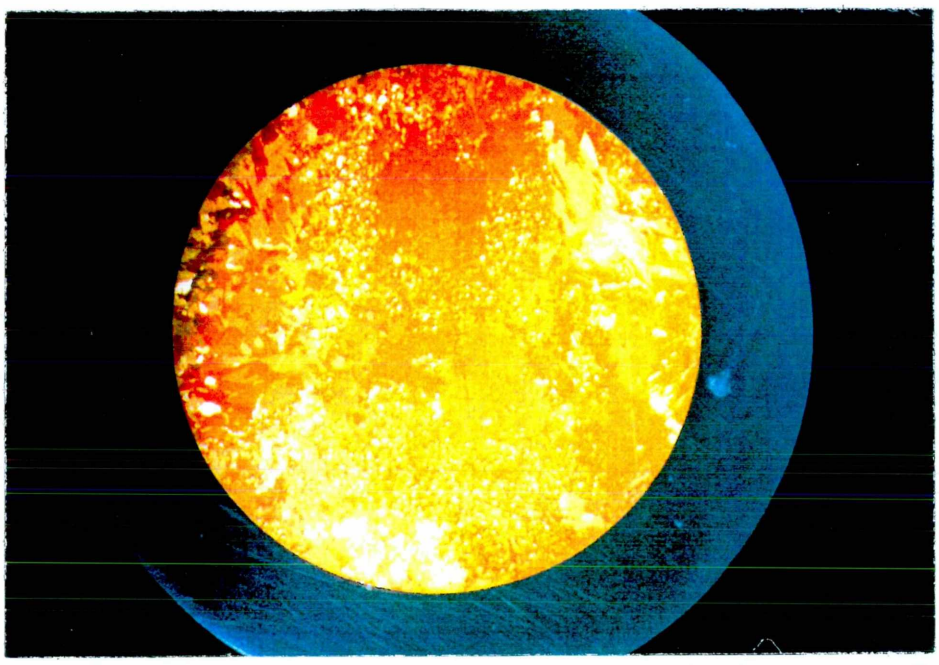
Table 7.3 shows that the gold dissolution rates obtained by adding iodide/iodine to the ferric thiocyanate lixiviant are as high as those obtained with similar concentrations of thiourea/formamidine disulphide [177] and also very close to those obtained with similar concentrations of the iodide/iodine lixiviant. Moreover, the mixed thiocyanate-iodine system has the advantage over the iodide-iodine system in terms of permitting a considerable diminution of the I_2 concentration in solution, which minimizes losses of I_2 by vaporization. In comparison with thiourea, thiocyanate has the advantage of being more stable towards oxidation. The overpotentials required for the oxidation of thiocyanate (see Chapter 3) are much higher than those for the

oxidation of thiourea [203]. The stability of thiocyanate was demonstrated by the volumetric analysis of the leach solutions from the experiments reported in this chapter, which indicated overall consumptions lower than 4%.

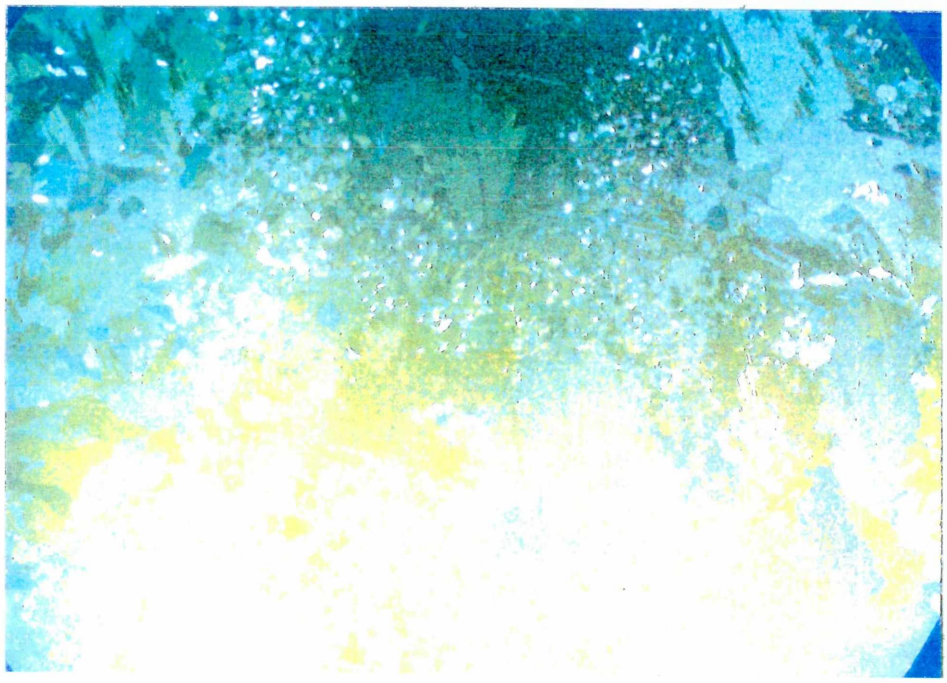
The intensity of leaching obtained with the iodide addition to the ferric thiocyanate lixiviant could even be noticed visually, as shown in **Figure 7.10**. Marked etching of the gold disc surface was observed in all the experiments with the mixed thiocyanate-iodine system. A picture of the gold disc after the polishing treatment is shown in **Figure 6.26**, Chapter 6, for comparison.

For practical hydrometallurgical systems it would be advisable to make additions of iodine (instead of iodide alone) and to maintain a percentage of the dissolved iron as Fe^{2+}, in order to slow down the overall autoreduction process. The optimum concentrations and percentages have to be found experimentally in each case.

Future experimental work in the mixed thiocyanate-iodine system should also be done with the X_3^- (X = I and/or SCN) species being generated by an oxidant other than Fe^{3+}, iodate being apparently the most adequate. This system, if successful, would probably extend the pH range at which the leaching could be done. The pH constraint in the present work was due to the necessity of avoiding iron precipitation from solution (see Appendix 4). Since the iodide/iodine system shows basically the same performance over the pH range from 2.7 to 10 [189-191], the leaching with the thiocyanate-iodine system over a wider pH range should therefore be investigated. Other alternatives that could be tried include the electrochemical reoxidation of iodide to iodine already mentioned in the literature [197], and of Fe^{2+} to Fe^{3+}.



(a)



(b)

Figure 7.10 - Gold rotating disc after leaching for 150 minutes at 25°C and pH 1.5 with 0.10 mol/dm^3 SCN^-, 0.0055 mol/dm^3 I^- and 0.055 mol/dm^3 Fe^{3+} (initial). Rotation speed: 75.4 rad/s (700 rpm). N_2 atmosphere. Magnifications: **(a)** 6 x and **(b)** 50 x.

The mechanistic views put forward in Chapter 6, Section 6.12, can be enlarged in order to include the mixed iodine-thiocyanate species. The intention here in not to postulate an accurate mechanism of dissolution of gold by mixed iodine-thiocyanate solutions, but only to describe several types of reaction steps which are likely to be involved in the actual dissolution process. This limited task is possible because of the complete analogy between the mechanism of oxidation of thiocyanate described in Section 6.12 and that of oxidation of iodide reported in the literature [113-119].

Thus, at lower potentials the aurous complex AuX_2^- would be formed (X = I and/or SCN) according to:

I. $$Au_{(s)} + X^- = Au(X^-)_{(ads)} \quad (7.8)$$

$$Au(X^-)_{(ads)} = Au(X)_{(ads)} + e \quad (7.9)$$

$$Au(X)_{(ads)} \longrightarrow AuX_{(ads)} \quad (7.10)$$

$$AuX_{(ads)} + X^- \longrightarrow AuX_2^- \quad (7.11)$$

The aurous complex could be produced by the direct attack of X_3^- on the metal surface without participation of the intermediate adsorbed compound $AuX_{(ads)}$. This would also produce the adsorbed free radical $X^{\cdot}$, as follows:

II. $$Au_{(s)} + X_3^- \longrightarrow AuX_2^- + X^{\cdot} \quad (712)$$

$$Au_{(s)} + X^{\cdot} \longrightarrow Au(X)_{(ads)} \quad (7.13)$$

The formation of the auric complex AuX_4^- would take place at higher potentials, as follows:

III. $$AuX_{(ads)} + X_3^- \longrightarrow AuX_4^- \quad (7.14)$$

In presence of iron(III), reaction 7.8 might be replaced by the adsorption of an iron(III)-thiocyanate complex, which is followed by its autoreduction yielding the adsorbed free radical $SCN^{\bullet}$. The formation of adsorbed free radicals, i.e. $Au(X)_{(ads)}$, could also result from the participation of X_2 species:

$$2Au_{(s)} + X_2 \longrightarrow 2Au(X)_{(ads)} \qquad (7.15)$$

The formation of $Au(X)_{(ads)}$ can lead either to the formation of $AuX_{(ads)}$ or, through further reaction steps, to the formation of X_2 and X_3^-.

This mechanistic view is rather generalized and there seems to be no sharp transition between stages I, II and III above. These stages may be ordered according to the increasing mixed potentials in the system, on which will depend the partial contributions of the aurous and auric complexes to the gold dissolution, as well as the fraction of the overall X which will be present in solution as either of the oxidized species X_2 or X_3^-. In all the steps above, X = SCN and/or I. Thus, X_3^- refers to the series I_3^-, I_2SCN^-, $I(SCN)_2^-$ and $(SCN)_3^-$, while X_2 refers to the series I_2, ISCN and $(SCN)_2$. The existence of all these species, under conditions similar to those existing in the gold rotating disc runs reported here, is well demonstrated in the specialized chemical literature quoted throughout this thesis. A less emphatic statement can be made about the mixed mononuclear complexes AuX_2^- and AuX_4^-. The inclusion of such species, for whose existence no documented evidence was found, is the only (although very feasible) assumption concerning the existence of chemical species made in this entire work, with the intention of generalizing the explanation of the experimental results. What is implied here is the existence of at least two series of mixed complexes. For the aurous complexes, AuI_2^-, $AuISCN^-$ and $Au(SCN)_2^-$, and for the auric complexes, AuI_4^-, AuI_3SCN^-, $AuI_2(SCN)_2^-$, $AuI(SCN)_3^-$ and $Au(SCN)_4^-$ The extremes of both series,

i.e. the aurous and auric complexes of iodide only or thiocyanate only are obviously well documented in the literature. On the other hand, iron(III)-iodide and mixed iron(III)-iodide-thiocyanate complexes have not been considered because of the scarcity of information about their existence and properties. It is obvious that, in the rotating disc experiments starting with SCN^- and I^- (without iodine addition), the primary oxidizing action was due to iron(III), whose initial concentration was 0.055 mol/dm^3 in all cases reported in this and in the previous section. The reduction of iron(III) to iron(II) was responsible for the production of the X_2 and X_3^- species mentioned above. However, the actual autoreduction mechanism can not be precisely described without a better knowledge about the existence and properties of iron(III)-iodide and iron(III)-iodide-thiocyanate complexes.

An interesting insight arising from the identification of species of the type X_3^- is that they may provide a criterion for the choice of a suitable oxidizing agent, apart from Fe^{3+}, to be used in the thiocyanate system. Oxidizing agents providing halides upon reduction seem to be adequate, depending on the overall compatibilities. Iodate, for instance, was one of the oxidants tried by Long and Skoog [200], who suggested that the ensuing reaction would be:

$$6SCN^- + IO_3^- + 2I^- + 6H^+ \longrightarrow 3I(SCN)_2^- + 3H_2O \qquad (7.16)$$

On the other hand, the action of iodate on a thiocyanate solution in the absence of iodide would be [200]:

$$IO_3^- + 6SCN^- + 6H^+ \longrightarrow I(SCN)_2^- + 2(SCN)_2 + 3H_2O \qquad (7.17)$$

This reaction was observed to be very fast. If, then, an excess of iodide ions was immediately added, the intensity of the absorption peak at 303 nm due to $I(SCN)_2^-$ would increase by a factor of three, suggesting the combination of the iodide ions with

the thiocyanogen formed initially, yielding more $I(SCN)_2^-$ as described by reaction 7.4. A lower peak intensity would be obtained if the iodide ions were added several minutes after reaction 7.17 having occurred, for then part of the $(SCN)_2$ generated would have been decomposed through hydrolysis [200].

CHAPTER 8: CONCLUSIONS. SUGGESTIONS FOR FURTHER WORK

8.1. Conclusions

The present work has led to the definition of several fundamental aspects of the thiocyanate leaching of gold, which can be summarized as follows:

(1) Thiocyanate is a viable and interesting lixiviant for gold. The high gold dissolution rates and the very low reagent consumptions observed in this work place thiocyanate as a strong competitor, if not a definitely advantageous option, with respect to thiourea, as an alternative system to cyanidation. Should iron(III) be used as the oxidizing agent, as was the case throughout this work, leaching should be performed below pH 3.0, above which iron(III) precipitation from solution starts to occur. Experimentation was carried out with a gold rotating disc arrangement under the following conditions:

Thiocyanate concentration (mol/dm^3):	0.05 to 0.50
Iron(III) concentration (mol/dm^3):	0.01 to 0.10
Temperature (°C):	25 to 85
Disc Rotating Speed (rd/s):	19-157

Thus, with 0.10 mol/dm^3 SCN^- and 0.055 mol/dm^3 Fe^{3+}, the initial gold dissolution rate at 85°C was 1.80×10^{-8} mol/cm^2 s. This rate decreased to 1.13×10^{-8} mol/cm^2 s when the thiocyanate concentration was reduced to 0.05 mol/dm^3.

(2) High rates of gold dissolution were obtained at 25°C by adding small amounts of iodide ions or iodine to the iron(III)-

thiocyanate lixiviant. For instance, with 0.10 mol/dm^3 SCN^-, 0.01 mol/dm^3 I^- and 0.055 mol/dm^3 Fe^{3+}, the initial dissolution rate at 25°C was 1.07×10^{-8} mol/cm^2 s. This rate decreased to 0.62×10^{-8} mol/cm^2 s when the SCN^- and I^- concentrations were reduced to 0.05 mol/dm^3 and 0.0055 mol/dm^3, respectively. The initial gold dissolution rate obtained at 25°C with 0.10 mol/dm^3 thiourea and 0.01 mol/dm^3 formamidine disulphide was 1×10^{-8} mol/cm^2 s. The fact that it is considerably more stable than thiourea towards oxidation is an important point in favour of thiocyanate. Furthermore, the rates obtained with 0.05 mol/dm^3 SCN^-, as above reported, are higher than those found in cyanidation practice, which are around 10^{-9} mol/cm^2 s.

(3) The experimental work was preceded by a thermochemical investigation on the thiocyanate systems relevant to the leaching of gold (and silver) ores. Gold was found to dissolve mainly as the auric, $Au(SCN)_4^-$, and the aurous, $Au(SCN)_2^-$, complexes. The minimum redox potentials required for gold dissolution to occur were estimated to be around 550-600 mV (vs. SHE), depending on the activity of free thiocyanate ion in solution. Thermodynamically, gold may dissolve as one of the thiocyanate complexes over a wide pH range, from 1 to 11, approximately. The pH constraint adopted in the present work was due to the use of Fe^{3+} as oxidizing agent. The gold-thiocyanate-water system was found to be metastable, the metal being dissolved at potentials at which the oxidation of thiocyanate was also expected to take place.

(4) The considerable stability shown by thiocyanate towards oxidation was not directly indicated by the thermodynamic calculations presented in Chapter 2, which only considered relatively stable oxidation products. However, it was found experimentally that a high overpotential was required for the

thiocyanate oxidation to take place, which clearly suggested that some intermediate step controls the overall oxidation process. This led to an extensive investigation into the intermediate species of thiocyanate oxidation. This turned out to be a rather complex subject, several intermediate species having been identified and described on the grounds of previous contributions to the chemistry and electrochemistry of thiocyanate, both in aqueous and organic media. The main oxidation intermediates were found to be thiocyanogen, $(SCN)_2$, and the trithiocyanate ion, $(SCN)_3^-$, which are responsible for the overpotentials observed in the oxidation of thiocyanate. These species, particularly $(SCN)_3^-$, proved to be more active than SCN^- itself in the process of gold dissolution. This fact became increasingly important as the results of the rotating disc runs were compared and analysed. A correlation was observed to exist between the autoreduction of the iron(III)-thiocyanate complexes in solution, which produces $(SCN)_2$ and $(SCN)_3^-$, and the rate of gold dissolution. Therefore, thiocyanogen and trithiocyanate ion were found to play an important role in the mechanism of gold dissolution.

(5) Due to its complexity, a detailed treatment, both theoretical and experimental, had to be given separately to the iron(III)-thiocyanate system. This part of the work, which is reported in Chapter 4, was important for two main reasons. First, because of the production, through the autoreduction of the iron(III)-thiocyanate complexes, of the species $(SCN)_2$ and $(SCN)_3^-$, which participate in the mechanism of gold dissolution. Second, because there is a direct relation between the Fe^{3+} reduction and the oxidation of SCN^-, which accounts for the reagent consumption during the leaching process. A series of six mononuclear iron(III)-thiocyanate complexes is formed in solution, whereas only one iron(II)-thiocyanate complex is known to exist. The description of this system through

thermodynamic calculations and distribution curves preceded the experimental part of the work. Both the thermodynamic calculations and practical potential measurements showed that the potentials provided by Fe^{3+} would allow the gold dissolution to take place in aqueous thiocyanate solutions. Moreover, as such potentials were higher than those at which thiocyanate would be oxidized, freshly prepared thiocyanate solutions were observed to undergo autoreduction until a certain Fe^{2+}/Fe^{3+} ratio was reached, a correspondence existing between the Fe^{3+} reduction and the SCN^- oxidation.

Several series of experiments were then performed to investigate the autoreduction process in iron(III)-thiocyanate solutions. The oxidation of SCN^- was found to proceed through the formation of $(SCN)_2$ and $(SCN)_3^-$ and their subsequent hydrolysis to more stable oxidation products such as sulphate, cyanide, cyanate or, ultimately, ammonia and carbonate. The hydrolysis of $(SCN)_2$ is faster than that of $(SCN)_3^-$, the latter being stabilized by H^+ in acidic conditions and/or by the interaction with other cations present in solution. The overall thiocyanate oxidation process to sulphate and cyanide or cyanate involves 6 electrons per SCN^- oxidized (or 8, when ammonia and carbonate are the final products). This means that 6 Fe^{3+} are reduced for each SCN^- oxidized. These experiments were extended over 18 days, in order to clarify the long-term behaviour of the iron(III)-thiocyanate solutions, information particularly important for prospective hydrometallurgical applications such as heap leaching and solution mining. Many potential (and pH) measurements were taken and correlated with the progress of the autoreduction process through spectrophotometric determinations of the reduction of Fe^{3+} to Fe^{2+}. Thiocyanate was analysed throughout the experiments, and the consumption observed after 18 days at 25°C was below 4% in most of the experiments.

(6) The mechanism of gold dissolution by iron(III)-thiocyanate solutions was discussed in detail. The most noticeable characteristic of the gold rotating disc experiments was the correlation between the rates of gold dissolution and the rates of autoreduction of the iron(III)-thiocyanate complexes. This correlation pointed to the participation of the intermediate species of thiocyanate oxidation, $(SCN)_2$ and $(SCN)_3^-$, in the mechanism of gold dissolution. In a typical rotating disc experiment, the auric complex, $Au(SCN)_4^-$, was considered to be formed at the potentials obtained when Fe^{3+} was added to an acidified thiocyanate solution. Under those initial conditions the rate of autoreduction was higher, providing larger yields of $(SCN)_3^-$, which is both an oxidant and, upon reduction, complexant for gold. The mechanism of gold dissolution was considered to proceed through the formation of an intermediate surface compound, $AuSCN_{(ads)}$, which is not stable in the presence of $(SCN)_3^-$, being removed into solution as the auric thiocyanate complex, $Au(SCN)_4^-$. The autoreduction rate decreased with time, due to the accumulation of Fe^{2+} in the system, causing corresponding decreases in the production of $(SCN)_3^-$ and in the mixed potential readings. The effect of this simultaneous and gradual decrease in the potential readings and $(SCN)_3^-$ yield was a transition from the predominant formation of $Au(SCN)_4^-$ to that of the aurous complex, $Au(SCN)_2^-$, which was accompaned by a decrease in the dissolution rate and a gradual stabilization of a thin layer of the adsorbed surface compound, $AuSCN_{(ads)}$, which was considered responsible for the passivating effect on the gold surface observed during the experiments (Section 6.7). At lower potentials, $Au(SCN)_2^-$ was formed by the action of non-oxidized SCN^- upon $AuSCN_{(ads)}$, and this part of the proposed mechanism corresponded to the lowest dissolution rates observed. The decrease in the initial rate of gold dissolution observed in experiments with iron(III)-thiocyanate solutions is in many respects similar to that observed in experiments with the iron(III)-thiourea system. In

fact, thiourea is even more unstable at the relatively high initial potentials promoted by Fe^{3+} additions, resulting in an analogous autoreduction process, with corresponding decreases in the gold dissolution rates.

(7) The gold dissolution process was greatly accelerated by raising the temperature from 25 to 85°C. Accordingly, the autoreduction of the iron(III)-thiocyanate complexes was found to be much faster at those higher temperatures and to proceed to a much greater extent, sometimes to almost complete Fe^{3+} reduction. This caused the dissolution of gold to proceed at high rates over longer times, the decrease in the initial dissolution rate being less pronounced as long as there was still Fe^{3+} present in the system. The dissolution rates at 85°C were among the highest obtained in this work, as quoted in the Item (1) of these conclusions.

(8) Experiments were conducted at constant potential in an attempt to maintain the high initial dissolution rates. In these experiments, the Fe^{2+} produced by the autoreduction process was reoxidized to Fe^{3+} with hydrogen peroxide. Several constant potentials were tried, corresponding to several percentages of Fe^{2+} over the total iron concentration in solution. Overall, the results were rather unsatisfactory .The dissolution rates obtained were lower than those expected by comparison with experiments with spontaneous autoreduction. Moreover, a decrease in the dissolution rates was still observed, despite the potentials being maintained constant by hydrogen peroxide additions. This behaviour was attributed to the modification of the overall chemistry of the system by the presence of H_2O_2, whose action takes place through the free radicals $OH^{\cdot}$ and $HO_2^{\cdot}$. Unfortunately, these highly reactive species not only oxidize Fe^{2+} but also interact with the active

intermediate thiocyanate species $(SCN)_2$ and $(SCN)_3^-$, which would otherwise participate in the mechanism of gold dissolution. Such interactions result in species such as $OSCN^-$, HOSCN, O_2SCN^-, HO_2SCN, etc. These species are considered to be less active in the gold dissolution mechanism than $(SCN)_2$ and $(SCN)_3^-$, hence the lowering of the gold dissolution rates in the presence of hydrogen peroxide. An additional drawback of H_2O_2 is the readiness with which it oxidizes thiocyanate. The unsuitability of H_2O_2 as a means of achieving high average gold dissolution rates at room temperature motivated an investigation into the effects of the addition of small amounts of iodide ions or iodine to the iron(III)-thiocyanate lixiviant.

(9) Experiments with addition of small amounts of I^- and/or I_2 revealed a synergistic effect of the thiocyanate-iodine mixture on the dissolution of gold. Thus, the dissolution rates obtained when these two chemicals were used together were substantially higher than those obtained when either iron(III)-thiocyanate or iron(III)-iodide were used separately. Investigation into the causes of this synergistic effect led to the proposition of the participation of mixed iodine-thiocyanate species, particularly I_2SCN^- and $I(SCN)_2^-$, in the mechanism of gold dissolution. A mechanistic view was then postulated in which species of the type X_3^- (where X = SCN, I) play an important role, as they not only oxidize but also provide the ligands to complex gold. The mixed species were visualized as forming the substitution series I_3^-, I_2SCN^-, $I(SCN)_2^-$ and $(SCN)_3^-$. Both I_3^- and the mixed iodine-thiocyanate species are stable at lower potentials than those of $(SCN)_2$ and $(SCN)_3^-$, which extends downwards the potential range for efficient leaching. Moreover, one of the most remarkable characteristics of these mixed species is their greater stability towards hydrolysis and decomposition, as compared to $(SCN)_2$. The

formation of $I(SCN)_2^-$ means a considerable stabilization of the thiocyanogen produced by the autoreduction of ferric thiocyanate complexes. The decrease in the potential readings observed with iron(III)-thiocyanate only, which was due to the simultaneous Fe^{3+} reduction and hydrolytic decomposition of the oxidized thiocyanate species produced, particularly of $(SCN)_2$, is much less pronounced in the presence of iodide/iodine. In these latter case, the oxidized species produced by the Fe^{3+} reduction contribute to several reversible equilibria between X_3^- and X_2 and X^- species (where X = SCN, I), which maintain the mixed potential of the system. The consequence of this behaviour is a substantial accumulation of species which are both oxidants and complexants for gold, hence the synergistic effect and the considerably higher gold dissolution rates. Hence, the use of iron(III)-thiocyanate with addition of iodide and/or iodine resulted in gold dissolution rates at 25°C as high as those obtainable with similar concentrations of thiourea, with the advantage of the higher stability of thiocyanate towards oxidation.

(10) The two main reactions which take place under the oxidizing action of Fe^{3+} on the mixed thiocyanate-iodide lixiviant are:

$$I^- + 2SCN^- = I(SCN)_2^- + 2e \qquad (8.1)$$

$$2I^- + SCN^- = I_2SCN^- + 2e \qquad (8.2)$$

These species, plus those resulting from the oxidation of I^- and SCN^- by Fe^{3+}, contribute to the following equilibria in solution:

$$I_{2(aq)} + I^- = I_3^- \qquad \log K = 2.86 \qquad (8.3)$$

$$I_{2(aq)} + SCN^- = I_2SCN^- \qquad \log K = 1.93 \qquad (8.4)$$

$$(SCN)_{2(aq)} + I^- = I(SCN)_2^- \qquad \log K = 4.10 \qquad (8.5)$$

$$(SCN)_{2(aq)} + SCN^- = (SCN)_3^- \qquad \log K = 3.04 \qquad (8.6)$$

Reactions 8.1 through 8.6 were considered to be the most relevant in terms of defining the composition of the mixed thiocyanate-iodide-iodine lixiviant. They constitute the framework for the optimization of leaching conditions such as mixed potential (i.e. oxidant addition), thiocyanate/iodide/iodine molar ratio, concentrations of these lixiviants, etc. It is evident from the equilibria above that thiocyanate works as a "carrier" for halogenic species in solution, which results in a considerable increase in the concentrations of X_3^- and X_2 (X = SCN, I) species in solution. The overall halogenic character of these (mixed) species is not impaired (in their reactivity towards gold) by the presence of thiocyanate in their structures, due the the pseudo-halide character of thiocyanate. This produces lixiviants with halogenic character, which can be used in relatively high concentrations, but which are mainly composed of thiocyanate. In fact, the thiocyanate/iodide molar ratios used in the present work varied from about 10 to 20, with gold dissolution rates of the same magnitude as those obtained with similar overall concentrations of iodide/iodine.

8.2. Suggestions for Further Work

The points stated above summarize the main contributions of this work to the knowledge of the thiocyanate leaching of gold. As mentioned in the Introduction, this is the first fundamental work on the leaching of gold by thiocyanate, and there is plenty of room for further research of both fundamental aspects and practical applications (with ores). Some of the possible directions for future work can be summarized as follows:

(a) Continuation of the work already done on the anodic behaviour of thiocyanate on vitreous carbon, platinum and gold electrodes. The combination of electrochemical and spectrophotometric techniques could lead to a more accurate determination of the relation between gold dissolution and thiocyanate oxidation. A relevant part of such work would be the investigation of the hydrolysis of the intermediate species $(SCN)_3^-$ and $(SCN)_2$. The kinetic data currently available on the hydrolysis of these species are scarce.

(b) A more detailed investigation of the mixed thiocyanate-iodine system is one of the immediate directions to be explored. The effectiveness of this system in dissolving gold and a first description of its chemistry are found in Chapter 7, but several questions remain to be answered. Some points of interest are: the stability of the mixed species I_2SCN^- and $I(SCN)_2^-$ over longer periods of time (several hours or days); the production of these species by other oxidizing agents, particularly iodate; the leaching behaviour of the mixed system as a function of potential and pH; the optimization of the overall thiocyanate/iodide/iodine ratio and concentrations for efficient leaching; and so on. A specific point of research concerns the mixed complexes of gold with thiocyanate and iodide. The aurous and auric complexes of thiocyanate have stability constants which are close to those of the homologous complexes with iodide, as reported in Appendix 3. This is a further indication of the feasibility of the existence of such mixed complexes, whose existence should be clarified on an experimental basis, as part of the overall investigation of this mixed leaching system.

(c) Iron(III) proved to be an efficient oxidizing agent, but it is constrained to pH values lower than 2.5 (see Appendix 4).

Furthermore, a second oxidizing agent is required due to the autoreduction processes in the systems discussed here. Hydrogen peroxide proved inadequate due to the action of the free peroxide radicals on the active thiocyanate intermediate species. Oxidants which would contribute to the chemistry of reactions 8.1 through 8.6 seem to be the immediate options to be tried. One such oxidant is iodate, which acts on a thiocyanate/iodide mixture as follows:

$$6SCN^- + IO_3^- + 2I^- + 6H^+ \longrightarrow 3I(SCN)_2^- + 3H_2O \qquad (8.7)$$

The action of iodate on a plain thiocyanate solution would be:

$$IO_3^- + 6SCN^- + 6H^+ \longrightarrow I(SCN)_2^- + 2(SCN)_2 + 3H_2O \qquad (8.8)$$

The extra thiocyanogen produced this way could be stabilized by iodide additions. The reactions above also indicate the possibility of using the mixed thiocyanate-iodine system without iron(III), which could probably extend the pH range for leaching. The use of halide-yielding oxidants seems to be a promising line of investigation connected with the overall thiocyanate-halide (or thiocyanogen-halogen) chemistry, as the $(SCN)_2$ formed by these oxidants may be readily stabilized by the halide ions resulting from their reduction, as in reaction 8.8.

(d) The electrochemical regeneration of the lixiviant, i.e. the reoxidation of iodide to iodine and of iron(II) to iron(III), should be considered. Peroxides tend to react with the active thiocyanate-halide intermediate species, lowering the gold dissolution rates. On the other hand, although oxidizing agents such as IO_3^- or BrO_3^- have advantages, their continual additions cause an undesirable build-up of halide species in the system. The electrochemical regeneration of the lixiviant could solve

both problems.

(e) It seems worthy investigating the relative stabilization of thiocyanogen or other thiocyanate species not only by I^- but also by Cl^- and Br^- (or the complexation of their halogens by thiocyanate). Mixed compounds of thiocyanate with these two halides are reported in the literature and have been studied to some extent [28, 65-67]. Halide additions could then be considered in different contexts. The thiocyanate-halide (or thiocyanogen-halogen) chemistry is a rather complex issue, and experimentation is required to prove its effectiveness under leaching conditions. Thiocyanate, however, is a mild chemical, highly soluble, easy to handle, non-corrosive and stable at potentials up to 550-600 mV. The thiocyanate-halide chemistry offers the prospect of lixiviants combining these thiocyanate characteristics with those of the halide/halogens as incorporated by the mixed thiocyanate-halide species, with a considerable attenuation of several of the inconveniences of the pure halide/halogen systems (corrosion, release to the gas phase, etc.), particularly when used in higher concentrations. Equilibria such as those indicated by reactions 8.3 to 8.6, considered together, indicate that considerable amounts of halogenic species can be held in solution as thiocyanate complexes without losing their reactivity, due to the pseudo-halide character of thiocyanate. On the other hand, halides may lend more stability to the intermediate thiocyanate species. As mentioned above, thiocyanate behaves (in the mixed thiocyanate-iodine system) both as a reactant and as a sort of "carrier" for the halogenic species in solution. Therefore, the behaviour of Cl and Br on this respect should be investigated.

(f) Another direction of research would be towards higher temperatures, with additions of iodide/iodine. It seems feasible, by using higher temperatures, to attain even faster gold dissolution rates and/or to reduce the concentrations of

the lixiviants below the minimum levels used in this work, while still maintaining satisfactory leaching rates. The mixed species I_2SCN^- and $I(SCN)_2^-$ are certainly much less stable at higher temperatures, but the overall result of the competition between the reactions involved in their decomposition and their effective participation in the gold dissolution process can only be established experimentally.

ACKNOWLEDGEMENTS

I wish to thank Dr. A. J. Monhemius for his supervision during the course of this investigation.

I am particularly grateful to Prof. Alfred R. Burkin for his many discussions, help and encouragement.

Especial thanks are due to Mr. John E. A. Burgess, whose constant technical advice and cooperation were invaluable aids for me to accomplish the experimental part of this work.

I wish to thank all the past and present members of the hydrometallurgy research group for their help, support and companionship at different stages of this investigation, which lasted almost five years. They listened patiently to my complaints during awkward times, tolerated many of my shortcomings, helped with my work, encouraged and criticized me, and gave me a fine birthday party which I hold as a lovely memory.

Thanks are also due to many other members of staff and colleagues from other departments, among which I wish to mention Mr. Vick Harris, Mr. Gordon Hicks, Mr. John Sullivan, Mr. Mike Haddon, Mr. Trevor Allen and Dr. Christine Butenuth, for their invaluable help in several aspects of this work.

Finally, I am most grateful to the Brazilian Research Council (CNPq) for the award of a scholarship without which it would not have been possible for me to undertake this course of studies. Thanks are also due to the Catholic University of Rio de Janeiro (PUC-RJ) and to the Peróxidos do Brasil Ltd., whose financial support I fully acknowledge.

APPENDIX 1: THERMODYNAMIC DATA AT 25°C USED IN THE PRESENT WORK

Species	State	ΔG° (kJ/mol)	Reference	Note
H_2	g	0	12, 13	
O_2	g	0	12, 13	
H_2O	l	-237.178	12, 13	1
H^+	aq	0	12, 13	
OH^-	aq	-157.293	12, 13	
H_2O_2	aq	-134.10	12, 13	
HO_2^-	aq	-67.4	12, 13	
H_2CO_3	aq	-623.42	12, 13	
HCO_3^-	aq	-587.06	12	
CO_3^{2-}	aq	-527.90	12, 13	
NH_3	aq	-26.6	12, 13	
NH_4^+	aq	-79.37	12, 13	
HCN	aq	112	12	
CN^-	aq	166	12	
HCNO	aq	-121	12	
CNO^-	aq	-98.7	12	
HSCN	aq	87.54	-	2
SCN^-	aq	92.68	12, 13	
$(SCN)_2$	-	334.0	-	3
$(SCN)_3^-$	aq	409.3	-	4
HOSCN	aq	66	-	5
Cl^-	aq	-131.0563	12	
HSO_4^-	aq	-756.01	12, 13	
SO_4^{2-}	aq	-744.63	12, 13	
Au	s	0	12, 14	
Au^+	aq	176	12	
Au^{3+}	aq	440	12	
AuO_3^{3-}	aq	-51.9	12, 14	
$HAuO_3^{2-}$	aq	-142	12, 14	
$H_2AuO_3^-$	aq	-218	12, 14	

Species	State	ΔG° (kJ/mol)	Reference	Note
$Au(OH)_3$	s	-317.0	12, 14	
$Au(OH)_3$	aq	-283.5	12, 14	
AuO_2	s	200.8	17	
$Au_2O_{3(hydr.)}$	s	131.7	17	
Au_2O_3 (anhydr.)	s	163.2	17	
AuSCN	aq	182	-	6
$Au(SCN)_2^-$	aq	252	12, 14	
$Au(SCN)_4^-$	aq	561.5	12, 14	
$Au(SCN)_5^{2-}$	aq	654.4	14	
$Au(SCN)_6^{3-}$	aq	746.8	14	
$Au(CN)_2^-$	aq	286	12, 14	
$AuCl_2^-$	aq	-151.0	12	
$AuCl_4^-$	aq	-234.6	12	
Ag	aq	37.26	12	
Ag	s	0	12, 14	
Ag^+	aq	77.16	12, 14	
Ag^{2+}	aq	269.16	12, 14	
AgO^+	aq	225.63	12	
AgO^-	aq	-22.98	12	
AgOH	aq	-80.21	12, 14	
$Ag(OH)_2^-$	aq	-260.37	12, 14	
Ag_2O	s	-11.22	12, 14	
Ag_2O_2	s	27.63	12, 14	
AgO	s	14.65	12	
Ag_2O_3	s	121.39	12, 14	
AgO_2	s	-10.99	12	
AgSCN	aq	142.7	14	
AgSCN	s	101.43	12, 14	
$Ag(SCN)_2^-$	aq	215.16	12, 14	
$Ag(SCN)_3^{2-}$	aq	300.97	12, 14	
$Ag(SCN)_4^{3-}$	aq	392.23	12, 14	
AgCN	aq	249.49	12, 14	
AgCN	s	156.97	12, 14	
$Ag(CN)_2^-$	aq	305.58	12, 14	
$Ag(CN)_3^{2-}$	aq	466.61	12	

Species	State	ΔG° (kJ/mol)	Reference	Note
AgCl	aq	-54.16	12, 14	
AgCl	s	-109.86	12, 14	
$AgCl_2^-$	aq	-215.58	12, 14	
$AgCl_3^{2-}$	aq	-345.97	12	
$AgCl_4^{3-}$	aq	-478.46	12	
Fe^{2+}	aq	-78.87	12, 14	
Fe^{3+}	aq	-4.6	12, 14	
$FeOH^{2+}$	aq	-229.41	12, 14	
$Fe(OH)_2^+$	aq	-438.1	12, 14	
$Fe(OH)_3^-$	aq	-615.0	12, 14	

(1) Most of the above ΔG° values given in [12] have been taken from [13] or [14] and for this reason both sources are mentioned. Whenever there is a slight discrepancy, the figures quoted are those given in [12].

(2) Calculated from the above ΔG° for thiocyanate ion and from $pK_{HSCN} = 0.9$ [16, 31, 32].

(3) Two inconsistent values, E° = 0.77 and 0.57 V are quoted on page 207 of [59] for the anodic reduction of thiocyanogen in aqueous solution. Calculations using these values and the above ΔG° for thiocyanate ion yield ΔG° = 334 and 295 kJ/mol, respectively, for aqueous thiocyanogen.

(4) Calculated from E° = 0.68 V for the couple $(SCN)_3^-/SCN^-$ estimated by Itabashi [91] and from the ΔG° quoted above for the thiocyanate ion.

(5) Derived from the equilibrium constant for the hydrolytic reaction:

$$(SCN)_2 + H_2O = H^+ + SCN^- + HOSCN \qquad K = 6 \times 10^{-13}$$

quoted on page 39 of [28] and from the above ΔG^o values for the remaining species.

(6) Derived from the stability constant $\beta_1 = 1.87 \times 10^{15}$ at 25°C and I = 3 ($NaClO_4$) given in [20] and from the $\Delta G°$ values for Au^+ and SCN^-. Attempts to correct this constant to zero ionic strength and to use the corrected value for calculating $\Delta G°$ for AuSCN resulted in figures within 1% of that derived from the uncorrected β_1, which was then adopted.

APPENDIX 2: EQUILIBRIA APPEARING ON THE Eh-pH DIAGRAMS

Note: The numbers of the following reactions correspond to those on the respective lines of the Eh-pH diagrams.

(1) $O_2\,(g) + 4\,H^+ + 4\,e^- = 2\,H_2O\,(l)$

$$E = 1.229 - 0.0591\ pH + 0.0148 \log P_{O_2}$$

(2) $2\,H^+ + 2\,e^- = H_2\,(g)$

$$E = -\,0.0591\ pH - 0.0295 \log P_{H_2}$$

(3) $HSO_4^- = SO_4^{2-} + H^+$

$$\log \frac{\{SO_4^{2-}\}}{\{HSO_4^-\}} = -1.99 + pH$$

(4) $H_2CO_3\,(aq) = HCO_3^- + H^+$

$$\log \frac{\{HCO_3^-\}}{\{H_2CO_3\}} = -\,6.37 + pH$$

(5) $NH_4^+ = NH_3\,(aq) + H^+$

$$\log \frac{\{NH_3\}}{\{NH_4^+\}} = -\,9.24 + pH$$

(6) $HCO_3^- = CO_3^{2-} + H^+$

$$\log \frac{\{CO_3^{2-}\}}{\{HCO_3^-\}} = -\,10.36 + pH$$

(7) $HSCN\,(aq) = SCN^- + H^+$

$$\log \frac{\{SCN^-\}}{\{HSCN\}} = -\,0.90 + pH$$

(8) $NH_4^+ + H_2CO_3\,(aq) + HSO_4^- + 8\,H^+ + 8\,e^- = HSCN\,(aq) + 7\,H_2O$

$$E = 0.1476 - 0.0591\ pH - 0.0074 \log \frac{\{HSCN\}}{\{NH_4^+\}\{H_2CO_3\}\{HSO_4^-\}}$$

(9) $NH_4^+ + H_2CO_3\,(aq) + HSO_4^- + 7\,H^+ + 8\,e^- = SCN^- + 7\,H_2O$

$$E = 0.1409 - 0.0517\ pH - 0.0074 \log \frac{\{SCN^-\}}{\{NH_4^+\}\{H_2CO_3\}\{HSO_4^-\}}$$

(10) $NH_4^+ + H_2CO_3\,(aq) + SO_4^{2-} + 8\,H^+ + 8\,e^- = SCN^- + 7\,H_2O$

$$E = 0.1557 - 0.0591\ pH - 0.0074 \log \frac{\{SCN^-\}}{\{NH_4^+\}\{H_2CO_3\}\{SO_4^{2-}\}}$$

(11) $NH_4^+ + HCO_3^- + SO_4^{2-} + 9\,H^+ + 8\,e^- = SCN^- + 7\,H_2O$

$$E = 0.2028 - 0.0665\ pH - 0.0074 \log \frac{\{SCN^-\}}{\{NH_4^+\}\{HCO_3^-\}\{SO_4^{2-}\}}$$

(12) $NH_3\,(aq) + HCO_3^- + SO_4^{2-} + 10\,H^+ + 8\,e^- = SCN^- + 7\,H_2O$

$$E = 0.2711 - 0.0739\ pH - 0.0074 \log \frac{\{SCN^-\}}{\{NH_3\}\{HCO_3^-\}\{SO_4^{2-}\}}$$

(13) $NH_3(aq) + CO_3^{2-} + 11\,H^+ + 8\,e^- = SCN^- + 7\,H_2O$

$$E = 0.3478 - 0.0813\ pH - 0.0074 \log \frac{\{SCN^-\}}{\{NH_3\}\{CO_3^{2-}\}\{SO_4^{2-}\}}$$

(14) $HCNO(aq) = CNO^- + H^+$

$$\log \frac{\{CNO^-\}}{\{HCNO\}} = -3.91 + pH$$

(15) $HCNO(aq) + HSO_4^- + 9\,H^+ + 8\,e^- = HSCN(aq) + 5\,H_2O$

$$E = 0.2868 - 0.0665\ pH - 0.0074 \log \frac{\{HSCN\}}{\{HCNO\}\{HSO_4^-\}}$$

(16) $HCNO(aq) + HSO_4^- + 8\,H^+ + 8\,e^- = SCN^- + 5\,H_2O$

$$E = 0.2801 - 0.0591\ pH - 0.0074 \log \frac{\{SCN^-\}}{\{HCNO\}\{HSO_4^-\}}$$

(17) $HCNO(aq) + SO_4^{2-} + 9\ H^+ + 8\ e^- = SCN^- + 5\ H_2O$

$$E = 0.2948 - 0.0665\ pH - 0.0074 \log \frac{\{SCN^-\}}{\{HCNO\}\{SO_4^{2-}\}}$$

(18) $CNO^- + SO_4^{2-} + 10\ H^+ + 8\ e^- = SCN^- + 5\ H_2O$

$$E = 0.3237 - 0.0739\ pH - 0.0074 \log \frac{\{SCN^-\}}{\{CNO\}\{SO_4^{2-}\}}$$

(19) $HCN(aq) + HSO_4^- + 7\ H^+ + 6\ e^- = HSCN\ (aq) + 4\ H_2O$

$$E = 0.3751 - 0.0690\ pH - 0.0099 \log \frac{\{HSCN\}}{\{HCN\}\{HSO_4^-\}}$$

(20) $HCN\ (aq) + HSO_4^- + 6\ H^+ + 6\ e^- = SCN^- + 4\ H_2O$

$$E = 0.3662 - 0.0591\ pH - 0.0099 \log \frac{\{SCN^-\}}{\{HCN\}\{HSO_4^-\}}$$

(21) $HCN(aq) + SO_4^{2-} + 7\ H^+ + 6\ e^- = SCN^- + 4\ H_2O$

$$E = 0.3859 - 0.0690\ pH - 0.0099 \log \frac{\{SCN^-\}}{\{HCN\}\{SO_4^{2-}\}}$$

(22) $CN^- + SO_4^{2-} + 8\ H^+ + 6\ e^- = SCN^- + 4\ H_2O$

$$E = 0.4792 - 0.0788\ pH - 0.0099 \log \frac{\{SCN^-\}}{\{CN^-\}\{SO_4^{2-}\}}$$

(23) $(SCN)_2\ (aq) + 2\ H^+ + 2\ e^- = 2\ HSCN\ (aq)$

$$E = 0.7816 - 0.0591\ pH - 0.0295 \log \frac{\{HSCN\}^2}{\{(SCN)_2\}}$$

(24) $(SCN)_2\ (aq) + 2\ e^- = 2\ SCN^-$

$$E = 0.7283 - 0.0295 \log \frac{\{SCN^-\}^2}{\{(SCN)_2\}}$$

(25) $2\ HOSCN\ (aq) + 2\ H^+ + 2\ e^- = (SCN)_2\ (aq) + 2H_2O$

$$E = 1.453 - 0.0591\ pH - 0.0295 \log \frac{\{(SCN)_2\}}{\{HOSCN\}^2}$$

(26) $HOSCN\ (aq) + H^+ + 2e^- = SCN^- + H_2O$

$$E = 1.091 - 0.0295\ pH - 0.0295 \log \frac{\{SCN^-\}}{\{HOSCN\}}$$

(27) $HCN\ (aq) = CN^- + H^+$

$$\log \frac{\{CN^-\}}{\{HCN\}} = -9.46 + pH$$

(28) $H_2CO_3\ (aq) + NH_4^+ + H^+ + 2\ e^- = HCN\ (aq) + 3H_2O$

$$E = -0.5351 - 0.0295\ pH - 0.0295 \log \frac{\{HCN\}}{\{H_2CO_3\}\{NH_4^+\}}$$

(29) $HCO_3^- + NH_4^+ + 2H^+ + 2e^- = HCN\ (aq) + 3\ H_2O$

$$E = -0.3467 - 0.0591\ pH - 0.0295 \log \frac{\{HCN\}}{\{HCO_3^-\}\{NH_4^+\}}$$

(30) $HCO_3^- + NH_3\ (aq) + 3H^+ + 2e^- = HCN\ (aq) + 3\ H_2O$

$$E = -0.0732 - 0.0887\ pH - 0.0295 \log \frac{\{HCN\}}{\{HCO_3^-\}\{NH_3\}}$$

(31) $HCO_3^- + NH_3\ (aq) + 2H^+ + 2e^- = CN^- + 3\ H_2O$

$$E = -0.3530 - 0.0591\ pH - 0.0295 \log \frac{\{CN^-\}}{\{HCO_3^-\}\{NH_3\}}$$

(32) $CO_3^{2-} + NH_3\ (aq) + 3\ H^+\ 2\ e^- = CN^- + 3\ H_2O$

$$E = -0.0465 - 0.0887\ pH - 0.0295 \log \frac{\{CN^-\}}{\{CO_3^{2-}\}\{NH_3\}}$$

(33) $HCNO\ (aq) + 2\ H^+ + 2\ e^- = HCN\ (aq) + H_2O$

$$E = 0.0217 - 0.0591\ pH - 0.0295 \log \frac{\{HCN\}}{\{HCNO\}}$$

(34) $CNO^- + 3\ H^+ + 2\ e^- = HCN\ (aq) + H_2O$

$$E = 0.1372 - 0.0887\ pH - 0.0295 \log \frac{\{HCN\}}{\{CNO\}}$$

(35) $CNO^- + 2\ H^+ + 2\ e^- = CN^- + H_2O$

$$E = -0.1426 - 0.0591\ pH - 0.0295 \log \frac{\{CN^-\}}{\{CNO^-\}}$$

(36) $AuO_2\ (s) + 4\ H^+ + e^- = Au^{3+} + 2\ H_2O$

$E = 2.437 - 0.2364\ pH - 0.0591\ \log \{Au^{3+}\}$

(37) $AuO_2\ (s) + H_2O + H^+ + e^- = Au(OH)_3\ (s)$

$E = 2.908 - 0.0591\ pH$

(38) $AuO_2\ (s) + H_2O + e^- = HAuO_3^{2-} + H^+$

$E = 1.095 + 0.0591\ pH - 0.0591\ \log \{HAuO_3^{2-}\}$

(39) $Au^{3+} + 3\ H_2O = Au(OH)_3\ (s) + 3\ H^+$

$\log \{Au^{3+}\} = - 7.97 - 3\ pH$

(40) $Au(OH)_3\ (s) = HAuO_3^{2-} + 2\ H^+$

$\log \{HAuO_3^{2-}\} = 2\ pH - 30.66$

(41) $Au^{3+} + 3\ e^- = Au\ (s)$

$E = 1.520 + 0.0197\ \log \{Au^{3+}\}$

(42) $Au(OH)_3\ (s) + 3\ H^+ + 3\ e^- = Au\ (s) + 3\ H_2O$

$E = 1.363 - 0.0591\ pH$

(43) $HAuO_3^{2-} + 5\ H^+ + 3\ e^- = Au(s) + 3\ H_2O$

$E = 1.968 - 0.0985\ pH + 0.0197\ \log \{HAuO_3^{2-}\}$

(44) $AuO_2\ (s) + H_2O + e^- = H_2AuO_3^-$

$E = 1.882 - 0.0591\ \log \{H_2AuO_3^-\}$

(45) $Au(OH)_3\ (s) = H_2AuO_3^- + H^+$

$\log \{H_2AuO_3^-\} = - 17.34 + pH$

(46) $H_2AuO_3^- = HAuO_3^{2-} + H^+$

$$\log \frac{\{HAuO_3^{2-}\}}{\{H_2AuO_3^-\}} = - 13.31 + pH$$

(47) $H_2AuO_3^- + 4\ H^+ + 3\ e^- = Au\ (s) + 3\ H_2O$

$E = 1.705 - 0.0788\ pH + 0.0197\ \log \{H_2AuO_3^-\}$

(48) $Au(SCN)_4^- + 2\ HSCN\ (aq) = Au\ (SCN)_6^{3-} + 2\ H^+$

$$\log \frac{\{Au(SCN)_6^{3-}\}}{\{Au(SCN)_4^{2-}\}\ \{HSCN\}^2} = -\ 1.79 + 2\ pH$$

(49) $AuO_2\ (s) + 6\ SCN^- + 4\ H^+ + e^- = Au(SCN)_6^{3-} + 2\ H_2O$

$$E = 5.021 - 0.2364\ pH - 0.0591\ \log \frac{\{Au(SCN)_6^{3-}\}}{\{SCN^-\}^6}$$

(50) $Au(SCN)_6^{3-} + 3\ H_2O = Au(OH)_3\ (s) + 6\ SCN^- + 3\ H^+$

$$\log \frac{\{SCN^-\}^6}{\{Au(SCN)_6^{3-}\}} = -35.71 + 3\ pH$$

(51) $Au(SCN)_4^- + 2\ H^+ + 2\ e^- = Au(SCN)_2^- + 2\ HSCN\ (aq)$

$$E = 0.6966 - 0.0591\ pH - 0.0591\ \log \{HSCN\}$$

(52) $Au(SCN)_6^{3-} + 4\ H^+ + 2\ e^- = Au(SCN)_2^- + 4\ HSCN\ (aq)$

$$E = 0.7495 - 0.1182\ pH - 0.1182\ \log \{HSCN\}$$

(53) $Au(SCN)_6^{3-} + 2\ e^- = Au(SCN)_2^- + 4\ SCN^-$

$$E = 0.6430 - 0.1182\ \log \{SCN^-\}$$

(54) $Au(OH)_3\ (s) + 2\ SCN^- + 3\ H^+ + 2e^- = Au(SCN)_2^- + 3\ H_2O$

$$E = 1.699 - 0.0887\ pH - 0.0295\ \log \frac{\{Au(SCN)_2^-\}}{\{SCN^-\}^2}$$

(55) $HAuO_3^{2-} + 2\ SCN^- + 5\ H^+ + 2\ e^- = Au(SCN)_2^- + 3\ H_2O$

$$E = 2.606 - 0.1478\ pH + 0.0591\ \log \{SCN^-\}$$

(56) $Au(SCN)_2^- + 2\ H^+ + e^- = Au(s) + 2\ HSCN\ (aq)$

$$E = 0.7972 - 0.1182\ pH - 0.0591\ \log \frac{\{HSCN\}^2}{\{Au(SCN)_2^-\}}$$

(57) $Au(SCN)_2^- + e^- = Au(s) + 2\ SCN^-$

$$E = 0.6907 - 0.0591\ \log \frac{\{SCN^-\}^2}{\{Au(SCN)_2^-\}}$$

(58) $AuO_2\ (s) + 4\ SCN^- + 4\ H^+ + e^- = Au(SCN)_4^- + 2\ H_2O$

$$E = 5.020 - 0.2364\ pH - 0.0591\ \log \frac{\{Au(SCN)_4^-\}}{\{SCN^-\}^4}$$

(59) $Au(SCN)_4^- + 3\ H_2O = Au(OH)_3\ (s) + 4\ SCN^- + 3\ H^+$

$$\log \frac{\{SCN^-\}^4}{\{Au(SCN)_4^-\}} = -\ 35.70 + 3\ pH$$

(60) $Au(SCN)_4^- + 4\ H^+ + 3\ e^- = Au\ (s) + 4\ HSCN\ (aq)$

$$E = 0.7301 - 0.0788\ pH - 0.0197 \log \frac{\{HSCN\}^4}{\{Au(SCN)_4^-\}}$$

(61) $Au(SCN)_4^- + 2\ e^- = Au(SCN)_2^- + 2\ SCN^-$

$$E = 0.6433 - 0.0295 \log \frac{\{Au(SCN)_2^-\}\ \{SCN^-\}^2}{\{Au(SCN)_4^-\}}$$

(62) $Au(SCN)_4^- + 3\ e^- = Au(s) + 4\ SCN^-$

$$E = 0.6591 - 0.0197 \log \frac{\{SCN^-\}^4}{\{Au(SCN)_4^-\}}$$

(63) $Au(SCN)_6^{3-} + 3\ H_2O = H_2AuO_3^- + 6\ SCN^- + 4\ H^+$

$$\log \frac{\{H_2AuO_3^-\}\ \{SCN^-\}^6}{\{Au(SCN)_6^{3-}\}} = -\ 53.05 + 4\ pH$$

(64) $H_2AuO_3^- + 2\ SCN^- + 4\ H^+ + 2\ e^- = Au(SCN)_2^- + 3\ H_2O$

$$E = 2.212 - 0.1182\ pH + 0.0591 \log \{SCN^-\}$$

(65) $Au(SCN)_4^- + 3\ H^+ + 2e^- = AuSCN^o\ (aq) + 3\ HSCN\ (aq)$

$$E = 0.6057 - 0.0887\ pH - 0.0295 \log \frac{\{AuSCN^o\}\ \{HSCN\}^3}{\{Au(SCN)_4^-\}}$$

(66) $Au(SCN)_4^- + 2\ e^- = AuSCN^o\ (aq) + 3\ SCN^-$

$$E = 0.5258 - 0.0295 \log \frac{\{AuSCN^o\}\ \{SCN^-\}^3}{\{Au(SCN)_4^-\}}$$

(67) $AuSCN^o\ (aq) + H^+ + e^- = Au\ (s) + HSCN\ (aq)$

$$E = 0.9790 - 0.0591\ pH - 0.0591 \log \frac{\{HSCN\}}{\{AuSCN^o\}}$$

(68) $AuSCN^{o}\ (aq) + e^{-} = Au(s) + SCN^{-}$

$$E = 0.9257 - 0.0591 \log \frac{\{SCN^{-}\}}{\{AuSCN^{o}\}}$$

(69) $Au(OH)_3\ (s) + SCN^{-} + 3\ H^{+} + 2\ e^{-} = AuSCN^{o}\ (aq) + 3\ H_2O$

$$E = 1.582 - 0.0887\ pH - 0.0295 \log \frac{\{AuSCN^{o}\}}{\{SCN^{-}\}}$$

(70) $Ag_2O_3\ (s) + 6\ H^{+} + 4\ e^{-} = 2\ Ag^{+} + 3\ H_2O$

$$E = 1.758 - 0.0887\ pH - 0.0295 \log \{Ag^{+}\}$$

(71) $AgO\ (s) + 2\ H^{+} + e^{-} = Ag^{+} + H_2O$

$$E = 1.810 - 0.1182\ pH - 0.0591 \log \{Ag^{+}\}$$

(72) $2\ Ag^{+} + H_2O = Ag_2O\ (s) + 2\ H^{+}$

$$\log \{Ag^{+}\} = 6.28 - pH$$

(73) $Ag^{+} + e^{-} = Ag\ (s)$

$$E = 0.7997 + 0.0591 \log \{Ag^{+}\}$$

(74) $Ag_2O_3\ (s) + 2\ H^{+} + 2\ e^{-} = 2\ AgO\ (s) + H_2O$

$$E = 1.706 - 0.0591\ pH$$

(75) $2\ AgO\ (s) + 2\ H^{+} + 2\ e^{-} = Ag_2O\ (s) + H_2O$

$$E = 1.439 - 0.0591\ pH$$

(76) $Ag_2O\ (s) + 3\ H_2O = 2\ Ag(OH)_2^{-} + 2\ H^{+}$

$$\log \{Ag(OH)_2^{-}\} = -17.70 + pH$$

(77) $Ag_2O\ (s) + 2\ H^{+} + 2\ e^{-} = 2\ Ag\ (s) + H_2O$

$$E = 1.171 - 0.0591\ pH$$

(78) $AgO\ (s) + H_2O + e^{-} = Ag\ (OH)_2^{-}$

$$E = 0.3922 - 0.0591 \log \{Ag(OH)_2^{-}\}$$

(79) $Ag(OH)_2^{-} + 2\ H^{+} + e^{-} = Ag\ (s) + 2\ H_2O$

$$E = 2.218 - 0.1182\ pH + 0.0591 \log \{Ag(OH)_2^{-}\}$$

(80) $Ag_2O_3\ (s) + 2\ HSCN\ (aq) + 4\ H^{+} + 4\ e^{-} = 2\ AgSCN(s) + 3\ H_2O$

$$E = 2.086 - 0.0591\ pH + 0.0295 \log \{HSCN\}$$

(81) $AgSCN\ (s) + 2\ HSCN\ (aq) = Ag(SCN)_3^{2-} + 2\ H^+$

$$\log \frac{\{Ag(SCN)_3^{2-}\}}{\{HSCN\}^2} = -\ 4.29 + 2\ pH$$

(82) $AgSCN\ (s) + H^+ + e^- = Ag\ (s) + HSCN\ (aq)$

$$E = 0.1440 - 0.0591\ pH - 0.0591\ \log \{HSCN\}$$

(83) $Ag_2O_3\ (s) + 6\ HSCN\ (aq) + 4\ e^- = 2\ Ag(SCN)_3^{2-} + 3\ H_2O$

$$E = 1.959 - 0.0148\ \log \frac{\{Ag(SCN)_3^{2-}\}^2}{\{HSCN\}^6}$$

(84) $Ag(SCN)_3^{2-} + HSCN\ (aq) = Ag(SCN)_4^{3-} + H^+$

$$\log \frac{\{Ag(SCN)_4^{3-}\}}{\{HSCN\}\ \{Ag(SCN)_3^{2-}\}} = -\ 0.65 + pH$$

(85) $Ag(SCN)_3^{2-} + 3\ H^+ + e^- = Ag(s) + 3\ HSCN\ (aq)$

$$E = 0.3975 - 0.1773\ pH - 0.0591\ \log \frac{\{HSCN\}^3}{\{Ag(SCN)_3^{2-}\}}$$

(86) $Ag_2O_3\ (s) + 8\ HSCN\ (aq) + 4\ e^- = 2\ Ag(SCN)_4^{3-} + 3\ H_2O + 2\ H^+$

$$E = 1.940 + 0.0295\ pH - 0.0148\ \log \frac{\{Ag(SCN)_4^{3-}\}^2}{\{HSCN\}^8}$$

(87) $Ag_2O_3\ (s) + 8\ SCN^- + 6\ H^+ + 4\ e^- = 2\ Ag(SCN)_4^{3-} + 3\ H_2O$

$$E = 2.047 - 0.0887\ pH - 0.0148\ \log \frac{\{Ag(SCN)_4^{3-}\}^2}{\{SCN^-\}^8}$$

(88) $Ag(SCN)_4^{3-} + e^- = Ag(s) + 4\ SCN^-$

$$E = 0.2229 - 0.0591\ \log \frac{\{SCN^-\}^4}{\{Ag(SCN)_4^{3-}\}}$$

(89) $Ag(SCN)_4^{3-} + 4\ H^+ + e^- = Ag\ (s) + 4\ HSCN\ (aq)$

$$E = 0.4360 - 0.2364\ pH - 0.0591\ \log \frac{\{HSCN\}^4}{\{Ag(SCN)_4^{3-}\}}$$

(90) $Ag_2O_3\ (s) + 6\ SCN^- + 6\ H^+ + 4\ e^- = 2\ Ag\ (SCN)_3^{2-} + 3\ H_2O$

$$E = 2.039 - 0.0887\ pH - 0.0148 \log \frac{\{Ag(SCN)_3^{2-}\}^2}{\{SCN^-\}^6}$$

(91) $Ag(SCN)_3^{2-} + e^- = Ag\ (s) + 3\ SCN^-$

$$E = 0.2377 - 0.0591 \log \frac{\{SCN^-\}^3}{\{Ag(SCN)_3^{2-}\}}$$

(92) $Ag_2O_3\ (s) + 2\ SCN^- + 6\ H^+ + 4\ e^- = 2\ AgSCN\ (s) + 3\ H_2O$

$$E = 2.113 - 0.0887\ pH + 0.0295 \log \{SCN^-\}$$

(93) $AgO\ (s) + SCN^- + 2\ H^+ + e^- = AgSCN\ (s) + H_2O$

$$E = 2.519 - 0.1182\ pH + 0.0591 \log \{SCN^-\}$$

(94) $AgSCN\ (s) + e^- = Ag\ (s) + SCN^-$

$$E = 0.0907 - 0.0591 \log \{SCN^-\}$$

(95) $Ag_2O_3\ (s) + 4\ HSCN\ (aq) + 2H^+ + 4e^- = 2\ Ag(SCN)_2^- + 3\ H_2O$

$$E = 1.951 - 0.0295\ pH - 0.0148 \log \frac{\{Ag(SCN)_2^-\}^2}{\{HSCN\}^4}$$

(96) $Ag(SCN)_2^- + HSCN\ (aq) = Ag(SCN)_3^{2-} + H^+$

$$\log \frac{\{Ag(SCN)_3^{2-}\}}{\{Ag(SCN)_2^-\}\{HSCN\}} = 0.30 + pH$$

(97) $Ag(SCN)_2^- + 2\ H^+ + e^- = Ag\ (s) + 2\ HSCN\ (aq)$

$$E = 0.4154 - 0.1182\ pH - 0.0591 \log \frac{\{HSCN\}^2}{\{Ag(SCN)_2^-\}}$$

(98) $AgSCN\ (s) + HSCN\ (aq) = Ag(SCN)_2^- + H^+$

$$\log \frac{\{Ag(SCN)_2^-\}}{\{HSCN\}} = -4.59 + pH$$

(99) $AgO\ (s) + 3\ SCN^- + 2H^+ + e^- = Ag(SCN)_3^{2-} + H_2O$

$$E = 2.372 - 0.1182\ pH - 0.0591 \log \frac{\{Ag(SCN)_3^{2-}\}}{\{SCN^-\}^3}$$

(100) $Ag(OH)_2^- + SCN^- + 2H^+ = AgSCN\ (s) + 2\ H_2O$

$$\log \{Ag(OH)_2^-\} + \log \{SCN^-\} = -35.96 + 2\ pH$$

(101) $Fe^{3+} + e^- = Fe^{2+}$

$$E = 0.7698 - 0.0591 \log \frac{\{Fe^{2+}\}}{\{Fe^{3+}\}}$$

(102) $FeOH^{2+} + H^+ + e^- = Fe^{2+} + H_2O$

$$E = 0.8979 - 0.0591\ pH - 0.0591 \log \frac{\{Fe^{2+}\}}{\{FeOH^{2+}\}}$$

(103) $Fe(OH)_2^+ + 2\ H^+ + e^- = Fe^{2+} + 2\ H_2O$

$$E = 1.193 - 0.1182\ pH - 0.0591 \log \frac{\{Fe^{2+}\}}{\{Fe(OH)_2^+\}}$$

(104) $Fe^{2+} + 3\ H_2O = Fe(OH)_3^- + 3\ H^+$

$$\log \frac{\{Fe(OH)_3^-\}}{\{Fe^{2+}\}} = -30.73 + 3\ pH$$

(105) $O_2\ (g) + 2\ H^+ + 2\ e^- = H_2O_2\ (aq)$

$$E = 0.6949 - 0.0591\ pH - 0.0295 \log \frac{\{H_2O_2\}}{P_{O_2}}$$

(106) $H_2O_2\ (aq) + 2\ H^+ + 2\ e^- = 2\ H_2O$

$$E = 1.763 - 0.0591\ pH + 0.0295 \log \{H_2O_2\}$$

(107) $HO_2^- + H_2O + 2\ e^- = 3\ OH^-$

$$E = 2.109 - 0.0887\ pH + 0.0295 \log \{HO_2^-\}$$

(108) $Au^{3+} + 2\ HCN\ (aq) + 2\ e^- = Au(CN)_2^- + 2\ H^+$

$$E = 1.959 + 0.0591\ pH - 0.0295 \log \frac{\{Au(CN)_2^-\}}{\{Au^{3+}\}\ \{HCN\}^2}$$

(109) $Au(OH)_3\ (s) + 2\ HCN\ (aq) + H^+ + 2\ e^- = Au(CN)_2^- + 3\ H_2O$

$$E = 1.723 - 0.0295\ pH - 0.0295 \log \frac{\{Au(CN)_2^-\}}{\{HCN\}^2}$$

(110) $Au(OH)_3\ (s) + 2\ CN^- + 3\ H^+ + 2\ e^- = Au(CN)_2^- + 3\ H_2O$

$$E = 2.283 - 0.0887\ pH - 0.0295 \log \frac{\{Au(CN)_2^-\}}{\{CN^-\}^2}$$

(111) $HAuO_3^{2-} + 2\ CN^- + 5\ H^+ + 2\ e^- = Au(CN)_2^- + 3\ H_2O$

$$E = 3.190 - 0.1478\ pH - 0.0295 \log \frac{\{Au(CN)_2^-\}}{\{HAuO_3^{2-}\}\ \{CN^-\}^2}$$

(112) $Au(CN)_2^- + e^- = Au\ (s) + 2\ CN^-$

$$E = -\ 0.4768 - 0.0591 \log \frac{\{CN^-\}^2}{\{Au(CN)_2^-\}}$$

(113) $Au(CN)_2^- + 2\ H^+ + e^- = Au\ (s) + 2\ HCN\ (aq)$

$$E = 0.6426 - 0.1182\ pH - 0.0591 \log \frac{\{HCN\}^2}{\{Au(CN)_2^-\}}$$

(114) $Ag^+ + HCN\ (aq) = AgCN\ (s) + H^+$

$$\log \{Ag^+\} + \log \{HCN\} = -\ 5.64 - pH$$

(115) $Ag_2O_3\ (s) + 2\ HCN\ (aq) + 4\ H^+ + 4\ e^- = 2\ AgCN\ (s) + 3\ H_2O$

$$E = 1.925 - 0.0591\ pH + 0.0295 \log \{HCN\}$$

(116) $AgCN\ (s) + HCN\ (aq) = Ag\ (CN)_2^- + H^+$

$$\log \frac{\{Ag(CN)_2^-\}}{\{HCN\}} = -\ 6.41 + pH$$

(117) $AgCN\ (s) + H^+ + e^- = Ag\ (s) + HCN\ (aq)$

$$E = 0.4661 - 0.0591\ pH - 0.0591 \log \{HCN\}$$

(118) $Ag_2O_3\ (s) + 4\ HCN\ (aq) + 2\ H^+ + 4\ e^- = 2\ Ag(CN)_2^- + 3\ H_2O$

$$E = 1.735 - 0.0295\ pH - 0.0148 \log \frac{\{Ag(CN)_2^-\}^2}{\{HCN\}^4}$$

(119) $Ag(CN)_2^- + HCN\ (aq) = Ag(CN)_3^{2-} + H^+$

$$\log \frac{\{Ag(CN)_3^{2-}\}}{\{Ag(CN)_2^-\}\ \{HCN\}} = -\ 8.59 + pH$$

(120) $Ag(CN)_2^- + 2\ H^+ + e^- = Ag\ (s) + 2\ HCN\ (aq)$

$$E = 0.8455 - 0.1182\ pH - 0.0591\ \log \frac{\{HCN\}^2}{\{Ag(CN)_2^-\}}$$

(121) $Ag_2O_3\ (s) + 6\ HCN\ (aq) + 4\ e^- = 2\ Ag(CN)_3^{2-} + 3\ H_2O$

$$E = 1.481 - 0.0148\ \log \frac{\{Ag(CN)_3^{2-}\}}{\{HCN\}^6}$$

(122) $Ag_2O_3\ (s) + 6\ CN^- + 6\ H^+ + 4\ e^- = 2\ Ag(CN)_3^{2-} + 3\ H_2O$

$$E = 2.321 - 0.0887\ pH - 0.0148\ \log \frac{\{Ag(CN)_3^{2-}\}^2}{\{CN^-\}^6}$$

(123) $Ag(CN)_3^{2-} + e^- = Ag\ (s) + 3\ CN^-$

$$E = -\ 0.3253 - 0.0591\ \log \frac{\{CN^-\}^3}{\{Ag(CN)_3^{2-}\}}$$

(124) $Ag(CN)_3^{2-} + 3\ H^+ + e^- = Ag\ (s) + 3\ HCN\ (aq)$

$$E = 1.354 - 0.1773\ pH - 0.0591\ \log \frac{\{HCN\}^3}{\{Ag(CN)_3^{2-}\}}$$

(125) $(SCN)_3^- + 2e^- = 3SCN^-$

$$E = 0.68 - 0.0295\ \log \frac{\{SCN^-\}^3}{\{(SCN)_3^-\}}$$

(126) $(SCN)_3^- + 3H^+ + 2e^- = 3HSCN$

$$E = 0.7599 - 0.0887\ pH - 0.0295\ \log \frac{\{HSCN\}^3}{\{(SCN)_3^-\}}$$

(127) $3(SCN)_2 + 2e^- = 2(SCN)_3^-$

$$E = 0.9500 - 0.0295\ \log \frac{\{(SCN)_3^-\}^2}{\{(SCN)_2\}^3}$$

(128) $3HOSCN + 3H^+ + 4e^- = (SCN)_3^- + 3H_2O$

$$E = 1.2963 - 0.0443\ pH - 0.0148\ \log \frac{\{(SCN)_3^-\}}{\{HOSCN\}^3}$$

APPENDIX 3: STABILITY CONSTANTS CONSIDERED IN THE PRESENT WORK

Metal Ion	Complex	log β_i	Conditions (Temp, Ionic Strength)		Ref.	Note
	$AuSCN_{(aq)}$	15.27	25°C	$3(NaClO_4)$	16, 20	-
	$Au(SCN)_2^-$	19.16	25°C	0	-	1
Au^+	AuI_2^-	21.14	"	"	-	7
	$Au(CN)_2^-$	38.89	"	"	-	1
	$AuCl_2^-$	11.37	"	"	-	1
	$Au(SCN)_4^-$	43.66	"	"	-	1
	$Au(SCN)_5^{2-}$	43.62	"	"	-	1
Au^{3+}	$Au(SCN)_6^{3-}$	43.67	"	"	-	1
	AuI_4^-	48.06	"	"	-	7
	$AuCl_4^-$	26.34	"	"	-	1
	$AgSCN_{(aq)}$	4.75	"	"	-	1, 2
	$Ag(SCN)_2^-$	8.30	"	"	-	1, 2
	$Ag(SCN)_3^{2-}$	9.50	"	"	-	1, 2
	$Ag(SCN)_4^{3-}$	9.75	"	"	-	1, 2
	AgSCN (s)	-12.00	"	"	16, 18	3
	AgCN (aq)	-1.11	"	"	-	1
Ag^+	$Ag(CN)_2^-$	18.15	"	"	-	1
	$Ag(CN)_3^{2-}$	19.02	"	"	-	1
	$Ag(CN)_4^{3-}$	20.8	30°C	1.0	16	-
	AgCN (s)	-15.66	25°C	0	16	4
	AgCl (aq)	0.05	"	"	-	1, 5
	$AgCl_2^-$	5.37	"	"	-	1
	$AgCl_3^{2-}$	5.25	"	"	-	1

Metal Ion	Complex	log β_i	Conditions (Temp, Ionic Strength)		Ref.	Note
Ag^+	$AgCl_4^{3-}$	5.50	"	"	-	1
	AgCl (s)	-9.74	"	"	16	6
Fe^{2+}	$FeNCS^+$	1.31	25°C	0	16	-
		0.81	"	3.0	16	-
	$FeNCS^{2+}$	3.02	25°C	0	16	-
		3.1	"	"	21	-
		2.21	"	3.0	16	-
		2.53	"	"	22	-
	$Fe(NCS)_2^+$	5.3	25°C	0	21	-
		3.64	"	3.0	16	-
		3.88	"	"	22	-
Fe^{3+}	$Fe(NCS)_{3(aq)}$	5.0	"	"	16	-
		6.2	"	0	21	-
		5.19	"	3.0	22	-
	$Fe(NCS)_4^-$	6.3	"	"	16	-
		6.52	"	"	22	-
	$Fe(NCS)_5^{2-}$	6.2	"	"	16	-
		6.20	"	"	22	-
	$Fe(NCS)_6^{3-}$	6.1	"	"	16	-

(1) Calculated from $\Delta G°$ data given in Appendix 1.

(2) This set of β_i values is consistent with that selected in [16] for 25°C and zero ionic strength which is: log β_i = 4.8, log β_2 = 8.23, log β_3 = 9.5 and log β_4 = 9.7.

(3) Calculation of this solubility product from $\Delta G°$ given in Appendix 1 yields the consistent figure log K_{SO} = - 11.98.

(4) Using $\Delta G°$ data from Appendix 1, log K_{SO} = - 15.10 is obtained.

(5) This figure disagrees with that quoted in [16] which is log β_1 = 3.31 (25°C, 0). It is possible that $\Delta G°_{AgCl}$ = - 54.16 kJ/mol for aqueous AgCl given by [12] and [14] is wrong. Assuming it to be so, and also assuming that $\Delta G°$ for Ag^+ and Cl^- in the same references are right, as well as log β_1 = 3.31, the figure $\Delta G°_{AgCl}$ = -72.79 kJ/mol is obtained. This figure, in its turn, is quite different from the -54.16 kJ/mol given in [12] and [14]. Thus, there is an inconsistency. The value log β_1 = 0.05, on the other hand, is consistent with all $\Delta G°$ provided by [12] and [14].

(6) Using $\Delta G°$ data from Appendix 1, log K_{SO} = - 9.80 is obtained.

(7) Calculated from $\Delta G°$ data given in [187].

APPENDIX 4: TESTS OF IRON PRECIPITATION FROM IRON(III)-THIOCYANATE SOLUTIONS

Experimental Procedure

The experiments were conducted in a stirred glass reactor open to the atmosphere and fitted with a pH electrode. An Ag/AgCl reference electrode and a Pt indicator electrode were also fitted into the reactor. Most of the experiments were performed at room temperature (23 ± 1°C). In the experiments at 60°C a heating mantle operated by a Fimonitor temperature controller was used. Freshly prepared potassium thiocyanate solutions were loaded into the reactor and the intended amount of Fe^{3+} stock solution (analytical grade ammonium iron(III) sulphate solution, 1 mol/dm^3) was added. The initial pH adjustment was made by adding either H_2SO_4 50% v/v or NaOH 4.0 mol/dm^3. After the initial adjustment the pH was kept constant by subsequent additions of NaOH when required. The NaOH consumption that appears in the table of results (see next page) corresponds to those subsequent additions and gives an indication of the extent of Fe^{3+} hydrolysis and precipitation during the experiments. Each experiment had a duration of 50 minutes.

The procedures for detection of precipitation are indicated in the table, in the last column to the right, and are described in the footnotes (1) to (3) of the same table. (1), (2) and (3) are successive steps for precipitate detection, each one comprising a decantation and a centrifugation test. (1) was performed immediately after (or even during) the experiment; (2) after 2 hours; and (3) after about 24 hours of its completion. Each step was taken only if no precipitate was detected in the previous one. A solution was considered to be stable when no precipitate at all could be found throughout the three steps reported.

RESULTS OF THE PRECIPITATION EXPERIMENTS:

Results at Room Temperature (23°C):

Run. No.	$[SCN^-]$ (mol/dm^3)	$[Fe^{3+}]$ (mol/dm^3)	pH	NaOH Consumed (cm^3)	Precipitate Detected (Yes/No)	Precipitation Detection (see Notes)
1	0.50	0.10	3.0	2.5	Yes	2a and 2b
2	0.24	"	"	11.6	Yes	1a
3	0.20	"	"	12.0	Yes	1a
4	0.10	"	"	14.7	Yes	1a
5	0.50	0.10	2.0	0	No	Soln. Stable
6	0.24	"	"	0	No	Soln. Stable
7	0.20	"	"	0	No	Soln. Stable
8	0.10	"	"	0	No	Soln. Stable
9	0.01	"	"	0	No	Soln. Stable
10	0.10	0.10	1.5	0	No	Soln. Stable
11	"	"	2.0	0	No	Soln. Stable
12	"	"	2.5	0.3	Yes	2a and 2b
13	"	"	2.6	2.8	Yes	1a
14	0.10	0.04	2.0	0	No	Soln. Stable
15	"	"	2.5	0	No	Soln. Stable
16	"	"	3.0	5.2	Yes	1a
17	0.10	0.02	1.5	0	No	Soln. Stable
18	"	"	2.0	0	No	Soln. Stable
19	"	"	2.5	0	No	Soln. Stable
20	"	"	3.0	2.1	Yes	1a
21	0.05	0.10	1.5	0	No	Soln. Stable
22	0.01	"	"	0	No	Soln. Stable

(Table continued next page)

Results at 60°C:

Run. No.	$[SCN^-]$ (mol/dm^3)	$[Fe^{3+}]$ (mol/dm^3)	pH	NaOH Consumed (cm^3)	Precipitate Detected (Yes/No)	Precipitation Detection (see Notes)
23	0.01	0.10	2.0	0.3	Yes	3a and 3b
24	"	0.02	"	0	No	Soln. Stable
25	0.10	0.10	1.5	0	No	Soln. Stable
26	"	0.02	"	0	No	Soln. Stable
27	0.05	0.10	"	0	No	Soln. Stable

NOTES: (1) (a) Precipitation visibly noticed even before finishing the experiment, or through a decantation test within ≈15 minutes of its completion.

(b) A precipitate was separated by centrifugation for ≈15 minutes at 4500 rpm performed immediately after the experiment was completed.

(2) (a) A precipitate was noticed after the solution from the experiment was left standing for ≈2 hours.

(b) A precipitate was separated by centrifugation for ≈15 minutes at 4500 rpm after the solution from the experiment was left standing for ≈2 hours.

(3) (a) A precipitate was noticed after the solution from the experiment was left standing overnight.

(b) A precipitate was separated by centrifugation (≈15 minutes at 4500 rpm) after the solution was left standing overnight.

Conclusions

The concentration ranges investigated were 0.01-0.50 mol/dm^3 SCN^- and 0.02-0.10 mol/dm^3 Fe^{3+}. The results reported above can be summarized as follows:

At room temperature (23°C), iron(III)-thiocyanate solutions are stable towards iron precipitation up to pH 2.5. The onset of precipitation as shown by experiments 12, 16 and 20 is around pH 2.5 or a little higher, depending on the particular concentrations of SCN^- and Fe^{3+} considered. In all conditions tried precipitation occurred below pH 3.0. The complexation by thiocyanate stabilizes Fe^{3+} in solution. Thus, the stability increases with increasing [SCN^-] and/or decreasing [Fe^{3+}].

Higher temperatures favour iron precipitation. The solutions tend to become unstable around pH 2.0, as shown by the run number 23, although the precipitation observed in this run was minimal, as indicated by the decantation and centrifugation tests and by the small consumption of NaOH (only 0.3 ml of 4.0 mol/dm^3 solution), and did not take place until several hours after the experiment.

Thus, for studies at 25°C, pH values up to 2.0 can be adopted safely. For higher temperatures, a pH below 2.0 is advisable. These conclusions relate to the gold rotating disc experiments with iron(III)-thiocyanate solutions, in which iron precipitation would be a disturbing factor for the monitoring of concentrations in solutions and the related mixed potential measurements.

Further tests revealed that the precipitates formed when the pH was raised promptly redissolved when the pH was lowered to a value within the stability limits.

There is also a lower pH constraint, although not as critical as

the upper one discussed above, which is due to the protonation of SCN^- to form HSCN. This causes a decrease in the availability of free SCN^- in solution. The pK_a for HSCN is around 0.9. Thus, a pH below 1.0 is not advisable.

Summarizing, the best pH range for gold dissolution by ferric thiocyanate solutions is from 1.0 to 2.0. Infrared analyses revealed that the precipitates obtained consisted basically of goethite, FeO(OH).

APPENDIX 5 - RESULTS OF THE EXPERIMENTS WITH IRON(III)-THIOCYANATE SOLUTIONS (CHAPTER 4)

A5.1. Experimental Conditions

Run Number	Initial Concentrations (mol/dm3)			Temperature (ºC)	Notes
	SCN^-	Iron(III)	Iron(II)		
TOF-1	0.275	0.055	0	25	
TOF-2	"	"	"	"	
TOF-3	"	"	"	"	
TOF-4	"	"	"	"	
TOF-5	"	"	"	"	1
TOF-6	"	"	"	"	2
TOF-7	0.275	0.011	0	25	
TOF-8	"	0.033	"	"	
TOF-9	"	0.055	"	"	
TOF-10	"	0.10	"	"	
TOF-11	0.05	0.01	0	25	
TOF-12	"	0.033	"	"	
TOF-13	"	0.055	"	"	
TOF-14	"	0.10	"	"	
TOF-15	0.50	0.01	0	25	
TOF-16	"	0.033	"	"	
TOF-17	"	0.055	"	"	
TOF-18	"	0.10	"	"	
TOF-19	0.163	0.01	"	25	
TOF-20	"	0.033	"	"	
TOF-21	"	0.06	"	"	
TOF-22	"	0.10	"	"	
TOF-23	0.275	0.0275	0.0275	25	
TOF-24	"	0.0385	0.0165	"	
TOF-25	"	0.0495	0.0055	"	

(Continued)

Run Number	Initial Concentrations (mol/dm^3)			Temperature (°C)	Notes
	SCN^-	Iron(III)	Iron(II)		
TOF-26	0.275	0.055	0	40	
TOF-27	"	"	"	"	
TOF-28	"	"	"	"	
TOF-29	"	"	"	"	
TOF-30	"	"	"	"	
TOF-31	0.05	0.01	0	55	
TOF-32	"	0.10	"	"	
TOF-33	0.50	0.01	0	55	
TOF-34	"	0.10	"	"	
TOF-35	0.275	0.055	0	55	
TOF-36	0.50	0.10	0	75	
TOF-37	0.275	0.055	0	25	
TOF-38	"	"	"	"	3
TOF-39	"	"	"	"	4
TOF-40	0.10	0.01	0	25	
TOF-41	"	0.033	"	"	
TOF-42	"	0.055	"	"	
TOF-43	"	0.10	"	"	
TOF-44	0.275	0.01	0	25	
TOF-45	"	0.03	"	"	
TOF-46	"	0.055	"	"	
TOF-47	"	0.10	"	"	
			"		
TOF-48	0.275	0.033	0	25	
TOF-49	"	0.055	"	"	

(1) Nitrogen atmosphere.
(2) Air sparged run.
(3) Initial pH = 1.0
(4) Initial pH = 2.0
(5) Other runs with initial pH = 1.5, which decreased to final values between 1.3 and 1.4.

A5.2. Potential Readings

Time (hours)	Potential (mV vs. SHE)							
	TOF-1	TOF-2	TOF-3	TOF-4	TOF-5	TOF-6	TOF-7	TOF-8
0	725	729	726	725	728	725	694	715
0.5	693	698	696	694	696	693		
1	681	685	683	682	684	682		
2	668	672	670	669	671	669	647	661
3	660	664	662	661	663	661		
4	656	658	656	656	657	656	636	647
6	651	652	649	649	649	650		
8	647	648	644	645	645	645	626	636
24	628	630	630	629			611	620
48			620	620			602	611
72			616	615			601	610
96			612	614			597	607
144			611	611			591	603
192			610	608			584	597
384			605	605			578	596
432			605	604			576	594

Time (hours)	Potential (mV vs. SHE)							
	TOF-9	TOF-10	TOF-11	TOF-12	TOF-13	TOF-14	TOF-15	TOF-16
0	723	736	740	757	765	774	676	689
0.5								
1								
2	669	686	727	744	752	761	624	631
3								
4	656	671	722	741	750	760	615	621
6								
8	644	657	713	732	744	754	609	615
24	628	638	694	717	731	746	596	602
48	620	629	685	708	721	738	588	595
72	619	628	673	694	710	727	586	593
96	616	624	665	688	704	722	583	592
144	612	621	662	683	700	718	580	591
192	608	616	655	676	689	709	576	589
384	603	613						
432	602	612	641	662	676	695	564	585

Time (hours)	Potential (mV vs. SHE)							
	TOF-17	TOF-18	TOF-19	TOF-20	TOF-21	TOF-22	TOF-23	TOF-24
0	697	710	710	727	735	745	609	632
0.5								
1								
2	636	645	674	693	705	721	612	636
3								
4	627	635	661	677	691	710	614	636
6								
8	620	626	649	663	676	695	614	633
24	608	616	630	644	655	672	613	626
48	602	612	625	638	648	664	612	622
72	601	610	618	630	640	655	610	617
96	600	609	613	627	637	650		
144	599	608	609	622	631	644		
192	598	607	603	617	626	638		
384								
432	595	604	587	606	617	625		

Time	Potential (mV vs. SHE)							
(hours)	TOF-25	TOF-26	TOF-27	TOF-28	TOF-29	TOF-30	TOF-31	TOF-32
0	665	723	723	725	725	718	728	763
0.5								
1								
2	660	645	647	645	646	647	703	743
3								
4	652	636	637	636	637	635	688	728
6								
8	644	625	625	624	625	626	673	714
24	630	612	612	611	612	611	611	670
48	624							
72	618							

Time	Potential (mV vs. SHE)						
(hours)	TOF-33	TOF-34	TOF-35	TOF-36	TOF-37	TOF-38	TOF-39
0	665	700	705	671	718	720	716
0.5				601			
1				588			
2	592	613	625	577	668	672	669
3				572			
4	575	604	614	569	657	660	655
6							
8	558	600	604	562	645	650	646
24	480	564	583	559	629	637	624
48					620	630	613
72					615	626	607

Time	Potential (mV vs. SHE)									
(hours)	TOF-40	TOF-41	TOF-42	TOF-43	TOF-44	TOF-45	TOF-46	TOF-47	TOF-48	TOF-49
0.0	715.0	736	748	753	690	715	725	736	715	721
0.25					659	672	680	693		
0.5	711.0	731	742	752	655	667	677	691		
1.0	708.0	728	737	747	646	659	669	683	660	670
1.5					642	655	664	681		
2.0	701.0	720	731	742	634	649	659	675	648	658
4.0			726							

A5.3. Iron(II) Spectrophotometric Determinations

Note: The iron(II) analyses are expressed in percentages of the total iron concentrations, which are reported in A5.1.

Time	Percentage of Iron(II) over Total Iron							
(hours)	TOF-1	TOF-2	TOF-3	TOF-4	TOF-5	TOF-6	TOF-7	TOF-8
0	0.00	0.00	0.00	0.00	0.00	0.00	0.00	0.00
1	6.41	6.08	6.25	6.25	6.58	6.25		
2	10.56	10.23	10.23	10.40	10.90	10.73		
4	16.21	16.21	16.21	16.04	16.88	16.54	23.11	19.28
6	19.70	20.20	20.03	19.86	20.03	20.53		
8	23.69	22.52	23.19	22.85	23.52	24.02	30.88	26.87
24	34.65	35.81	35.64	34.81			43.21	38.40
48			43.12	41.96			52.34	46.83
72			46.44	45.28			57.37	49.92
96			49.76	47.93			62.39	54.42
144			51.75	50.59			66.05	57.23
192			52.09	52.59			70.16	59.76
384			57.73	55.41			76.10	63.10
432			58.23	56.37			77.47	63.97

Time	Percentage of Iron(II) over Total Iron							
(hours)	TOF-9	TOF-10	TOF-11	TOF-12	TOF-13	TOF-14	TOF-15	TOF-16
0	0	0	0	0	0	0	0	0
1								
2	10.4		1.19	0.45	0.27	0.05	16.99	17.03
4	16.88	11.8	3.01	1.01	0.6	0.24	21.56	21.81
6								
8	23.85	18.8	5.76	2.14	1.26	0.51	27.95	27.43
24	35.31	31.35	13.98	5.79	3.26	1.33	38.92	38.4
48	41.96	38.84	22.29	10.29	5.82	2.54	46.22	44.3
72	45.44	42.31	28.14	13.94	8.07	3.53	50.79	47.11
96	49.33	45.79	33.16	17.88	10.4	4.62	52.62	47.64
144	52.69	48.71	39.56	22.09	13.39	6.27	58.1	51.33
192	54.68	50.17	45.49	26.59	17.04	8.09	62.67	52.73
384	57.67	54.72						
432	58.42	55.88	60.11	41.21	27.67	14.67	70.89	55.54

Time	Percentage of Iron(II) over Total Iron							
(hours)	TOF-17	TOF-18	TOF-19	TOF-20	TOF-21	TOF-22	TOF-23	TOF-24
0	0	0	0	0	0	0	50.03	30.1
1								
2	16.21	14.95	10.78	6.63	4.58	2.34	50.03	30.99
4	20.7	19.15	16.72	11.97	8.24	4.26	50.03	32.75
6								
8	26.08	25.3	25.85	18.72	13.72	7.73	50.36	34.41
24	36.08	35.19	41.84	33.9	27.17	17.41	50.69	39.73
48	41.39	39.03	51.89	44.58	37.8	27.37	51.69	43.72
72	44.05	40.49	59.2	50.2	45.71	34.28	54.01	48.37
96		41.25	60.84	53.27	48	36.68		
144	46.76	43.3	68.15	58.54	54.23	44.21		
192	48.37	44.32	70.89	61.35	55.89	46.95		
384								
432	51.32	47.41	78.2	66.62	61.29	55.63		

Time (hours)	Percentage of Iron(II) over Total Iron							
	TOF-25	TOF-26	TOF-27	TOF-28	TOF-29	TOF-30	TOF-31	TOF-32
0	10.07	0.00	0.00	0.00	0.00	0.00	0.00	0.00
1								
2	15.15	35.48	37.29	38.95	36.67	35.41	33.43	5.41
4	19.35	47.59	45.93	43.43	43.02	46.04	42.57	10.01
6								
8	24.12	54.65	52.57	53.40	54.65	54.01	59.01	16.22
24	33.75	63.37	63.37	63.61	63.37	64.31	78.20	29.89
48	40.39							
72	45.04							

Time (hours)	Percentage of Iron(II) over Total Iron						
	TOF-33	TOF-34	TOF-35	TOF-36	TOF-37	TOF-38	TOF-39
0	0.00	0.00	0.00		0.00	0.00	0.00
1							
2	73.63	56.13	52.69		8.07	9.07	7.57
4	90.07	71.99	67.52		13.55	14.05	12.22
6							
8	90.90	74.73	70.42		19.95	19.37	19.86
24	97.75	77.42	85.95		33.32	28.50	34.32
48					39.07	33.42	44.38
72					44.05	36.41	50.36

Time (hours)	Percentage of Iron(II) over Total Iron									
	TOF-40	TOF-41	TOF-42	TOF-43	TOF-44	TOF-45	TOF-46	TOF-47	TOF-48	TOF-49
0.0	0.00	0.00	0.00	0.00	0.00	0.00	0.00	0.00	0.00	0.00
0.25	0.00	0.45	0.33	0.05	1.46	2.42	2.09	1.24		
0.5	0.55	0.73	0.60	0.15	4.20	4.67	3.75	2.16		
1.0	1.46	1.57	0.96	0.33	7.86	7.76	6.41	3.98	8.04	6.41
1.5					10.60	10.29	8.74	5.54		
2.0	4.20	2.84	1.69	0.62	12.42	12.59	10.73	7.09	12.82	10.73

A5.4. Thiocyanate Analyses

Time (hours)	Thiocyanate Analyses (mol/dm^3)							
	TOF-1	TOF-2	TOF-3	TOF-4	TOF-5	TOF-6	TOF-7	TOF-8
0	0.277	0.276	0.275	0.275	0.274	0.275	0.275	0.275
2	0.274	0.274						
4	0.274	0.274						
8	0.273	0.273	0.274	0.272	0.274	0.270		
24	0.273	0.273	0.272	0.272				
72			0.272	0.272			0.274	0.273
192							0.274	0.271
384			0.271	0.270			0.273	0.270
432								
720			0.268					

Time (hours)	Thiocyanate Analyses (mol/dm^3)							
	TOF-9	TOF-10	TOF-11	TOF-12	TOF-13	TOF-14	TOF-15	TOF-16
0	0.275	0.275	0.050	0.050	0.050	0.050	0.500	0.500
2								
4								
8								
24								
72	0.271	0.269	0.049	0.049	0.049	0.049	0.499	0.497
192	0.270	0.269	0.049	0.049	0.049	0.049	0.498	0.496
384	0.268	0.268						
432			0.049	0.048	0.047	0.048	0.497	0.494

Time (hours)	Thiocyanate Analyses (mol/dm^3)							
	TOF-17	TOF-18	TOF-19	TOF-20	TOF-21	TOF-22	TOF-23	TOF-24
0	0.500	0.500	0.164	0.164	0.164	0.164	0.275	0.275
2								
4								
8								
24								
72	0.499	0.493	0.161	0.159	0.158	0.157	0.274	0.272
192	0.498	0.492	0.161	0.159	0.156	0.154		
384								
432	0.493	0.491	0.161	0.159	0.156	0.154		

Time (hours)	Thiocyanate Analyses (mol/dm^3)							
	TOF-25	TOF-26	TOF-27	TOF-28	TOF-29	TOF-30	TOF-31	TOF-32
0	0.275	0.275	0.275	0.275	0.275	0.275	0.050	0.050
2								
4								
8		0.271	0.271	0.271	0.271	0.271	0.049	0.048
24		0.271	0.270	0.270	0.270	0.271	0.049	0.046
72	0.271							

Time (hours)	Thiocyanate Analyses (mol/dm^3)							
	TOF-33	TOF-34	TOF-35	TOF-36	TOF-37	TOF-38	TOF-39	
0	0.500	0.500	0.275	0.499	0.275	0.275	0.275	
2				0.488				
4				0.482				
8	0.497	0.488	0.270	0.484				
24	0.496	0.487	0.270	0.475	0.272	0.272	0.272	
72					0.271	0.271	0.270	

APPENDIX 6 - RESULTS OF THE GOLD ROTATING DISC EXPERIMENTS

A6.1. Runs with Spontaneous Autoreduction

A6.1.a. Experimental Conditions

Run Number	Initial Concentrations (mol/dm^3)		Rotation Speed (rpm)	Temperature (°C)	Notes
	SCN^-	Iron(III)			
Au-1	0.275	0.055	720	25	
Au-2	"	"	"	"	
Au-3	"	"	"	"	
Au-4	0.275	0.055	720	25	1
Au-5	"	"	"	"	1
Au-6	"	"	"	"	1
Au-7	"	"	"	"	1
Au-8	0.275	0.055	180	25	
Au-9	"	"	420	"	
Au-10	"	"	1020	"	
Au-11	"	"	1500	"	
Au-12	0.05	0.055	720	25	
Au-13	0.10	"	"	"	
Au-14	0.163	"	"	"	
Au-15	0.50	"	"	"	
Au-16	"	"	"	"	
Au-17	"	"	"	"	
Au-18	0.10	0.01	720	25	
Au-19	"	0.033	"	"	
Au-20	"	0.055	"	"	
Au-21	"	0.10	"	"	
Au-22	0.275	0.01	"	"	
Au-23	"	0.033	"	"	
Au-24	"	0.10	"	"	

(Continued)

Run Number	Initial Concentrations (mol/dm^3)		Rotation Speed (rpm)	Temperature (ºC)	Notes
	SCN^-	Iron(III)			
Au-25	0.05	0.055	720	48	
Au-26	"	"	"	55	
Au-27	"	"	"	85	
Au-28	0.10	0.055	720	40	
Au-29	"	"	"	48	
Au-30	"	"	"	55	
Au-31	"	"	"	"	
Au-32	"	"	"	85	
Au-33	"	"	"	"	
Au-34	0.275	0.055	720	40	
Au-35	"	"	"	48	
Au-36	"	"	"	55	
Au-37	"	"	"	"	
Au-38	"	"	"	85	
Au-39	"	"	"	"	1

(1) Run in aerated atmosphere. Other runs in nitrogen atmosphere.

(2) Initial pH was 1.5, decreasing to a final value of c. a. 1.4 in most cases.

A6.1.b. Gold Dissolution Results

Note: The gold rotating disc area was 1.54 cm^2. Initial volume of liquid: 180 cm^3. Sample size: 5 cm^3.

Time (min)	Gold Dissolved (mg)							
	Au-1	Au-2	Au-3	Au-4	Au-5	Au-6	Au-7	Au-8
0	0.0000	0.0000	0.0000	0.0000	0.0000	0.0000	0.0000	0.0000
8	0.1492	0.1480	0.1443	0.0992	0.0954	0.1042	0.0980	0.1492
15	0.2135	0.2118	0.2143	0.1420	0.1366	0.1492	0.1402	0.1946
30	0.2810	0.2821	0.2794	0.1682	0.1785	0.1823	0.1856	0.2504
45	0.3277	0.3299	0.3206	0.1970	0.2157	0.2230	0.2262	0.2865
60	0.3646	0.3696	0.3554	0.2232	0.2420	0.2541	0.2557	0.3151
75	0.3891	0.4000	0.3812	0.2597		0.2732	0.2779	0.3442
90	0.4172	0.4277	0.4074	0.2827	0.2864	0.2947	0.2994	0.3605
120	0.4668	0.4806	0.4533	0.3242	0.3310	0.3302	0.3484	0.3992
150	0.5086	0.5202	0.4795	0.3543	0.3725	0.3717	0.3770	0.4322
180	0.5228	0.5564	0.5312	0.3846	0.4042	0.4048	0.4141	
210	0.5760	0.5882	0.5668	0.4150	0.4401	0.4260	0.4459	

Time	Gold Dissolved (mg)							
(min)	Au-9	Au-10	Au-11	Au-12	Au-13	Au-14	Au-15	Au-16
0	0.0000	0.0000	0.0000	0.0000	0.0000	0.0000	0.0000	0.0000
8	0.1492	0.1456	0.1438	0.0917	0.1132	0.1276	0.1744	0.1654
15	0.2085	0.1997	0.1874	0.1301	0.1534	0.1678	0.2389	0.2125
30	0.2593	0.2555	0.2416	0.1758	0.2092	0.2326	0.3083	0.2785
45	0.2954	0.2982	0.2859	0.2151	0.2486	0.2726	0.3428	0.3343
60	0.3208	0.3283	0.3113	0.2358	0.2803	0.3053	0.3856	0.3851
75	0.3453	0.3483	0.3450	0.2619	0.3080	0.3324	0.4240	0.4280
90	0.3587	0.3750	0.3643	0.2782	0.3302	0.3559	0.4566	0.4784
120	0.3873	0.4107	0.3929	0.3182	0.3731	0.3998	0.5252	0.5585
150	0.4231	0.4397	0.4273	0.3513	0.4144	0.4361	0.5872	0.6370

Time	Gold Dissolved (mg)							
(min)	Au-17	Au-18	Au-19	Au-20	Au-21	Au-22	Au-23	Au-24
0	0.0000	0.0000	0.0000	0.0000	0.0000	0.0000	0.0000	0.0000
8	0.1905	0.0752	0.0809	0.1132	0.0953	0.1150	0.1330	0.1564
15	0.2429	0.1064	0.1071	0.1534	0.1371	0.1622	0.1766	0.1895
30	0.3072	0.1518	0.1578	0.2092	0.1913	0.2112	0.2410	0.2454
45	0.3580	0.1793	0.1874	0.2486	0.2290	0.2440	0.2738	0.2815
60	0.3993	0.2137	0.2175	0.2803	0.2560	0.2742	0.3039	0.3085
75	0.4469	0.2256	0.2405	0.3080	0.2867	0.2942	0.3315	0.3392
90	0.4766	0.2488	0.2628	0.3302	0.3090	0.3179	0.3538	0.3584
120	0.5538	0.2736	0.3028	0.3731	0.3490	0.3593	0.3995	0.4013
150	0.6240	0.3014	0.3428	0.4144	0.3862	0.3952	0.4395	0.4413

Time	Gold Dissolved (mg)							
(min)	Au-25	Au-26	Au-27	Au-28	Au-29	Au-30	Au-31	Au-32
0	0.0000	0.0000	0.0000	0.0000	0.0000	0.0000	0.0000	0.0000
8	0.2545	0.3804	1.6428	0.2254	0.3315	0.5224	0.5179	2.6252
15	0.3640	0.5724	2.7753	0.3242	0.4591	0.7675	0.7688	3.9798
30	0.5508	0.8653	4.3588	0.4718	0.6357	1.0923	1.1218	6.0636
45	0.6860	1.0476	5.4611	0.5657	0.7770	1.3360	1.3735	7.2045
60	0.8024	1.1984	6.2905	0.6406	0.8850	1.4770	1.5521	8.6129
75		1.3482	6.9129	0.7068	0.9709	1.6186	1.6742	9.4910
90	0.9874	1.4380	7.5852	0.7603	1.0447	1.7299	1.7694	10.1832
120	1.1346	1.5802	8.2839	0.8545	1.1902	1.9036	1.9389	11.2901
150	1.2521	1.7145	8.8770	0.9325	1.3114	2.0422	2.0735	11.9894

Time	Gold Dissolved (mg)							
(min)	Au-33	Au-34	Au-35	Au-36	Au-37	Au-38	Au-39	
0	0.0000	0.0000	0.0000	0.0000	0.0000	0.0000	0.0000	
8	2.2691	0.2885	0.3577	0.4590	0.5453	2.9943	2.7217	
15	3.5122	0.4093	0.4818	0.6925	0.7730	4.4317	3.9695	
30	5.3315	0.5645	0.6682	0.9245	1.1181	6.2293	5.5837	
45	6.6428	0.6709	0.8078	1.1794	1.3963	7.2755	6.6039	
60	7.6213	0.7594	0.9455	1.5240	1.6927	8.0536	7.3417	
75	8.8864	0.8317	1.0707	1.8711	2.1324	8.5210	7.8086	
90	9.5185	0.9068	1.2057	2.7993	2.9232	8.7253	8.0344	
120	10.7411	1.0373	1.4912	4.3233	4.3130	8.7706	8.0869	
150		1.1712	1.8310	5.7942	5.6082		8.0499	

A6.1.c. Potential Readings

Note: The figures under Au are the potentials at the surface of the gold rotating disc and those under Pt at a platinum electrode. Both were measured against an Ag/AgCl reference electrode and appear in the tables after convertion to SHE.

Time (min)	Potential (mV vs. SHE)							
	Au-1		Au-2		Au-3		Au-4	
	Au	Pt	Au	Pt	Au	Pt	Au	Pt
0	713	725	710	723	713	723	726	728
4	708	711	708	712	708	712	716	719
8	700	701	699	701	700	700	706	706
15	689	690	689	689	689	690	695	694
30	679	679	679	679	679	679	684	683
45	672	672	671	671	672	672	677	676
60	667	666	666	666	668	667	672	671
75	663	662	663	662	664	664	668	666
90	661	660	659	659	662	661	664	663
120	655	654	654	654	657	656	659	657
150	651	650	650	650	653	652	655	654
180	649	648	647	647			652	650
210	647	645	645	645			649	648

Time (min)	Potential (mV vs. SHE)							
	Au-5		Au-6		Au-7		Au-8	
	Au	Pt	Au	Pt	Au	Pt	Au	Pt
0	724	729	719	729	723	726	715	705
4	717	717	714	716	717	715		
8	706	706	704	704	707	706	696	701
15	696	695	694	693	695	695	689	688
30	682	681	683	682	682	682	680	680
45	676	675	676	675	675	675	675	675
60	671	670	671	670	670	669	670	670
75			667	665	666	665	667	667
90	663	662	663	662	663	662	665	665
120	658	657	659	657	658	657	661	660
150	654	653	654	652	653	653	657	657
180	651	650	651	650	651	650		
210	649	648	648	647	649	648		

Time (min)	Potential (mV vs. SHE)							
	Au-9		Au-10		Au-11		Au-12	
	Au	Pt	Au	Pt	Au	Pt	Au	Pt
0	713	717	714	719	718	725	774	765
4								
8	694	696	700	699	702	700	781	764
15	688	688	690	690	693	692	779	762
30	679	678	681	680	683	681	773	759
45	673	673	675	674	676	675	769	757
60	669	669	670	670	672	670	765	755
75	666	666	666	667	669	667	763	754
90	664	663	662	662	666	664	762	753
120	660	660	663	661	661	660	759	751
150	657	657	660	658	658	657	755	747

Time (min)	Potential (mV vs. SHE)							
	Au-13		Au-14		Au-15		Au-16	
	Au	Pt	Au	Pt	Au	Pt	Au	Pt
0	758	747	742	735	684	695	685	697
4			738	730	676	679		
8	756	745	727	727	664	664	664	665
15	749	739	725	720	653	653	655	656
30	740	734	716	713	643	643	646	646
45	735	730	710	708	640	640	643	643
60	731	727	706	705	637	637	641	641
75	729	725	702	701	635	635	640	639
90	726	723	700	698	634	633	639	638
120	722	719	694	692	632	631	638	637
150	719	716	690	688	630	629	636	635

Time (min)	Potential (mV vs. SHE)							
	Au-17		Au-18		Au-19		Au-20	
	Au	Pt	Au	Pt	Au	Pt	Au	Pt
0	690	699	725	729	752	745	758	747
4								
8	664	665	726	726	750	742	756	745
15	655	655	721	720	742	736	749	739
30	647	647	707	706	731	727	740	734
45	645	644	698	698	726	723	735	730
60	643	642	693	693	721	719	731	727
75	641	641	690	689	718	716	729	725
90	640	640	685	685	715	713	726	723
120	637	637	681	681	711	709	722	719
150	633	632	677	677	707	706	719	716

Time (min)	Potential (mV vs. SHE)							
	Au-21		Au-22		Au-23		Au-24	
	Au	Pt	Au	Pt	Au	Pt	Au	Pt
0	771	765	678	698	708	716	734	736
4								
8	772	763	675	680	687	688	718	717
15	768	759	664	666	678	679	710	709
30	761	753	653	653	667	667	701	701
45	756	750	648	647	661	661	695	694
60	753	748	645	644	657	657	690	689
75	751	746	643	642	655	654	687	686
90	748	744	641	641	653	652	684	683
120	744	740	639	639	650	649	678	677
150	741	738	638	638	648	647	674	673

Time (min)	Potential (mV vs. SHE)							
	Au-25		Au-26		Au-27		Au-28	
	Au	Pt	Au	Pt	Au	Pt	Au	Pt
0	780	768	785	780	747	749	765	761
4			785	779	733	736	762	758
8	780	765	782	775	720	723	758	754
15	774	763	776	770	708	712	751	747
30	766	757	764	761	697	699	741	739
45	759	753	756	754	687	690	734	732
60	754	749	750	749	679	682	729	727
75			745	745	676	678	724	723
90	746	743	741	740	671	673	720	720
120	740	738	735	734	663	666	715	714
150	735	734	729	728	657	659	710	709

Time (min)	Potential (mV vs. SHE)							
	Au-29		Au-30		Au-31		Au-32	
	Au	Pt	Au	Pt	Au	Pt	Au	Pt
0	754	751	754	760	758	761	705	712
4	754	746			754	754	690	694
8	747	742	744	744	747	747	679	683
15	738	734	734	735	736	737	666	670
30	725	724	721	721	721	721	650	652
45	717	716	712	712	712	712	641	643
60	711	711	707	707	706	706	632	635
75	706	705	701	701	700	700	627	629
90	701	701	697	697	692	692	621	623
120	695	695	691	691	687	687	611	614
150	690	690	684	684	683	683	605	608

Time (min)	Potential (mV vs. SHE)							
	Au-33		Au-34		Au-35		Au-36	
	Au	Pt	Au	Pt	Au	Pt	Au	Pt
0	686	690	715	727	706	712	712	722
4			705	707	695	697	696	698
8	656	652	695	697	684	686	682	684
15	642	645	686	685	672	672	672	673
30	629	633	673	673	661	662	659	660
45	622	624	666	666	655	655	652	652
60	612	615	660	660	650	651	646	647
75	605	607	657	657	647	647	640	641
90	600	603	655	655	644	644	637	638
120	591	593	650	650	639	639	628	629
150			645	645	633	634	624	625

Time (min)	Potential (mV vs. SHE)							
	Au-37		Au-38		Au-39			
	Au	Pt	Au	Pt	Au	Pt		
0	700	702	654	671	655	665		
4	684	686	625	633				
8	677	679	609	617	615	623		
15	667	668	597	604	602	609		
30	654	655	584	590	585	592		
45	646	647	575	580	576	582		
60	641	641	572	576	568	573		
75	636	637	562	566	562	567		
90	631	633	558	560	557	561		
120	626	628	543	544	547	549		
150	623	624			533	536		

A6.1.d. Iron(II) Spectrophotometric Determinations

Note: The iron(II) analyses are expressed in percentages of the total iron concentrations, which are reported in A6.1.a.

Time	Percentage of Iron(II) over Total Iron							
(min)	Au-1	Au-2	Au-3	Au-4	Au-5	Au-6	Au-7	Au-8
0	0.00	0.00	0.00	0.00	0.00	0.00	0.00	0.00
8			2.92					2.92
15	4.88	4.54	4.67	3.92	3.92	4.25	3.75	4.75
30	7.68	6.99	7.25	6.08	6.41	6.58	6.41	7.24
45	9.47	9.10	9.27	7.91	8.40	8.24	8.40	9.40
60	11.26	11.20	11.17	9.73	10.23	10.07	10.07	11.23
75	13.04	12.80	12.85	11.39		11.73	11.73	12.89
90	14.49	14.71	14.42	12.89	13.22	12.89	13.22	14.38
120	17.20	17.19	16.98	15.38	16.04	15.55	15.55	16.71
150	19.08	19.81	19.03	17.54	18.37	17.54	17.87	18.87
180	20.94	20.47	20.71	19.53	19.86	19.37	19.86	
210	22.28	21.90	22.09	20.53	21.86	20.86	20.53	

Time	Percentage of Iron(II) over Total Iron							
(min)	Au-9	Au-10	Au-11	Au-12	Au-13	Au-14	Au-15	Au-16
0	0.00	0.00	0.00	0.00	0.00	0.00	0.00	0.00
8	2.92	2.92	2.76	0.10	0.60	1.26	5.91	5.58
15	4.75	4.75	4.42	0.27	1.10	2.09	8.57	8.90
30	7.24	7.41	7.08	0.60	1.76	3.26	11.89	12.22
45	9.23	9.23	9.28	0.76	2.26	4.15	13.89	13.55
60	11.06	11.06	11.06	0.93	2.76	4.92	15.21	15.21
75	12.72	12.72	12.89	1.10	2.92	5.75	16.38	16.21
90	14.22	14.22	14.60	1.18	3.26	6.58	17.21	17.04
120	16.71	16.71	17.21	1.43	3.92	8.07	18.70	18.37
150	18.70	18.87	19.20	1.59	4.42	9.57	19.53	19.53

Time	Percentage of Iron(II) over Total Iron							
(min)	Au-17	Au-18	Au-19	Au-20	Au-21	Au-22	Au-23	Au-24
0	0.00	0.00	0.00	0.00	0.00	0.00	0.00	0.00
8	5.58	0.82	0.45	0.60	0.24	5.12	3.68	1.70
15	8.24	2.38	1.29	1.10	0.42	8.77	6.35	2.61
30	11.73	5.12	2.70	1.76	0.79	14.62	10.57	3.98
45	13.72	7.86	3.37	2.26	1.06	17.91	13.38	5.08
60	15.05	9.68	4.10	2.76	1.15	20.65	15.35	6.27
75	16.04	11.24	4.67	2.92	1.33	21.92	17.31	7.27
90	16.88	12.70	5.23	3.26	1.52	23.39	19.00	8.28
120	18.54	15.16	6.35	3.92	1.79	25.21	21.53	10.10
150	19.53	17.36	7.20	4.42	2.06	27.04	23.22	11.84

Time (min)	Percentage of Iron(II) over Total Iron							
	Au-25	Au-26	Au-27	Au-28	Au-29	Au-30	Au-31	Au-32
0	0.00	0.00	0.00	0.00	0.00	0.00	0.00	0.00
1		0.10	12.72			1.42	0.93	18.58
4		0.76		0.76	1.91	4.06	3.57	
8	0.93	1.59	31.36	1.75	3.23	5.71	6.05	
15	1.42	2.41		2.75	4.88	9.00	8.85	56.76
30	2.41	4.22	46.37	4.39	8.15	14.41	14.44	63.67
45	3.24	5.70	56.46	5.87	11.09	19.13	20.02	71.25
60	3.90	7.40		7.35	13.36	22.35	22.94	77.89
75		8.63	76.30	8.49	15.94	24.89	27.49	83.17
90	5.38	9.59	80.13	9.79	18.01	27.76	32.34	86.78
120	6.52	11.52	87.12	11.90	22.14	30.93	34.19	89.80
150	7.99	14.72	89.46	14.54	24.29	34.29	41.53	90.57

Time (min)	Percentage of Iron(II) over Total Iron							
	Au-33	Au-34	Au-35	Au-36	Au-37	Au-38	Au-39	
0	0.00	0.00	0.00	0.00	0.00	0.00	0.00	
1	24.74	1.25	2.57	6.72	7.53	55.92	51.05	
4		5.87	10.97	17.63	18.08			
8	46.11	9.49	16.07	26.54	25.33	72.62	68.25	
15	55.65	13.77	22.97	36.52	36.67	84.32	82.54	
30	62.56	20.82	34.42	50.29	41.30	92.15	90.37	
45	71.51	26.87	36.91	53.47	48.43	94.21	92.43	
60	79.35	31.26	41.41	56.30	54.87	95.12	93.34	
75	85.17	33.65	46.21		58.99	95.25	93.47	
90	89.96	37.68	49.36	66.75	61.75	96.76	94.98	
120	93.14	43.42	54.00	68.04	69.26	98.18	96.40	
150		50.10	59.55	68.88	73.74		97.25	

A6.2. Runs at Constant Potential

A6.2.a. Experimental Conditions

Run Number	Initial Concentrations (mol/dm^3)			Potential (mV vs. SHE)
	SCN^-	Iron(III)	Iron(II)	
Au-40	0.275	0.0539	0.0011	703
Au-41	"	0.0495	0.0055	670
Au-42	"	0.044	0.011	650
Au-43	"	"	"	"
Au-44	0.10	0.0539	0.0011	735
Au-45	"	0.044	0.011	675

(1) Initial pH was 1.5, decreasing to a final value of c. a. 1.4.
(2) Temperature, 25ºC.
(3) Disc Rotating Speed, 720 rpm.

A6.2.b. Gold Dissolution Results

Note: Initial volume of liquid: 180 cm^3. Sample size: 5 cm^3.

Time (min)	Gold Dissolved (mg)					
	Au-40	Au-41	Au-42	Au-43	Au-44	Au-45
0	0.0000	0.0000	0.0000	0.0000	0.0000	0.0000
8	0.1319	0.0360	0.0505	0.0611	0.0683	0.0234
15	0.1962	0.0709	0.0809	0.0978	0.1015	0.0373
30	0.2892	0.1286	0.1297	0.1587	0.1479	0.0678
45	0.3591	0.1732	0.1638	0.1981	0.1858	0.0908
60	0.4188	0.2083	0.1966	0.2377	0.2145	0.1146
75	0.4627	0.2470	0.2268	0.2654	0.2392	0.1330
90	0.5084	0.2845	0.2529	0.2921	0.2667	0.1493
120	0.5892	0.3367	0.3021	0.3407	0.3085	0.1808
150	0.6680	0.3846	0.3510	0.3848	0.3461	0.2055

A6.3. Runs with Addition of Iodide or Iodine Solution

A6.3.a. Experimental Conditions

Run Number	Initial Concentrations (mol/dm^3)		
	SCN^-	I^-	I_2 Solution
Au-46	0	0.0022	0
Au-47	0	0.0055	0
Au-48	0	0.0110	0
Au-49	0.10	0.0022	0
Au-50	"	0.0055	0
Au-51	"	"	0
Au-52	"	0.0110	0
Au-53	0.05	0.0055	0
Au-54	0.10	0	0.001 N
Au-55	"	0	0.005 N

(1) Initial Iron(III) Concentration, 0.055 mol/dm^3.
(2) Initial pH was 1.5, decreasing to a final value of c. a. 1.4.
(3) Temperature, 25ºC.
(4) Disc Rotating Speed, 75.4 rad/s (720 rpm).

A6.3.b. Gold Dissolution Results

Note: Initial volume of liquid: 180 cm^3. Sample size: 5 cm^3.

Time (min)	Gold Dissolved (mg)					
	Au-46	Au-47	Au-48	Au-49	Au-50	Au-51
0	0.0000	0.0000	0.0000	0.0000	0.0000	0.0000
8	0.0462	0.1289	0.2798	0.6444	1.1894	1.2637
15	0.0840	0.2469	0.5336	0.9946	1.9196	2.0304
30	0.1757	0.5462	1.1250	1.5253	3.2462	3.3520
45	0.2722	0.8501	1.6892	1.9527	4.3042	4.4622
60	0.3560	1.1342	2.2642	2.2935	5.3052	5.4385
75	0.4322	1.3948	2.7652	2.6092	6.1567	6.3228
90	0.5070	1.6281	3.2048	2.9155	7.3717	7.6770
120	0.6294	2.0242	3.9926	3.4623	8.9749	9.2901
150	0.7331	2.3249	4.5732	3.9875	10.6220	10.7393

Time (min)	Gold Dissolved (mg)					
	Au-52	Au-53	Au-54	Au-55		
0	0.0000	0.0000	0.0000	0.0000		
8	1.5534	0.8975	0.7142	1.6065		
15	2.6652	1.5265	1.1367	2.6695		
30	4.7974	2.5710	1.8361	4.6096		
45	6.6765	3.4192	2.4298	6.2618		
60	8.4120	4.1832	2.9469	8.2320		
75	10.0688	4.8743	3.4323	9.7507		
90	11.6605	5.5048	3.8691	11.6081		
120	14.5740	6.6254	4.7055	14.3946		
150	17.3245	7.7666	5.4753	17.4979		

A6.3.c. Potential Readings

Time (min)	Potential (mV vs. SHE)							
	Au-46		Au-47		Au-48		Au-49	
	Au	Pt	Au	Pt	Au	Pt	Au	Pt
0	644	668	622	640	620	630	698	706
4					629	637	689	697
8	655	674	640	653	635	642	685	690
15	659	675	648	657	642	647	680	684
30	664	678	657	664	651	655	672	675
45	668	680	663	667	657	660	668	670
60	673	685	668	671	660	663	665	667
75	675	686	670	672	664	666	663	665
90	677	677	672	674	666	668	662	664
120	681	690	676	677	670	672	662	663
150	684	692	678	679	675	676	661	662

Time (min)	Potential (mV vs. SHE)							
	Au-50		Au-51		Au-52		Au-53	
	Au	Pt	Au	Pt	Au	Pt	Au	Pt
0	678	683	679	683	665	671	687	681
4	677	682	678	682	667	674	690	689
8	674	678	674	678	665	672	688	688
15	670	673	670	673	663	668	685	685
30	666	669	665	667	659	664	679	680
45	664	666	662	664	656	661	675	676
60	662	664	660	662	655	659	673	673
75	661	662	660	662	656	659	670	671
90	659	661	659	661	656	660	669	669
120	657	659	658	660	656	660	666	667
150	657	658	657	658	656	659	665	665

Time (min)	Potential (mV vs. SHE)							
	Au-54		Au-55					
	Au	Pt	Au	Pt	Au	Pt	Au	Pt
0	695	705	672	677				
4	691	697	672	679				
8	685	689	668	674				
15	681	685	664	670				
30	672	675	660	665				
45	668	670	658	662				
60	665	668	657	660				
75	663	664	657	660				
90	662	663	655	657				
120	661	662	655	657				
150	661	662	656	658				

A6.3.d. Iron(II) Spectrophotometric Determinations

Time (min)	Percentage of Iron(II) over Total Iron					
	Au-46	Au-47	Au-48	Au-49	Au-50	Au-51
0	0.00	0.00	0.00	0.00	0.00	0.00
1	0.10	0.60	1.42	2.59	4.74	5.41
4	0.26	1.09	2.74	5.91	10.36	10.40
8	0.43	1.59	3.56	9.07	14.66	15.05
15	0.59	2.09	4.38	13.39	20.11	19.70
30	0.92	2.75	5.85	19.03	25.38	25.01
45	1.08	3.40	7.15	22.85	28.56	28.17
60	1.24	3.56	7.63	25.51	30.94	30.16
75	1.40	3.89	8.10	28.00	32.87	31.82
90	1.56	4.21	8.73	30.33	34.31	33.32
120	1.72	5.02	9.82		36.12	35.98
150	1.87	5.50	10.80	34.48	37.19	37.14

Time (min)	Percentage of Iron(II) over Total Iron					
	Au-52	Au-53	Au-54	Au-55		
0	0.00	0.00	0.00	0.00		
1	11.50	3.42	1.92	4.25		
4	16.13	6.58	5.55	10.56		
8	18.44	9.57	8.86	14.28		
15	23.22	13.72	13.31	20.53		
30	26.83	20.20	18.74	26.01		
45	29.94	24.18	22.52	28.83		
60	31.56	27.17	25.63	30.99		
75	33.17	29.66	27.90	32.99		
90	34.45	31.66	29.84	34.81		
120	36.84	34.48	32.41	37.30		
150	39.05	36.81	34.96	38.47		

APPENDIX 7 - REAGENTS USED IN THE PRESENT WORK

Note: Unless otherwise specified, analytical grade reagents were used.

(1) Potassium Thiocyanate - M. W. 97.18
Minimum assay, 99.0 % - BDH Chemicals.

(2) Potassium Iodide - M. W. 166.00
Minimum assay, 99.8 % - BDH Chemicals.

(3) Iodine - At. W. 126.90
Minimum assay, 99.9 % - BDH Chemicals.

(4) Ammonium Iron(III) Sulphate, 12-hydrate - M. W. 482.18
Minimum assay, 99.0 % - BDH Chemicals.

(5) di-Ammonium Iron(II) Sulphate, 6-hydrate - M. W. 392.13
Minimum assay, 99.0 % - BDH Chemicals.

(6) Iron(III) Sulphate - M. W. 399.87
BDH Chemicals.

(7) Iron(II) Sulphate, 7-hydrate - M. W. 278.01
Minimum assay, 99.5 % - BDH Chemicals.

(8) Iron(III) Nitrate, 9-hydrate - M. W. 404.00
Minimum assay, 98.0 % - BDH Chemicals.

(9) Ammonium Acetate - M. W. 77.08
Minimum assay, 98.0 % - BDH Chemicals.

(10) Ammonium Fluoride - M. W. 37.04
Minimum assay, 95.0 % - BDH Chemicals.

(11) 1,10-Phenanthroline Hydrate - M. W. 198.22
Minimum assay, 99.5 % - BDH Chemicals.

(12) Formaldehyde Solution - M. W. 30.03
Assay, 37.0-40.0 % - BDH Chemicals.

(13) Acetonitrile - M. W. 41.05
Minimum assay, 99.5 % - BDH Chemicals.

(14) Silver Nitrate - M. W. 169.87
Minimum assay, 99.9 % - BDH Chemicals.

(15) Potassium Dichromate - M. W. 294.18
Minimum assay, 99.9 % - BDH Chemicals.

(16) Tin(II) Chloride, 2-hydrate - M. W. 225.63
Minimum assay, 97.0 % - BDH Chemicals.

(17) Mercury(II) Chloride - M. W. 271.50
Minimum assay, 99.5 % - BDH Chemicals.

(18) Diphenylaminesulphonic Acid Solution (Redox Indicator)
33.0 % w/w solution - BDH Chemicals.

(19) Sulphuric Acid - M. W. 98.07 - Sp. Gr. 1.84
Minimum assay, 98.0 % - BDH Chemicals.

(20) Hydrochloric Acid - M. W. 36.46 - Sp. Gr. 1.18
Minimum assay, 35.4 % - BDH Chemicals.

(21) Nitric Acid - M. W. 63.01 - Sp. Gr. 1.42
Minimum assay, 98.0 % - BDH Chemicals.

(22) Acetic Acid - M. W. 60.05
Minimum assay, 99.8 % - BDH Chemicals.

(23) Orthophosphoric Acid - M. W. 98.00
Minimum assay, 69.0-70.5 % - BDH Chemicals.

(24) Hydrogen Peroxide Solution - M. W. 34.01
About 30 % w/v H_2O_2 - BDH Chemicals.

(25) Potassium Permanganate 0.1 N 'Convol' - M. W. 158.03
BDH Chemicals.

(26) Gold Standard Solution (1000 ppm) 'SpectrosoL'
Solute: chloroauric acid. Matrix: HCl - BDH Chemicals.

(27) Sodium Carbonate, anhydrous - M. W. 105.99
Minimum assay, 99.9 % - BDH Chemicals.

(28) Sodium Hydroxide, pearl - M. W. 40.00
Minimum assay, 98.0 % - BDH Chemicals.

REFERENCES

1. Nicol, M. J., Fleming, C. A. and Paul, R. L., Chap. 15: The Chemistry of the Extraction of Gold, in "The Extractive Metallurgy of Gold in South Africa", Stanley, G. G., ed., The Chamber of Mines of South Africa, Johannesburg, 1987, Vol. 2, 517 pp.

2. White, H. A., The Solubility of Gold in Thiosulphates and Thiocyanates, *The Journal of the Chem. Metall. and Min. Soc. of S. Africa*, **6**, 109-111 (1905).

3. Fleming, C. A., A Process for Simultaneous Recovery of Gold and Uranium from South African Ores, in "Gold 100 - Procedings of the International Conference on Gold. Volume 2: Extractive Metallurgy of Gold", S. Afr. Inst. Min. Metall., Johannesburg, 1986, pp. 301-319.

4. Finkelstein, N. P., Chap. 10: The Chemistry of the Extraction of Gold from its Ores, in "Gold Metallurgy in South Africa", Adamson, R. J., ed., Chamber of Mines of S. Africa, Cape Town, 1972, 452 pp.

5. Finkelstein, N. P. and Hancock, R. D., A New Approach to the Chemistry of Gold, *Gold Bulletin*, **7** (3) 72-77 (1974).

6. Nicol, M. J., The Anodic Behaviour of Gold. Part I. Oxidation in Acidic Solutions, *Gold Bulletin*, **13** (2) 46-55 (1980).

7. Nicol, M. J., The Anodic Behaviour of Gold. Part II. Oxidation in Alkaline Solutions, *Gold Bulletin*, **13** (3) 105-111 (1980).

8. Nicol, M. J., Fleming, C. A. and Preston, J. S., Chap. 63: Application to Extractive Metallurgy, in "Comprehensive Coordination Chemistry - Vol. 6", Wilkinson, G., Gillard, R. D. and McCleverty, J. A., eds., Pergamon Press, Oxford, 1987.

9. Hill, S. D., Summary of Bureau of Mines Research on Improved Precious Metals Recovery for Conventional Processing Facilities, in "Practical Hydromet'83 - 7th AIME Annual Symposium on Uranium and Precious Metals", Colorado, USA, August 22-24, 1983.

10. Avraamides, J., Prospects for Alternative Leaching Systems for Gold: a Review, in "Carbon-in-Pulp Technology for the Extraction of Gold", Austr. I.M.M., July 1982, pp.379-398.

11. Barbosa Fº, O. and Monhemius, A. J., Thermochemistry of Thiocyanate Systems for Leaching Gold and Silver Ores, in: "Precious Metals'89", Jha, M. C. and Hill, S. D., eds., TMS-AIME, U.S.A., 1989, pp.307-357.

12. Bard, A. J., Parsons, R. and Jordan, J., eds., "Standard Potentials in Aqueous Solution", Marcel Dekker, Inc., New York and Basel, 1985, 834 pp.

13. Wagman, D. D. et al., "Selected Values of Chemical Thermodynamic Properties", Nat. Bur. Stand. Tech. Note 270-3, U.S. Government Printing Office, Washington, D.C., 1968.

14. Wagman, D. D. et al., "Selected Values of Chemical Thermodynamic Properties", Nat. Bur. Stand. Tech. Note 270-4, U.S. Government Printing Office, Washington, D.C., 1969.

15. Wagman, D. D. et al., "The NBS Tables of Chemical Thermodynamic Properties", Nat. Bur. of Standards, U.S.A., 1982.

16. Smith, R. M. and Martell, A. E., "Critical Stability Constants - Vol. 4: Inorganic Complexes", Plenum Press, New York, 1976, 257 pp.

17. Pourbaix, M., ed., "Atlas d'Equilibres Electrochimiques à 25ºC", Gauthier-Villars, Paris, 1963.

18. Sillén, L. G. and Martell, A. E., "Stability Constants of Metal-Ion Complexes", Special Publication No. 17, The Chemical Society, London, 1964.

19. Latimer, W. M., "The Oxidation States of the Elements and their Potentials in Aqueous Solutions", 2nd ed., Prentice-Hall, Englewood Cliffs, N.J., 1952, 392 pp.

20. Kiehl, C., Bestimmung der Stabilitätskonstanten von in wäbriger Lösung existierenden Komplexverbindungen zwischen Gold (1+) - und Rhodanidionen, *Z. Phys. Chem. (Leipzig)*, **232**, 384-390 (1966).

21. Vasilev, V. P. and Mukhina, P. S., Equilibria in Aqueous Solutions of Thiocyanato-Complexes of Iron, *Russian J. Inorg. Chem.*, **9** (5), 620 - 623 (1964).

22. Korondan, I. and Nagypal, I., NMR Relaxation Studies in Solutions of Transition Metal Complexes. X. The Stepwise Equilibria in the Iron (III) - Thiocyanate System Studied by NMR Relaxation, *Inorg. Chim. Acta*, **73**, 131-134 (1983).

23. Jolly, W. L., "The Inorganic Chemistry of Nitrogen", Benjamin Inc., New York, 1964, 124 pp.

24. Jensen, M. B., On the Kinetics of the Decomposition of Cyanic Acid, *Acta Chemica Scandinavica*, **12**, 1657-1670 (1958).

25. Amell, A. R., Kinetics of the Hydrolysis of Cyanic Acid, *J. Am. Ch. Soc.*, **78**, 6234-6238 (1956).

26. Kemp, I. A. and Kohnstam, G., The Decomposition of Inorganic Cyanates in Water, *J. Chem. Soc.*, 900-911 (1956).

27. Warner, J. C. and Stitt, F. B., The Conversion of Ammonium Cyanate into Urea. Mechanism and Kinetic Salt Effect, *J. Am. Chem. Soc.*, **55**, 4087-4812 (1933).

28. Hughes, M. N., Chap. 1: General Chemistry, in "Chemistry and Biochemistry of Thiocyanic Acid and its Derivatives", Newman, A. A., ed., Academic Press, New York and London, 1975, pp. 1 - 67.

29. Burmeister, J. L., Chap. 2: Coordination Chemistry, in "Chemistry and Biochemistry of Thiocyanic Acid and its Derivatives", Newman, A. A., ed., Academic Press, New York and London, 1975, pp. 68 - 130.

30. Griffith, W. P., Chap IV: Nitrogen Ligands, in "Developments in Inorganic Nitrogen Chemistry - Vol. 1", Colburn, C. B., ed., Elsevier, Amsterdam, 1966.

31. Golub, A. M., Köhler, H. and Skopenko, V. V., eds., "Chemistry of Pseudohalides", Elsevier, Amsterdam, 1986, 479 pp.

32. Boughton, J. H. and Keller, R. N., Dissociation Constants of Hydropseudohalic Acids, *J. Inorg. Nucl. Chem.*, **28**, 2851-2859 (1966).

33. Suzuki, T. and Hagisawa, H., *Bull. Inst. Phys. Chem. Res. (Tokyo)*, **21**, 601 (1942); Chem Abstr. 43, 2074 (1949).

34. Morgan, T. D. B., Stedman, G. and Whincup, P. A. E., The Ionisation Constant of Thiocyanic Acid, *J. Chem. Soc.*, 4813-4822 (1965).

35. Crowell, T. I. and Hankins, M. G., The Hydrolysis of Thiocyanic Acid. I. Dependence of Rate on Acidity Function, *J. Phys. Chem.*, **73**, 1380 - 1383 (1969).

36. Wilson, I. R. and Harris, G. M., The Oxidation of Thiocyanate Ion by Hydrogen Peroxide. I. The pH-Independent Reaction, *J. Am. Chem. Soc.*, **82**, 4515-4517 (1960).

37. Wilson, I. R. and Harris, G. M., The Oxidation of Thiocyanate Ion by Hydrogen Peroxide. II. The Acid-catalyzed Reaction, *J. Am. Chem. Soc.*, **83**, 286-289 (1961).

38. Smith, R. H. and Wilson, I. R., The Mechanism of the Oxidation of Thiocyanate Ion by Peroxomonosulphate in Aqueous Solution. I.Stoicheiometry of the Reaction, *Aust. J. Chem.*, **19**, 1357-1363 (1966).

39. Smith, R. H. and Wilson, I. R., The Mechanism of the Oxidation of Thiocyanate Ion by Peroxomonosulphate in Aqueous Solution. II. Kinetics of the Reaction, *Aust. J. Chem.*, **19**, 1365-1375 (1966).

40. Smith, R. H. and Wilson, I. R., The Mechanism of the Oxidation of Thiocyanate Ion by Peroxomonosulphate in Aqueous Solution. III.Interpretation of Results, *Aust. J. Chem.*, **20**, 1353-1366 (1967).

41. Betts, R. H. and Dainton, F. S., Electron Transfer and Other Processes Involved in the Spontaneous Bleaching of Acidified Aqueous Solutions of Ferric Thiocyanate, *J. Am. Chem. Soc.*, **75**, 5721-5727 (1953).

42. Stedman, G. and Whincup, P. A. E., Oxidation of Metal Thiocyanates by Nitric and Nitrous Acids. Part I: Products, *J. Chem. Soc. (A)*, 1145-1148 (1969).

43. Hughes, M. N., Phillips, E. D., Stedman, G. and Whincup, P. A. E., Oxidation of Metal Thiocyanates by Nitric and Nitrous Acids. Part II: Kinetics, *J. Chem. Soc. (A)*, 1148-1151 (1969).

44. Muralikrishna, U. and Bapanaiah, K. V., Kinetics of the Oxidation of Thiocyanate by Chromic Acid, *Z. Phys. Chemie, Leipzig,* **255** (1) 16-22 (1974).

45. Stanbury, D. M., Wilmarth, W. K., Khalaf, S., Po, H. N. and Byrd, J. E., Oxidation of Thiocyanate and Iodide by Iridium (IV), *Inorg. Chem.*,**19**, 2715-2722 (1980).

46. Ng, F. T. T. and Henry, P. M., Kinetics and Mechanism of the Oxidation of Thiocyanate by Tris(1,10-phenanthroline)iron(III) and its Derivatives, *Can. J. Chem.*, **53** (22) 3319-3326 (1975).

47. Gauguin, R., Etude Potentiométrique des Propriétés Réductrices de l'Ion Thiocyanique, *J. Chim. Phys.*, **42**, 136-148 (1945).

48. Gauguin, R., Propriétés Réductrices des Ions Thiocyaniques et Cyanidriques; Remarques sur les Potentiels d'Oxydo-Réduction des Systemes Irréversibles, *Annal. Chim. Phys.* (12) **4**, 832-880 (1949).

49. Gauguin, R., Oxydation Electrochimique de l'Ion Thiocyanique; Application aux Dosages et à l'Etude des Réactions, *Anal. Chim. Acta,* **5**, 200-214 (1951).

50. Nicholson, M. M., Voltammetry of Thiocyanate Ion at the Stationary Platinum Electrode, *Analytical Chemistry*, **31** (1) 128-132 (1959).

51. Bjerrum, N. and Kirschner, A., Die Rhodanide des Goldes und das Freie Rhodan, *Kongelige Dansk Videnskabernes Selskab.,* **8** (1) 1-77 (1918); Thiocyanates of Gold and Free Thiocyanogen, *Chemical Abstracts*, **13**, 1057-1060 (1919).

52. Kerr, D. F. and Wilson, I. R., Reaction of Sulphur Dicyanide with Thiocyanate Ion, *J. Chem. Soc. (Dalton Trans.)*, 459-461 (1973).

53. Kitching, W., Smith, R. H. and Wilson, I. R., Kinetics of the Decomposition of Sulphur Dicyanide in Aqueous Solution, *Austral. J. Chem.*, **15**, 211-217 (1962).

54. Muylder, J. and Pourbaix, M., Sec. 14.3: Or, in "Atlas d'Equilibres Electrochimiques à 25°C", Pourbaix, M., ed., Gauthier-Villars, Paris, 1962.

55. Puddephatt, R. J., "The Chemistry of Gold", Elsevier, Amsterdam, 1978, 274 pp.

56. Schmid, G. M. and Curley-Fiorino, M. E., Chap. IV-3: Gold, in"Encyclopedia of Electrochemistry of the Elements - Vol. IV", Bard, A. J., ed., Marcel Dekker, Inc., New York and Basel, 1975.

57. Vanleugenhaghe, C., Pourbaix, M. and Rysselberghe, P., Sec. 14.2: Argent, in "Atlas d'Equilibres Electrochimiques à 25°C", Pourbaix, M., ed., Gauthier-Villars, Paris, 1963.

58. Shumilova, N. A. and Zhutaeva, G. V., Chap. VIII-1: Silver, in "Encyclopedia of Electrochemistry of the Elements - Vol. VIII", Bard, A. J., ed., Marcel Dekker, Inc., New York and Basel, 1978.

59. Randin, J. P., Chap. VII-1: Carbon, in "Encyclopedia of Electrochemistry of the Elements - Vol. VII", Bard, A.J., ed., Marcel Dekker, Inc., New York and Basel, 1976, pp. 206-221.

60. Pouradier, J. and Gadet, M., Electrochimie des Sels d'Or. VI. Acides Auro et Aurothiocyaniques et Sels Correspondants, *J. Chim. Phys.*, **63**, 1467-1473 (1966).

61. Goolsby, A. D. and Sawyer, D. T., Electrochemistry of Gold(I) and its Complexes in Acetonitrile, *Anal. Chem.*, **40** (13), 1978-1983 (1968).

62. Söderbäck, E., Studien über Freie Rhodan, *Ann. Chem., Liebigs.*, **419**, 217-322 (1919).

63. Seel, F. and Wesemann, D., Eine neue Darstellungsweise für Dirhodan, *Chem. Ber.*, **86**, 1107-1110 (1953).

64. Seel, F. and Müller, E., Zur Kenntnis des Rhodans und seiner Verbindungen, *Chem. Ber.*, **88**, 1747-1755 (1955).

65. Angus, A. B. and Bacon, R. G. R., Thiocyanogen Chloride. Part I. Chemical Evidence of the Existence of the Monomeric Compound in Solutions in Organic Solvents, *J. Chem. Soc.*, 774-778 (1958).

66. Bacon, R. G. R. and Irwin, R. S., Thiocyanogen Chloride. Part II. Some Physical Properties of its Solutions, *J. Chem. Soc.*, 778-784 (1958).

67. Nelson, M. J. and Pullin, A. D. E., The Infrared Spectrum of Thiocyanogen and Thiocyanogen Halides, *J. Chem. Soc.*, 604-612 (1960).

68. Vanderzee, C. E. and Quist, A. S., Thiocyanogen: Its Spectra and Heat of Formation in Relation to Structure, *Inorganic Chemistry*, **5** (7) 1238-1242 (1966).

69. Gardner, W. H. and Weinberger, H., Thiocyanogen Solution, *Inorg. Synth.*, **1**, 84-86 (1939).

70. Kerstein, H. and Hoffmann, R., Gewinnung von freiem Rhodan aus Alkalirhodaniden durch Elektrolyse, *Chem. Ber.*, **57** (1) 491-496 (1924).

71. Söderbäck, E., Über Katalytische Rhodanierung von Aromatischen Kernen, *Acta Chemica Scandinavica*, **8**, 1851-1858 (1954).

72. Schöneshöfer, Von M., Beck, G. and Henglein, A., Pulsradiolytische Untersuchung der Hydrolyse des Dirhodans, *Ber. Bunsen-Ger. Phys. Chem.*, **74**, 1011-1015 (1970).

73. Baxendale, J. H., Bevan, P. L. T. and Stott, D. A., Pulse Radiolysis of Aqueous Thiocyanate and Iodide Solutions, *Trans. Far. Soc.*, **64** (3) 2389-2397 (1968).

74. Nord, G., Pedersen, B., Floryan-Lφvborg, E. and Pagsberg, P., Pulse Radiolysis Study of the Rates of Reaction of the I_2^- and $(SCN)_2^-$ Radical Anions with the Tris(2,2'-bipyridyl)^2 Complexes of Os(II) and Os(III), *Inorg. Chem.*, **21**, 2327-2330 (1982).

75. Duonghong, D., Ramsden, J. and Grätzel, M., Dynamics of Interfacial Electron-Transfer Processes in Colloidal Semiconductor Systems, *J. Am. Chem. Soc.*, **104**, 2977-2985 (1982).

76. Behar, D., Bevan, P. L. T. and Scholes, G., Pulse Radiolysis of Aqueous Thiocyanate Solutions. Nature of the Intermediate Transient Species, *J. Phys. Chem.*, **76** (11) 1537-1542 (1972).

77. Schöneshöfer, Von M. and Henglein, A., Pulsradiolytische Untersuchung der Dissoziationsgleichgewichte des gemischten Radikal-Anion-Komplexes $BrSCN^-$, *Ber. Bunsenges. Phys. Chem.*, **73**, 289-293 (1969).

78. Adams, G. E., Boag, J. W., Currant, J. and Michael, B. D., "Pulse Radiolysis", Academic Press, New York, 1965.

79. Pikaev, A. K., "Pulse Radiolysis of Water and Aqueous Solutions", Indiana University Press, 1967, 295 pp.

80. Matheson, M. S. and Dorfman, L. M., "Pulse Radiolysis", The M. I. T. Press, Cambridge, MA, U. S. A., 1969, 202 pp.

81. Pereiro, R., Arvía, A. J. and Calandra, A. J., Kinetics of the SCN^- /$(SCN)_2$ Couple on Platinum in Acetonitrile, *Electrochimica Acta*, **17**, 1723-1734 (1972).

82. Martinez, C., Calandra, A. J. and Arvía, A. J., The Anodic Oxidation of Thiocyanate Ion Dissolved as KSCN in Dimethylsulphoxide, *Electrochimica Acta*, **17**, 2153-2179 (1972).

83. Holtzen, D. A. and Allen, A. S., Kinetic Parameters for the Anodic Oxidation of Thiocyanate at the Glassy Carbon Electrode, *Analytica Chimica Acta*, **69**, 153-160 (1974).

84. Cauquis, G. and Pierre, G., La Formation Transitoire de l'Ion Complexe $(SCN)_3^-$ au Cours de l'Oxidation Electrochimique de l'Ion Thiocyanate dans l'Acétonitrile, *Bull. Soc. Chim. France*, **6**, 2244 (1972).

85. Cauquis, G. and Pierre, G., L'Oxidation Electrochimique de l'Ion Sélénocyanate en Milieu Organique. Existence d'un Complexe $(SeCN)_3^-$, *Bull. Soc. Chim. France*, **3**, 1225-1228 (1972).

86. Cauquis, G. and Pierre, G., Le Propriétés Electrochimiques de l'Ion Thiocyanate et du Thiocyanogène au Sein de l'Acetonitrile et la Thiocyanation par Voie Electrochimique, *C. R. Acad. Sci. Paris*, **266** (C), 883-886 (1968).

87. Martins, M. E., Castellano, C., Calandra, A. J. and Arvía, A. J., The Electrochemistry of Gold in Acetonitrile Solutions Containing Thiocyanate Ions, *J. Electroanal. Chem.*, **81**, 291-300 (1977).

88. Martins, M. E., Castellano, C., Calandra, A. J. and Arvía, A. J., Electrochemical Kinetics of Gold Electrodes in SCN^- /Dimethylsulfoxide Solutions, *J. Electroanal. Chem.*, **92**, 45-53 (1978).

89. Gallego, J. H., Castellano, C. E., Calandra, A. J. and Arvía, A. J., The Electrochemistry of Gold in Acid Aqueous Solutions Containing Chloride Ions, *J. Electroanal. Chem.*, **66**, 207-230 (1975).

90. Itabashi, E., Identification of Electrooxidation Products of Thiocyanate Ion in Acidic Solutions by Thin-Layer Spectroelectrochemistry, *J. Electroanal. Chem.*, **177**, 311-315 (1984).

91. Itabashi, E., Spectroelectrochemical Characterization of Iron(III)-Thiocyanate Complexes in Acidic Thiocyanate Solutions at an Optically Transparent Thin-Layer-Electrode Cell, *Inorg. Chem.*, **24**, 4024-4027 (1985).

92. Sandell, E. B., "Colorimetric Determination of Traces of Metals", 3rd. ed., Interscience Publishers Inc., New York, 1965.

93. Miyake, C., Magnetic and Spectrophotometric Studies on Decoloration of Thiocyanate Iron (III) Complexes in Solutions. I, *Bull. Chem. Soc. Japan*, **33**, 867-871 (1960).

94. Miyake, C., Magnetic and Spectrophotometric Studies on Decoloration of Thiocyanate Iron (III) Complexes in Solutions. II. Effect of Acids, *Bull. Chem. Soc. Japan*, **34**, 471-474 (1961).

95. Miyake, C., Magnetic and Spectrophotometric Studies on Decoloration of Thiocyanate Iron (III) Complexes in Solutions. III. Structure of Thiocyanatoiron (III) Complex in Organic Solvents, *Bull. Chem. Soc. Japan*, **34**, 475-476 (1961).

96. Mussini, T. and Faita, G., Chap. I-1: Chlorine, in: "Encyclopedia of Electrochemistry of the Elements - Vol. I", Bard, A. J., ed., Marcel Dekker, Inc., New York, 1973.

97. Mussini, T. and Faita, G., Chap. I-2: Bromine, in: "Encyclopedia of Electrochemistry of the Elements - Vol. I", Bard, A. J., ed., Marcel Dekker, Inc., New York, 1973.

98. Desideri, P. G., Lepri, L. and Heimler, D., Chap. I-3: Iodine and Astatine, in: "Encyclopedia of Electrochemistry of the Elements - Vol. I", Bard, A. J., ed., Marcel Dekker, Inc., New York, 1973.

99. Raspi, G., Pergola, F. and Cozzi, D., Anodic Oxidation of Chlorides, Bromides and Iodides on a Platinum Microelectrode with Periodical Renewal of the Diffusion Layer, *J. Electroanal. Chem.*, **15**, 35-48 (1967).

100. Kolthoff, I. M. and Coetzee, J. F., Polarography in Acetonitrile. II. Metal Ions Which Have Significantly Different Polarographic Properties in Acetonitrile and Water. Anodic Waves. Voltammetry at Rotating Platinum Electrode, *J. Am. Chem. Soc.*, **79**, 1852-1858 (1957).

101. Marchon, J. C., Potentiels d'Oxydoréduction d'Ions Halogénures e Trihalogénures dans le Nitrométhane et l'Acétonitrile, *C. R. Acad. Sci. Paris*, **267** (C) 1123-1126 (1968).

102. Nelson, I. V. and Iwamoto, R. T., Voltammetric Evaluation of the Stability of Trichloride, Tribromide, and Triiodide Ions in Nitromethane, Acetone, and Acetonitrile, *J. Electroanal. Chem.*, **7**, 218-221 (1964).

103. Zimmerman, G. and Strong, F. C., Equilibria and Spectra of Aqueous Chloride Solutions, *J. Am. Chem. Soc.*, **79**, 2063-2066 (1957).

104. Cerquetti, A., Longhi, P., Mussini, T. and Natta, G., Thermodynamics of the $Cl_2/Cl^-/Cl_3^-$ System in Aqueous Solution, *J. Electroanal. Chem.*, **20**, 411-418 (1969).

105. Sherrill, M. S. and Izard, E. F., The Solubility of Chlorine in Aqueous Solutions of Chlorides and the Free Energy of Trichloride Ion, *J. Am. Chem. Soc.*, **53**, 1667-1674 (1931).

106. Cerquetti, A., Longhi, P. and Mussini, T., Thermodynamics of Aqueous Hydrochloric Acid from E.M.F.'s of Hydrogen-Chlorine Cells, *J. Chem. Eng. Data*, **13** (4) 458-461 (1968).

107. Faita, G., Longhi, P. and Mussini, T., Standard Potentials of the Cl_2/Cl^- Electrode at Various Temperatures with Related Thermodynamic Functions, *J. Electrochem. Soc.*, **114** (4) 340-343 (1967).

108. Sereno, L., Macagno, V. A. and Giordano, M. C., Electrochemical Behaviour of the Chloride/Chlorine System at Platinum Electrodes in Acetonitrile Solutions, *Electrochimica Acta*, **17**, 561-575 (1972).

109. Iwasita, T. and Giordano, M. C., Kinetics of the Bromine-Tribromide-Bromide Redox Processes on Platinum Electrodes in Acetonitrile Solutions, *Electrochimica Acta*, **14**, 1045-1059 (1969).

110. Iwamoto, R. T., Solvent Effects on the Electrooxidation of Iodide Ion, *Analyt. Chem.*, **31**, 955 (1959)

111. Popov, A. I. and Geske, D. H., Studies on the Chemistry of Halogen and Polyhalides. XVI. Voltammetry of Bromine and Interhalogen Species in Acetonitrile, *J. Am. Chem. Soc.*, **80**, 5346-5349 (1958).

112. Toren, E. C. and Driscoll, C. P., Polarographic Study of the Iodine-Iodide Couple at the Rotating Platinum Electrode, *Analyt. Chem.*, **38**, 872-876 (1966).

113. Katzin, L. I. and Gebert, E., The Iodide-Iodine-Triiodide Equilibrium and Ion Activity Coefficient Ratios, *J. Am. Chem. Soc.*, **77**, 5814-5819 (1955).

114. Kolthoff, I. M. and Jordan, J., Voltammetry of Iodine and Iodide at Rotated Platinum Wire Electrodes, *J. Am. Chem. Soc.*, **75**, 1571-1575 (1953).

115. Popov, A. I. and Geske, D. H., Studies on the Chemistry of Halogen and of Polyhalides. XIII. Voltametry of Iodine Species in Acetonitrile, *J. Amer. Chem. Soc.*, **80**, 1340 (1958).

116. Dané, L. M., Janssen, J. J. and Hoogland, J. G., The Iodine-Iodide Redox Couple at a Platinum Electrode, *Electrochimica Acta*,**13**, 507-518 (1968).

117. Giordano, M. C., Bazán, J. C. and Arvía, A. J., Study of the Iodide-Tri-Iodide Redox Electrode in Dimethylsulphoxide, *Electrochimica Acta*, **11**, 1553-1578 (1966).

118. Macagno, V. A. and Giordano, M. C., Kinetics and Mechanisms of Electrochemical Reactions on Platinum with Solutions of Iodine-Sodium Iodide in Acetonitrile, *Electrochimica Acta*, **14**, 335-357 (1969).

119. Arvia, A. J., Giordano, M. C. and Podestá, J. J.,Kinetics and Mechanisms of Electrochemical Reactions on Platinum with Solutions of Iodine-Sodium Iodide in Dimethylsulphoxide, *Electrochimica Acta*, **14**, 389-403 (1969).

120. Bent, H. E. and French, C. L., The Structure of Ferric Thiocyanate and its Dissociation in Aqueous Solution, *J. Am. Chem. Soc.*, **63**, 568-572 (1941).

121. Mϕller, M., *Kem. Maanedsblad*, **18**, 138-140 (1937); Investigation of Aqueous Solutions of Iron Thiocyanate, *Chemical Abstracts*, **33**, 9179 (1939)

122. Edmonds, S. M. and Birnbaum, N., Ferric Thiocyanate, *J. Am. Chem. Soc.*, **63**, 1471-1472 (1941).

123. Schlesinger, H. I., Ferric Thiocyanate, *J. Am. Chem. Soc.*, **63**, 1765-1767 (1941).

124. Gould, R. K. and Vosburgh, W. C., Complex Ions III. A Study of Some Complex Ions in Solution by Means of the Spectrophotometer, *J. Am. Chem. Soc.*, **64**, 1630-1634 (1942).

125. Frank, H. S. and Oswalt, R., The Stability and Light Absorption of the Complex Ion $FeSCN^{++}$, *J. Am. Chem. Soc.*, **69**, 1321-1325 (1947).

126. Polchlopek, S. E. and Smith, J. H., Composition of Ferric Thiocyanate at High Concentrations, *J. Am. Chem. Soc.*, **71**, 3280-3283 (1949).

127. Lewin, S. Z. and Wagner, R. S., The Nature of Iron(III) Thiocyanate in Solution, *J. Chem. Education*, **30**, 445-450 (1953).

128. Perrin, D. D., The Ion $Fe(CNS)^{2+}$. Its Association Constant and Absorption Spectrum, *J. Am. Chem. Soc.*, **80**, 3852-3856 (1958).

129. Mironov, V. E. and Rutkovskii, Yu. I., Distribution of Iron(III) between Aqueous Salt Solutions and Ether, *Russian J. Inorg. Chem.*, **10** (5) 580-583 (1965).

130. Mironov, V. E. and Rutkovskii, Yu. I., Thiocyanato-Complexes of Iron(III), *Russian J. Inorg. Chem.*, **10** (12) 1450-1453 (1965).

131. Sultan, S. M. and Bishop, E., A Study of the Formation and Stability of the Iron(III)-Thiocyanate Complex in Acidic Media, *Analyst*, **107**, 1060-1064 (1982).

132. Below, J. F., Jr., Connick, R. E. and Coppel, C. P., Kinetics of the Formation of the Ferric Thiocyanate Complex, *J. Am. Chem. Soc.*, **80**, 2961-2967 (1958).

133. Goodall, D. M., Harrison, P. W., Hardy, M. J. and Kirk, C. J., Relaxation Kinetics of Ferric Thiocyanate, *J. Chem. Education*, **49**, 675-678 (1972).

134. Butler, J. N., "Ionic Equilibrium: A Mathematical Approach", Addison-Wesley, Reading, MA, 1964, 547 pp.

135. Stumm, W. and Morgan, J. J., "Aquatic Chemistry", John Wiley, 1981, 780 pp.

136. Kolthoff, I. M., Sandell, E. B., Meehan, E. J. and Bruckenstein, S., "Quantitative Chemical Analysis", The Macmillan Co., London, 1969, 1199 pp.

137. Ellis, K. J. and Laurence, G. S., Photolysis of $FeSCN^{2+}$ Complex Ion in Aqueous Solution, *Trans. Far. Soc.*, **63**, 91-100 (1967).

138. Yatsimirskii, K. B. and Korableva, V. D., Thiocyanate Complexes of Manganese, Iron, Cobalt and Nickel, *J. Inorg. Chem. USSR*, **3** (2), 139-148 (1958); *Zhur. Neorg. Khim.*, **3**, 339 (1958).

139. Conocchioli, T. J. and Sutin, N., The Kinetics of the Iron(II)-Catalyzed Dissociation of the Monothiocyanate Complex of Iron(III), *J. Am. Chem. Soc.*, **89**, 282-286 (1967).

140. ZoBell, C. E., Studies on the Redox Potential of Marine Sediments, *Bull. Amer. Assoc. Petr. Geol.*, **30** (4), 477-513 (1946).

141. Natarajan, K. A. and Iwasaki, I., Eh Measurements in Hydrometallurgical Systems, *Minerals Sci. Eng.*, **6** (1), 35-44 (1974).

142. Vogel, A. I., " A Text-Book of Quantitative Inorganic Analysis", 3rd. edn., Longmans, London, 1961, 1216 pp.

143. Belcher, R. and Nutten, A. J., "Quantitative Inorganic Analysis", 3rd edn., Butterworths, London, 1970, 425 pp.

144. Williams, W. J., "Handbook of Anion Determination", Butterworths, London, 1979, 630 pp.

145. Charlot, G., "Les Méthodes de la Chimie Analytique. Analyse Quantitative Minérale", 5th. edn., Masson et C^{ie} Éditeurs, Paris, 1966, 1023 pp.

146. Fortune, W. B. and Mellon, M. G., Determination of Iron with o-Phenanthroline, *Ind. Eng. Chem., Anal. Ed.*, **10**, 60-64 (1938).

147. Commission on Spectrochemical and other Optical Methods for Analysis, International Union of Pure and Applied Chemistry, "Tables of Spectrophotometric Absorption Data of Compounds used for the Colorimetric Determination of Elements", Butterworths, London, 1963, 626 pp.

148. Burkin, A. R., "The Chemistry of Hydrometallurgical Processes", E. & F. Spon Ltd., London, 1966, 157 pp.

149. Flynn, Jr., C. M., Hydrolysis of Inorganic Iron(III) Salts, *Chem. Rev.*, **84**, 31-41 (1984).

150. Basolo, F. and Pearson, R. G., "Mechanisms of Inorganic Reactions: A Study of Metal Complexes in Solution", 2nd Ed., John Wiley & Sons, Inc., New York, 1967, 701 pp.

151. Halpern, J., Mechanisms of Electron Transfer and Related Processes in Solution, *Quart. Rev.*, **15**, 207-236 (1961).

152. Southhampton Electrochemistry Group, "Instrumental Methods in Electrochemistry", Ellis Horwood Ltd., Chichester, U. K., 1985, 443 pp.

153. Kastle, J. H. and Smith, C. R., On the Oxidation of Sulphocyanic Acid and its Salts by Hydrogen Peroxide, *Am. Chem. journal*, **32**, 376-385 (1904).

154. Sant, B. R., Kinetics of the Oxidation of Thiocyanate by Hydrogen Peroxide, *Naturwissenschaften*, **44**, 180 (1957).

155. Harber, F. and Weiss, J., The Catalytic Decomposition of Hydrogen Peroxide by Iron Salts, *Proc. Royal Soc. London*, **147**(A), 332-351 (1934).

156. Medalia, A. I. and Kolthoff, I. M., Redox Recipes. I. Reaction between Ferrous Iron and Peroxides. General Considerations, *J. Polymer Sci.*, **4**, 377-398 (1949).

157. Kolthoff, I. M. and Medalia, A. I., The Reaction between Ferrous Iron and Peroxides. I. Reaction with Hydrogen Peroxide in the Absence of Oxygen, *J. Am. Chem. Soc.*, **71**, 3777-3783 (1949).

158. Kolthoff, I. M. and Medalia, A. I., The Reaction between Ferrous Iron and Peroxides. II. Reaction with Hydrogen Peroxide in the Presence of Oxygen, *J. Am. Chem. Soc.*, **71**, 3784-3788 (1949).

159. Barb, W. G., Baxendale, J. H., George, P. and Hargrave, K. R., Reactions of Ferrous and Ferric Ions with Hydrogen Peroxide. Part I - The Ferrous Ion Reaction, *Trans. Far. Soc.*, **47**, 462-500 (1963).

160. Sobkowski, J., The Kinetics of Oxidation of Ferrous Ions by Hydrogen Peroxide in Perchloric, Sulphuric, and Phosphoric Acid Solutions, *Roczniki Chemii Ann. Soc. Chim. Polonorum*, **36**, 1503-1510 (1962).

161. Lindsay Smith, J. R. and Norman, R. O. C., Hydroxylation. Part I. The Oxidation of Benzene and Toluene by Fenton's Reagent, *J. Chem. Soc.*, 2897-2905 (1963).

162. Walling, C. and Kato, S., The Oxidation of Alcohols by Fenton's Reagent. The Effect of Copper Ion, *J. Am. Chem. Soc.*, **93**, 4275-4281 (1971).

163. Walling, C., El-Taliawi, G. M., and Johnson, R. A., Fenton's Reagent. IV. Structure and Reactivity Relations in the Reactions of Hydroxyl Radicals and the Redox Reactions of Radicals, *J. Am. Chem. Soc.*, **96**, 133-139 (1974).

164. Fenton, H. J. H., *J. Chem. Soc.*, **65**, 899 (1894) (quoted in reference 156).

165. Bailey, R. and Boltz, D. F., Differential Spectrophotometric Determination of Hydrogen Peroxide Using 1,10-Phenanthroline and Bathophenanthroline, *Anal. Chem.*, **31**, 117-119 (1959).

166. Bruckenstein, S., Sharkey, J., and Yip, J. Y., Effect of Polishing with Different Size Abrasives on the Current Response at a Rotating Disk Electrode, *Anal. Chem.*, **57**, 368-371 (1985).

167. Cadle, S. H. and Bruckenstein, S., Ring-Disk Electrode Study of the Anodic Behaviour of Gold in 0.2M Sulfuric Acid, *Anal. Chem.*, **46**, 16-20 (1974).

168. Hoare, J. P., A Cyclic Voltammetric Study of the Gold-Oxygen System, *J. Electrochem. Soc.*, **131**, 1808-1815 (1984).

169. Levich, V. G., "Physicochemical Hydrodynamics", Prentice-Hall, Inc., Englewood Cliffs, N. J., 1962, 700 pp.

170. Levich, V. G., *Acta Phys. Chim. URSS*, **17**, 257 (1942) (quoted in reference 169).

171. Churchill, M. and Laxen, P. A., The Rotating Disc System and its Applications in the Dissolution of Gold, Research Report No. 16, National Institute for Metallurgy, South Africa, 1966.

172. Bard, A. J. and Faulkner, L. R., "Electrochemical Methods", John Wiley & Sons, New York, 1980, 718 pp.

173. Wadsworth, M. E. and Miller, J. D., Chap.3: Hydrometallurgical Processes in "Rate Processes in Extractive Metallurgy", Sohn, H. Y. and Wadsworth, M. E. (eds.), Plenum Press, New York, 1979, 472 pp.

174. Opekar, F. and Beran, P., Rotating Disk Electrodes, *J. Electroanal. Chem.*, **69**, 1-105 (1976).

175. Albery, W. J. and Hitchman, M. L., "Ring-Disc Electrodes", Claredon Press, Oxford, 1971, 175 pp.

176. Gregory, D. P. and Riddiford, A. C., Transport to the Surface of a Rotating Disc, *J. Chem. Soc.*, 3756-3764 (1956).

177. Groenewald, T., The Dissolution of Gold in Acidic Solutions of Thiourea, *Hydrometallurgy*, **1**, 277-290 (1976).

178. Weiss, R. F., The Solubility of Nitrogen, Oxygen and Argon in Water and Seawater, *Deep-Sea Research*, **17**, 721-735 (1970).

179. Awakura, Y., Iwai, M. and Majima, H., Oxidation of Fe(II) in HCl and H_2SO_4 Solutions with Dissolved Molecular Oxygen in the Presence and Absence of a Cupric Catalyst, in "Iron Control in Hydrometallurgy", Dutrizac, J. E. and Monhemius, A. J., eds., 1986.

180. Mathews, C. T. and Robins, R. G., The Oxidation of Aqueous Ferrous Sulphate Solutions by Molecular Oxygen, *Proc. Aust. Inst. Min. Met.*, **242**, 47-56 (1972).

181. Huffman, R. E. and Davidson, N., Kinetics of the Ferrous Iron-Oxygen Reaction in Sulfuric Acid Solution, *J. Amer. Chem. Soc.*, **78**, 4836-4842 (1956).

182. Colborn, R. P. and Nicol, M. J., An Investigation into the Kinetics and Mechanism of the Oxidation of Iron(II) by Oxygen in Aqueous Chloride Solutions, *J. S. Afr. Inst. Min. Met.*, 281-289 (1973).

183. Thurgood, C. P., Kirk, D. W., Foulkes, F. R. and Graydon, W. F., Activation Energies of Anodic Gold Reactions in Aqueous Alkaline Cyanide, *J. Electrochem. Soc.*, **128**, 1680-1685 (1981).

184. Kirk, D. W., Foulkes, F. R. and Graydon, W. F., A Study of Anodic Dissolution of Gold in Aqueous Alkaline Cyanide, *J. Electrochem. Soc.*, **125**, 1436-1443 (1978).

185. Mac Arthur, D. M., A Study of Gold Reduction and Oxidation in Aqueous Solutions, *J. Electrochem. Soc.*, **119**, 672-676 (1972).

186. Cathro, K. J. and Koch, D. F. A., The Anodic Dissolution of Gold in Cyanide Solutions, *J. Electrochem. Soc.*, **111**, 1416-1420 (1964).

187. Brent Hiskey, J. and Atluri, V. P., Dissolution Chemistry of Gold and Silver in Different Lixiviants, *Min. Proc. and Extr. Met. Rev.*, **4**, 95-134 (1988).

188. Qi, P. H. and Brent Hiskey, J., Leaching and Electrochemical Behaviour of Gold in Iodide Solutions, Part I: Dissolution Kinetics, Dept. of Materials Science and Engineering, Univ. of Arizona, Tucson, AZ (in press).

189. Qi, P. H. and Brent Hiskey, J., Leaching and Electrochemical Behaviour of Gold in Iodide Solutions, Part II: Electrochemistry, Dept. of Materials Science and Engineering, Univ. of Arizona, Tucson, AZ (in press).

190. Brent Hiskey, J. and Qi, P. H., Leaching Behavior of Gold in Iodide Solutions, in "World Gold'91 Proceedings", The Aust. Inst. Min. Met., Australia, 1991, pp. 115-120.

191. Davis, A. and Tran, T., Gold Dissolution in Iodide Electrolytes, *Hydrometallurgy*, **26**, 163-177 (1991).

192. McGrew, K. J. and Murphy, J. W., Iodine Leach for the Dissolution of Gold, U. S. Pat. 4,557,759 (1985).

193. Homick, R. P., Gold Reclamation Process, U. S. Pat. 3,957,505 (1976).

194. Falanga et al., Recovery of Gold and/or Palladium from an Iodide-Iodine Etching Solution, U. S. Pat. 4,319,923 (1982).

195. Wilson, H. W., Noble Metals Solvation Agents - Hydroxyketones and Iodine and Iodide, U. S. Pat. 3,826,750 (1974).

196. Wilson, H. W., Process for Separation and Recovery of Gold, U. S. Pat. 3,778,252 (1973).

197. Jacobson, R., Murphy, J. and Whitman, D., The Economics of Small Metallic In-Situ Mining Operations, including Uranium, Gold, Silver and Copper, "Proceedings of the Small Mines Conference", Royal School of Mines, Imperial College, London, 1987.

198. Fleming, C. A., Private Communication, 1988.

199. Országh, I., Bazsa, Gy. and Beck, M. T., Spectrophotometric Study of the Reversible Iodine-Thiocyanate Interaction, *Inorg. Chim. Acta*, **6**, 271-274 (1972).

200. Long, C. and Skoog, D. A., A Thiocyanate Complex of Iodine(I), *Inorg. Chem.*, **5**, 206-210 (1966).

201. Lewis, C. and Skoog, D. A., Spectrophotometric Study of a Thiocyanate Complex of Iodine, *J. Am. Chem. Soc.*, **84**, 1101-1106 (1962).

202. Griffith, R. O. and McKeown, A., Kinetics of the Reaction Between Potassium Thiocyanate and Iodine in Aqueous Solution, *Trans. Faraday Soc.*, **31**, 868-875 (1935).

203. Groenewald, T., Electrochemical Studies on Gold Electrodes in Acidic Solutions of Thiourea Containing Gold(I) Thiourea Complex Ions, *J. Appl. Electrochem.*, **5**, 71-78 (1975).

204. Adams, R. N., "Electrochemistry at Solid Electrodes", Marcel Dekker, Inc., New York, 1969, 402 pp.